# Organometallic Chemistry

ELSEVIER

# JOURNAL OF ORGANOMETALLIC CHEMISTRY


**Emeritus Board**

H.C. Brown (*Lafayette, IN, USA*)
G.P. Chiusoli (*Parma, Italy*)
E.O. Fischer (*Munich, Germany*)
M. Kumada (*Kyoto, Japan*)
J. Lewis (*Cambridge, UK*)
M.G. Voronkov (*Irkutsk, Russian Federation*)
G. Wilke (*Mülheim/Ruhr, Germany*)

**Editorial Board**

J.L. Atwood (*Columbia, MO, USA*)
T. Bitterwolf (*Moscow, ID, USA*)
P. Braunstein (*Strasbourg, France*)
H. Brunner (*Regensburg, Germany*)
F. Calderazzo (*Pisa, Italy*)
E. Carmona (*Sevilla, Spain*)
R.J.P. Corriu (*Montpellier, France*)
A.H. Cowley (*Austin, TX, USA*)
A.G. Davies (*London, UK*)
C. Eaborn (*Brighton, UK*) *
J.J. Eisch (*Binghamton, NY, USA*)
C. Floriani (*Lausanne, Switzerland*)
S. Gambarotta (*Ottawa, Ont., Canada*)
M.L.H. Green (*Oxford, UK*)
W.A. Herrmann (*Munich, Germany*) *
P. Jutzi (*Bielefeld, Germany*)
R.B. King (*Athens, GA, USA*) *
G. van Koten (*Utrecht, The Netherlands*)*
M.F. Lappert (*Brighton, UK*)
G.J. Leigh (*Brighton, UK*)
P.M. Maitlis (*Sheffield, UK*)
F. Mathey (*Palaiseau, France*)*
D.M.P. Mingos (*London, UK*)*
A. Nakamura (*Osaka, Japan*) *
J.F. Normant (*Paris, France*)
J.P. Oliver (*Detroit, MI, USA*) *
S. Pasynkiewicz (*Warsaw, Poland*)
P.L. Pauson (*Glasgow, UK*)
C. Raston (*Clayton, Vic., Australia*)
M.D. Rausch (*Amherst, MA, USA*)
O.A. Reutov (*Moscow, Russian Federation*)
H. Sakurai (*Chiba, Japan*)
V.I. Sokolov (*Moscow, Russian Federation*)
F.G.A. Stone (*Waco, TX, USA*)
R.M. Waymouth (*Stanford, CA, USA*)
H. Werner (*Würzburg, Germany*)
A. Yamamoto (*Tokyo, Japan*)
H. Yamazaki (*Tokyo, Japan*)

* Denotes Regional Editor, Deputy Regional Editor, Subject Reviews Editor or Book Reviews Editor.


## Aims and Scope

The *Journal of Organometallic Chemistry* publishes original papers, preliminary communications, priority communications and subject reviews dealing with theoretical aspects, structural chemistry, synthesis, physical and chemical properties including reaction mechanisms, and practical applications, of organoelement compounds in a sense corresponding essentially to Section 29 ("Organometallic and Organometalloidal Compounds") of *Chemical Abstracts*.

Papers on the following classes of compounds will be considered for publication:

(a) Compounds containing at least one direct bond between carbon and other elements excluding H, N, O, halogens and noble gases. Borderline cases can be expected among certain compounds containing S; these will be considered but not encouraged, and will be judged on their own merits. Carbonates and carbides will be excluded, as will also organometallic compounds in which the metal has no significant role.

(b) Metal hydrides and carbonyls.

(c) Metallocenes and similar complexes.

(d) In exceptional cases, compounds containing no direct carbon–metal (or –metalloid) bond in the sense as described in (a) but which exhibit distinct organometallic character.

(e) New uses of compounds mentioned under (a)–(d) in synthetic organic chemistry, with the exclusion of their use for well-known routine purposes.

(f) Papers consisting wholly or mainly of reports of spectroscopic data (including fragmentation patterns from mass spectral studies) will be accepted only if the interpretation of such data has clear general implications.


## Subscription information 1996

Volumes 506–526, each containing 2 issues, are scheduled for publication. Prices are available from the publishers upon request. Subscriptions are accepted on a prepaid basis only. Issues are sent by SAL (Surface Air Lifted) mail wherever this service is available. Airmail rates are available upon request. Please address all requests regarding orders and subscriptions to:

**ELSEVIER SCIENCE S.A.**
P.O. Box 564, 1001 Lausanne, Switzerland.
Telephone: (21) 3 20 73 81
Telex: 450 620 ELSA CH; Telefax: (21) 3 235 444

*Customers in the United States and Canada may obtain information from:*

**ELSEVIER SCIENCE, INC.**
Attn.: Journal Information Center, 655 Avenue of the Americas, New York, NY 10010, USA.
Telephone: (212) 633–3750
Telex: 420643 AEP UI; Telefax: (212) 633–3764

**US mailing notice:** *Journal of Organometallic Chemistry* (ISSN 0022-328X) is published biweekly by Elsevier Science S.A. (P.O. 564, 1001 Lausanne). Annual subscription price in the USA is US$ 6283.- (valid in North, Central and South America), including air speed delivery. Second class postage is paid at Jamaica N.Y. 11431.

**USA POSTMASTERS:** Send address changes to *Journal of Organometallic Chemistry*, Publications Expediting, Inc., 200 Meacham Avenue, Elmont, NY 11003. **AIRFREIGHT AND MAILING** in the USA by Publication Expediting Inc., 200 Meacham Avenue, Elmont, NY 11003.



## Abstracting Organizations

Articles in this journal will be indexed and abstracted in Chemical Abstracts, Chemischer Informationsdienst, Current Abstracts of Chemistry and Index Chemicus, Current Contents, Physical, Chemical and Earth Sciences, Pascal (Centre de Documentation Scientifique et Technique), Research Alert™ and the Science Citation Index.

Full texts are incorporated in CJELSEVIER, a file in the Chemical Journals Online database which is available on STN® International.

# Journal of Organometallic Chemistry

Volume 508 (1996)

# Journal of Organometallic Chemistry

Volume 508 (1996)

**Emeritus Board**
H.C. Brown *(Lafayette, IN, USA)*
G.P. Chiusoli *(Parma, Italy)*
E.O. Fischer *(Munich, Germany)*
M. Kumada *(Kyoto, Japan)*
J. Lewis *(Cambridge, UK)*
M.G. Voronkov *(Irkutsk, Russian Federation)*
G. Wilke *(Mülheim/Ruhr, Germany)*

**Editorial Board**
J.L. Atwood *(Columbia, MO, USA)*
T. Bitterwolf *(Moscow, ID, USA)*
P. Braunstein *(Strasbourg, France)*
H. Brunner *(Regensburg, Germany)*
F. Calderazzo *(Pisa, Italy)*
E. Carmona *(Sevilla, Spain)*
R.J.P. Corriu *(Montpellier, France)*
A.H. Cowley *(Austin, TX, USA)*
A.G. Davies *(London, UK)*
C. Eaborn *(Brighton, UK)* *
J.J. Eisch *(Binghamton, NY, USA)*
C. Floriani *(Lausanne, Switzerland)*
S. Gambarotta *(Ottawa, Ont., Canada)*
M.L.H. Green *(Oxford, UK)*
W.A. Herrmann *(Munich, Germany)* *
P. Jutzi *(Bielefeld, Germany)*
R.B. King *(Athens, GA, USA)* *
G. van Koten *(Utrecht, The Netherlands)**
M.F. Lappert *(Brighton, UK)*
G.J. Leigh *(Brighton, UK)*
P.M. Maitlis *(Sheffield, UK)*
F. Mathey *(Palaiseau, France)**
D.M.P. Mingos *(London, UK)**
A. Nakamura *(Osaka, Japan)* *
J.F. Normant *(Paris, France)*
J.P. Oliver *(Detroit, MI, USA)* *
S. Pasynkiewicz *(Warsaw, Poland)*
P.L. Pauson *(Glasgow, UK)*
C. Raston *(Clayton, Vic., Australia)*
M.D. Rausch *(Amherst, MA, USA)*
O.A. Reutov *(Moscow, Russian Federation)*
H. Sakurai *(Chiba, Japan)*
V.I. Sokolov *(Moscow, Russian Federation)*
F.G.A. Stone *(Waco, TX, USA)*
R.M. Waymouth *(Stanford, CA, USA)*
H. Werner *(Würzburg, Germany)*
A. Yamamoto *(Tokyo, Japan)*
H. Yamazaki *(Tokyo, Japan)*

* Denotes Regional Editor, Deputy Regional Editor, Subject Reviews Editor or Book Reviews Editor.

ELSEVIER AMSTERDAM – LAUSANNE – NEW YORK – OXFORD – SHANNON – TOKYO

*Abstracting Organizations*
Articles in this journal will be indexed and abstracted in Chemical Abstracts, Chemischer Informationsdienst, Current Abstracts of Chemistry and Index Chemicus, Current Contents, Physical, Chemical and Earth Sciences, Pascal (Centre de Documentation Scientifique et Technique), Research Alert™ and the Science Citation Index.
Full texts are incorporated in CJELSEVIER, a file in the Chemical Journals Online database which is available on STN® International.

International Standard Serial Number 0022-328X

© 1996 – Elsevier Science S.A. All rights reserved 0022-328X/96/$15.00
No part of this publication may be reproduced, stored in a retrieval system or transmitted in any form or by any means, electronic, mechanical, photocopying, recording or otherwise, without the prior written permission of the publisher, Elsevier Science S.A., P.O. Box 564, 1001 Lausanne, Switzerland.
Submission of an article for publication implies the transfer of the copyright from the author(s) to the publisher and entails the author(s) irrevocable and exclusive authorization of the publisher to collect any sums or considerations for copying or reproduction payable by third parties. Upon acceptance of an article by the journal, the author(s) will be asked to transfer copyright of the article to the publisher. This transfer will ensure the widest possible dissemination of information.

**For Material Subject to US Copyright Law**
*Special regulations for readers in the USA* – This journal has been registered with the Copyright Clearance Center, Inc. Consent is given for copying of articles for personal or internal use, or for the personal use of specific clients. This consent is given on the condition that the copier pays through the Center the per-copy fee stated in the code on the first page of each article for copying beyond that permitted by Sections 107 or 108 of the US Copyright Law. The appropriate fee should be forwarded with a copy of the first page of the article to the Copyright Clearance Center, Inc., 222 Rosewood Drive, Danvers, MA 01923, USA. If no code appears in an article, the author has not given broad consent to copy and permission to copy must be obtained directly from the author. The fee indicated on the first page of an article in this issue will apply retroactively to all articles published in the journal, regardless of the year of publication. This consent does not extend to other kinds of copying, such as for general distribution, resale, advertising and promotion purposes, or for creating new collective works. Special written permission must be obtained from the publisher for such copying.

No responsibility is assumed by the Publisher for any injury and/or damage to persons or property as a matter of products liability, negligence or otherwise, or from any use or operation of any methods, products, instructions or ideas contained in the material herein.

⊖ The paper used in this publication meets the requirements of ANSI/NISO 239.48-1992 (Permanence of Paper).

Printed in The Netherlands

ELSEVIER

Volume 508, Numbers 1–2, 8 February 1996

Journal of Organometallic Chemistry

# Contents

*Regular Papers*

Reaction of sodium amalgam with carbenium ions species stabilised by two adjacent organometallic moieties
J.-F. Capon, N. Le Berre-Cosquer and R. Kergoat (Brest, France) . . . . . 1

Reactions of $(THF)W(CO)_5$ with some diphosphenes carrying bulky aryl and phenoxy groups
D.-L. An, K. Toyota, M. Yasunami and M. Yoshifuji (Sendai, Japan) . . . . . 7

Zirkoniumorganische Chemie mit anorganischen Donorliganden N,N′-Bis(trimethylsilyl)benzamidinat (Siam) in Verbindungen des Typs $(Siam)_2ZrX_2$ (X = Methyl, Benzyl, Allyl, Chlorid oder Iodid) und $(Siam)_3ZrX$ (X = Chlorid)
D. Walther, R. Fischer, H. Görls, J. Koch and B. Schweder (Jena, Deutschland) . . . . . 13

Comparison of the oxidation of dinuclear cyclopentadienyl iron diphosphine complexes with the bridging ligands –CN and $-C{\equiv}C(CH_2)_2CN$
G.A. Carriedo (Oviedo, Spain), A. Arancibia, C. Díaz-Valenzuela, N. Yutronic (Santiago, Chile), E. Pérez-Carreño and S. García-Granda (Oviedo, Spain) . . . . . 23

Synthesis of secondary allenylidene–molybdenum complexes with a ferrocenyl substituent from carbenium ions species stabilized by two organometallic moieties
J.-F. Capon, N. Le Berre-Cosquer, B. Leblanc and R. Kergoat (Brest, France) . . . . . 31

Protonation of triosmium clusters $Os_3(CO)_9(\mu\text{-}CO)(\mu_3\text{-}2\sigma,\eta^2\text{-}HC{\equiv}CR)$ and $Os_3(\mu\text{-}H)(CO)_9(\mu_3\text{-}\sigma,2\eta^2\text{-}C{\equiv}CR)$ ($R = CH_2OH$, $CMe_2OH$, $C(Me){=}CH_2$)
V.V. Krivykh, O.A. Kizas, E.V. Vorontsov, F.M. Dolgushin, A.I. Yanovsky, Yu.T. Struchkov and A.A. Koridze (Moscow, Russia) . . . . . 39

Reaction of pentaarylantimony with acid halide, aldehyde and ketone
M. Fujiwara, M. Tanaka, A. Baba, H. Ando and Y. Souma (Osaka, Japan) . . . . . 49

Synthesis of some $\mu$-hydroxo-, phenoxo- and O,O-acetylacetonato-arylgold(III) complexes. Crystal structure of $[Au(C_6H_4NO_2-2)_2(\mu\text{-}OH)]_2 \cdot 2Et_2O$
J. Vicente (Murcia, Spain), M.D. Bermúdez, F.J. Carrión (Cartagena, Spain) and P.G. Jones (Braunschweig, Germany) . . . . . 53

Catalytic hydroformylation of (1*S*,5*S*)-(−)- and (1*R*,5*R*)-(+)-$\beta$-pinene: stereoselective synthesis and spectroscopic characterization of (1*S*,2*R*,5*S*)-, (1*S*,2*S*,5*S*)-, (1*R*,2*R*,5*R*)- and (1*R*,2*S*,5*R*)-10-formylpinane
F. Azzaroni, P. Biscarini, S. Bordoni, G. Longoni and E. Venturini (Bologna, Italy) . . . . . 59

Synthesis and spectroscopic studies of new hydridoruthenium complexes: catalytic reactions of [RuHCl(bpzm)(cod)] (bpzm = bis(pyrazol-1-yl)methane, cod = cycloocta-1,5-diene)
F.A. Jalón, A. Otero, A. Rodríguez (Ciudad Real, Spain) and M. Pérez-Manrique (Burgos, Spain) . . . . . 69

Properties and reactivity of the new $[Ir_4(\mu\text{-}CO)_3(CO)_5(\mu\text{-}PR_3)(PR_3)_2]$ clusters, ($PR_3 = PPh_xpyl_{3-x}$, pyl = 2-pyridyl)
K. Wajda-Hermanowicz, F. Pruchnik and M. Zuber (Wrocław, Poland) . . . . . 75

Molecular oxygen promoted oxidative cleavage of carbon–palladium bonds — catalytic cyclization of allylic 2-alkynoates to $\alpha$-alkylidene-$\gamma$-butyrolactones by a $Pd^{II}$ complex
G. Zhu and X. Lu (Shanghai, China) . . . . . 83

Preparation of Group 4 metal complexes of a bulky amido-fluorenyl ligand
H.V.R. Dias, Z. Wang (Arlington, TX, USA) and S.G. Bott (Denton, TX, USA) . . . . . 91

Mechanism of oxidative allyl transfer from allylic ammonium cations to palladium(0) $\alpha$-diimine complexes
L. Canovese, F. Visentin, P. Uguagliati, F. Di Bianca (Venezia, Italy), A. Fontana (Palermo, Italy) and B. Crociani (Rome, Italy) . . . . . 101

Insertion reactions involving palladium complexes with nitrogen ligands. I. Reactivity towards carbon monoxide of methylpalladium(II) complexes containing bidentate $\alpha$-diimine ligands: crystal structures of four methylpalladium (II) and acylpalladium(II) complexes
R.E. Rülke, J.G.P. Delis, A.M. Groot, C.J. Elsevier, P.W.N.M. Van Leeuwen, K. Vrieze, K. Goubitz and H. Schenk (Amsterdam, Netherlands) . 109

Synthetic studies of permethylcyclopentadienyl ruthenium(II) complexes involving dppf, (±)-BINAP and (±)-DIOP ligands
M. Sato and M. Asai (Saitama, Japan) . . . . . 121

$^{55}Mn$ and $^{187}Re$ NQR spectral studies of modulation effects of mutual motions of electrons and atomic nuclei in cyclopentadienyl tricarbonyl manganese and rhenium complexes
G.K. Semin, S.I. Kuznetsov, E.V. Bryukhova and T.L. Khotsyanova (Moscow, Russia) . . . . . 129

The reactions of tricobalt alkylidyne complexes $[Co_3(\mu_3\text{-}CR)(CO)_9]$ (R = Me, $CO_2Me$) with the vinyl phosphine ligands $PPh_2CH{=}CH_2$ and *cis*-$Ph_2PCH{=}CHPPh_2$; crystal structure of $[Co_3(\mu_3\text{-}CCO_2Me)(\mu\text{-}Ph_2PCH{=}CHPPh_2)(CO)_7]$
G.A. Acum, M.J. Mays, P.R. Raithby and G.A. Solan (Cambridge, UK) . . . . . 137

Katalytische Hydrierung von Halogenmonoosilanen mit Tributylzinnhydrid
U. Pätzold, G. Roewer und U. Herzog (Freiberg/Sa., Deutschland) . . . . . 147

General valence force fields of the free and the coordinated cyclopentadienyl anion
T. Polzer and W. Kiefer (Würzburg, Germany) . . . . . 153

Preparation and some properties of Pt(II) ruthenocenylacetylide complexes
M. Sato and E. Mogi (Saitama, Japan) . . . . . 159

Ring slippage in indenyl derivatives of molybdenum and tungsten
J.R. Ascenso (Lisboa, Portugal), I.S. Gonçalves (Oeiras, Portugal), E. Herdtweck (Garching, Germany) and C.C. Romão (Oeiras, Portugal) . . . 169

Elsevier Science S.A.

Diphenylphosphine derivatives of $Co(NO)(CO)_3$, $Fe(NO)_2(CO)_2$ and $Mn(NO)(CO)_4$
J.T. Lin (Taipei, Taiwan), S.Y. Wang (Chung Hua, Taiwan), Y.C. Chou, M.L. Gong, Y.-M. Shiow (Taipei, Taiwan), H.-M. Gau (Taichung, Taiwan) and Y.S. Wen (Taipei, Taiwan) . . . 183
Isomeric diphosphines of a heteroannularly bridged ferrocene: preparation, chromatographic separation and structure elucidation
G. Kutschera (Wien, Austria), C. Kratky (Graz, Austria), W. Weissensteiner and M. Widhalm (Wien, Austria) . . . 195
Synthesis and molecular structure of enantiopure 1-(diphenylphosphino)-2,1'-[(1-*N*,*N*-dimethylamino)-1,3-propanediyl]-ferrocene and its palladium dichloride complex, a new ligand for enantioselective catalysts
A. Mernyi (Wien, Austria), C. Kratky (Graz, Austria), W. Weissensteiner and M. Widhalm (Wien, Austria) . . . 209
Optically active transition-metal complexes. III. Synthesis of optically active ($\eta^4$-aminodiolefin)tricarbonyl iron complexes. Kinetic resolution of a chiral amine by means of an optically active dienyl iron cation
M. Käser and A. Salzer (Aachen, Germany) . . . 219
Syntheses of tungsten-substituted oligosilanes
A. Zechmann and E. Hengge (Graz, Austria) . . . 227
Multiply substituted cyclopentadienyl metal complexes: I. Solid-state and solution conformational studies on ($\eta^5$-$C_5Me_4R$)Fe(CO)(L)I (R = H, $^t$Bu)
K.E. Du Plooy, J. Du Toit, D.C. Levendis and N.J. Coville (Johannesburg, South Africa) . . . 231
Reactions of trimethylaluminium with aliphatic diols
W. Ziemkowska and S. Pasynkiewicz (Warsaw, Poland) . . . 243
Synthesis, properties and crystal structure of bis(cyclopentadienyl)aluminium complex [$\eta^1$-$(C_5H_5)_2$AlO–$^i$Pr]$_2$
A. Kunicki, R. Sadowski and J. Zachara (Warsaw, Poland) . . . 249
Palladium-catalyzed reaction of 1-aza-5-germa-5-organobicyclo[3.3.3]undecane with aryl bromide
M. Kosugi, T. Tanji, Y. Tanaka, A. Yoshida, K. Fugami (Gunma, Japan), M. Kameyama (Tochigi, Japan) and T. Migita (Shizuoka, Japan) . . . 255
Electron density distribution in the vanadocene crystal on the basis of X-ray diffraction data at 108 K
M.Yu. Antipin, K.A. Lyssenko (Moscow, Russia) and R. Boese (Essen, Germany) . . . 259

*Preliminary Communications*
Hydride abstraction from ($\eta^2$-acetaldehyde)zirconocene dimer using $B(C_6F_5)_3$
D. Röttger, S. Schmuck and G. Erker (Münster, Germany) . . . 263
Vergleichende Dimerisierung der Enantiomere von Oct-1-in-3-ol mit chiralen Rhodium-Phosphan-Komplexen
H. Singer und M. Steigerwald (Mainz, Deutschland) . . . 267
Crown compounds for anions. A polymeric complex of cyclic trimeric perfluoro-*o*-phenylenemercury with thiocyanate anion containing an infinite helical chain of alternating molecules of mercury-containing macrocycle and $SCN^-$ ions
I.A. Tikhonova, F.M. Dolgushin, A.I. Yanovsky, Yu.T. Struchkov, A.N. Gavrilova, L.N. Saitkulova, E.S. Shubina, L.M. Epstein, G.G. Furin and V.B. Shur (Moscow, Russia) . . . 271
Zur Elektronenstruktur metallorganischer Komplexe der f-Elemente. XXXVIII. Halbsandwich-Komplexe der Stöchiometrien (COT)Ln($HBpz_3$) und (COT)Ln[$HB(3,5\text{-}Me_2pz)_3$]-ideale Systeme für die experimentelle Bestimmung der Kristallfeld-Aufspaltungseffekte des Cyclooctatetraenyl-Liganden
H.-D. Amberger (Hamburg, Deutschland) und F.T. Edelmann (Magdeburg, Deutschland) . . . 275

*Book Review* . . . 281

*Author Index* . . . 283

*Subject Index* . . . 285

The publisher encourages the submission of articles in electronic form thus saving time and avoiding rekeying errors. A leaflet describing our requirements is available from the publisher upon request.

ELSEVIER

Journal of Organometallic Chemistry 508 (1996) 1–6

Journal of Organometallic Chemistry

# Reaction of sodium amalgam with carbenium ions species stabilised by two adjacent organometallic moieties

J.-F. Capon, N. Le Berre-Cosquer, R. Kergoat *

*URA CNRS No. 322, Chimie, Electrochimie Moléculaires et Chimie Analytique, Equipe de Chimie Inorganique Moléculaire, Université de Bretagne Occidentale, 6 Avenue le Gorgeu, BP 809, 29285 Brest Cédex, France*

Received 9 February 1995

**Abstract**

The ionic complexes $[Cp_2Mo_2(CO)_4\{\mu\text{-}\eta^2\text{:}\eta^3\text{-}HC{\equiv}C\text{–}C(H)(Fc)\}][BF_4]$ (1) and $[\{Cp_2Mo_2(CO)_4(\mu\text{-}\eta^2\text{:}\eta^3\text{-}HC{\equiv}C\text{–}C(H)\}_2Fc][(BF_4)_2]$ (5) react with Na–Hg in toluene solution. The results are interpreted in terms of a radical mechanism involving intramolecular and intermolecular coupling reactions.

*Keywords:* Carbenium ions; Molybdenum clusters; Ferrocenyl; Ferrocenophane

## 1. Introduction

Recently we have been interested in the reactivity of carbon-centred organometallic radicals formed from the carbenium ions $[Cp_2Mo_2(CO)_4\{\mu\text{-}\eta^2\text{:}\eta^3\text{-}HC{\equiv}C\text{–}C(R_1)(R_2)\}]^+$ [1,2]. Free radical intermediates are assumed to be present during the reductive dimerization of such compounds (Scheme 1) [1–3]. The structures of the dimers $[Mo_2Cp_2(CO)_4(\mu\text{-}\eta^2\text{:}\eta^2\text{-}HC{\equiv}CCH_2\text{–})]_2$ [3] and $[Mo_2Cp_2(CO)_4(\mu\text{-}\eta^2\text{:}\eta^2\text{-}HC{\equiv}CC(H)(Et)\text{–}]_2$ [2] were established by X-ray diffraction. The work also shows that for the best results in the coupling reactions the $R_1$ and $R_2$ groups should be free from acidic protons: for example, if $R_1 = R_2$ = Methyl or Cyclohexyl, the formation of $\mu$-enyne complexes $[Cp_2Mo_2(CO)_4\{\mu\text{-}\eta^2\text{:}\eta^2\text{-}HC{\equiv}C\text{–}C(R) = C(R')(R'')\}]$ is favoured (Scheme 1 (b)).

Similar reactions of ferricinium ions involving a carbonium-ion-centre $C^+$ stabilised by an organometallic fragment have been known for many years [4]. They are interpreted as proceeding through the reduction of the ferricinium ion by electron transfer from the reducing agent with the formation of a radical, followed by a coupling reaction to produce a dimer. More recently, photolysis of ferrocenyl ethers has been shown to give ferricinium ion radicals that can dimerise or abstract a proton from the solvent [5].

Here, we describe coupling reactions involving free radical intermediates of the carbenium ions $[Cp_2Mo_2(CO)_4\{\mu\text{-}\eta^2\text{:}\eta^3\text{-}HC{\equiv}C\text{–}C(R_1)(R_2)\}]^+$ with a ferrocenyl group ($R_1$ = Fc:$(C_5H_4)Fe(C_5H_5)$). The carbon atom bearing the positive charge is adjacent both to a ferrocenyl group and an acetylenic cluster. Such compounds, lacking any acidic protons ($R_1$ = Fc and $R_2$ = H), cannot give $\mu$-enyne complexes. The nature of the stabilisation of the $C^+$ atom has already been discussed for the complex $[Cp_2Mo_2(CO)_4\{\mu\text{-}\eta^2\text{:}\eta^3\text{-}CH_3(CH_2)_4\text{–}C{\equiv}C\text{–}C(H)(Fc)\}][BF_4]$ [6].

## 2. Results and discussion

### 2.1. Reduction of $[Cp_2Mo_2(CO)_4\{\mu\text{-}\eta^2\text{:}\eta^3\text{-}HC{\equiv}C\text{–}C(H)(Fc)\}][BF_4]$ (1)

Treatment of $[Cp_2Mo_2(CO)_4\{\mu\text{-}\eta^2\text{:}\eta^3\text{-}HC{\equiv}C\text{–}C(H)(Fc)\}][BF_4]$ (1) (Scheme 2) with Na–Hg (in toluene 18°C, 18 h) gives a mixture of $[Cp_2Mo_2(CO)_4\{\mu\text{-}\eta^2\text{:}\eta^2\text{-}HC{\equiv}C\text{–}C(H)_2(Fc)\}]$ (2) (yield 23%), $[\{Cp_2Mo_2(CO)_4\}_2(\mu\text{-}\eta^2\text{:}\eta^2\text{-}HC{\equiv}C\text{–}C(H)(Fc)\text{–}C(H)(Fc)\text{–}C{\equiv}CH)]$ (4) (yield 7%) and $[Cp_2Mo_2(CO)_4\{\mu\text{-}\sigma\text{:}\eta^3\text{-}HC{=}CH{-}C(H)(Fc)\}]$ (3) (yield 10%), which can easily be separated ($SiO_2$, $CH_2Cl_2$–hexane). The compounds (2) and (4) result from a typical radical mechanism; com-

* Corresponding author.

0022-328X/96/$15.00 © 1996 Elsevier Science S.A. All rights reserved
*SSDI* 0022-328X(95)05776-5

pound (4) comes from a coupling reaction between two free radicals (an intermolecular coupling reaction) and compound (2) is formed by abstraction of protons from the solvent or traces of moisture. Complex (4) contains two asymmetric centres, and the dl/meso diastereomers obtained in equal amount cannot be separated. Product (3) probably comes from fragmentation or rearrangement reaction of the $\mu$-alkyne complex (2) which may react with the excess Na. Such processes were discussed previously for the reduction of $\mu$-enyne [1,2] or $\mu$-alkyne complexes [7].

### 2.2. Reduction of $[\{Cp_2Mo_2(CO)_4(\mu\text{-}\eta^2\text{:}\eta^3\text{-}HC{\equiv}C\text{-}C(H)\}_2Fc][\{BF_4\}_2]$ (5)

The reaction of Na–Hg with the dication $[\{Cp_2Mo_2(CO)_4(\mu\text{-}\eta^2\text{:}\eta^3\text{-}HC{\equiv}C\text{-}C(H)\}_2Fc][\{BF_4\}_2]$ (5) (Scheme 3) yields a mixture of products which can be separated by column-chromatography on silica. Use of the above conditions in the case of dication (5) again gives both coupling and H-atom abstraction, to form compounds (6) and (7). The two main features are that (a) complex (6) is obtained by an intramolecular radical

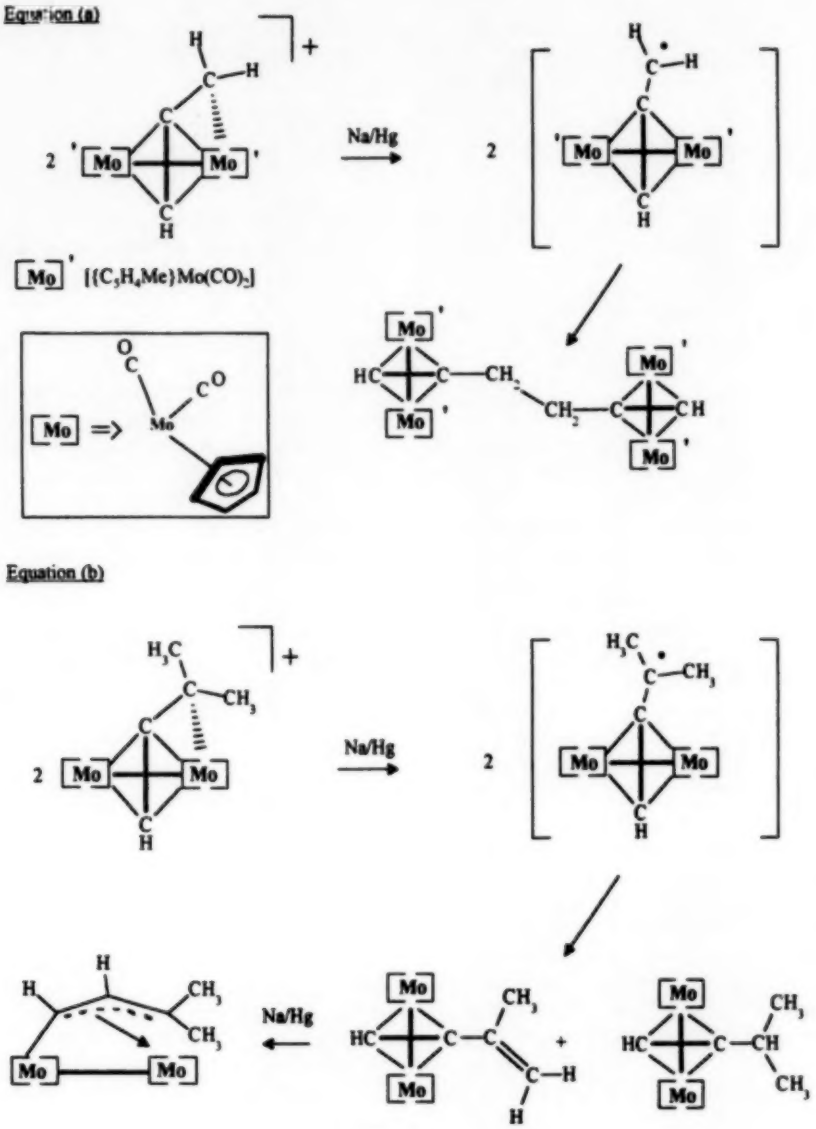


Scheme 1.

process (unlike the formation of (4) which involved an intermolecular radical process), and (b) only one diastereomer is obtained (diastereoselectivity 100%).

This reaction generates chiral carbon atoms $\alpha$ to the organometallic moieties, and as a consequence the $^1H$ NMR spectrum of (6) displays two signals for cyclopentadienyl ligands linked to molybdenum atoms; the $C_5H_5$–Mo groups are diastereotopic [8]. Moreover, all the protons of the $C_5H_4$–Fe ring display different chemical shifts (ABCD spin system) as expected for molecules with a stereogenic carbon atom [9]. Compound (6) is an ansa-ferrocene with two carbon atoms as bridging substituents; it belongs to the [2] (1,1') ferrocenophane class of compounds which attract much attention because of their ability to give access to polyferrocenylethylenes by ring-opening polymerization [10]. These results have to be compared with those for reductive cyclization of $Co_2(CO)_6$-complexed propargyl cations which provided a new route to cycloalkadiynes by a radical intramolecular process [11].

Preliminary electrochemical studies on (6) show that the presence of a C–C bond has a marked influence on the mechanism of oxidation, making it a quasi-reversible process ($Ep_{ox} = -0.08$ V versus ferrocene) leading to the dication (5). In contrast, two reversible oxidations were observed in the case of 1,1,12,12-tetramethyl-[1.1]silaferrocenophane [12] and its carbon or tin analogue [13]. More complete electrochemical studies of the behaviour of the various carbenium ions, including the nature of the radical intermediate, are in progress in our laboratory.

Recent examination by McClain et al. [14] of the reduction of the dicarbenium complex (A) $[Cp_2Mo_2(CO)_4(CH_2CCCH_2)][BF_4]_2$ with Na–Hg in the hope of making a polymer was unsuccessful, whereas reduction of the monocarbenium complex (B) $[(C_5H_4Me)_2Mo_2(CO)_4(\mu\text{-}\eta^2\text{:}\eta^3\text{-}HC{\equiv}C\text{–}CH_2)][BF_4]$ [3] gave a C–C coupled product. Unlike that in (B), the LUMO of the dicarbenium complex (A) places no electron density on the ligand upon reduction, so avoiding C–C coupling reactions. Complex (A) is a binuclear compound with a '$C_4H_4$' ligand, whereas the dication (5) $[\{Cp_2Mo_2(CO)_4(\mu\text{-}\eta^2\text{:}\eta^3\text{-}HC{\equiv}C\text{–}C(H)\}_2Fc][BF_4]_2$ is a tetranuclear compound that can be considered as two independent carbenium complexes linked by a ferrocenyl substituent. Therefore the behaviour of (5) in one elec-

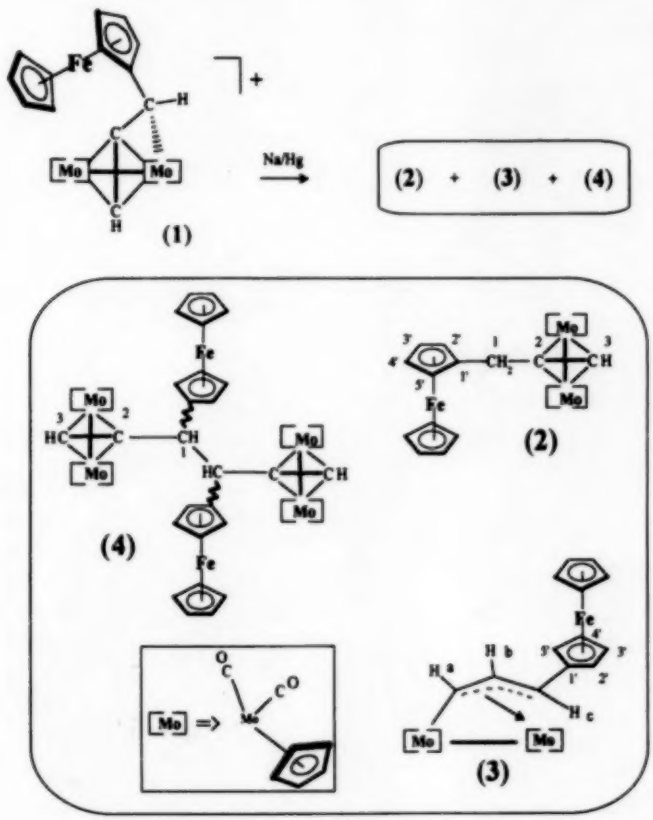


Scheme 2.

tron reduction is expected to be closer to compound (**B**) than to (**A**). A C–C coupling reaction occurs fortunately by an intramolecular process; in the case of an intermolecular process, the reaction would probably have been uncontrollable.

In conclusion the results described above show how carbenium ions stabilized by $[Cp_2Mo_2(CO)_4]$ can be used as precursors of dimers $[Mo_2Cp_2(CO)_4(\mu\text{-}\eta^2\text{:}\eta^2\text{-}HC{\equiv}CC(R_1)(R_2)\text{–})]_2$ by inter- or intramolecular C–C coupling.

## 3. Experimental details

### 3.1. General

All reactions and purifications were performed under dinitrogen using Schlenk techniques. The solvents were freshly distilled under dinitrogen from sodium–benzophenone for toluene and from $CaH_2$ for dichloromethane and hexane.

The infrared spectra were obtained with a Perkin–Elmer 1430 spectrometer, using solutions in $CH_2Cl_2$ or KBr pellets. Infrared frequencies are reported in wavenumbers ($cm^{-1}$).

The $^1H$ and $^{13}C$ NMR spectra were recorded on a Bruker AC 300 instrument ($^1H$, 300.13 MHz; $^{13}C$, 75.47 MHz). Chemical shifts are reported as $\delta$ in units of parts per million (ppm) relative to a tetramethylsilane internal reference. Coupling constants are reported in hertz.

The starting materials (**1**) and (**5**) were prepared by treating the alcohol precursors $[Cp_2Mo_2(CO)_4\{\mu\text{-}\eta^2\text{:}\eta^2\text{-}HC{\equiv}C\text{–}C(H)(OH)(Fc)\}]$ and $[\{Cp_2Mo_2(CO)_4(\mu\text{-}\eta^2\text{:}\eta^2\text{-}HC{\equiv}C\text{–}C(H)(OH)\}_2Fc]$ [15] with an excess of $HBF_4$ by the standard procedure used for the carbenium ions stabilized by $[Cp_2Mo_2(CO)_4]$ [6,16].

### 3.2 Reduction of compound $[Cp_2Mo_2(CO)_4\{\mu\text{-}\eta^2\text{:}\eta^3\text{-}HC{\equiv}C\text{–}C(H)(Fc)\}][BF_4]$ (1)

To a 2% Na–Hg amalgam prepared from 0.3 g of Na and 14.7 g of Hg was added a suspension of $[Cp_2Mo_2(CO)_4\{\mu\text{-}\eta^2\text{:}\eta^3\text{-}HC{\equiv}C\text{–}C(H)(Fc)\}][BF_4]$ (**1**) (2 g, 2.7 mmol) in 60 ml of toluene. The mixture was stirred at room temperature for 18 h. After filtration, the solvent was removed from the filtrate in vacuo and the residue was chromatographed on silica gel using mixtures of hexane–dichloromethane as eluent.

The first red band eluted with hexane–dichloromethane (70:30 in volume) was shown to contain compound (**2**) (0.41 g, yield 23%).

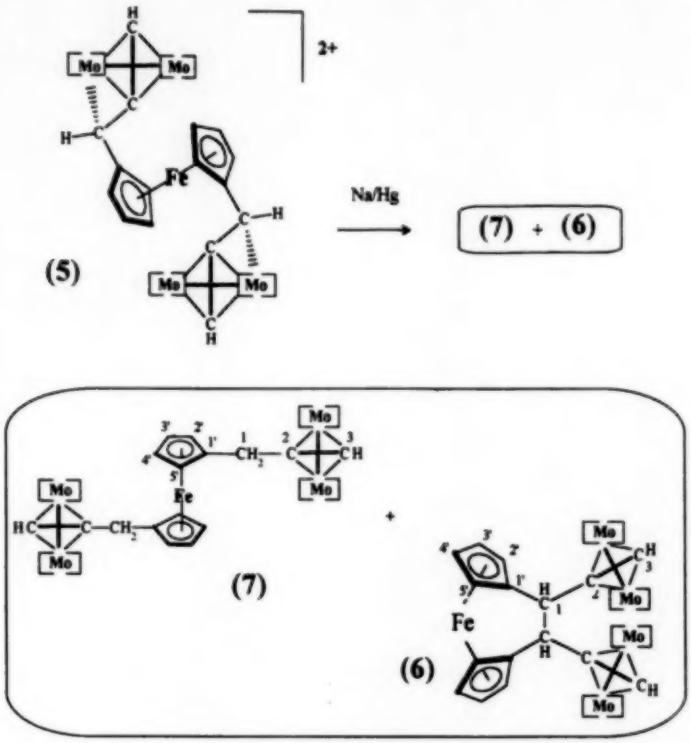


Scheme 3.

The second band containing the red complex (**4**) (0.12 g, yield 7%) was eluted with hexane–dichloromethane (30:70).

The third orange band, eluted with dichloromethane, gave complex (**3**) (0.18 g, yield 10%).

Spectroscopic data for $[Cp_2Mo_2(CO)_4\{\mu\text{-}\eta^2\text{:}\eta^2\text{-}HC{\equiv}C\text{-}C(H)_2(Fc)\}]$ (**2**):

$^1$H NMR ($CD_2Cl_2$): 5.81 (s, 1H, HC3); 5.13 (s, 10H, 2 $C_5H_5$–Mo); 4.08 (s, 5H, $C_5H_5$–Fe); 3.94 (t, 2H, (H2′–5′), $^3J$(H–H) = 1.85); 3.88 (t, 2H, (H3′–4′), $^3J$(H–H) = 1.85); 3.53 (s, 2H, $CH_2$). $^{13}$C NMR ($CD_2Cl_2$): 233.5 (CO); 91.5 ($C_5H_5$–Mo); 90.2 (C1′); 88.7 (C3); 88.3 (C2); 68.8 ($C_5H_5$–Fe); 67.7 and 67.6 ($C_5H_4$, C2′, C3′, C4′, C5′); 36.4 ($CH_2$). IR ($CH_2Cl_2$): $\nu$(CO): 1995, 1900, 1825. Anal. Found: C, 48.76; H, 3.27. $C_{27}H_{22}FeMo_2O_4$. Calc.: C, 49.27; H, 3.37%.

Spectroscopic data for $[Cp_2Mo_2(CO)_4\{\mu\text{-}\sigma\text{:}\eta^3\text{-}HC{=}CH{-}C(H)(Fc)\}]$ (**3**):

$^1$H NMR (acetone $d_6$): 10.15 (dd, 1H, Ha, $^3J$(Ha–Hb) = 8.8; $^4J$(Ha–Hc) = 1.0); 6.5 (dd, 1H, Hb, $^3J$(Hb–Ha) = 8.8; $^3J$(Hb–Hc) = 10.6); 5.4 (s, 5H, $C_5H_5$–Mo); 5.3 (s, 5H, $C_5H_5$–Mo); 2.5 (d, 1H, Hc, $^3J$(Hb–Hc) = 11.0); 4.1 (m, 4H, $C_5H_4$); 4.16 (s, 5H, $C_5H_5$–Fe). $^{13}$C NMR (acetone $d_6$): 250.2, 246.8, 242.0 and 241.3 (4 CO); 168.1 (Ca, d, $^1J$(C–Ha) = 144.3); 131.8 (Cc, d, $^1J$(C–Hc) = 164.4); 129.4 (Cb, d, $^1$J( C–Hb ) = 162.9); 95.8 ($C_5H_5$–Mo, d, $^1J$(C–H) = 176.0); 92.9 ($C_5H_5$–Mo, d, $^1J$(C–H) = 178.6); 84.0 (C1′); 70.1 ($C_5H_5$–Fe, d, $^1J$(C–H) = 175.6); 69.9, 69.3, 68.1 and 65.9 ($C_5H_4$, C2′, C3′, C4′, C5′, d, $^1J$(C–H) = 174.8). IR ($CH_2Cl_2$) $\nu$(CO): 1940, 1900, 1835. Ca, Cb and Cc represent the carbon atom bearing the Ha, Hb and Hc protons respectively (Scheme 2). Anal. Found: C, 49.71; H, 2.96. $C_{27}H_{22}FeMo_2O_4$. Calc.: C, 49.27; H, 3.37%.

Spectroscopic data for $[\{Cp_2Mo_2(CO)_4\}(\mu\text{-}\eta^2\text{:}\eta^2\text{-}HC{\equiv}C\text{-}C(H)(Fc)\text{-}C(H)(Fc)\text{-}C{\equiv}CH)]$ (**4**):

$^1$H NMR spectrum consists of two sets of peaks of about equal intensity, one set corresponding to the R*S* compound and the other to the SS–RR compound. Attempts to obtain a high quality $^{13}$C NMR spectrum of (**4**) were unsuccessful owing to its very poor solubility in a range of deuterated solvents. $^1$H NMR (THF $d_8$): 7.57 (s, 4H, HC3); 5.64 (s, 10H, 2 $C_5H_5$–Mo); 5.47 (s, 10H, 2 $C_5H_5$–Mo); 5.29 (s, 10H, 2 $C_5H_5$–Mo); 4.90 (s, 10H, 2 $C_5H_5$–Mo); 4.42 (s, 10H, 2 $C_5H_5$–Fe); 4.26 (s, 10H, 2 $C_5H_5$–Fe); 5.68, 5.10, 4.87, 4.66, 4.63, 4.26, 4.25, 4.13, 3.99, 3.95 (m, $C_5H_4$ and HC1). IR (THF): $\nu$(CO): 1985, 1900, 1890, 1830. Anal. Found: C, 48.90; H, 3.33. $C_{54}H_{42}Fe_2Mo_4O_8$. Calc.: C, 49.35; H, 3.22%.

### *3.3. Reduction of compound $[\{Cp_2Mo_2(CO)_4(\mu\text{-}\eta^2\text{:}\eta^3\text{-}HC{\equiv}C\text{-}C(H)\}_2(Fc)][BF_4]_2$ (5)*

The procedure described for compound (**1**) was used: a suspension of $[\{Cp_2Mo_2(CO)_4(\mu\text{-}\eta^2\text{:}\eta^3\text{-}HC{\equiv}C\text{-}C(H)\}_2(Fc)][BF_4]_2$ (**5**) (1.5 g, 1.15 mmol) in 50 ml of toluene was added to 15 g of 2% Na–Hg amalgam. After stirring 18 h and filtration, the solution was filtered and solvent removed in vacuo to leave a residue which was chromatographed on silica gel with using mixtures of hexane and dichloromethane as eluent.

The first red band was eluted with hexane–dichloromethane (60:40) and gave compound (**7**) (0.27 g, yield 21%).

The second band eluted with hexane–dichloromethane (40:60) yielded compound (**6**) (0.23 g, 18%). Owing to the rather similar chromatographic properties of the products, elutions had to be developed very slowly.

Spectroscopic data for $[\{Cp_2Mo_2(CO)_4(\mu\text{-}\eta^2\text{:}\eta^2\text{-}HC{\equiv}C\text{-}C(H)\text{-}\}_2(Fc)]$ (**6**):

$^1$H NMR (acetone $d_6$): 6.11 (s, 2H, 2 HC3); 5.40 (s, 10H, 2 $C_5H_5$–Mo); 5.30 (s, 10H, 2 $C_5H_5$–Mo); 4.72 (s, 2H, 2 HC1); 4.92 (m, 2H), 4.56 (m, 2H), 4.05 (m, 2H) and 3.82 (m, 2H): 2 (H2′–3′–4′–5′). IR ($CH_2Cl_2$) $\nu$(CO): 1995, 1910, 1830. Anal. Found: C, 46.72; H, 3.37. $C_{44}H_{32}FeMo_4O_8$. Calc.: C, 46.84; H, 2.86%.

Spectroscopic data for $[\{Cp_2Mo_2(CO)_4(\mu\text{-}\eta^2\text{:}\eta^2\text{-}HC{\equiv}C\text{-}CH_2\}_2(Fc)]$ (**7**):

$^1$H NMR (acetone $d_6$): 6.06 (s, 2H, 2 HC3); 5.22 (s, 20H, 2 $C_5H_5$–Mo); 3.99 (t, 4H, 2 (H2′–5′), $^3J$(H–H) = 1.8); 3.96 (t, 4H, 2 (H3′–4′), $^3J$(H–H) = 1.8); 3.62 (s, 4H, 2 $CH_2$). $^{13}$C NMR (acetone $d_6$): 233.6 (CO); 230.1 (CO); 93.5 (C1′); 92.0 ($C_5H_5$–Mo); 90.5 (C3); 89.1 (C2); 69.8 and 68.6 ($C_5H_4$, C2′, C3′, C4′, C5′); 36.5 ($CH_2$). IR ($CH_2Cl_2$) $\nu$(CO): 1995, 1900, 1825. Anal. Found: C, 45.97; H, 3.12. $C_{44}H_{34}FeMo_4O_8$. Calc.: C, 46.75; H, 3.03%.

## Acknowledgement

We thank Dr. Jean Talarmin (University of Brest) for the electrochemical studies.

## References

[1] N. Le Berre-Cosquer, R. Kergoat and P. L'Haridon, *Organometallics, 11* (1992) 721.

[2] J.-F. Capon, S. Cornen, N. Le Berre-Cosquer, R. Kergoat, R. Pichon and P. L'Haridon, *J. Organomet. Chem., 470* (1994) 137.

[3] A. Meyer, D. McCabe, M.D. Curtis, *Organometallics, 6* (1987) 1491.

[4] T.G. Taylor and J.C. Ware, *J. Am. Chem. Soc., 89* (1967) 2304; M. Cais and A. Eisenstadt, *J. Am. Chem. Soc., 86* (1964) 1148; K.L. Rinehart, Jr., C.J. Michejda and P.A. Kittle, *J. Am. Chem. Soc., 81* (1959) 3162; V. Weinmayr, *J. Am. Chem. Soc., 77* (1955) 309; P.L. Pauson and W.E. Watts, *J. Chem. Soc.* (1962) 3880.

[5] C. Baker and W.M. Horspool, *J. Chem. Soc. Perkin Trans., 1* (1979) 2294; C. Imrie, T.A. Modro and C.C.P. Wagner, *J. Chem. Soc. Perkin Trans., 2* (1994) 1379; R.A. Jackson, M. Scarmoutsos and A.K. Zarkadis, *J. Chem. Soc. Perkin Trans., 2* (1991) 809.

[6] L.L. Troitskaya, V.I. Sokolov, V.I. Bakhmutov, O.A. Reutov, M. Gruselle, C. Cordier and G. Jaouen, *J. Organomet. Chem., 364* (1989) 195; C. Cordier, M. Gruselle, J. Vaissermann, L.L. Troitskaya, V.I. Bakhmutov, V.I. Sokolov and G. Jaouen, *Organometallics, 11* (1992) 3825.

[7] S.F.T. Froom, M. Green, K.R. Nagle and D.J. Williams, *J. Chem. Soc. Chem.Commun.*, (1987) 1305.

[8] M. Savignac, G. Jaouen, C.A. Roger, R.E. Perrier, B.G. Sayer and M.J. McGlinchey, *J. Org. Chem., 51* (1986) 2328; M. Gruselle, H. El Hafa, M. Nikolski and G. Jaouen, J. Vaisserman, L. Li and M.J.McGlinchey, *Organometallics, 12*, (1993), 4917.

[9] P. Braunstein, T.G. Carnciro, D. Matt, F. Balegroune and D. Grandjean, *J. Organomet. Chem., 367* (1989) 117; G. Doisneau, G. Balavoine, T. Fellebeen-Khan, J.-C. Cliret, J. Delaire, I. Ledoux, R. Loucif and G. Puccetti, *J. Organomet. Chem., 421* (1991) 299.

[10] J.M. Nelson, H. Rengel and I. Manners, *J. Am. Chem. Soc., 115* (1993) 7035.

[11] G.G. Melikyan, R.C. Combs, J. Lamirand, M. Khan and K.M. Nicholas, *Tetrahedron Lett., 35* (1994) 363.

[12] J. Park, Y. Seo, S. Cho, D. Whang, K. Kim and T. Chang, *J. Organomet. Chem., 489* (1995) 23.

[13] T.Y. Dong, M.Y. Hwang and Y.S. Wen, *J. Organomet. Chem., 391* (1990) 377.

[14] M.D. McClain, M.S. Hay, M.D. Curtis and J.W. Kampf, *Organometallics, 13* (1994) 4377.

[15] J.-F. Capon, N. Le Berre-Cosquer, B. Leblanc and R. Kergoat, *J. Organomet. Chem.*, in press.

[16] V.I. Sokolov, I.V. Barinov, O.A. Reutov, *Isv. Akad. Nauk SSSR, Ser. Khim.*, (1982) 1992.

ELSEVIER

Journal of Organometallic Chemistry 508 (1996) 7–12

Journal of Organometallic Chemistry

# Reactions of (THF)W(CO)$_5$ with some diphosphenes carrying bulky aryl and phenoxy groups

De-Lie An, Kozo Toyota, Masafumi Yasunami, Masaaki Yoshifuji *

*Department of Chemistry, Faculty of Science, Tohoku University, Aoba, Sendai 980-77, Japan*

Received 2 November 1994; in revised form 19 July 1995

**Abstract**

The reaction of (THF)W(CO)$_5$ (THF = tetrahydrofuran) with asymmetrical diphosphenes carrying bulky aryl and phenoxy groups gave end-on-type complexes on either phosphorus atom. One of the complexes was analyzed by X-ray crystallography indicating that the major complex suffers less from the steric bulk.

*Keywords:* Carbonyl; Chromium; Molybdenum; Phosphorus; Tungsten; X-ray diffraction

## 1. Introduction

Physicochemical properties of low coordinated phosphorus compounds such as diphosphenes are of current interest. We have previously reported the preparation, characterization, and crystal structure of 1,2-bis(2,4,6-tri-tert-butylphenyl)diphosphene (**1**) utilizing the 2,4,6-tri-tert-butylphenyl group (abbreviated to Ar) as a sterically protecting group [1,2]. Moreover, we and others have also described some diphosphenes with the >N–P=P– skeleton [3–5], as well as diphosphene **2** containing the –O–P=P– skeleton [6]. We reported some results on the reaction of several kinds of phenoxydiphosphenes with sulfur, dichlorocarbene and selenium, and now we report the results on the reaction of such diphosphenes having the –O–P=P– skeleton with (THF)W(CO)$_5$ (THF = tetrahydrofuran) to give complexes of end-on type coordination.

## 2. Results and discussion

### 2.1. Preparation of diphosphenes carrying bulky phenoxy and the Ar groups

Some stable diphosphenes carrying bulky phenoxy and the Ar groups were prepared as previously reported [6] as follows. Sterically hindered phenyl phosphorodichloridites **3a–3c** were prepared from the corresponding phenols **4a–4c**. Reaction of **3a–3c** with lithium 2,4,6-tri-tert-butylphenylphosphide [7], followed by the dehydrochlorination reaction with 1,8-diazabicyclo-[5.4.0]undec-7-ene (DBU) gave the corresponding asymmetrical diphosphenes **2a–2c** (Scheme 1). Diphosphenes **2a–2c** were stable towards air and moisture during the silica-gel column-chromatography procedure.

The $^{31}$P NMR spectra of the diphosphenes **2a–2c** showed an AB pattern, unequivocally characteristic of asymmetrical diphosphenes. The signals due to the P$^A$ of the diphosphenes **2a–2c** appear at slightly higher field ($\delta_P$ = 409–411 ppm) compared with those for **1** ($\delta_P$ = 490 ppm), where P$^A$ denotes the Ar-substituted phosphorus atom and P$^B$ denotes the other phosphorus atom except for the symmetrical **1**. The phenoxy-group-substituted phosphorus atoms (P$^B$) of **2a–2c** resonate at significantly low field ($\delta_P$ = 533–535 ppm) compared with the P$^A$ for **2a–2c** or P$^A$ for **1**. These

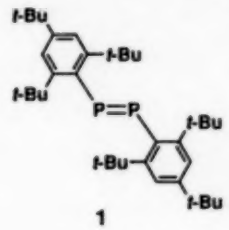


**1**

Form 1.

* Corresponding author.

0022-328X/96/$15.00 © 1996 Elsevier Science S.A. All rights reserved
*SSDI* 0022-328X(95)05843-5

Form 2.

facts can be interpreted by considering resonance structures of the –O–P=P– π system involving the P=P double bond perturbed by the lone-pair electrons of the oxygen atom [3,4,6].

### 2.2. Reaction of the diphosphenes 2a–2c with (THF)W(CO)$_5$

The reaction of **2a–2c** with a large excess amount of (THF)W(CO)$_5$ at room temperature in THF for 3 days led to the formation of the end-on complexes **5a–5c** and **6a–6c** (Scheme 2), when the starting diphosphenes **2a–2c** were completely consumed. During the reaction of **2** with (THF)W(CO)$_5$, two sets of AB-pattern signals appeared in an almost equal amount. Either peak $\delta_{P^B}$ in a lower field for **5** or $\delta_{P^A}$ in a higher field for **6** was accompanied with satellite peaks due to $^{183}$W, clearly indicating the position of the coordination site of the end-on-type coordination [8]. It seems likely that the P$^A$ atom is more electron donating than P$^B$ but that **5** is less hindered than **6**. The $^{31}$P NMR data for **2**, **5** and **6** are listed in Table 1 together with **1** as a reference. The two complexes **5** and **6** were isolated after silica gel column chromatography as a mixture of the major **5** and the minor **6**, but attempted further purification of the minor complex **6** failed. The major complexes **5** were successfully obtained as crystalline materials in every case and **5b** could be analyzed by X-ray crystallography. Although some transition metal complexes of the phenoxy-substituted diphosphene with a side-on-type coordination or mixed side-on- and end-on-type coordination have been reported [9,10], the complex formation with single end-on-type coordination such as **5** or **6** has not been reported so far. Similar results were obtained for **2b** with the other Group 6 metal carbonyls such as chromium and molybdenum to give the end-on coordination complexes **7b–10b**. Table 1 also lists the $^{31}$P NMR data for compounds **7b–10b**.

### 2.3. Structure analysis of tungsten carbonyl complex 5b

Fig. 1 is an ORTEP drawing [11] of **5b**. Some selected bond lengths and bond angles are listed in Table 2 and Table 3 respectively. The atoms (W(1), P(1), P(2), O(1), C(1), C(16)) are coplanar within 0.012(2) Å and the atoms O(6) and C(38) are slightly off this plane by 0.339 and 0.184 Å respectively. The aromatic rings of the Ar and the bulky phenoxy groups are almost perpendicular to the diphosphene P=P π system, making an angle of 90.84° and 86.06° respectively. The dihedral angles of C(16)–P(2)–P(1)–O(1), C(16)–P(2)–P(1)–W(1), P(2)–P(1)–O(1)–C(1) are 179.7(3)°, 1.1(3)° and −2.7(6)° respectively. The bond length P(1)–P(2) is 2.025(3) Å, which falls into the shortest lengths reported for diphosphenes so far [12]. The coordination

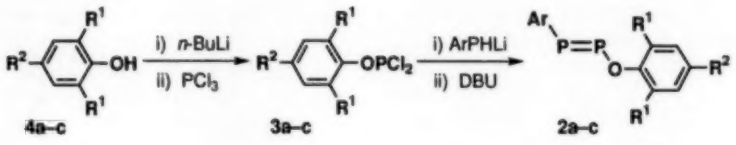


a: R$^1$ = R$^2$ = t-Bu; b: R$^1$ = t-Bu, R$^2$ = Me; c: R$^1$ = t-Bu, R$^2$ = H;
Ar = 2,4,6-t-Bu$_3$C$_6$H$_2$; DBU = 1,8-diazabicyclo[5.4.0]undec-7-ene.

Scheme 1.

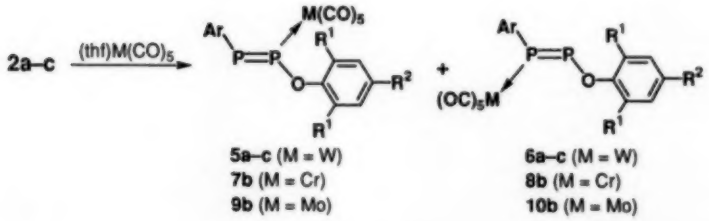


a: R$^1$ = R$^2$ = t-Bu; b: R$^1$ = t-Bu, R$^2$ = Me; c: R$^1$ = t-Bu, R$^2$ = H.

Scheme 2.

Table 1
$^{31}$P NMR data of diphosphenes **1** and **2** and the Group 6 metal carbonyl complexes **5–10** (in $CDCl_3$)

| Compound [a] | $\delta_{P^B}$ (ppm) | $^1J_{P^BW}$ (Hz) | $\delta_{P^A}$ (ppm) | $^1J_{P^AW}$ (Hz) | $^1J_{PP}$ (Hz) |
|---|---|---|---|---|---|
| **1** | 490.0 [b] | — | 490.0 [b] | — | — |
| **2a** | 534.1 | — | 409.8 | — | 572.2 |
| **2b** | 534.4 | — | 409.7 | — | 572.3 |
| **2c** | 533.2 | — | 410.4 | — | 572.5 |
| **5a** | 444.6 | 289.5 | 343.2 | — | 564.3 |
| **5b** | 443.4 | 291.3 | 339.6 | — | 568.9 |
| **5c** | 443.2 | 291.6 | 339.9 | — | 569.1 |
| **6a** | 491.2 | — | 311.3 | 243.5 | 510.8 |
| **6b** | 491.7 | — | 311.8 | 243.6 | 510.6 |
| **6c** | 491.0 | — | 312.9 | 244.0 | 510.9 |
| **7b** | 501.1 | — | 378.1 | — | 572.9 |
| **8b** | 516.0 | — | 363.4 | — | 512.6 |
| **9b** | 484.2 | — | 362.9 | — | 565.0 |
| **10b** | 501.8 | — | 378.2 | — | 573.2 |

[a] $P^A$ denotes the Ar-substituted phosphorus atom and $P^B$ denotes the other except for **1**.
[b] $\delta_P$ value in $C_6D_6$ for **1**: 492.4 [1].

length P(1)–W(1) of 2.456(2) Å is much shorter than 2.531(2) Å of $[ArP{=}C{=}CPh_2]W(CO)_5$ [13], 2.506(1) Å of $[ArP{=}C{=}C{=}CPh_2]W(CO)_5$ [14] and 2.522(6) and 2.517(5) Å of $[ArP{=}C{=}PAr][W(CO)_5]_2$ [15]. The two tert-butyl groups of the phenoxy moiety are disordered, and the structure with a dominant occupancy is shown in Fig. 1.

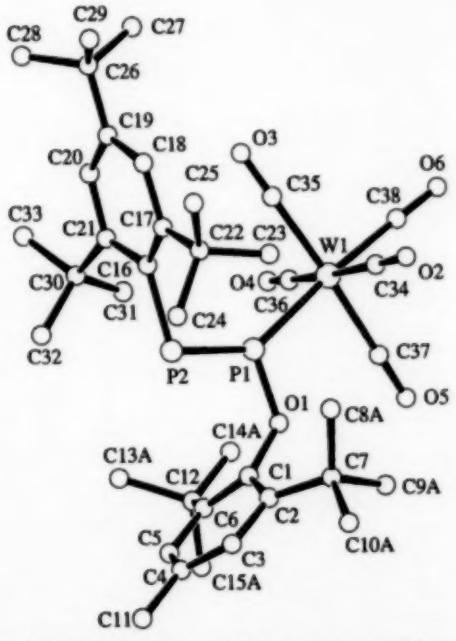


Fig. 1. Molecular structure of **5b** with atom-labeling scheme. The atoms C(8)–C(10) and C(13)–C(15) are disordered and the molecular structure with a dominant occupancy (0.76) for each is shown for clarity.

## 3. Experimental details

All experiments were carried out under an argon atmosphere with dry solvents, unless otherwise specified. All melting points were determined with a Yanagimoto MP-J3 micromelting point apparatus and were uncorrected. $^1$H and $^{13}$C NMR spectra were measured by either a Bruker AC-200P or AM-600 spectrometer. $^{31}$P NMR spectra were obtained with a Bruker AC-200P spectrometer using 85% $H_3PO_4$ as an external standard. IR spectra were recorded on a Horiba FT-300 spectrometer. The UV–visible spectra were obtained with a Hitachi U-3210 spectrometer. X-ray reflections were recorded on a Rigaku AFC-7S four-circle diffractometer using graphite-monochromated Mo Kα radiation.

Table 2
Some selected bond distances (Å) for **5b** (numbers in parentheses are estimated standard deviations).

| | | | |
|---|---|---|---|
| W(1)–P(1) | 2.456(2) | C(2)–C(7) | 1.57(1) |
| W(1)–C(34) | 2.028(9) | C(3)–C(4) | 1.39(1) |
| W(1)–C(35) | 2.062(9) | C(4)–C(5) | 1.38(1) |
| W(1)–C(36) | 2.026(10) | C(4)–C(11) | 1.50(1) |
| W(1)–C(37) | 2.050(9) | C(5)–C(6) | 1.40(1) |
| W(1)–C(38) | 2.021(9) | C(6)–C(12) | 1.55(1) |
| P(1)–P(2) | 2.025(3) | C(16)–C(17) | 1.423(10) |
| P(1)–O(1) | 1.629(5) | C(16)–C(21) | 1.424(9) |
| P(2)–C(16) | 1.858(7) | C(17)–C(18) | 1.399(10) |
| O(1)–C(1) | 1.414(8) | C(17)–C(22) | 1.555(10) |
| O(2)–C(34) | 1.153(9) | C(18)–C(19) | 1.373(10) |
| O(3)–C(35) | 1.124(9) | C(19)–C(20) | 1.372(10) |
| O(4)–C(36) | 1.151(10) | C(19)–C(26) | 1.535(10) |
| O(5)–C(37) | 1.122(9) | C(20)–C(21) | 1.401(10) |
| O(6)–C(38) | 1.145(9) | C(21)–C(30) | 1.56(1) |
| C(1)–C(2) | 1.402(10) | | |
| C(1)–C(6) | 1.407(10) | | |
| C(2)–C(3) | 1.40(1) | | |

### 3.1. Synthesis of diphosphenes (2a–2c)

Diphosphenes **2** were prepared according to the method reported previously [6].

**2a**: yellow needles; melting point (m.p.), 186.5–187.5°C (hexane). $^{31}P\{^1H\}$ NMR (81 MHz, $CDCl_3$): $\delta$ 409.8 and 534.1 (AB, $^1J_{PP} = 572.2$ Hz) ppm.

**2b**: yellow needles; m.p., 171.5–172.5°C (hexane). $^{31}P\{^1H\}$ NMR ($CDCl_3$): $\delta$ 409.7, 534.4 (AB, $^1J_{PP} = 572.3$ Hz) ppm.

**2c**: yellow needles; m.p., 167–168°C (hexane). $^{31}P\{^1H\}$ NMR ($CDCl_3$): $\delta$ 410.4, 533.2 (AB, $^1J_{PP} = 572.5$ Hz) ppm.

### 3.2. Synthesis of tungsten carbonyl complexes (5a–5c and 6a–6c)

A typical synthetic procedure is described for **5a** and **6a**. Diphosphene **2a** (210 mg, 0.37 mmol) was dissolved in THF (25 ml) and stirred at room temperature for 3 days in the presence of a large excess (about 50-fold excess) of $(THF)W(CO)_5$, prepared from photolysis of hexacarbonyltungsten in THF [16], when the starting diphosphene was almost consumed. During the reaction of **2a** with $(THF)W(CO)_5$, two sets of AB-pattern signals appeared in an almost equal intensity owing to the two complexes **5a** and **6a**. The reaction mixture was subjected to silica-gel column chromatography to give **5a** and **6a**, but the ratio of the complexes changed to about 1:0.5, probably because of some decomposition of **6a**. The further attempted purification of **6a** has failed so far but the pure **5a** was isolated as a crystalline material with 38% yield based on the diphosphene **2a** used. Similarly, **5b** and **5c** were prepared and isolated with yields of 46 and 48% from the corresponding diphosphenes **2b** and **2c** respectively, together with the corresponding **6b** and **6c**. However, attempted purification of both **6b** or **6c** was unsuccessful.

**5a**: yellow prisms; m.p., 145–146°C ($CH_3CN$). $^1H$ NMR ($CDCl_3$, 200 MHz): $\delta$ 1.28 (9H, s, *p*-$^t$Bu), 1.32 (9H, s, *p*-$^t$Bu), 1.49 (18H, s, *o*-$^t$Bu), 1.54 (18H, s, *o*-$^t$Bu), 7.30 (2H, s, arom.), 7.43 (2H, bs, arom.) ppm. $^{31}P\{^1H\}$ NMR ($CDCl_3$): $\delta_{P^A}$ 343.2, $\delta_{P^B}$ 444.6 (satellite, $^1J_{PW} = 289.5$ Hz) (AB, $^1J_{PP} = 564.3$ Hz) ppm. $^{13}C\{^1H\}$ NMR ($CDCl_3$, 50 MHz): $\delta$ 31.06 (s, *p*-C*Me*$_3$), 31.47 (s, *p*-C*Me*$_3$), 33.07 (s, *o*-C*Me*$_3$), 33.36 (d, $J_{PC} = 6.47$ Hz, *o*-C*Me*$_3$), 34.62 (s, *p*-C*Me*$_3$), 34.90 (s, *p*-C*Me*$_3$), 36.58 (s, *o*-C*Me*$_3$), 38.85 (s, *o*-C*Me*$_3$), 123.13 (d, $^3J_{PC} = 2.31$ Hz, *m*-arom.), 123.83 (s, *m*-arom.), 124.00 (d, $^1J_{PC} = 66.8$ Hz, *ipso*-arom.), 140.12 (s, arom.), 146.48 (s, arom.), 151.16 (d, $J_{PC} = 4.62$ Hz, arom.), 155.57 (d, $^2J_{PC} = 12.49$ Hz, *ipso*-arom.), 163.62 (s, arom.), 193.99 (d, $^2J_{PC} = 7.86$ Hz, 4 × CO), 198.20 (d, $^2J_{PC} = 37.49$ Hz, CO) ppm. UV ($CH_2Cl_2$): $\Delta_{max}$ 289 (log $\epsilon = 4.18$), 409 (log $\epsilon = 4.05$) nm. IR (KBr): $\nu$ 2077 (s), 1998, 1957 (vs) $cm^{-1}$. Anal. Found: C, 54.92; H, 6.60%. $C_{41}H_{58}O_6P_2W$ calc.: C, 55.16; H, 6.55%.

**6a**: $^{31}P\{^1H\}$ NMR ($CDCl_3$): $\delta_{P^A}$ 311.3 (satellite,

Table 3
Some selected bond angles (°) for **5b** (numbers in parentheses are estimated standard deviations)

| | | | |
|---|---|---|---|
| P(1)–W(1)–C(34) | 92.0(2) | C(3)–C(4)–C(11) | 120.3(9) |
| P(1)–W(1)–C(35) | 92.7(2) | C(5)–C(4)–C(11) | 121.8(9) |
| P(1)–W(1)–C(36) | 94.7(2) | C(4)–C(5)–C(6) | 123.7(8) |
| P(1)–W(1)–C(37) | 87.1(2) | C(1)–C(6)–C(5) | 115.1(7) |
| P(1)–W(1)–C(38) | 174.1(2) | C(1)–C(6)–C(12) | 126.5(7) |
| C(34)–W(1)–C(35) | 92.4(4) | C(5)–C(6)–C(12) | 118.2(7) |
| C(34)–W(1)–C(36) | 173.3(3) | P(2)–C(16)–C(17) | 121.1(5) |
| C(34)–W(1)–C(37) | 93.8(3) | P(2)–C(16)–C(21) | 120.2(6) |
| C(34)–W(1)–C(38) | 83.2(3) | C(17)–C(16)–C(21) | 118.3(6) |
| C(35)–W(1)–C(36) | 88.0(4) | C(16)–C(17)–C(18) | 118.9(7) |
| C(35)–W(1)–C(37) | 173.7(3) | C(16)–C(17)–C(22) | 126.3(7) |
| C(35)–W(1)–C(38) | 90.8(3) | C(18)–C(17)–C(22) | 114.8(7) |
| C(36)–W(1)–C(37) | 85.8(4) | C(17)–C(18)–C(19) | 123.2(7) |
| C(36)–W(1)–C(38) | 90.1(3) | C(18)–C(19)–C(20) | 117.2(7) |
| C(37)–W(1)–C(38) | 89.9(3) | C(18)–C(19)–C(26) | 121.9(7) |
| W(1)–P(1)–P(2) | 142.2(1) | C(20)–C(19)–C(26) | 120.8(7) |
| W(1)–P(1)–O(1) | 110.0(2) | C(19)–C(20)–C(21) | 123.8(7) |
| P(2)–P(1)–O(1) | 107.8(2) | C(16)–C(21)–C(20) | 118.2(7) |
| P(1)–P(2)–C(16) | 104.3(2) | C(16)–C(21)–C(30) | 125.7(7) |
| P(1)–O(1)–C(1) | 124.4(4) | C(20)–C(21)–C(30) | 116.1(6) |
| O(1)–C(1)–C(2) | 117.8(6) | W(1)–C(34)–O(2) | 175.0(7) |
| O(1)–C(1)–C(6) | 119.1(6) | W(1)–C(35)–O(3) | 175.7(9) |
| C(2)–C(1)–C(6) | 123.0(7) | W(1)–C(36)–O(4) | 178.2(8) |
| C(1)–C(2)–C(3) | 116.3(7) | W(1)–C(37)–O(5) | 177.3(8) |
| C(1)–C(2)–C(7) | 124.2(7) | W(1)–C(38)–O(6) | 177.2(8) |
| C(3)–C(2)–C(7) | 119.3(7) | | |
| C(2)–C(3)–C(4) | 122.5(8) | | |
| C(3)–C(4)–C(5) | 117.8(7) | | |

$^1J_{PW}$ = 243.5 Hz), $\delta_{P^B}$ 491.2 (AB, $^1J_{PP}$ = 510.8 Hz) ppm.

**5b**: yellow prisms; m.p., 201–202°C ($CH_3CN$). $^1H$ NMR ($CDCl_3$, 600 MHz): $\delta$ = 1.30 (9H, *s*, *p*-$^t$Bu), 1.51 (18H, s, *o*-$^t$Bu), 1.56 (18H, s, *o*-$^t$Bu), 2.36 (3H, s, *p*-Me), 7.12 (2H, s, arom.), 7.45 (2H, s, arom.) ppm. $^{31}P\{^1H\}$ NMR ($CDCl_3$): $\delta_{P^A}$ 339.6, $\delta_{P^B}$ 443.4 (satellite, $^1J_{PW}$ = 291.3 Hz) (AB, $^1J_{PP}$ = 568.9 Hz) ppm. $^{13}C\{^1H\}$ NMR ($CDCl_3$, 150 MHz): $\delta$ 21.37 (s, *p*-Me), 31.06 (s, *p*-C*Me*$_3$), 33.08 (s, *o*-C*Me*$_3$), 33.37 (s, *o*-C*Me*$_3$), 34.90 (s, *p*-*C*Me$_3$), 36.36 (s, *o*-C*Me*$_3$), 38.86 (s, *o*-*C*Me$_3$), 123.19 (s, *m*-arom.), 124.28 (d, $^1J_{PC}$ = 66.55 Hz, *ipso*-arom.), 127.90 (s, *m*-arom.), 133.37 (s, *p*-arom.), 140.72 (s, *o*-arom.), 151.20 (s, *p*-arom.), 151.56 (d, $^2J_{PC}$ = 14.79 Hz, *ipso*-arom.), 155.73 (d, $J_{PC}$ = 9.51 Hz, *o*-arom.), 194.02 (d, $^2J_{PC}$ = 5.28 Hz and satellite, $^1J_{WC}$ = 122.08 Hz, 4 × CO), 198.14 (d, $^2J_{PC}$ = 37.58 Hz, CO) ppm. UV ($CH_2Cl_2$): $\Delta_{max}$ 289 (log $\epsilon$ = 4.20), 408 (log $\epsilon$ = 4.09) nm. IR (KBr): $\nu$ 2077 (s), 2000, 1958 (vs), 1944 (vs) cm$^{-1}$. Anal. Found: C, 53.60; H, 6.22%. $C_{38}H_{52}O_6P_2W$ calc.: C, 53.66; H, 6.16%.

**6b**: $^{31}P\{^1H\}$ NMR ($CDCl_3$): $\delta_{P^A}$ 311.8 (satellite, $^1J_{PW}$ = 243.6 Hz), $\delta_{P^B}$ 491.7 (AB, $^1J_{PP}$ = 510.6 Hz) ppm.

**5c**: yellow prisms; m.p., 176–178°C ($CH_3CN$). $^1H$ NMR ($CDCl_3$, 600 MHz): $\delta$ 1.28 (9H, s, *p*-$^t$Bu), 1.49 (18H, s, *o*-$^t$Bu), 1.56 (18H, s, *o*-$^t$Bu), 7.14 (1H, t, $^3J_{HH}$ = 7.74 Hz, arom.), 7.34 (2H, d, $^3J_{HH}$ = 7.77 Hz, arom.), 7.44 (2H, bs, arom.) ppm. $^{31}P\{^1H\}$ NMR ($CDCl_3$): $\delta_{P^A}$ 339.9, $\delta_{P^B}$ 443.2 (satellite, $^1J_{PW}$ = 291.6 Hz) (AB, $^1J_{PP}$ = 569.1 Hz) ppm. $^{13}C\{^1H\}$ NMR ($CDCl_3$, 150 MHz): $\delta$ 31.04 (s, *p*-C*Me*$_3$), 33.04 (s, *o*-C*Me*$_3$), 33.34 (bs, *o*-C*Me*$_3$), 34.89 (s, *p*-*C*Me$_3$), 36.51 (s, *o*-*C*Me$_3$), 38.85 (s, *o*-*C*Me$_3$), 123.20 (s, arom.), 124.06 (d, $^1J_{PC}$ = 66.25 Hz, *ipso*-arom.), 124.46 (s, arom.), 127.08 (s, arom.), 141.31 (s, arom.), 151.28 (d, $J_{PC}$ = 3.70 Hz, arom.), 153.63 (dd, $^3J_{PC}$ = 6.47 Hz and $^2J_{PC}$ = 16.18 Hz, *ipso*-arom.), 155.73 (d, $J_{PC}$ = 10.26 Hz, arom.), 193.96 (d, $^2J_{PC}$ = 6.49 Hz and satellite, $^1J_{WC}$ = 125.98 Hz, 4 × CO), 198.07 (d, $^2J_{PC}$ = 38.18 Hz, CO) ppm. UV ($CH_2Cl_2$): $\Delta_{max}$ 289 (log $\epsilon$ = 4.16), 408 (log $\epsilon$ = 4.11) nm. IR (KBr): $\nu$ 2079 (s), 2000, 1965 (vs), 1936 (vs) cm$^{-1}$. Anal. Found: C, 53.46; H, 6.31. $C_{37}H_{50}O_6P_2W$ calc.: C, 53.12; H, 6.02%.

**6c**: $^{31}P\{^1H\}$ NMR ($CDCl_3$): $\delta_{P^A}$ 312.9 (satellite, $^1J_{PW}$ = 244.0 Hz), $\delta_{P^B}$ 491.0 (AB, $^1J_{PP}$ = 510.9 Hz) ppm.

### 3.3. Synthesis of the other Group 6 metal carbonyl complexes (7b, 8b, 9b and 10b)

Similarly to the preparation of tungsten complexes, the following chromium and molybdenum complexes of diphosphene **2b** were prepared and characterized.

**7b**: yield, 53%; orange prisms; m.p., 182.5–183.5°C ($CH_3CN$). $^1H$ NMR ($CDCl_3$, 200 MHz): $\delta$ 1.31 (9H, s, *p*-$^t$Bu), 1.52 (18H, s, *o*-$^t$Bu), 1.58 (18H, s, *o*-$^t$Bu), 2.38 (3H, s, *p*-Me), 7.14 (2H, s, arom.), 7.46 (2H, s, arom.) ppm. $^{31}P\{^1H\}$ NMR ($CDCl_3$): $\delta_{P^A}$ 378.1, $\delta_{P^B}$ 501.1 (AB, $^1J_{PP}$ = 572.9 Hz) ppm. $^{13}C\{^1H\}$ NMR ($CDCl_3$, 50 MHz): $\delta$ 21.37 (s, *p*-Me), 31.06 (s, *p*-C*Me*$_3$), 33.09 (s, *o*-C*Me*$_3$), 33.21 (dd, $J_{PC}$ = 6.95 Hz and $J_{PC}$ = 2.14 Hz, *o*-C*Me*$_3$), 34.88 (s, *p*-*C*Me$_3$), 36.39 (s, *o*-*C*Me$_3$), 38.76 (s, *o*-*C*Me$_3$), 123.06 (d, $J_{PC}$ = 3.02 Hz, *m*-arom.), 124.95 (d, $^1J_{PC}$ = 58.43 Hz, *ipso*-arom.), 127.93 (d, $J_{PC}$ = 1.66 Hz, *m*-arom.), 133.29 (d, $J_{PC}$ = 1.61 Hz, arom.), 140.55 (s, *o*-arom.), 151.34 (d, $J_{PC}$ = 4.03 Hz, arom.), 151.80 (dd, $^2J_{PC}$ = 17.69 Hz and $^3J_{PC}$ = 7.62 Hz, *ipso'*-arom.), 155.69 (dd, $J_{PC}$ = 11.25 Hz and $J_{PC}$ = 3.25 Hz, arom.), 213.00 (dd, $^2J_{PC}$ = 14.34 Hz and $^3J_{PC}$ = 2.62 Hz, 4 × CO), 220.58 (s, CO) ppm. UV ($CH_2Cl_2$): $\Delta_{max}$ 282 (log $\epsilon$ = 4.23), 410 (log $\epsilon$ = 3.95) nm. IR (KBr): $\nu$ 2071, 1963, 1948 cm$^{-1}$.

**8b**: $^{31}P\{^1H\}$ NMR ($CDCl_3$): $\delta_{P^A}$ 363.4, $\delta_{P^B}$ 516.0 (AB, $^1J_{PP}$ = 512.6 Hz) ppm.

**9b**: yield, 33%; yellow prisms; m.p., 174–175°C ($CH_3CN$). $^1H$ NMR ($CDCl_3$, 200 MHz): $\delta$ 1.32 (9H, s, *p*-$^t$Bu), 1.52 (18H, s, *o*-$^t$Bu), 1.57 (18H, s, *o*-$^t$Bu), 2.38 (3H, s, *p*-Me), 7.14 (2H, s, arom'.), 7.49 (2H, s, arom.) ppm. $^{31}P\{^1H\}$ NMR ($CDCl_3$): $\delta_{P^A}$ 362.9, $\delta_{P^B}$ 484.2 (AB, $^1J_{PP}$ = 565.0 Hz) ppm. $^{13}C\{^1H\}$ NMR ($CDCl_3$, 50 MHz): $\delta$ 21.38 (s, *p*-Me), 31.09 (s, *p*-C*Me*$_3$), 33.09 (s, *o*-C*Me*$_3$), 33.39 (dd, $J_{PC}$ = 6.89 Hz and $J_{PC}$ = 2.42 Hz, *o*-C*Me*$_3$), 34.89 (s, *p*-*C*Me$_3$), 36.35 (s, *o*-*C*Me$_3$), 38.83 (s, *o*-*C*Me$_3$), 123.19 (d, $J_{PC}$ = 2.77 Hz, *m*-arom.), 124.14 (dd, $^1J_{PC}$ = 66.33 Hz and $^2J_{PC}$ = 1.72 Hz, *ipso*-arom.), 127.85 (d, $J_{PC}$ = 1.56 Hz, *m*-arom.), 133.27 (d, $J_{PC}$ = 1.56 Hz, arom.), 140.72 (s, arom.), 151.01 (d, $J_{PC}$ = 3.87 Hz, *o*-arom.), 151.66 (dd, $^2J_{PC}$ = 16.71 Hz and $^3J_{PC}$ = 7.25 Hz, *ipso'*-arom.), 155.66 (dd, $J_{PC}$ = 11.30 Hz and $J_{PC}$ = 2.94 Hz, arom.), 202.76 (dd, $^2J_{PC}$ = 10.37 Hz and $^3J_{PC}$ = 1.14 Hz, 4 × CO), 209.86 (dd, $^2J_{PC}$ = 37.09 Hz and $^3J_{PC}$ = 0.95 Hz, CO) ppm. UV ($CH_2Cl_2$): $\Delta_{max}$ 283 (sh,log $\epsilon$ = 4.23), 316 (sh,log $\epsilon$ = 3.89, 406 (log $\epsilon$ = 4.11) nm. IR (KBr): $\nu$ 2079, 1963, 1950 cm$^{-1}$. Anal. Found: C, 59.87; H, 6.64. $C_{38}H_{52}O_6P_2Mo$ calc.: C, 59.84; H, 6.87%.

**10b**: $^{31}P\{^1H\}$ NMR ($CDCl_3$): $\delta_{P^A}$ 378.2, $\delta_{P^B}$ 501.8 (AB, $^1J_{PP}$ = 573.2 Hz) ppm.

### 3.4. X-ray structure determination of 5b

The compound **5b** was recrystallized from acetonitrile.

Crystal data for **5b**: $C_{38}H_{52}O_6P_2W$; $M_r$ = 850.62; triclinic, space group, $P\bar{1}$; $a$ = 11.358(3), $b$ = 18.508(3) and $c$ = 10.087(4) Å; $\alpha$ = 97.81(3)°, $\beta$ = 105.16(3)° and $\gamma$ = 97.81(2)°; $U$ = 1994(1) Å$^3$; $Z$ = 2; $D_c$ = 1.416 g cm$^{-3}$; $\mu$ = 30.20 cm$^{-1}$. Unique 7015 reflections with $2\theta \leq 50.0°$ were recorded and 6105 of these with $I > 3.00\sigma(I)$ were judged as observed. The structure was solved using SHELXS86 [17]. Non-hydrogen atoms were refined anisotropically except for the disordered carbon atoms of C(8)–C(10) and C(13)–C(15). Both of the

occupancy factors for the dominant tert-butyl group were 0.76. Hydrogen atoms were included but not refined. $R = 0.038$ and $R_w = 0.049$.

### 3.5. Supplementary material available

Tables of atomic coordinates, anisotropic thermal parameters, H-atom coordinates, bond distances and angles, and structure factors for **5b** (31 pages) are available on request from the Cambridge Crystallographic Data Centre, University Chemical Laboratory, Lensfield Road, Cambridge CB2 1EW, UK.

## Acknowledgments

This work was supported in part by the Grant-in-Aid for Scientific Research 06227209 from the Ministry of Education, Science and Culture, Japanese Government. The authors also thank Tosoh Akzo Co., Ltd. for the donation of organolithium reagents.

## References

[1] M. Yoshifuji, I. Shima, N. Inamoto, K. Hirotsu and T. Higuchi, *J. Am. Chem. Soc., 103* (1981) 4587; *104* (1982) 6167.

[2] M. Yoshifuji, K. Shibayama, N. Inamoto, T. Matsushita and K. Nishimoto, *J. Am. Chem. Soc., 105* (1983) 2495.

[3] (a) M. Abe, K. Toyota and M. Yoshifuji, *Chem. Lett.*, (1992) 2349; (b) M. Abe, K. Toyota and M. Yoshifuji, *Heteroatom Chem., 4* (1993) 427.

[4] (a) L.N. Markovskii, V.D. Romanenko, E.O. Klebanskii and S.V. Iksanova, *Zh. Obshch. Khim., 55* (1985) 1867; *Chem. Abstr., 105* (1986) 24355g; (b) E. Niecke, B. Kramer and M. Nieger, *Angew. Chem., Int. Edn. Engl., 28* (1989) 215; E. Niecke, O. Altmeyer and M. Nieger, *Angew. Chem., Int. Edn. Engl., 30* (1991) 1136.

[5] L.N. Markovskii, V.D. Romanenko, M.I. Povolotskii, A.V. Ruban and E.O. Klebanskii, *Zh. Obshch. Khim., 56* (1986) 2157; *Chem. Abstr., 106* (1987) 176522t; L.N. Markovskii, V.D. Romanenko and A.V. Ruban, *Phosphorus Sulfur, 30* (1987) 447.

[6] D.-L. An, K. Toyota, M. Yasunami and M. Yoshifuji, *Heteroatom Chem., 6* (1995) 53.

[7] K. Issleib, H. Schmidt and Chr. Wirkner, *Z. Anorg. Allg. Chem., 488* (1982) 75; M. Yoshifuji, K. Toyota, K. Shibayama and N. Inamoto, *Chem. Lett.*, (1983) 1653.

[8] M. Yoshifuji, K. Shibayama, T. Hashida, K. Toyota, T. Niitsu, I. Matsuda, T. Sato and N. Inamoto, *J. Organomet. Chem., 311* (1986) C63.

[9] (a) K.M. Flynn, H. Hope, B.D. Murray, M.M. Olmstead and P.P. Power, *J. Am. Chem. Soc., 105* (1983) 7750; (b) R.A. Bartlett, H.V.R. Dias, K.M. Flynn, M.M. Olmstead and P.P. Power, *J. Am. Chem. Soc., 109* (1987) 5699.

[10] R.B. King, F.-J. Wu and E.M. Holt, *J. Am. Chem. Soc., 109* (1987) 7764.

[11] C.K. Johnson, ORTEP II, *Oak Ridge National Laboratory Rep., ORNL-TM-5138*, 1976. (Oak Ridge National Laboratory, Oak Ridge, TN).

[12] M. Yoshifuji, in M. Regitz and O.J. Scherer (eds.), *Multiple Bonds and Low Coordination in Phosphorus Chemistry*, Georg Thieme, Stuttgart, 1990, pp. 321–337.

[13] M. Yoshifuji, K. Toyota, T. Sato, N. Inamoto and K. Hirotsu, *Heteroatom Chem., 1* (1990) 339.

[14] M. Yoshifuji, K. Toyota, T. Uesugi, I. Miyahara and K. Hirotsu, *J. Organomet. Chem., 461* (1993) 81; 469 (1994) C24.

[15] M. Yoshifuji, K. Toyota, T. Niitsu, N. Inamoto and K. Hirotsu, *J. Organomet. Chem., 389* (1990) C12.

[16] W. Strohmeier and F.-J. Müller, *Chem. Ber., 102* (1969) 3608.

[17] G.M. Sheldrick, SHELX86, *Program for the Automatic Solution of Crystal Structures*, University of Göttingen, Göttingen, 1986.

ELSEVIER

Journal of Organometallic Chemistry 508 (1996) 13–22

Journal of Organometallic Chemistry

# Zirkoniumorganische Chemie mit anorganischen Donorliganden N,N′-Bis(trimethylsilyl)benzamidinat (Siam) in Verbindungen des Typs $(Siam)_2ZrX_2$ (X = Methyl, Benzyl, Allyl, Chlorid oder Iodid) und $(Siam)_3ZrX$ (X = Chlorid)

D. Walther [a,*], R. Fischer [a], H. Görls [b], J. Koch [a], B. Schweder [a]

[a] *Friedrich-Schiller-Universität Jena, Institut für Anorganische und Analytische Chemie, August-Bebel-Straße 2, Jena D-07743, Deutschland*
[b] *Max-Planck-Arbeitsgruppe $CO_2$-Chemie, Lessing-Straße 12, D-07743 Jena, Deutschland*

Eingegangen am 25. November 1994

**Abstract**

Organometallic compounds of the type $(Siam)_2ZrX_2$ (Siam = *N,N′*-bis(trimethylsilyl)benzamidinat; *X* = methyl, benzyl or allyl) have been synthesized by reaction of $(Siam)_2ZrCl_2$ and Grignard reagents. The structures of $(Siam)_2ZrX_2$ (X = Cl, I, $CH_3$ or $CH_2$–$C_6H_5$) and $(Siam)_3ZrCl$ have been investigated by X-ray crystal structure analysis. $(Siam)_3ZrCl$ shows a capped octahedral structure with the coordination number 7 at the zirconium. $(Siam)_2ZrX_2$ compounds have distorted octahedral structures and the ligands occupy *cis*-positions. The distortion depends on the bulkiness of the ligand X.

The systems $(Siam)_2ZrCl_2$–methylalumoxan (MAO) and $(Siam)_3ZrCl$–MAO polymerize at 30°C reactive olefins such as ethylene or norbornene. Less reactive olefins (e.g. propene) can be reacted with $(Siam)ZrCl_3$–MAO to yield oligomers and polymers. The same catalytic system is able to convert 1,5-hexadiene selectively under formation of methylene–cyclopentane.

**Zusammenfassung**

Organometallverbindungen des Typs $(Siam)_2ZrX_2$ (Siam = *N,N′*-Bis(trimethylsilyl)benzamidinat; X = Methyl, Benzyl oder Allyl) wurden durch Reaktion von $(Siam)_2ZrCl_2$ mit den entsprechenden Grignard-Verbindungen synthetisiert. Die Strukturen der Verbindungen $(Siam)_2ZrX_2$ (X = Cl, I, $CH_3$ oder $CH_2$–$C_6H_5$) und $(Siam)_3ZrCl$ wurden durch Röntgenkristallstrukturanalyse aufgeklärt. $(Siam)_3ZrCl$ besitzt eine "capped" oktaedrische Struktur mit der Koordinationszahl 7 am Zirkonium. Die Verbindungen $(Siam)_2ZrX_2$ sind verzerrt oktaedrisch aufgebaut und die Liganden besetzen *cis*-Positionen. Das Ausmaß der Verzerrung ist vom Raumbedarf von X abhängig.

Die Systeme $(Siam)_2ZrCl$–Methylalumoxan (MAO) und $(Siam)_3ZrCl$–MAO polymerisieren bei 30°C reaktive Olefine wie Ethylen oder Norbornen. Weniger reaktive Olefine (z.B. Propen) können mit $(Siam)ZrCl_3$–MAO zu Oligomeren und Polymeren reagieren. Das gleiche katalytische System kann 1,5-Hexadien selektiv zu Methylen–cyclopentan umwandeln.

*Keywords:* Zirconium; Alkyl; Allyl; X-ray diffraction; Catalysis

## 1. Einleitung

Im Rahmen von Untersuchungen zum Einfluß von Chelatliganden mit anorganischen Haftatomen auf die katalytische Reaktivität von Metallorganoverbindungen der 4. Nebengruppe [1] haben wir auch Verbindungen mit dem N,N′-Bis(trimethylsilyl)benzamidinato-Liganden (Siam) einbezogen. Die anorganische Zirkoniumchemie mit diesem Liganden wurde 1988 mit den Arbeiten von Dehnicke und Mitarbeitern [2] ([Siam]$ZrCl_3$) beziehungsweise Roesky et al. [3] ($[Siam]_2ZrCl_2$) eingeleitet. Edelmann hat die stereochemische Analogie zum Pentamethylcyclopentadienylanion festgestellt [4] und an Lanthanoidkomplexen die "elektronische Äquivalenz" zum Cyclopentadienylsystem untersucht [5].

* Corresponding author.

0022-328X/96/$15.00 © 1996 Elsevier Science S.A. All rights reserved
*SSDI* 0022-328X(95)05853-2

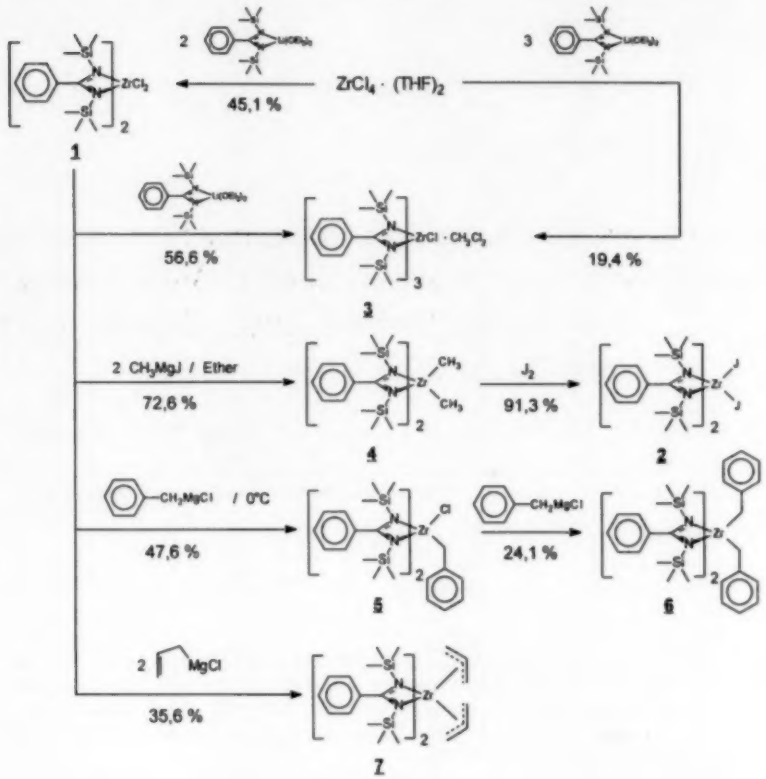


Reaktionsschema 1.

Metallorganische Verbindungen des Typs Cp(Siam) $MX_2$ (M = Ti, Zr oder Hf [6], $(Siam)_3UCH_3$ des Uran (IV) [7] und $(Siam)_2Ti(allyl)$ des Titan(III) [8] sind in jüngster Zeit beschrieben worden. Teuben insbesondere hat die Metallorganochemie des Yttriums mit diesem Liganden intensiv studiert und die Wirkung von Siam auf die katalytische Aktivität dieser Verbindungen im Vergleich zu Cp-stabilisierten Verbindungen untersucht [9].

Gegenstand dieser Arbeit sind Synthese und Struktur von metallorganischen Verbindungen des Typs $(Siam)_2ZrR_2$ (R = Me [10], Benzyl oder Allyl) und von Halogeniden der Zusammensetzung $(Siam)_{4-n}ZrX_n$ ($n = 1$, 2; X = Cl oder I), sowie erste Untersuchungen zur

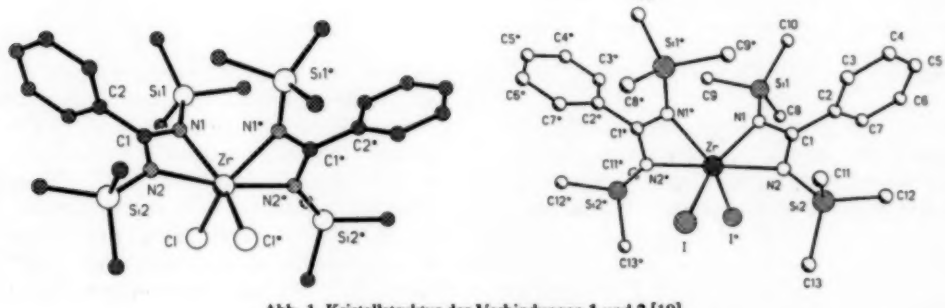


Abb. 1. Kristallstruktur der Verbindungen 1 und 2 [19].

katalytischen Aktivität in Ziegler–Natta-Systemen mit Methylalumoxanen (MAO).

## 2. Synthese und Strukturen der N,N'-Bis(trimethylsilyl)benzamidinato-zirkoniumhalogenide (1–3)

Das Reaktionsschema 1 informiert über die Synthesewege zu den Halogenverbindungen, die als Edukte auch für sterische Vergleiche dienen und daher durch Röntgenstrukturanalysen charakterisiert wurden.

$(Siam)_2ZrCl_2$ wurde bereits von Roesky aus Lithium-*N,N'*-bis(trimethylsilyl)benzamidinat und Zirkoniumtetrachlorid synthetisiert und H-NMR-spektroskopisch untersucht [3]. Verbindung **1**, die NMR-spektroskopisch mit der von Roesky et al. beschriebenen identisch ist, zeigt nach Ausweis der Kristallstrukturanalyse eine *cis*-Struktur der Chloroliganden und ist daher strukturell mit $Cp_2ZrCl_2$ vergleichbar. (Abb. 1).

Auch in der Verbindung **2** nehmen die Iodoliganden die *cis*-Position im verzerrt oktaedrischen Komplex ein. Der Übergang zu dem deutlich größeren Halogenid führt also nicht zu einem *trans*-Komplex, sondern lediglich zu einem Zusammendrängen der Benzamidinatoliganden am Zirkonium.

Für weitere stereochemische Vergleiche und für katalytische Untersuchungen ist auch die Verbindung $(Siam)_3ZrCl$ **3** bedeutsam, die durch Reaktion von **1** oder Zirkoniumtetrachlorid mit einem Überschuß an Lithium-*N,N'*-bis(trimethylsilyl)-benzamidinat zugänglich ist. Die Röntgenstrukturanalyse von **3** zeigt, daß es zu einer Aufweitung der Koordinationssphäre am Zirkonium auf die Koordinationszahl 7 kommt (Abb. 2). Die Koordinationsgeometrie um das Zirkonium läßt sich annähernd als "capped" oktaedrisch beschreiben. Damit wird verständlich, daß die $SiMe_3$-Gruppen in den NMR-Spektren nicht mehr chemisch äquivalent sind. In der Elementarzelle liegen zwei strukturunabhängige Moleküle im Verhältnis 1:1 vor. Es handelt sich dabei um die zwei optischen Antipoden, in denen die Benz-

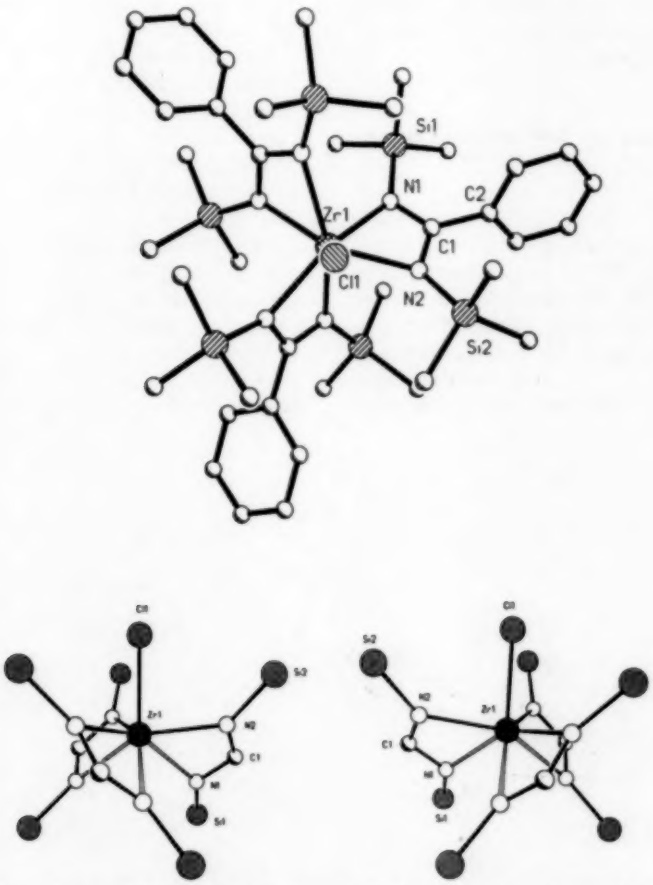


Abb. 2. Kristallstrukturanalyse von **3** (Methyl- und Phenylgruppen sind im unteren Teil zur besseren Übersicht weggelassen).

Tabelle 1
Ausgewählte Bindungslängen und -winkel der Röntgenkristallstrukturen von **1–4**

| | **1** X = Cl | **3** X = Cl | **2** X = I | **4** X = $CH_3$ |
|---|---|---|---|---|
| *Bindungslängen* | | | | |
| Zr–X (Å) | 2.4002(9) | 2.464(2) | 2.8099(5) | 2.248(2) |
| Zr–N(1) (Å) | 2.209(2) | 2.325(4) | 2.174(2) | 2.240(1) |
| Zr–N(2) (Å) | 2.239(2) | 2.249(4) | 2.265(2) | 2.312(2) |
| N(1)–C(1) (Å) | 1.333(3) | 1.330(7) | 1.346(2) | 1.337(2) |
| N(2)–C(1) (Å) | 1.323(3) | 1.329(5) | 1.326(2) | 1.323(2) |
| C(1)–C(2) (Å) | 1.502(4) | 1.503(7) | 1.501(3) | 1.497(2) |
| *Bindungswinkel* | | | | |
| X–Zr–X* (°) | 103.38(7) | – | 107.76(2) | 106.4(2) |
| N(1)–Zr–N*(1) (°) | 90.1(1) | 89.84(13) | 92.77(9) | 92.76(8) |
| N(2)–Zr–N*(2) (°) | 168.9(1) | 118.14(4) | 178.82(9) | 176.31(7) |
| Zr, N(1), N(2)–Phenyl (°) | 74.6 | 86.0 | 81.0 | 79.9 |
| C(1)–Zr–C*(1) (°) | 125.1(1) | 115.24(7) | 131.87(9) | 131.5(2) |

amidinatliganden propellerartig rechts- beziehungsweise linksdrehend angeordnet sind. Die wichtigsten Bindungslängen und -winkel der drei mittels Kristallstrukturanalyse charakterisierten Halogenide sind unter andern in Tabelle 1 zusammengefaßt.

## 3. Synthese und Strukturen der zirkoniumorganischen Verbindungen 4–7

Die Umsetzung von $(Siam)_2ZrCl_2$ mit Organolithium- oder Grignard-Verbindungen verläuft nur mit $\beta$-wasserstoffreien und schlanken organischen Gruppen (Methyl, Benzyl und Allyl) erfolgreich. In den anderen bisher untersuchten Fällen (Ethyl, Butandiyl, Butadiendiyl und Phenyl) erfolgten Zersetzungsreaktionen, ohne daß eine definierte Verbindung isoliert werden konnte. Die Dimethylverbindung **4** läßt sich in guten Ausbeuten durch Umsetzung von **1** mit zwei Äquivalenten Methylmagnesiumiodid darstellen, über ihre Synthese und ihr H-NMR-Spektrum wurde kürzlich berichtet [10].

Die Festkörperstruktur von **4** ist in Abb. 3 wiedergegeben, und Bindungslängen beziehungsweise -winkel sind in Tabelle 1 aufgelistet. Das Zirkonium ist verzerrt oktaedrisch von zwei Benzamidinatliganden und zwei Methylgruppen umgeben. Somit liegt, wie auch in den Dihalogeniden **1** und **2**, eine *cis*-Anordnung der Liganden vor.

In den H-NMR-Spektren wird bis zu einer Temperatur von −90°C nur ein Singulett für die $SiMe_3$-Gruppen gefunden, d.h. in Lösung rotieren die Benzamidinato-Liganden offenbar so schnell, daß sie in der NMR-Zeitskala nicht aufgelöst sind. Die Lage der NMR-Resonanzen für die Zr–$CH_3$-Gruppe legt nahe, daß der Benzamidinato-Ligand Siam im Vergleich zu dem Cp-

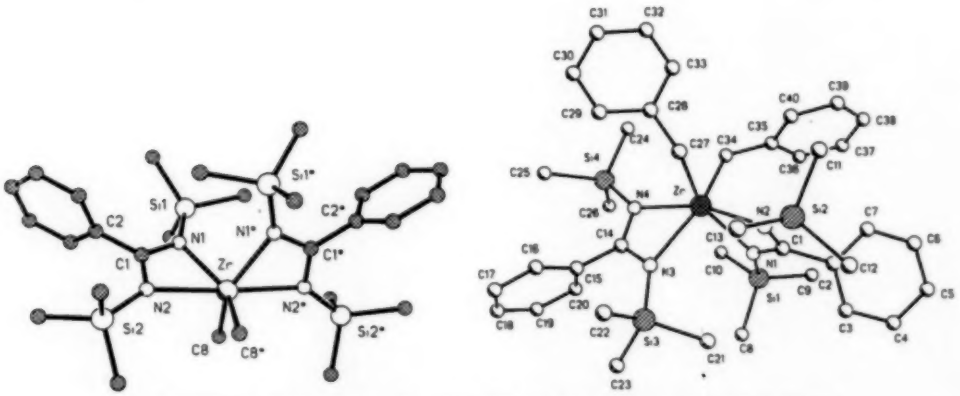


Abb. 3. Kristallstrukturanalysen von $(Siam)_2$-$Zr(CH_3)_2$ (**4**) und $(Siam_2Zr(CH_2C_6H_5)_2$ (**6**) [19].

Tabelle 2
Ausgewählte Bindungslängen (Å) der Röntgenkristallstruktur von **6**

| | | | |
|---|---|---|---|
| Zr–C(27) | 2.315(4) | Zr–C(34) | 2.301(3) |
| C(27)–C(28) | 1.488(5) | C(34)–C(35) | 1.432(5) |
| Zr–N(3) | 2.257(3) | Zr–N(1) | 2.224(3) |
| Zr–N(4) | 2.271(3) | Zr–N(2) | 2.283(3) |
| N(3)–C(14) | 1.336(4) | N(1)–C(1) | 1.339(4) |
| N(4)–C(14) | 1.331(4) | N(2)–C(1) | 1.335(4) |
| C(14)–C(15) | 1.506(4) | C(1)–C(2) | 1.497(4) |

Tabelle 3
Ausgewählte Bindungswinkel (°) der Röntgenstruktur von **6**

| | | | |
|---|---|---|---|
| C(27)–Zr–C(34) | 96.2(2) | | |
| C(27)–Zr–N(3) | 101.11(14) | C(34)–Zr–N(2) | 107.61(12) |
| C(27)–Zr–N(4) | 98.27(12) | C(34)–Zr–N(1) | 89.50(12) |
| C(27)–Zr–N(1) | 144.92(12) | C(34)–Zr–N(3) | 147.89(12) |
| C(27)–Zr–N(2) | 85.05(12) | C(34)–Zr–N(4) | 90.60(12) |
| Zr–C(27)–C(28) | 117.6(2) | Zr–C(34)–C(35) | 116.6(2) |
| N(3)–Zr–N(1) | 91.60(10) | N(1)–Zr–N(4) | 116.31(10) |
| N(3)–Zr–N(2) | 100.71(10) | N(2)–Zr–N(4) | 161.11(9) |
| N(3)–Zr–N(4) | 60.40(10) | N(1)–Zr–N(2) | 60.37(9) |
| N(3)–C(14)–N(4) | 117.3(3) | N(1)–C(1)–N(2) | 115.9(3) |
| C(1)–Zr–C(14) | 126.1 | | |

Liganden einen stärkeren Elektronenzug am Zentralatom bewirkt.

Bei der Reaktion von **1** mit einem Äquivalent Benzylmagnesiumchlorid gelingt es bei 0°C zunächst nur, einen Chloroliganden zu substituieren. Es entsteht die hellgelbe Verbindung $(Siam)_2ZrCl(benzyl)$ **5**. Bei der Umsetzung von **1** mit zwei Äquivalenten Benzyl-Grignard-Reagenz bildet sich bei 36°C neben **5** auch die Dibenzylverbindung **6** (Tabellen 2 und 3). Deren Kristallstrukturanalyse zeigt, daß das Zirkonium wiederum verzerrt oktaedrisch von zwei Benzamidinatliganden und zwei Benzylgruppen in *cis*-Anordnung umgeben ist (Abb. 3). Die Verbindung weist jedoch eine niedrigere Symmetrie als die vergleichbare Dimethylverbindung **4** auf. Die zweizählige Drehachse ist verloren gegangen, weil sich offenbar die größeren Benzylgruppen gerade noch so zwischen die Benzamidinato-Liganden hineindrängen können. Dieser sterische Effekt führt auch dazu, daß die beiden Benzylgruppen $\eta^1$-koordiniert sind.

In den $^1$H-NMR-Spektren tritt bei Raumtemperatur nur jeweils ein Singulett für die Protonen der $SiMe_3$- und $Zr–CH_2$-Gruppen auf. Während das Signal für die $SiMe_3$-Gruppen bis −90°C erhalten bleibt, beginnt sich das Signal der benzylischen $CH_2$-Protonen bei 0°C zu verbreitern, bei −35°C tritt Koaleszenz ein, und bei tieferen Temperaturen ist ein Dublett zu sehen. Aus den NMR-Daten ist eine Rotationsbarriere um die Zr–C-Bindung von 47.6 kJ mol$^{-1}$ zu berechnen.

Bei der Umsetzung von **1** mit zwei Äquivalenten Allylmagnesiumchlorid entsteht in glatter Reaktion die Diallylverbindung $(Siam)_2Zr(allyl)_2$ **(7)**, deren $^1$H-NMR-Spektrum bei Raumtemperatur für die $SiMe_3$-Gruppen ein Singulett bei 0.01 ppm zeigt. Das Quintett bei 6.70 ppm und das Dublett bei 3.71 ppm sind den

Tabelle 4
Vergleich von ausgewählten Daten der Kristallstrukturanalysen von $L_2ZrX_2$
(L = Cp oder Cp*; Siam X = Cl, I, $CH_3$ oder $CH_2–C_6H_5$)

| X | Bindungswinkel X–Zr–X (°) | | | Bindungswinkel L–Zr–L (°) | | Bindungslänge Zr–X (Å) | | |
|---|---|---|---|---|---|---|---|---|
| | Cp | Cp* | Siam | Cp | Siam | Cp | Cp* | Siam |
| Cl | 97.1 [11]<br>97.7 | | 103.4 | 126.0<br>128.3 | 125.1 | 2.44<br>2.45 | | 2.40 |
| I | 96.2 [12a] | 93.5 [12b] | 107.8 | 126.3 | 131.8 | 2.85 | 2.83 | 2.81 |
| $CH_3$ | 95.6 [13] | | 106.4 | 132.5 | 131.5 | 2.27<br>2.28 | | 2.25 |
| $CH_2$–Ph | – | | 96.2 | – | 126.1 | – | | 2.30<br>2.31 |

Tabelle 5
Vergleich der $^1$H-NMR- und $^{13}$C-NMR-Spektren der zirkonorganischen Verbindungen $Cp_2ZrR_2$, $Cp^*_2ZrR_2$ und $(Siam)_2ZrR_2$ in $C_6D_6$

| Zr–R | $Cp_2ZrR_2$ | | $Cp^*_2ZrR_2$, | $(Siam)_2ZrR_2$ | |
|---|---|---|---|---|---|
| | $^1$H-NMR, δ (ppm) | $^{13}$C-NMR, δ (ppm) | $^1$H-NMR, δ (ppm) | $^1$H-NMR, δ (ppm) | $^{13}$C-NMR, δ (ppm) |
| $Zr–CH_3$ | −0.39 [14a] | | −0.62 [14b] | 0.93 | 44.8 |
| $Zr–CH_2$–Ph | 1.84 [15a] | 60.6 | 1.59 [15b] | 2.82 | 78.3 |
| $Zr–\eta^3–C_3H_5$ | | | | | |
| $=CH_2$ | 2.89 [16] | | | 3.71 | 86.7 |
| =CH– | 5.63 [16] | | | 6.70 | 143.3 |

mittelständigen beziehungsweise den endständigen Protonen der $\eta^3$-gebundenen Allylgruppen zuzuordnen. Das Singulett der $SiMe_3$-Gruppen beginnt sich bei −20°C zu verbreitern und bei −27.5°C tritt Koaleszenz auf. Bei noch tieferen Temperaturen treten dann zwei Singuletts auf, d.h. die Rotation der Benzamidinatoliganden ist eingefroren. Aus den NMR-Daten ist eine Rotationsbarriere von 49.3 kJ $Mol^{-1}$ zu berechnen. Die Signale für die Allylgruppen bleiben bis −80°C praktisch unverändert.

## 4. Diskussion

Die vorliegenden Strukturanalysen von **1–4** und **6** unterstützen die Annahme, daß das $(Siam)_2Zr$-Fragment sterische Ähnlichkeit zum $Cp_2Zr$ beziehungsweise $Cp^*_2$-Zr-Fragment hat. In Tabelle 4 sind die wichtigsten Strukturdaten der entsprechenden Verbindungen gegenübergestellt.

Der Benzamidinatoligand Siam ist etwas voluminöser und hat im Vergleich zum Cp beziehungsweise $Cp^*$ eine mehr elliptische Peripherie. Das zeigt sich in den generell kleineren X–Zr–X-Bindungswinkeln der Cp- und $Cp^*$-Komplexe. Dagegen sind die Bindungslängen Zr–X der Benzamidinatokomplexe kürzer als bei den analogen Cp- und $Cp^*$-Verbindungen. Diese Befunde sind durch einen stärkeren Elektronenzug der Benzamidinatoliganden mit ihren anorganischen Donorgruppen und damit einem größeren ionischen Bindungsanteil erklärbar. Auch in Lösung gelten diese Aussagen, wie anhand der NMR-Spektren geschlossen werden kann (Tabelle 5). In den Siam-Zirkoniumverbindungen liegt also—vereinfachend ausgedrückt—ein Metallzentrum vor, das im Vergleich zu analogen $Cp_2Zr$-Komplexen eine stärkere Lewis-Säure ist.

## 5. Orientierende Versuche zur katalytischen Aktivität der 1, 3 und $[(Siam)ZrCl_3]_2$ mit Methylalumoxan als Cokatalysator

Erste vergleichende Untersuchungen von Ziegler–Natta-Katalysatoren aus **1**, **3** oder dem ligandärmsten Komplex $[(Siam)ZrCl_3]_2$ mit MAO als Cokatalysator wurden mit Ethylen, Propylen, Norbornen und Hexadien-1,5 durchgeführt. (Molverhältnis, Katalysator : MAO : Substrat, 1 : 100 : 200–1000). Ethylen wird bei 30°C in einer langsamen Reaktion von allen drei Katalysatorsystemen katalytisch zu Polyethylen umgesetzt. Dabei werden nach 24 h Umsatzzahlen von 600–700 erreicht. Im Vergleich mit dem Katalysatorsystem $Cp_2ZrCl_2$–MAO ist die Aktivität um mehr als den Faktor $10^3$ geringer.

Propylen wird lediglich mit dem ligandärmsten Katalysatorsystem $[(Siam)ZrCl_3]_2$–MAO mit erwartungsgemäß noch geringerer Reaktionsgeschwindigkeit (ungefähr 100–110) umgesetzt, wobei als Hauptprodukt neben geringen Mengen ataktischen Polypropylen oligomere Produkte durch "gas chromatography–mass spectroscopy" (GC–MS) identifiziert werden, und zwar neben wenig Dimeren, Trimere, Tetramere und Pentamere.

Norbornen bildet unter Ringöffnungspolymerisation mit Umsatzzahlen bis 480–24 h Polynorbornen. Das entstandene Produkt ist sehr schwer löslich, so daß es nur IR-spektroskopisch und thermogravimetrisch untersucht wurde. Erstere liefert den Hinweis auf das überwiegende Vorliegen von *trans*-Strukturen [17]. Das Produkt beginnt sich bei 150°C teilweise zu zersetzen (36% Masseverlust), vollständige Zersetzung tritt bei 420°C ein.

Die erhaltenen Ergebnisse erlauben den Schluß, daß die geprüften Komplexe generell C–C-Verknüpfungsreaktionen nur sehr langsam katalysieren, so daß sie als Polymerisationskatalysatoren ungeeignet sind.

1,5-Hexadien kann mit $[(Siam)ZrCl_3]_2$–MAO überraschend selektiv zu Methylen–cyclopentan cyclisiert werden, wenn bei 40°C gearbeitet wird. Die Bildung von Dimeren oder höheren Oligomeren bzw. Polymeren wird nicht beobachtet. Siam-reichere Komplexe sind inaktiv. Im Vergleich dazu wird 1,5-Hexadien mit dem $Cp_2ZrCl_2$–MAO-System unter vergleichbaren Bedingungen in einer schnelleren Reaktion unselektiv zu einem Oligomerengemisch umgesetzt, das zu 33% aus Monomeren, 37% aus Dimeren, 23% Trimeren mit 7% Tetrameren besteht.

Unter anderen Bedingungen werden aus Hexadien (1,5) Polymere erhalten [18]. Auch in der Reaktion mit 1,5-Hexadien zeigt sich der generelle Unterschied zwischen Zirconocen-Typ–MAO-Katalysatoren und (Siam)-Zr-Komplexen, aktiviert mit MAO. Letztere reagieren auch hier langsam in C–C-Verknüpfungsreaktionen, und das ermöglicht, die Reaktion mit Hexadien (1,5) im monomere-Regime zu halten.

## 6. Experimenteller Teil

Alle Arbeiten wurden unter einer Argonschutzgasatmosphäre ausgeführt. Die NMR-Spektren wurden auf einem 200 MHz-Spektrometer der Firma Bruker aufgenommen. Die kristallographischen Strukturbestimmungen erfolgten auf einem Enraf–Nonius CAD4-Diffraktometer mit Mo K$\alpha$-Strahlung ($\lambda = 0.710\ 69$ Å; Graphit-Monochromator) mittels "least-squares"-Verfeinerung der $2\theta$-Werte von 25 Reflexen. Röntgenintensitäten wurden in $\omega$–$2\theta$-Abtastung gemessen. Eine Lorentz und Polarisationskorrektur wurde durchgeführt [19]. Eine Absorptionskorrektur erfolgte bei Verbindung **2**.

Die Strukturen wurden mittels direkter Methoden gelöst (SHELXS-86) [20], wodurch der größte Teil der Nichtwasserstoffatome lokalisiert wurde. Durch Differenzfouriersynthesen konnten die restlichen Nichtwasserstoffatome ermittelt werden. Das erhaltene vorläufige Strukturmodell wurde im Vollmatrix-LSQ-Verfahren anisotrop verfeinert (Verbindung **1**, **2** und **4** mittels [19]; Verbindung **3** und **6** durch [21,22]. In der Tabelle 6 sind einige kristallographische Daten zu den Kristallstrukturen zusammengefaßt. Weitere Einzelheiten zur Kristallstrukturanalyse können beim Fachinformationszentrum Energie, Physik, Mathematik GmbH, W-7513 Eggenstein-Leopoldshafen 2, unter Angabe der Hinterlegungsnummer CSD-58769, der Autoren und des Zeitschriftenzitats angefordert werden.

Das Edukt Bis-*N,N'*-bis(trimethylsilyl)benzamidinatozirkoniumdichlorid **1** wurde durch folgende abgewandelte Literaturvorschrift dargestellt (vgl. [3]).

### 6.1. *Bis-(N,N'-bis(trimethylsilyl)benzamidinato)-zirkonium-IV-dichlorid ($(Siam)_2ZrCl_2$) (1)*

Zu einer gerührten Lösung von 62,5 ml n-Butyllithium (1.6 m) in Hexan (0.1 mol) werden bei 0°C in folgender Reihenfolge 16.1 g (0.1 mol) Hexamethyldisilazan 25 ml Ether und 10.3 g (0.1 mol) Benzonitril tropfenweise zugegeben. Die entstandene Reaktionslösung wird bei 0°C während 2 h in eine kräftig gerührte Suspension von 18.9 g (0.05 mol) $ZrCl_4(THF)_2$ in 50 ml Ether getropft. Nach erfolgter Zugabe erwärmt man auf Raumtemperatur, läßt noch 4 h ausreagieren und sammelt die ausgeschiedene Substanz auf einer G4-Fritte. Nun wird mit Methylenchlorid extrahiert. Aus dem Extrakt kristallisieren in der Kälte 15.6 g (45.3%) reines **1**.

$^1$H-NMR ($C_6D_6$): $\delta$ 0.05 (36H, s, Si–$CH_3$); 7.2–8.0 (10H, m, Ph) ppm. $^{13}$C-NMR ($C_6D_6$): $\delta$ 2.0 (Si–$CH_3$); 126.2; 128.4; 139.6 (Ph); 184.9 ($CN_2$) ppm.

Die Mutterlauge enthält neben **1** noch etwas **3**.

### 6.2. *Bis-(N,N'-bis(trimethylsilyl)benzamidinato)-zirkonium-IV-diiodid ($(Siam)_2ZrI_2$) (2)*

In eine Suspension von 4.2 g (6.48 mmol) **4** in 20 ml Ether wird bei 0°C unter Rühren langsam 30 ml einer etherischen Lösung von 3.3 g (13.0 mmol) frisch sublimiertem Iod tropfenweise zugegeben. Die Iodlösung wird entfärbt, und der Bodenkörper löst sich auf. Das

Tabelle 6
Kristallographische Daten

| | 1 | 2 | 3 | 4 | 6 |
|---|---|---|---|---|---|
| Kristallmorphologie | farbloses Prisma | farbloses Prisma | farblose hexagonales Prisma | farbloses Prisma | gelbe Quader |
| Kristallgröße (mm) | 0.44 × 0.32 × 0.28 | 0.40 × 0.38 × 0.36 | 0.40 × 0.40 × 0.36 | 0.60 × 0.60 × 0.48 | 0.40 × 0.38 × 0.36 |
| Summenformel | $C_{26}H_{46}Cl_2Si_4N_4Zr$ | $C_{26}H_{46}I_2Si_4N_4Zr$ | $C_{40}H_{77}Cl_3Si_6N_6Zr$ | $C_{28}H_{52}Si_4N_4Zr$ | $C_{40}H_{60}Si_4N_4Zr$ |
| Molekulargewicht ($gmol^{-1}$) | 689.2 | 872.1 | 1008.2 | 648.3 | 800.5 |
| Kristallsystem | monoklin | monoklin | hexagonal | monoklin | monoklin |
| Raumgruppe | $C2/c$ | $C2/c$ | $P\bar{3}c1$ | $C2/c$ | $C2/c$ |
| Gitterparameter | | | | | |
| $a$ (Å) | 21.284(5) | 21.767(3) | 21.580(3) | 21.701(6) | 34.434(7) |
| $b$ (Å) | 9.335(2) | 9.582(2) | 21.580(3) | 9.384(2) | 13.648(3) |
| $c$ (Å) | 18.056(3) | 17.670(6) | 20.260(1) | 17.809(2) | 19.911(4) |
| $\beta$ (°) | 94.91(1) | 99.23(1) | | 95.12(1) | 108.36(8) |
| Elementarzellenvolumen $V$ (Å$^3$) | 3574(1) | 3638(1) | 8171(2) | 3612(1) | 8881(3) |
| Dichte $\rho_c$ ($g\,cm^{-3}$) | 1.28 | 1.59 | 1.23 | 1.19 | 1.20 |
| Anzahl der Formeleinheiten $Z$ | 4 | 4 | 6 | 4 | 8 |
| Absorptionskoeffizient $\mu$(Mo K$\alpha$) ($cm^{-1}$) | 6.1 | 21.3 ($\psi$-scan) | 5.1 | 4.5 | 3.9 |
| Temperatur (°C) | 20(1) | −90(1) | 20(1) | 20(1) | −90(1) |
| $2\theta_{max}$ (°) | 55.0 | 64.0 | 55.0 | 50.0 | 55.0 |
| gemessene Reflexe | 4452 | 6785 | 4954 | 4495 | 10249 |
| symmetrieunabhängige Reflexe | 4319 | 6303 | 4800 | 4108 | 10086 |
| beobachtete Reflexe mit $I > 2\sigma(I)$ | 3553 | 5283 | 3450 | 3812 | 7116 |
| verfeinerte Parameter | 168 | 169 | 316 | 168 | 682 |
| $R_1$ | 0.039 | 0.027 | 0.065 | 0.031 | 0.038 |
| $wR_2$ ($Rw$) | (0.057) | (0.038) | 0.124 | (0.050) | 0.094 |
| "Goodness of fit" | 2.02 | 1.36 | 1.24 | 2.03 | 1.08 |
| Restelektronendichte (electrons Å$^{-3}$) | 0.44 | 0.46 | 0.33 | 0.24 | 0.60 |

Lösungsmittel wird im Vakuum abdestilliert. Im Destillat ist gaschromatographisch Methyliodid nachweisbar. Der Rückstand wird aus n-Hexan umkristallisiert. Ausbeute: 5.2 g (92.0%) **2** in Form farbloser Kristalle.

Elementaranal. Gef.: C, 35.8; H, 5.3; N, 6.4. $C_{26}H_{46}I_2N_4Si_4Zr$ (872.0 g $mol^{-1}$) ber.: C, 37.0; H, 5.4; N, 6.0%. $^1$H-NMR ($CD_2Cl_2$): $\delta$ 0.05 (36H, s, Si–$CH_3$); 7.2–8,0 (10H, m, Ph) ppm. $^{13}$C-NMR ($CD_2Cl$): $\delta$ 2.4 (Si–$CH_3$); 126.3; 129.0; 130.1; 139.1 (Ph); 184.2 ($CN_2$) ppm.

### 6.3. Tris-(N,N'-bis(trimethylsilyl)benzamidinato-zirkoniumchlorid ((Siam)$_3$ZrCl · $CH_2Cl_2$) (3)

#### 6.3.1. Variante A

Zu einer gerührten Lösung von 62.5 ml *n*-Butyllithium (1.6 m) in Hexan (0.1 mol) werden bei 0°C nacheinander 16.1 g (0.1 mol) Hexamethyldisilazan, 25 ml Ether und 10.3 g (0.1 mol) Benzonitril tropfenweise zugegeben. Nun werden in kleinen Portionen insgesamt 9.4 g (0.025 mol) $ZrCl_4(THF)_2$ bei 0°C zugesetzt. Nach erfolgter Zugabe erwärmt man auf Raumtemperatur, läßt noch 4 h ausreagieren und vervollständigt die Kristallisation bei −25°C. Die ausgeschiedene Substanz wird auf einer G4-Fritte gesammelt und mit Methylenchlorid extrahiert. Aus der Lösung kristallisieren in der Kälte 4.9 g (19.6%) **3** als weiße hexagonale Kristalle.

Elementaranal. Gef.: C, 47.4; H, 7.1; N, 8.4; Cl, 10.6. $C_{40}H_{71}Cl_3N_6Si_6Zr$ (1002.12 g $mol^{-1}$) ber.: C, 46.3; H, 6.9; N, 7.6; Cl, 9.7%. $^1$H-NMR ($C_6D_6$): $\delta$ 0.20 (27H, s, Si–$CH_3$); 0.40 (27H, s, Si–$CH_3$); 7.2–8.0 (15H, m, Ph) ppm. $^{13}$C-NMR ($C_6D_6$): $\delta$ 3.9 (Si–$CH_3$); 4.2 (Si–$CH_3$); 140.2; 129.0; 128.4; 126.2 (Ph); 182.2 ($CN_2$) ppm.

#### 6.3.2. Variante B

Zu einer gerührten Lösung von 30 ml *n*-Butyllithium (1.6 m) in Hexan (48 mmol) werden bei 0°C 7.7 g (48 mmol) Hexamethyldisilazan, 15 ml Ether und 4.95 g (48 mmol) Benzonitril tropfenweise zugegeben. Nun werden in kleinen Portionen insgesamt 11.0 g (16 mmol) **1** bei 0°C zugesetzt. Nach erfolgter Zugabe erwärmt man auf Raumtemperatur, läßt noch 4 h ausreagieren und vervollständigt die Kristallisation im Tiefkühlschrank. Die ausgeschiedene Substanz wird auf einer G4-Fritte gesammelt und mit Methylenchlorid extrahiert. Aus der Lösung kristallisieren in der Kälte 9.0 g (56.2%) **3**.

### 6.4. Bis-(N,N'-bis(trimethylsilyl)benzamidinato)-dimethylzirkonium-IV ((Siam)$_2$Zr($CH_3$)$_2$) (4) (vgl. [10])

Bei −78°C wird in eine Suspension von 12.3 g (17.85 mmol) **1** in 180 ml Ether unter Rühren 29.0 ml (35.67 mmol) Methylmagnesiumiodid (1.23 m) in Ether tropfenweise zugegeben. Nun wird langsam auf Raumtemperatur erwärmt und noch 2 h weitergerührt. Nach Zugabe von Dioxan werden die ausgefallenen Magnesiumsalze auf einer G4-Fritte abgetrennt. Der Filterkuchen wird nochmals mit 100 ml Ether ausgewaschen und die vereinigten Filtrate werden im Vakuum bis zur beginnenden Kristallisation eingeengt. Ausbeute: 8.5 g (73.5%) **4** weiße lichtempfindliche Kristalle.

Elementaranal. Gef.: C, 51.9, H, 8.1; N, 8.7. $C_{28}H_{52}N_4Si_4Zr$ (648.3 g $mol^{-1}$) ber.: C, 52.0; H, 8.2; N, 9.0%. $^1$H-NMR ($C_6D_6$): $\delta$ 0.05 (36H, s, Si–$CH_3$); 0.93 (6H, s, Zr–$CH_3$); 6.9–7.2 (10H, m, Ph) ppm. $^{13}$C-NMR ($C_6D_6$): $\delta$ 2.2 (Si–$CH_3$); 44.8 (Zr–$CH_3$); 126.2; 1283; 128.6; 141.0 (Ph); 184.4 ($CN_2$) ppm.

### 6.5. Bis-(N,N'-bis(trimethylsilyl)benzamidinato)$\eta_2$-benzyl-zirkonium-IV-chlorid ((Siam)$_2$ZrCl($CH_2C_6H_5$) (5)

In 4.2 g (6.09 mmol) **1**—in 50 ml Ether suspendiert—werden bei −78°C unter Rühren 8.7 ml (6.09 mmol) Benzylmagnesiumchlorid (0.7 m) in Ether zugetropft. Nun wird langsam erwärmt. Bei −20°C beginnt sich die Lösung gelb zu färben. Die Reaktion wird durch vierstündiges Rühren bei 20°C vervollständigt. Nun wird Dioxan zugetropft und das ausgefallene Magnesiumchlorid auf einer G4-Fritte abgetrennt. Der Filterkuchen wird mit 50 ml Ether gründlich ausgewaschen. Die vereinigten Filtrate werden im Vakuum bis zur Trockne eingeengt, der Rückstand wird in 70 ml n-Hexan aufgenommen und klar filtriert. Bei −30°C kristallisieren 2.15 g (47.6%) **5** als hellgelbe, schuppenförmige Kristalle.

Elementaranal. Gef.: C, 53.2; H, 7.2; N, 7.5. $C_{33}H_{53}ClN_4Si_4Zr$ (744.8 g $mol^{-1}$) ber.: C, 52.3; H, 8.2; N, 7.2%. $^1$H-NMR ($C_6D_6$): $\delta$ 0.09 (36H, s, Si–$CH_3$); 3.02 (2H, s, $CH_2$–Zr); 6.9–7.5 (15H, m, Ph) ppm. $^{13}$C-NMR ($C_6D_6$): $\delta$ 2.4 (Si–$CH_3$); 76.7 ($CH_2$–Zr); 121.8; 126.3; 128.6; 129.0; 130.1; 147.9 (Ph); 185.6 ($CN_2$) ppm.

### 6.6. Bis-(N,N'-bis(trimethylsilyl)benzamidinato)di-$\eta^1$-benzyl-zirkonium-IV ((Siam)$_2$Zr($CH_2C_6H_5$)$_2$ (6)

Bei −78°C werden in eine Suspension von 4.5 g (6.23 mmol) **1** in 100 ml Ether unter Rühren 19.0 ml (13.3 mmol) Benzylmagnesiumchlorid (0.7 m) in Ether zugegeben, danach wird langsam auf Raumtemperatur erwärmt und dann 5 h am Rückfluß gekocht. Nun wird durch Zugabe von Dioxan Magnesiumchlorid ausgefällt und über eine G4-Fritte abgetrennt. Der Filterkuchen wird mit 50 ml Ether ausgewaschen, und die vereinigten Filtrate werden bis zur Trockne eingeengt. Der Rückstand wird mit 70 ml *n*-Hexan aufgenommen, filtriert und bei −20°C zur Kristallisation gebracht. Man erhält als erste Fraktion 0.7 g (15.1%) **5**. Die zweite Fraktion kristallisiert bei −45°C. Ausbeute, 1.2 g (24.1%) **6** als zitronengelbe Kristalle.

Elementaranal. Gef.: C, 60.0; H, 7.6; N, 7.0. $C_{40}H_{60}N_4Si_4Zr$ (800.5 g $mol^{-1}$) ber.: C, 57.8; H, 7.3; N, 7.3%. $^1$H-NMR ($C_6D_6$): $\delta$ 0.00 (36H, s, Si–$CH_3$); 2.82 (4H, s, $CH_2$–Zr); 6.9–7.5 (15H, m, Ph) ppm. $^{13}$C-NMR ($C_6D_6$): $\delta$ 2.8 (Si–$CH_3$); 78.3 ($CH_2$–Zr); 121.1, 126.2; 128.3; 128.6; 129.0; 130.1; 140.5; 149.9; (Ph); 187.4 ($CN_2$) ppm.

Das scharfe Signal der benzylischen Methylengruppen bei 2.70 ppm beginnt sich beim Abkühlen in $d^7$-Toluol ab 0°C zu verbreitern. Bei −35°C tritt Koaleszenz auf. Bei −40°C sind zwei grundliniengetrennte Signale zu sehen. NMR-Daten ($\Delta\delta$ = 80 Hz; $T_c$ = 238 K).

### 6.7. Bis-(N,N'-bis(trimethylsilyl)benzamidinato)di-allyl-zirkonium-IV ((Siam)$_2$Zr($C_3H_5$)$_2$) (7)

Bei 0°C werden in eine Suspension von 4.7 g (6.82 mmol) **1** in 100 ml Ether unter Rühren tropfenweise 7.0 ml (14.0 mmol) Allylmagnesiumchlorid (2.0 m) in THF zugegeben. Die Reaktionslösung nimmt sofort eine gelbe Farbe an. Nun wird langsam auf Raumtemperatur erwärmt. Das ausgefallene Magnesiumchlorid wird auf einer Schlenk-Glasfritte abgetrennt. Der Filterkuchen wird mit 50 ml Ether ausgewaschen, und die vereinigten Filtrate werden bis zur Trockne eingeengt. Der Rückstand wird mit 70 ml *n*-Hexan aufgenommen, und nach Filtration kristallisiert **7** bei −20°C aus. Ausbeute, 1.7 g (35.6%) **7** als gelb–orange lichtempfindliche Kristalle.

Elementaranal. Gef.: C, 54.87; H, 8.06. $C_{32}H_{56}N_4Si_4Zr$ (700.4 g $mol^{-1}$) ber.: C, 55.80; H, 8.22%. $^1$H-NMR ($C_6D_6$): $\delta$ 0.01 (36H, s, Si–$CH_3$); 3.71 (8H, d, $J$ = 11.9 Hz, $CH_2$=); 6.70 (2H, q, $J$ = 11.9 Hz, CH=); 6.97–7.21 (10H, m, Ph) ppm. $^{13}$C-NMR ($C_6D_6$): $\delta$ 3.5 (Si–$CH_3$); 86.7 (=$CH_2$); 127.1; 129.4; 141.3 (Ph); 143.3 (CH=); 182.0 ($CN_2$) ppm.

Das scharfe Signal der Silylgruppen bei 0.01 ppm beginnt sich beim Abkühlen ab −20°C in $d^7$-Toluol zu verbreitern. Bei −27.5°C tritt Koaleszent auf. Bei noch tieferen Temperaturen sind zwei grundliniengetrennte Signale zu sehen. NMR-Daten ($\Delta\delta$ = 75 Hz; $T_c$ = 245.5 K).

### 6.8. Katalytische Reaktionen

#### 6.8.1. Reaktion mit Ethylen

0.1 mmol der Verbindungen **1**, **3** beziehungsweise [(Siam)$ZrCl_3$]$_2$ in 50 ml Toluol werden mit 10 mmol MAO, eingesetzt als 30%ige Lösung in Toluol, Fa. Witco) in einem 200 ml-Stahlautoklaven bei 30°C unter Rühren umgesetzt. Nach 24 h wird unumgesetztes Ethylen abgelassen und die Mischung unter Eiskühlung mit halbkonzentrierter kalter wäßriger Salzsäure hydrolisiert. Nach Filtration, Waschen mit Toluol, Ethanol und Trocken erhält man 1.7–2 g nahezu farbloses Polymer; das entspricht einer Umsatzzahl von 600–700 (24 h). Das erhaltene Polyethylen wurde nicht näher charakterisiert. Im Toluol-filtrat sind durch GC–MS keine weiteren oligomeren Produkte nachweisbar.

#### 6.8.2. Reaktion mit Propylen

In einem 200 ml-Stahlautoklaven werden bei −50°C etwa 10 g Propylen einkondensiert, danach wird eine Lösung von 0.1 mmol der Verbindung **1**, **3** oder [(Siam)$ZrCl_3$]$_2$ und 10 mmol MAO in 20 ml Toluol zudosiert. Nach 24 h Rühren bei 30°C wird unumgesetztes Gas abgelassen, danach wird die Mischung unter Eiskühlung mit halbkonzentrierter Salzsäure hydrolysiert. Die organische Phase wird abgetrennt, mit Natriumcarbonat getrocknet und danach im Vakuum destilliert. Lediglich im Falle von [(Siam)$ZrCl_3$]$_2$ konnten im Destillat die oligomeren Produkte (Dimere bis Pentamere $C_{15}H_{30}$) durch GC–MS indiziert werden. Der Gesamtgehalt dieser Oligomeren entspricht einer Umsatzzahl von ungefähr 100 (etwa 500 mg Produkt). Der ölige Destillationsrückstand ist ein Gemisch von höheren Oligomeren beziehungsweise ataktischen Polymeren, wie NMR-spektroskopische Vergleiche zeigen.

Unter gleichen Bedingungen wird mit dem System $Cp_2ZrCl_2$–MAO eine nahezu quantitative Umsetzung bereits nach 2 h beobachtet. Es entsteht ein Oligomerengemisch, das Dimere bis Heptamere enthält, die durch GS–MS dedektierbar sind. Dabei sind Tetramere mit 40% Anteil die Hauptprodukte. Polymeres Produkt wird unter diesen Bedingungen nur in sehr geringen Mengen beobachtet.

#### 6.8.3. Reaktion mit Norbornen

Die Reaktion wird wie beim Ethylen beschrieben mit 5 g Norbornen ($5.3 \times 10^{-2}$ mol) als Substrat, durchgeführt. Man erhält mit **1** und mit [(Siam)$ZrCl_3$]$_2$ 1.4–2.8 g von farblosem Polymer, das in Lösungsmitteln extrem schwer löslich ist.

IR: ($\delta$(C–H), trans) 965 $cm^{-1}$ [17]. Thermogravimetrie: Bei 150°C 36% Masseverlust, bei 420°C vollständige Zersetzung.

#### 6.8.4. Reaktion mit 1,5-Hexadien

0.1 mmol Komplexverbindung **1**, **3** oder [(Siam)$ZrCl_3$]$_2$ werden mit 10 mmol MAO und 17 mmol Substrat bei 40°C in 20 ml Toluol umgesetzt. Durch Probenentnahme während der Reaktion wird der Verlauf mittels GC–MS verfolgt. Umsatz nach 24 h 10%, nach 15 d 42% (Umsatzzahl, 80). Es wird selektiv Methylencyclopentan gebildet. Dimere beziehungsweise Oligomere oder Polymere werden nicht gefunden.

Unter vergleichbaren Bedingungen erfolgt mit $Cp_2ZrCl_2$–MAO nach 3 h vollständiger Umsatz. Das Produktgemisch enthält 33% Monomere (einschließlich 19% Methylen–cyclopentan, der Rest besteht aus Methyl–cyclopenten und Methyl–cyclopentan), 37%

Dimerengemisch, 23% Trimere, 7% Tetramere, jeweils durch GC–MS bestimmt).

## Dank

Dem Bundesministerium für Forschung und Technologie gilt unser herzlicher Dank für die großzügige Förderung dieser Arbeit.

## Literatur

[1] B. Schweder, D. Walther, R. Fischer, G. Bischof, B. Stang und H. Görls, *Proc. Eur. Jpn. Symp. on Selective Processes and Catalysis Involving Small Molecules, Rennes, Frankreich, 14.–16. September 1994*, 1994, Abstract S. 61.

[2] D. Fenske, E. Hartmann und K. Dehnicke, *Z. Naturforsch. 43b* (1988) 1611.

[3] H.W. Roesky, B. Meller, M. Noltemeyer, U. Scholz und G.M. Sheldrick, *Chem. Ber., 121* (1988) 1403.

[4] M. Wedler, F. Knösel, M.N. Noltemeyer, F.T. Edelmann und U. Behrens, *J. Organomet. Chem., 388* (1990) 21.

[5] C. Hagen, H. Reddmann, H.-D. Amberger und F. Edelmann, *J. Organomet. Chem., 462* (1993) 69.

[6] A.N. Chenega, R. Gomez und M.L.H. Green, *J. Chem. Soc., Chem., Commun.*, (1993) 1415.

[7] M. Wedler, F. Knösel, F.T. Edelmann und U. Behrens, *Chem. Ber., 125* (1992) 1313.

[8] D.G. Dick, R. Duchateau, J.J.H. Edema und S. Gamborotta, *Inorg. Chem., 32* (1993) 1959.

[9] J.H. Teuben, R. Duchateau, C.T. van Wee und A. Meetsma, *J. Am. Chem. Soc., 115* (1993) 4931.

[10] (a) J.C. Flores, I.C.W. Chien und H.D. Rausch, *Organometallics, 14* (1995) 1827.
(b) I.R. Hagadorn und J. Arnold, *Organometallics, 13* (1994) 4670.

[11] K. Prout, T.S. Cameron, R.A. Forder, S.R. Critchley, B. Denton und G.V. Rees, *Acta Crystallogr. Sect. B, 30* (1974) 2290.

[12] (a) G.A. Sim und M.A. Bush, *J. Chem. Soc. A*, (1971) 2225.
(b) Z. Hou, T.L. Breen und D.W. Stephan, *Organometallics, 12* (1993) 3158.

[13] W.E. Hunter, D.C. Hrncir, R.A. Vann Bynum, R.A. Penttila und J.L. Atwood, *Organometallics, 2* (1983) 750.

[14] (a) E. Sammuel und M.D. Rausch, *J. Am. Chem. Soc., 95* (1973) 6263.
(b) J.M. Manriquez, D.R. McAlister, R.D. Sanner und J.E. Bercan, *J. Am. Chem. Soc., 100* (1978) 2716.

[15] (a) J. Scholz, F. Rehbaum, K.-H. Thiele, R. Goddard, P. Betz und C. Krüger, *J. Organomet. Chem., 443* (1993) 93.
(b) J.M. Atkison und P.B. Brindey, *J. Organomet. Chem., 411* (1991) 131.

[16] H.A. Martin, T.J. Lemare und F. Jellinek, *J. Organomet. Chem., 14* (1968) 149.

[17] (a) T. Oshika und H. Tabichi, *Bull. Chem. Soc. Jpn., 41* (1968) 211.
(b) T.J. Katz und N. Acton, *Tetrahedron Lett., 43* (1976) 4251.

[18] G.W. Coates und R.M. Waymouth, *J. Am. Chem. Soc., 115* (1993) 91.

[19] *MOLEN, An Interactive Structure Solution Procedure*, Enraf–Nonius, Delft, 1990.

[20] G.M. Sheldrick, *SHELXS-86, ein Programm zur Lösung von Kristallstrukturen*, Universität Göttingen, Göttingen, 1980.

[21] G.M. Sheldrick, *SHELXL-93, ein Programm zur Verfeinerung von Kristallstrukturen*, Universität Göttingen, Göttingen, 1993.

[22] G.M. Sheldrick, *Molekülstruktur, SHELXTL / PC*, Siemens Analytical X-Ray Instruments, Inc., Madison, WI, 1992.

ELSEVIER

Journal of Organometallic Chemistry 508 (1996) 23–30

Journal of Organometallic Chemistry

# Comparison of the oxidation of dinuclear cyclopentadienyl iron diphosphine complexes with the bridging ligands –CN and $-C{\equiv}C(CH_2)_2CN$

Gabino A. Carriedo [a,*], Alejandra Arancibia [b], Carlos Díaz-Valenzuela [b,*], Nicolás Yutronic [b], Enrique Pérez-Carreño [c], Santiago García-Granda [c]

[a] *Departamento de Química Orgánica e Inorgánica, Facultad de Química, Universidad de Oviedo, Oviedo 33071, Spain*
[b] *Departamento de Química, Facultad de Ciencias, Universidad de Chile, Santiago, Chile*
[c] *Departamento de Química Física y Analítica, Facultad de Química, Universidad de Oviedo, Oviedo 33071, Spain*

Received 10 February 1995

**Abstract**

The alkynyliron complex $[Fe(C{\equiv}C{-}CH_2CH_2{-}CN)(dppe)(C_5H_5)]$ (**2**) (dppe = $Ph_2PCH_2CH_2PPh_2$), prepared from $[Fe(C{\equiv}C{-}CH_2CH_2{-}CN)(CO)_2(C_5H_5)]$ (**1**) and dppe under UV irradiation, reacted with $HBF_4.Et_2O$ in tetrahydrofuran and with $NH_4[PF_6]$ in $CH_2Cl_2$ to give the cationic vinylidene derivative $[Fe(=C{=}CH{-}CH_2CH_2{-}CN)(dppe)(C_5H_5)]A$ (A = $BF_4$ (**3a**) or $PF_6$ (**3b**)), which can be reconverted to **2** with $K_2CO_3$ in $CH_2Cl_2$. The compound $[(C_5H_5)(dppe)Fe{-}NC{-}CH_2CH_2{-}C{\equiv}CH]PF_6$ (**4**), which is a tautomeric form of **3** was prepared by reaction of $[Fe(I)(dppe)(C_5H_5)]$ with the alkyne $HC{\equiv}C{-}CH_2CH_2CN$ in the presence of $NH_4[PF_6]$ in $CH_2Cl_2$. The dinuclear compound $[(C_5H_5)(dppe)Fe{-}C{\equiv}C{-}CH_2CH_2{-}CN{-}Fe(dppe)(C_5H_5)][PF_6]$ (**5**), which is unstable, can be formed by reaction of **2** with $[Fe(NCMe)(dppe)(C_5H_5)]PF_6$ in $CH_2Cl_2$. Its electrochemical oxidation shows that there is no electronic interaction between the two metal centres. Extended Hückel molecular orbital calculations have been carried out on the model complexes $[(C_5H_5)(PH_3)_2Fe{-}C{\equiv}C{-}CH_2CH_2{-}CN{-}Fe(PH_3)_2(C_5H_5)]^+$ (**7**) and $[(C_5H_5)(PH_3)_2Fe{-}CN{-}Fe(PH_3)_2(C_5H_5)]^+$ (**8**).

*Keywords:* Iron; Alkynyl; Cyanide; Ligand bridged; Electrochemistry; EHMO calculations

## 1. Introduction

In previous studies [1] we have shown that the binuclear cyanide-bridged complex $[(C_5H_5)(dppe)Fe{-}CN{-}Fe(dppe)(C_5H_5)][PF_6]$ undergoes two one-electron oxidations, the first affecting mainly the *N*-bonded Fe atom, with electrode potentials that suggested an extended electronic communication between the two iron atoms mediated by the CN bridge.

Here we wish to report how the electron delocalization in this species can be further shown by comparison with the oxidation behaviour of the related binuclear complex $[(C_5H_5)(dppe)Fe{-}C{\equiv}C{-}CH_2CH_2{-}CN{-}Fe(dppe)(C_5H_5)][PF_6]$ containing the asymmetric bidentate cyanoalkynyl $-C{\equiv}C{-}CH_2CH_2{-}CN$, which is an isolating bridging ligand, and by a molecular orbital (MO) study carried out on the model complexes $[(C_5H_5)(PH_3)_2Fe{-}C{\equiv}C{-}CH_2CH_2{-}CN{-}Fe(PH_3)_2(C_5H_5)]^+$ and $[(C_5H_5)(PH_3)_2Fe{-}CN{-}Fe(PH_3)_2(C_5H_5)]^+$.

## 2. Results and discussion

The orange iron alkynyl complex $[Fe(C{\equiv}CCH_2CH_2CN)(dppe)(C_5H_5)]$ (**2**) was prepared from the dicarbonyl precursor $[Fe(C{\equiv}CCH_2CH_2CN)(CO)_2(C_5H_5)]$ (**1**) and dppe under UV irradiation. Compound **2** can be stored under dinitrogen in the solid state for several months, but it decomposes in solution.

As might be expected [2], the neutral complex **2** can be protonated with $HBF_4$ in diethyl ether to give the cationic vinylidene complex $[Fe(=C{=}CH{-}CH_2CH_2{-}CN)(dppe)(C_5H_5)]BF_4$ (**3a**) (Scheme 1). The protonation can be also achieved in dichloromethane solution under very mild conditions using $NH_4[PF_6]$ to give the $[PF_6]$ salt (**3b**). The cationic complex **3** could be reconverted to **2** with $K_2CO_3$ in $CH_2Cl_2$.

* Corresponding authors.

0022-328X/96/$15.00 © 1996 Elsevier Science S.A. All rights reserved
*SSDI* 0022-328X(95)05829-X

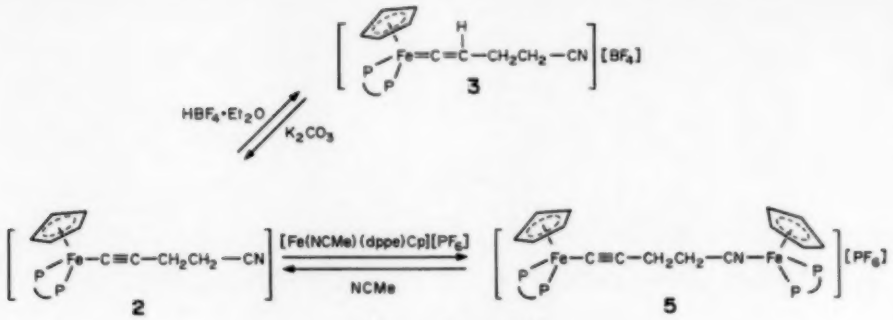

Scheme 1. (PP = dppe).

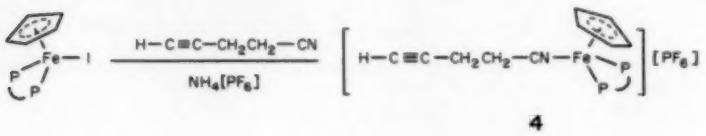

Scheme 2.

The alkyne H–C≡C–$CH_2CH_2$–CN reacted very easily with [FeI(dppe)($C_5H_5$)] and $NH_4[PF_6]$ in $CH_2Cl_2$ or methanol (Scheme 2) to give the cationic nitrile complex [($C_5H_5$)(dppe)Fe–NC–$CH_2CH_2$–C≡CH][$PF_6$] (**4**), which is a tautomeric form of **3b**.

These compounds were characterized by the analytical and spectroscopic data given in Tables 1 and 2 and Section 3.

The changes in $\nu$(CN) and $\nu$(CC), and the chemical shifts of the phosphorus atoms in the $^{31}$P NMR spectra are consistent with the formulations proposed. For example, **2** had a very similar $\nu$(CN) frequency to, but a significantly lower $\nu$(CC) frequency than the free alkyne H–C≡C–$CH_2CH_2$–CN (2251 and 2134 $cm^{-1}$ respectively), while for **4** both frequencies are slightly higher than in the alkyne.

The IR spectrum of the cationic vinylidene complex **3** did not show any absorption attributable to $\nu$(H–C≡) stretching (the alkyne H–C≡C–$CH_2CH_2$–CN has a band at 3294 $cm^{-1}$, and **4** at 3293 $cm^{-1}$) but had an intense band at 1657 $cm^{-1}$, owing to the C=C double bond, and a $\nu$(CN) band almost identical with that of **2**. More significantly, the $^{13}$C NMR spectrum of **3** showed a triplet at 355.3 ppm ($J$(P–C) = 34 Hz), which corresponds to the α-vinylidene carbon atom.

In contrast, the $^{13}$C NMR spectrum of **2** shows the signal of the –CN carbon atom at almost the same frequency as in the free alkyne, while for **4** the chemical

Table 1
Spectroscopic and voltammetric data for the compounds

| Compound [a] | IR, $\nu$($cm^{-1}$) [b] | | $^{31}$P NMR, $\delta$ [c] (ppm) | | $E_{1/2}$ (V) | |
|---|---|---|---|---|---|---|
| | $\nu$(CN) | $\nu$(CC) | | | $E_1$ | $E_2$ |
| [Fe(C≡$CCH_2CH_2CN$)(CO)$_2$($C_5H_5$)] (**1**) | 2246 | 2134 [e] | | | | |
| [Fe(C≡$CCH_2CH_2CN$)(dppe)($C_5H_5$)] (**2**) | 2243 | 2087 | 106.6 [f] | | 0.02 | |
| [Fe(=C=$CHCH_2CH_2CN$)(dppe)($C_5H_5$)][$PF_6$] (**3**) | 2244 | 1657 | 95.9 [g] | | > 1.2 | |
| [Fe(NC–$CH_2CH_2$C≡CH)(dppe)($C_5H_5$)][$PF_6$] (**4**) | 2263 | 2153 [h] | 98.0 [i] | | 0.77 | |
| [(Fe(dppe)($C_5H_5$))$_2$(μ-(C≡$CCH_2CH_2CN$))][$PF_6$] (**5**) | 2253 | 2085 | 106.5 [j] | 97.7 | 0.05 | 0.73 |

[a] The free alkyne H–C≡C–$CH_2CH_2$–CN has IR absorptions at 3294 (CH), 2251 (CN) and 2134 (CC) $cm^{-1}$.
[b] Nujol mull.
[c] Measured in $CD_2Cl_2$ downfield to external 85% aqueous $H_3PO_4$.
[d] In $CH_2Cl_2$ with reference to a saturated calomel electrode.
[e] $\nu$(CO) in THF at 2036s. 1987s $cm^{-1}$.
[f] In acetone 107.6.
[g] In acetone 96.7.
[h] $\nu$(CH) at 3293 $cm^{-1}$.
[i] In $CDCl_3$ 98.4.
[j] In acetone 107.4, 98.6.

Table 2
$^1H$ and $^{13}C$ NMR data for the compounds

| Compound | $^1H$ NMR, $\delta$ [a] (ppm) | | | | $^{13}C$ NMR, $\delta$ [a,b] (ppm) | | | | | |
|---|---|---|---|---|---|---|---|---|---|---|
| | P–$CH_2CH_2$–P | –$CH_2CH_2$– | $C_5H_5$ | Other | P–$CH_2CH_2$–P | –$CH_2CH_2$– | $C_5H_5$ | CN | Cα | Cβ |
| **2** | 2.16 (m) | 2.65 (m), 1.65 (t) | 4.14 (t, $J$ = 1.05 Hz) | 7–8 (m, Ph) | 28.4 (t, $J_{CP}$ = 22.4 Hz) | 20.3, 19.4 | 79.2 | 120.8 | 108.2 (t, $J$ = 40 Hz) | 113.6 |
| **3** | 3.00 (m) | 2.00 (m), 1.52 (m) | 5.13s | 7–8 (m, Ph), 4.33 (CH) | 30.0 (t, $J_{CP}$ = 23 Hz) | 20.99, 18.77 | 90.96 | 122.4 | 355.3 (t, $J_{CP}$ = 34 Hz) | c |
| **4** | 2.40 (m) | 1.90 (m), 1.45 (m) | 4.33 | 7–8 (m, Ph), 1.70 (m, CH) | 28.3 (t, $J_{CP}$ = 21.2 Hz) | 20.3, 15.3 | 79.7 | 136.2 | 71.7 (=CH) | 80.4 (–C=) |
| **5** | 2.2–2.5 | | 4.09, 4.26 | 7–8 (m, Ph) | | | | | | |

[a] In $CD_2Cl_2$ unless otherwise stated.
[b] Other signals from the $C_6H_5$ rings are between 129 and 134 ppm.
[c] Hidden by the $C_6H_5$ signals.
For the free alkyne HCC–$CH_2CH_2$CN: $^1H$ NMR: $\delta$ 2.59m(4H), 2.20m(1H) ppm. $^{13}C$ NMR: $\delta$120.5(CN), 82.2 (–C–), 72.6 (CH), 18.48, 16.58($CH_2CH_2$) ppm.

shift of the –CN carbon atom is to a higher field which is the expected effect of coordination to the iron [3]. The assignment of the signals corresponding to the $C_\alpha$ and $C_\beta$ alkynyl carbon atoms was made by comparison with the literature data [4].

The formation of **4** by the reaction shown in Scheme 2 suggested to us the possibility of synthesizing the binuclear compound $[(C_5H_5)(dppe)Fe–C{\equiv}C–CH_2–CH_2–CN–Fe(dppe)(C_5H_5)][PF_6]$ (**5**) in a similar manner, using the iron-alkynyl derivative **2**. However, the reaction in the presence of $NH_4[PF_6]$ gave a mixture of the expected **5**, together with its protonated form **3b**, and another species having two $^{31}P$ NMR signals in a 1:1 ratio at 97.7 and 95.5 ppm, which most probably arose from the binuclear vinylidene derivative $[(C_5H_5)(dppe)Fe{=}C{=}CH–CH_2CH_2–CN–Fe(dppe)(C_5H_5)][PF_6]_2$ (**6**). Monitoring the reaction by $^{31}P$ NMR spectroscopy revealed that the mononuclear vinylidene complex **3b** is formed first, and that the slow reaction of this latter with $[FeI(dppe)(C_5H_5)]$ and $NH_4[PF_6]$ gives **6**. The addition of $K_2CO_3$ to the mixture gave mainly **5**, but with other decomposition products.

The use of $Tl[PF_6]$ as iodine abstractor in place of $NH_4[PF_6]$ in the reaction of $[FeI(dppe)(C_5H_5)]$ with **2** was also accompanied by extended decomposition and could not be used to obtain pure **5**.

In another attempt to synthesize **5**, we observed that the alkynyl **2** reacts with the acetonitrile complex $[Fe(NCMe)(dppe)(C_5H_5)][PF_6]$ in $CH_2Cl_2$ with partial replacement of the coordinated acetonitrile, generating an equilibrium shown in Scheme 1. (We also observed that the cationic vinylidene complex **3** reacts similarly with $[Fe(NCMe)(dppe)(C_5H_5)]$, partially replacing the acetonitrile to give **6** but, in the reaction, **5** is also formed alongside other products.)

The formation of **5** in the equilibrium represented in Scheme 1 was shown by the appearance of a signal at 97.7 ppm in the $^{31}P$ NMR spectrum of the reaction mixture. In $CH_2Cl_2$ it is well separated from the signal corresponding to the complex $[Fe(NCMe)(dppe)(C_5H_5)][PF_6]$ (97.9 ppm). The equilibrium could be shifted to the species **5** by periodically evaporating the volatiles to remove the free acetonitrile. Unfortunately, all the attempts to isolate **5** from the final mixture failed, yielding red to brown solids that contained it together with $[Fe(NCMe)(dppe)(C_5H_5)][PF_6]$ and other mononuclear nitrile complexes of the type of **4**. However, the presence of **5** as the main product in the materials isolated was clearly demonstrated by the $^{31}P$ and $^1H$ NMR spectra (Tables 1 and 2). As expected, the $^{31}P$ NMR spectrum showed two signals at very similar positions to those of **2** and **4**, but the signal at 106.5 ppm was broad, and the relative intensities indicated an excess of 0.4–1 mmol of mononuclear nitrile complexes per millimole of **5**, increasing with the time in solution.

In order to examine the oxidation behaviour of the dinuclear compound **5**, we measured the cyclic voltammograms of the reaction products containing it (see Section 3). The voltammograms showed two thermodynamically controlled oxidation waves, with chemical irreversibility. The oxidation peak of the wave at higher potential was about 1.3–1.5 times more intense than that of the other, which is due to the presence of the mononuclear nitrile complexes $[Fe(NCR)(dppe)(C_5H_5)]^+$ (we checked that the electrode potential of the complex $[Fe(NCMe)(dppe)(C_5H_5)][PF_6]$ under the same experimental conditions was 0.77 V). We have observed repeatedly that the compound $[Fe(NCMe)(dppe)(C_5H_5)][PF_6]$, as similar nitrile complexes, decomposes slowly in dichloromethane solution with formation of an unidentified product that has an oxidation wave centred at 0.06 V. As a consequence, after a while the wave at 0.05 V may be mixed with the product wave of the decomposition of the iron cationic nitrile complexes. No other waves were detected in the voltammograms.

These results unambiguously confirmed that the binuclear cation $[(C_5H_5)(dppe)Fe–C{\equiv}C–CH_2CH_2–CN–Fe(dppe)(C_5H_5)]^+$ undergoes two one-electron oxidations with electrode potentials almost identical with those of the mononuclear compounds **2** and **4** (see Table 1). These were obtained by measuring their cyclic voltammograms and were as expected [4,5]. This coincidence indicates that the first oxidation of the binuclear monocation affects only the neutral Fe–C≡C– site, and the second the cationic –CN–Fe moiety, demonstrating that the electronic interaction between the two iron atoms is almost non-existent. This is to be expected considering that the two metallic centres are separated in the binuclear compound by an isolating $CH_2CH_2$ group.

The behaviour of **5** towards oxidation is markedly different to that of the diiron cyano-bridged cationic complex $[(C_5H_5)(dppe)Fe–CN–Fe(dppe)(C_5H_5)][PF_6]$

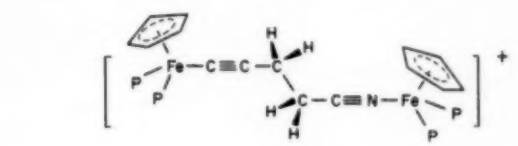


7

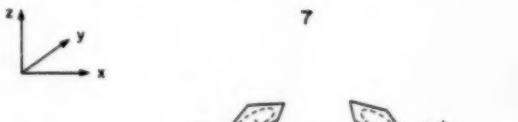


8

Fig. 1. Model complexes $[(C_5H_5)(PH_3)_2Fe–C{\equiv}C–CH_2CH_2–CN–Fe(PH_3)_2(C_5H_5)]^+$ (**7**) and $(C_5H_5)(PH_3)_2Fe–CN–Fe(PH_3)_2(C_5H_5)]^+$ (**8**).

reported previously [1]. In the latter case the two electrode potentials (0.34 and 1.00 V) are significantly different from those of the non-interacting sites $(C_5H_5)$(dppe)Fe–C and N–Fe(dppe)$(C_5H_5)$, as estimated from the electrode potentials of the mononuclear species [MeCN–Fe(dppe)$(C_5H_5)$][$PF_6$](0.77 V), and [$(C_5H_5)$(dppe)Fe–CNMe][$PF_6$] (1.15 V). For this work the methyl isocyanide complex was obtained by reaction of [$(C_5H_5)$(dppe)Fe–CN] with MeI in tetrahydrofuran (THF) in the presence of K[$PF_6$], and the cyclic voltammograms was recorded in $CH_2Cl_2$.

Although the differences between the isolated Fe(dppe)Cp fragments in **5** and the interconnected fragments in the μ-cyanide [$(C_5H_5)$(dppe)Fe–CN–Fe(dppe)$(C_5H_5)$][$PF_6$] complex can be understood intuitively, we examined the electronic effects more quantitatively by carrying out MO calculations at the extended Hückel (EH) level on the model complexes [$(C_5H_5)$-$(PH_3)_2$Fe–C≡C–$CH_2CH_2$–CN–Fe$(PH_3)_2(C_5H_5)$]$^+$ (**7**) and [$(C_5H_5)(PH_3)_2$Fe–CN–Fe$(PH_3)_2(C_5H_5)$]$^+$ (**8**) (Fig. 1).

As might be expected, the calculations (Table 3) showed that the highest occupied molecular orbital (HOMO) of the cation **7** (−11.87 eV), which is mainly formed by the Fe $d_{xy}$ and the π-bonding combination of the $p_y$ orbitals of the –C≡C– group (Fig. 2), is totally located on the Fe–C≡C– alkynyl moiety without significant participation of the other Fe atom orbitals. However, the second- and third-highest occupied MOs are also located in the Fe–C≡C alkynyl fragment, and only the fourth-highest occupied MO (MO 65) with $\varepsilon = -12.02$ eV is totally localized on the –CN–Fe moiety. This might suggest that the second oxidation of the complex should also occur at the Fe-alkynyl fragment although, as indicated by the experimental results, it must be related to the MO 65 that is located on the CN–Fe moiety of the molecule. This is because, after the first oxidation, the d-orbital energies of the oxidized iron atom should be more negative, making the MOs 63 and 64 of the monocation lower in energy than the MO 65 of the dication.

The ordering in the energy of the MOs localized at the Fe–C≡C, and Fe–NC– moieties in **7** were the same as those corresponding to the mononuclear models [Fe(C≡CMe)$(PH_3)_2(C_5H_5)$]$^+$ ($\varepsilon$(HOMO) = −11.87 eV) and [Fe(NCMe)$(PH_3)_2(C_5H_5)$]$^+$ ($\varepsilon$(HOMO) = −12.02 eV), which have also been studied by Fenske–Hall calculations with H in place of Me [6].

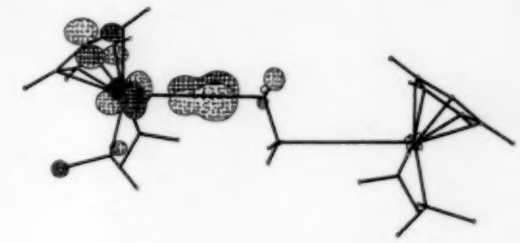

MO 62 - HOMO

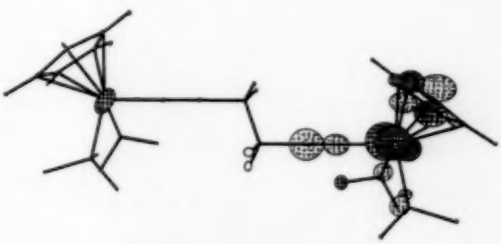

MO 65

Fig. 2. Selected MOs for **7**.

In the cyanide-bridged model **8** and in contrast with the alkynyl-cyano-bridged complex **2** the HOMO (−11.94 eV), which again is mainly formed by the combination of the Fe $d_{xy}$ orbitals of both fragments, and the $p_y$ component of the π occupied MO of the CN ligand (Fig. 3), is delocalized, although mainly located (62.55%) on the *N*-bonded Cp$(PH_3)_2$Fe– fragment and significantly less (30.21%) on the other fragment. This is totally analogous to the case of the complex *trans-trans*-[$\{PH_3\}_3(CO)_2$Mn–CN–Mn$(CO)_2\{PH_3\}_3$]$^+$, where the HOMO is more localized on the *N*-bonded site [7]. In both cases the effect is due to the higher electronegativity of the N atom. However, in **8** the second-highest occupied orbital (−11.96 eV) is very delocalized, being located more on the *N*-bonded site (47.03%), but with a similar contribution of the *C*-bonded iron fragment

Table 3
Localization of selected molecular orbitals in the model molecules, as measured by the charge matrix elements

| Model molecule | Orbital | ε (eV) | N–Fe$(PH_3)_2$Cp | | | | C–Fe$(PH_3)_2$Cp | | | | NC– (%) | CC (%) |
|---|---|---|---|---|---|---|---|---|---|---|---|---|
| | | | Fe (%) | $(PH_3)_2$ (%) | $C_p$ (%) | Total (%) | Fe (%) | $(PH_3)_2$ (%) | $C_p$ (%) | Total (%) | | |
| **7** | 1.HOMO | −11.87 [a] | 1.31 | 0.06 | 0.14 | 1.51 | 53.93 | 4.70 | 11.86 | 70.49 | 0.25 | 25.08 |
| | 4.HOMO | −12.02 | 61.73 | 6.18 | 16.61 | 84.52 | 3.15 | 0.33 | 1.47 | 4.95 | 9.04 | 0.47 |
| **8** | 1.HOMO | −11.94 | 45.75 | 4.68 | 12.12 | 62.55 | 22.03 | 2.24 | 5.94 | 30.21 | 7.25 | |
| | 2.HOMO | −11.96 | 39.29 | 1.93 | 5.81 | 47.03 | 33.39 | 2.36 | 8.64 | 44.39 | 8.58 | |

[a] When the Fe–C distance ranged from 1.80 to 2.00 Å, the energy varied from −11.74 to −11.94 eV.

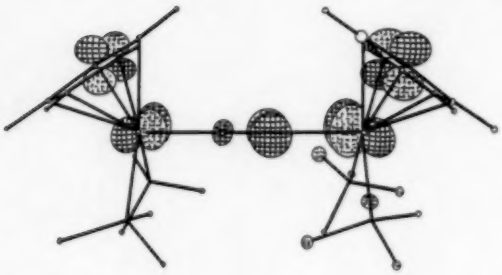

MO 52 - HOMO

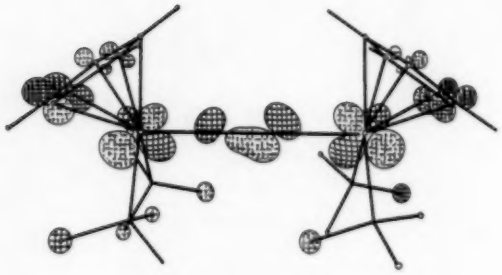

MO 53

Fig. 3. Selected MOs for **8**.

(44.39%). Therefore the first oxidation affects mainly the *N*-bonded iron atom, but the second may affect both metal atoms to nearly the same extent.

The two electrode potentials for the oxidations of $[(C_5H_5)(dppe)Fe-CN-Fe(dppe)(C_5H_5)][PF_6]$ differ by about 0.7 V, whereas the orbital energies of the MOs of the model **8** involved in each ionization process are almost the same. However, as observed in other cases [7], the potentials for the oxidation of **2**, **4**, **5**, $[Fe(CNMe)(dppe)(C_5H_5)]^+$, and the first $[(C_5H_5)(dppe)Fe-CN-Fe(dppe)(C_5H_5)]^+$ increase almost linearly with the orbital energies of the corresponding HOMOs of the models (for the molecule $[Fe(CNMe)(dppe)(C_5H_5)]^+$ the computed HOMO energy is −12.09 eV). Therefore the potential for the second oxidation of $[(C_5H_5)(dppe)Fe-CN-Fe(dppe)(C_5H_5)]^+$ appears to be much higher than the value expected for the orbital energy of the corresponding HOMO of this cation. This is due to the extended electron delocalization in the cyanide bridged species. It shows that, after the first oxidation of the molecule, not only the d-orbital parameters of the *N*-bonded iron atom, but also those of the *C*-bonded ion atom must become more negative to account for the second oxidation. In other words, the oxidation of the monocation markedly affects both Fe atoms.

It is unfortunate that the instability of the binuclear cyanide-bridged dications and trications prevents good experimental examination of its magnetic and spectroscopic properties.

## 3. Experimental part

All reactions were carried out under dry dinitrogen with standard Schlenk techniques. The IR spectra were recorded with a Perkin–Elmer FT 1720-X spectrometer. NMR spectra were recorded on a Bruker AC-300 instrument. Elemental analyses were performed with a Perkin–Elmer 240 microanalyser. The cyclic voltammograms were measured with a PAR M273 instrument. The auxiliary electrode was a platinum wire, and the working electrode was a platinum bead. The reference was a calomel electrode separated from the solution by a a fine-porosity frit and an agar–agar bridge saturated with KCl. Solutions were $0.5 \times 10^{-3}$ M in the complexes and 0.1 M in $[^nNBu_4][PF_6]$ as supporting electrolyte. Under the same experimental conditions $E_{1/2}$ for the ferrocene–ferrocenium couple was 0.46 V, with a peak separation of 76 mV.

The alkyne $NC-CH_2CH_2-C\equiv C-H$ [8], and the complex $[FeI(dppe)(C_5H_5)]$ [1] were prepared as described. The two-step preparation of **2** (see below) is based on similar published methods for Fe alkynyls with CO or diphosphines [4,5,9]. The red complex $[Fe(NCMe)(dppe)(C_5H_5)][PF_6]$ [10,11], was prepared with a good yield by reaction overnight at room temperature of the neutral complex $[FeI(dppe)(C_5H_5)]$ with an excess of NCMe in $CH_2Cl_2$ in the presence of $NH_4[PF_6]$ filtering and precipitating with ether. Anal. Found: C, 55.7; H, 4.29; N, 1.70, Calc.; C, 56.2; H, 4.54; N, 1.89%. The yellow $[Fe(CNMe)(dppe)(C_5H_5)][PF_6]$ was obtained also with a good yield by adding MeI and $K[PF_6]$ to a solution of $[Fe(CN)(dppe)(C_5H_5)]$ in THF and stirring overnight at room temperature, filtering and precipitating with ether. Anal. Found: C, 55.5; H, 4.47; N, 1.72. Calc.: C, 56.2; H, 4.54; N, 1.89%.

### *3.1. Preparation of $[Fe(C\equiv C-CH_2CH_2-CN)(dppe)(C_5H_5)]$ (2)*

A solution of $HC\equiv CCH_2CH_2-CN$ (0.33 ml, 4.17 mmol) in THF (20 ml) was cooled to −20°C, and 2.7 ml of 1.6 N LiBu in hexane (4.32 mmol) were added dropwise with stirring. Stirring was continued for $\frac{1}{2}$ h, and the mixture was cooled to −80°C. A solution of $[FeCl(CO)_2(C_5H_5)]$ (0.9 g, 4.24 mmol) in THF (25 ml) was added dropwise and, after 1 h, the mixture was allowed to reach room temperature, stirred for two more hours and filtered through 1 cm of alumina, to give a

yellow solution of $[FeC{\equiv}C{-}CH_2CH_2{-}CN)(CO)_2(C_5H_5)]$ (**1**) (IR: $\nu$(CO) 2036s 1987s $cm^{-1}$) (occasionally mixed with some $[Fe_2(CO)_4(C_5H_5)_2]$). This solution was concentrated to 30 ml, dppe (1.73 g, 4.34 mmol) was added, and the mixture was irradiated at −20°C until no $\nu$(CO) absorptions could be observed in the IR spectrum (about 5 h). The resulting red solution was filtered through Celite and evaporated to dryness. The residue was extracted with diethyl ether and the extracts were filtered through alumina (1 cm) and evaporated to dryness, to give a red solid that contained some dppe. This was washed five times with 20 ml of hot hexane to give **2** (Yield, 0.6 g, 1 mmol (23.7%). Anal. Found: C, 72.1; H, 5.53; N, 2.30. Calc. 72.4; H, 5.53; N, 2.35%.

### 3.2. Preparation of $[(C_5H_5)(dppe)Fe{=}C{=}CH{-}CH_2{-}CH_2{-}CN][BF_4]$ (3)

A mixture of **2** (0.106 g, 0.177 mmol) in THF (15 ml) and $HBF_4 \cdot Et_2O$ (0.03 ml, 0.0286 g of solution of 85%, $d = 1.1$ g $cm^{-3}$, equivalent to 0.2 mmol of acid) was stirred for 30 min. The volatiles were evaporated in vacuo, and the residue was washed once with diethyl ether and dissolved in $CH_2Cl_2$. The solution was treated with dried $K_2CO_3$, filtered and concentrated. Addition of diethyl ether gave a red–orange precipitate of **3a** (yield, 0.08 g (66%)). Anal. Found: C, 62.9; H, 4.76; N, 1.56. Calc.: C, 631; H, 4.97; N, 2.00%.

### 3.3. Preparation of $[(C_5H_5)(dppe)Fe{-}NC{-}CH_2CH_2{-}CCH][PF_6]$ (4)

A mixture of $[FeI(dppe)(C_5H_5)]$ (0.2 g, 0.31 mmol), and the alkyne $HC{\equiv}CCH_2CH_2CN$ (0.5 ml, 6.32 mmol) in $CH_2Cl_2$ (20 ml) was stirred overnight with solid $NH_4[PF_6]$ (0.2 g, 1.2 mmol) at room temperature. The mixture was filtered (Celite) and evaporated to dryness. The resulting solid was washed with ether and dried in vacuo to give **4** as a red microcrystalline powder (yield, 0.15 g (65%)). Anal. Found: C, 58.4; H, 4.47; N, 1.97. Calc.: C, 58.2; H, 4.58; N, 1.88%.

### 3.4. The formation of $[(C_5H_5)(dppe)Fe{-}C{\equiv}C{-}CH_2{-}CH_2{-}CN{-}Fe(dppe)(C_5H_5)][PF_6]$ (5)

A mixture of **2** (0.09 g, 0.15 mmol) and $[Fe(NCMe)(dppe)(C_5H_5)]$ (0.056 g, 0.1 mmol) in $CH_2Cl_2$ (15 ml) was stirred in the absence of light overnight and evaporated to dryness in vacuo. The residue was redissolved in 15 ml of $CH_2Cl_2$ and the treatment was repeated three more times. The final residue was dissolved in 20 ml of $CH_2Cl_2$, filtered and concentrated to 2 ml. Addition of a large excess of diethyl ether and stirring gave a red–brown solid that was repeatedly washed with diethyl ether until no neutral **2** was detected in the extracts (yields, about 0.07 g). This product was used for the cyclic voltammograms.

Table 4
Bonding distances used in the models

| Model cation [a] | Fe–N (Å) | FeC (Å) | NC (Å) | C≡C (Å) |
|---|---|---|---|---|
| [Fe]–C≡C–$CH_2CH_2$–CN–[Fe] | 1.946 | 1.920 | 1.130 | 1.181 |
| [Fe]–NC–Me | 1.946 | | 1.130 | |
| [Fe]–C≡C–Me | | 1.920 | | 1.181 |
| [Fe]–CN–Me | | 1.860 | 1.150 | |
| [Fe]–CN–[Fe] | 2.083 | 1.914 | 1.107 | |

[a] [Fe] = $Fe(PH_3)_2Cp$.

### 3.5. Computational details

EH MO calculations [12] were carried out using the modified Wolfsberg–Helmholz formula [13]. The atomic parameters were taken from the literature [14]. The bonding distances used in the models [15] are indicated in Table 4. Other distances were as follows: Fe–P, 2.214; P–H, 1.437; Fe–Cp–centre, 1.706; $C_{Cp}$–$C_{Cp}$, 1.500; CC–$CH_2$, 1.460; $CH_2$–$CH_2$, 1.514; $CH_2$–CN, 1.470; C–H, 1.080.

The angles around the $CH_2$ carbon atoms were 109.5° and between the Fe–CC vector and the Fe–$PH_3$ bonds, and between the two Fe–$PH_3$ bonds were 90°. The calculation showed that changing the last to 109° did not modify substantially the results. The HPH angles were the tetrahedral.

The calculations were carried out on a Micro VAX 3400 computer at the Scientific Computer Center of the University of Oviedo with a locally modified version of the program ICON. MO drawing were generated with the use of the program CACAO [16].

## Acknowledgments

We are very grateful to the Spanish Instituto de Cooperacion Iberoamericana, to the Oficina de Relaciones Internacionales de la Universidad de Oviedo for a joint Project between Chile and Spain, and to FONDECYT (Chile)(Grant 1950305) for support.

## References

[1] G. Barrado, G.A. Carriedo, C. Diaz-Valenzuela and V. Riera. *Inorg. Chem., 30* (1991) 4416.
[2] M.I. Bruce, *Chem. Rev., 91* (1991) 197.
[3] J. Ruiz, M.T. Garland, E. Román and D. Astruc, *J. Organomet. Chem., 377* (1989) 30.
[4] N.G. Connelly, M.P. Gamasa, J. Gimeno, C. Lapinte, E. Lastra, J.P. Maher, N. Le Narvor, A.L. Rieger and P.H. Rieger, *J. Chem. Soc. Dalton Trans.*, (1993) 2575.

[5] C. Bitcan and M.W. Whiteley, *J. Organomet. Chem., 336* (1987) 385.
[6] N.M. Kostic and R.F. Fenske, *Organometallics, 1* (1982) 974.
[7] G.A. Carriedo, N.G. Connelly, S. Alvarez, E. Pérez-Carreño and S. García-Granda, *Inorg. Chem., 32* (1993) 272.
[8] L. Brandsma, *Preparative Acetilenic Chemistry*, Elsevier, New York, 2nd edn., 1988.
[9] M.P. Gamasa, J. Gimeno, E. Lastra, M. Lanfranchi and A. Tiripicchio, *J. Organomet. Chem. 404* (1991) 333.
[10] J. Ruiz, E. Román and D. Astruc, *J. Organomet. Chem., 322* (1987) C13.
[11] P.E. Riley, C.E. Capshew, R. Pettit and R.E. Davies, *Inorg. Chem., 17* (1978) 408.
[12] R. Hoffman, *J. Chem. Phys., 39* (1963) 1397.
[13] J.H. Ammeter, H.B. Bürgi, J.C. Thibeault and R. Hoffman, *J. Am. Chem. Soc., 100* (1978) 3686.
[14] B.E.R. Scilling, R. Hoffman and D.L. Lichtenberger, *J. Am. Chem. Soc., 101* (1979) 585.
[15] A.G. Orpen, L. Brammer, F.H. Allen, O. Kennard, D.G. Watson and R. Taylon, *J. Chem. Soc., Dalton Trans.*, (1989) S1.
[16] C. Mealli and M. Proserpio, *J. Chem. Educ., 67* (1990) 399.

ELSEVIER

Journal of Organometallic Chemistry 508 (1996) 31–37

Journal of Organometallic Chemistry

# Synthesis of secondary allenylidene–molybdenum complexes with a ferrocenyl substituent from carbenium ions species stabilized by two organometallic moieties

J.-F. Capon, N. Le Berre-Cosquer, B. Leblanc, R. Kergoat *

*URA CNRS No. 322, Chimie, Electrochimie Moléculaires et Chimie Analytique, Equipe de Chimie Inorganique Moléculaire, Université de Bretagne Occidentale, 6 Avenue le Gorgeu, BP 809, 29285 Brest Cédex, France*

Received 27 February 1995

**Abstract**

The monoallenylidene complex $[Cp_2Mo_2(CO)_4\{\mu\text{-}\sigma:\eta^2\text{-}C{=}C{=}C(Fc)(H)\}]$ (**5**) and the diallenylidene complex $[\{Cp_2Mo_2(CO)_4(\mu\text{-}\sigma:\eta^2\text{-}C{=}C{=}C(H))\}_2Fc]$ (**6**) have been obtained from the corresponding monocarbenium ion $[Cp_2Mo_2(CO)_4\{\mu\text{-}\eta^2:\eta^3\text{-}HC{\equiv}C\text{-}C(H)(Fc)\}][BF_4]$ (**3**) and the dicarbenium ion $[\{Cp_2Mo_2(CO)_4(\mu\text{-}\eta^2:\eta^3\text{-}HC{\equiv}C\text{-}C(H))_2Fc\}][BF_4]_2]$ (**4**) respectively, and their spectroscopic data are determined.

*Keywords:* Iron; Ferrocene; Molybdenum; Carbenium ions; Allenylidene complexes

## 1. Introduction

In the cationic compounds $[Cp_2Mo_2(CO)_4\{\mu\text{-}\eta^2:\eta^3\text{-}HC{\equiv}C\text{-}C(R_1)(R_2)\}][BF_4]$ the metal exerts a powerful stabilizing effect at the adjacent propargylic carbenium ion centre [1–12]. Various nucleophiles can alkylate these cations [1,6,13]. We have previously described the unexpected selective abstraction of the acetylenic proton in the carbenium ions by the acetylide reagent $LiC{\equiv}C\text{-}C(CH_3){=}CH_2$ [14] (Scheme 1). The resulting compounds were $\mu\text{-}\sigma:\eta^2$ allenylidene species $[Cp_2Mo_2(CO)_4\{\mu\text{-}\sigma:\eta^2\text{-}C{=}C{=}C(R_1)(R_2)\}]$. The first example of such a compound was made by Green and co-workers by a different procedure [15].

Secondary ($R_1$ or $R_2 = H$) and primary ($R_1 = R_2 = H$) allenylidene complexes are thermally unstable (unlike the tertiary derivatives) and must be kept in solution below −35°C to prevent degradation. The secondary allenylidene complexes A ($R_1 = Et$, $R_2 = H$) and B ($R_1 = Me$, $R_2 = H$) (Scheme 2) exist as two diastereoisomers depending on the relative position of the substituents on the $C_\gamma$ atom.

We describe herein further secondary allenylidene compounds with a ferrocenyl substituent ($R = Fc$, $\{(C_5H_4)Fe(C_5H_5)\}$). We hoped that the presence of a bulky substituent on the carbon chain could lead to the formation of only one diastereomer of a thermally stable allenylidene complex. Increasing demand for new materials, and particularly metallocene compounds, which might exhibit properties essential for second-order nonlinear optical (NLO) behaviour [16,17], could make allenylidene complexes with a ferrocenyl substituent very attractive. We also report the synthesis of interesting starting materials and synthetic intermediates, which we have described elsewhere [18].

## 2. Results and discussion

The route to dimolybdenum allenylidene complexes involves the activation of 2-propyn1-ol ($HC{\equiv}C\text{-}C(OH)(R_1)(R_2)$) and comprises three steps (method A, Scheme 3):

(1) formation of the alkyne adduct with a tetrahedral $C_2Mo_2$ by treatment of the triply metal–metal bonded species $[Cp_2Mo_2(CO)_4]$ with the appropriate alkyne;

* Corresponding author.

0022-328X/96/$15.00 © 1996 Elsevier Science S.A. All rights reserved
*SSDI* 0022-328X(95)05777-3

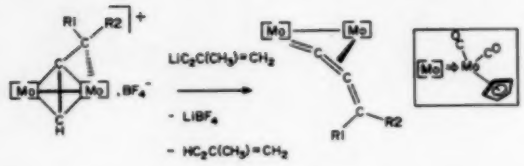

Scheme 1.

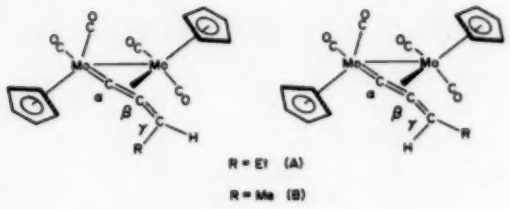

Scheme 2.

(2) protonation of $[Cp_2Mo_2(CO)_4\{\mu\text{-}\eta^2\text{:}\eta^2\text{-}RC{\equiv}C\text{–}C(OH)(R_1)(R_2)\}]$ followed by elimination of water gives the carbenium ion;

(3) addition of $LiC{\equiv}C\text{–}C(CH_3){=}CH_2$ to the carbenium ion in $[Cp_2Mo_2(CO)_4\{\mu\text{-}\eta^2\text{:}\eta^3\text{-}HC{\equiv}C\text{–}C(R_1)(R_2)\}][BF_4]$ leads to the allenylidene complex $[Cp_2Mo_2(CO)_4\{\mu\text{-}\sigma\text{:}\eta^2\text{-}C{=}C{=}C(R_1)(R_2)\}]$.

An important feature of method B (Scheme 3) is that treatment of the $\mu$-alkyne compound $[Cp_2Mo_2(CO)_4\{\mu\text{-}\eta^2\text{:}\eta^2\text{-}(HC{\equiv}C\text{–}C(OH)(H)(Fc)\}]$ (1) with $Al_2O_3$ or $SiO_2$ (chromatography) causes direct elimination of $H_2O$ to yield an allenylidene complex. These various features are described separately below.

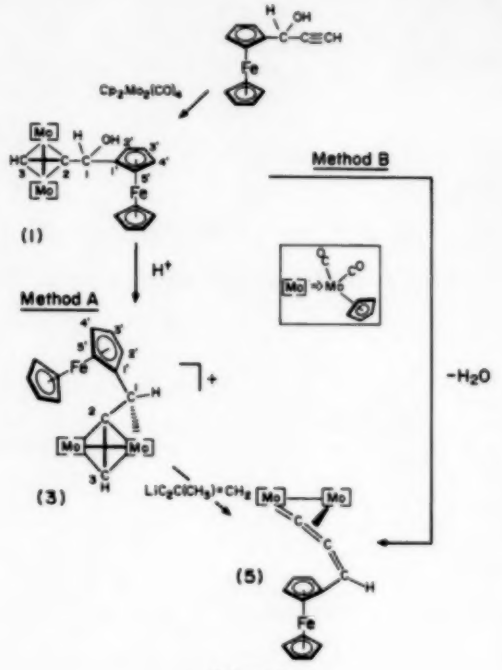

Scheme 3.

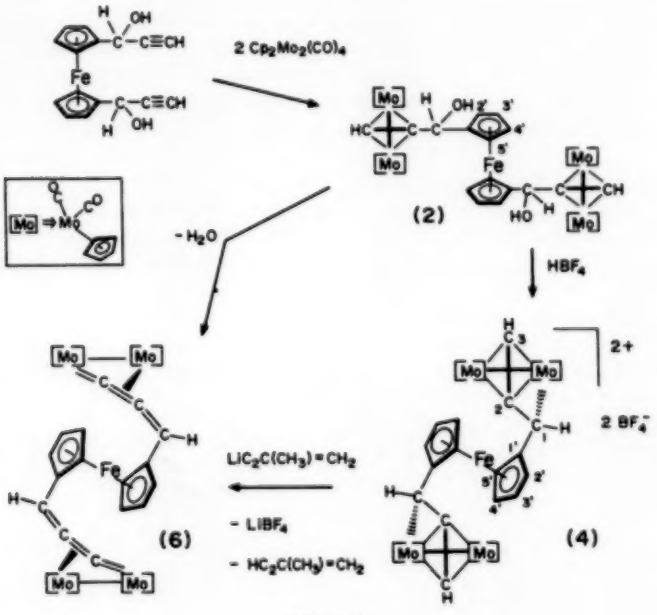

Scheme 4.

### 2.1. Coordination by $[Cp_2Mo_2(CO)_4]$

The classical procedure for the synthesis of $\mu$-alkyne compounds is used [19], involving addition of $[Cp_2Mo_2(CO)_4]$ to a solution of the alkyne (HC≡C–C(OH)(H)(Fc)) followed by stirring for 18 h at room temperature yields the compound $[Cp_2Mo_2(CO)_4\{\mu\text{-}\eta^2\text{:}\eta^2\text{-}(HC{\equiv}C\text{–}C(OH)(H)(Fc))\}]$ (**1**) (80%). In contrast, heating of the solution is necessary in the case of bulky alkynes [20].

For (**1**) the shift of the acetylenic proton resonance (H–C≡) is, as expected, upfield from that of the free alkyne, i.e. 5.50 ppm for complex (**1**) compared with 2.60 ppm for HC≡C–C(OH)(H)(Fc). The $^1J$(≡C–H) coupling constant is also changed, being 212 Hz for compound (**1**) and 250 Hz for HC≡C–C(OH)(H)(Fc).

The dipropargyl alcohol derivative complex $[\{Cp_2Mo_2(CO)_4(\mu\text{-}\eta^2\text{:}\eta^2\text{-H–C}{\equiv}C\text{–C(OH)(H)})\}_2(Fc)]$ (**2**), was obtained from the diyne compound $\{H\text{–}C{\equiv}C\text{–}C(OH)(H)\}_2(Fc)$, by a procedure very similar to that used for complex (**1**) (Scheme 4).

A mixture of monocoordinated and dicoordinated compounds is usually formed in the reaction of $[Cp_2Mo_2(CO)_4]$ with diynes, as for example in the case of octa-1,7 diyne [21] or hexa-1,5 diyne [22]. The mixture obtained from the diol $[\{Cp_2Mo_2(CO)_4(\mu\text{-}\eta^2\text{:}\eta^2\text{-H–C}{\equiv}C\text{–C(OH)(H)})\}_2(Fc)]$ (**2**) is expected to be difficult to separate chromatographically because compound (**2**) decomposes on silica or alumina columns. In order to avoid this complication the formation of the monocoordinated compound was prepared by stirring the solution of the diyne compound $\{H\text{–}C{\equiv}C\text{–}C(OH)(H)\}_2(Fc)$ in the presence of an excess of $[Cp_2Mo_2(CO)_4]$ for 36 h.

A very important feature of ferrocene compound (**2**) is the presence of two stereogenic functionalized side chains, which means that theoretically both racemic (RR + SS) and meso (RS≡SR) forms are possible. The $^1$H NMR spectrum for the crude product mixture displays a complex profile of ($C_5H_5$–Mo) and ($C_5H_4$–Fe) resonances due to the presence of the two stereoisomers. Repeated extractions with cold pentane gave a single isomer, but analysis of its spectroscopic data does not allow us to conclude whether it is the RS or the (RR + SS) diastereoisomer. As alcohol (**2**) contains stereogenic carbon atoms, two resonances are observed for the ($C_5H_5$–Mo) groups, as in the case of other diynes complexes $[Mo_2Cp_2(CO)_4(\mu\text{-}\eta^2\text{:}\eta^2\text{-HC}{\equiv}CC(R_1)(R_2)\text{–}]_2$ ($R_1$ = H, $R_2$ = Me [6]; $R_1$ = H, $R_2$ = Et [7]).

### 2.2. Synthesis of the carbenium ions

Addition of $HBF_4$ to compounds (**1**) and (**2**) leads to formation of the corresponding carbenium ion salts $[Cp_2Mo_2(CO)_4\{\mu\text{-}\eta^2\text{:}\eta^3\text{-HC}{\equiv}C\text{–C(H)(Fc)}\}][BF_4]$ (**3**) and $[\{Cp_2Mo_2(CO)_4(\mu\text{-}\eta^2\text{:}\eta^3\text{-HC}{\equiv}C\text{–C(H)})\}_2Fc][BF_4]_2$ (**4**) by elimination of $H_2O$. The carbon atom bearing the positive charge in compounds (**3**) and (**4**) is adjacent both to a ferrocenyl substituent and to an acetylenic cluster. It has been demonstrated that the dimolybdenum cluster is mainly responsible for the stabilization of the $C^+$ centre in the salt $[Cp_2Mo_2(CO)_4\{\mu\text{-}\eta^2\text{:}\eta^3\text{-}CH_3(CH_2)_4\text{–C}{\equiv}C\text{–C(H)(Fc)}\}][BF_4]$ [23,24]. The cation in the latter compound and that in the complex (**3**) both contain secondary carbenium ions; the signals from the ($C^+$–*H*) protons in acetone $d_6$, 8.16 ppm and 7.88 ppm respectively, both lie upfield, as expected for a proton on a positively charged centre. Examination of the non-decoupled $^{13}$C NMR spectrum of compound (**3**) and comparisons with NMR data for various carbenium ions previously reported allowed us to assign the various signals.

Although less extensively studied, several dicarbenium ions (essentially dimetallic complexes) have been described [25]. The dication (**4**) is a tetrametallic dicarbenium ion whereas that in the compound $[Cp_2Mo_2(CO)_4(CH_2C{\equiv}CCH_2)][BF_4]_2$ [26] is a bimetallic dication with a $(C_4H_4)^{2+}$ ligand. Compound (**4**) behaves as if it were two independent carbenium ions, like the $Co_2(CO)_6$ complexed propargyl dication described by Nicholas and co-workers [27]. The dicarbenium complex (**4**) and the monocarbenium compound (**3**) display quite similar $^1$H NMR spectra between 4.3 and 8 ppm. The very low solubility of compound (**4**) has so far prevented us obtaining suitable crystals for an X-ray study.

As expected for secondary carbenium ions [23,24,28], the $^1$H and $^{13}$C NMR spectra of compounds (**3**) and (**4**) recorded in acetone $d_6$ solution at room temperature indicate that these molecules show no chiral features: the ($C_5H_5$–Mo) groups display only one signal and two pseudotriplets appear for the ($C_5H_4$–Fe) protons with a AA′BB′ spin system with $J_{AB} \approx 2$ Hz.

### 2.3. Synthesis of the allenylidene complexes

Addition of $LiC{\equiv}C\text{–}C(CH_3){=}CH_2$ to a cooled suspension of $[Cp_2Mo_2(CO)_4\{\mu\text{-}\eta^2\text{:}\eta^3\text{-HC}{\equiv}C\text{–C(H)(Fc)}\}][BF_4]$ (**3**) caused an immediate colour change from violet to green (Scheme 3). Elemental analysis, IR and NMR spectral data are consistent with the formation of a $\mu\text{-}\sigma\text{:}\eta^2(4e^-)$ allenylidene complex $[Cp_2Mo_2(CO)_4\{\mu\text{-}\sigma\text{:}\eta^2\text{-C=C=C(Fc)(H)}\}]$ (**5**).

When solutions of the secondary allenylidene compounds previously described are warmed to room temperature fast decomposition occurs, the green solution turning to red and an intractable mixture being formed. In contrast, compound (**5**) is thermally stable for a short time in solution even at room temperature. Electron release by the ferrocenyl group should stabilize the

allenylidene moiety as in allenylidene compounds without H-substituents on the Cγ atom.

The $^{13}C$ NMR spectrum of (5)recorded at −10°C exhibits one signal for the Cα atom, at 282 ppm, four signals for the carbonyl ligands, between 239 and 230 ppm, and two peaks in the ($C_5H_5$–Mo) region. Compound (5) exists as only one diastereomer. We assume that for these reasons the most favoured isomer is that shown in Fig. 1, in which the H-substituent is closer to the $CpMo(1)(CO)_2$ group; the ferrocenyl ligand and the $CpMo(1)(CO)_2$ group are probably in a trans disposition. It is noteworthy that only one isomer (the thermodynamically preferred diastereomer) is also observed in the case of vinylidene compounds $[Cp_2Mo_2(CO)_4\{\mu\text{-}\sigma:\eta^2\text{-}(C{=}C(R)(R'))\}]$ containing two different substituents R and R′ [15].

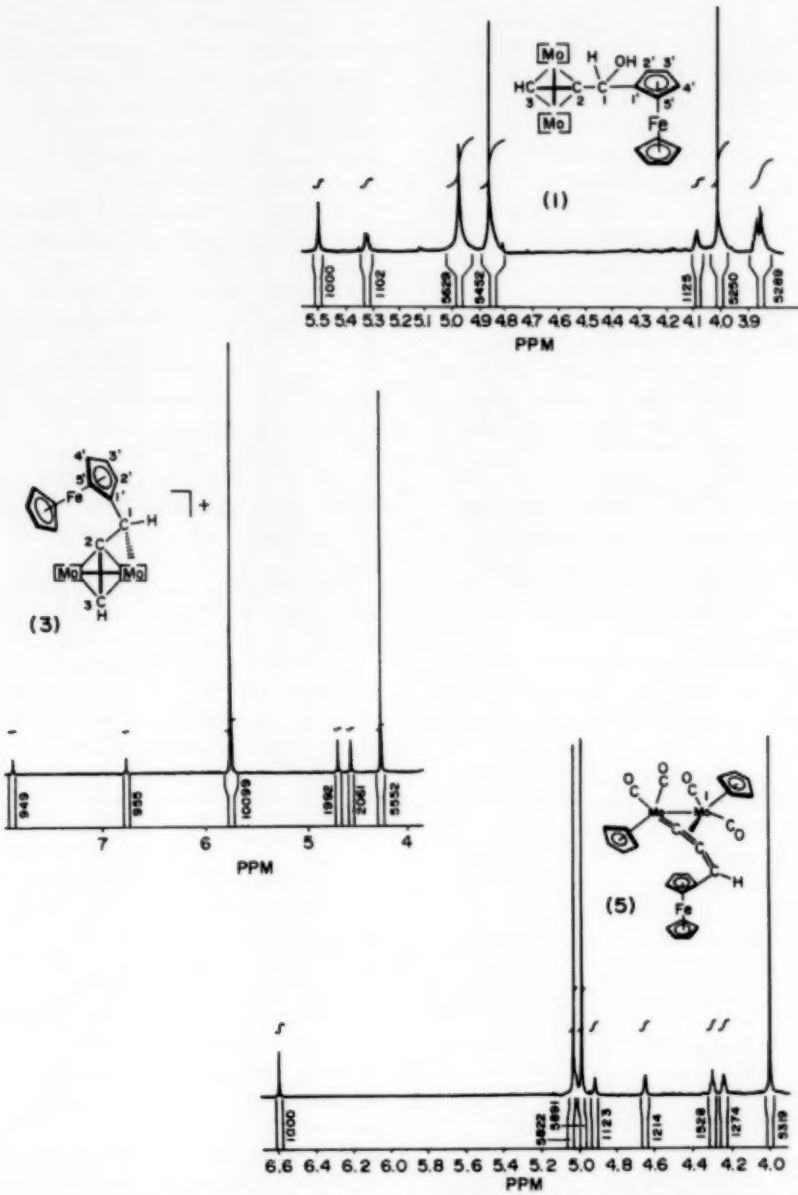


Fig. 1. $^1H$ NMR spectra of compounds $[Cp_2Mo_2(CO)_4\{\mu\text{-}\eta^2:\eta^2\text{-}HC{\equiv}C\text{-}C(OH)(H)(Fc)\}]$ (1), $[Cp_2Mo_2(CO)_4\{\mu\text{-}\eta^2:\eta^3\text{-}HC{\equiv}C\text{-}C(H)(Fc)\}][BF4]$ (3) and $[Cp_2Mo_2(CO)_4\{\mu\text{-}\sigma:\eta^2C{=}C{=}C(Fc)(H)\}]$ (5).

Owing to the presence of asymmetrically bridged allenylidene ligand, the effective symmetry for compound (**5**) is $C_1$ at room temperature: the two cyclopentadienyl ligands linked to a molybdenum centre are in a different environment [15] and so two signals are observed in the $^1H$ and $^{13}C$ NMR spectra. The four protons of the ($C_5H_4$–Fe) group are all magnetically inequivalent and form an ABCD spin system, as in the case of ferrocenyl compounds containing a stereogenic centre.

The diallenylidene compound [{$Cp_2Mo_2(CO)_4$($\mu$-$\sigma$:$\eta^2$-C=C=C(H))}$_2$Fc] (**6**) is obtained by the same procedure as that used for complex (**5**) but using an excess of LiC≡C–C(CH$_3$)=CH$_2$. The thermal instability of compound (**6**) prevents satisfactory elemental analysis (see Section 3). This instability is like that of the diacetylenic compound Fc–(C≡C–H)$_2$, whereas the characterisation of the monoacetylenic compound Fc–C≡C–H is easier [29]. Except for the ($C_5H_5$–Fe) signal, the $^1H$ NMR spectrum of compound (**6**) has twice as many peaks as the monoallenylidene complex (**5**): there are two singlets, at 6.60 and 6.65 ppm, corresponding to the (C$\gamma$H) protons, four inequivalent cyclopentadienyl resonances and eight multiplets (not always well resolved) from the ($C_5H_4$–Fe) protons. Compound (**6**) exists in solution as a mixture of two diastereomers, the meso and racemic forms. This is also the case for the diol Fc–{C(OH)(H)(Ph)}$_2$ which possesses two stereogenic centres [30]. However, in the case of the diallenylidene complex (**6**) the chirality arises from the presence of the asymmetrically bridged allenylidene ligands. Attempts to separate the two isomers by fractional crystallization have been unsuccessful due to decomposition.

### 2.4. One step synthesis of allenylidene compounds

An alternative way of preparing complex (**5**) involves chromatography of compound [$Cp_2Mo_2$-(CO)$_4$($\mu$-$\eta^2$:$\eta^2$-HC≡C–C(OH)(H)(Fc))] (**1**) on a silica column. Small amounts of [$Cp_2Mo_2(CO)_6$] were first eluted with a hexane–dichloromethane mixture. A second band containing traces of the starting material (**1**) was eluted with pure dichloromethane. When diethyl ether was added to the column it turned green and the complex (**5**) formed was eluted in moderate yields (17%).

By using the same procedure, but starting from the diol [{$Cp_2Mo_2(CO)_4$($\mu$-$\eta^2$:$\eta^2$-HC≡C–C(OH)(H))}$_2$-(Fc)] (**2**), only very low yields of diallenylidene complex (**6**) were isolated because of its instability.

This type of reaction has only been observed previously for the $\mu$-alkyne complexes with a ferrocenyl substituent. Probably the mild acidity of the silica gel suffices to produce the ferrocenyl carbocation [31], which rearranges to the allenylidene compound.

In conclusion, a convenient method for the preparation of monoallenylidene and diallenylidene compounds of ferrocene is outlined in this paper. The diallenylidene compound [{$Cp_2Mo_2(CO)_4$($\mu$-$\sigma$:$\eta^2$-C=C=C(H))}$_2$-(Fc)] (**6**) is unstable. Incorporation of metals into NLO systems has much potential in this field of study [15,16], and so we are seeking methods of obtaining more stable allenylidene complexes of ferrocene.

## 3. Experimental details

All reactions and purifications were performed under dinitrogen using Schlenk techniques. The solvents were freshly distilled under dinitrogen from drying agents as follows: sodium–benzophenone for THF and toluene, $CaH_2$ for dichloromethane, hexane and diethyl ether. The deuterated solvents were dried over activated molecular sieves prior to use.

The infrared spectra were obtained with a Perkin–Elmer 1430 spectrometer, using solutions in $CH_2Cl_2$ or KBr pellets. Infrared frequencies are reported in wavenumbers (cm$^{-1}$).

The $^1H$ and $^{13}C$ NMR spectra were recorded on a Bruker AC 300 instrument ($^1H$, 300.13 MHz; $^{13}C$, 75.47 MHz). Chemical shifts are reported in units of parts per million (ppm) relative to a tetramethylsilane internal reference. Coupling constants are reported in hertz.

Mass spectra were obtained with an HP 5695 gas chromatography–mass spectroscopy apparatus. The *m/e* values were based on the $^{96}Mo$ isotope.

Analyses were performed at the Service Central d'Analyses of the CNRS.

The complex [$Cp_2Mo_2(CO)_4$] was obtained by a published method [32]. The starting compounds H–C≡C–C(OH)(H)(Fc) and {H–C≡C–C(OH)(H)}$_2$(Fc) were readily made from ferrocene aldehyde and 1,1′-ferrocene dialdehyde [33,34] by standard procedures [35]. LiC≡C–C(CH$_3$)=CH$_2$ was prepared from Li$^n$Bu (2.5 M in hexane) and HC≡C–C(CH$_3$)=CH$_2$ in THF [36].

### 3.1. Synthesis of [$Cp_2Mo_2(CO)_4$\{$\mu$-$\eta^2$:$\eta^2$-HC≡C–C(OH)(H)(Fc)\}] (1)

H–C≡C–C(OH)(H)(Fc) (0.44 g, 1.84 mmol) was added to a solution of [$Cp_2Mo_2(CO)_4$] (0.8 g, 1.84 mmol) in toluene (60 ml). The mixture was stirred at room temperature for 18 h. The solvent was removed in vacuo and the residue was chromatographed on a Florisil column. Elution with a hexane–dichloromethane mixture (70:30 in volume) afforded complex (**1**) (yield, 1 g; 80%).

Spectroscopic data for (**1**):

$^1H$ NMR (toluene $d_8$ solution): 5.50 (d, 1H, HC≡,

$^4J$(H–H) = 0.5 Hz); 5.32 (d, 1H, HC, $^3J$(H–H) = 2.25 Hz); 4.97 (s, 5H, $C_5H_5$–Mo); 4.86 (s, 5H, $C_5H_5$–Mo); 4.09 (m, 1H, $C_5H_4$); 3.85 (m, 3H, $C_5H_4$); 4.01 (s, 5H, $C_5H_5$–Fe). $^{13}$C NMR ($C_6D_6$ solution): 233.3, 233.1, 229.1 (CO); 96.8 (C1'); 91.2 ($C_5H_5$–Mo); 91.1 ($C_5H_5$–Mo); 75.2 (C1, d $^1J$(C–H) = 147 Hz); 87.9 (C3, d, $^1J$(C–H) = 212 Hz); 59.5 (C2); 68.8 ($C_5H_5$–Fe); 69.5 ($C_5H_4$, d, $^1J$(C–H) = 176 Hz); 64.2 ($C_5H_4$, d, $^1J$(C–H) = 176 Hz); 67.6 ($C_5H_4$, d, $^1J$(C–H) = 176 Hz); 67.4 ($C_5H_4$, d, $^1J$(C–H) = 175 Hz). IR (KBr pellet): $\nu$(CO): 1995, 1910, 1830. MS: (*m/e*) 656: $[M-H_2O]^+$; 600: $[M-H_2O-2CO]^+$; 544: $[M-H_2O-4CO]^+$. Anal. Found: C, 47.13; H, 3.78. $C_{27}H_{22}FeMo_2O_5$. Calc.: C, 48.10; H, 3.22%.

### 3.2. Synthesis of [{$Cp_2Mo_2(CO)_4$($\mu$-$\eta^2$:$\eta^2$-H–C≡C–C(OH)(H))}$_2$(Fc)] (2)

[$Cp_2Mo_2(CO)_4$] (4.7 g, 10.9 mmol) was added to a freshly prepared solution of {H–C≡C–C(OH)(H)}$_2$(Fc) (1.28 g, 4.4 mmol) in toluene (40 ml) and the mixture stirred for 36 h. Work-up as for compound (1) gave 3.3 g (yield 65%) of (2).

Spectroscopic data for (2):

$^1$H NMR ($CDCl_3$ solution). After extraction with pentane, only one diastereoisomer was recovered: 5.89 (s, 2H, 2 HC≡); 5.09 (s, 10H, 2 $C_5H_5$–Mo); 4.93 (s, 10H, 2 $C_5H_5$–Mo); 4.13 (s, 2H, 2 HO or 2 HC); 4.01 (t, 4H, $C_5H_4$, (H2'–5'), $^3J$(H–H) = 2.1 Hz); 3.89 (t, 4H, $C_5H_4$, (H3'–4'), $^3J$(H–H) = 2.0 Hz); 3.84 (s, 2H, 2 HO or 2 HC). $^{13}$H NMR ($CD_2Cl_2$ solution, 272 K) (below 272 K coalescence occurred; at higher temperatures compound (2) decomposed in the solution before the spectrum could be fully recorded): 233.1, 232.6, 229.0 (CO); 97.1 (C1'); 92.3 (C3, d, $^1J$(C–H) = 185 Hz); 91.3, 91.2 ($C_5H_5$–Mo); 74.7 (C1, d, $^1J$(C–H) = 141 Hz); 74.5–67.7 ($C_5H_4$–Fe); 60.3 (C2).IR (KBr pellet): $\nu$(CO): 1995, 1910, 1830. Anal. Found: C, 45.91; H, 3.22. $C_{44}H_{34}FeMo_4O_{10}$. Calc.: C, 45.47; H, 2.95%.

### 3.3. Synthesis of [$Cp_2Mo_2(CO)_4$($\mu$-$\eta^2$:$\eta^3$-HC≡C–C(H)(Fc)}][$BF_4$] (3)

To a stirred solution of (1) (1 g, 1.84 mmol) in diethyl ether (80 ml) was added dropwise a solution of 0.5 ml of $HBF_4$ in diethyl ether. The violet precipitate was filtered off and washed with diethyl ether (3 × 7 ml) to leave 1.33 g (yield 97%) of (3).

Spectroscopic data for (3):

$^1$H NMR (acetone $d_6$ solution): 7.88 (s, 1H, HC1); 6.76 (s, 1H, HC3); 5.76 (s, 10H, 2 $C_5H_5$–Mo); 4.69 (t, 2H, $C_5H_4$, (H2'–5'), $^3J$(H–H) = 1.85 Hz); 4.56 (t, 2H, $C_5H_4$, (H3'–4'), $^3J$(H–H) = 1.85 Hz); 4.26 (s, 5H, $C_5H_5$–Fe). $^{13}$C NMR (acetone $d_6$): 223.0 (CO); 120.8 (C1, d, $^1J$(C–H) = 168.4 Hz); 102.3 (C1'); 94.1 ($C_5H_5$–Mo, d, $^1J$(C–H) = 183.0 Hz); 86.2 (C2); 76.9 (C3, d, $^1J$(C–H) = 224.3 Hz; $^3J$(C–H) = 5.6 Hz); 71.0 ($C_5H_5$–Fe, d, $^1J$(C–H) = 176.9 Hz); 72.5 (C3'–C4', d, $^1J$(C–H) = 177.5 Hz); 65.8 (C5'–C2', d, $^1J$(C–H) = 180.1 Hz). IR (KBr pellet) $\nu$(CO): 2015, 2000, 1875; $\nu$(BF): 1100. Anal. Found: C, 43.80; H, 2.93; F, 10.72. $C_{27}H_{21}BF_4FeMo_2O_4$. Calc.: C, 43.59; H, 2.85; F, 10.21%.

### 3.4. Synthesis of [{$Cp_2Mo_2(CO)_4$($\mu$-$\eta^2$:$\eta^3$-HC≡C–C(H))}$_2$Fc][{$BF_4$}$_2$] (4)

To a solution of (2) (2 g, 1.7 mmol) in 30 ml of dichloromethane (complex (2) is less soluble than (1)). was added 0.3 ml of a solution of $HBF_4$ in diethyl ether. An immediate change of colour from red to violet occurred. Addition of 60 ml of diethyl ether and cooling to −15°C yielded a violet precipitate of compound (4) (1.9 g, 88%).

Spectroscopic data for (4):

$^1$H NMR (acetone $d_6$): 7.7 (s, 2H, 2 HC1); 6.73 (s, 2H, 2 HC3); 5.72 (s, 20H, 4 $C_5H_5$–Mo); 4.75 (t, 4H, $C_5H_4$, 2 (H2'–5'), $^3J$(H–H) = 1.87 Hz); 4.56 (t, 4H, $C_5H_4$, 2 (H3'–4'). $^{13}$C NMR (acetone $d_6$): 116.3 (C1); 105.5 (C1'); 94.3 ($C_5H_5$–Mo); 88.0 (C2); 77.6 (C3); 74.1 and 74.0 ($C_5H_4$, C2', C3', C4', C5'); CO not observed. IR ($CH_2Cl_2$): $\nu$(CO): 2040, 1995, 1875; $\nu$(BF): 1050. Anal. Found: C, 40.07; H, 3.01; F, 9.98. $C_{44}H_{32}B_2F_8FeMo_4O_8$. Calc.: C, 40.59; H, 2.47; F, 11.67%.

### 3.5. Synthesis of [$Cp_2Mo_2(CO)_4$($\mu$-$\sigma$:$\eta^2$-C=C=C(Fc)(H)}] (5)

Method A: compound (3) (1 g, 1.34 mmol) was added to a suspension of LiC≡C–C($CH_3$)=$CH_2$ generated from HC≡C–C($CH_3$)=$CH_2$ (0.15 ml, 1.6 mmol) and Li$^n$Bu (0.54 ml, 1.34 mmol) in THF frozen in liquid nitrogen. The excess of HC≡C–C($CH_3$)=$CH_2$ was used to prevent oligomerisation [35]. Dichloromethane (50 ml) was added, causing a rapid colour change from violet to green. The solution was allowed to warm to room temperature and was then filtered quickly through a Celite pad (3 × 5 cm) to remove $LiBF_4$. After removal of the solvent in vacuo the crude solid was extracted with diethyl ether and yielded 0.38 g (43%) of (5).

Method B: a solution of complex (1) (0.5 g, 0.74 mmol) in dichloromethane was rapidly eluted through a silica gel column made up with hexane. Small amounts of [$Cp_2Mo_2(CO)_6$] (elution hexane–dichloromethane, 4:1 in volume) and traces of unchanged compound (1) (elution dichloromethane) were first collected. Elution with diethyl ether then afforded the green allenylidene complex (5) (0.08 g, yield 17%).

Spectroscopic data for (5):

$^1$H NMR ($C_6D_6$): 6.59 (s, 1H, =C(*H*)–Fc); 5.02 (s, 5H, $C_5H_5$–Mo); 4.98 (s, 5H, $C_5H_5$–Mo); 4.91 (m, 1H,

$C_5H_4$); 4.64 (m, 1H, $C_5H_4$); 4.29 (m, 1H, $C_5H_4$); 4.23 (m, 1H, $C_5H_4$); 3.99 (s, 5H, $C_5H_5$–Fe). $^{13}C$ NMR (acetone $d_6$) −10°C: 281.9 (Mo=*C*); 239.0, 235.8, 232.8 and 230.8 (4 CO); 149.2 (Mo=C=*C*); 137.6 (Mo=C=C=*C*(H), d, $^1J$(C–H) = 165 Hz); 98.5 (C, ($C_5H_4$) quaternary carbon atom); 96.2 ($C_5H_5$–Mo, d, $^1J$(C–H) = 177.7 Hz); 94.5 ($C_5H_5$–Mo, d, $^1J$(C–H) = 177.1 Hz); 70.6 ($C_5H_5$–Fe, d, $^1J$(C–H) = 175.8 Hz); 71.9, 69.1, 69.9 and 69.2 ($C_5H_4$, d, $^1J$(C–H) = 176 Hz). IR (KBr pellet) $\nu$(CO): 1960, 1910, 1850; $\nu$(C=C=C): 1650. MS: (*m/e*) 656: $[M]^+$; 600: $[M-2CO]^+$; 544: $[M-4CO]^+$. Anal. Found: C, 50.22; H, 3.10. $C_{27}H_{20}FeMo_2O_4$. Calc.: C, 49.42; H, 3.07%.

### *3.6. Synthesis of [{$Cp_2Mo_2(CO)_4(\mu$-$\sigma$:$\eta^2$-C=C=C(H))}$_2$Fc] (6)*

Compound (**4**) (0.53 g, 0.41 mmol) was added to a suspension of an excess of LiC≡C–C($CH_3$)=$CH_2$ generated from HC≡C–C($CH_3$)=$CH_2$ (0.2 ml, 2.1 mmol) and Li$^n$Bu (0.75 ml, 1.9 mmol) in THF frozen in liquid nitrogen. Addition of dichloromethane initiated the reaction and the solution turned green. The mixture was filtered at −30°C and removal of the solvent from the filtrate in vacuo left a crude solid which was extracted with cold dichloromethane. The extract was concentrated in vacuo to 15 ml and diethyl ether was added to give a green precipitate (0.18 g, yield 38%).

The procedure used for (**5**), but starting from (**2**) gave [$Cp_2Mo_2(CO)_6$] and small amounts of (**6**).

Spectroscopic data for (**6**):

$^1H$ NMR (toluene $d_8$): 6.60 (s, 2H, 2 =C(*H*)); 6.65 (s, 2H, 2 =C(*H*)); 5.08 and 5.05 (2s, 20H, 4 $C_5H_5$–Mo); 5.01 and 4.98 (2s, 20H, 4 $C_5H_5$–Mo); between 4.9 and 4.2 ppm eight multiplets (16H, 4 $C_5H_4$). $^{13}C$ NMR data (because of the poor stability of compound (**6**) only some peaks could be assigned): 297.6, 296.4 (Mo=*C*); 95.9, 94.1, 92.2, 91.5 ($C_5H_5$–Mo). IR ($CH_2Cl_2$): $\nu$(CO): 1965, 1905, 1850; $\nu$(C=C=C): 1650.

## Acknowledgements

We thank Dr. R. Pichon for recording the NMR spectra.

## References

[1] A. Meyer, D. McCabe and M.D. Curtis, *Organometallics, 6* (1987) 1491.
[2] S.F.T. Froom, M. Green, K.R. Nagle and D.J. Williams, *J. Chem. Soc. Chem. Commun.*, (1987) 1305.
[3] O.A. Reutov, I.V. Barinov, V.A. Chertkov and V.I. Sokolov, *J. Organomet. Chem., 297* (1985) C25.
[4] M. Gruselle, C. Cordier, M. Salmain, H. El Amouri, C. Guérin, J. Vaissermann and G. Jaouen, *Organometallics, 9* (1990) 2993.
[5] C. Cordier, M. Gruselle, V.I. Bakhmutov, M.V. Galakhov, L.L. Troitskaya and V.I. Sokolov, *Organometallics, 10* (1991) 2303.
[6] N. Le Berre-Cosquer, R. Kergoat and P. L'Haridon, *Organometallics, 11* (1992) 721.
[7] J.-F. Capon, S. Cornen, N. Le Berre-Cosquer, R. Kergoat, R. Pichon and P. L'Haridon, *J. Organomet. Chem., 470* (1994) 137.
[8] H. El Amouri, J. Vaisserman, Y. Besace, K.P.C. Vollhardt and G.E. Ball, *Organometallics, 12* (1993) 605.
[9] M. Gruselle, H. El Hafa, M. Nikolski, G. Jaouen, J. Vaisserman, L. Li and M.J. McGlinchey, *Organometallics, 12* (1993) 4917.
[10] H. El Amouri, Y. Besace, J. Vaisserman, M.J. McGlinchey and G. Jaouen, *Organometallics, 13* (1994) 4426.
[11] L. Girard, P.E. Lock, H. El Amouri and M.J. McGlinchey, *J. Organomet. Chem., 478* (1994) 189.
[12] H. El Hafa, C. Cordier, M. Gruselle, Y. Besace, G. Jaouen and M.J. McGlinchey, *Organometallics, 13* (1994) 5149.
[13] M. Gruselle, V. Philomin, F. Chaminant, G. Jaouen and K.M. Nicholas, *J. Organomet. Chem., 399* (1990) 317.
[14] J.-F. Capon, S. Bernier, N. Le Berre-Cosquer, R. Kergoat, R. Pichon and P. L'Haridon, *J. Organomet. Chem., 487* (1995) 201.
[15] S.F.T. Froom, M. Green, R.J. Mercer, K.R. Nagle, A.G. Orpen and R.A. Rodrigues, *J. Chem. Soc. Dalton Trans.*, (1991) 3171.
[16] M.L.H. Green, S.R. Marder, M.E. Thompson, J.A. Bandy, D. Bloor, P.V. Kolinsky and R.J. Jones, *Nature, 330* (1987) 360.
[17] N.J. Long, *Angew. Chem. Int. Ed. Engl., 34* (1995) 21.
[18] J.F. Capon, N. Le Berre-Cosquer and R. Kergoat, *J. Organomet. Chem*, in press.
[19] W.I. Bailey, M.H. Chishholm, F.A. Cotton and L.A. Rankel, *J. Am. Chem. Soc., 100* (1978) 5764.
[20] J.A. Beck, S.A.R. Knox, R.F.D. Stansfield, F.G.A. Stone, M.J. Winter and P.Woodwart, *J. Chem. Soc. Dalton Trans.*, (1982) 195.
[21] N. Le Berre-Cosquer and R. Kergoat, *J. Organomet. Chem., 427* (1992) 325.
[22] S.A.R. Knox, R.F.D. Stansfield, F.G.A. Stone, M.J. Winter and P. Woodwart, *J. Chem. Soc. Dalton Trans.*, (1982) 173.
[23] L.L Troitskaya, V.I. Sokolov, V.I. Bakhmutov, O.A. Reutov, M Gruselle, C.Cordier and G. Jaouen, *J. Organomet. Chem., 364* (1989) 195.
[24] C. Cordier, M. Gruselle, J. Vaissermann, L.L Troitskaya, V.I. Bakhmutov, V.I. Sokolov and G. Jaouen, *Organometallics, 11* (1992) 3825.
[25] S.C. Bennett, A. Gelling and M.J. Went, *J. Organomet. Chem., 439* (1992) 189.
[26] M.D. McClain, M.S. Hay, M.D. Curtis and J.W. Kampf, *Organometallics, 13* (1994)4377.
[27] G.G. Melikyan, R.C. Combs, J. Lamirand, M. Khan and K.M. Nicholas, *Tetrahedron Lett., 35* (1994) 363.
[28] M.V. Galakhov, V.I. Bakhmutov, I.V. Barinov and O.A. Reutov, *J. Organomet. Chem., 421* (1991) 65.
[29] G. Doisneau, G. Balavoine and T. Fillebeen-Khan, *J. Organomet. Chem., 425* (1992) 113.
[30] M.N. Nefedova, I.A. Mamedyarova, P.P. Petrovski, V.I. Sokolov, *J. Organomet. Chem., 425* (1992) 125.
[31] A.N. Nesmeyanov and I.I. Kritskaya, *Izv. Akad. Nauk SSSR Ser. Khim.*, (1964) 2160.
[32] M.D. Curtis, N.A. Fotinos, L. Messerle and A.P. Sattelberger, *Inorg. Chem., 22* (1983) 1559.
[33] C.G.A. Balavoine, G. Doisneau and T. Fellebeen-Khan, *J. Organomet. Chem., 412* (1991) 381.
[34] U.T. Mueller-Westerhoff, Z. Yang and G. Ingram, *J. Organomet. Chem., 463* (1993) 163.
[35] M.M. Midland, *J. Org. Chem., 40* (1975) 2250.
[36] L. Bransdma, *Preparative Acetylenic Chemistry*, Elsevier, Amsterdam, 1988, 2nd edn.

ELSEVIER

Journal of Organometallic Chemistry 508 (1996) 39–47

Journal of Organometallic Chemistry

# Protonation of triosmium clusters $Os_3(CO)_9(\mu\text{-}CO)(\mu_3\text{-}2\sigma,\eta^2\text{-}HC{\equiv}CR)$ and $Os_3(\mu\text{-}H)(CO)_9(\mu_3\text{-}\sigma,2\eta^2\text{-}C{\equiv}CR)$ ($R = CH_2OH$, $CMe_2OH$, $C(Me){=}CH_2$)

V.V. Krivykh *, O.A. Kizas, E.V. Vorontsov, F.M. Dolgushin, A.I. Yanovsky, Yu.T. Struchkov, A.A. Koridze *

*A.N. Nesmeyanov Institute of Organoelement Compounds, Russian Academy of Sciences, Vavilov Str., 28, 117813 Moscow, Russia*

Received 17 March 1995

**Abstract**

Protonation of $Os_3(CO)_9(\mu\text{-}CO)(\mu_3\text{-}2\sigma,\eta^2\text{-}HC{\equiv}CR)$ ($R = CH_2OH$ (**1**), $R = CMe_2OH$ (**2**), and $Os_3(\mu\text{-}H)(CO)_9(\mu_3\text{-}\sigma,2\eta^2\text{-}C{\equiv}CR)$ ($R = CH_2OH$ (**3**), $R = CMe_2OH$ (**4**), $R = C(Me){=}CH_2$ (**5**)) affords cationic complexes with the 5e-and 6e-propargyl ligands $[Os_3(CO)_9(\mu\text{-}CO)(\mu_3\text{-}3\sigma,\eta^2\text{-}HC{\equiv}CCR'_2)]^+$ ($R' = H$ (**6**), $R' = Me$ (**7**)) and $[Os_3(\mu\text{-}H)(CO)_9(\mu_3\text{-}2\sigma,2\eta^2\text{-}CCCR'_2)]^+$ ($R' = H$ (**8**), $R' = Me$ (**9**)) respectively. Reactions of the cationic complexes with $PPh_3$ were studied. The treatment of solutions of complexes **6–9** with triphenylphosphine leads to the phosphonium derivatives of the $Os_3$ clusters $Os_3(CO)_9(\mu\text{-}CO)(\mu_3\text{-}2\sigma,\eta^2\text{-}HC{\equiv}CCR'_2\overset{+}{P}Ph_3)$ ($R' = H$, (**10**); $R' = Me$, (**11**)) as well as complexes $Os_3(\mu\text{-}H)(CO)_9(\mu_3\text{-}\sigma,2\eta^2\text{-}\overset{+}{P}Ph_3C{=}C{=}CR'_2)$ ($R' = H$ (**12**), $R' = Me$ (**13**)) with the novel phosphonium allenyl ligand. The cluster $Os_3(CO)_8(\mu\text{-}CO)\{HC_2[C(Me){=}CH_2]COC[C(Me){=}CH_2]CH\}$ (**14**) was synthesized and its X-ray study was carried out ($R = 0.0504$ for 5510 observed reflections). Crystals of **14** are triclinic, at 20°C: $a = 8.591(2)$, $b = 11.437(2)$, $c = 12.642(3)$ Å, $\alpha = 93.17(2)$, $\beta = 104.67(2)$, $\gamma = 101.83(2)°$, $V = 1168.6(4)$ Å$^3$, $d_{calc} = 2.793$ g cm$^{-3}$, $Z = 2$, space group $P\bar{1}$.

*Keywords:* Triosmium clusters; Protonation; Six-electronic propargyl ligand; Phosphonium complexes; Phosphonium allenyl ligand; Crystal structure

## 1. Introduction

Recently, interest has grown in complexes containing the $\eta^3$-propargyl ligand coordinated to one [1] or two [2] transition metal atoms. At the same time, there is less information on the coordination of this ligand to three metal atoms. Protonation of compounds containing coordinated propargyl alcohols or vinylacetylenes is known as a route to the synthesis of complexes containing the $\eta^3$-propargyl ligand. It is also well known that the acetylenic ligand can coordinate to the $Os_3$ cluster in various fashions, namely in the $\sigma,\eta^2$-, $2\sigma$-, $\eta^2$-, and $\sigma,2\eta^2$-modes [3]. Such compounds can be suitable objects for the generation of the propargyl cation and for the study of its stabilization by the $Os_3(CO)_9$ and $Os_3(CO)_{10}$ fragments. As early as 1981, some preliminary results of protonation of $2\sigma,\eta^2$- and $\sigma,2\eta^2$-coordinated $HC{\equiv}CCMe_2OH$ by $Os_3$ clusters in $CF_3COOH$ were published [4]. To continue our investigations of $\eta^3$-propargyl ligands coordinating mono- and polynuclear species we attempted to study the protonation of $HC{\equiv}CCR_2OH$ ($R = H$, Me) bound to the $Os_3$ core in more detail. Our preliminary results on the protonation of the $Os_3$ clusters containing the $HC{\equiv}CCMe_2OH$ and $HC{\equiv}CC(Me){=}CH_2$ ligands have been reported elsewhere [5].

In the present paper, we report the protonation of $Os_3(CO)_9(\mu\text{-}CO)(\mu_3\text{-}2\sigma,\eta^2\text{-}HC{\equiv}CR)$ ($R = CH_2OH$ (**1**), $R = CMe_2OH$ (**2**) and $Os_3(\mu\text{-}H)(CO)_9(\mu_3\text{-}\sigma,2\eta^2\text{-}C{\equiv}CR)$ ($R = CH_2OH$ (**3**), $R = CMe_2OH$ (**4**), $R = C(Me){=}CH_2$ (**5**) clusters, as well as the reactions of generated cationic complexes with triphenylphosphine.

* Corresponding authors.

Elsevier Science S.A.
*SSDI* 0022-328X(95)05871-0

## 2. Experimental

All reactions were carried out in an argon atmosphere using anhydrous solvents. IR spectra were recorded on a Specord IR-75 spectrophotometer. $^1H$ and $^{13}C$ NMR spectra were measured on a Bruker WP-200 SY instrument at the operation frequency of 200.13 MHz using $C_6D_6$ as a solvent at 25°C and $CD_2Cl_2$ in the temperature range from −60 to −20°C. Chromatography was performed using silica gel of the 40/100 grade (Chechiya) as an adsorbent.

Clusters **2** and **4** were prepared according to the published procedure [4]; cluster **5** was prepared from the $Os_3(CO)_{10}(MeCN)_2$ [5] in 90% yield.

### 2.1. Preparation of $Os_3(CO)_9(\mu\text{-}CO)(\mu_3\text{-}2\sigma,\eta^2\text{-}HC{\equiv}CCH_2OH)$ (1)

$HC{\equiv}CCH_2OH$ (0.3 g, 5.27 mmol) was added to a solution of $Os_3H_2(CO)_{10}$ (0.5 g, 1.758 mmol) in diethyl ether and stirred at 25°C until the initial osmium cluster disappeared (chromatography with hexane–ether, 5:1). The solvent was removed in vacuo; the residue was poured into the column. The broad orange band containing a mixture of **1** and the vinyl cluster $Os_3(\mu\text{-}H)(CO)_{10}(\mu_2\text{-}\sigma,\eta^2\text{-}HC{=}CHCH_2OH$ (**15**) was eluted by the solvent mixture mentioned. The reaction products were chromatographed in 0.02 g portions through a layer of silica gel ($d$ = 10 mm, $l$ = 550 mm). Crystallization of the first band from hexane yielded the dark-yellow crystalline compound **1** (0.18 g, 34%). IR (hexane): 2100 w, 2062 vs, 2060 vs, 2021 s, 2008 m, 1848 br $cm^{-1}$. $^1H$ NMR ($C_6D_6$): 1.80 (1H, s, OH), 3.82 (1H, d, $J$(HH) = 13.5 Hz, C$H$H), 4.31 (1H, d, $J$(HH) = 13.5 Hz, CH$H$), 9.31 (1H, s, =CH). The product from the second band was crystallized from hexane to give the orange crystalline compound **15** (0.05 g, 9.4%). IR: 2103 m, 2061 vs, 2052 vs, 2025 vs, 2013 vs, 1992 s, 1982 m $cm^{-1}$. $^1H$ NMR ($C_6D_6$): −19.31 (1H, s, Os–H–Os), 0.61 (1H, t, $J$(HH) = 4.6 Hz, OH), 3.26 (2H, t, $J$(HCCH) ~ $J$(HCOH) ~ 3.9 Hz, C$H$H), 4.02 (1H, dt, $J$(HH) = 13.8 Hz, $J$(HH) = 3.6 Hz, =C$H$CH$_2$), 7.24 (1H, d, $J$(HH) = 13.8 Hz).

### 2.2. The reaction of $Os_3H_2(CO)_{10}$ with isopropenylacetylene

$HC{\equiv}CC(Me){=}CH_2$ (0.005 g, 0.07 mmol) was added to a solution of $Os_3H_2(CO)_{10}$ (0.02 g, 0.023 mmol) in hexane and stirred for about 3 h until the initial cluster disappeared (chromatography with hexane–ether, 5:1). The solvent was removed in vacuo. The column chromatography with a mixture of hexane–ether 5:1 gave two dark yellow crystalline compounds. One of them, $Os_3(\mu\text{-}H)(CO)_{10}(\mu_2\text{-}\sigma,\eta^2\text{-}HC{=}CHC(Me){=}CH_2)$ (**16**) was crystallized from hexane (0.01 g, 47%). IR (hexane): 2104 w, 2074 m, 2061 vs, 2052 s, 2031 w, 2022 vs, 2010 s, 1992 m, 1986 w, 1980 w $cm^{-1}$. $^1H$ NMR ($C_6D_6$): −18.44 (1H, s, Os–H–Os), 1.43 (3H, s, $CH_3$), 4.83 (1H, s, =C$H$H), 5.13 (1H, s, =CH$H$), 5.16 (1H, d, $J$(HH) = 14.0 Hz, =CH), 7.13 (1H, d, J(HH) = 14.0 Hz, =CH). The other one also crystallized from hexane represents the complex $Os_3(CO)_{10}$ ($\eta^4$-$H_2C{=}C(Me)$-$CH{=}CH_2$) (**17**) [6] (0.01 g, 47%). IR (hexane): 2112 m, 2064 vs, 2032 vs, 2027 s, 2009 s, 1996 w, 1986 m, 1978 sh $cm^{-1}$. $^1H$ NMR ($CD_2Cl_2$): 0.21 (1H, dd, $J$(HH) = 8.1, 3.0 Hz, =C$H$H), 0.56 (1H, d, $J$(HH) = 3.0 Hz, MeC=C$H$H), 2.09 (1H, dd, $J$(HH) = 6.8 Hz, $J$(HH) = 3.0 Hz, HC=CH$H$), 2.31 (1H, s, MeC=CH$H$), 2.68 (3H, s, $CH_3$), 5.24 (1H, dd, $J$(HH) = 7.7 Hz, =CH).

### 2.3. Preparation of $Os_3(\mu\text{-}H)(CO)_9(\mu_3\text{-}\sigma,2\eta^2\text{-}C{\equiv}CCH_2OH)$ (3)

A solution of complex **1** (0.3 g) in octane (25 ml) was refluxed for 10 min. Octane was removed in vacuo. The column chromatography with a mixture hexane–ether 5:1 gave pale-cream crystalline compound **3** (0.23 g, 80%), which was crystallized from hexane. IR: 2101 m, 2079 vs, 2058 vs, 2023 vs, 2019 s, 1982 m $cm^{-1}$. $^1H$ NMR ($CD_2Cl_2$): −23.30 (1H, s, Os–H–Os), 2.46 (1H, t, $J$(HH) = 5.0 Hz, OH), 5.09 (2H, d, $J$(HH) = 5.0 Hz, $CH_2$).

### 2.4. Preparation of $Os_3(CO)_8(\mu\text{-}CO)\{HC_2[C(Me){=}CH_2]COC[C(Me)CH_2]CH\}$ (14)

A solution of complex $Os_3(CO)_9(\mu\text{-}CO)(\mu_3\text{-}2\sigma,\eta^2\text{-}HC{\equiv}CC(Me){=}CH_2)$ **19** (0.22 g) in octane (20 ml) was refluxed for 10 min. Octane was removed in vacuo; the residue was column chromatographed, and eluted with heptane. Cluster **5** (90%) was isolated as a major product [5]. The second band contained the orange crystalline compound **14** (0.02 g, 10%). IR (heptane): 2095 s, 2074 w, 2057 vs, 2024 w, 2016 s, 2002 m, 1992 w, 1851 m $cm^{-1}$. $^1H$ NMR ($C_6D_6$): 1.80 (3H, s, $CH_3$), 1.96 (3H, s, $CH_3$), 5.00 (1H, s, =$CH_2$), 5.04 (1H, s, =$CH_2$), 5.15 (1H, s, =$CH_2$), 5.60 (1H, s, =$CH_2$), 7.27 (1H, s, =CH), 8.05 (1H, s, HC=).

### 2.5. Preparation of the phosphonium clusters $[Os_3(CO)_9(\mu\text{-}CO)(\mu_3\text{-}2\sigma,\eta^2\text{-}HC{\equiv}CCMe_2\overset{+}{P}Ph_3)]BF_4^-$ (11)

$HBF_4 \cdot Et_2O$ (0.3 g, 0.04 ml, 0.194 mmol) was added to a solution of cluster **1** (0.06 g, 0.065 mmol) in $CH_2Cl_2$ (5 ml) cooled to −60°C. After 5 min, triphenylphosphine (0.02 g, 0.24 mmol) was added, and the mixture was stirred at the mentioned temperature for 20 min. Then the temperature was brought to 25°C. The phosphonium complex was precipitated from methylene

chloride with ether. The yellow powder **11** was obtained (0.04 g, 66%). IR ($CH_2Cl_2$): 2106 m, 2070 vs, 2058 s, 2035 m, 1845 br $cm^{-1}$. $^1H$ NMR ($CD_2Cl_2$): 1.65 (3H, d, $J(HP) = 6.8$ Hz $CH_3$), 1.74 (3H, d, $J(HP) = 6.8$ Hz, $CH_3$), 7.71 (15H, m, Ph), 9.29 (1H, s, =CH).

All the protonation reactions followed by the treatment of cationic intermediates with triphenylphosphine and the isolation of the phosphonium compounds were performed under similar conditions. Only in the case of complexes **4** and **5** was a 30% solution of trifluoromethanesulfonic acid in nitromethane used as a protonating agent.

*$[Os_3(CO)_9(\mu\text{-}CO)(\mu_3\text{-}2\sigma,\eta^2\text{-}HC{\equiv}CCH_2\overset{+}{P}Ph_3)]BF_4^-$ (10)*

Yellow powder (0.025 g, 65.5%). IR ($CH_2Cl_2$): 2105 m, 2070 vs, 2058 vs, 2032 s, 2005 m, 1849 br $cm^{-1}$. $^1H$ NMR: 3.95 (1H, dd, $J_{av}$(HH) (HP) = 15 Hz, CHH), 4.25 (1H, dd, $J_{av}$(HH) (HP) = 15.0 Hz, CHH), 7.7 (15H, m, Ph), 8.55 (1H, s, =CH).

*$[Os_3(\mu\text{-}H)(CO)_9(\mu_3\text{-}\sigma,2\eta^2\text{-}\overset{+}{P}Ph_3C{=}C{=}CH_2)]BF_4^-$ (12)*

White powder (0.05 g, 65.3%). IR ($CH_2Cl_2$): 2110 m, 2082 vs, 2060 vs, 2042 s, 2015 s $cm^{-1}$. $^1H$ NMR ($CD_2Cl_2$): −22.0 (1H, s, Os–H–Os), 2.93 (1H, dd, $J(HH) \sim J(HP) = 2.8$ Hz, =C*H*H), 4.07 (1H, dd, $J(HH) = 2.5$ Hz, $J(HP) = 3.7$ Hz, =CHH), 7.8 (15H, m, Ph).

*$[Os_3(\mu\text{-}H)(CO)_9(\mu_3\text{-}\sigma,2\eta^2\text{-}Ph_3\overset{+}{P}C{=}C{=}CMe_2)]BF_4^-$ (13)*

White powder (0.05 g, 65%). IR ($CH_2Cl_2$): 2105 m, 2080 vs, 2059 vs, 2030 s, 2010 m $cm^{-1}$. $^1H$ NMR: −23.17 (1H, s, Os–H–Os), 1.99 (3H, s, $CH_3$), 2.09 (3H, s, $CH_3$), 7.8 (15H, m, Ph).

### 2.6. Preparation of $\bar{O}s_3(\mu\text{-}H)(CO)_9(\mu_3\text{-}2\sigma,\eta^2\text{-}Ph_3\overset{+}{P}C{\equiv}CCH_2OH)$ (18)

$HBF_4 \cdot Et_2O$ (0.03 g, 0.04 ml, 0.194 mmol) was added to a solution of cluster **3** (0.06 g, 0.068 mmol) in $CH_2Cl_2$ at −78°C. After 5 min triphenylphosphine (0.02 g, 0.24 mmol) was added, and the mixture was stirred at this temperature for 1 h. The reaction mixture was slowly brought to 25°C. The solution was chromatographed through a layer of silica gel ($l = 3$ cm, $d = 1$ cm) at −78°C, then washed with methylene chloride at the mentioned temperature. After such treatment, there were no traces of the phosphonium cluster **10** (chromatography with $CH_2Cl_2$–acetone, 5:1). The solvent was removed in vacuo, and the residue was crystallized from the ether–hexane mixture. Colourless transparent crystals of the zwitter-ionic cluster **18** were obtained (0.04 g, 50.8%). IR ($CH_2Cl_2$): 3606 br, 2073 s, 2046 vs, 2015 vs, 1993 s, 1968 s, 1944 m $cm^{-1}$. $^1H$ NMR ($CD_2Cl_2$): −19.12 (1H, d, $J(HP) = 3.3$ Hz, Os–H–Os), 3.15 (1H, d, $J(HH) = 13.0$ Hz, CHH), 3.79 (1H, d, $J(HH) = 13.0$ Hz, CHH), 7.8 (15H, m, Ph).

Table 1
Atomic coordinates ($\times 10^4$) in **14**

| | x | y | z |
|---|---|---|---|
| Os(1) | 2783(1) | 2025(1) | 2822(1) |
| Os(2) | 2105(1) | 2939(1) | 801(1) |
| Os(3) | 5358(1) | 3708(1) | 2307(1) |
| O(1) | 6462(9) | 1600(5) | 3162(6) |
| O(12) | 2008(17) | 4265(10) | 3793(10) |
| O(13) | 4390(15) | 1347(11) | 5061(8) |
| O(14) | −518(13) | 321(10) | 2634(10) |
| O(15) | −1518(12) | 2016(9) | 663(10) |
| O(16) | 1535(16) | 2557(11) | −1676(9) |
| O(17) | 1678(11) | 5546(7) | 994(10) |
| O(18) | 5213(12) | 3630(8) | −133(8) |
| O(19) | 8708(12) | 4674(10) | 1907(10) |
| O(20) | 5045(15) | 6225(8) | 3099(10) |
| C(1) | 2528(13) | 1221(8) | 1118(8) |
| C(2) | 3952(12) | 936(7) | 1792(9) |
| C(3) | 5237(12) | 1932(8) | 2395(8) |
| C(4) | 7369(12) | 2558(8) | 3962(9) |
| C(5) | 7020(13) | 3637(9) | 3823(9) |
| C(6) | 4130(14) | −351(8) | 1867(10) |
| C(7) | 5401(18) | −669(11) | 1444(17) |
| C(8) | 2999(20) | −1145(11) | 2280(14) |
| C(9) | 8554(14) | 2219(10) | 4888(9) |
| C(10) | 9566(20) | 3236(12) | 5771(11) |
| C(11) | 8711(17) | 1085(12) | 4942(11) |
| C(12) | 2336(19) | 3423(12) | 3445(12) |
| C(13) | 3808(14) | 1588(10) | 4237(9) |
| C(14) | 709(16) | 969(11) | 2718(10) |
| C(15) | −155(14) | 2380(9) | 723(11) |
| C(16) | 1704(16) | 2737(11) | −757(10) |
| C(17) | 1889(14) | 4594(10) | 930(10) |
| C(18) | 4745(14) | 3546(9) | 654(9) |
| C(19) | 7443(15) | 4317(10) | 2067(10) |
| C(20) | 5115(16) | 5309(9) | 2747(11) |

### 2.7. An X-ray study of $Os_3(CO)_8(\mu\text{-}CO)\{HC_2[C(Me){=}CH_2]COC[C(Me)CH_2]CH\}$ (14)

Crystals of **14** are triclinic at 20°C: $a = 8.591(2)$, $b = 11.437(2)$, $c = 12.642(3)$ Å, $\alpha = 93.17(2)$, $\beta = 104.67(2)$, $\gamma = 101.83(2)°$, $V = 1168.6(4)$ Å$^3$, $d_{calc} = 2.793$ g $cm^{-3}$, $Z = 2$, space group $P\bar{1}$. Unit cell parameters and intensities of 7463 independent reflections were measured on a Siemens P3/PC automatic diffractometer (20°C, Mo K$\alpha$ radiation, graphite monochromator, $\theta/2\theta$-scans, $\theta < 31°$).

The structure was solved by direct methods and refined by the full-matrix least squares technique, first in the isotropic and then in the anisotropic approximation. The hydrogen atoms were not located. The correction for absorption ($\mu = 163$ $cm^{-1}$) was based on the azimuthal scans ($T_{min} = 0.270$). The final discrepancy factors $R = 0.0504$, $R_w = 0.0506$ for 5510 reflections with $I \geq 3\sigma(I)$. All calculations were carried out with

the SHELXTL PLUS programs (PC version) [7] on an IBM PC. Coordinates of non-hydrogen atoms are given in Table 1. A table of thermal parameters and a complete list of bond lengths and angles has been deposited at the Cambridge Crystallographic Data Centre.

## 3. Results and discussion

### 3.1. The synthesis of clusters with acetylenic ligands

Cluster $Os_3(CO)_9(\mu\text{-}CO)(\mu_3\text{-}2\sigma,\eta^2\text{-}HC{\equiv}CCH_2OH)$ (**1**) was obtained as a hard-to-separate mixture with the vinyl derivative $Os_3(\mu\text{-}H)(CO)_{10}(\mu_2\text{-}\sigma,\eta^2\text{-}HC{=}CHCH_2OH)$ (**15**) by the treatment of osmium carbonylhydride with propargyl alcohol in ether at 25°C. Column chromatography of this mixture in small batches and recrystallization gave clusters **1** and **15** in the 34.0% and 9.4% yields respectively. In the IR spectrum of **1**, there are six CO bands of the terminal CO groups and a band at 1848 $cm^{-1}$ of the bridging carbonyl group. In the $^1H$ NMR spectrum, there is a broad signal at 1.8 ppm associated with the hydroxyl group, two signals at 3.8 and 4.3 ppm with $J_{AB} = 13.5$ Hz associated with the magnetically non-equivalent protons of the $CH_2$ group, and a low-field signal at 9.3 ppm of the methyne proton. Thus, spectral characteristics are in accord with the proposed structure of cluster **1**.

All attempts to obtain cluster $Os_3(\mu\text{-}CO)(CO)_9(\mu_3\text{-}2\sigma,\eta^2\text{-}HC{\equiv}CC(Me){=}CH_2)$ (**19**) using the same method were unsuccessful. The treatment of $Os_3H_2(CO)_{10}$ with vinylacetylene in a 1:1 ratio provided the vinyl compound $Os_3(\mu\text{-}H)(CO)_{10}(\mu\text{-}\sigma,\eta^2\text{-}HC{=}CHC(Me){=}CH_2)$ (**16**) and the product of the selective enyne hydrogenation, namely the diene cluster $Os_3(CO)_{10}(\eta^4\text{-}H_2C{=}C(CH_3){-}CH{=}CH_2)$ (**17**), which was obtained earlier [6] directly from 2-methyl-1,3-butadiene and $H_2Os_3(CO)_{10}$. After crystallization, clusters **16** and **17** were each obtained in 47% yield. In the IR spectrum of the vinyl compound **16**, there are ten bands of the terminal CO groups; in the $^1H$ NMR spectrum, there are the following signals: −18.44 of the bridging hidride, a singlet at 1.43 ppm of the methyl group protons, and the other signals corresponding to the structure of **16**, namely two signals at 4.83 and 5.15 ppm ($=CH_2$), and two doublets at 5.16 and 7.13 ppm with $J = 14.0$ Hz (HC=CH). In the IR spectrum of the diene cluster **17**, there are eight bands of the terminal CO groups. The $^1H$ NMR spectrum contains the signals: 0.21 (dd, $J(HH)$ = 8.1, 3.0 Hz, C*H*H), 0.56 (1H, d, $J(HH) = 3.0$ Hz, MeC=CH*H*), 2.68 (1H, s, $CH_3$), and 5.24 (1H, dd, $J(HH) = 7.7$ Hz, HC=).

Cluster **19** was obtained in high yield (85%) by the treatment of $Os_3(CO)_{10}(MeCN)_2$ with isopropenylacetylene in an ether solution at 25°C [5].

The thermolysis of **1** and **19** in boiling octane yielded the clusters with the five electron acetylide ligands $Os_3(\mu\text{-}H)(CO)_9(\mu_3\text{-}\sigma,2\eta^2\text{-}C{\equiv}CCH_2OH)$ (**3**) and $Os_3(\mu\text{-}H)(CO)_9(\mu_3\text{-}\sigma,2\eta^2\text{-}C{\equiv}CC(Me){=}CH_2)$ (**5**) in high yield (90%). IR spectra of both compounds contain the bands of the terminal carbonyl groups; in $^1H$ NMR spectra, there are signals of the bridging hydrogen ligands at −23.30 and −23.43 ppm, which are characteristic of clusters with the $\mu_3\text{-}\sigma,2\eta^2$-acetylide ligands.

The thermolysis of complex **19** provides, along with **5**, another compound **14** in low yield (10%), the IR spectrum of which has, apart from seven bands of the terminal CO groups, a band at 1850 $cm^{-1}$ of the bridging carbonyl group. The $^1H$ NMR spectrum contains two singlets of the methyl groups at 1.80 and 1.96 ppm, four singlets at 5.00, 5.04, 5.15 and 5.60 ppm associated with two $=CH_2$ groups as well as two singlets at 7.27 and 8.05 ppm associated with two fragments of =CH. The spectral data allowed to assign the formula of $Os_3(CO)_8(\mu\text{-}CO)\{HC_2[C(Me){=}CH_2]\text{-}COC[C(Me)CH_2]CH\}$ to this compound. Its structure was unambiguously established by an X-ray study. The compound has a complex ligand formed by a combination of the allyl fragment and the oxygen-containing five-membered metallacycle and is analogous both to complex $Os_3(CO)_8(\mu\text{-}CO)\{H_2CPhCOCPhCH\}$ reported in Ref. [8] and cluster $Os_3(CO)_8(\mu\text{-}CO)\{H_2CFc\text{-}COCFcCH\}$, which we described earlier [9]. The thermolysis of clusters containing a terminal alkyne and the bridging carbonyl group as ligands, usually proceeds via the decarbonylation followed by the oxidative addition of the C–H bond to the metal atom, thus changing the ligand coordination mode from $2\sigma,\eta^2$ to $\sigma,2\eta^2$ and yielding acetylide clusters.

However, as seen from the examples cited, in a number of cases, complexes of the same type as **14** are formed (the mechanism is still uncertain) in which the bridging carbonyl group is retained and a complex organic ligand involving the former terminal CO group is formed.

The molecular structure of **14** is shown in Fig. 1. Selected bond distances and angles in **14** are listed in Tables 2 and 3. The structure is identical with that of the complex with the phenyl substituents reported earlier [8]. Three osmium atoms form a triangle with the Os(1)–Os(2), Os(1)–Os(3), Os(2)–Os(3) distances equal to 2.785(1), 2.854(1) and 2.885(1) Å respectively (the corresponding distances in $Os_3(CO)_8(\mu\text{-}CO)\{H_2\text{-}CPhCOCPhCH\}$ [8], are 2.794, 2.857 and 2.880 Å).

Like the complex with the phenyl substituents, the dimerized acetylene ligand is bound to the triosmium core by three $\sigma$-bonds Os(2)–C(1), Os(3)–C(3) and Os(3)–C(5) and its allyl moiety C(1)C(2)C(3) is $\pi$-coordinated by the Os(1) atom. Two five-membered cycles Os(2)C(1)C(2)C(3)Os(3) and Os(3)C(3)O(1)C(4)C(5) are fused via the Os(3)–C(3) bond and do not show considerable deviations from planarity (maximum devi-

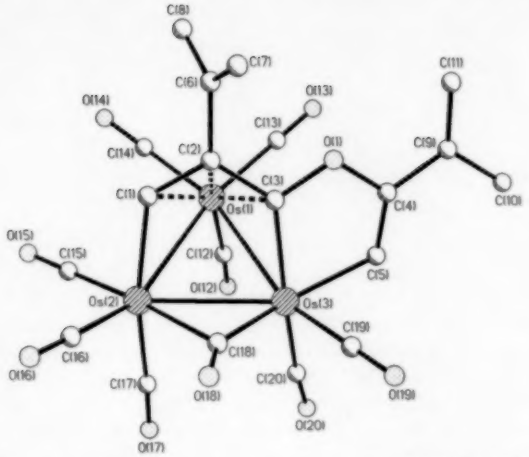


Fig. 1. The molecular structure of $Os_3(CO)_8(\mu\text{-}CO)\{HC_2[C(Me)=CH_2]COC[C(Me)=CH_2]CH\}$ (**14**).

Table 3
Selected bond angles (deg) in **14**

| | | | |
|---|---|---|---|
| C(1)–Os(1)–C(2) | 36.3(4) | C(1)–Os(1)–C(3) | 64.1(3) |
| C(2)–Os(1)–C(3) | 36.2(3) | C(1)–Os(2)–C(18) | 90.0(4) |
| C(3)–Os(3)–C(5) | 75.7(4) | C(3)–Os(3)–C(18) | 94.2(4) |
| C(5)–Os(3)–C(18) | 150.7(5) | C(3)–O(1)–C(4) | 111.7(7) |
| Os(1)–C(1)–Os(2) | 79.6(3) | Os(1)–C(1)–C(2) | 74.0(6) |
| Os(2)–C(1)–C(2) | 128.1(6) | Os(1)–C(2)–C(1) | 69.7(6) |
| Os(1)–C(2)–C(3) | 73.2(6) | C(1)–C(2)–C(3) | 116.4(8) |
| Os(1)–C(2)–C(6) | 127.8(8) | C(1)–C(2)–C(6) | 122.0(7) |
| C(3)–C(2)–C(6) | 121.5(9) | Os(1)–C(3)–Os(3) | 81.7(4) |
| Os(1)–C(3)–O(1) | 119.0(7) | Os(3)–C(3)–O(1) | 118.1(5) |
| Os(1)–C(3)–C(2) | 70.6(6) | Os(3)–C(3)–C(2) | 128.1(7) |
| O(1)–C(3)–C(2) | 113.6(8) | O(1)–C(4)–C(5) | 117.5(9) |
| O(1)–C(4)–C(9) | 114.2(8) | C(5)–C(4)–C(9) | 128.3(9) |
| Os(3)–C(5)–C(4) | 114.3(7) | C(2)–C(6)–C(7) | 115.8(10) |
| C(2)–C(6)–C(8) | 118.6(12) | C(7)–C(6)–C(8) | 125.5(11) |
| C(4)–C(9)–C(10) | 115.7(10) | C(4)–C(9)–C(11) | 121.6(9) |
| C(10)–C(9)–C(11) | 122.6(11) | Os(2)–C(18)–Os(3) | 84.0(5) |
| Os(2)–C(18)–O(18) | 129.3(8) | Os(3)–C(18)–O(18) | 146.7(9) |

ations from their mean planes are 0.03 and 0.11 Å respectively); the dihedral angle formed by their planes is equal to 20° (the same value was found for the phenyl analog).

It should be noted that the isopropenyl substituents in **14** are non-equivalent. In one of them, which is bound to the oxygen-containing chelate metallacycle, there is a distinct difference in the double C(9)=C(11) bond (1.33(2) Å) and the ordinary C(9)–C(10) bond (1.52(2) Å) lengths. Moreover, this substituent is trans-conjugated with the C(4)=C(5) double bond (1.34(1) Å) of the metallacycle; the torsion angle C(11)C(9)C(4)C(5) is equal to 176°. In contrast, the isopropenyl group bound to the allenyl fragment of the other metallacycle has almost equal C(6)–C(7) and C(6)–C(8) bond lengths (1.43 (2) and 1.41(2) Å respectively). However, this feature most probably does not have any chemical implications and should be attributed to the effect of a disorder in the crystal. The dihedral angle formed by the planes of the isopropenyl and allyl groups in this case is equal to 64°. The lack of the conjugation in this system seems to be associated with the strong electron density transfer from the $\pi$-system of the allyl fragment to the coordinating metal atom. However, the atomic coordinates for the phenyl substituted complex are not available, either in the original paper [8] or in the Cambridge Structural Database, so that we could not check whether the same is true in the case of phenyl derivative. However, as can be seen from the figure given in Ref. [8], one may anticipate the same effect in the structure of phenyl derivative.

Table 2
Selected bond lengths (angstroms) in **14**

| | | | |
|---|---|---|---|
| Os(1)–Os(2) | 2.785(1) | Os(1)–Os(3) | 2.854(1) |
| Os(1)–C(1) | 2.235(10) | Os(1)–C(2) | 2.291(11) |
| Os(1)–C(3) | 2.325(11) | Os(2)–Os(3) | 2.885(1) |
| Os(2)–C(1) | 2.112(10) | Os(2)–C(18) | 2.289(12) |
| Os(3)–C(3) | 2.023(9) | Os(3)–C(5) | 2.097(10) |
| Os(3)–C(18) | 2.009(11) | O(1)–C(3) | 1.371(12) |
| O(1)–C(4) | 1.399(10) | O(18)–C(18) | 1.166(16) |
| C(1)–C(2) | 1.412(14) | C(2)–C(3) | 1.435(11) |
| C(2)–C(6) | 1.517(13) | C(4)–C(5) | 1.339(14) |
| C(4)–C(9) | 1.472(15) | C(6)–C(7) | 1.432(23) |
| C(6)–C(8) | 1.410(20) | C(9)–C(10) | 1.519(15) |
| C(9)–C(11) | 1.334(18) | | |

### *3.2. Protonation of clusters $Os_3(CO)_9(\mu\text{-}CO)(\mu_3\text{-}2\sigma,\eta^2\text{-}HC{\equiv}CCR)$ ($R = CH_2OH$ (**1**), $R = CMe_2OH$ (**2**)) and $Os_3(\mu\text{-}H)(CO)_9(\mu_3\text{-}\sigma,2\eta^2\text{-}C{\equiv}CR$ ($R = CH_2OH$ (**3**), $R = CMe_2OH$ (**4**), $R = C(Me){=}CH_2$ (**5**))*

If one drop of $CF_3COOH$ is added to a solution of **1** in $CD_2Cl_2$ at $-50$°C, the $^1H$ NMR spectrum is changed in the following way. The signal of the OH group at 1.8 ppm is shifted low-field, and two broad signals appear corresponding to the slowly exchanging OH and $CF_3COOH$. The signals of two non-equivalent protons of the $CH_2$ group at 3.80 and 4.30 ppm are drawn closer together (3.95, 4.25 ppm) with the coupling constant being retained ($J_{AB}$ = 13.5 Hz), although the high field component already contains an additional splitting with $J^2$ = 3.5 Hz. At the same time, the low-field signal at 9.3 ppm is practically unchanged. The addition of five more drops of trifluoroacetic acid leads to the collapse of the AB system components and to the appearance of a new singlet at 4.3 ppm, but only on addition of two drops of trifluoromethanesulfonic acid; the latter signal transforms to two doublets at 3.70 and 4.93 ppm with $J$ = 5.0 Hz, thus evidencing for the formation of the cationic complex **6**.

R' = H; 1
R' = Me; 2

R' = H; 6
R' = Me; 7

Scheme 1.

A B

Scheme 2.

The proton signal at 9.3 ppm is 0.5 ppm down-shifted. In this case, the previous set of signals is still observed, which corresponds to a high concentration of $CF_3COOH$ in the ratio 1 : 1. Protonation of **1** was carried out within the temperature range −50– −20°C. As the temperature is increased, the signals of decomposition products appear in the spectrum. At 17°C, the reversible broadening of the $CH_2$ group signals was observed, but a further increase in the temperature caused the degradation of the cationic cluster **6**. Spectral changes occurring upon the gradual additions of acids to **1** might be rationalized as follows. Trifluoroacetic acid forms a solvate with cluster **1** resulting in an additional signal with $J = 3.5$ Hz due to the interaction of the $CH_2OH$ group with $CF_3COOH$ through the oxygen atom. An increase in the acid concentration facilitates the exchange process bringing the signals of the $CH_2$ group protons together and finally causing the collapse of these signals; only the addition of a stronger acid leads to the cationic complex **6**. The structure of this complex can be described as a resonance hybrid of structures **A** and **B** (Scheme 2).

Protonation of $Os_3(CO)_9(\mu\text{-}CO)(\mu_3\text{-}2\sigma,\eta^2\text{-}HC{=}CCMe_2OH)$ (**2**) was studied earlier by the $^1H$ NMR method [4]. We studied the protonation of **2** by the $^{13}C$ NMR method. Comparison of the $^{13}C$ NMR spectra of the initial **2** (29.49 (q, $J(CH) = 127$ Hz, Me), 33.40 (q, $J(CH) = 127$ Hz, Me), 79.53 (s, $C{-}Me_2$), 117.0 (d, $J(CH) = 163$ Hz, $=CH$), 168.52 (s, $=C$), 171.8, 174.43, 176.0 (br), 179.38, 179.86 (CO), 202.85 ($\mu$-CO)) and its protonated form after the addition of $HBF_4 \cdot Et_2O$ in a $CD_2Cl_2$ solution at −60°C (14.0 (s, Me), 19.92 (s, Me), 110.24 (d, $J(CH) = 162$ Hz, $HC=$), 117.02 (s, $C{-}Me_2$), 152.99 (s, $=C$), 158.97, 174.02, 174.74, 175 (br), 175.23, 178.82, (CO), 207.15 ($\mu$-CO)), shows that the formation of the cationic complex causes a low-field shift of the carbon signal of $CMe_2$ group by 37 ppm. The other signals of the $C_3$ ligand are only slightly shifted, thus indicating the retention, to a great extent, of the $2\sigma,\eta^2$-bonding mode in the fragment H–C=C– (structure **A**) though the contribution of the structure **B** should also be taken into account. It is remarkable that the signal of the bridging CO group is retained although it is shifted low-field by 4 ppm. Hence the protonation of the complexes with four electron acetylene ligands, such as propargyl alcohol and its derivatives, coordinated to the $Os_3$ cluster in the $2\sigma,\eta^2$ fashion, gives the cationic complexes with the five electron propargyl ligand.

We were successful in detecting the formation of the cationic cluster with the six-electron propargyl ligand on protonation of clusters containing the acetylide ligand coordinated in the $\sigma,2\eta^2$-fashion (Scheme 3)

If a solution of trifluoromethanesulfonic acid in $CD_3NO_2$ is added to solutions of complexes **4** and **5** in $CD_2Cl_2$ at −50°C [5], the $^1H$ NMR spectra are changed in the following way: the hydride signals at −23.5 ppm **4** and −23.34 ppm **5** gradually disappear and a new signal at −22.9 ppm appears. In the low-field range of the spectra the following signals disappear: the singlet of the magnetically equivalent methyl groups at 1.8 ppm for **4** and the signal of the methyl group at 2.19 ppm for **5**, as well as the signals in the range of 5.0–5.3 ppm, responsible for the protons of the $=CH_2$ group in **5**. In both cases, the same set of signals appears, namely the signal of the $\mu$-hydride at −22.9 ppm and two signals of two magnetically non-equivalent methyl groups at 2.24 and 2.64 ppm, the spectral pattern evi-

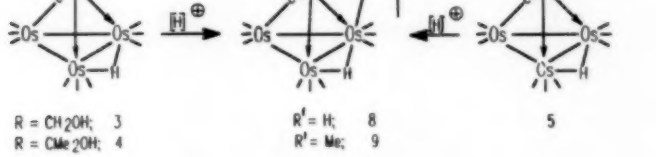

R = $CH_2OH$; 3
R = $CMe_2OH$; 4

R' = H; 8
R' = Me; 9

5

Scheme 3.

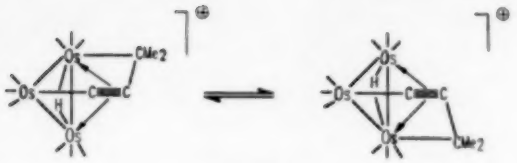

Scheme 4.

dences for the formation of the cationic cluster **9** in the solution. With an increase in the temperature, the signals of the methyl groups are gradually broadened; they coalesce at 17°C and a further temperature increase leads to the sharpening of the signal. Temperature changes in the spectrum may be interpreted in the following way. The protonation of **4** or **5** generates the carbenium ion in the $\alpha$-position with respect to the triple bond. The cation is stabilized due to the direct interaction of the carbocationic center with one of the osmium atoms bearing the hydrogen bridge (Scheme 4) (the same situation takes place in mono-[1a] and binuclear [2a,b,c] propargyl complexes). Such direct participation of the metal atom in the stabilization of the $\alpha$-cationic center is a general property for $\alpha$-metallocenylcarbenium ions and related cationic complexes [10]. Since the probability of bonding to both osmium atoms mentioned is equal, the degenerate exchange process takes place resulting in the observed temperature dependence. The free activation energy of this process is $G^{\neq}_{290\ K} = 13.3 \pm 0.3$ kcal mol$^{-1}$. Recently, a similar exchange process has been observed in the neutral complex $CpWRe_2(CO)_8(OR)(C_3Me_2)$ [11]. The cationic cluster **9** is not stable enough for isolation; moreover, as the temperature of a solution of **9** is increased to 25°C, another set of signals appears in the spectrum, namely two singlets in the range of the methyl groups at 2.23 and 2.47 ppm, and the hydride signal at −19.5 ppm. The chemical shift value of the hydride signal is not in line with that for similar clusters with the five-electron acetylide ligand of the $\sigma,2\eta^2$ type. The intensities of these signals depend on the exposure time of the solution of **9**. These signals seem to have been observed earlier [4] upon dissolving of **4** in $CF_3COOH$ at room temperature.

If the protonation is carried out at low temperatures, a different spectrum is observed. At −10°C, the $^1$H spectrum contains the following signals: the singlet at 2.13 ppm of two methyl groups, the signal of the hydride ligand at −23.62 ppm as well as another signal set of two methyl groups and the corresponding signal of the hydride ligand at −23.52 ppm in the ratio of 5:1. An increase in the acid concentration leads to a change in the intensity ratio of the signal sets to 1:2. An addition of one drop of trifluoromethanesulfonic acid in nitromethane to this solution causes the appearance of the signals of the cationic cluster **9**: 2.28 (1H, s, $CH_3$), 2.68 (1H, s, $CH_3$), and −22.99 (1H, s, Os–H–Os), the signals at −23.52 (Os–H–Os) and 2.09 of the methyl groups still being observed in the spectrum in the ratio of 3:1. At low temperatures, trifluoroacetic acid does not seem to generate the cationic complex **9** but only $Os_3(\mu\text{-H})(CO)_9(\mu_3\text{-}\sigma,2\eta^2\text{-C}{\equiv}CCMe_2OC\text{-}OCF_3)$ (**19**) is formed showing the signals at −23.52 ppm and 2.13 ppm of the methyl groups.

Protonation of **3** yields the cationic cluster $[Os_3(\mu\text{-H})(CO)_9(\mu_3\text{-}2\sigma,2\eta^2\text{-C}{\equiv}CCH_2]^+$ (**8**), which appeared to be even less stable than **9**. The addition of $CF_3COOH$ in $CD_3NO_2$ to a solution of **3** in $CD_2Cl_2$ at −50°C results in the features of **8** in the $^1$H NMR spectrum, that is the signals at −21.99 ppm and two singlets of the magnetically non-equivalent protons of the $CH_2$ group at 5.14 and 6.07 ppm. The ratio of the neutral and cationic clusters is 5:1. The addition of two more and then three more drops of trifluoromethanesulfonic acid changes this ratio from 1:1 to 1:3 respectively. In the latter case, the spectrum indicates the degradation products. At −20°C, the initial complex **3** gradually disappears, and on further temperature increase (20°C), the cationic cluster **8** is completely decomposed.

### 3.3. Preparation of phosphonium clusters

The treatment of solutions of the cationic clusters **6–9** with triphenylphosphine in the temperature range −50– −60°C gives new phosphonium derivatives of the $Os_3$ clusters. The cationic complexes **6** and **7** yield $2\sigma,\eta^2$-coordinated derivatives **10** and **11** respectively with four-electron acetylene ligands, while the treatment of cations **8** and **9** with phosphine allowed clusters **12** and **13** respectively to be obtained with the new five-electron phosphonium allenyl ligand (Scheme 5).

IR spectra of **10** and **11** in the carbonyl region exhibit the bands at 1849 and 1845 cm$^{-1}$, respectively, characteristic of the bridging carbonyl groups. The $^1$H NMR spectrum of **10** at −20°C exhibits two doublets of doublets at 3.95 and 4.25 ppm with $J(HH) \sim J(HP) \sim 15$ Hz belonging to the protons of the $CH_2$ group, the multiplet of the phenyl substituent at 7.7 ppm, and the low-field singlet signal of the methyne proton at 8.55 ppm. The $^1$H NMR spectrum of **11** at −20°C shows two doublets of the methyl group at 1.65 and 1.74 pp, with $J(HP) = 6.8$ Hz, the multiplet of the phenyl group, and the low-field singlet signal at 9.29 ppm. With an increase in the temperature to 17°C, two doublet signals of the methyl groups collapse into one broad signal, probably, due to the migration of the $C_3$ ligand relative to the metal core of the cluster. Similar processes were reported for alkyne complexes [4,12]. The addition of triphenylphosphine to solutions of **8** and **9** at −50°C generates the phosphoniumallenyl clusters $Os_3(\mu\text{-H})(CO)_9(\mu_3 - \sigma,2\eta^2\text{-}\overset{+}{P}h_3PC{=}C{=}CR'_2)$ (R′ = H (**12**)) and (R′ = Me (**13**)). The site of the nucleophilic

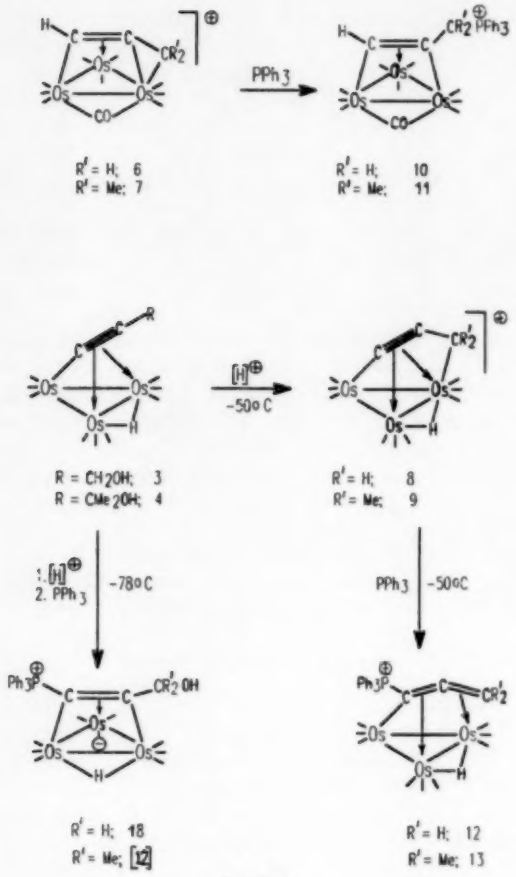


Scheme 5.

attack of the six-electron propargyl ligand can be derived from the $^1$H NMR spectra of complexes **12** and **13**. In the case of **12**, the protons of the $=CH_2$ group give rise to two double doublets with $J(HH) \sim J(HP) \sim 2.8$ Hz, $J(HH) = 2.5$ Hz, $J(HP) = 3.7$ Hz, and the hydride ligand gives rise to singlet at $-22.0$ ppm. The same picture is observed in the case of **13**. The $^1$H NMR spectrum exhibits two singlets at 1.99 and 2.09 ppm of the methyl groups and a singlet at $-23.17$ ppm of the hydride ligand. A small $J$ value for 'H'–'P' interaction in **12**, as well as the lack of the 'H'–'P' interaction in **13**, evidence for the attack of the $\alpha$-carbon atom of the ligand by phosphine which is in accord with the structure involving the phosphonium allenyl ligand proposed for **12** and **13**.

If the reaction of **3** or **4** with an acid is performed at $-78$°C, the ionization does not take place and, therefore, the cationic complexes **8** and **9** are not formed. However, a known reaction of phosphine addition to acetylenic ligands takes place, that is the interaction of the neutral cluster with the neutral nucleophile to form zwitter-ionic derivatives [12]. In our case, compounds $Os_3(\mu\text{-}H)(CO)_9(\mu_3\text{-}2\sigma,\eta^2\text{-}Ph_2PC{\equiv}CCR'_2OH)$ (R' = H (**18**)) and (R' = Me [12]) were obtained.

Thus, in the present paper, protonation of the $Os_3$ clusters coordinated to propargyl alcohol and its derivatives in the $2\sigma,\eta^2$- and $\sigma,2\eta^2$-fashion has been studied. Labile cationic complexes with 5e- and 6e-propargyl ligands were generated and studied by $^1$H and $^{13}$C NMR spectroscopy.

In conclusion, we may state that depending on the nuclearity and coordination mode of the propargyl ligand, the nucleophilic attack can be selectively directed to $C_1$, $C_2$, or $C_3$ ligand atoms.

## Acknowledgment

The authors are deeply grateful to Professor V.I. Bakhmutov for help in measuring and interpreting the NMR spectra. This work was in part supported by the Russian Foundation for Basic Research (project No. 94-03-08167 and 94-03-08338) and the International Science Foundation (grant No. M04300).

## References

[1] (a) V.V. Krivykh, E.S. Taits, P.V. Petrovskii and M.I. Rybinskaya, *Metalloorg. Khim., 2* (1989) 939; (b) V.V. Krivykh, E.S. Taits, P.V. Petrovskii, Yu.T. Struchkov and A.I. Yanovskii, *Mendeleev Commun.*, (1991) 103; (c) V.V. Krivykh, *Metalloorg. Khim., 5* (1992) 213 (*Organomet. Chem. USSR 5* (1992), 113 Engl. Trans. (d) C.P. Casey and C.S. Yi, *J. Am. Chem. Soc., 114* (1992) 6597; (e) P.W. Blosser, J.C. Gallucci and A. Wojcicki, *J. Am. Chem. Soc., 115* (1993) 2994; (f) P.W. Blosser, D.G. Schimpff and A. Wojcicki, *Organometallics, 12* (1993) 1993; (g) T.-M. Huang, J-T. Chen, G.-H. Lee and Y. Wang, *J. Am. Chem. Soc., 115* (1993) 1170; (h) P.I. Stang, C.M. Crittel and A.M. Arif, *Organometallics, 12* (1993) 4799; (i) A. Wojcicki, *New J. Chem., 18* (1994) 61.

[2] (a) K.M. Nicholas, *Acc. Chem. Res., 20* (1987) 207; (b) V.I. Sokolov, I.V. Barinov and O.A. Reutov, *J. Organomet. Chem., 297* (1985) C25; (c) A. Meyer, D.J. McCabe and M.D. Curtis, *Organometallics, 6* (1987) 1491; (d) G.H. Young, N.V. Raphael, A. Wojcicki, M. Calligaris, G. Nardin and N. Bresciani-Rahor, *Organometallics, 10* (1991) 1934; (e) A. Wojcicki, *J. Cluster Sci., 4* (1993) 59.

[3] A.J. Deeming, *Adv. Organomet. Chem., 26* (1986) 1.

[4] S. Aime and A.J. Deeming, *J. Chem. Dalton Trans.*, (1981) 828.

[5] O.A. Kizas, V.V. Krivykh, E.V. Vorontsov and A.A. Koridze, *Izv. Akad. Nauk, Ser. Khim.*, (1993) 1144 (*Bull. Acad. Sci., 42* (1993) 1102).

[6] M. Tachikawa, J.R. Shapley, R.C. Haltiwanger and C.G. Pierpont, *J. Am. Chem. Soc., 98* (1976) 4851.

[7] W. Robinson and G.M. Sheldrick, SHELX, in N.V. Isaacs and M.R. Taylor (eds.), Crystallographic Computing Techniques and New Technologies, Oxford University Press, Oxford, 1988, p.366.

[8] G. Gervasio, *J. Chem. Soc., Chem. Commun.*, (1976) 25.
[9] A.A. Koridze, O.A. Kizas, P.V. Petrovskii, M.G. Ezernitskaya and B.V. Lokshin, *Metalloorgan. Khim. 1* (1988) 1237 (*Organomet. Chem. USSR, 6* (1988) 676).
[10] A.A. Koridze, *Usp. Khim., 5* (1986) 277.
[11] P.-S. Cheng, Y. Chi, S.-M. Peng and G.-H. Lee, *Organometallics, 12* (1993) 250.
[12] R. Henrik, M. McPartlin, A.J. Deeming, S. Hasso and P. Manning, *J. Chem. Soc. Dalton Trans.*, (1982) 899.

ELSEVIER

Journal of Organometallic Chemistry 508 (1996) 49–52

Journal of Organometallic Chemistry

# Reaction of pentaarylantimony with acid halide, aldehyde and ketone

Masahiro Fujiwara [a,*], Mutsuo Tanaka [a], Akio Baba [b], Hisanori Ando [a], Yoshie Souma [a]

[a] *Osaka National Research Institute, AIST, MITI, Ikeda, Osaka 563, Japan*
[b] *Department of Applied Chemistry, Faculty of Engineering, Osaka University, Suita, Osaka 565, Japan*

Received 29 March 1995; in revised form 18 May 1995

**Abstract**

Pentaarylantimony (pentaphenylantimony, penta-*p*-tolylantimony and penta-*p*-chlorophenylantimony) was found to be a mild arylation reagent. The arylation was chemoselective toward aromatic acid halides to give the corresponding aromatic ketones. No direct addition to ketone and acid anhydride occurred. Arylation reactions of aldehyde or ketone were promoted by the addition of Lewis acid. The nucleophilicities of aromatic antimony compounds depend on the number of antimony–aromatic carbon bonds.

*Keywords:* Pentaarylantimony; Acid halide; Aldehyde; Ketone; Chemoselective reaction; Antimony

## 1. Introduction

The reaction behaviors of organoantimony compounds have been recently applied for synthetic organic reactions [1]. Most of studies are performed using trivalent antimony compounds such as triphenyl- [2] and tributylstibine [3] and pentavalent stibonium compounds such as tetraphenylstibonium iodide [4] and methoxide [5]. Recently it was found [3,6] that alkyl organoantimony compounds with five antimony–carbon bonds exhibited unique reactivities for carbon–carbon bond formation different from other 15 group elements such as phosphorus [7], arsenic [8] and bismuth [9]. Although these observations presage novel synthetic reactions using pentavalent organoantimony compounds, their utilization in situ is inevitable because of their extremely low stability so that they can be identified only by using mass spectrometry [10]. On the other hand, aromatic organoantimony compounds bearing five antimony–aromatic carbon bonds (pentaarylantimony) are comparatively stable and can be isolated and purified by recrystallization [11–13]. Although their reaction behaviors and synthetic applications were seldom examined because of their relatively poor reactivity [14], their stable character is more advantageous in the fundamental studies on the properties of organoantimony compounds with five antimony–carbon bonds. In this paper, we wish to report the reactivities of pentaarylantimony to acid halides, aldehydes and a ketone.

## 2. Results and discussion

The results of the reaction of pentaarylantimony with acid halides

$$Ar_5Sb + RCOX \longrightarrow ArCOR \quad (1)$$

are summarized in Table 1. Without any additives pentaphenylantimony [11] reacted with benzoyl chloride to give benzophenone in 79% yield (run 1). This is the first example of the coupling reaction of pentaarylantimony with acid halides, although dipropynyltriphenylantimony [15] and triphenyldimethylantimony [6] have been reported to react with acid halides. Acetonitrile was the solvent of choice, and neither benzene (45%) nor DMF (~0%) were suitable. In contrast to pentaphenylantimony, triphenylstibine and tetraphenylstibonium bromide gave no benzophenone. Although other *para*-substituted benzoyl chloride derivatives and cinnamoyl chloride also afforded the corresponding ketones in good yields (runs 2–5), alkyl derivatives such as hexanoyl chloride gave the coupling product only in low yield (run 6).

* Corresponding author.

0022-328X/96/$15.00 © 1996 Elsevier Science S.A. All rights reserved
*SSDI* 0022-328X(95)05793-0

Table 1
Reaction of pentaarylantimony with acid halides [a]

| run | Antimony | Acid halide | Yield (%) [b,c] |
|---|---|---|---|
| 1 | $Ph_5Sb$ | PhCOCl | 79 |
| 2 | $Ph_5Sb$ | $p$-$ClC_6H_4COCl$ | 77 |
| 3 | $Ph_5Sb$ | $p$-$NO_2C_6H_4COCl$ | 78 |
| 4 | $Ph_5Sb$ | $p$-$MeOC_6H_4COCl$ | 83 |
| 5 | $Ph_5Sb$ | PhCH = CHCOCl | 64 (33) |
| 6 | $Ph_5Sb$ | $n$-$C_5H_{11}COCl$ | 13 |
| 7 | $p$-$Tol_5Sb$ | PhCOCl | 35 |
| 8 [d] | $p$-$Tol_5Sb$ | PhCOBr | 68 |
| 9 [e] | $(p\text{-}ClC_6H_4)_5Sb$ | PhCOCl | 76 |
| 10 | $Ph_5Sb$ | PhCOF | tr (39) |
| 11 [d] | $Ph_5Sb$ | PhCOBr | 87 |
| 12 | $Ph_5Sb$ | EtOCOCOCl | ~100 |
| 13 | $LiSbPh_6$ | $n$-$C_5H_{11}COCl$ | 28 (18) |
| 14 [f] | $Ph_5Sb$ | $n$-$C_5H_{11}COCl$ | 50 |

[a] Reaction conditions: antimony/acid halide = 1/3 mmol, solv. acetonitrile 1 ml, 80°C, 24 h.
[b] Determined by GLC based on an aryl group in pentaarylantimony.
[c] Yields of biphenyl were in parentheses; in other runs, trace amounts of biphenyl were obtained.
[d] 3 h.
[e] Penta-$p$-chlorophenylantimony slightly dissolved in acetonitrile.
[f] Tetrakis (triphenylphosphine) palladium (0.05 mmol) was added.

*Para*-substituted aromatic antimony compounds, penta-*p*-tolylantimony [12] and penta-*p*-chlorophenylantimony [13] were also applicable to give the corresponding ketones in moderate to good yields (runs 7–9). The effect of the substituents in the aryl group to the reactivity of pentaarylantimony was clearly observed. In the case of the homogeneous benzene solvent reaction, the yields of the products with benzoyl chloride increased in the following order, penta-*p*-tolylantimony (29%) < pentaphenylantimony (45%) < penta-*p*-chlorophenylantimony (79%). This tendency is in accord with the stability of aryl anion. The comparison of reactivity of three acid halides, benzoyl fluoride, chloride and bromide is also suggestive (runs 1, 10, 11). The good agreement of the reactivity order, Br > Cl > F, was observed between pentaarylantimony, and organozinc and -cadmium reagents [16]. In the cases of zinc and cadmium reagents, the coordination of carbonyl oxygen to the metal is excluded, and a direct substitution reaction is suggested [16]. As the Lewis acidity of pentaarylantimony is thought to be very poor [17], the reaction of pentaarylantimony with acid halides seems to proceed in a nucleophilic manner similar to organozinc and -cadmium reagents.

This arylation procedure could be expanded to ethyl oxalyl chloride, yielding ethyl benzoylformate quantitatively (run 12). Ethyl benzoylformate is very susceptible to organometallic compounds, even those such as organocadmium reagents which are known to be versatile for chemoselective ketone synthesis from acid halides [18]. Ethyl benzoylformate was recovered quantitatively in the reaction with an equimolar amount of pentaphenylantimony under the same reaction conditions. The formation of triphenylmethanol was not naturally observed at all in the reaction of benzoyl chloride with pentaphenylantimony. Benzoic and phthalic anhydride were also recovered completely, while it was known that they readily reacted with organocadmium reagents to afford the corresponding ketones [16]. Furthermore, a nitro function tolerated this arylation by pentaphenylantimony, furnishing the corresponding phenyl ketone in a good yield (run 3). This high chemoselectivity has not been observed in other organometallic compounds.

For the sake of improving the yield of the coupling product with hexanoyl chloride, we attempted two modifications. Pentaphenylantimony is known to react with phenyllithium to form lithium hexaphenylantimonate [11]. When this ate-complex was used for the coupling reaction, the product yield increased from 13% to 28% (run 13), although it is hard to dissolve in acetonitrile. On the other hand, the addition of tetrakis(triphenylphosphine)palladium obviously improved the yield of the *n*-pentyl phenyl ketone (run 14) [18]. It is well known that the coupling reaction of various organometallic compounds with acid halides is catalyzed by palladium complexes [19].

The reaction of pentaphenylantimony with aldehydes was next studied

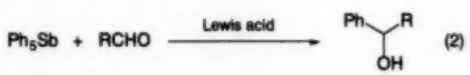

(2)

and the results are summarized in Table 2. Although no benzhydrol was obtained in the absence of any promoter (run 1), the nucleophilic addition to aldehydes was effected by Lewis acid. Benzaldehyde (run 2) and *n*-hexanal (run 6) produced the corresponding phenylated alcohols in 95 and 56% yields, respectively, in the presence of an equimolar amount of titanium tetrachloride to the aldehydes. Boron trifluoride etherate also

Table 2
Reaction of pentaphenylantimony with aldehydes [a]

| Run | Aldehyde | Lewis acid | Temp. | Yield (%) [b] |
|---|---|---|---|---|
| 1 | PhCHO | – | 40°C | 0 |
| 2 | PhCHO | $TiCl_4$ | −78°C → rt | 95 |
| 3 | PhCHO | $BF_3 \cdot Et_2O$ | −78°C → rt | 54 |
| 4 | PhCHO | $AlCl_3$ | −78°C → rt | 7 |
| 5 | PhCHO | $SnCl_4$ | −78°C → rt | 0 |
| 6 | $n$-$C_5H_{11}CHO$ | $TiCl_4$ | −78°C → rt | 56 |

[a] Reaction conditions: antimony/aldehyde/Lewis acid = 1.5/0.5/0.5 mmol, solv. dichloromethane 4 ml, 3 h.
[b] Determined by GLC based on a phenyl group in pentaphenylantimony.

promoted the reaction moderately (run 3). However, other Lewis acids such as aluminum chloride and tin tetrachloride were not effective at all (run 4, 5). Even in the case of aldehyde, neither triphenylstibine nor tetraphenylstibonium bromide gave any benzhydrol. On the other hand, 1-phenylcyclohexanol was obtained in a modest yield (38%) in dichloromethane at reflux for 3 h

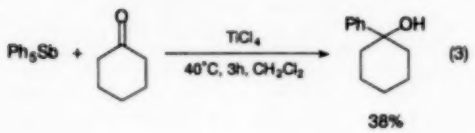


although cyclohexanone did not react with pentaphenylantimony under similar conditions to the reaction with aldehyde.

The best yield (95%; run 2) of benzhydrol was observed in the reaction where benzaldehyde and titanium tetrachloride were first mixed to form a complex. The addition of benzaldehyde to the mixed solution of pentaphenylantimony and titanium tetrachloride afforded the product in low yield (18%). Moreover, no benzhydrol was obtained in the reaction of titanium tetrachloride with the solution of pentaphenylantimony and the aldehyde. It seems that the formation of the complex of aldehyde with Lewis acid is essential to accomplish this addition reaction. Titanium tetrachloride-mediated reaction of pentaphenylantimony with aldehyde may proceed by nucleophilic attack of one phenyl group of pentaphenylantimony on the carbonyl carbon of aldehyde activated by the coordination of titanium tetrachloride (Fig. 1).

From the results of the reactions using three types of organoantimony compound, the nucleophilicities of aryl groups of those organoantimony compounds seem to be different. Triarylantimony is regarded as a base rather than a nucleophile. In the case of tetraarylstibonium bromide, the anionic species is bromide and all aryl groups are included in the cationic stibonium moiety. Therefore, the nucleophilicity of these aryl groups seems to be very poor. On the other hand, aryl groups of pentaarylantimony have enough nucleophilicity. However, the reaction of one aryl group of pentaarylantimony forms tetraarylstibonium-type compounds which are inactive for the reaction. Therefore, only one aryl group of pentaarylantimony reacted in all cases.

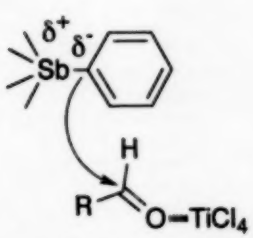


Fig. 1. A plausible reaction scheme of pentaphenylantimony with aldehyde mediated by titanium tetrachloride.

In conclusion, arylation utilizing pentaarylantimony, which has been hardly employed in organic synthesis, could be applicable for acid halides, aldehydes or a ketone. The direct arylation has a high chemoselectivity to aromatic acid halides. On the other hand, the reactions with aldehydes or a ketone were promoted by the addition of titanium tetrachloride.

## 3. Experimental section

### 3.1. Materials

All acid halides, aldehydes, Lewis acids and cyclohexanone, which are commercially available, were used without further purification. All solvents were used after distillation. Triphenylantimony was a commercial product, which was purified by recrystallization (ethanol). Tetraphenylstibonium bromide was prepared by the described method [20]. Pentaphenylantimony, penta-*p*-tolylantimony and penta-*p*-chlorophenylantimony were obtained by a modified method [21]. Tetrakis(triphenylphosphine)palladium was purchased from Tokyo Kasei Industry. NMR spectra were determined on a JEOL $\alpha$-500 (500 MHz) spectrometer.

#### 3.1.1. Pentaphenylantimony

The THF solution (50 ml) of triphenylantimony dibromide (38 mmol) obtained from triphenylantimony and bromine [22] was added dropwise to a THF solution (100 ml) of phenylmagnesium bromide (80 mmol) for 30 min in ice bath. The resulting solution was refluxed for 3 h. After cooling, the THF solution was poured into a 2 M HCl aqueous solution (130 ml) with some ice. The precipitate formed was filtrated, washed with water and dried under reduced pressure. The crude product was recrystalized from acetonitrile; purified isolated yield was 80%; m.p. 170–172 °C (lit. 168.5–170 °C) [11]; $^1$H NMR ($CDCl_3$): $\delta$ 7.0–7.2 (m, Ph) ppm. Penta-*p*-tolylantimony and penta-*p*-chlorophenylantimony were obtained in a similar manner to pentaphenylantimony.

#### 3.1.2. Penta(p-tolyl)antimony

Purified isolated yield was 55%; m.p. 201–203 °C (hexane) (lit. 189 °C) [12], $^1$H NMR ($CDCl_3$): $\delta$ 2.3 (s, 15H, $CH_3$); 7.0–7.1 (m, 10H, $C_6H_4$); 7.2–7.3 (m, 10H, $C_6H_4$) ppm.

*3.1.3. Penta(p-chlorophenyl)antimony*

Purified isolated yield was 26%, mp. 218–222 °C (benzene/petroleum ether) (lit. 197 °C) [13], $^1$H NMR ($CDCl_3$): δ 7.0–7.1 (m, $ClC_6H_4$) ppm.

*3.2. Reaction procedure*

*Typical procedure of the reaction of pentaarylantimony with acid halide*

To a solvent solution (1 ml) of pentaarylantimony (1 mmol) was added an acid halide (3 mmol) at room temperature. The resulting mixture was stirred for 24 h at 80 °C under nitrogen atmosphere. After removing the solvent under reduced pressure, the residue was subjected to silica-gel column chromatography, giving the crude product (benzene). Purification was performed by recrystallization using benzene/hexane (benzophenone, *p*-chlorobenzophenone, *p*-nitrobenzophenone, *p*-methoxybenzophenone, chalcone) or distillation (*n*-pentyl phenyl ketone and ethyl benzoylformate). All products were identified by $^1$H NMR and GLC by reference to commercial standards.

*Typical procedure of the reaction of pentaphenylantimony with aldehyde*

To the dichloromethane solution (2 ml) of an aldehyde (0.5 mmol) was added at −78 °C a Lewis acid (0.5 mmol), and then the dichloromethane solution (2 ml) of pentaphenylantimony (1.5 mmol) was mixed. Temperature was gradually increased and finally reached room temperature after 3 h. The resulting mixture was washed with an aqueous solution of sodium bicarbonate and organic materials were extracted by diethyl ether. The organic layer was dried over anhydrous magnesium sulfate. After removing the solvent under reduced pressure, the residue was subjected to silica-gel column chromatography, giving the crude product (benzene). Purification was performed by recrystallization using benzene/hexane (benzhydrol) or distillation (1-phenyl-1-hexanol). All products were identified by $^1$H NMR and GLC satisfactorily.

*The procedure of the reaction of pentaphenylantimony with cyclohexanone*

To the dichloromethane solution (2 ml) of cyclohexanone (0.5 mmol) was added at room temperature titanium tetrachloride (0.5 mmol), and then the dichloromethane solution (2 ml) of pentaphenylantimony (1.5 mmol) was mixed. The resulting solution was refluxed for 3 h. The work-up procedure was the same as that in the reaction with aldehyde.

## References and notes


[1] L.D. Freedman and G.O. Doak, in F.R. Hartley (ed.), *The Chemistry of the Metal–Carbon Bond*, Vol. 5, Wiley, New York, 1989, p. 397.

[2] D.H.R. Barton, N. Ozbalik and M. Ramesh, *Tetrahedron, 44* (1989) 5661; C.S. Cho, K. Tanabe and S. Uemura, *Tetrahedron Lett., 35* (1994) 1275; C.S. Cho, K. Tanabe, O. Itoh and S. Uemura, *J. Org. Chem., 60* (1995) 274.

[3] Y.-Z. Huang, *Acc. Chem. Res., 25* (1992) 182.

[4] M. Fujiwara, M. Imada, A. Baba and H. Matsuda, *J. Org. Chem., 53* (1988) 5974; M. Fujiwara, A. Baba and H. Matsuda, *Bull. Chem. Soc. Jpn., 63* (1990) 1069.

[5] M. Fujiwara, K. Hitomi, A. Baba and H. Matsuda, *Synthesis* (1990) 106; M. Fujiwara, K. Hitomi, A. Baba and H. Matsuda, *Chem. Lett.* (1994) 875.

[6] Y.-Z. Huang and Y. Liao, *J. Org. Chem., 56* (1991) 1381; L.-J. Zhang, Y.-Z. Huang, H.-X. Jiang, J. Duan-Mu and Y. Liao, *J. Org. Chem., 57* (1992) 774.

[7] B.E. Maryanoff and A.B. Reitz, *Chem. Rev., 89* (1989) 863.

[8] D. Lloyd, I. Gorney and R.A. Orimiston, *Chem. Soc. Rev., 16* (1987) 45.

[9] J.-P. Finet, *Chem. Rev., 89* (1989) 1487.

[10] L. Yu, G.-X. Fu, Y. Liao, C.-W. Xu and Y.-Z. Huang, *Org. Mass Spectrom., 25* (1990) 645.

[11] W. Wittig and K. Clauss, *Liebigs Ann. Chem., 577* (1952) 26.

[12] C. Brabant, J. Hubert and A.L. Beauchamp, *Can. J. Chem., 51* (1973) 2951.

[13] B. Raynier, B. Waegell, R. Commandeur and H. Mathais, *Nouv. J. Chim., 3* (1979) 393.

[14] G.A. Razuvaev, N.A. Osanova and Y.A. Sangalov, *J. Gen. Chem. USSR, 37* (1967) 197; K.W. Shen, W.E. McEwen and A.P. Wolf, *J. Am. Chem. Soc., 91* (1969) 1283; M. Schlosser, T. Kadibelban and G. Steinhoff, *Liebigs Ann. Chem., 743* (1971) 25; W.E. McEwen and C.-T. Chung, *Phosphorus, 4* (1974) 91; G.F. Lanneau, R.J. Wikholm, C.T. Lin and W.E. McEwen, *J. Organomet. Chem., 85* (1975) 179; M.S. Raizada and H.L. Nigam, *J. Indian Chem. Soc., 63* (1986) 722; V.A. Dodonov, O.P. Bolatova and A.V. Gushchin, *J. Gen. Chem. USSR, 58* (1988) 629.

[15] A palladium-catalyzed coupling reaction of dipropynyltrimethylantimony with acid chlorides has been reported: Y. Yamamoto, T. Okinaka, M. Nakatani and K. Akiba, *Nippon Kagaku Kaishi* (1987) 1286.

[16] D.A. Shirley, in R. Adams (ed.), *Organic Reactions*, Vol. 8, Wiley, New York, 1954, p. 28.

[17] The reaction using pentavalent organoantimony compounds as Lewis acid was reported. Even tetraphenylstibonium triflate with an excellent leaving group is inert to the carbonyl group; M. Fujiwara, M. Imada, A. Baba and H. Matsuda, *Tetrahedron Lett., 30* (1989) 739.

[18] H. Gilman and J.F. Nelson, *Rec. Trav. Chim., 55* (1936) 518.

[19] J.K. Stille, *Angew. Chem. Int. Ed. Engl., 25* (1986) 508, J. Yamada and Y. Yamamoto, *J. Chem. Soc., Chem. Commun.* (1987) 1302, D.H.R. Barton, N. Ozbalik and M. Ramesh, *Tetrahedron, 44* (1988) 5661, C.S. Cho, K. Itotani and S. Uemura, *J. Organomet. Chem., 443* (1993) 253.

[20] J. Chatt and F.G. Mann, *J. Chem. Soc.* (1940) 1195.

[21] T.C. Thepe, R.J. Garascia, M.A. Selvoski and A.N. Patel, *Ohio J. Sci., 77* (1977) 134.

[22] W.J. Lile and R.J. Menzies, *J. Chem. Soc.* (1950) 617.

ELSEVIER

Journal of Organometallic Chemistry 508 (1996) 53–57

Journal of Organometallic Chemistry

# Synthesis of some $\mu$-hydroxo-, phenoxo- and O,O-acetylacetonato-arylgold(III) complexes. Crystal structure of $[Au(C_6H_4NO_2-2)_2(\mu\text{-}OH)]_2 \cdot 2Et_2O$

José Vicente [a,*], María Dolores Bermúdez [b,*], Francisco J. Carrión [b], Peter G. Jones [c]

[a] *Grupo de Química Organometálica, Departamento de Química Inorgánica, Facultad de Química, Universidad de Murcia, Apdo 4021, Murcia 30071, Spain*

[b] *Grupo de Ciencia de Materiales e Ingeniería Metalúrgica, Departamento de Ingeniería de Materiales y Fabricación, Escuela Politécnica Superior, Universidad de Murcia, 30203 Cartagena, Spain*

[c] *Institut für Anorganische und Analytische Chemie, Technische Universität Braunschweig, Postfach 3329, 38023 Braunschweig, Germany*

Received 29 March 1995

**Abstract**

A new synthesis of *cis*-$Me_4N[Au(C_6H_4NO_2-2)_2Cl_2]$ (**1**) is reported, involving the reaction of $[Hg(C_6H_4NO_2-2)Cl]$ with $Me_4N[AuCl_4]$ in the presence of $Me_4NCl$. Reaction of **1** with NaOPh or with Tlacac (acac = acetylacetonate) in the presence of $NaClO_4$ yields $Na[Au(C_6H_4NO_2-2)_2(OPh)_2]$ (**2**) or *cis*-$[Au(C_6H_4NO_2-2)_2(O,O\text{-}acac)]$ (**3**), respectively. Complex **3** reacts with $PPh_3$ to give *trans*-$[Au(C_6H_4NO_2-2)_2(C\text{-}acac)(PPh_3)]$ (**4**). Treatment of **2** in acetone with NaOH gives $[Au(C_6H_4NO_2-2)_2(\mu\text{-}OH)]_2$ (**5**), which is also formed when a solution of **2** in $CHCl_3$/hexane is exposed to water. The crystal structure of $\mathbf{5} \cdot 2Et_2O$ shows that it is a centrosymmetric dimer with two hydroxo groups bridging two $Au(C_6H_4NO_2-2)$ moieties. The features of the structure include short Au–C bond distances (1.992(5) Å, 1.995(5) Å) and hydrogen bonding between the bridging OH groups and diethyl ether molecules.

*Keywords:* Gold; Crystal structure; Acetylacetonato $\mu$-hydroxo complexes

## 1. Introduction

Few organogold(III) complexes with oxoanionic ligands are known and many of them are unstable or moisture sensitive [1]. Thus, $[AuMe_2(OH)]_4$ detonates when dry just by touching [2], and the complexes $[AuMe_2(X)L]$, where X = $ClO_4$, $CF_3SO_3$, *p*-$MeC_6H_4SO_3$ or $NO_3$ and L = $PPh_3$, decompose at room temperature to give ethane and [Au(X)L] [3]. $[AuMe_2(OSiMe_3)]_2$ is thermally stable but sensitive to moisture [4]. As far as we are aware, only three O,O-acetylacetonato- complexes are known [5], and no HO- or RO-arylgold(III) complexes. This paper reports the synthesis of new O,O-acetylacetonato- and the first HO- and RO-arylgold(III) complexes, advantage being taken of the high stability of the C–Au bonds in *ortho*-nitrophenyl gold complexes [6].

## 2. Results and discussion

The synthesis of *cis*-$Me_4N[Au(C_6H_4NO_2-2)_2Cl_2]$ (**1**) has been achieved by transmetallation (1:1, refluxing 18 h in acetone) [7]:

$$2[Hg(C_6H_4NO_2-2)_2] + [AuCl_4]^- \rightarrow [Au(C_6H_4NO_2-2)_2Cl_2]^- + 2[Hg(C_6H_4NO_2-2)Cl]$$

However, because $Me_4NCl$ symmetrizes the by-product $[Hg(C_6H_4NO_2-2)Cl]$,

$$2[Hg(C_6H_4NO_2-2)Cl] + Cl^- \rightarrow [Hg(C_6H_4NO_2-2)_2] + [HgCl_3]^-$$

it is possible to improve the yield of **1**, with respect to the nitrophenyl group, by carrying out the reaction of $Me_4N[AuCl_4]$ with $[Hg(C_6H_4NO_2-2)Cl]$ in the presence of $Me_4NCl$ (1:2:2, EtOH, refluxing 5 h, see Scheme

* Corresponding authors.

Elsevier Science S.A.
*SSDI* 0022-328X(95)05772-2

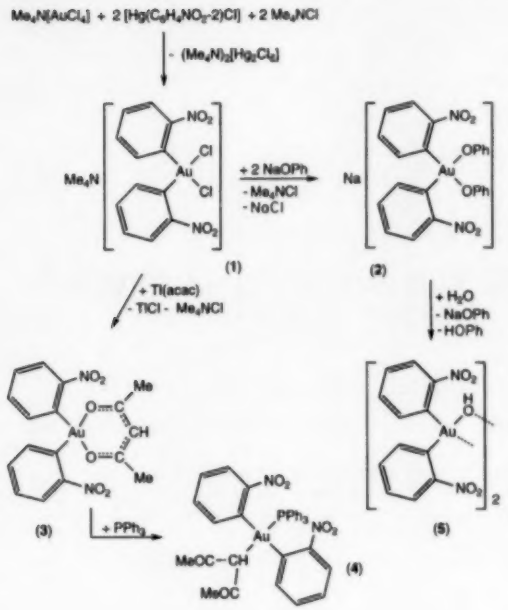


Scheme 1.

1). We have previously used a similar method to prepare $[Au(C_6H_4NO_2-2)Cl]^-$ [8].

Reactions of **1** with NaOR (R = Me, Et) gave metallic gold even at low temperature and under an inert atmosphere. However, **1** reacts with NaOPh (1:3, $CH_2Cl_2$, room temperature) to give $Na[Au(C_6H_4NO_2-2)_2(OPh)_2]$ (**2**). As far as we are aware, **2** is the first arylgold(III) species containing an $RO^-$ ligand. Some aryl- or alkyl-oxodimethylgold(III) complexes ($AuMe_2(OR)PPh_3$) (R = Ph, tolyl, $CH_2CF_3$, $CH(CF_3)_2$) have recently been reported [9]. The complex $[AuMe_2(OH)]_4$ dissolves in aqueous NaOH to give a solution which is believed to contain $Na[AuMe_2(OH)_2]$ [10].

Tlacac (acac = acetylacetonate) reacts with **1**, in the presence of $NaClO_4$, (1:1, acetone) to give *cis*-$[Au(C_6H_4NO_2-2)_2(O,O\text{-}acac)]$ (**3**). If the reaction is carried out in the absence of $NaClO_4$, a mixture of **1** and **3** is obtained, probably because formation of the partially soluble $Me_4NCl$ leads to establishment of the equilibrium $\mathbf{3} + 2Cl^- \leftrightarrow \mathbf{1} + acac^-$. When $NaClO_4$ is present formation of the insoluble NaCl and $Me_4NClO_4$ displaces the equilibrium towards **3**. As far as we are aware, only two other (O,O-acac)diarylgold(III) complexes (*cis*-$[Au(R)_2(O,O\text{-}acac)]$ (R = 2,2′-biphenyl [5a], $C_6F_5$ [5b]) and one cationic (O,O-acac)monoarylgold(III) complex ($[Au(C,N'\text{-}C_6H_4N{=}NPh-2)(O,O\text{-}acac)]ClO_4$ [5c]) have been described. The complex $[AuMe_2(O,O\text{-}acac)]$ was reported long ago [11]. Addition of $PPh_3$ to **3** (1:1, $CH_2Cl_2$, room temperature) gives *trans*-$[Au(C_6H_4NO_2-2)_2(C\text{-}acac)(PPh_3)]$ (**4**) in which the acac ligand is C-bonded rather than O,O-bonded and the cis geometry has changed to trans (as indicated by $^1H$ NMR spectroscopy, as described below). The reaction of $[AuMe_2(O,O\text{-}acac)]$ with tertiary phosphines results in formation of an equilibrium with *cis*-$[AuMe_2(C\text{-}acac)(PR_3)]$. Only in the case of $PMe_2Ph$ could the C-acac complex be isolated [12]. Activation of C–H bonds in ketones (MeCOR) takes place with some (C-acac)(2-phenylazophenyl)gold(III) derivatives to give ketonyl complexes [5c]. The fact that **3** and **4** are stable in acetone is in accordance with the proposed pathway for this C–H activation process [5c].

Attempts were made to grow single crystals of **2** by the liquid diffusion method using $CH_2Cl_2$/n-hexane. The only suitable crystals obtained for X-ray diffraction turned out to be of $[Au(C_6H_4NO_2-2)_2(\mu\text{-}OH)]_2 \cdot 2Et_2O$ (**5**), presumably as a result of reaction with traces of water. This hydroxo-bridged complex was also made, although in low yield because of partial reduction to metallic gold, by reaction of **1** with NaOH. The homologous methylgold(III) derivative is a tetramer $[AuMe_2(\mu\text{-}OH)]_4$ [2] whereas 1-hydroxo-2,3,4,5-tetraphenylauracyclopentadiene is, like complex **5**, a dimer [13]. When dilute aqueous HCl was added to **5**, reaction took place with decomposition and no pure chloro complex was isolated.

Reactions between complex **2** and various protic acids did not lead to new complexes. Thus, **2** was stirred in acetone in an attempt to obtain new acetonylgold(III) complexes by C–H activation [5c], but no reaction was observed. Although some reaction took place with phenylacetylene in solution, as indicated by a change in colour from colourless to yellow, the starting complex was recovered unchanged after partial removal of the solvent and addition of $Et_2O$/n-hexane. Equilibrium reactions have previously been described between phenoxogold(III) complexes, *cis*-$[AuMe_2(OPh)(PPh_3)]$, and RH = methylcyanoacetate, malononitrile or phenylacetylene [9]. However, while the first gave a mixture of the starting complex and *cis*-$[AuMe_2(R)(PPh_3)]$, the latter two gave the corresponding R–Au(III) complexes. Complexes **3** and **4** were also recovered unchanged after treatment with phenylacetylene. This is in contrast with the observed behaviour of acetylacetonatogold(I) complexes towards alkynes [14].

### *2.1. Spectroscopic properties and structure of the complexes.*

#### *2.1.1. IR spectra*

The phenoxo derivative **2** shows strong bands in the region 1250–1300 $cm^{-1}$ assignable to $\nu$(C–O) [9], and strong bands at 690 and 760 $cm^{-1}$, typical of monosub-

stituted phenyl groups (PhO). This last set of bands is not observed for the hydroxo species **5**. The acac complex **3** shows $\nu$(CO) at 1550 and 1570 $cm^{-1}$, while the phosphine adduct **4** shows broad bands at 1650 and 1675 $cm^{-1}$ as expected for chelating O,O-acac and terminal C-acac groups, respectively [5c]. All the complexes show bands at 1330–1340 $cm^{-1}$ and ca. 1510 $cm^{-1}$, which have been shown to correspond to $\nu_{sym}(NO_2)$ and to $\nu_{asym}(NO_2)$, respectively, when the nitrophenyl group is not coordinated to the metal centre [15].

### 2.1.2. NMR spectra

The $^1H$ NMR spectrum of the acac complex **3** shows a singlet resonance at 2.0 ppm for methyl groups and at 5.5 ppm for the methynic proton. This resonance appears in **4** as a doublet at 4.2 ppm ($^3J_{HP}$ = 12 Hz). $^{13}C$ NMR of **4** shows only one resonance for the C attached to the nitro group (151.8 ppm) and 12 resonances in the range 122–135 ppm. The methyne carbon gives a doublet at 67.62 ppm with $^2J_{CP}$ = 86 Hz. These data indicate a trans geometry for **4**. The antisymbiotic effect has proved useful in understanding some related changes in geometry in arylpalladium(II) complexes [16]. In terms of this effect, an aryl and a phosphine ligand should have a destabilizing effect on each other when attached to class b metal ions such as palladium(II). No resonance assignable to $\mu$-hydroxo protons was observed in the $^1H$ NMR spectrum of **5**. The same feature has been reported for other bridging hydroxo complexes [17].

### 2.2. Crystal structure of complex 5

The crystal structure of **5** is the first for a nitroarylgold(III) complex (see Fig. 1). The complex displays crystallographic inversion symmetry and the central $Au_2O_2$ ring is thus exactly planar; the transannular Au...Au distance is 3.150(1) Å. The coordinate at gold is, as expected, planar, with a mean deviation of 0.06 Å. The Au–C bond distances (1.992(5) Å, 1.995(5) Å) are among the shortest Au(III)–C bond distances so far reported [18]. The only two other crystal structures reported of hydroxoorganogold(III) complexes ($[AuMe_2(OH)]_4$ [19] and 1-hydroxo-2,3,4,5-tetraphenylauracyclopentadiene [13b]) were not of sufficient accuracy to allow comparison with the data for complex **5**. The Au–O distances (2.073(4) Å, 2.075(4) Å) in **5** are longer than in $Sr[Au(OH)_4]_2$ (1.980(8) Å) [20]. This difference can partly be attributed to the change from a bridging to a terminal OH ligand. Thus, in $[Au_2O_6]^{6-}$ the Au–O distances are 2.17 Å and 2.12 Å, respectively [21]. Additionally, the greater trans influence of an aryl than of an OH ligand must be taken into account.

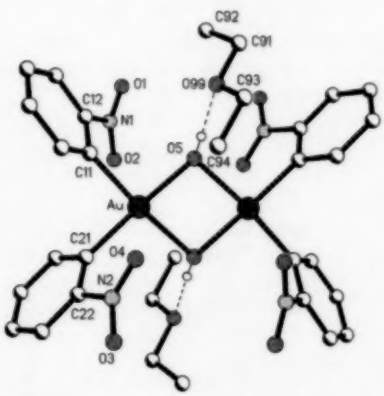


Fig. 1. The structure of compound **5** in the crystal. Radii are arbitrary.

Each nitro group is inclined to its own aryl ring (N1 by 35°, N2 by 20°) and in an anti disposition with respect to the hydrogen of the neighbouring *cis*-OH group. The OH hydrogen atoms are (necessarily) mutually trans and both are hydrogen bonded to a diethyl ether molecule (O...O 2.700(5) Å, O–H...O 178°).

The presence of the nitro group causes significant widening of the corresponding C–C($NO_2$)–C angle (123.0(5)°, 123.9(5)°) with little change in the bond distances of the aryl ring (1.375(8)–1.404(8) Å). The opposite effect is observed for the C–C(Au)–C bond angle (117.0(5)°, 115.6(5)°). Both facts have been attributed to the operation of the -I rather than the -M effect of the nitro group [22]. The C–N (1.477(7) Å, 1.498(7) Å) and N–O (1.211(6)–1.230(7) Å) bond distances are similar to those previously reported [22]. The short intramolecular ONO...Au distances (Au...O2 2.866 Å, Au...O4 2.845 Å) correspond to weak axial interactions.

## 3. Experimental section

The compound [Hg($C_6H_4NO_2$ – 2)Cl] was prepared as previously described [23]. Reactions were carried out at room temperature and NMR spectra were recorded on a Bruker AC-200 or a Varian XL-300 spectrometer, and referenced to internal $SiMe_4$ ($^1H$, $^{13}C$) or external $H_3PO_4$ ($^{31}P$) unless otherwise stated.

### 3.1. Cis-$Me_4N[Au(C_6H_4NO_2 - 2)_2Cl_2]$ (1)

To a yellow solution of $Me_4N[AuCl_4]$ (530 mg, 1.30 mmol) in EtOH (50 $cm^3$) were added solid [Hg($C_6H_4NO_2$ – 2)Cl] (919 mg, 2.60 mmol) and $Me_4NCl$ (2.64 mg, 2.70 mmol). The mixture was stirred under reflux until complete (ca. 5 h). The solvent was removed decoloration and the residue extracted with $CH_2Cl_2$ (3 × 5 $cm^3$). The extract was filtered through anhydrous $MgSO_4$ and the filtrate evaporated to ca. 1 $cm^3$. Addition of $Et_2O$ (15 $cm^3$) afforded a white

precipitate which was recrystallized from $CH_2Cl_2$/$Et_2O$ (629 mg, 1.10 mmol) to give **1** [7]. Yield, 84%; $^1H$ NMR (DMSO): δ 3.10 (s, 12 H, $Me_4N^+$), 7.22 (m, 2H, $C_6H_4$), 7.33 (m, 2H, $C_6H_4$), 7.52 (m, 2H, $C_6H_4$), 7.87 (m, 2H, H3) ppm; $^{13}C$ NMR (DMSO): δ 150.97 (C2), 125.32, 126.27, 133.74, 135.12 (C1, C3–C6, two nuclei must be accidentally isochronous), 54.58 ($Me_4N^+$), ppm.

### 3.2. *Na[Au(C$_6$H$_4$NO$_2$ − 2)$_2$(OPh)$_2$]* (2)

Solid **1** (189 mg, 0.33 mmol) was added to a suspension of NaOPh (170 mg, 0.99 mmol) in $CH_2Cl_2$ (30 $cm^3$), and the mixture stirred for 6 h. The solution was then filtered through anhydrous $MgSO_4$ and the filtrate evaporated to ca. 1 $cm^3$. Addition of $Et_2O$/n-hexane (1:1, 10 $cm^3$) produced a pale yellow precipitate which was filtered off, washed with $Et_2O$ and dried under vacuum. Yield, 64%; M.p. 100°C (decomp.); $\Lambda_M = 87$ $\Omega^{-1}$ $cm^2$ $mol^{-1}$ ($5 \times 10^{-4}$ mol $dm^{-3}$); $^1H$ NMR: δ 6.44 (m, 2H), 6.73 (m, 4H), 7.55 (m, 10H, $C_6H_4$ + PhO), 7.85 (m, 2H, H3) ppm. Anal. Calc. for $C_{24}H_{18}AuN_2NaO_6$: C, 44.3; H, 2.8; N, 4.3; Au, 30.3%. Found: C, 43.9; H, 3.0; N, 4.1; Au, 30.7%.

### 3.3. *[Au(C$_6$H$_4$NO$_2$ − 2)$_2$(O,O-acac)]* (3)

To an acetone solution (50 $cm^3$) of **1** (56 mg, 0.10 mmol) were added solid Tl(acac) (acac = acetylacetonate) (29.5 mg, 0.10 mmol) and $NaClO_4$ (13.2 mg, 0.09 mmol). The mixture was stirred for 7 h and the solvent was then removed. The residue was extracted with $CH_2Cl_2$ ($2 \times 5$ $cm^3$) and the solid filtered through anhydrous $MgSO_4$. Evaporation of the filtrate to a volume of ca. 1 $cm^3$ and addition of $Et_2O$ (10 $cm^3$) gave a white precipitate (40 mg, 0.07 mmol) which was recrystallized from $CH_2Cl_2$/$Et_2O$. Yield, 75%; M.p., 205°C (decomp.); $^1H$ NMR: δ 2.00 (s, 6H, Me), 5.47 (s, 1H, CH), 7.30 (m, 4H, H4, H5), 7.52 (m, 2H, H6), 8.00 (m, 2H, H3) ppm. Anal. Calc. for $C_{17}H_{15}AuN_2O_6$: C, 37.8; H, 2.8; N, 5.2; Au, 36.5%. Found: C, 37.6; H, 2.4; N, 5.1; Au, 36.8 %.

Table 1
Atomic coordinates ($\times 10^4$) and equivalent isotropic displacement parameters ($Å^2 \times 10^3$) for **5**. *U*(eq) is defined as one third of the trace of the orthogonalized $U_{ij}$ tensor

| | *x* | *y* | *z* | *U*(eq) |
|---|---|---|---|---|
| Au | 5185.7(1) | 5783.4(1) | 5619.9(1) | 15.1(1) |
| C(11) | 4935(4) | 7109(4) | 5626(3) | 17.0(12) |
| C(12) | 4071(4) | 7437(4) | 5503(4) | 21.3(13) |
| C(13) | 3882(5) | 8349(4) | 5413(3) | 29(2) |
| C(14) | 4583(5) | 8959(4) | 5455(4) | 33(2) |
| C(15) | 5461(4) | 8654(4) | 5572(4) | 30.0(15) |
| C(16) | 5637(4) | 7746(4) | 5651(4) | 22.2(12) |
| N(1) | 3293(3) | 6812(4) | 5499(3) | 28.0(13) |
| O(1) | 2650(3) | 7001(4) | 5071(3) | 44.3(13) |
| O(2) | 3321(3) | 6156(3) | 5945(3) | 31.7(11) |
| C(21) | 5695(4) | 5873(4) | 6726(3) | 17.5(12) |
| C(22) | 6590(4) | 5774(4) | 6930(3) | 21.9(12) |
| C(23) | 6905(4) | 5780(5) | 7710(4) | 30.5(15) |
| C(24) | 6313(4) | 5928(5) | 8327(4) | 34(2) |
| C(25) | 5398(4) | 6031(4) | 8156(4) | 27(2) |
| C(26) | 5101(4) | 6010(4) | 7370(3) | 24.7(14) |
| N(2) | 7281(3) | 5622(4) | 6286(3) | 30.9(14) |
| O(3) | 8010(3) | 5295(4) | 6492(3) | 60(2) |
| O(4) | 7107(3) | 5846(3) | 5603(3) | 42.5(12) |
| O(5) | 4558(3) | 5587(3) | 4519(2) | 17.2(9) |
| C(91) | 4349(5) | 6695(5) | 2671(4) | 38(2) |
| C(92) | 3519(5) | 7018(5) | 3095(5) | 50(2) |
| C(93) | 5912(5) | 6417(5) | 2885(4) | 39(2) |
| C(94) | 6598(5) | 6298(6) | 3544(5) | 50(2) |
| O(99) | 5054(3) | 6613(3) | 3250(3) | 30.3(11) |

Table 2
Selected bond lengths (Å) and angles (deg.) for **5**

| | | | |
|---|---|---|---|
| Au–C(21) | 1.992(5) | C(22)–N(2) | 1.498(7) |
| Au–C(11) | 1.995(5) | C(23)–C(24) | 1.367(9) |
| Au–O(5) | 2.073(4) | C(24)–C(25) | 1.392(8) |
| Au–O(5)#1 | 2.075(4) | C(25)–C(26) | 1.381(9) |
| C(12)–N(1) | 1.477(7) | O(5)...O(99) | 2.700(7) |
| N(1)–O(1) | 1.221(6) | Au...Au#1 | 3.150(1) |
| N(1)–O(2) | 1.222(6) | | |
| C(21)–Au–C(11) | 90.0(2) | O(1)–N(1)–O(2) | 124.2(6) |
| C(21)–Au–O(5) | 173.8(2) | O(1)–N(1)–C(12) | 117.9(5) |
| C(11)–Au–O(5) | 93.3(2) | O(2)–N(1)–C(12) | 117.9(5) |
| C(21)–Au–O(5)#1 | 95.7(2) | O(4)–N(2)–O(3) | 123.7(5) |
| C(11)–Au–O(5)#1 | 173.9(2) | O(4)–N(2)–C(22) | 118.9(5) |
| O(5)–Au–O(5)#1 | 81.2(2) | O(3)–N(2)–C(22) | 117.3(5) |
| C(12)–C(11)–C(16) | 117.0(5) | Au–O(5)–Au#1 | 98.8(2) |
| C(11)–C(12)–C(13) | 123.0(5) | C(14)–C(13)–C(12) | 118.6(6) |
| C(13)–C(14)–C(15) | 120.0(6) | C(16)–C(15)–C(14) | 120.5(6) |
| C(15)–C(16)–C(11) | 120.8(6) | C(22)–C(21)–C(26) | 115.6(5) |
| C(21)–C(22)–C(23) | 123.9(5) | C(24)–C(23)–C(22) | 119.3(6) |
| C(23)–C(24)–C(25) | 119.3(6) | C(26)–C(25)–C(24) | 120.0(6) |
| C(25)–C(26)–C(21) | 121.9(6) | | |

Symmetry transformation used to generate equivalent atoms: #1; $-x+1, -y+1, -z+1$.

### 3.4. *Trans-[Au(C$_6$H$_4$NO$_2$ − 2)$_2$(C-acac)(PPh$_3$)]* (4)

Solid $PPh_3$ (26 mg, 0.10 mmol) was added to a $CH_2Cl_2$ solution (30 $cm^3$) of **3** (53 mg, 0.10 mmol) and the mixture stirred for 3 h. The solvent was evaporated to a volume of ca. 1 $cm^3$ and $Et_2O$/n-hexane (1:1, 10 $cm^3$) added to give a pale yellow precipitate (68 mg, 0.09 mmol). Yield, 89%; M.p., 165°C; $^1H$ NMR: δ 2.00 (s, 6H, Me), 4.23 [d, 1H, CH, $^3J_{HP} = 12$ Hz], 7.28–7.77 (m, 21H, $C_6H_4$ + $PPh_3$), 8.40 [d, 2H, H3, $^3J_{HH} = 8$ Hz] ppm; $^{31}P$ NMR, δ 24.93 ppm; $^{13}C$ NMR, δ 206.00 (CO), 151.87 (C2), 134.38, 134.12, 133.90, 132.59, 131.84, 131.79, 130.99, 129.25, 128.97, 128.75, 126.34, 122.97 (C1, C3–C6, Ph), 67.62 (CH), 30.62 (Me) ppm. Anal. Calc. for $C_{35}H_{30}AuN_2O_6P$: C, 52.4; H, 3.8; N, 3.5; Au, 24.5%. Found: C, 52.4; H, 3.9; N, 3.2; Au, 24.1 %.

### 3.5. *[Au(C$_6$H$_4$NO$_2$ − 2)$_2$(μ-OH)$_2$]$_2$* (5)

Solid NaOH (31.2 mg, 0.78 mmol) was added to an acetone solution (25 $cm^3$) of **1** (150 mg, 0.26 mmol)

and the suspension was stirred for 15 h, during which decomposition to metallic gold was observed. Evaporation of the solvent, extraction of the residue with $CH_2Cl_2$ and filtration of the extract through Celite gave a yellow solution which was concentrated to a volume of ca. 1 $cm^3$. Addition of n-hexane (20 $cm^3$) gave a pale yellow precipitate which was recrystallized from $CH_2Cl_2$/n-hexane. Yield, 35%; M.p., 210°C (decomp.). $^1H$ NMR: $\delta$ 7.9–6.4 (m, aryl) ppm. Anal. Calc. for $C_{24}H_{18}Au_2N_4O_{10}$: C, 31.5; H, 2.0; N, 6.1; Au, 43.0%. Found: C, 32.1; H, 2.3; N, 5.7; Au, 43.4%.

Crystal data. $C_{32}H_{38}Au_2N_4O_{12}$, $M_r = 1064.6$, orthorhombic, Pbca, $a = 14.801(2)$ Å, $b = 14.788(3)$ Å, $c = 16.627(2)$ Å, $V = 3639.4$ Å$^3$, $Z = 4$, $D_x = 1.943$ Mg m$^{-3}$, $\lambda$(Mo K$\alpha$) = 0.71073 Å, $\mu = 8.2$ mm$^{-1}$, $F(000) = 2048$, $T = -130$°C.

Data collection and reduction. A colourless flattened pyramid ca. $0.45 \times 0.4 \times 0.2$ mm$^3$ was mounted in inert oil and transferred to the cold gas stream of the diffractometer (Siemens P4 with LT-2 low temperature attachment). A total of 3671 unique intensities were measured to $2\theta = 50°$. Cell constants were refined from setting angles of 65 reflections to $2\theta = 25°$. An absorption correction based on $\psi$-scans gave transmission factors 0.55–0.97.

Structure solution and refinement. The structure was solved by the heavy-atom method and refined on $F^2$ using the program SHELXL-93. The hydroxyl H atom was refined with DFIX; others were included with a riding model. The weighting scheme was $w^{-1} = [\sigma^2(F_o^2) + (0.034P)^2]$, with $P = (F_o^2 + 2F_c^2)/3$. The final $wR(F^2)$ for all reflections was 0.059, with a conventional $R(F)$ of 0.026 for 2201 reflections with $I > 2\sigma I$, for 230 parameters; $S = 0.88$, max. $\Delta/\sigma = 0.001$, max. $\Delta\rho = 1.0$ e Å$^{-3}$. Final atomic coordinates are given in Table 1, with selected bond lengths and angles in Table 2.

Full details of the structure determination have been deposited at the Fachinformationszentrum Karlsruhe, Gesellschaft für wissenschaftlich-technische Information mbH, D-76344 Eggenstein-Leopoldshafen, Germany, from where this material can be obtained on quoting the full literature citation and the reference number CSD 401615.

## Acknowledgments

We thank Dirección General de Investigación Científica y Técnica (PB92-0982-C) and the Fonds der Chemischen Industrie for financial support. FJC is grateful to Ministerio de Educación y Ciencia (Spain) for a grant.

## References

[1] Schmidbaur, *Gmelin Handbuch der Anorganischen Chemie, Organogold Compounds*, Springer, Berlin, 1980; R. Usón and A. Laguna, *Coord. Chem. Rev.*, *70* (1986) 1.
[2] S.J. Harris and R.S. Tobias, *Inorg. Chem.*, *8* (1969) 2259.
[3] S. Komiya and J.K. Kochi, *J. Am. Chem. Soc.*, *98* (1976) 7599.
[4] H. Schmidbaur and M. Bergfeld, *Inorg. Chem.*, *5* (1966) 2069.
[5] (a) R. Usón, J. Vicente, J.A. Cirac and M.T. Chicote, *J. Organomet. Chem.*, *198* (1980) 105; (b) R. Usón, A. Laguna, M. Laguna and M. Abad, *J. Organomet. Chem.*, *249* (1983) 437; (c) J. Vicente, M.D. Bermúdez, M.P. Carrillo and P.G. Jones, *J. Chem. Soc., Dalton Trans.*, (1992) 1975, and references cited therein.
[6] J. Vicente, M.D. Bermúdez, J. Escribano, M.P. Carrillo and P.G. Jones, *J. Chem. Soc., Dalton Trans.*, (1990) 3083, and references cited therein.
[7] J. Vicente, M.T. Chicote, A. Arcas, M. Artigao and R. Jiménez, *J. Organomet. Chem.*, *247* (1983) 123.
[8] J. Vicente, A. Arcas and M.T. Chicote, *J. Organomet. Chem.*, *252* (1983) 257.
[9] T. Sone, M. Iwata, N. Kasuga and S. Komiya, *Chem. Lett.*, (1991) 1949.
[10] M.G. Miles, G.E. Glass, R.S. Tobias, *J. Am. Chem. Soc.*, *88* (1966) 5738.
[11] F.H. Brain and G.S. Gibson, *J. Chem. Soc.*, (1939) 762.
[12] S. Komiya and J.K. Kochi, *J. Am. Chem. Soc.*, *99* (1977) 3695.
[13] (a) E.H. Braye, W. Hübel and I. Caplier, *J. Am. Chem. Soc.*, *83* (1961) 4406; (b) M. Peteau-Boisdenghien, J. Meunier-Piret and M. van Meerssche, *Crys. Struct. Commun.*, *4* (1975) 375.
[14] J. Vicente, M.T. Chicote, I. Saura-Llamas and M.C. Lagunas, *J. Chem. Soc. Chem. Commun.*, (1992) 915; J. Vicente, M.T. Chicote and M.D. Abrisqueta, *J. Chem. Soc., Dalton Trans.*, (1995) 497.
[15] J. Vicente, M.T. Chicote, J. Martin, P.G. Jones, C. Fittschen and G.M. Sheldrick, *J. Chem. Soc., Dalton Trans.*, (1986) 2215.
[16] R.G. Pearson, *Inorg. Chem.*, *12* (1973) 712; J. Dehand, J. Jordanov, M. Pfeffer and M. Zinsius, *C.R. Acad. Sci., Ser. C*, *281* (1975) 651; M. Pfeffer, D. Grandjean and G. Le Borgne, *Inorg. Chem.*, *20* (1981) 4426; C. Arlen, M. Pfeffer, O. Bars and G. Le Borgne, *J. Chem. Soc., Dalton Trans.*, (1986) 359.
[17] See, for example, J. Vicente, M.T. Chicote, M.C. Ramírez de Arellano and P.G. Jones, *J. Chem. Soc. Dalton Trans.*, (1992) 1839.
[18] P.G. Jones, *Gold Bull.*, *14* (1981) 159.
[19] C.E. Glass, J.H. Konnert, M.G. Miles, D. Britton and R.S. Tobias, *J. Am. Chem. Soc.*, *90* (1968) 1131.
[20] P.G. Jones and G.M. Sheldrick, *Acta Crystallogr.*, *C40* (1984) 1776.
[21] H. Klassen and R. Hoppe, *Nature*, *63* (1976) 387.
[22] J. Vicente, A. Arcas, M.V. Borrachero, E. Molíns and C. Miravitlles, *J. Organomet. Chem.*, *441* (1992) 487, and references cited therein.
[23] A.N. Nesmeyanov, *Selected Works in Organic Chemistry*, Pergamon, Oxford 1963.

ELSEVIER

Journal of Organometallic Chemistry 508 (1996) 59–67

Journal of Organometallic Chemistry

# Catalytic hydroformylation of (1*S*,5*S*)-(−)- and (1*R*,5*R*)-(+)-β-pinene: stereoselective synthesis and spectroscopic characterization of (1*S*,2*R*,5*S*)-, (1*S*,2*S*,5*S*)-, (1*R*,2*R*,5*R*)- and (1*R*,2*S*,5*R*)-10-formylpinane

Fabrizio Azzaroni, Paolo Biscarini, Silvia Bordoni, Giuliano Longoni *, Emanuela Venturini

*Dipartimento di Chimica Fisica ed Inorganica, viale del Risorgimento 4, 40136 Bologna, Italy*

Received 6 March 1995

**Abstract**

(1*S*,5*S*)-(−)- and (1*R*,5*R*)-(+)-β-pinene have been hydroformylated in toluene to give (1*S*,2*R*,5*S*)- and (1*R*,2*S*,5*R*)-10-formylpinane with up to 95% diastereoselectivity using bimetallic $CoRh(CO)_7$ as a catalyst; the latter was generated in situ from preformed $Co_2Rh_2(CO)_{12}$ or a stoichiometric mixture of either $[Rh_4(CO)_{12}]$ or $[Rh_6(CO)_{16}]$ and $[Co_2(CO)_8]$. At 70–125°C and under 60 atm of syngas, the yields of hydroformylated products do not exceed 30% because of the concomitant isomerization of β- to α-pinene. In all cases the catalyst is recovered as a mixture of soluble cobalt carbonyl derivatives and a crystalline precipitate that contains most of the rhodium, mainly as $[Rh_6(CO)_{16}]$. Comparable yields and diastereoselectivities were obtained from reactions in tetrahydrofuran with a mixture of $[Rh_4(CO)_{12}]$ and $[N(PPh_3)_2]Cl$ as the catalyst precursor.

The corresponding (1*S*,2*S*,5*S*)- and (1*R*,2*R*,5*R*)-10-formylpinanes, along with the corresponding alcohols, were obtained diastereoselectively by use of bimetallic Co–Rh or homometallic Rh carbonyl catalysts modified with bis(diphenylphosphine)ethane (dppe). When unidentate phosphines such as triphenylphosphine were used in place of dppe, as the ligand/metal (L/M) ratio was raised the diastereoselectivity of both the hetero- and the homo-metallic catalytic system fell progressively, and was completely lost for $L/M \geq 4$. However, a further increase in L/M to ca. 70–100 allows chemio- and diastereo-selective synthesis of both the (1*S*,2*S*,5*S*)- and (1*R*,2*R*,5*R*)-10-formylpinane.

The (1*S*,2*R*,5*S*)-, (1*S*,2*S*,5*S*)-, (1*R*,2*R*,5*R*)- and (1*R*,2*S*,5*R*)-10-formylpinane diastereomers were isolated by distillation under reduced pressure and fully characterized by IR, UV, $^1H$ and $^{13}C$ NMR and circular dicroism (CD) spectroscopy, and mass spectrometry.

The possible factors favouring the diastereoselective hydroformylation of β-pinenes under the conditions used are discussed.

*Keywords:* Pinene; Hydroformylation; Cobalt; Carbonyl; Rhodium; Stereoselectivity

## 1. Introduction

Naturally occurring terpenes are a source of inexpensive olefins that upon hydroformylation give aldehydes of relevance to the perfume industries, and some show antimicrobial activity [1–5]. Stereoselective hydroformylation of chirally pure terpenes could be of value for the industrial production of optically active intermediates that could be employed for optical resolution or asymmetric synthesis [6,7]. Enantiomerically pure (+) and (−) 3-formyl pinanes and 2-formylbornane were obtained several years ago by catalytic hydroformylation of α-pinenes, and spectroscopically characterized [8,9]. The hydroformylation of β-pinene has been investigated with several Co and Rh homometallic catalysts in the 60–140°C temperature range and under 35–300 atm of syngas [1,8,10–12]. However, owing to the isomerization of β-pinene during catalysis to the thermodynamic mixture of β- and α-pinene ($\beta/\alpha \approx 4:96$) and to a less pronounced difference in the steric hindrance of the two enantiotopic faces of the olefin, a complex mixture of several regio-isomeric and diastereomeric aldehydes was often obtained.

These are shown in Fig. 1, with the adopted numbering scheme. For instance, $[Rh_6(CO)_{16}]$ catalyzes the hydroformylation of β-pinene to the *cis*-10-for-

* Corresponding author.

0022-328X/96/$15.00 © 1996 Elsevier Science S.A. All rights reserved
*SSDI* 0022-328X(95)05778-1

mylpinane with a good diastereoselectivity, but the activity was very low and β-pinene was found to isomerize to α-pinene [12]. When $[Co_2(CO)_8]$ was used as catalyst, it displayed even lower hydroformylation *TF* values, and the rate of isomerization of β- to α-pinene was increased, the thermodynamic ratio being reached within 3 h starting from pure β-pinene. Furthermore, probably as a consequence of the greater ability of cobalt to catalyze the hydroformylation of cyclic olefins [1], *trans*-3-formylpinane became the major product [12]. Low activity and ready isomerization of β- to α-pinene was also observed with the dinuclear $[\{Rh(\mu\text{-}S^tBu)(CO)P(OPh)_3\}_2]$, which afforded a ca. 1:1 mixture of *cis*-10- and *trans*-3-formylpinane [10]. In contrast, both $[RhCl(CO)(PPh_3)_2]$ and $[HRh(CO)(PPh_3)_3]$, in the presence of free phosphine, are very active [1,11]. At a low phosphine/rhodium ratio ($PPh_3/Rh = 11$), $[HRh(CO)(PPh_3)_3]$ shows very little stereoselectivity, and the *cis*- and *trans*-10-formylpinanes are obtained in comparable amounts. However, at higher $PPh_3/Rh$ ratios (78–79), whereas $[RhCl(CO)(PPh_3)_2]$ remained only weakly stereoselective, $[HRh(CO)(PPh_3)_3]$ catalyzed the synthesis of *cis*-10-formylpinane with good selectivity [1]. Replacement of triphenylphosphine by tris(2-t-butylphenyl)phosphite as the ancillary ligand on rhodium caused a significant drop in the activity but allowed the *trans*-10-formylpinane, which is usually obtained only in minor amounts, to be produced with a very high selectivity [1].

Since only a very few spectroscopic data for these 10-formylpinanes were available and the selectivity displayed by some catalysts appeared puzzling, we decided to undertake an investigation of the hydroformylation of (1*S*,5*S*)-(−)- and (1*R*,5*R*)-(+)-β-pinene, with the aim of gaining a better understanding of the factors favouring diastereospecific hydroformylation. An outcome of the work was that we obtained in high optical purity (> 90%) the (1*S*,2*R*,5*S*)-(−)-, (1*S*,2*S*,5*S*)-(−)-, (1*R*,2*S*,5*R*)-(+)- and (1*R*,2*R*,5*R*)-(+)-10-formylpinane diastereomers, which were characterized spectroscopically by IR, UV, and $^1H$ and $^{13}C$ NMR spectroscopic studies, and by mass spectrometry and circular dichroism (CD) investigations.

## 2. Results

### 2.1. Hydroformylation of (1S,5S)-(−)- and (1R,5R)-(+)-β-pinene

The high diastereoselectivity observed in the hydroformylation of α-pinene [6,10,11], and more recently of a t-butyl-oxazoline derivative [13], was attributed to the difference in steric hindrance between the two enan-

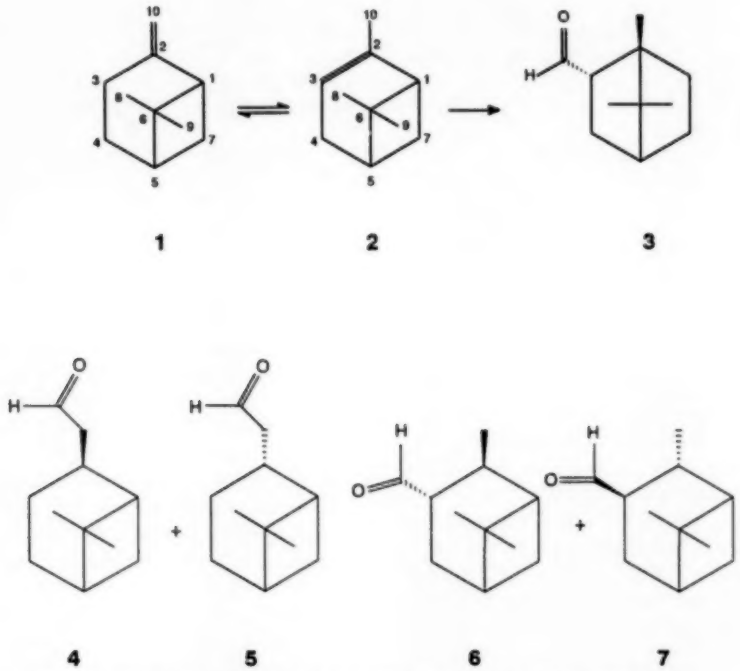


Fig. 1. Possible products of the hydroformylation of β-pinene with Co and Rh catalysts.

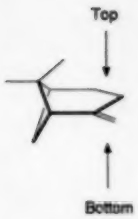


Fig. 2.

tiotopic faces of the olefin. This difference for the exocyclic double bond of β-pinene is small and so the diastereoselective hydroformylation should be less but not trivial. It seemed puzzling, however, that metal carbonyl centres without substituents [12] and completely substituted metal centres [1,11] could both selectively attack the olefin from the least hindered face (i.e. from the bottom in Fig. 2), whereas increased steric hindrance by the ancillary ligand favoured attack on the most hindered face (i.e. from the top in Fig. 2) [1]. We therefore, undertook a study of the hydroformylation of β-pinene with a series of catalysts which could be expected to be very active and which could be thought to involve either metal carbonyl centres without substituents or those bearing ancillary ligands of a size comparable to CO, viz. the bimetallic Co–Rh carbonyl catalysts [14,15] and the $[Rh_4(CO)_{12}]/Cl^-$ system [16]. Indeed, it is known that bimetallic Co–Rh catalytic systems derived either from preformed $[Co_2Rh_2(CO)_{12}]$ or from stoichiometric mixtures of $[Co_2(CO)_8]$ and $[Rh_4(CO)_{12}]$ or $[Rh_6(CO)_{16}]$ often give hydroformylation rates much higher than those observed for the corresponding homometallic catalysts [14,15]. One possible explanation of this synergetic effect can be derived from the observation that under a carbon monoxide or a syngas atmosphere the bimetallic Co–Rh cluster mentioned above, and also mixtures of Co and Rh homometallic clusters, readily undergo equilibration with $CoRh(CO)_7$ [17]. As can also be inferred from studies carried out on carbonyl-substituted derivatives under syngas, $[CoRh(CO)_{7-x}L_x]$ ($x = 0$–2) [18] probably activate hydrogen by oxidative addition to the M–M bond leading to the formation of $[HCo(CO)_4]$ and $[HRh(CO)_3]$ [19,20] without the requirement of carbon monoxide elimination as for $[Co_2(CO)_8]$ [21], or the breaking of several Rh–Rh bonds as for both $[Rh_4(CO)_{12}]$ and $[Rh_6(CO)_{16}]$. Moreover, it is known that on increasing the temperature and in the absence of sufficient CO soluble $[Rh_4(CO)_{12}]$ is converted into $[Rh_6(CO)_{16}]$ which separates out from catalytic solutions owing to its very low solubility. Therefore, a second reason for this synergetic effect may be the ability of $[Co_2(CO)_8]$ to maintain most of the rhodium in solution through the above equilibrium with $[CoRh(CO)_7]$. Consequently, it appeared conceivable that attainment of a high hydroformylation rate through the generation of the catalyst precursor $[CoRh(CO)_7]$ under experimental conditions in which Rh carbonyls are diastereoselective and the isomerization rate of β- to α-pinene mainly catalyzed

Table 1
Hydroformylation of (1*S*,5*S*)-(−)-β-pinene [a]

| Catalyst | Pressure (atm) | Temp. (°C) | Time (h) | Conversion (%) | Selectivity (%) [b] | | |
|---|---|---|---|---|---|---|---|
| | | | | | 4 | 5 | 3+6+7 |
| $[Co_2Rh_2(CO)_{12}]$ | 60 | 100 | 1 | 32 [c] | 1.6 | 95 | 3 |
| $[Rh_4(CO)_{12}] + [Co_2(CO)_8]$ | 60 | 70 | 5 | 17 [c] | 1.9 | 88 | 4.5 |
| $[Rh_4(CO)_{12}] + [Co_2(CO)_8]$ | 60 | 100 | 1 | 31 [c] | 1.6 | 92 | 4.4 |
| $[Rh_4(CO)_{12}] + [Co_2(CO)_8]$ [d] | 60 | 100 | 3 | 30 [c] | 2.2 | 91 | 4.8 |
| $[Rh_4(CO)_{12}] + [Co_2(CO)_8]$ | 60 | 125 | 0.5 | 32 [c] | 0.6 | 76 | 12.5 |
| $[Rh_4(CO)_{12}]/2Cl^-$ | 60 | 125 | 8 | 30 [c] | 7.4 | 64 | 10.6 |
| $[Rh_4(CO)_{12}]/2Cl^-$ [e] | 60 | 125 | 8 | 33 [c] | 10.6 | 82 | 5.4 |
| $[Rh_4(CO)_{12}] + PPh_3$ [f] | 60 | 150 | 5 | 20 | 52 | 46 | <1 |
| $[Rh_4(CO)_{12}] + PPh_3$ [g] | 60 | 100 | 5 | 62 | 94 | 2 | <1 |
| $[Rh_4(CO)_{12}] + PPh_3$ [g] | 60 | 125 | 5 | 96 | 94 | 4 | <1 |
| $[Rh_4(CO)_{12}] + PCy_3$ [h] | 60 | 125 | 5 | 51 | 85 | 12 | 2 |
| $[Rh_4(CO)_{12}]$ + dppe [i] | 60 | 150 | 5 | 15 | 93 [l] | 4 [l] | <1 |

[a] $[M] = 5 \times 10^{-3}$ M, [pinene] = 1 M, toluene as solvent and $CO/H_2 = 1$, if not otherwise stated.
[b] A difference from 100% selectivity is due to the presence of hydrogenated products.
[c] Due to isomerization of β- to α-pinene, only conversion into oxygenated products is given.
[d] $CO/H_2 = 2$.
[e] THF as solvent.
[f] $PPh_3/M = 4$; the activity dropped after ca. 3 h due to progressive deactivation of the catalyst.
[g] $PR_3/M = 100$.
[h] $PR_3/M = 20$.
[i] dppe/Rh = 2; dppe = bis(diphenylphosphine)ethane.
[l] Approximately 1:1.5 mixture of aldehyde and alcohol.

by Co is relatively slow [12], could facilitate an efficient and diastereoselective synthesis of 10-formylpinanes.

A few selected results obtained with the above mixed metal catalysts in the 70–150°C temperature range and under 60 atm of syngas in the hydroformylation of (1*S*,5*S*)-(−)- and (1*R*,5*R*)-(+)-2-methylene-6,6-dimethyl-bicyclo[3.1.1]heptane [**1**, (1*S*,5*S*)-(−)-β-pinene and **1'**, (1*R*,5*R*)-(+)-β-pinene] enantiomers are collected in Tables 1 and 2, respectively.

First, the overall catalysis of preformed $[Co_2Rh_2(CO)_{12}]$ and of 2:1 molar mixtures of $[Co_2(CO)_8]$ and $[Rh_4(CO)_{12}]$ were very similar in activity and selectivity. In both cases, after depressurization and cooling to ambient temperature at the end of each catalytic run, the rhodium was recovered almost quantitatively as a crystalline precipitate essentially of pure $[Rh_6(CO)_{16}]$ while most of the cobalt remained in solution as a mixture of carbonyl compounds. The segregation of the two metals when also starting from $[Co_2Rh_2(CO)_{12}]$, and the consequent loss of heterometallic Co–Rh bonds, is in keeping with the known reactivity of both $[Co_2Rh_2(CO)_{12}]$ and $[CoRh(CO)_7]$ under CO and $H_2$ [19,20]. Secondly, the performances of the above catalytic systems were almost unchanged upon adding fresh substrate, repressurization to 60 atm with syngas and heating at 100°C. In contrast, in both cases the reaction solutions separated from $[Rh_6(CO)_{16}]$ precipitate showed very poor activity upon addition of fresh substrate and recycling. As a consequence, only 2:1 molar mixtures of $[Co_2(CO)_8]$ and $[Rh_4(CO)_{12}]$ were routinely used for most of the subsequent experiments.

As shown in Tables 1 and 2, under 60 atm of syngas the activity of these systems increases with temperature. The average hydroformylation *TF* values with a 1 M concentration of (1*S*,5*S*)-(−)-β-pinene and a $5 \times 10^{-3}$ M overall concentration of metal were 5–6 $h^{-1}$ at 70°C, ca. 50–60 $h^{-1}$ at 100°C and in the 100–120 $h^{-1}$ range at 125°C. Unfortunately, under these conditions the rate of isomerization of β- to α-pinene is about twice as fast and the yields of hydroformylated products never exceed 30–35%. Both the reaction rates and the selectivities are insensitive to the composition of the gas composition over a wide range of $CO/H_2$ molar ratios. Significant drops in activity were only observed on increasing the $CO/H_2$ molar ratio to 4–6. It appears likely that the hydroformylation is almost exclusively carried out by $[HRh(CO)_x]$ rather than by $[HCo(CO)_x]$ species (see below), otherwise the selectivity of the bimetallic Co–Rh system would be surprising in view of the reported [8,12] performances of $[Co_2(CO)_8]$ in related experiments. Evidently, under the experimental conditions adopted hydroformylation at cobalt is almost completely depressed by the combination of mild temperature and relatively high CO partial pressure. It is well known that the apparent order of CO partial pressure in Co-catalyzed hydroformylation reactions is −1 at $p_{CO} > 10$ atm and is > 0 only for $p_{CO} < 10$ atm, whereas rhodium shows a similar inversion of the apparent reaction order of CO at ca. 40 atm [21,22].

The bimetallic Co–Rh system under 60 atm of syngas starts to lose its high selectivity only at reaction temperatures above 125°C, and this is only partially offset by a concomitant increase of the partial pressure of syngas or of CO. In all conditions, the major product (85%–96%) of the catalysis consists of (1*S*,2*R*,5*S*)-(−)-10-formylpinane (**5**) from (−)-β-pinene and (1*R*,2*R*,5*R*)-(+)-10-formylpinane (**5'**) from (+)-β-pinene. The products were isolated in a pure state by fractional distillation under vacuum. The epimeric (1*S*,2*S*,5*S*)-(**4**) and (1*R*,2*R*,5*R*)-10-formylpinane (**4'**) are only detected in small amounts (gas chromatographic analysis) and are undetectable in the $^1H$ and $^{13}C$ NMR spectra of distilled samples. These attributions are based on full spectroscopic characterization (see below) and retention times, since **4** and **5** (as well as **4'** and **5'**), often referred to as *cis* and *trans* diastereomers, can be separated by gas chromatography using capillary columns.

Table 2
Hydroformylation of (1*R*,5*R*)-(+)-β-pinene [a]

| Catalyst | Pressure (atm) | Temp. (°C) | Time (h) | Conversion (%) | Selectivity (%) [b] | | |
|---|---|---|---|---|---|---|---|
| | | | | | **4'** | **5'** | **3 + 6 + 7** |
| $[Rh_4(CO)_{12}] + [Co_2(CO)_8]$ | 60 | 100 | 5 | 21 [c] | 2.1 | 87 | 8 |
| $[Rh_4(CO)_{12}] + [Co_2(CO)_8]$ | 60 | 125 | 2 | 34 [c] | 3.3 | 82 | 12.5 |
| $[Rh_4(CO)_{12}]/2Cl^-$ [d] | 60 | 125 | 8 | 27 [c] | 4.5 | 78 | 12.1 |
| $[Rh_4(CO)_{12}] + PPh_3$ [e] | 60 | 125 | 8 | 94 | 95 | 4 | < 1 |
| $[Rh_4(CO)_{12}] + PCy_3$ [f] | 60 | 125 | 8 | 28 | 93 | 4 | < 1 |

[a] [M] = $5 \times 10^{-3}$ M, [pinene] = 0.5 M, toluene as solvent and $CO/H_2 = 1$, if not otherwise stated.
[b] A difference from 100% selectivity is due to hydrogenated products.
[c] Due to isomerization of β- to α-pinene, only conversion into oxygenated products is given.
[d] THF as solvent.
[e] $PPh_3/Rh = 100$.
[f] $PCy_3/Rh = 20$.

In addition to alcohols, the impurities which accompany **5** (or **5'**) are isomeric aldehydes which show rather different retention times and slightly different fragmentation patterns but identical mass peaks in the mass spectrum. For instance, the M − 15 fragment is systematically more abundant in these aldehydes than in **4** and **5**. Consequently, structures such as **3**, **6** and, to a minor extent **7**, appear the most likely. Unfortunately, since these isomeric aldehydes were always produced in small amounts in mixtures, our attempts at fractional distillation under vacuum to isolate a sample suitable for NMR spectroscopy failed.

Since our attribution of a *trans* stereochemistry to **5** was in contrast with previous findings in the hydroformylation of β-pinene with $[Rh_6(CO)_{16}]$ [12], we extended our investigations to a second active catalytic system, which can be generated from $[Rh_4(CO)_{12}]$ by addition of stoichiometric amounts of halide ions. CIR studies have shown that under syngas (60–150 atm) and in the presence of 1–3 equiv. of chloride ions, $[Rh_4(CO)_{12}]$ and $[Rh_6(CO)_{16}]$ readily disproportionate to mixtures of $[Rh(CO)_2Cl_2]^-$, $[Rh(CO)_4]^-$, $[Rh_5(CO)_{15}]^-$ and, possibly, $[HRh(CO)_4]$ [16]. The above mixtures are active in the hydroformylation of formaldehyde to glycolaldehyde [16]. As shown in Tables 1 and 2, the above mixtures with an $[N(PPh_3)_2]Cl/[Rh_4(CO)_{12}]$ molar ratio of 1:2 were also active in the hydroformylation of β-pinene both in toluene and in THF solution. Although their activity is less than that of the Co–Rh bimetallic system, the selectivity is comparable. The *trans* diastereomers **5** and **5'** are obtained stereoselectively. As with the Co–Rh system, and in keeping with the acidity of the rhodium carbonyl hydride derivatives, the hydroformylation yields do not exceed ca. 30% because of concomitant isomerization of β- to α-pinene.

The most notable difference in selectivity between the unsubstituted bimetallic Co–Rh carbonyl, as well as the $Cl^-[Rh_4(CO)_{12}]$ catalytic system investigated by us, and the homometallic carbonyl-substituted or unsubstituted rhodium catalysts previous investigated is the almost exclusive formation of the *trans* isomer **5** (or **5'**) in our experiments, rather than the *cis* isomer **4** (or **4'**) generally obtained by other workers [1,8,10,12]. To gain some understanding of the factors effecting selectivity, as well as to evaluate their effect on activity, we investigated the hydroformylation of β-pinene with $[Co_2(CO)_8]/[Rh_4(CO)_{12}]$ mixtures or with $[Rh_4(CO)_{12}]$ in the presence of phosphines. Since the phosphine-modified bimetallic system did not display any significant synergetic effect attributable to the presence of both Co and Rh, only the homometallic rhodium system was investigated in detail. A few significant results are collected at the bottom of Tables 1 and 2. First, the triphenylphosphine-modified $[Rh_4(CO)_{12}]$ catalytic systems, under experimental conditions identical to those adopted for the $[Co_2(CO)_8]$-modified $[Rh_4(CO)_{12}]$ catalyst, display less activity. For instance, with $PPh_3/Rh$ molar ratios $\leq 4$, the observed initial *TF* values were in the range 8–30 $h^{-1}$. Furthermore, within 3 or 4 h significant deactivation of all catalysts occurred. Concomitantly, the selectivity toward the *trans* diastereomer **5** decreased on increasing the $PPh_3/Rh$ molar ratio, so that with $PPh_3/Rh = 4$ a ca. 1:1 mixture of the diastereomers **4** and **5** is obtained. As expected from previous reports [1], upon increasing the $PPh_3/Rh$ ratio to 100, an almost complete switch of selectivity towards the *cis* diastereomer **4** (or **4'**) was observed, with *TF* values of ca. 20 $h^{-1}$. Although the activities are not directly comparable with those observed with $[HRh(PPh_3)_3(CO)]$ in the presence of free $PPh_3$ as catalyst, due to differences in the experimental conditions [1], the selectivities observed with $[Rh_4(CO)_{12}]$ modified with triphenylphosphine are exactly the same. This is in keeping with the known chemistry of $[Rh_4(CO)_{12}]$ and triphenylphosphine. Indeed, it has been reported that progressive substitution of the carbonyls of $[Rh_4(CO)_{12}]$ gives $[Rh_4(CO)_8(PPh_3)_4]$ [23]. Further addition of triphenylphosphine results in degradation to the binuclear $[Rh_2(CO)_4(PPh_3)_4]$ that oxidatively adds dihydrogen to give $[HRh(CO)_2(PPh_3)_2]$ [24].

As shown in Tables 1 and 2, diastereomers **4** and **4'** were also obtained with a selectivity up to 93% on replacing the unidentate triphenylphosphine with the bidentate bis(diphenylphosphine)ethane (dppe) even at relatively low dppe/Rh molar ratios (dppe/Rh ≥ 2). However, on increasing the temperature to 150°C, the activity of the catalyst remains rather low, with average *TF* values of 4–10 $h^{-1}$.

An enhanced selectivity toward the *cis* isomer was also observed on increasing the cone angle of the unidentate phosphine, as when using the tricyclohexylphosphine ($PCy_3$) instead of $PPh_3$. For instance, the stereoselectivity toward *cis*-10-formylpinane of the $[Rh_4(CO)_{12}]/PCy_3$ catalytic system is 85% with an L/Rh ratio of 20. Unfortunately, the activity of the system drops significantly as the L/Rh ratio is increased and, under the experimental conditions used, this system was practically inactive for a ratio of 100.

In addition to the switch from *trans* to *cis* selectivity, the addition of phosphine also prevents catalysis of the isomerization of β- to α-pinene at the lowest L/Rh ratios. This is attributed to the decreased acidity of the phosphine-modified carbonyl hydrides $[HRh(CO)_{3-x}L_x]$.

### 2.2. Spectroscopic characterization of the (1S, 2R, 5S)-, (1S, 2S, 5S)-, (1R, 2R, 5R)- and (1R, 2S, 5R)-10-formylpinanes

As previously reported, the *trans*- and *cis*-10-formylpinanes are clearly distinguishable by $^1H$ NMR

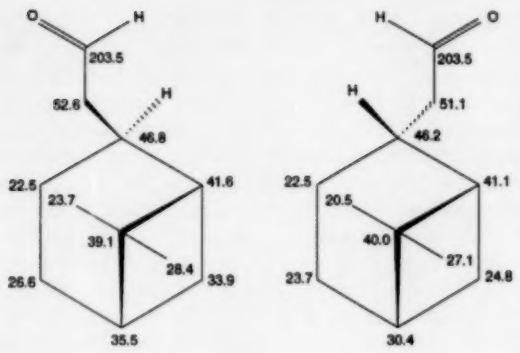


Fig. 3. $^{13}C$ NMR data for the (1*S*,2*S*,5*S*)- (**4**) and (1*S*,2*R*,5*S*)- (**5**) epimers of 10-formylpinane. The corresponding (1*R*,2*R*,5*R*)- (**4'**) and (1*R*,2*S*,5*R*)- (**5'**) enantiomers of 10-formylpinane show identical chemical shifts to within experimental error.

spectroscopy, through the chemical shifts of the methyl protons ($\delta$ 1.05 ppm for **4** and **4'**, $\delta$ 0.9 ppm for **5** and **5'**) [1], and by $^{13}C$ NMR spectroscopy. The $^{13}C$ chemical shifts have been assigned guided by those of the related *cis*- and *trans*-myrtenal [25]. As shown in Fig. 3, where the assignments of the $^{13}C$ resonances of the two diastereomers are reported, the most significant difference between the (1*S*,2*R*,5*S*)-(−)- and (1*S*,2*S*,5*S*)-(−)-10-formylpinane epimers consists in the chemical shift of carbon atom 7. This in the *cis* diastereomer **4**, because the methylene bridge is *trans* to the $-CH_2-C(=O)H$ moiety which lies on the same side of the *gem*-dimethyl carbon bridge and falls in a region where the *trans* isomer **5** does not show any absorption. The corresponding (1*R*,2*R*,5*R*)-(+)- and (1*R*,2*S*,5*R*)-(+)-10-formylpinane enantiomers show identical NMR spectra to the above, as expected. Consistent with the capillary column gas chromatography results, the $^{13}C$ NMR spectra allow us to calculate ca. 95% optical purity for the various distilled samples.

The optical rotatory powers ($\alpha_D$) of the above diastereomers are collected in Table 3. As expected, the introduction of a third asymmetric carbon has little effect on the optical rotatory power. Therefore, the $\alpha_D$ values allow us to distinguish between each pair of diastereomers (**4**–**4'** or **5**–**5'**), but do not enable us to discriminate between the **4**–**5**, and presumably **4'**–**5'**, pair of epimers which derive from the hydroformylation of (−)- or (+)-$\beta$-pinene, respectively. This led us to study their optical behaviour in more detail.

The spectroscopic behaviour of aldehydes has been investigated both experimentally and theoretically [26,27] but, to our knowledge, no circular dichroism (CD) study of asymmetric aldehydes has so far been reported [28]. For instance, the isotropic ultraviolet and visible (UV–vis) spectra of formaldehyde and higher aldehydes show absorptions at ca. 300 and 190 nm. Both absorptions have been assigned to excitations to triplet valence and Rydberg states, although the particular transition involved may be controversial [26,27]. Thus, while there is complete agreement in assigning the weak absorption at ca. 300 nm (molar extinction coefficient $\varepsilon = 100$ in formaldehyde) to a symmetry forbidden $n \rightarrow \pi^*$ transition, several controversial single–triplet promotions (e.g. valence $n \rightarrow \sigma^*$, $n \rightarrow \pi^*$ or $\pi \rightarrow \pi^*$, as well as $n \rightarrow 3s$ Rydberg transitions) have been proposed in the past as being responsible for the second excitation at ca. 190 nm. Nowadays, the latter absorption is thought to arise from a mixing of $\pi \rightarrow \pi^*$ and $n \rightarrow 3s$ Rydberg transitions [27].

The availability of the *trans* (**5**) and *cis*- (**4** and **4'**) 10-formylpinane diastereomers in a satisfactory optical purity made possible an investigation of their chiroptical behaviour to further confirm the assigned absolute configuration. In any case, a study of the aldehydic chromophore by UV–vis and CD spectra appeared desirable in view of the lack of previous studies.

The UV and CD spectra of **5**, **4** and **4'** are shown in Fig. 4 and selected parameters for **4**, **4'** and **5** are listed in Table 3. The UV spectrum of **5** in the top part of Fig.

Table 3
Chiroptical behaviour of the **4**, **4'** and **5** diastereomers [a]

| Compound | Solvent | $M \times 10^2$ | $[\alpha_D]$ (wt.%) | $\varepsilon$ (λ,nm) | $\Delta\varepsilon$ (λ,nm) | $g \times 10^3$ |
|---|---|---|---|---|---|---|
| **4** | $CHCl_3$ | | −17.1 (1.2%) | | | |
| | heptane | 0.759 | −15.4 (1.0%) | 30 (300) | +0.127 (300) | +6.0 |
| | | | | | −0.438 (193) | |
| **4'** | $CHCl_3$ | | +15.2 (1.2%) | | | |
| | heptane | 1.217 | +15.0 (1.0%) | 31 (300) | −0.143 (300) | −5.0 |
| | | | | 1314 (192) | +0.468 (191) | +0.4 |
| **5** | $CHCl_3$ | | | 20 (298) | −0.082 (298) | −4.0 |
| | heptane | 0.985 | −17.4 (1.0%) | 18 (300) | −0.092 (300) | −5.1 |
| | | | | | −0.150 (192) | |
| **5*** [b] | heptane | 3.28 | | 148 (212) | −0.187 (212) | |

[a] Slight discrepancies between the $\varepsilon$ and $\Delta\varepsilon$ values for the diastereomeric aldehydes are due partially to air oxidation during prolonged handling in dilute solution.
[b] Compound **5*** is the acid obtained by oxidation of **5**.

4 shows one band at ca. 300 nm and one inflection lower than 200 nm, corresponding to two electronic transitions, as evident in the isotropic spectra. The bottom part of the figure, which reports the CD spectrum of **5**, shows two corresponding Cotton effects. The first band at ca. 300 nm shows vibronic structure with an apparent progression of ca. 900 $cm^{-1}$. The absorption of ca. 300 nm is unambiguously due to the $n \rightarrow \pi^*$ electronic transition of the –C(=O)H chromophore in an aliphatic chiral substrate, since upon oxidation of the aldehyde to the corresponding acid, this absorption is replaced by a new, more intense absorption at ca. 220 nm (dotted plot in Fig. 4) arising from the –C(=O)OH chromophore. As a result of the observed induction of optical activity by the chiral aliphatic radical on the $n \rightarrow \pi^*$ electronic transition of the formyl chromophore, the negative sign of the corresponding multiple Cotton effect seems to relate mainly to the absolute configuration, *R*, of the asymmetric carbon atom in position 2 of the aliphatic cycle. Thus, both **5** (Fig. 4) and **4'** (Fig. 5) show a negative sign. In contrast, the second band, only noticeable as an inflection in the continuously rising energy curve of the isotropic spectra, is partly resolved into a Cotton effect at ca. 190 nm in the CD experiments. The related sign of the Cotton effect seems to be determined mainly by the absolute configurations of carbon atoms 1 and 5 of the aliphatic cycle, since it is negative for both **4** and **5** (1*S*,5*S*), and positive for **4'** (1*R*,5*R*). The octant rule, which has been often successfully applied to interpret the sign of the Cotton effect in cyclic ketones such as (*S*)-(+)-3-methylcyclopentanone [28] seems to be of little use in this case.

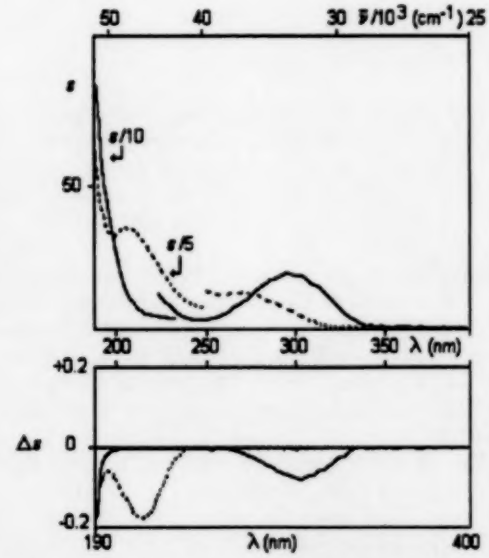


Fig. 4. UV (top) and CD (bottom) spectra of (1*S*,2*R*,5*S*)-10-formylpinane (**5**, continuous plot) and its corresponding acid (**5***, dotted plot) in heptane.

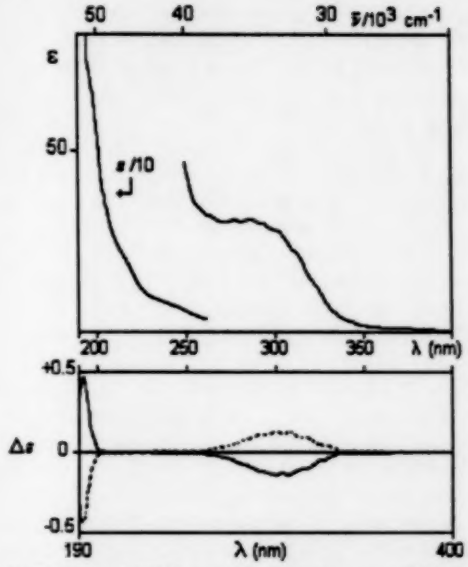


Fig. 5. UV (top) and CD (bottom, dotted plot) spectra of (1*S*,2*S*,5*S*)-10-formylpinane (**4**), and CD spectrum (bottom, continuous plot) of (1*R*,2*R*,5*R*)-10-formylpinane (**4'**) in heptane.

## 3. Discussion

The hydroformylation results reported here clearly show that as the steric hindrance of the probable active species $[HRh(CO)_{3-x}L_x]$ increases on progressive replacement of carbonyl groups by bulkier triphenylphosphine and tricyclohexylphosphine, the activity drops and the stereoselectivity switches from **5** to **4** (or from **5'** to **4'**). The stereochemistry of hydroformylation has been shown to result from a formal *syn* addition of a H–M moiety in all cases involving both cobalt and rhodium investigated [22], and, more recently, in the case of a platinum catalyst [29]. Either $\pi$-complexation of the olefin to the metal followed by insertion into the H–M bond or direct *syn* addition of a H–M moiety to the O=C double bond in a 4-centre transition state should have identical stereochemical consequences. As inferred from Fig. 2, steric considerations suggest that $\pi$-complexation *anti* to the *gem*-dimethyl carbon bridge (attack from the bottom or to the least hindered face of the olefin) should always be the most favourable. Such an attack would give rise to the *cis* **4** and **4'** diastereomers, as occurs with the bulkier $[HRh(CO)_{3-x}L_x]$ catalysts. In contrast, the least bulky $[HRh(CO)_3]$ species, generated in situ via fragmentation either of heterometallic Co–Rh clusters or of $[Rh_4(CO)_{12}]$, evi-

dently attacks from the top on to the most hindered face of the olefin, as shown by the stereoselectivity of the hydroformylation in the *trans* **5** and **5'** diastereomers. Moreover, it has also been reported that the hydrogenated pinane obtained as a by-product of the hydroformylation of β-pinene with $[Rh_6(CO)_{16}]$ consists only of the diastereomer having the methyl group *anti* to the *gem*-dimethyl carbon group [12]. Although it is reasonable that such an attack should be available preferentially only to the least crowded carbonyl $[HRh(CO)_3]$, it raises the question of why the expected products from the addition on to the opposite least-hindered face of the olefin are so disfavoured. A greater electron density or the *exo* face of the endocyclic double bond of norbornene [30] has been suggested to be the origin of the preference for *exo* attack in its hydroformylation reactions [29]. Such an unbalance in the electron density on the two faces of an exocyclic double bond appears less probable and is contradicted by the results of the hydroformylation of *R*-(+)-camphene which show very little discrimination between the two faces [31]. We therefore suggest that in the case of β-pinene, discrimination between the two enantiotopic faces of the substrate made by an unsubstituted $[HRh(CO)_3]$ species is not only a straightforward consequence of the different steric hindrance which they present to approach of the catalyst, but is also greatly influenced by the relative energies of the transition states which are traversed on the way to the corresponding σ-alkylrhodium derivatives. In other words, attack from the bottom should give rise to a π-complex which is more favoured thermodynamically than that derived from a top addition. However, the former leads to the σ-alkyl intermediate complex more slowly than the latter, probably because it forces the methylene group closer to the methyl of the *gem*-dimethyl group, rather than away, and traverses a higher-energy transition state. A related crossing of the reaction profiles of diastereomers has been demonstrated to be at the origin of the stereospecific hydrogenation of olefinic substrates [32].

The various hindrances that the catalyst should experience on approaching the two faces of the olefin become most different on increasing the crowding at the metal centre. In this case, energy differences between π-complexes arising from bottom and top attack may become so large that only the former remains possible. As a consequence, selectivity should switch from the *trans* to the *cis* diastereomers and the rate of hydroformylation should slow down because of steric hindrance of the π-complex, and within the transition state. Accordingly, at relatively low $PPh_3$/Rh molar ratios, which should favour the presence of $[HRh(CO)_2(PPh_3)]$, a mixture of **4** and **5** is obtained, with a rate lower than those displayed by the Co–Rh and the Rh–$Cl^-$ systems. Moreover, with high $PPh_3$/Rh molar ratios (70–100) or with bidentate ligands, which should favour disubstituted $[HRh(CO)(PPh_3)_2]$ [33], diastereomer **4** was obtained stereoselectively, although at an even lower rate.

## 4. Experimental details

All preparations of reaction solutions were performed under dinitrogen or using a standard Schlenk tube technique. $[Rh_4(CO)_{12}]$ and $[Co_2Rh_2(CO)_{12}]$ were prepared by literature methods [34,35]. $[Co_2(CO)_8]$ was purchased from Strem and crystallized from heptane. (1*S*,5*S*)-(−)-β-Pinene and (1*R*,5*R*)-(+)-β-pinene were obtained from Fluka and used as purchased. Toluene was dried over sodium and distilled prior to use.

### 4.1. Hydroformylation reactions

Hydroformylation reactions were carried out in 250 ml Parr autoclave reactors equipped with mechanical stirrers, internal thermocouples, addition ports, sampling valves and a cooling coil. In a typical experiment, the autoclave was charged with a solution made as following: $[Co_2(CO)_8]$ (43 mg), $[Rh_4(CO)_{12}]$ (47 mg), mesitylene (2 g, as internal standard), and olefin (16 g) were dissolved in toluene (ca. 50 ml). The resulting solution was brought to a final volume of 100 ml with toluene and charged into the autoclave glass reactor. The autoclave was pressurized to 60 atm with a 1:1 mixture of CO and $H_2$, and thermostatted at 100°C. The hydroformylation reactions were run at constant pressure and were stopped by rapid cooling to ca. 20°C and depressurization.

### 4.2. Analysis of the products

The product distributions of each olefin during the catalytic reactions were analyzed every 30 min by sampling. Analyses were performed on Hewlett Packard HP5890 GC-FID and 5971 GC-MSD instruments. Standard and capillary (50 m) Carbowax 20M columns were used respectively.

The final diastereomeric distribution was determined by $^1H$ and $^{13}C$ NMR spectroscopy after vacuum distillation. NMR spectra were recorded for $CDCl_3$ solutions containing TMS as internal standard on Varian Gemini 200 and 300 spectrometers. The assignments are based on DEPT studies and comparisons with related derivatives [25].

The IR spectra were recorded on a Perkin-Elmer 1600 interferometer. Ultraviolet and visible spectra (UV–vis) were measured on a Jasco UVIDEC-650 spectrophotometer between 20000 and 52600 $cm^{-1}$ (400–190 nm), both in heptane and chloroform solutions. Circular dichroism (CD) spectra were obtained from the same solutions on a Jasco 500A spectropo-

larimeter equipped with a Jasco Data Processor, by repeated scannings (60 times) and averaging of the accumulated data. Optical rotation ($\alpha_D$) was measured with a Bendix 143C polarimeter.

## Acknowledgment

We thank the CNR (Progetto Finalizzato-Chimica Fine II) for a grant.

## References

[1] A.J. Chalk, *Chem. Ind. (Dekker)*, *33* (1988) 43, and references cited therein.
[2] B. Auger, J.A. Bajgrowicz and E. Giraudi, W.O. Pat. 9 311 094 A1, 1993 (to Givaudan-Roure); [*Chem. Abs.*, *119* (1993) 146 389f].
[3] W.K. Giersch and K.H. Schulte, Swiss Pat. 680 852 A, 1992 (to Firmenich S.A.); [*Chem. Abs.*, *118* (1992) 175 539q].
[4] K. Aoshima, M. Tsunakawa, H. Miyawaki, C. Yugawa and I. Yumoto, Jpn. Pat. 04 108 755 A2, 1992 (to Taiyo Perfumery Co.); [*Chem. Abs.*, *117* (1992) 178 140t].
[5] J. Hagen, R. Lehman and K. Bansemir, Ger. Pat. 2 914 090, 1980 (to Henkel K.-G.a.A.); [*Chem. Abs.*, *94* (1981) 128].
[6] A. Siegel and W. Himmele, *Angew. Chem., Int. Ed. Engl.*, *19* (1980) 178.
[7] Tse-Lok Ho, *Enantioselective Synthesis: Natural Products from Chiral Terpenes*, John Wiley & Sons, New York, 1992.
[8] W. Himmele and H. Siegel, *Tetrahedron Lett.*, (1976) 907.
[9] W. Himmele and H. Siegel, *Tetrahedron Lett.*, (1976) 911.
[10] I. Ciprés, P. Kalck, D.C. Park and F. Serein-Spirau, *J. Mol. Catal.*, *66* (1991) 399.
[11] J. Hagen and K. Bruns, Ger. Pat. 2 849 742, 1980 (to Henkel K.-G.a.A.); [*Chem. Abs.*, *93* (1980) 691].
[12] E.N. dos Santos, C.U. Pittman, Jr. and H. Toghiani, *J. Mol. Catal.*, *83* (1993) 51.
[13] L. Kollar and P. Sandor, *J. Organomet. Chem.*, *445* (1993) 257.
[14] P. Pino, *Proc. Symp. Rhodium Homog. Catal.*, Veszprem, 1978, 98F.
[15] A. Ceriotti, L. Garlaschelli, G. Longoni, M.C. Malatesta, D. Strumolo, A. Fumagalli and S. Martinengo, *J. Mol. Catal.*, *24* (1984) 309.
[16] M. Marchionna and G. Longoni, *J. Chem. Soc., Chem. Commun.*, (1987) 1097.
[17] I.T. Horvath, G. Bor, M. Garland and P. Pino, *Organometallics*, *5* (1986) 1441.
[18] I.T. Horvath, *Polyhedron*, *7* (1988) 2345.
[19] M. Garland, I.T. Horvath, G. Bor and P. Pino, *J. Organomet. Chem.*, *358* (1988) C17.
[20] M. Garland and P. Pino, *Organometallics*, *9* (1990) 1943.
[21] P. Pino, A. Major, F. Spindler, R. Tannenbaum, G. Bor and I. Horvath, *J. Organomet. Chem.*, *417* (1991) 65.
[22] P. Pino, *J. Organomet. Chem.*, *200* (1980) 223.
[23] B.L. Booth, M.J. Else, R. Fields and R.N. Hazseldine, *J. Organomet. Chem.*, *27* (1971) 119.
[24] D. Evans, G. Yagupsky and G. Wilkinson, *J. Chem. Soc. A*, (1968) 2660.
[25] J.K. Whitesell and M.A. Minton, *Stereochemical Analysis of Alicyclic Compounds by Carbon-13 NMR Spectroscopy*, Chapman & Hall, London, 1987.
[26] H.H. Jaffé and M. Orchin, *Theory and Applications of Ultraviolet Spectroscopy*, John Wiley & Sons, New York, 1962.
[27] M.B. Robin, *Higher Excited States of Polyatomic Molecules*, Academic Press, New York, 1985, Vol. III, and references cited therein.
[28] S.F. Mason, *Molecular Optical Activity and Chiral Discriminations*, Cambridge University Press, Cambridge, UK, 1982.
[29] C. Botteghi, S. Paganelli, A. Perosa, R. Lazzaroni and G. Uccello-Barretta, *J. Organomet. Chem.*, *447* (1993) 153.
[30] S. Inagaki, H. Fujimoto and K. Fukui, *J. Am. Chem. Soc.*, *98* (1976) 4054.
[31] S. Bordoni, E. Venturini and G. Longoni, unpublished work.
[32] C.R. Landis and J. Halpern, *J. Am. Chem. Soc.*, *109* (1987) 1746.
[33] C.P. Casey, G.T. Whiteker, M.G. Melville, L.M. Petrovich, J.A. Gavney and D.R. Powell, *J. Am. Chem. Soc.*, *114* (1992) 5535.
[34] S. Martinengo, P. Chini and G. Giordano, *J. Organomet. Chem.*, *27* (1971) 389.
[35] S. Martinengo, P. Chini, V.G. Albano, F. Cariati and T. Salvatori, *J. Organomet. Chem.*, *59* (1973) 379.

ELSEVIER

Journal of Organometallic Chemistry 508 (1996) 69–74

Journal of Organometallic Chemistry

# Synthesis and spectroscopic studies of new hydridoruthenium complexes: catalytic reactions of [RuHCl(bpzm)(cod)] (bpzm = bis(pyrazol-1-yl)methane, cod = cycloocta-1,5-diene)

Félix A. Jalón [a,*], Antonio Otero [a,*], Ana Rodríguez [a], Mercedes Pérez-Manrique [b]

[a] *Departamento de Química Inorgánica, Orgánica y Bioquímica, Facultad de Químicas, Campus Universitario, Universidad de Castilla-La Mancha, 13071 Ciudad Real, Spain*

[b] *Facultad de CyTA y Ciencias Químicas, Plaza Misael Bañuelos s / n, Universidad de Burgos, 09001 Burgos, Spain*

Received 11 April 1995

**Abstract**

The reaction of [RuHCl(bpzm)(cod)] (**1**) (bpzm = bis(pyrazol-1-yl)methane, cod = cycloocta-1,5-diene) with one equivalent of $AgCF_3SO_3$ afforded the triflate-containing [RuH($CF_3SO_3$)(bpzm)(cod)] (**2**). The reaction of **2** with $PMe_2Ph$ allowed the synthesis of *trans*-[RuH($PMe_2Ph$)(bpzm)(cod)]$CF_3SO_3$ (**3a**), which isomerizes easily to *cis*-[RuH($PMe_2Ph$)(bpzm)(cod)]$CF_3SO_3$ (**3b**), while a similar reaction of **1**, in the presence of $AgCF_3SO_3$, gave a series of phosphine-containing complexes such as [RuH($CF_3SO_3$)(cod)($PMe_2Ph$)$_2$] (**4**), the products of this process greatly depending on the reaction conditions. The complex *trans*-[RuH{$P(OMe)_3$}(bpzm)(cod)]$CF_3SO_3$ (**5a**), which also readily isomerizes to *cis*-[RuH{$P(OMe)_3$}(bpzm)(cod)]$CF_3SO_3$ (**5b**), was isolated from the reaction of **2** with $P(OMe)_3$, or alternatively from the reaction of **1** with $P(OMe)_3$ and $AgCF_3SO_3$. Finally, the reaction of **2** or **1** (in the presence of $AgCF_3SO_3$) with *N*-donors pyridine, 4-methylpyridine (4-picoline) or 3,5-dimethylpyridine (3,5-lutidine) yielded a mixture of products which we believe to contain both *cis*- and *trans*-[RuHL(bpzm)(cod)]$CF_3SO_3$ (L = pyridine, 4-picoline, or 3-5-lutidine). Spectroscopic data are provided for these compounds. Complex **1** catalyzes both the hydrogenation of the unsaturated substrates cyclohexene, cyclohexanone, acetone and propanal, with turn-over rates of up to 1506 $h^{-1}$ for cyclohexanone in the presence of NaOH at 130°C, and the efficient transfer hydrogenation of cyclohexanone by propan-2-ol in the presence of NaOH at 80°C, with a turn-over rate of 880 $h^{-1}$.

*Keywords:* Ruthenium; BPZM; Cod; Hydride; Catalysis; Hydrogenation

## 1. Introduction

Although the chemistry of metal poly(pyrazol-1-yl)-borato complexes has been extensively studied in recent years [1], comparable development of the isosteric poly(pyrazol-1-yl)alkanes is unknown [2]. We have recently reported [3] a family of poly(pyrazol-1-yl)-alkaneruthenium complexes and one of them, [$RuCl_2$-(bpzm)(cod)], was found to be a saturated species with a bpzm that could be replaced easily by phosphines and CO. This compound and $Li[BEt_3H]$ gave [RuHCl-(bpzm)(cod)] [4] which was a good starting material in substitution processes with hydrogen and *N*-donors [5]. We subsequently became interested in the behaviour of this compound, and this paper focusses on the study of its reactivity towards some phosphorus donors as well as its catalytic activity in hydrogenation and transfer hydrogenation processes of several unsaturated substrates.

## 2. Results and discussion

The reaction of [RuHCl(bpzm)(cod)] (**1**) with $AgCF_3SO_3$ was investigated first. The standard procedure involved the addition of one equivalent of silver triflate to a suspension of **1** in acetone to give, after appropriate work-up, the complex [RuH($CF_3SO_3$)-(bpzm)(cod)] (**2**):

$$[RuHCl(bpzm)(cod)] + AgCF_3SO_3 \rightarrow [RuH(CF_3SO_3)(bpzm)(cod)] + AgCl \quad (1)$$

Complex **2** was isolated as a white crystalline air-stable solid, which was stable for several hours, although solutions in polar solvents such as acetone and tetrahydrofuran (THF) are air sensitive. In halogenated sol-

* Corresponding authors.

0022-328X/96/$15.00 © 1996 Elsevier Science S.A. All rights reserved
*SSDI* 0022-328X(95)05836-2

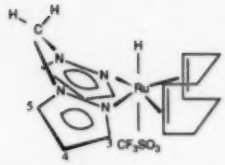

Fig. 1. Proposed structure for **2**.

vents, for example chloroform, a quantitative transformation of **2** to the known $[RuCl_2(bpzm)(cod)]$ was observed.

IR and especially NMR spectroscopy have proved useful tools for the characterization of **2** and the remaining complexes. The IR spectrum of **2** shows the characteristic bands for the bpzm, cod and triflate as well as a band at 2051 $cm^{-1}$ which corresponds to $\nu$(Ru–H) of a terminal hydride [6]. However, more extensive structural information was obtained from NMR spectroscopy. The $^1H$ NMR spectrum of **2** is in accordance with the presence of a symmetrical bpzm ligand with two equivalent pyrazolyl rings, and a cycloocta-1,5-diene with $C_s$ symmetry. Two additional ligands, hydride and triflate, complete the coordination sphere for ruthenium(II) in an octahedral geometry (Fig. 1). Selective irradiations of certain ancillary ligand signals in a series of nuclear Overhauser enhancement (NOE) experiments were carried out in order to assign the resonances of different protons in **2** and in other complexes (see below). This method has previously been successfully employed by us in other ruthenium complexes [3,4]. The application of this method allowed the assignment of the pyrazole $H^3$ and $H^5$ resonances by irradiation of the $CH_2$ group [7] and it is in accordance with the usual criterion for pyrazoles where $^3J_{45} > {}^3J_{34}$ [8].

A complete assignment of the six resonances (see Section 3) for the olefinic (two) and aliphatic (four) protons of the cod was performed by two consecutive irradiations. The first, at the hydride proton whose resonance appears at −8.77 ppm, led to enhancement of the signals of the closer olefinic and *exo* aliphatic protons at 3.62 and 2.33 ppm respectively. A second selective irradiation of the latter gave an obvious enhancement of the signal at 3.62 ppm, and of that of the geminal aliphatic *endo* proton at 1.99 ppm. The $^{13}C$ NMR spectrum is in accordance with the proposed structure and shows (see Section 3) four signals for the bpzm and also four signals for the cod (two for the methylene and two for the olefinic carbon atoms).

Reactivity studies on **1** and **2** with *N* and *P* donors were then carried out.

### 2.1. Reactivity of 1 and 2 with $PMe_2Ph$

This reactivity was found to be highly dependent on molar ratio, temperature and reaction time. Thus the reaction of **2** with $PMe_2Ph$ in a 1:1 molar ratio for 15 min at room temperature in acetone gives *trans*-$[RuH(PMe_2Ph)(bpzm)(cod)]CF_3SO_3$ (**3a**) as the only product:

$$[RuH(CF_3SO_3)(bpzm)(cod)] + PMe_2Ph \rightarrow \textit{trans}\text{-}[RuH(PMe_2Ph)(bpzm)(cod)]CF_3SO_3 \quad (2)$$

Complex **3a** was isolated as a white crystalline air-sensitive solid, which is soluble in polar solvents and insoluble in non-polar solvents. When solutions of **3a** were kept, both at room temperature for a long time or at 45°C for 15 h, *cis*-$[RuH(PMe_2Ph)(bpzm)(cod)]CF_3SO_3$ (**3b**) was formed as the main product, although it was always contaminated with non-hydride-containing byproducts and all attempts to isolate a pure sample of **3b** were unsuccessful. It was also impossible to collect variable-temperature NMR data to establish the kinetics of the isomerization process. Surprisingly, neither **3a** nor **3b** was isolated from the reaction of **1** with $AgCF_3SO_3$ and $PMe_2Ph$ in acetone in an 1:1:1 molar ratio at room temperature, but rather an unresolved mixture of phosphine containing complexes was observed (monitored by $^1H$ NMR). This suggests that several substitutions of both bpzm and cod by $PMe_2Ph$ had taken place. This behaviour was also observed when the reactions were carried out in 1:1:2 and 1:1:3 molar ratios. Attempts to isolate pure samples of the complexes from the reaction mixtures were unsuccessful. However, when the reaction in 1:1:1 molar ratio was carried out at −80°C and the solution was allowed to warm to room temperature, $[RuH(CF_3SO_3)(cod)(PMe_2Ph)_2]$ (**4**) was isolated after appropriate work-up as a light-green solid, although always contaminated with byproducts. As previously pointed out, the reaction of **1** with $AgCF_3SO_3$ in the presence of $PMe_2Ph$ is not very selective and, under various conditions, mixtures of products resulting from chloride abstraction were obtained, leading to the formation of AgCl and the substitution of bpzm and cod by $PMe_2Ph$.

Some of these phosphine complexes have been fully characterized spectroscopically. Complex **3a** shows in its IR spectrum a terminal hydride band at 1981 $cm^{-1}$. The $^1H$ NMR spectrum displays three sets of low field signals for the aromatic protons of two equivalent pyrazol-1-yl groups and two signals of an AB system for the diastereotopic $CH_2$ group of the bpzm. Four signals for the aliphatic protons and two signals for the olefinic protons of the cod are also present, consistent with $C_s$ symmetry. The assignment of proton signals was again facilitated by NOE experiments.

Both the hydride and the methyl phosphine resonances are doublets because of coupling with $^{31}P$. The

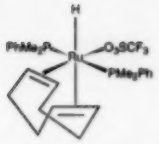

Fig. 2. Proposed structure for **4**.

value of $J_{PH} = 96.9$ Hz for the hydride resonance at −0.68 ppm indicates a *trans* disposition arrangement of the H and $PMe_2Ph$ [9]. This value is higher than the value of 23.7 Hz found in the *cis*-isomer **3b** where the hydride signal appears at −7.43 ppm (see Section 3). The $^{31}P$ NMR spectrum shows a resonance at −1.63 ppm ($J_{PH} = 96.9$ Hz). The data are in accordance with an octahedral geometry for **3a** similar to that previously found for **2** (see Fig. 1) where both H and $PMe_2Ph$ are apical.

The $^{13}C$ NMR spectrum of **3a** shows resonances for the carbon atoms of the bpzm and the cod (see Section 3). The phosphine resonances are a set of four signals for the phenyl groups and one signal for the methyl groups. In order to assign some of the resonances, a two-dimensional heteronuclear chemical shift correlation ($^1H$–$^{13}C$ COSY) experiment was carried out and some $J_{PC}$ values in the $^{13}C\{^1H\}$ NMR spectrum were determined. The $J_{PC}$ values for the olefinic and carbon atoms close to the phosphine are larger than those of the more distant atoms. The IR spectrum of **4** shows $\nu$(Ru–H) at 1992 $cm^{-1}$ and the $^1H$ NMR spectrum displays six resonances for the cod, in accordance with $C_s$ symmetry, while the hydride signal appears as a triplet at −11.31 ppm ($J_{PH} = 24.0$ Hz). This relatively small coupling constant value suggests a *cis*-disposition of the hydride and two equivalent phosphines. The phosphine resonances appear as two sets of signals for the phenyl groups and two pseudotriplets for the methyl groups which is the standard pattern observed for two mutually *trans*-phosphines [10]. The data are in accordance with the octahedral structure depicted in Fig. 2. The lack of solubility of **4** has prevented the recording of the $^{13}C$ NMR spectrum.

### 2.2. Reactivity of 1 and 2 towards $P(OMe)_3$

The reaction of **2** with one equivalent of $P(OMe)_3$ was carried out in a similar way to that previously described for $PMe_2Ph$ (see above) and gave *trans*-$[RuH(P(OMe)_3)(bpzm)(cod)]CF_3SO_3$ (**5a**). This was prepared alternatively from the reaction of **1** with $AgCF_3SO_3$ and $P(OMe)_3$ in a 1:1:1 molar ratio at −80°C in acetone. In both procedures, **5a** was isolated as an air-stable white crystalline solid, although solutions in polar solvents such as acetone or THF, in which it is moderately soluble, are very air sensitive. Complex **5a** reacts with halogenated solvents to give $[RuCl_2(bpzm)(cod)]$. The IR spectrum of **5a** shows $\nu$(Ru–H) at 1976 $cm^{-1}$, and $^1H$ and $^{13}C$ NMR data support the structure depicted in Fig. 1 for **2**, with the hydride and phosphite *trans*. The assignment of proton and carbon signals was also carried out by NOE and $^1H$–$^{13}C$ COSY experiments, which also allowed the assignment of some of $J_{PC}$ values in the $^{13}C\{^1H\}$ NMR spectrum. Complex **5a** isomerizes to *cis*-$[RuH(P(OMe)_3)(bpzm)(cod)]CF_3SO_3$ (**5b**) after heating a solution of the former for 40 h (monitored by $^1H$ NMR spectroscopy), although other byproducts were detected which were not afterwards identified. It was again impossible to determine the kinetics of the isomerization process. The hydride resonance for **5b** appears as a doublet at −8.0 ppm, $J_{PH}$ = 24 Hz, in contrast with the values of −0.31 ppm, $J_{PH} = 48.5$ Hz, found for **5a**.

The behaviour of **1** with $AgCF_3SO_3$ and $P(OMe)_3$, in a molar ratio 1:1:1, is clearly different from that previously described for $PMe_2Ph$, where substitution of the bpzm by the phosphine was observed.

### 2.3. Reactivity of 1 and 2 towards pyridine and related donors

The reaction of **1** with $AgCF_3SO_3$ and pyridine, 4-methylpyridine (4-picoline) or 3,5-dimethylpyridine (3,5-lutidine) or **2** with the *N*-donors in molar ratios 1:1:1 and 1:1 respectively, at room temperature or at −80°C, affords a mixture of two products which are tentatively identified as isomers $[RuHL(bpzm)(cod)]CF_3SO_3$ (L = py, 4-picoline or 3,5-lutidine) judged by spectroscopic and analytical data. The mixture of products was isolated as yellow solids, which were soluble in common polar solvents. Attempts to resolve the mixtures were unsuccessful because of similar solubilities. We cannot explain the isolation of the mixture of the isomers under these conditions and we have not

Table 1
$^1H$ NMR data for the *cis* and *trans* isomers $[RuH(4\text{-picoline})(bpzm)(cod)]CF_3SO_3$

| Isomer | $^1H$ NMR, $\delta$ (ppm) | | | | | | |
|---|---|---|---|---|---|---|---|
| | Bis(pyrazolyl)methane | | | | Picoline | | Hydride |
| | $CH_2$ | $H^3$ | $H^4$ | $H^5$ | Aromatic | Methyl | |
| *trans* | 7.02 (s) | 8.85 (d, $^3J_{34} = 2.0$ Hz) | 6.84 (pt) | 8.39 (d, $^3J_{45} = 2.5$ Hz) | 8.21 (d), 7.29 (d, $^3J = 5.4$ Hz) | 2.35 (s) | −5.61 (s) |
| *cis* | 6.03 ($J_{AX} = 14.5$ Hz) | 8.21 (d, $^3J_{34} = 1.7$ Hz), 8.13 (d, $^3J_{34} = 2.0$ Hz) | 6.47 (pt) | 8.27 (d, $^3J_{45} = 2.7$ Hz), 8.13 (d, $^3J_{45} = 2.6$ Hz) | 7.98 (d, $^3J = 6.1$ Hz), 7.14 (d, $^3J = 5.9$ Hz) | 2.28 (s) | −4.50 (s) |

observed an interconversion of isomers when the temperature was raised. The $^1$H NMR spectra show two hydride resonances. However, the assignment of the remaining signals is very difficult. In order to obtain additional structural data an exhaustive $^1$H NMR study on the mixture derived from 4-picoline was carried out. Double-resonance experiments, $J_{HH}$ values and relative intensities of the signals resulted in the assignments depicted in Table 1.

We conclude that the reactions of **1** and **2** with *N*-donors are not selective and we believe that a mixture of products, corresponding to *cis* and *trans* isomers form.

### 2.4. Catalytic hydrogenation processes

Complex **1** was used as a catalyst in catalytic hydrogenations of the following substrates: cyclohexene, cyclohexanone, acetone and propanal, because of the well-known activity of several hydride ruthenium complexes in this kind of process [11]. In a typical procedure, solutions of the mixture of reagents, using as solvent either THF for the hydrogenation of cyclohexene or the corresponding carbonyl compound in the case of the remaining substrates, were placed in a steel reactor and $H_2$ was introduced at the pressure. The reaction conditions for the different experiments required, as well as the observed catalytic activity, are shown in Table 2.

The ability of ruthenium complex **1** to hydrogenate the substrates is greatest for cyclohexene and is especially low for cyclohexanone. This may be due to the higher coordination capacity of the olefin. The low activity towards cyclohexanone occurs in spite of its greater basicity than acetone. In addition, electronic and steric factors may be responsible for the greater catalytic activity for the hydrogenation of propanal than of acetone. The rates of hydrogenation clearly show a temperature dependence, and the highest turn-over rates were obtained at 130°C. With the aim of generating coordination sites, silver or thallium salts were added to the mixtures employing cyclohexene and acetone (see Table 2) but, surprisingly, in both cases a decrease in the catalytic activity was found.

Table 3
Catalytic activity in basic medium [a]

| | Catalytic activity (turn-over per hour) | | |
|---|---|---|---|
| Cyclohexene | 965 | | |
| Cyclohexanone | 174 | 1506 [b] | 880 [c] |
| Acetone | 1091 | | |

[a] Reaction conditions: $H_2$ pressure, 30 bar; [substrate]/[precursor] = 2000:1; reaction time, 2 h without previous activation of the precursor; 80°C; NaOH–MeOH, 0.1 M.
[b] 130°C.
[c] Transfer hydrogenation from 2-propanol; 80°C; NaOH–/$^i$PrOH (0.05 M); reaction time, 3 h.

Owing to the favourable effect on the rates of hydrogenation, especially for ketones, strong bases, such as NaOH or KOH, are frequently added as cocatalysts [12], although their function is not well understood [13]. We decided to study the effect of base in some of our hydrogenation processes. In a typical procedure a solution of NaOH in MeOH was used, and the reaction conditions and the observed values for the turn-over rates are shown in Table 3. The hydrogenation of propanal under these experimental conditions did not take place and the formation of condensation products was observed. A marked increase in activity in the presence of base was found and the turn-over rate for the hydrogenation of cyclohexanone at 130°C is, to the best of our knowledge, among the largest described.

The results prompted us to study the transfer hydrogenation of cyclohexanone, which showed a low hydrogenation activity (see Table 2). Ruthenium complexes are useful in the dehydrogenation of alcohols and in transferring hydrides to ketones in transfer hydrogenation catalytic processes [14]. When cyclohexanone was treated with the catalytic system [RuHCl(bpzm)(cod)]–NaOH] in propan-2-ol at 80°C, an efficient reduction of the ketone took place, and a dramatic improvement in the catalytic activity compared with previously described hydrogenations at the same temperature (174 turn-overs per hour) was found (Table 3). An appreciа-

Table 2
Catalytic activity [a]

| | Catalytic activity (turn-over per hour) | | | | | |
|---|---|---|---|---|---|---|
| Cyclohexene | 9 [b] | 400 [c] | 540 [d] | 0.4 [b,e] | 10 [c,e] | 115 [d,e] |
| Cyclohexanone | 0 [b] | 0 [c] | 14 [d] | | | |
| Acetone | 4 [b] | 80 [c] | 200 [d] | | 16 [c,f] | 16.4 [d,f] |
| Acetaldehyde | 44 [b] | 82 [c] | 260 [d] | | | |

[a] Reaction conditions: $H_2$ pressure, 30 bar; [substrate]/[precursor] = 2000:1; reaction time, 2 h without previous activation of the precursor.
[b] Room temperature.
[c] 80°C.
[d] 130°C.
[e] With addition of TlBF4.
[f] With addition of AgBF4.

ble enhancement in the rates of hydrogen transfer to many ketones when a small quantity of base was added to the system has previously observed [14c,d,15].

## 3. Experimental details

All reactions were performed using standard Schlenk-tube techniques in dry dinitrogen. Solvents were distilled from appropriate drying agents and degassed before use. Ruthenium materials $[\{RuCl_2(cod)\}_n]$ [16] and [RuHCl(cod)(bpzm)] [4] were prepared as previously reported. Microanalyses were performed with a Perkin–Elmer 2400 CHN analyser. IR spectra were obtained in the region 4000–200 $cm^{-1}$ using a Perkin–Elmer 883 spectrophotometer. $^1H$ (300 MHz) and $^{13}C$ (75 MHz) NMR and NOE difference spectra were recorded at 19°C on a Unity Varian FT300 spectrometer and referenced to the residual deuteriated solvents. NOE difference spectra were recorded with the following acquisition parameters: spectral width, 5000 Hz; acquisition time, 3.27 s; pulse width, 90°; relaxation delay, 4 s; irradiation power, 5–10 L; number of scans, 120. The two-dimensional NMR spectra were acquired using standard Varian FT sofware, and processed using an IPC-Sun computer. The gas chromatograph (GC) analyses for the reaction products in the catalytic experiments were carried out on a Hewlett–Packard 5890 chromatograph with a flame ionization detector connected to a Hewlett–Packard 3395 integrator, and using a HP-FFAP (12 m × 0.2 mm × 0.33 pm) glass capillary column at 70°C. The hydrogenation reactions were carried out in an autoclave under $H_2$ at 30 bar and in a thermostatic bath with magnetic stirring.

### 3.1. Preparations

#### 3.1.1. [RuH($CF_3SO_3$)(bpzm)(cod)] EtOH (2).

$AgCF_3SO_3$ (65 mg, 0.25 mmol) was added to an acetone (20 ml) suspension of [RuHCl(bpzm)(cod)] (100 mg, 0.25 mmol) at −80°C in a darkened Schlenk tube. The mixture was stirred and allowed to warm to room temperature. The yellowish solution was filtered and evaporated to dryness. Complex **2** was obtained as a white microcrystalline solid from ethanol diethyl ether (yield, 98.2 mg (71%)).

Anal. Found: C, 39.61; H, 5.00; N, 10.44. $C_{18}H_{27}F_3N_4O_4RuS$ calc.: C, 39.02; H, 4,88; N, 10.12%. IR (KBr $cm^{-1}$): $\nu$(Ru–H) 2051 $cm^{-1}$. $^1H$ NMR ($[^2H_6]$-acetone, tetramethylsilane (TMS)) $\delta$ 8.27 (d, 2H, $^3J_{45}$ = 2.5 Hz, $H^5$); 7.58 (d, 2H, $^3J_{34}$ = 1.7 Hz, $H^3$); 7.19 (s, 2H, $CH_2$bpzm); 6.50 (pt, 2H, $H^4$); 3.70 (bs, 2H, $H^{olef}$cod); 3.62 (bs, 2H, $H^{olef}$cod); 2.72 (m, 2H, $H^{exo}$cod); 2.33 (m, 2H, $H^{exo}$cod); 1.99 (d, 2H, $J_{gem}$ = 7.5 Hz, $H^{endo}$cod); 1.93 (d, 2H, $J_{gem}$ = 8.1 Hz, $H^{endo}$cod); −8.77 (s, 1H, hydride) ppm. $^{13}C$ NMR ($[^2H_4]$-methanol, TMS): $\delta$ 143.78 ($^1J_{CH}$ = 187.5 Hz, $C^3$); 134.66 ($^1J_{CH}$ = 195.9 Hz, $C^5$); 108.6 ($^1J_{CH}$ = 181.9 Hz, $C^4$); 76.4 ($^1J_{CH}$ = 159.7 Hz, $C^{sp2}$cod); 73.7 ($^1J_{CH}$ = 153.7 Hz, $C^{sp2}$cod); 64.92 ($^1J_{CH}$ = 151.7 Hz, $CH_2$bpzm); 34.18 ($^1J_{CH}$ = 125.2 Hz, $C^{sp3}$cod); 29.05 ($^1J_{CH}$ = 126.0 Hz, $C^{sp3}$cod) ppm.

#### 3.1.2. trans-[RuH($PMe_2Ph$)(bpzm)(cod)]$CF_3SO_3$ (3a).

$PMe_2Ph$ (35.22 μl, 0.25 mmol) was added to an acetone solution (20 ml) of [RuH($CF_3SO_3$)(bpzm)(cod)] (126 mg, 0.25 mmol) and the solution was stirred for 15 min. The initial yellow solution turned pale and was evaporated to 2 ml. Complex **3a** crystallized as a white solid when diethyl ether was slowly added (yield, 119.4 mg (74%)).

Anal. Found: C, 44.36; H, 4.84; N, 8.93. $C_{24}H_{32}F_3N_4O_3PRuS$ calc.: C, 44.65; H, 4.99; N, 8.68%. IR (KBr): $\nu$(Ru–H) 1981 $cm^{-1}$ $^1H$ NMR ($[^2H_6]$-acetone, TMS): $\delta$ 8.19 (d, 2H, $^3J_{45}$ = 2.7 Hz, $H^5$); 7.27 (d, 2H, $^3J_{34}$ = 1.2 Hz, $H^3$); 7.27 (m, 2H, $H^2$Ph); 6.98 (m, 3H, $H^{3,4}$ Ph); 6.88 (AX system, 2H, $J_{AX}$ = 13.9 Hz, $CH_2$bpzm); 6.49 (pt, 2H, $H^4$); 3.17 (bs, 2H, $H^{olef}$cod); 2.92 (bs, 2H, $H^{olef}$cod); 2.56 (m, 2H, $H^{exo}$cod); 2.41 (m, 2H, $H^{exo}$cod); 1.86 (m, 2H, $H^{endo}$cod); 1.80 (m, 2H, $H^{endo}$cod); 1.51 (d, 6H, $^2J_{PH}$ = 6.9 Hz, Me); −0.68 (d, 1H, $^2J_{PH}$ = 96.9 Hz, hydride) ppm. $^{31}P$ NMR ($[^2H_6]$-acetone, $H_3PO_4$): $\delta$ −1.63 (d, $J_{PH}$ = 96.9 Hz) ppm. $^{13}C$ NMR ($[^2H_6]$-acetone, TMS): $\delta$ 144.09 ($^1J_{CH}$ = 189.0 Hz, $^3J_{PC}$ = 2.55 Hz, $C^3$); 136.90 ($C^1$Ph); 135.60 ($^1J_{CH}$ = 194.3 Hz, $C^5$); 130.10 ($C^2$Ph); 129.5 ($C^4$Ph); 128.50 ($C^3$Ph); 108.66 ($^1J_{CH}$ = 182.2 Hz, $C^4$); 72.90 ($^1J$ = 161.3 Hz, $^3J_{PC}$ = 2.02 Hz, $C^{sp2}$cod); 64.90 ($^1J_{CH}$ = 160.7 Hz, $^3J_{PC}$ = 3.75 Hz, $C^{sp2}$cod); 64.29 ($^1J_{CHA}$ = 150.6 Hz, $^1J_{CHX}$ = 151.27 Hz, $CH_2$bpzm); 32.25 ($^1J_{CH}$ = 125.4 Hz, $C^{sp3}$cod); 29.37 ($^1J_{CH}$ = 125.4 Hz, $^4J_{PC}$ = 3.0 Hz, $C^{sp3}$cod); 11.84 ($^1J_{PC}$ = 19.05 Hz, Me) ppm.

#### 3.1.3. [RuH($CF_3SO_3$)(cod)($PMe_2Ph$)$_2$] (4).

$PMe_2Ph$ (71.57 μl, 0.51 mmol) was added to an acetone (20 ml) suspension of [RuHCl(bpzm)(cod)] (100 mg, 0.25 mmol). The mixture was stirred for 10 min, and a light-green solution was obtained. $AgCF_3SO_3$ (97.6 mg, 0.38 mmol) was added to this solution at −80°C in a light-protected Schlenk tube and the mixture was stirred and allowed to warm to room temperature. The solution was filtered and evaporated to dryness to give a white solid which corresponds to **4** (yield, 63.5 mg (40%)). No satisfactory analytical data were observed.

IR (KBr): $\nu$(Ru–H) 1992 $cm^{-1}$. $^1H$ NMR ($[^2H_6]$-acetone, TMS): $\delta$ 7.69 (bs, 4H, $H^2$Ph); 7.32 (bs, 6H, $H^{3,4}$ Ph); 3.73 (bs, 2H, $H^{olef}$cod); 3.27 (bs, 2H, $H^{olef}$cod); 2.57 (m, 2H, $H^{exo}$cod); 2.17 (m, 2H, $H^{exo}$cod); 2.03 (bs, 2H, $H^{endo}$cod); 1.85 (bs, 2H, $H^{endo}$cod); 1.51 (pt, 6H, Me); 1.36 (pt, 6H, Me); −11.53 (t, $^1H$, $^2J_{PH}$ = 24.0 Hz, hydride) ppm.

*3.1.4. trans-[RuH{P(OMe)$_3$}(bpzm)(cod)]CF$_3$SO$_3$ (5a).*

P(OMe)$_3$ (22.40 μl, 0.19 mmol) was added to an acetone solution (20 ml) of [RuH(CF$_3$SO$_3$)(bpzm)(cod)] (100 mg, 0.19 mmol). After stirring at room temperature for 15 min, the solution was evaporated down to 2 ml and, following cooling at −180°C, **7a** as a white solid was isolated (yield, 62.5 mg (52%)).

Anal. Found: C, 36.38; H, 4.85; N, 8.58. $C_{19}H_{31}F_3N_4O_6PRuS$ calc.: C, 36.11; H, 4.75; N, 8.87%. IR (KBr): ν(Ru–H) 1976 cm$^{-1}$. $^1$H NMR ([$^2H_6$]-acetone, TMS): δ 8.32 (d, 2H, $^3J_{45}$ = 2.1 Hz, H$^5$); 7.43 (d, 2H, $^3J_{34}$ = 1.5 Hz, H$^3$); 7.19 (AB system, 2H, $J_{AB}$ = 12.0 Hz, CH$_2$); 6.52 (pt, 2H, H$^4$); 3.36 (d, 11H, $^2J_{PH}$ = 9.9 Hz, H$^{olef}$cod, Me); 3.18 (bs, 2H, H$^{olef}$cod); 2.57 (bs, 4H, H$^{exo}$cod); 1.84 (m, 2H, H$^{endo}$cod); 1.78 (m, 2H, H$^{endo}$cod); −0.31 (d, 1H, $^2J_{PH}$ = 148.5 Hz, hydride) ppm. $^{31}$P NMR ([$^2H_6$]-acetone, $H_3PO_4$): 5.00 (d, $J_{PH}$ = 148.5 Hz) ppm. $^{13}$C NMR ([$^2H_6$]-acetone, TMS): δ 145.33 ($^1J$ = 190.8 Hz, $^3J_{PC}$ = 2.5 Hz, C$^3$); 135.29 ($^1J_{CH}$ = 200.0 Hz, C$^5$); 108.28 ($^1J_{CH}$ = 181.8 Hz, C$^4$); 71.46 ($^1J_{CH}$ = 150.73 Hz, C$^{sp2}$cod); 66.00 ($^1J_{CH}$ = 123.9 Hz, $^2J_{PC}$ = 7.0 Hz, C$^{sp2}$cod); 64.50 ($^1J_{CH}$ = 157.7 Hz, $^3J_{PC}$ = 2.03 Hz, CH$_2$bpzm); 52.38 ($^1J_{CH}$ = 146.2 Hz, $^2J_{PC}$ = 8.03 Hz, Me); 34.58 ($^1J_{CH}$ = 121.9 Hz, C$^{sp3}$cod); 30.33 ($^1J_{CH}$ = 123.9 Hz, $^4J_{PC}$ = 3.0 Hz, C$^{sp3}$cod) ppm.

### *3.2. Catalytic hydrogenation processes*

In a typical experiment, a solution of [RuHCl(bpzm)(cod)] (6 mg, 0.015 mmol) in 10 ml of THF to which 3 ml(30 mmol) of cyclohexene had been added was introduced under dinitrogen into the reactor and the reaction vessel was pressurized at 30 bar. After heating at the appropriate temperature and stirring the reaction for 2 h, the autoclave was cooled, and the products analysed by GC.

The hydrogenation procedures for the carbonyl-containing products were carried out in a similar way.

In the experiments with the cocatalyst NaOH, the precursor [RuHCl(bpzm)(cod)] was dissolved in methanol solutions containing base. For example **1** (6 mg, 0.015 mmol) was dissolved in 10 ml of NaOH–MeOH (0.1 M) and 3 ml of cyclohexene were subsequently added. The remaining operations were similar to those described above.

### *3.3. Catalytic transfer hydrogenation of cyclohexanone*

A solution of [RuHCl(bpzm)(cod)] (6 mg, 0.015 mmol) in 10 ml of propan-2-ol and 5 ml of NaOH Pr$^i$OH (0.05 M) was heated at 80°C. Cyclohexanone (3 ml) was added, the mixture was heated under reflux at 80°C for 3 h, and then the reaction products were analysed by GC.

## Acknowledgement

The authors gratefully acknowledge financial support from the Dirección General de Investigación Científica y Técnica (Grant. PB92-0715).

## References and notes

[1] S. Trofimenko, *Chem. Rev., 93* (1993) 943.
[2] Selected examples: (a) A. Llobet, D.J. Hodgson and T.J. Meyer, *Inorg. Chem., 29* (1990) 3760; (b) A. Llobet, M.A. Curry, H.T. Evans and T.J. Meyer, *Inorg. Chem., 28* (1989) 3131; (c) A. Llobet, P. Doppelt and T.J. Meyer, *Inorg. Chem., 27* (1988) 514.
[3] M. Fajardo, A. de la Hoz, E. Diez-Barra, F.A. Jalón, A. Otero, A. Rodriguez, J. Tejeda, D. Belleti, M. Lanfranchi and M.A. Pellinghelli, *J. Chem. Soc., Dalton Trans.*, (1993) 1935.
[4] F.A. Jalón, A. Otero and A. Rodriguez, *J. Chem. Soc., Dalton Trans.*, (1995) 1629.
[5] B. Moreno, S. Sabo-Etienne, B. Chaudret, A. Rodriguez, F. Jalón and S. Trofimenko, *J. Am. Chem. Soc., 116* (1994) 2635.
[6] G.K.N. Reddy and N.M. Nanje Gowda, *J. Indian Chem. Soc., 54* (1977) 289.
[7] W. Holser, *Tetrahedron, 47* (1991) 1393.
[8] (a) L.A. Oro, M. Esteban, R.M. Claramunt, J. Elguero, C. Fóces-Fóces and F.H. Cano, *J. Organomet. Chem., 276* (1984) 79; (b) J. Elguero, R. Jacquier and D. Tizané, *Bull. Soc. Chim. Fr., 5* (1969) 1687; (c) G. Minghetti, M.A. Cinellu, A.L. Bandini, G. Banditelli, F. Demartin and M. Manassero, *J. Organomet. Chem., 315* (1986) 387.
[9] H.D. Kaesz and R.B. Saillant, *Chem. Rev., 72* (1972) 231.
[10] (a) J. Chatt, and R.G. Wilkins, *J. Chem. Soc.*, (1952) 4300; (b) J. Chatt and R.G. Wilkins, *J. Chem. Soc.*, (1953) 70; (c) J. Chatt and R.G. Wilkins, *J. Chem. Soc.*, (1956) 525; (d) J.M. Jenkins and B.L. Shaw, *J. Chem. Soc. A*, (1966) 770.
[11] F.H. Jardine, (*Prog. Inorg. Chem., 31* (1984) 265 and references cited therein.)
[12] (a) P. Chaloner, *Handbook of Coordination Catalysis in Organic Chemistry*, Butterworths, London, 1986; (b) G. Zassinovich and G. Mestroni, *Chem. Rev., 92* (1992) 1054.
[13] P. Kvintovics, B.R. James and B. Heil, *J. Chem. Soc., Chem. Commun.*, (1986) 1811.
[14] Selected examples: (a) R. Noyori and H. Takaya, *Acc. Chem. Res., 23* (1990) 345, and references cited therein; (b) D.E. Linn, J. Halpern, *J. Am. Chem. Soc., 109* (1987) 2969; (c) L.R. Chowdhury and J-E. Bäckvall, *J. Chem. Soc., Chem. Commun.*, (1991) 1063; (d) D. Morton and D.J. Cole-Hamilton, *J. Chem. Soc., Chem. Commun.*, (1988) 1154; (e) C. Bianchini, E. Farnetti, M. Graziani, M. Perozzini and A. Polo, *Organometallics, 12* (1993) 3753.
[15] See for example B. Graser and H. Steigerwald, *J. Organomet. Chem., 193* (1980) C67.
[16] M.A. Bennet and G. Wilkinson. *Chem. Ind. (London)*, (1959) 1516.

ELSEVIER

Journal of Organometallic Chemistry 508 (1996) 75–81

Journal of Organometallic Chemistry

# Properties and reactivity of the new $[Ir_4(\mu\text{-}CO)_3(CO)_5(\mu\text{-}PR_3)(PR_3)_2]$ clusters, ($PR_3 = PPh_xpyl_{3-x}$, pyl = 2-pyridyl)

K. Wajda-Hermanowicz, F. Pruchnik *, M. Zuber

*Institute of Chemistry, University of Wrocław, 14 F. Joliot-Curie, 50-383 Wrocław, Poland*

Received 12 April 1995

**Abstract**

The complex $Ir_4(CO)_{12}$ was shown to react with pyridylphosphines to give $[Ir_4(\mu\text{-}CO)_3(CO)_5(\mu\text{-}PPh_2pyl)(PPh_2pyl)_2]$ **(1)** $[Ir_4(\mu\text{-}CO)_3(CO)_5(\mu\text{-}PPhpyl_2)(PPhpyl_2)_2]$ **(2)** and $[Ir_4(\mu\text{-}CO)_3(CO)_5(\mu\text{-}Ppyl_3)(Ppyl_3)_2]$ **(3)** in which one of the phosphine ligands bridges through coordination of P and N atoms. Clusters **1–3** were characterized by $^1H$, $^{31}P$ NMR and IR spectroscopy. Variable-temperature $^1H$, $^{31}P$ and $^{13}C$ NMR spectra of **1–3** were investigated and the results are discussed. In solution under CO complexes **1–3** are in equilibrium with the clusters $[Ir_4(\mu - CO)_3(CO)_6(PR_3)_3]$.

*Keywords:* Iridium; Carbonyl; Phosphine; Pyridyl; Clusters; NMR spectroscopy

## 1. Introduction

The synthesis and reactivity of metal carbonyl clusters is attracting increasing attention [1–3]. These species show a rich substitution, catalytic and structural chemistry. Substitution of the carbonyl groups by other ligands exerts an influence on the reactivity of the clusters [4–8]. Very interesting ligands in this respect could be the potentially multidentate 2-pyridylphosphines of the type $PPh_xpyl_{3-x}$ ($x = 0, 1, 2$). It is known that they can act as unidentate terminal ligands [9–11] bridging ligands [12,13] or chelating ligands [14,15]. Changes in coordination on going from the solid to solutions are also known [16]. Recently we made $[Ir_4(CO)_9(PR_3)_3]$-type complexes ($PR_3 = PPh_xpyl_{3-x}$, pyl = 2-pyridyl, $x = 0, 1, 2$) [17]; in solution under argon the clusters lose one CO ligand and are transformed into complexes $[Ir_4(\mu\text{-}CO)_3(CO)_5(\mu\text{-}PR_3)(PR_3)_2]$ ($PR_3 = PPh_xpyl_{3-x}$, pyl = 2-pyridyl). We report below the results of studies of the synthesis, properties, reactivity and fluxional behaviour of the clusters.

## 2. Experimental details

### 2.1. Materials and apparatus

The NMR spectra were recorded on a Bruker AMX-300 spectrometer and IR spectra on Specord M-80 and Bruker IFS 113V spectrometers using KBr pellets. $(NH_4)_2IrCl_6$ was purchased from Fluka.

### 2.2. Preparation of complexes

#### 2.2.1. $[Ir_4(CO)_{12}]$

The complex was prepared as previously described [18].

#### 2.2.2. $[Ir_4(\mu - CO)_3(CO)_5(\mu\text{-}PPh_2pyl)(PPh_2pyl)_2]$ (1)

A sample of $[Ir_4(CO)_{12}]$ (0.2 g, 0.18 mmol) was placed in a bulb equipped with a reflux condenser, dropping funnel and CO inlet. The apparatus was filled with CO and a KOH/MeOH solution (0.6 M, 20 ml), carefully deaerated with nitrogen, was added. The suspension was stirred at 60–70°C until a clear solution was obtained, and then a solution of $PPh_2pyl$ (0.2 g, 0.76 mmol) $[Ir_4(CO)_{12}/PR_3 = 1:4.2]$ in 6 ml of MeOH (carefully deaerated with nitrogen) was added. The mix-

* Corresponding author.

0022-328X/96/$15.00 © 1996 Elsevier Science S.A. All rights reserved
*SSDI* 0022-328X(95)05779-X

ture was stirred at 70°C for 1 h under a CO atmosphere until the orange product separated out. The precipitate was filtered off, washed with methanol and heptane, and dried under nitrogen. Yield, 87%.

*2.2.3. $[Ir_4(\mu\text{-}CO)_3(CO)_5(\mu\text{-}PPhpyl_2)(PPhpyl_2)_2]$ (2) and $[Ir_4(\mu\text{-}CO)_3(CO)_5(\mu\text{-}Ppyl_3)(Ppyl_3)_2]$ (3)*

These clusters were prepared analogously using $PPhpyl_2$ and $Ppyl_3$, respectively. Yields of obtained products were similar.

### 2.3. Spectroscopic data

The IR data [1] ($cm^{-1}$) in the region 4000–400 $cm^{-1}$ were as follows:

Complex **1**: 1769 vs**; 1786 vs**; 1814 w; 1934 vs*; 1950 vs*; 1961 vs*; 1980 vs(sh)*; 2007 vs*; 2040 w*; 3050 m.

Complex **2**: 1775 vs**; 1780 vs**; 1842 vw; 1943 vs*; 1972 vs*; 1993 vs*; 2006 s*; 3045 w.

Complex **3**: 1771 vs**; 1788 vs**; 1844 vw; 1938 s*; 1974 vs*; 1990 vs*; 2004 s*; 2040 vw*; 2850 vw; 2920 w; 2990 vw; 3040 w; 3435m.

The 121.5 MHz $^{31}P\{^1H\}$ NMR spectra [2] ($\delta$, ppm) of $[Ir_4(\mu\text{-}CO)_3(CO)_5(\mu\text{-}PR_3)(PR_3)_2]$ in $CD_2Cl_2$ (with 85% $H_3PO_4$ as standard) were as follows:

Complex **1**: 28.3 [dd, $^3J(\mathbf{P_r},P_b) = 48.2$ Hz, $^3J(\mathbf{P_r},P_a) = 2.4$ Hz, $\mathbf{P_r}$]; −12.2 [dd, $^3J(\mathbf{P_b},P_r) = 48.2$ Hz, $^3J(\mathbf{P_b},P_a) = 2.4$ Hz, $\mathbf{P_b}$]; −13.4 [t, $^3J(\mathbf{P_a},P_r) = {}^3J(\mathbf{P_a},P_b) = 2.4$ Hz, $\mathbf{P_a}$] ppm.

Complex **2**: 28.9 [dd, $^3J(\mathbf{P_r},P_b) = 46.7$ Hz, $^3J(\mathbf{P_r},P_a) = 2.2$ Hz, $\mathbf{P_r}$]; −7.4 [dd, $^3J(\mathbf{P_b},P_r) = 46.7$ Hz, $^3J(\mathbf{P_b},P_a) = 2.2$ Hz, $\mathbf{P_b}$]; −11.2 [t, $^3J(\mathbf{P_a},P_r) = {}^3J(\mathbf{P_a},P_b) = 2.2$ Hz, $\mathbf{P_a}$] ppm.

Complex **3**: 31.9 [dd, $^3J(\mathbf{P_r},P_b) = 44.0$ Hz, $^3J(\mathbf{P_r},P_a) = 2.4$ Hz, $\mathbf{P_r}$]; −3.8 [dd, $^3J(\mathbf{P_b},P_r) = 44.0$ Hz, $^3J(\mathbf{P_b},P_a) = 2.4$ Hz, $\mathbf{P_b}$]; −9.4 [t, $^3J(\mathbf{P_a},P_r) = {}^3J(\mathbf{P_a},P_b) = 2.4$ Hz, $\mathbf{P_a}$] ppm.

The 300 MHz $^1H$ NMR spectra [3] ($\delta$, ppm) of $[Ir_4(\mu\text{-}CO)_3(CO)_5(\mu\text{-}PR_3)(PR_3)_2]$ in $CD_2Cl_2$ were as follows:

Complex **1**: 8.72 [m(10), $^3J(6,5) = 4.7$ Hz, $J(6,4) = 1.9$ Hz, $J(6,3) = 0.8$ Hz, $J(6,P) = 0.9$ Hz, H6(a)]; 8.55 [m(10), $^3J(6,5) = 4.8$ Hz, $J(6,4) = 1.7$ Hz, $J(6,3) = 1.0$ Hz, $J(6,P) = 0.9$ Hz, H6(a)]; 8.49 [m(10), $^3J(6,5) = 5.4$ Hz, $^4J(6,4) = 1.3$ Hz, $^5J(6,3) = 0.9$ Hz, $J(6,P) = 0.6$ Hz, H6(b)]; 7.15 [m(14), $^3J(5,4) = 7.5$ Hz, $^3J(5,6) = 4.8$ Hz, $^4J(5,3) = 1.3$ Hz, $J(5,P) = 2.7$ Hz, H5(a)]; 7.03 [m(12), $^3J(5,6) = 5.4$ Hz, $^3J(5,4) = 7.2$ Hz, $^4J(5,3) = 1.8$ Hz, $J(5,P) = 2.2$ Hz, H5(b)]; 6.54 [m(16), $^3J(3,4) = 7.8$ Hz, $^4J(3,5) = 1.8$ Hz, $^5J(3,6) = 0.9$ Hz, $J(3,P) = 4.1$ Hz, H3(b)] ppm; Ph and remaining pyl protons overlapped in the range 7.7–7.2 ppm (not resolved).

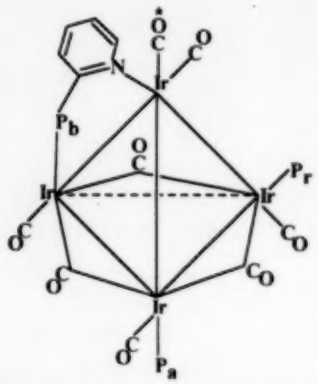


Fig. 1. Schematic structure of the $[Ir_4(\mu\text{-}CO)_3(CO)_5(\mu\text{-}PR_3)(PR_3)_2]$-type clusters.

Complex **2**: 8.73 [m(10), $^3J(6,5) = 4.7$ Hz, $^4J(6,4) = 1.7$ Hz, $^5J(6,3) = 1.0$ Hz, $J(6,P) = 0.9$ Hz, H6(a)]; 8.54 [m(10), $^3J(6,5) = 4.7$ Hz, $^4J(6,4) = 1.9$ Hz, $^5J(6,3) = 1.0$ Hz, $J(6,P) = 0.9$ Hz, H6(a)]; 8.51 [m(10), $^3J(6,5) = 4.8$ Hz, $^4J(6,4) = 1.7$ Hz, $^5J(6,3) = 1.0$ Hz, $J(6,P) = 0.9$ Hz, H6(a)]; 8.42–8.36 [H6(b) and H6(a), overlapping, not resolved]; 7.92 [m(12), $^3J(3,4) = 7.8$ Hz, $^4J(3,5) = 1.3$ Hz, $^5J(3,6) = 1.1$ Hz, $J(3, P) = 4.2$ Hz, H3(a)]; 7.83 [m(12), $^3J(4,3) = 7.8$ Hz, $^3J(4,5) = 7.8$ Hz, $^4J(4,6) = 1.7$ Hz, $J(4,P) = 4.2$ Hz, H4(a)]; 6.98 [m(10), $^3J(5,4) = 7.7$ Hz, $^3J(5,6) = 5.3$ Hz, $^4J(5,3) = 1.6$ Hz, $J(5,P) = 2.2$ Hz H5(b)]; 6.54 [m(12), $^3J(3,4) = 8.0$ Hz, $^4J(3,5) = 1.7$ Hz, $^5J(3,6) = 1.0$ Hz, $J(3,P) = 4.4$ Hz, H3(b)] ppm; Ph and remaining pyl protons overlapped in the range 7.7–7.09 ppm (not resolved).

Complex **3** 8.63 [m(10), $^3J(6,5) = 4.8$ Hz, $^4J(6,4) = 1.7$ Hz, $^5J(6,3) = 1$Hz, $J(6,P) = 0.8$ Hz, H6(a)]; 8.58 [m(10), $^3J(6,5) = 4.8$ Hz, $^4J(6,4) = 1.7$ Hz, $^5J(6,3) = 1$ Hz, $J(6,P) = 0.8$ Hz, H6(a)]; 8.50 [m(10), $^3J(6,5) = 4.7$ Hz, $^4J(6,4) = 1.8$ Hz, $^5J(6,3) = 1.1$ Hz, $J(6,P) = 0.8$ Hz, H6(a)]; 8.41 [*H6*(b), overlapping, not resolved]; 8.34 [m(10), $^3J(6,5) = 4.8$ Hz, $^4J(6,4) = 1.9$ Hz, $^5J(6,3) = 1.0$ Hz, $J(6,P) = 0.7$ Hz, H6(a)]; 8.03–7.88 (H3 overlapping, not resolved); 7.76 [m(12), $^3J(4,3) = 7.8$ Hz, $^3J(4,5) = 7.6$ Hz, $^4J(4,6) = 1.7$ Hz, $J(4,P) = 4.4$ Hz, H4(a)]; 7.72–7.61 (H4, overlapping, not resolved); 7.49 [m(12), $^3J(4,5) = 7.7$ Hz, $^3J(4,3) = 7.9$ Hz, $^4J(4,6) = 1.7$ Hz, $J(4,P) = 2.6$ Hz, H4(b)]; 7.31 [m(14), $^3J(5,4) = 7.6$ Hz, $^3J(5,6) = 4.6$ Hz, $^4J(5,3) = 1.2$ Hz, $J(5,P) = 2.8$ Hz, H5(a)]; 7.26–7.13 ppm [H5(a), overlapping, not resolved]; 7.00 [m(12), $^3J(5,4) = 7.7$ Hz, $^3J(5,6) = 5.3$ Hz, $^4J(5,3) = 1.5$ Hz, $J(5,P) = 2.2$ Hz, *H5*(b)]; 6.70 [m(16), $^3J(3,4) = 7.9$ Hz, $^4J(3,5) = 1.6$ Hz, $^5J(3,6) = 0.9$ Hz, $J(3,P) = 3.8$ Hz, *H3*(b)] ppm.

[1] Designation: *, $\nu$(CO) terminal; **, $\nu$(CO) bridging.

[2] Designation: $\mathbf{P_r}$ = radial; $\mathbf{P_b}$ = bridging; and $\mathbf{P_a}$ = axial phosphine ligand (Fig. 1).

[3] Designation: (a) protons of pyridyl ring non-coordinated with iridium; (b) protons of pyridyl ring coordinated with iridium (see Fig. 1).

## 3. Results and discussion

The $[Ir_4(\mu\text{-}CO)_3(CO)_5(\mu\text{-}PR_3)(PR_3)_2]$ clusters ($PR_3 = PPh_xpyl_{3-x}$, pyl = 2-pyridyl, $x = 0, 1, 2$) were prepared by reaction of $Ir_4(CO)_{12}$ with the appropriate phosphine in 0.6 M KOH solution in methanol at 75°C under CO with a $Ir_4(CO)_{12}/PR_3/KOH$ ratio of 1 : 4 : 10, or from $[Ir_4(CO)_9(PR_3)_3]$ in $CHCl_3$ under argon at 20–50°C. The reactions are shown in Fig. 2.

The clusters of type $[Ir_4(\mu\text{-}CO)_3(CO)_5(\mu\text{-}PR_3)(PR_3)_2]$ are very interesting because of their crystal structures and fluxional behaviour in solution. A single-crystal X-ray study of **1** [19] revealed that it contains one phosphine ligand bridging through P and N atoms and two phosphines (radial and axial, see Fig. 1) coordinated through the phosphorus atom only. However $[Ir_4(\mu\text{-}CO)_3(CO)_6(PPh_2pyl)_3]$ contains only terminal phosphines. The carbonyl ligands in $Ir_4[(\mu\text{-}CO)_3(CO)_5(\mu\text{-}PR_3)(PR_3)_2]$ and in $[Ir_4(\mu\text{-}CO)_3(CO)_6(PR_3)_3]$ are present as both terminal and bridging ligands. In both types of clusters there are three carbonyls bridging Ir–Ir bonds in the basal plane of the cluster.

In the IR spectra of **1–3** both the terminal and bridging CO stretching frequencies have lower values than those in $[Ir_4(\mu\text{-}CO)_3(CO)_6(PR_3)_3]$ [17]. This is due to the stronger $\sigma$-donor and weaker $\pi$-acceptor properties of the N atom of pyridyl ring compared with that of the CO ligand. Thus coordination via N atom increases the electron density on Ir atoms in the cluster. This leads to weakening of the C–O bond in coordinated carbonyls and so to a lowering of the $\nu$(CO) frequencies.

The $^1$H NMR spectrum of tris(2-pyridyl)phosphine [20] consists of four well-separated multiplets, assigned to four non-equivalent pyridyl protons (H6, 8.70 ppm; H3, 7.18 ppm; H4, 7.60 ppm; and H5, 7.40 ppm). Four multiplets are also present in the spectrum of tris(2-pyridyl)phosphine oxide or sulphide. Relative to those for the phosphine, the resonances of protons 3, 4 and 6 in the phosphine oxide are shifted towards lower field by about 0.1–0.2 ppm. The resonance of proton 5 is shifted towards lower field by about 0.8 ppm.

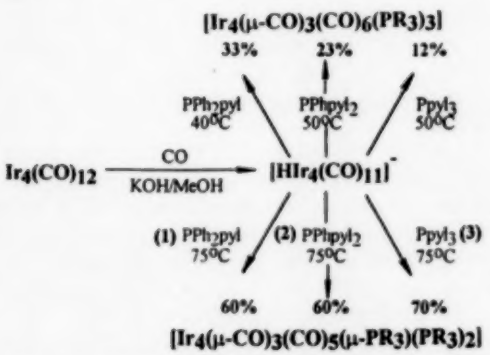


Fig. 2. Preparation of $[Ir_4(\mu\text{-}CO)_3(CO)_5(\mu\text{-}PR_3)(PR_3)_2]$ and $[Ir_4(\mu\text{-}CO)_3(CO)_6(PR_3)_3]$.

For rhodium complexes of the type $[RhCl(CO)(PR_3)_2]$ [16] (where $PR_3 = PPhpyl_2$ and $Ppyl_3$) it was found that, because of coordination of phosphine via phosphorus, pyridyl resonances are shifted towards lower fields relative to those for the free phosphine. This is because the electron density on coordinated phosphine is lower (similar to phosphine oxide) than in the free ligand. In contrast, the resonances of the protons of the pyridyl ring coordinated via nitrogen and phosphorus appear at higher field than those for pyridylphosphines coordinated via phosphorus only. This effect is also observed for the iridium clusters $[Ir_4(\mu\text{-}CO)_3(CO)_5(\mu\text{-}PR_3)(PR_3)_2]$ considered below.

The 121.5 MHz $^{31}P\{^1H\}$ and 300 MHz $^1$H NMR spectra of $[Ir_4(\mu\text{-}CO)_3(CO)_5(\mu\text{-}PR_3)(PR_3)_2]$ clusters indicate they have the same structure in the solid and in solution. Two pyridylphosphine ligands are coordinated to iridium via P atoms only. The remaining phosphine is coordinated via the phosphorus and the nitrogen of one of pyridyl rings. The $^{31}P\{^1H\}$ NMR spectra in $CDCl_3$ exhibit two double doublets for the radial and bridging ligands as well as a triplet for the axial phosphine ligand (see NMR data above). The triplet results from overlapping of two doublets with the same $^3J(P_r, P_a)$ and $^3J(P_b, P_a)$ coupling constants. The $^1$H NMR spectra indicate that the chemical shifts of protons of the non-coordinated pyridyl rings are approximately the same for both $[Ir_4(\mu\text{-}CO)_3(CO)_6(PR_3)_3]$ and $[Ir_4(\mu\text{-}CO)_3(CO)_5(\mu\text{-}PR_3)(PR_3)_2]$ compounds. However, the proton resonances for the pyridyl rings of the P, N-bonded bridging phosphine ligand always appear at the highest fields (see NMR data). The 2D homo- (H, H) and hetero-correlated (H, C) COSY spectra confirm a very characteristic shift of the H3 resonance of the bridging pyridyl ring in $PPh_xpyl_{3-x}$ ($x = 0, 1, 2$) ligands. For the bridging $Ppyl_3$ ligand, the H3 resonance is shifted by ca. 1.15–1.38 ppm towards higher field (in this case the signals of the H3 protons of non-coordinating pyridyls overlap, and the exact values of the chemical shifts were not determined) (see $^1$H NMR data). For complexes with $PPhpyl_2$ and $PPh_2pyl$ ligands, the H3 resonances of the non-bridging phosphines were not resolved. The H4 and H5 resonances undergo analogous shifts of ca. 0.27–0.12 ppm and 0.12 ppm, respectively (as was found for complexes containing the $PPh_2pyl$ ligand). The resonance for H6 proton is shifted only slightly (as in the case of complexes with $PPh_2pyl$ and $Ppyl_3$ ligands; in the case of the cluster with a $PPhpyl_2$ ligand this resonance overlaps with the H6 resonance of the uncoordinated pyridyl ring). Thus the most characteristic difference between bridging and non-bridging phosphines in $[Ir_4(\mu\text{-}CO)_3(CO)_5(\mu\text{-}PR_3)(PR_3)_2]$ clusters lies in the large shift (towards higher field) of their

H3 pyridyl protons. It was also found that the lines in resonances of the protons in the pyridyl ring in P,N-bonded phosphine ligands are broader than those for the remaining protons, probably because of the interaction with the iridium atom which possesses a quadrupole moment.

The $^{1}H$ and $^{31}P$ NMR spectra of **1** and **2** are temperature-dependent (Figs. 3 and 4). The $^{1}H$ spectra of both compounds in $CH_2Cl_2$ do not change significantly between +20°C and −40°C. The only effects observed in this range involve changes in the chemical shifts for some resonances and some broadening of resonance lines at temperatures down to −40°C. This is clearly seen for **2** in the range 8.2–8.8 ppm (where only signals of the H6 pyridyl protons appear). However at lower temperatures, between −50°C and −90°C, new broad resonances appear. For the cluster with $PPh_2pyl$ [21] the new signals appear at δ 6.7, 7.7 ppm and at δ 6.3, 8.0 ppm. In the case of $PPhpyl_2$ the new resonances are at δ 6.7 ppm and δ 7.9 ppm (Fig. 3). The $^{1}H$ NMR spectra of **3** exhibit no significant changes in the range +20°C to −90°C. We thus suggest that the observed changes are due to rotation of the ligand around the Ir—P bond or of the phenyl group around the P—C bond.

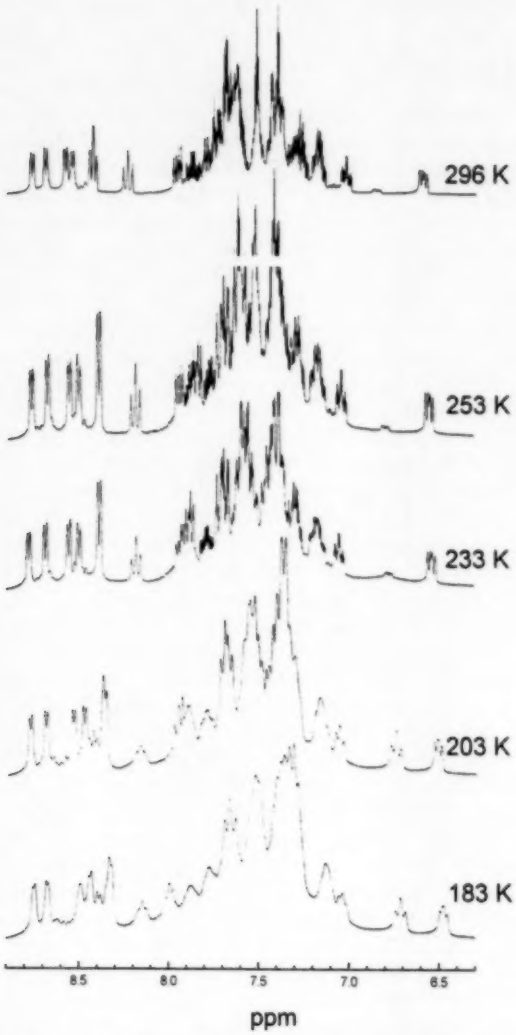


Fig. 3. The 300 MHz $^{1}H$ variable-temperature NMR spectra of **2** in $CD_2Cl_2$.

Complexes **1** and **2** display averaged signals in their $^{31}P\{^{1}H\}$ NMR spectra down to about −70°C. The spectra at room temperature, in $CD_2Cl_2$ or $CDCl_3$ as solvent, contain three resonances: $P_r$ = dd, $P_b$ = dd, $P_a$ = t (for designations and values of chemical shifts and coupling constants, see Experimental details). However, the line width depends on the solvent used as well as on the temperature. In $CCl_4/CDCl_3/CH_2Cl_2$ (13:27:60 volume ratio) (used as a solvent for measurements at temperatures up to −115°C), and also in $CD_2Cl_2$ and $CDCl_3$ at temperatures below 0°C, $J(P_r, P_a)$ and $J(P_b, P_a)$, couplings are not observed. As a result the spectrum consist of a $P_r$ doublet, a $P_b$ doublet and a $P_a$ singlet. At −70°C, collapse of the $P_r$ doublet is observed for the cluster with $PPh_2pyl$ as ligand. In the case of the cluster with $PPhpyl_2$, merging of $P_r$ into a singlet takes place at −80°C.

At −90°C, substantial broadening of the $P_r$ resonance at δ 30 ppm is observed for the complex with $PPh_2pyl$. Below −90°C, two broad signals appear in this region. For **1**, their chemical shifts are δ 33.5 ppm and 29.0 ppm. In the case of the cluster with $PPhpyl_2$, the coalescence temperature is lower by about 5°C. At −110°C, resonances for $P_r$ are observed at δ 32.0 and 26.0 ppm. For the bridging phosphine ligand broadening of the $P_b$ doublet is also observed, and this finally merges into a singlet. In the cluster with $PPh_2pyl$, collapse of the $P_b$ doublet takes place at −90°C (for the corresponding $P_r$ resonance collapse of the doublet occurs at −70°C), while for the complex with $PPhpyl_2$ the same behaviour is observed at lower temperatures (the $P_r$ doublet becomes a singlet at −80°C while merging of the bridging doublet is observed at about −110°C).

Cluster **3** exhibits dynamic properties only at much lower temperatures. At −113°C, merging of the $P_r$ doublet into a singlet is observed, while the remaining resonances do not essentially change. Because of the sparing solubility of the clusters in solvents with very low freezing points, we were not able to examine the $^{31}P\{^{1}H\}$ NMR spectra at lower temperatures.

The temperature-dependent $^{31}P\{^{1}H\}$ NMR spectra for the clusters suggest that the observed changes are due to the change in the coordination sphere of the Ir atom

bound to radial phosphine. It is also noteworthy that the coalescence temperatures depend on the number of pyridyl rings in the phosphine molecules (the larger the number of pyridyl rings, the lower the coalescence temperatures).

The natural abundance $^{13}C$ NMR spectra of the complexes are very complicated. For illustration, the $^{13}C$ NMR spectra of **1** in $CD_2Cl_2$ at +20°C and −90°C are shown in Fig. 5. The low-field resonances at $\delta$ 221.1, 214.3 and 212.7 ppm can be assigned, by analogy with data for known compounds, to the three bridging carbonyls [22–27]. It is known that in the $^{13}C$ NMR spectra of $Ir_4$ clusters the chemical shifts of the ligand resonances decrease in the sequence bridging > radial > axial ≈ apical [26]. From the 2D heterocorrelated (H, C) COSY spectra we can also assign the signals in the range $\delta$ 179.3–170.0 ppm to the remaining carbonyl groups. The doublet at $\delta$ 175.6 ppm can probably be assigned to the apical carbonyl group (designated as * in Fig. 1); the observed $J$(C–P) coupling constant for this carbonyl group is 30.5 Hz. Such large coupling constants are observed for analogous com-

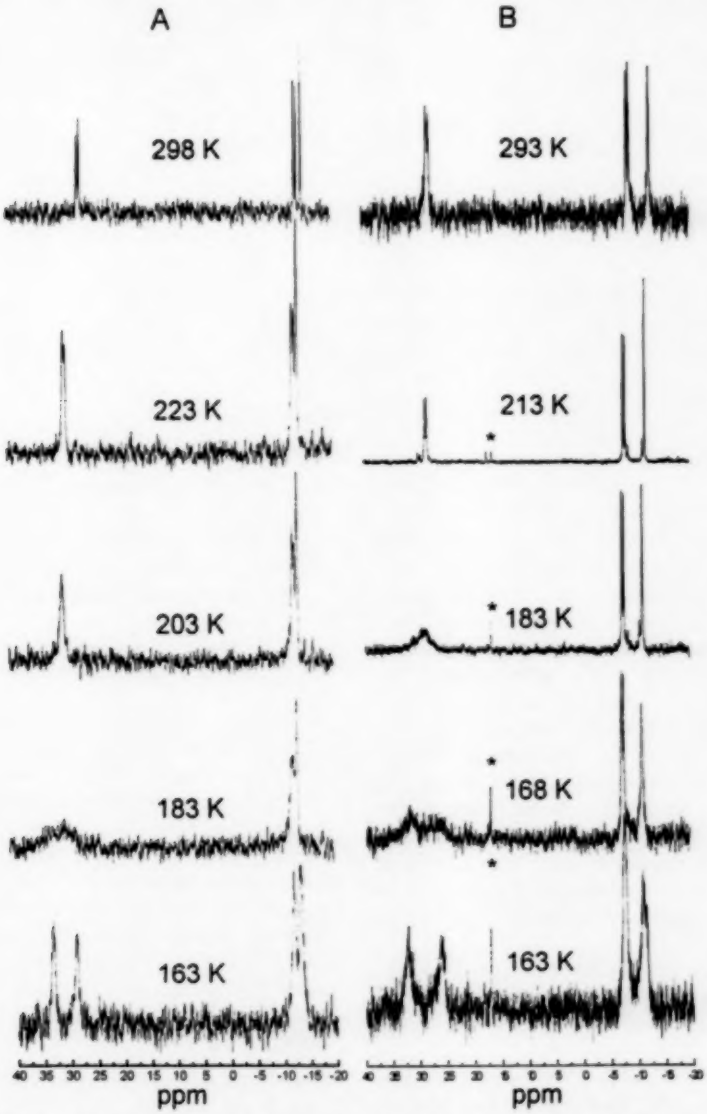


Fig. 4. The 121.5 MHz $^{31}P\{^1H\}$ variable-temperature NMR spectra (A) of **1** and (B) of **2** in $CCl_4/CDCl_3/CH_2Cl_2$ (13:27:60 volume ratio); * = impurity.

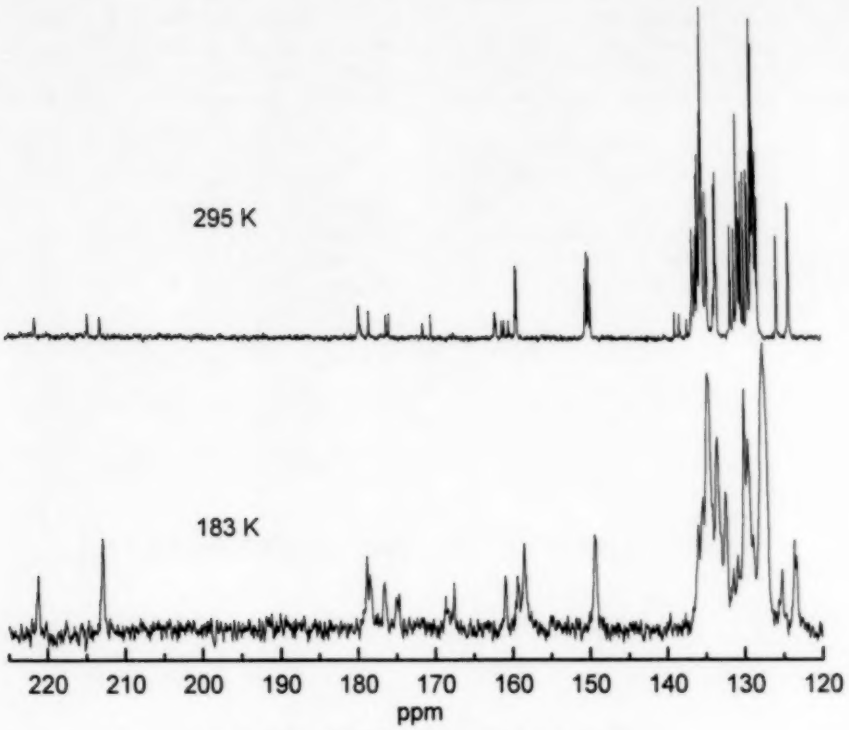


Fig. 5. The 75.5 MHz $^{13}C$ NMR spectra of **1** in $CD_2Cl_2$.

pounds when the ligands are pseudo-*trans* to each other in apical and basal–axial positions [8,22,24]. The remaining carbonyl resonances proved more difficult to assign. The signals in the range $\delta$ 161.7–120 ppm belong to the carbons of the phenyl and pyridyl rings. They are coupled with P atoms and were not resolved.

As is shown in Fig. 5, lowering of the temperature causes only slight changes in $^{13}C\{^1H\}$ NMR spectrum in the carbonyl region. At −90°C the lines are broader and there is some change in the chemical shifts of some resonances. However at −90°C only two resonances are observed above $\delta$ 210 ppm ($\delta$ 221.1 and 212.8 ppm, intensity ratio 1:2). Taking account of the nature of the changes with temperature, we suggest that the two bridging carbonyl resonances observed at −90°C are due to coincidential overlapping of signals at $\delta$ 214.3 and 212.7 ppm as a result of a shift of the first of these signals.

In the light of the $^1H$, $^{31}P\{^1H\}$ and $^{13}C\{^1H\}$ NMR spectra, and of the temperature-dependent spectra, we conclude that:

1. The $[Ir_4(\mu\text{-}CO)_3(CO)_5(\mu\text{-}PR_3)(PR_3)_2]$-type clusters have the same geometry in the solid state and in solution, since the $^{31}P$ NMR spectrum of **1** at room temperature is consistent with the X-ray structure.
2. Carbonyl scrambling is not observed in the temperature range +90°C to −115°C.
3. The 2-pyridyl rings (both coordinated and non-coordinated) are not involved in the exchange process and their resonances do not coalescence. Therefore the dynamic properties at low temperatures are due to rotation of the ligand around the Ir—P bond or of the phenyl group around the P—C bond.

There is a very interesting reaction of the $[Ir_4(\mu\text{-}CO)_3(CO)_5(\mu\text{-}PR_3)(PR_3)_2]$ clusters with CO [21]. Even with only a stoichiometric amount of CO splitting of the Ir—N bond is observed and a carbonyl ligand is coordinated to the apical iridium atom. These reactions can be monitored by $^{31}P\{^1H\}$ and $^1H$ NMR spectroscopy. The rate of consumption of a stoichiometric amount of CO is slow at room temperature. The reverse processes were also observed. In solution under argon, the $[Ir_4(\mu\text{-}CO)_3(CO)_6(PR_3)_3]$ clusters one carbonyl ligand at the apical iridium atom is substituted by the N atom of one of the pyridyl groups. Thus the following equilibrium exists in solution:

$$[Ir_4(CO)_8(\mu\text{-}PR_3)(PR_3)_2] \underset{Ar}{\overset{CO}{\rightleftharpoons}} [Ir_4(CO)_9(PR_3)_3]$$

Similar behaviour was observed for $[Ir_2Rh_2(CO)_{10}(\eta^4\text{-}COD)]$ [25]. Displacement of the second carbonyl

ligand at the apical iridium atom was not observed by use of NMR spectroscopy even at 90°C. No displacement of a CO ligand in $[Ir_4(\mu\text{-}CO)_3(CO)_5(\mu\text{-}PR_3)(PR_3)_2]$ to give $[Ir_4(\mu\text{-}CO)_3(CO)_4(\mu\text{-}PR_3)_2(PR_3)]$ was observed also in a basic medium.

## Acknowlegment

This research was supported by the Committee of Scientific Research, Grant No. 2 0703 91 01.

## References

[1] D. Braga and F. Grepioni, *J. Organometal. Chem., 336* (1987) C9.
[2] J.D. Atwood, *Coord. Chem. Rev., 83* (1988) 93.
[3] B.C. Gates, L. Guczi and H. Knözinger, *Metal Clusters in Catalysis*, Elsevier Amsterdam, 1986.
[4] J.P. Kennedy, P. Selz, A.L. Rheingold, W.C. Trogler and F. Basolo, *J. Am. Chem. Soc., 111* (1989) 3615.
[5] G.F. Holland, D.E. Ellis, D.R. Tyler, H.B. Gray and W.C. Trogler, *J. Am. Chem. Soc., 109* (1987) 4276.
[6] K. Dahlinger, F. Falcone and A.J. Poë, *Inorg. Chem., 25* (1986) 2654.
[7] J.D. Atwood, *J. Organometal. Chem., 383* (1990) 59.
[8] B.E. Mann, M.D. Vargas and R. Khadar, *J. Chem. Soc., Dalton Trans.*, (1992) 1725.
[9] K. Wajda, F. Pruchnik and T. Lis, *Inorg. Chim. Acta*, 40 (1980) 207.
[10] K. Wajda-Hermanowicz and F.P. Pruchnik, *Transition Metal Chem., 13* (1988) 22.
[11] J.P. Farr, M.M. Olmstead and A.L. Balch, *J. Am. Chem. Soc., 102* (1980) 6654.
[12] A. Maisonnat, J.P. Farr and A.L. Balch, *Inorg. Chim. Acta, 53* (1981) L217.
[13] A.J. Deeming and M.B. Smith, *J. Chem. Soc., Chem. Commun.*, (1993) 844.
[14] M.M. Olmstead, A. Maisonnat, J.P. Farr and A.L. Balch, *Inorg. Chem., 20*, (1981) 4060.
[15] J.P. Farr, M.M. Olmstead, F.E. Wood and A.L. Balch, *J. Am. Chem. Soc., 105* (1983) 792.
[16] K. Wajda-Hermanowicz and F.P. Pruchnik, *Transition Metal Chem., 13* (1988) 101.
[17] K. Wajda-Hermanowicz, M. Koralewicz and F.P. Pruchnik, *Appl. Organomet. Chem., 4* (1988) 73.
[18] F.P. Pruchnik, K. Wajda-Hermanowicz and M. Koralewicz, *J. Organometal. Chem., 381* (1990) 384.
[19] E. Gałdecka, Z. Gałdecki, K. Wajda-Hermanowicz and F.P. Pruchnik, *J. Chem. Crystallogr.*, in press.
[20] G.E. Griffin and W.A. Thomas, *J. Chem. Soc. B*, (1970) 477.
[21] K. Wajda-Hermanowicz, F. Pruchnik, M. Zuber, G. Rusek, E. Gałdecka and Z. Gałdecki, *Inorg. Chim. Acta, 232* (1995) 207.
[22] G.F. Stuntz and J.R. Shapley, *J. Am. Chem. Soc., 99* (1977) 607.
[23] P.E. Cattermole, K.G. Orrell and A.G. Osborne, *J. Chem. Soc., Dalton Trans.*, (1974) 328.
[24] B.E. Mann, B.T. Pickup and A.K. Smith, *J. Chem. Soc., Dalton Trans.*, (1989) 889.
[25] G. Bondietti, G. Suardi, R. Ros, R. Roulet, F. Grepioni and D. Braga, *Helv. Chim. Acta, 76* (1993) 2913.
[26] R. Ros, A. Scrivanti, V.G. Albano, D. Braga and L. Garlaschelli, *J. Chem. Soc., Dalton Trans.*, (1986) 2411.
[27] A. Strawczynski, G. Suardi, R. Ros and R. Roulet, *Helv. Chim. Acta, 76* (1993) 2210.

ELSEVIER

Journal of Organometallic Chemistry 508 (1996) 83–90

Journal of Organometallic Chemistry

# Molecular oxygen promoted oxidative cleavage of carbon–palladium bonds — catalytic cyclization of allylic 2-alkynoates to $\alpha$-alkylidene-$\gamma$-butyrolactones by a $Pd^{II}$ complex

Guoxin Zhu, Xiyan Lu *

*Shanghai Institute of Organic Chemistry, Chinese Academy of Sciences, 354 Fenglin Lu, Shanghai 200032, China*

Received 13 April 1995

**Abstract**

Molecular oxygen was used as the oxidant to promote the $Pd^{II}$ and $Cu^{II}$ catalyzed cyclization of acyclic allylic 2-alkynoates, yielding $\alpha$-haloalkylidene-$\gamma$-butyrolactones with high stereoselectivity. The stereochemistry of halopalladation of the carbon–carbon triple bond, 1,2-induction in the intramolecular carbon–carbon double insertion and oxidative cleavage of carbon–palladium bonds in the cyclization reaction were studied in detail.

*Keywords:* Palladium(II); Molecular oxygen; Oxidative cleavage; Butyrolactone; Cyclization; Stereoselectivity

## 1. Introduction

The stereoselective process has played a central role in the synthesis of compounds possessing medicinal or theoretical significance [1]. Recently, transition metal-catalyzed reactions, especially those that construct cyclic structures from easily available acyclic precursors, have received much attention owing to the template action of the transition metals [2].

The $\alpha$-methylene-$\gamma$-butyrolactone ring is an integral building block of many important naturally occurring compounds which exhibit many interesting biological activities such as cytotoxicity, antitumority, etc. [3]. Also, $\gamma$-butyrolactones are versatile intermediates in organic synthesis and are widely used in natural product synthesis [4]. Thus, it is of common interest to study the construction of $\gamma$-butyrolactones. We have been engaged in the development of new synthetic methods for $\alpha$-alkylidene-$\gamma$-butyrolactone derivatives from readily available acyclic allylic 2-alkynoates [5]. In our reaction, the lactone ring is constructed by carbon–carbon bond formation, which is quite different from the other methodologies reported. Based on this strategy, the carbon–carbon triple bond was first halopalladated to generate a vinylpalladium species, followed by intramolecular carbon–carbon double-bond insertion to form a new carbon–palladium bond which was quenched using different methods, such as dehalopalladation [5b], deacetoxypalladation [5c], dehydroxypalladation [5d], carbonylation [5e] and oxidative cleavage by $CuX_2$ [5f], etc., to complete the catalytic cycle. Thus, a series of $\alpha$-methylene-$\gamma$-butyrolactone derivatives were synthesized stereoselectively (Scheme 1).

Recently, considerable attention has been devoted to the development of aerobic oxidation catalysts for economical and environmental reasons [6]. The $CuCl_2$ assisted cleavage of the carbon–palladium bond by molecular oxygen in a Waker-type oxidation reaction has been extensively studied [7]. We wondered if oxidative cleavage of the carbon–palladium bond by molecular oxygen in the presence of a nucleophile would take place in our cyclization reaction. Should this be possible, the $\alpha$-alkylidene-$\gamma$-butyrolactone derivatives could be synthesized from acyclic precursors in a very simple manner. In this paper, we wish to report our recent results on the molecular oxygen promoted palladium(II) and cupric salt catalyzed cyclization of 2′-alkenyl 2-alkynoates in the presence of lithium halide.

* Corresponding author.

0022-328X/96/$15.00 © 1996 Elsevier Science S.A. All rights reserved
*SSDI* 0022-328X(95)05781-1

Table 1
Cyclization of allyl 2-alkynoates (1) under oxygen

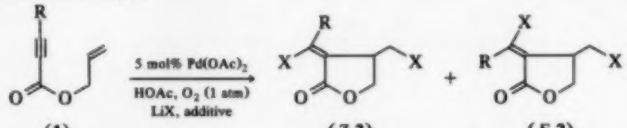


(1) (Z-2) (E-2)

| Entry no. | 1; R | LiX (equiv.) | Additive (equiv.) | Isolated yield (%) | |
|---|---|---|---|---|---|
| | | | | Z-2 | E-2 |
| 1 [a] | Me (1a) | LiCl(3) | – | 40.5 (Z-2a) | – |
| 2 | Me (1a) | LiCl(5) | CuCl(0.4) | 64.0 (Z-2a) | 3 (E-2a) |
| 3 [b] | Me (1a) | LiCl(5) | CuCl(0.4) | 38.0 (Z-2a) | 3 (E-2a) |
| 4 | Me (1a) | LiCl(5) | $CuCl_2$(0.4) | 73.0 (Z-2a) | 6 (E-2a) |
| 5 | Me (1a) | LiCl(5) | $Cu(OAc)_2$(0.4) | 83.0 (Z-2a) | 8 (E-2a) |
| 6 | i-$C_7H_{15}$(1b) | LiCl(6) | $Cu(OAc)_2$(0.4) | 68.0 (Z-2b) | 14.5 (E-2b) |
| 7 | i-$C_7H_{15}$(1b) | LiCl(6) | $CuCl_2$(0.4) | 61.0 (Z-2b) | 12.5 (E-2b) |
| 8 | $^n$Pr (1c) | LiCl(6) | $Cu(OAc)_2$(0.4) | 68.0 (Z-2c) | 12.0 (E-2c) |
| 9 | $^n$Pr (1c) | LiCl(10) | $Cu(OAc)_2$(0.4) | 71.5 (Z-2c) | 7.0 (E-2c) |
| 10 | $^n$Pr (1c) | LiBr(8) | $Cu(OAc)_2$(0.4) | 80.5 (Z-2'c) | 14.5 (E-2'c) |
| 11 | Me (1a) | LiBr(8) | $Cu(OAc)_2$(0.4) | 70.0 (Z-2'a) | 6.5 (E-2'a) |

[a] $PdCl_2(PhCN)_2$ as the catalyst.
[b] Reaction using ultrasonic means (100 W).

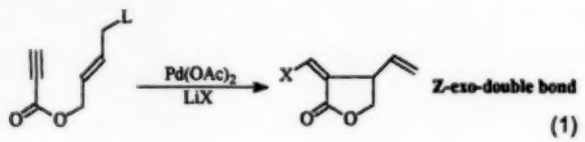


(1)

## 2. Results and discussion

### 2.1. Cyclization of allyl 2-alkynoates (1) promoted by molecular oxygen

We first tried the $PdCl_2(PhCN)_2$-catalyzed reaction of allyl 2-butynoate (**1a**) under $O_2$ in HOAc. The reaction afforded α-chloromethylene-β-chloromethyl-γ-butyrolactone (**2a**) with *Z*-selectivity in the exocyclic double bond, which was similar to the result found in the reaction of allyl 2-butynoate with a stoichiometric amount of $CuCl_2$ [5f]. When a catalytic amount of co-oxidant, e.g. CuCl, $CuCl_2$, etc. was added, the cyclization reaction occurred with improved yield. Finally, the cyclization reaction in HOAc catalyzed by $Pd(OAc)_2$ (0.05 equiv.) and $Cu(OAc)_2$ (0.4 equiv.) in the presence of LiCl (5 equiv.) gave the best results (Table 1).

Using the similar catalytic system, the cyclization of other allyl 3-substituted 2-alkynoates also proceeded smoothly under oxygen at room temperature (entries 6–9, Table 1).

When lithium bromide was used as the nucleophile

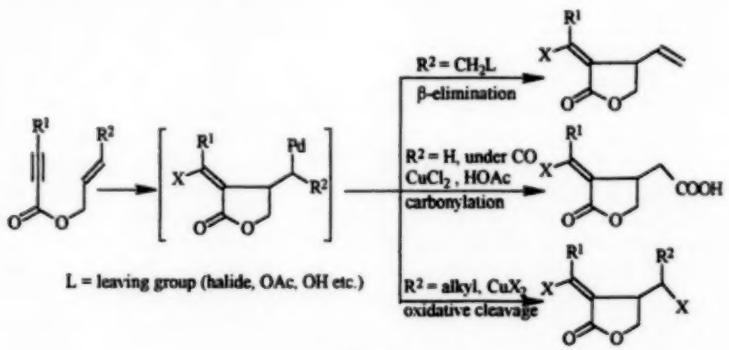


Scheme 1.

Table 2
Oxygen-mediated cyclization of allyl propynoate (3) [a]

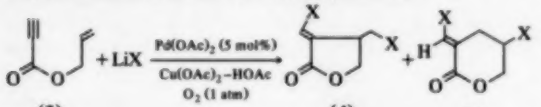


(3) (4) (5)

| Entry no. | LiX (equiv.) | $Cu(OAc)_2$ (equiv.) | Isolated yield (%) | | |
|---|---|---|---|---|---|
| | | | 4 | 5 | (4/5) [b] |
| 1 | LiCl(6) | 0 | 8.5 | 14 | 38:62 |
| 2 | LiCl(6) | 0.4 | 33 | 16.5 | 67:33 |
| 3 | LiCl(2) | [c] | 58 | 0 | – |
| 4 | LiBr(6) | 0.4 | 42.5 [d] | 37 [e] | 53.5:46.5 |

[a] All reaction were carried out at 40°C. [b] Isolated ratio.
[c] $CuCl_2$ (5 equiv.) was used in the reaction. [d] Brominated γ-butyrolactone product **4'**.
[e] Brominated δ-valerolactone product **5'**.

instead of lithium chloride, the oxygen-promoted cyclization also took place with the same catalytic system affording brominated α-alkylidene-γ-butyrolactone derivatives (entries 10, 11, Table 1).

### 2.2. Cyclization of allyl propynoate (3) — stereochemistry of halopalladation of terminal carbon–carbon triple bonds

We found that halopalladation of the carbon–carbon triple bond of propynoates exhibited a different stereochemical behaviour in the two catalytic systems {Eq. (1) [5b] and Eq. (2) [5f]}.

In the first reaction, *trans*-halopalladation of the carbon–carbon triple bond occurred to afford a *Z*-exocyclic double bond in the lactone product [5b], while *cis*-halopalladation of the carbon–carbon triple bond affording an *E*-exocyclic double bond was found in the second reaction [5f]. The only difference is that in the second reaction, $CuCl_2$ was used as the oxidant in the oxidative cleavage of the carbon–palladium bond [Eq. (2)]. It is suggested that the cupric salt may play an important role in the halopalladation step in the second reaction. To demonstrate the role of the $Cu^{II}$ salt, the palladium acetate-catalyzed reaction of allyl propynoate (**3**) with LiCl in HOAc under oxygen was carried out in the absence of $CuCl_2$ (entry 1, Table 2). We found that the exocyclic double bond of the isolated γ-butyrolactone product was still in the *E* form, implying that halopalladation still occurred in a *cis* manner under the oxygen even in the absence of a cupric salt. It is possible that the oxidant caused the halopalladation to occur in a different way. In this reaction, besides the five-membered γ-butyrolactone product **4**, a six-membered δ-valerolactone (**5**) was also obtained in 14% yield; this was not found in the reaction using 5 equiv. of $CuCl_2$ (entry 3, Table 2). Also, the cyclization of allyl 2-propynoate could be improved by a catalytic amount of $Cu(OAc)_2$ (entry 2, Table 2).

The reaction of **3** with LiBr under oxygen in the absence of $CuCl_2$ yielded a brominated acyclic product **6** rather than the expected cyclic product [Eq. (3)]. It is possible that the bromide ion is easily oxidized in the reaction system to give molecular bromine, which added readily to the carbon–carbon triple bond.

In the presence of a catalytic amount of $Cu(OAc)_2$, the palladium-catalyzed cyclization reaction of **3** with

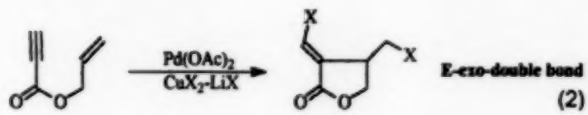


(2)

Table 3
Oxygen-mediated cyclization of 1'-substituted allylic 2-alkynoates

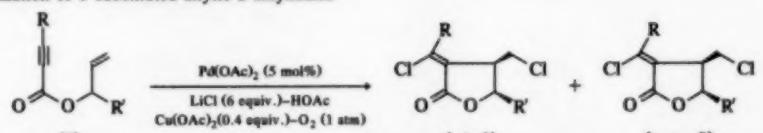


(7) (*cis*-8) (*trans*-8)

| Entry No. | 7 | R | R' | Yield (%) | *cis*-8/*trans*-8 [a] | |
|---|---|---|---|---|---|---|
| 1 | *rac*-7a | $CH_3$ | $C_5H_{11}$ | 53 | (>97:3) | *cis*-8a/*trans*-8a [b] |
| 2 | (*S*)-7a | $CH_3$ | $C_5H_{11}$ | 58 | (>97:3) | (4*S*,5*S*)-8a/(4*R*,5*S*)-8a [b] |
| 3 | *rac*-7b | H | $^iPr$ | 42 | (<3:97) | *cis*-8b/*trans*-8b [c] |

[a] Determined by 300 MHz $^1H$ NMR spectroscopy. [b] *Z*-Exocyclic double bond.
[c] *E*-Exocyclic double bond.

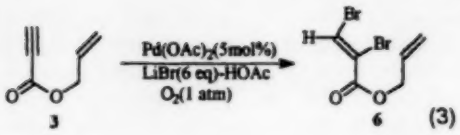

(3)

LiBr under oxygen also occurred smoothly, affording two cyclic products **4'** and **5'** in reasonable yield with good stereoselectivity (entry 4, Table 2).

### 2.3. 1,2-Stereoinduction of intramolecular carbon–carbon double-bond insertion in the oxygen-mediated cyclization reaction

Our recent research has revealed that the $Pd^{II}$-catalyzed reaction of 1'-alkyl 3-unsubstituted 2-propynoates with $CuCl_2$/LiCl gave *trans* selectivity for the $\beta,\gamma$-substituents in the lactones, while 1'-alkyl 3-substituted 2-alkynoates afforded *cis* selectivity for the $\beta,\gamma$-substituents in the lactones [5f,8].

The reaction under oxygen showed a similar stereochemistry. For the allylic 3-substituted 2-alkynoate, only *cis*-$\beta,\gamma$-disubstituted-$\alpha$-($Z$)-alkylidene-$\gamma$-butyrolactone was obtained (entry 1, Table 3). Starting from a homochiral substrate, an enantiomerically pure $\beta,\gamma$-substituted-$\alpha$-alkylidene-$\gamma$-butyrolactone could be obtained (entry 2, Table 3). However, cyclization of 1'-isopropyl-allyl propynoate only gave the *trans* product (relative to the $\beta,\gamma$-substituents) with an $E$-exocyclic double bond (entry 3, Table 3). Such stereochemistry indicates that the substituent R in substrate **7** plays an important role, not only in the stereochemistry of halopalladation of the carbon–carbon triple bond but also in the diastereoselectivity of the intramolecular carbon–carbon double-bond insertion reaction. The stereochemical results arising from the cyclization reaction may be rationalized on the basis of steric/conformational effects in the transition state for intramolecular carbon–carbon double-bond insertion, as proposed in our previous paper [5f].

### 2.4. Stereochemistry of oxidative cleavage of the carbon–palladium bond under oxygen

Oxidative cleavage of the carbon–palladium $\sigma$-bond takes place in a number of palladium-catalyzed oxidation reactions in the presence of nucleophiles [9]. The oxidizing agent usually weakens the palladium–carbon bonds, so that the palladium is converted into a good leaving group [10]. Although oxidative cleavage of carbon–palladium bonds has been studied extensively, the detailed mechanisms of these reactions are still unclear. Recently, we established the cleavage of carbon–palladium bonds by cupric chloride with predominant retention of configuration at the carbon atom [11], which is different from results reported in the literature [9,12].

The palladium-catalyzed cyclization of the 2-butynoate $E$-**9** with LiCl under oxygen in the presence of 0.4 equiv. of $Cu(OAc)_2$ afforded the cyclic product **10** selectively [Eq. (4)]; for the $Z$-substrate $Z$-**9**, the cyclization reaction afforded **10'** as the major product

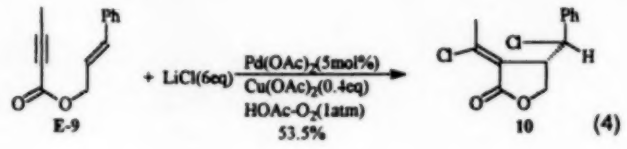

(4)

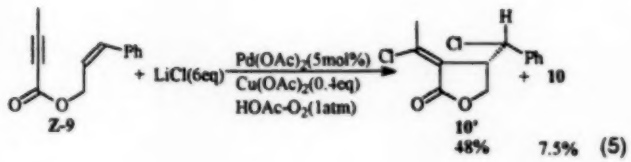

(5)

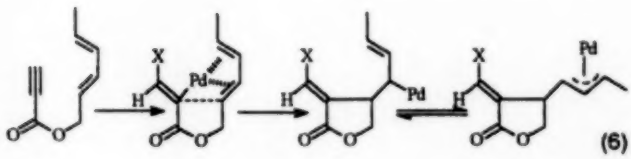

(6)

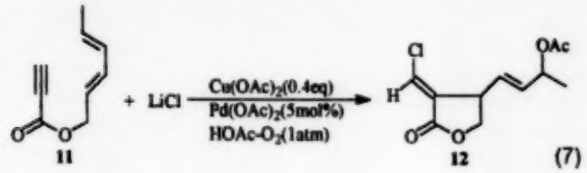


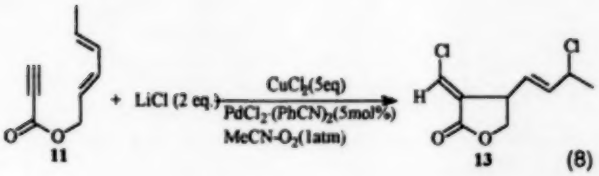


[Eq. (5)]. The structure of the products was determined by comparing the spectral data with those for the authentic compounds. This result indicates that oxidative cleavage of the carbon–palladium bond under oxygen also occurs with predominant retention of the configuration at the carbon atom [11].

### 2.5. Cyclization of 2,4-hexadienyl propynoate

In the cyclization reactions discussed so far, a $\sigma$-carbon–palladium bond is formed through intramolecular carbon–carbon double-bond insertion into the vinyl–palladium bond. If a conjugated dienyl propynoate is used, a $\pi$-allyl palladium intermediate could be formed which could also be quenched by a nucleophile in the presence of an oxidant [Eq. (6)].

We first tried the palladium-catalyzed reaction of 2,4-hexadienyl propynoate with LiCl under oxygen in HOAc. Reaction occurred to afford a mixture of cyclic diasteromers. With product **12**, we found the allyl–palladium species could be quenched by $OAc^-$, possibly derived from the solvent [Eq. (7)]. When the reaction was carried out in MeCN, the chlorinated cyclization product **13** was obtained [Eq. (8)]. However, the stereoselectivity of this reaction was poor with a mixture of isomers being obtained.

Reaction of 2,3-butadienyl propynoate with LiCl catalyzed by palladium(II) and the cupric salt under oxygen led to no cyclic product being isolated.

### 2.6. Mechanism

A possible mechanism for this palladium-catalyzed cyclization is given in Scheme 2. Halopalladation of the carbon–carbon triple bond in the presence of the oxidant and LiCl (*cis* addition for R = H and *trans* addition for R = alkyl) would produce a vinyl–palladium species which can be inserted intramolecularly by a

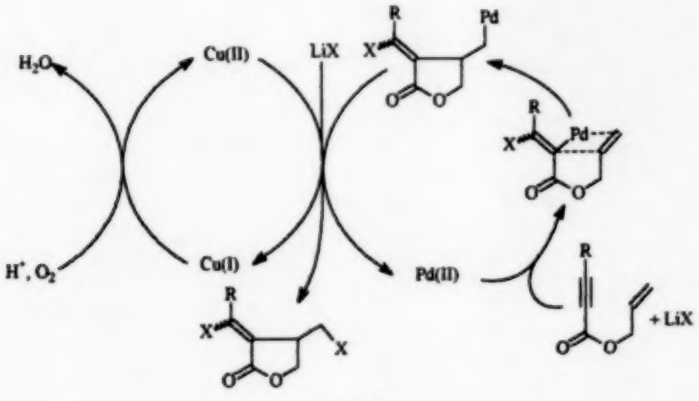


Scheme 2.

carbon–carbon double bond. The latter reaction would yield a cyclic intermediate containing a $\sigma$-carbon–palladium bond which may then be further oxidatively cleaved directly by oxygen in the presence of a catalytic amount of cupric salt to generate $Pd^{II}$ catalytic species and afford the cyclic product. Here, the role of the oxidant is not limited to re-oxidation of the low-valent palladium species, but it may also labilize the palladium–carbon bond in such a way that palladium is converted into a good leaving group. As a result, nucleophilic substitution of the metal may take place readily. The second catalytic circle involving oxidation of $Cu^{I}$ to $Cu^{II}$ by oxygen then takes place to complete the cycle.

In summary, we have studied the chemical behavior of the molecular oxygen mediated oxidative cleavage of the carbon–palladium bond and the stereochemistry of the reaction in detail. The present method provides a facile catalytic system capable of synthesizing functionalized $\alpha$-alkylidene-$\gamma$-butyrolactone derivatives from readily available acyclic allylic 2-alkynoates, thus avoiding the use of a large excess of cupric salt. Due to its simplicity, both in terms of the starting materials and the reaction conditions, the present reaction could be of utility in organic synthesis, especially in large-scale reactions.

## 3. Experimental details

The starting allylic 2-alkynoates were synthesized according to the reported procedure [5,13]. Analytical samples were further purified by Kugelrohr distillation using the stated oven temperatures (ot).

### *3.1. General procedure for oxygen-mediated palladium-catalyzed cyclization of allylic 2-alkynoates*

Under an oxygen atmosphere, $Pd(OAc)_2$ (11 mg, 0.05 mmol) was added to a solution of allylic 2-alkynoate (1 mmol), $Cu(OAc)_2$ (75 mg, 0.4 mmol) and lithium halide (6 mmol) in HOAc (5 ml), and the reaction was monitored by TLC (eluent: petroleum ether/ethyl acetate = 10:3). After reaction was complete, ethyl acetate (60 ml) was added and the mixture washed with water (3 × 5 ml) and dried ($MgSO_4$). Preparative TLC on silica gel (eluent: petroleum ether/ethyl acetate = 10:2) afforded the pure cyclic product. The results obtained are described in the text. The spectral and analytical data for compounds *Z*-**2a**, *E*-**2a**, *Z*-**2′a**, *E* − **2′a**, **4** and **4′** have been reported previously [5,10].

$\alpha$-(*E*)-(1′-Chloro-6′-methylheptylidene)-$\beta$-chloromethyl-$\gamma$-butyrolactone (*E*-**2b**): Oil. $^1$H NMR (300 MHz, $CDCl_3$) $\delta$: 4.43–4.33 (m, 2H); 3.82–3.77 (m, 1H); 3.66–3.60 (m, 2H); 3.19–3.12 (m, 1H); 3.09–3.02 (m, 1H); 1.64–1.51 (m, 3H); 1.39–1.18 (m, 4H); 0.89 ~ 0.85 (m, 6H) ppm. MS *m/e*: 282 (7.22); 281 (48.90); 280 (13.07); 279 (79.69); 277 (5.38); 245 (33.82, M $-^{35}$Cl); 243 (100.00, M $-^{37}$Cl); 209 (30.96); 207 (52.36); 193 (37.85); 175 (12.48); 173 (19.68); 160 (28.39); 151 (12.62); 149 (11.58); 147 (25.25); 145 (31.02); 99 (7.93). IR (neat)(cm$^{-1}$): 2950; 1765; 1680; 1470; 1380; 1230; 1080; 800; 740; 690. HRMS for $C_{13}H_{20}O_2Cl_2$: calc: 278.0840; found: 278.0851.

$\alpha$-(*Z*)-(1′-Chloro-6′-methylheptylidene)-$\beta$-chloromethyl-$\gamma$-butyrolactone (*Z*-**2b**): Oil. $^1$H NMR (300 MHz, $CDCl_3$) $\delta$: 4.93 (dd, $J$ = 0.69 Hz, $J$ = 9.73 Hz, 1H); 4.27 (m, 1H); 3.54 (m, 3H); 2.53 (m, 2H); 1.75–1.54 (m, 3H); 1.40–1.26 (m, 2H); 1.24–1.18 (m, 2H); 0.90–0.87 (m, 6H) ppm. MS *m/e*: 281 (0.47); 209 (1.91); 207 (2.64); 1.75 (1.96); 173 (1.05); 151 (1.16); 149 (1.05); 121 (1.21) 119 (1.11); 58 (27.26); 43 (100.00). IR (neat)(cm$^{-1}$): 2960; 2765; 1645; 1470; 1380; 1230; 1140; 1000; 750. Analysis: Calc. for $C_{13}H_{20}O_2Cl_2$:C, 55.92; H, 7.22%. Found: C, 55.90; H, 7.04%.

$\alpha$-(*E*)-(1′-Chlorobutylidene)-$\beta$-chloromethyl-$\gamma$-butyrolactone (*E*-**2c**): Oil. $^1$H NMR (300 MHz, $CDCl_3$) $\delta$: 4.44–4.36 (m, 2H); 3.82–3.80 (m, 1H); 3.66–3.62 (m, 2H); 3.18–3.11 (m, 1H); 3.07–3.00 (m, 1H); 1.72–1.64 (m, 2H); 0.96 (t, $J$ = 7.37 Hz, 3H) ppm. MS *m/e*: 227 (10.32); 226 [M$^+$(2 × $^{37}$Cl), 8.13]; 225 (61.92); 224 [M$^+$($^{37}$Cl, $^{35}$Cl), 21.72]; 223 (100.00); 222 [M$^+$(2 × $^{35}$Cl), 19.36); 189 [M$^+$($^{37}$Cl) − Cl, 5.77]; 187 [M$^+$($^{37}$Cl) − Cf, 16.20]; 175 [M$^+$($^{37}$Cl) − $CH_2Cl$, 17.86]; 173 [M$^+$($^{35}$Cl) − $CH_2Cl$, 53.52]; 147 (1.72); 145 (4.63); 137 (18.13); 109 (17.54); 93 (21.49); 91 (36.08). IR (neat)(cm$^{-1}$): 2980; 1760; 1660; 1440; 1380; 1230; 1070; 800; 740. HRMS: Calc. for $C_9H_{12}O_2Cl_2$: 224.01849 ($^{37}$Cl, $^{35}$Cl); 222.0214 (2 × $^{35}$Cl). Found: 224.0153 ($^{37}$Cl, $^{35}$Cl); 222.0177 (2 × $^{35}$Cl).

$\alpha$-(*Z*)-(1′-Chlorobutylidene)-$\beta$-chloromethyl-$\gamma$-butyrolactone (*Z* − **2c**): Oil. $^1$H NMR (300 MHz, $CDCl_3$) $\delta$: 4.39 (dd, $J_1$ = 0.72 Hz, $J_2$ = 9.83 Hz, 2H); 4.31–4.26 (m, 1H); 3.60–3.52 (m, 3H); 2.52 (dt, $J_1$ = 1.92 Hz, $J_2$ = 7.67 Hz, 2H); 1.78 (hexa, $J$ = 7.64 Hz, 2H); 1.01 (t, $J$ = 7.41 Hz, 3H) ppm. MS *m/e*: 227 (5.10); 226 [M$^+$(2 × $^{37}$Cl), 4.74]; 225 (31.51); 224 [M$^+$($^{37}$Cl, $^{35}$Cl), 15.07]; 223 (49.75); 222 [M$^+$(2 × $^{35}$Cl), 16.03]; 209 (4.58); 207 (7.61); 189 [M$^+$($^{37}$Cl) − Cl, 4.55]; 187 [M$^+$($^{37}$Cl) − Cl, 13.37]; 175 [M$^+$($^{37}$Cl) − $CH_2Cl$, 33.41]; 173 [M$^+$($^{35}$Cl) − $CH_2Cl$, 100.00]; 147 (2.70); 145 (75.7); 137 (24.30); 109 (33.97); 93 (44.56); 91 (63.91). IR (neat)(cm$^{-1}$): 2980; 2880; 1765; 1645; 1460; 1380; 1240; 1215; 1140; 910; 750. HRMS: Calc. for $C_9H_{12}O_2Cl_2$: 226.01553 (2 × $^{37}$Cl); 224.01849 ($^{37}$Cl, $^{35}$Cl); 222.02143 (2 × $^{35}$Cl). Found: 226.0131 (2 × $^{37}$Cl); 224.0186 ($^{37}$Cl, $^{35}$Cl); 222.0257 (2 × $^{35}$Cl).

$\alpha$-(*E*)-(1′-Bromobutylidene)-$\beta$-bromomethyl-$\gamma$-butyrolactone (*E* − **2′c**): Oil. $^1$H NMR (300 MHz, $CDCl_3$) $\delta$: 4.44 (m, 2H); 3.71–3.59 (m, 1H); 3.48 (t,

$J$ = 9.61 Hz, 1H); 3.33–3.26 (m, 1H); 3.19–3.13 (m, 1H); 1.66 (hexa, $J$ = 7.37 Hz, 2H); 0.96 (t, $J$ = 7.28 Hz, 3H) ppm. MS $m/e$: 315 [$M^+(2\times{}^{80}Br)+1$, 32.73]; 314 [$M^+(2\times{}^{80}Br)$, 7.83); 313 [$M^+({}^{80}Br, {}^{79}Br)+1$, 68.33]; 312 [$M^+(2\times{}^{79}Br)$, 6.14]; 311 [$M^+(2\times{}^{79}Br)+1$, 36.37]; 310 [$M^+(2\times{}^{79}Br)$, 1.64]; 233 [$M^+({}^{80}Br)-Br$, 97.91]; 231 [$M^+({}^{79}Br)-Br$, 100.00]; 219 [$M^+({}^{80}Br)-CH_2Br$, 5.29]; 217 [$M^+({}^{79}Br)-CH_2Br$, 2.08]; 203 (4.75); 201 (8.04); 199 (4.65); 177 (9.51); 175 (12.38); 137 (13.64); 135 (13.24); 107 (16.34); 105 (13.19); 79 (21.63). IR (neat)($cm^{-1}$): 2960; 2880; 1760; 1645; 1460; 1435; 1380; 1220; 1140; 1060; 780. HRMS: Calc. for $C_9H_{11}O_2Br_2$: 311.9183 [$M^+({}^{79}Br, {}^{80}Br)-1$]; 309.9204 [$M^+({}^{79}Br, {}^{79}Br)-1$]. Found: 311.9136 [$M^+({}^{79}Br, {}^{80}Br)-1$]; 309.9271 [$M^+({}^{79}Br, {}^{80}Br)-1$].

α-(*Z*)-(1′-Bromobutylidene)-β-bromomethyl-γ-butyrolactone (*Z*−**2′c**): Oil. $^1H$ NMR (300 MHz, $CDCl_3$) δ: 4.35 (dd, $J_1$ = 1.11 Hz, $J_2$ = 9.96 Hz, 1H); 4.26 (dd, $J_1$ = 6.24 Hz, $J_2$ = 9.40 Hz, 1H); 3.60–3.55 (m, 1H); 3.44–3.31 (m, 2H); 2.63 (dt, $J_1$ = 1.85 Hz, $J_2$ = 7.77 Hz, 2H); 1.84–1.69 (m, 2H); 0.99 (t, $J$ = 7.42 Hz, 3H) ppm. MS $m/e$: 315 [$M^+(2\times{}^{80}Br)+1$, 17.20]; 314 [$M^+(2\times{}^{80}Br)$; 4.21]; 313 [$M^+({}^{80}Br, {}^{79}Br)+1$, 35.85]; 312 [$M^+(2\times{}^{79}Br)$, 3.20]; 311 [$M^+(2\times{}^{79}Br)+1$, 18.25]; 233 [$M^+({}^{80}Br)-Br$, 94.55]; 231 [$M^+({}^{79}Br)-Br$, 100.00]; 219 [$M^+({}^{80}Br)-CH_2Br$, 3.14]; 217 [$M^+({}^{79}Br)-CH_2Br$, 3.40]; 203 (3.39); 201 (3.19); 175 (2.40); 173 (6.03); 137 (6.05); 135 (1.74); 109 (14.28); 107 (22.66); 105 (19.82). IR (neat)($cm^{-1}$): 2960; 2880; 1760; 1640; 1460; 1430; 1375; 1235; 1210; 1130; 770; 740. Analysis: Calc. for $C_9H_{12}O_2Br_2$: C, 34.64; H, 3.88%. Found: C, 34.68; H, 3.84%.

α-(*E*)-(1′-Chloromethylene)-γ-chloro-δ-valerolactone (**5**): Oil. $^1H$ NMR (300 MHz, $CDCl_3$) δ: 7.32 (t, $J$ = 3.19 Hz, 1H); 4.87 (m, 1H); 3.73 (d, $J$ = 4.5 Hz, 2H); 3.15 (ddd, $J_1$ = 3.20 Hz, $J_2$ = 8.23 Hz, $J_3$ = 18.45 Hz, 1H); 2.94 (ddd, $J_1$ = 3.09 Hz, $J_2$ = 4.81 Hz, $J_3$ = 18.32 Hz, 1H) ppm; radiating at δ 4.87 ppm: 3.73 (s); 3.15 (dd, $J_1$ = 3.10 Hz, $J_2$ = 18.8 Hz); 2.94 (dd, $J_1$ = 3.13 Hz, $J_2$ = 18.5 Hz) ppm. MS $m/e$: 184 [$M^+(2\times{}^{37}Cl)$, 0.70]; 182 [$M^+({}^{37}Cl, {}^{35}Cl)$, 3.71]; 180 [$M^+(2\times{}^{35}Cl)$, 5.53]; 147 [$M^+({}^{37}Cl)-Cl$, 0.85]; 145 [$M^+({}^{35}Cl)-Cl$, 2.27]; 133 [$M^+({}^{37}Cl)-CH_2Cl$, 32.36]; 131 [$M^+({}^{35}Cl)-CH_2Cl$, 100.00]; 105 (11.27); 103 (34.23); 87 (2.42); 75 (19.0); 63 (2.49). IR (neat)($cm^{-1}$): 3050; 2920; 1760; 1600; 1425; 1340; 1300; 1190; 840. HRMS: Calc. for $C_6H_6O_2Cl_2$: 181.9715 ($^{35}Cl$, $^{37}Cl$); 179.9714 ($2\times{}^{35}Cl$). Found: 181.9713 ($^{35}Cl$, $^{37}Cl$); 179.9714 ($2\times{}^{35}Cl$).

α-(*E*)-(1′-Bromomethylene)-γ-bromo-δ-valerolactone (**5′**): Oil. $^1H$ NMR (300 MHz, $CDCl_3$) δ: 7.56 (t, $J$ = 3.17 Hz, 1H); 4.85 (m, 1H); 3.58 (m, 2H); 3.08 (ddd, $J_1$ = 3.15 Hz, $J_2$ = 8.24 Hz, $J_3$ = 18.5 Hz, 1H); 2.81 (ddd, $J_1$ = 3.20 Hz, $J_2$ = 4.88 Hz, $J_3$ = 18.51 Hz, 1H) ppm. MS $m/e$: 272 [$M^+(2\times{}^{80}Br)$, 7.05]; 270 [$M^+({}^{80}Br, {}^{79}Br)$, 14.17]; 268 [$M^+(2\times{}^{79}Br)$, 7.35]; 191 [$M^+({}^{80}Br)-Br$, 12.14]; 189 [$M^+({}^{79}Br)-Br$, 12.80]; 177 [$M^+({}^{80}Br)-CH_2Br$, 97.87]; 175 [$M^+({}^{79}Br)-CH_2Br$, 100.00]; 149 (24.94); 147 (27.14); 121 (14.51); 119 (15.43); 109 (4.58). IR (neat)($cm^{-1}$): 3080; 2940; 1765; 1650; 1430; 1285; 1185; 1020; 710. HRMS: Calc. for $C_6H_6O_2Br_2$: 269.8697 [$M^+({}^{79}Br, {}^{80}Br)-1$]; 267.8735 [$M^+({}^{79}Br, {}^{79}Br)-1$]. Found: 269.8738 [$M^+({}^{79}Br, {}^{80}Br)-1$]; 267.8721 [$M^+({}^{79}Br, {}^{80}Br)-1$].

*cis*-β-Chloromethyl-γ-pentyl-α-(*Z*)-(1′-chloroethylidene)-γ-butyrolactone (*cis*-**8a**): M.p. 57–58°C. $^1H$ NMR (300 MHz, $CDCl_3$) δ: 4.37 (dt, $J_1$ = 9.86 Hz, $J_2$ = 4.93 Hz, 1H); 3.75 (dd, $J_1$ = 5.59 Hz, $J_2$ = 11.39 Hz, 1H); 3.54–3.43 (m, 2H); 2.40 (s, 3H); 1.85–1.59 (m, 4H); 1.43–1.34 (m, 4H); 0.91 (t, $J$ = 6.64 Hz, 3H) ppm; radiating at δ 4.37 ppm: 3.50 (dd, $J_1$ = 6.60 Hz, $J_2$ = 11.10 Hz); 3.46 (t, $J$ = 5.60 Hz) ppm. MS $m/e$: 268 [$M^+(2\times{}^{37}Cl)$, 1.02]; 266 [$M^+({}^{35}Cl, {}^{37}Cl)$, 4.75]; 264 [$M^+(2\times{}^{35}Cl)$, 6.19]; 231 (2.14); 229 (2.77); 219 [$M^+(2\times{}^{37}Cl)-CO_2-1$, 0.01]; 217 [$M^+$ ($^{37}Cl$, $^{35}Cl$) $-CO_2-1$, 3.37]; 215 [$M^+(2\times{}^{35}Cl)-CO_2-1$, 8.83]; 197 [$M^+(2\times{}^{37}Cl)-C_5H_{11}$, 3.48]; 195 [$M^+({}^{37}Cl, {}^{35}Cl)-C_5H_{11}$, 15.22]; 193 [$M^+(2\times{}^{35}Cl)-C_5H_{11}$, 25.59]; 167 (5.59); 165 (56.11); 163 (32.12); 133 (2.66); 131 (51.26); 129 (100.00); 65 (41.67). IR (Nujol film) ($cm^{-1}$) 2900; 2840; 1740; 1660; 1470; 1160. Analysis: Calc. for $C_{12}H_{18}Cl_2O_2$: C, 54.30; H, 6.84%. Found: C, 54.32; H, 7.09%.

(4*S*)-Chloromethyl-(5*S*)-pentyl-(2*Z*)-(1′-chloroethylidene)-γ-butyrolactone (4*S*, 5*S*)-**8a**: Oil. $[\alpha]_D^{25}$ = −26.0° (*c*, 1.33; $CHCl_3$).

*trans*-β-Chloromethyl-γ-isopropyl-α-(*E*)-(1′-chloromethylene)-γ-butyrolactone (*trans*-**8b**): Oil. $^1H$ NMR (300 MHz, $CDCl_3$) δ: 6.88 (d, $J$ = 1.65 Hz, 1H); 4.16 (dd, $J_1$ = 2.83 Hz, $J_2$ = 5.99 Hz, 1H); 3.59 (m, 2H); 3.19 (m, 1H); 1.87 (m, 1H); 0.99 (d, $J$ = 6.73 Hz, 6H) ppm. MS $m/e$: 227 [$M^+(2\times{}^{37}Cl)+1$, 4.29]; 225 [$M^+({}^{37}Cl, {}^{35}Cl)+1$, 25.19]; 223 [$M^+(2\times{}^{35}Cl)$, 39.62]; 189 [$M^+({}^{37}Cl)-Cl$, 4.73]; 187 [$M^+({}^{37}Cl)-Cl$, 14.37]; 183 (10.61); 181 (62.62); 179 (100.00); 153 (19.11); 151 (34.24); 145 (33.89); 143 (99.76); 117 (20.54); 115 (63.63); 109 (1.97); 107 (4.62); 89 (16.66); 87 (50.44). IR (neat)($cm^{-1}$): 3050; 2960; 2880; 1760; 1640; 1465; 1440; 1180; 1090; 1000; 860. HRMS: Calc. for $C_9H_{12}O_2Cl_2$: 224.01849 ($^{37}Cl$, $^{35}Cl$); 222.02143 ($2\times{}^{35}Cl$). Found: 224.0153 ($^{37}Cl$, $^{35}Cl$); 222.0237 ($2\times{}^{35}Cl$).

α-(*Z*)-(1′-Chloroethylidene)-β(*S**)-[1″(*R**)-chlorobenzyl]-γ-butyrolactone (**10**) [5f]: M.p. 119 ~ 121°C. $^1H$ NMR (600 MHz, $CDCl_3$) δ: 7.45 ~ 7.20 (m, 5H); 5.00 (d, $J$ = 7.10 Hz, 1H); 4.23 (d, $J$ = 9.70 Hz, 1H); 4.15 (dd, $J_1$ = 7.10 Hz, $J_2$ = 9.70 Hz, 1H); 3.75 (t, $J$ = 7.10 Hz, 1H); 2.31 (s, 3H) ppm. IR (Nujol film)($cm^{-1}$): 1760; 1650; 1240; 1140. MS $m/e$: 275 [$M^+(2\times{}^{37}Cl)+1$, 0.12]; 273 [$M^+({}^{35}Cl, {}^{37}Cl)+1$, 0.25]; 271 [$M^+(2\times{}^{35}Cl$, 0.31].

α-(*Z*)-(1′-Chloroethylidene)-β(*S**)-[1″(*S**)-chloro-

benzyl]-γ-butyrolactone (**10'**) [5f]: M.p. 134 ~ 136°C. $^1$H NMR (600 MHz, $CDCl_3$) δ: 7.42 ~ 7.32 (m, 5H); 4.88 (d, $J$ = 8.76 Hz, 1H); 4.68 (d, $J$ = 9.54 Hz, 1H); 4.25 (dd, $J_1$ = 6.12 Hz, $J_2$ = 9.54 Hz, 1H); 3.56 (dd, $J_1$ = 6.12 Hz, $J_2$ = 8.76 Hz, 1H); 1.60 (s, 3H) ppm. IR (neat)($cm^{-1}$): 2950; 1740; 1630; 1460; 1370. MS $m/e$: 273 [$M^+$($^{35}$Cl, $^{37}$Cl) + 1, 0.45]; 271 [$M^+$(2 × $^{35}$Cl) + 1, 0.87]; 127 ($^{37}$ClPhCH$^+$, 30.23); 125 ($^{35}$ClPhCH$^+$, 100.00).

α-(*E*)-(1'-Chloromethylene)-β-(3'-chloro-1'-butenyl)-γ-butyrolactone (**13**) [14]: Oil. $^1$H NMR (300 MHz, $CDCl_3$) δ: 6.59 (d, $J$ = 2.71 Hz); 6.56 (d, $J$ = 2.69 Hz, 1H); 5.90–5.83 (m, 1H); 5.66–5.40 (m, 1H); 4.58–4.30 (m, 2H); 4.04–3.97 (m, 1H); 3.90–3.81 (m, 1H); 1.64–1.61 (m, 3H) ppm. MS $m/e$: 225 [$M^+$(2 × $^{37}$Cl) + 1, 2.29]; 224 [$M^+$(2 × $^{37}$Cl), 1.56]; 223 (12.62); 222 (3.22); 221 (18.01); 220 (2.53); 194 (3.15); 192 (17.91); 190 (29.00); 187 [$M^+$($^{37}$Cl) − Cl, 4.26]; 185 [$M^+$($^{35}$Cl) − Cl, 6.74]; 178 (1.74); 176 (1.92); 157 [$M^+$($^{37}$Cl) − $CHClCH_3$, 16.59]; 155 [$M^+$($^{35}$Cl) − $CHClCH_3$, 40.55]; 141 (12.61); 132 (27.70); 130 (5.11); 119 (22.43); 105 (2.22); 91 ($CH{=}CHCHClCH_3$, 100.00). IR (neat)($cm^{-1}$) : 3050; 2980; 2900; 1770; 1640; 1480; 1450; 1380; 1320; 1180; 1020; 970.

## Acknowledgments

We thank the National Natural Science Foundation of China and Chinese Academy of Sciences for financial support.

## References

[1] D. Seebach, *Angew. Chem., Int. Ed. Engl., 29* (1990) 1320; T. Mukaiyama, *Challenges in Organic Chemistry*, Clarendon Press, Oxford, UK, 1990; C.P. Jasperse, D.P. Curran and T.L. Fevig, *Chem. Ber., 91* (1991) 1237.

[2] A.F. Nobels, M. Graziani and A.J. Hubert, *Metal Promoted Selectivity in Organic Synthesis*, Kluwer, Dordrecht, The Netherlands, 1991; B.M. Trost, *Pure Appl. Chem., 64* (1992) 315; E. Negishi, *Pure Appl. Chem., 64* (1992) 323; J.-E. Bäckvall, *Pure Appl. Chem., 64* (1992) 429; Y. Kishi, *Pure Appl. Chem., 64* (1992) 343; R. Noyori, *J. Synth. Org. Chem. Jpn., 50* (1992) 113.

[3] W. Tang and G. Eisenbrand, *Chinese Drugs of Plant Origin*, Springer-Verlag, Berlin, 1992; N.H. Fisher, E.J. Oliver and H.D. Fisher, in W. Herz, H. Grisebach and G.W. Kriby (eds.), *Progress in the Chemistry of Organic Natural Products*; Springer-Verlag, New York, 1979, p. 47; P.A. Grieco, *Synthesis*, (1975) 67; H.M.R. Hoffmann and J. Rabe, *Angew. Chem., Int. Ed. Engl., 24* (1985) 94; N. Petragnani, H.M.C. Ferraz and G.V.J. Silva, *Synthesis*, (1986) 157.

[4] S.C. Koch and A.R. Chamberlin, *J. Org. Chem., 58* (1993) 2725, and references cited therein; M. Menges and R. Bruckner, *Synlett*, (1993) 901; D.W. Ribbons and A.G. Sutherland, *Tetrahedron, 50* (1994) 3587, and references cited therein; Y. Nagao, W. Dai, M. Ochiai and M. Shiro, *J. Org. Chem., 54* (1989) 5211, and references cited therein; J. Rojo, M. Oarcia and J.C. Carretero, *Tetrahedron, 49* (1993) 9787; M.M. Murta, M.B.M. de Azevedo and A.E. Greene, *J. Org. Chem., 58* (1993) 2537; J. Cossy, J.L. Ranaivosata and V. Bellosta, *Tetrahedron Lett., 35* (1994) 1205; J. Ariza, J. Font and R.M. Ortuno, *Tetrahedron, 46* (1990) 1931.

[5] (a) X. Lu, S. Ma, J. Ji, G. Zhu and H. Jiang, *Pure Appl. Chem., 66* (1994) 1501; (b) S. Ma and X. Lu, *J. Chem. Soc., Chem. Commun.*, (1990) 733; S. Ma and X. Lu, *J. Org. Chem., 56* (1991) 5120; S. Ma, G. Zhu and X. Lu, *J. Org. Chem., 58* (1993) 3692; (c) G. Zhu, S. Ma and X. Lu, *J. Chem. Res. S*, (1993) 366; G. Zhu, S. Ma and X. Lu, *J. Chem. Res. M*, (1993) 2467; (d) S. Ma and X. Lu, *J. Organomet. Chem., 447* (1993) 305; (e) J. Ji and X. Lu, *Tetrahedron, 50* (1994) 9067; (f) S. Ma and X. Lu, *J. Org. Chem., 58* (1993) 1245; X. Lu and G. Zhu, *Synlett*, (1993) 68; J. Ji, C. Zhang and X. Lu, *J. Org. Chem., 60* (1995) 1160.

[6] S.I. Murahashi, T. Naota and N. Hirai, *J. Org. Chem., 58* (1993) 7318; G. Wang, U. Andreasson and J.-E. Bäckvall, *J. Chem. Soc., Chem. Commun.*, (1994) 1037; M. Hamamoto, K. Nakayama, Y. Nishiyama and Y. Ishii, *J. Org. Chem., 58* (1993) 6421; T.M. Meulemans, N.H. Kiers, B.L. Ferina and P.W.N.M. van Leeuwen, *Tetrahedron Lett., 35* (1994) 455.

[7] P.M. Henry, *Palladium Catalyzed Oxidation of Hydrocarbons*, Reidel, Boston, MA, 1980; H. Grennberg and J.-E. Bäckvall, *J. Chem. Soc., Chem. Commun.*, (1993) 1331.

[8] R.C. Larock and T.R. Hightower, *J. Org. Chem., 58* (1993) 5298.

[9] G.W. Daub, *Prog. Inorg. Chem., 22* (1977) 409, J.-E. Bäckvall, *Acc. Chem. Res., 16* (1983) 335, and references cited therein.

[10] P.K. Wong and J.K. Stille, *J. Organomet. Chem., 70* (1974) 121.

[11] G. Zhu, S. Ma, X. Lu and Q. Huang, *J. Chem. Soc., Chem. Commun.*, (1995) 271.

[12] J.-E. Bäckvall, Tetrahedron Lett., (1977) 467.

[13] G. Zhu and X. Lu, Tetrahedron: Asym., 6 (1995) 345; G. Zhu and X. Lu, *Tetrahedron: Asym., 6* (1995) 885.

[14] J.-E. Bäckvall, Y.I.M. Nilsson, P.G. Andersson, R.G.P. Gatti and J. Wu, *Tetrahedron Lett., 35* (1994) 5713.

ELSEVIER

Journal of Organometallic Chemistry 508 (1996) 91–99

Journal of Organometallic Chemistry

# Preparation of Group 4 metal complexes of a bulky amido-fluorenyl ligand

H.V. Rasika Dias [a,*], Ziyun Wang [a], Simon G. Bott [b]

[a] Department of Chemistry and Biochemistry, The University of Texas at Arlington, Arlington, TX 76019, USA
[b] Department of Chemistry, University of North Texas, Denton, TX 76203, USA

Received 18 April 1995; in revised form 13 June 1995

**Abstract**

The synthesis, spectroscopic and structural characterization of new amido-fluorenyl ligand [$(Me_3CN(H)–Si(Me)_2CH_2–C_{13}H_8)Li(THF)$] (**1**) is reported. The treatment of **1** with BuLi followed by the reaction with Group 4 metal chlorides led to crystalline, solvent free, metal complexes [$(\eta^1\text{-}NCMe_3)Si(Me)_2CH_2(\eta^5\text{-}C_{13}H_8)MCl_2$] (where M = Ti (**3**), Zr (**4**) or Hf (**5**)) in good yield. The X-ray crystal structures of **4** and **5** are also reported. Both these compounds possess monomeric structures with relatively short M–N and M–Cl bonds. The M–N distances of **4** and **5** are 2.060(3) Å and 2.065(3) Å respectively. The metal ion is coordinated to the fluorene group in $\eta^5$-fashion. The X-ray data also indicate the presence of a relatively unstrained ligand backbone in these metal complexes.

*Keywords:* Alkali metals; Group 4; Crystal structure; Amide; Metallocene

## 1. Introduction

The *ansa*-metallocene complexes of Group 4 metals are of importance in many areas including in catalytic alkene polymerizations and in the asymmetric induction [1–16]. Recently there has been increasing interest in the synthesis of ligands where one of the cyclopentadiene groups of *ansa*-metallocene has been replaced with groups such as amido or alkoxy donors [17–25]. The Group 3 and 4 metal complexes of these monocyclopentadiene-amido or -alkoxy ligands have also been found to act as catalysts for olefin polymerization reactions [17–19,21,26–30]. Furthermore, metal complexes of such amido-cyclopentadienyl ligands show higher Lewis acidity compared to the corresponding bis(cyclopentadienyl)metal complexes [19]. This increased electrophilicity of the metal center has been attributed largely to the reduction in the number of electrons donated to the metal center by the ligands [17,31]. In the absence of adequate steric protection, the metal complexes derived from these hybrid *ansa*-ligands often tend to form adducts with solvents, Lewis bases, alkali metal halides, or to form aggregates [17,21,25]. In certain instances, this increased reactivity even leads to the formation of bis-ligand complex. For example, irrespective of the molar ratio, the reaction between $[Me_3CNSi(Me)_2\text{-}C_5H_4]Li_2$ and $ZrCl_4$ leads exclusively to $[Me_3CNSi(Me)_2C_5H_4]_2Zr$ [24].

We have focused our attention on the synthesis of sterically demanding *ansa*-ligand systems containing fluorene [32]. In this paper, we describe the synthesis of an amido-fluorenyl ligand with a $-Si(Me)_2CH_2-$ backbone and its use in the synthesis of the dichloro metal complexes of Ti, Zr and Hf. Such systems could be expected to have relatively less strained ligand backbone compared to systems with $-CR_2-$ or $-SiR_2-$ (where R = alkyl or aryl group) bridges and should offer better protection to the central metal ion.

## 2. Experimental details

All operations were carried out under an atmosphere of purified nitrogen using either standard Schlenk techniques or in a Vacuum Atmospheres single station dry box equipped with a −25°C refrigerator. Solvents were distilled from conventional drying agents and degassed twice prior to use [33]. Glassware was oven-dried at 150°C overnight. The $^1H$ and $^{13}C$ NMR spectra were recorded in $C_6D_6$ at 25°C on a Bruker MSL-300 spec-

* Corresponding author.

0022-328X/96/$15.00 © 1996 Elsevier Science S.A. All rights reserved
SSDI 0022-328X(95)05803-6

trometer ($^1$H, 300.15 MHz; $^{13}$C, 75.47 MHz) or Nicolet NT-200 spectrometer ($^1$H, 200.06 MHz; $^{13}$C, 50.31 MHz), unless otherwise noted. Chemical shifts for $^1$H NMR spectra are relative to internal $Me_4Si$ or to residual protium in the deuterated solvents ($C_6D_6$, 7.15 ppm). The $^{13}$C NMR spectra were run with $^1$H decoupling and the chemical shifts are reported in ppm vs. $Me_4Si$ ($C_6D_6$ at 128.0 ppm). Melting points were obtained on a Mel-Temp II apparatus and were not corrected. Elemental analyses were performed by Texas Analytical Laboratories, Inc., Houston, TX.

Fluorene ($C_{13}H_{10}$), $^n$BuLi (1.6 M solution in hexanes), $TiCl_4$, $ZrCl_4$ and $HfCl_4$ were obtained from Aldrich and used as received. $TiCl_4(THF)_2$ was prepared according to literature method [34]. The $ClCH_2Si(Me)_2N(H)CMe_3$ was synthesized from $Me_3CNH_2$ and $ClCH_2Si(Me)_2Cl$ as described for the related species, purified by vacuum distillation and used immediately in the synthesis of **1** [35,36].

### 2.1. [{$Me_3CN(H)Si(Me)_2CH_2$–$C_{13}H_8$}Li(THF)] (1)

Fluorene (2.0 g, 12.0 mmol) in thf (20 ml) was cooled to 0°C and treated with $^n$BuLi in hexane (7.5 ml of 1.6 M solution, 12.0 mmol) over a period of 15 min. The color of the solution became red immediately. The solution was then allowed to warm up to room temperature and stirred for further 30 min. This mixture was added dropwise into $ClCH_2Si(Me)_2N(H)CMe_3$ (1.08 g, 6.0 mmol, 20 ml) in THF (20 ml) at 0°C, allowed to warm up to room temperature and stirred overnight. All of the volatiles were removed under vacuum and the residue was extracted into toluene. The mixture was filtered and the toluene was removed from the filtrate to obtain a red solid. This red solid was rinsed several times with hexane and dried under vacuum to obtain **1** in 67% yield. The product was recrystallized from toluene–hexane at −25°C. m.p. 105–108°C. $^1$H $\delta$ = 0.22 (s, 6H, SiMe), 0.67 (s, 9H, $^t$Bu), 1.01 (m, 4H, THF), 2.48 (m, 4H, THF), 2.62 (s, 2H, $CH_2$), 7.08–8.37 (m, 8H, $C_{13}H_8$); $^{13}$C{$^1$H} $\delta$ = 2.72 (SiMe), 14.87 ($SiCH_2$), 25.08 (THF), 32.93 ($^t$Bu), 50.24 ($^t$Bu), 67.53 (THF), 85.06, 111.78, 115.57, 119.41, 120.83, 121.77, 130.73 ($C_{13}H_8$). Anal. Calc. for $C_{24}H_{34}NOSiLi$: C, 74.38; H, 8.84; N, 3.61. Found: C, 74.32; H, 8.81; N, 3.58.

### 2.2. [{($\eta^1$-$NCMe_3$)$Si(Me)_2CH_2$($\eta^5$-$C_{13}H_8$)}$TiCl_2$] (3)

A solution of **1** (0.50 g, 1.29 mmol) in toluene (20 ml) was treated with $^n$BuLi in hexane (0.8 ml of 1.6 M solution, 1.29 mmol) at 0°C and allowed to stir for 10 min. After 30 min stirring at room temperature, this mixture was added dropwise to $TiCl_4(THF)_2$ (0.45 g, 1.34 mmol) in toluene (15 ml) over a period of 15 min at −78°C. The color of the mixture changed from red to dark green. The solution was allowed to warm up to room temperature and stirred overnight. The resulting mixture was filtered and the filtrate was concentrated to ca. 5 ml. Hexane was added and the solution was cooled to −25°C to obtain a dark green microcrystalline precipitate. A second crop of crystals were obtained from the concentrated filtrate. Yield 0.34 g (63%), m.p. 205–210°C. $^1$H $\delta$ = 0.40 (s, 6H, SiMe), 1.28 (s, 9H, $^t$Bu), 2.61 (s, 2H, $CH_2$), 7.16–7.60 (m, 8H, $C_{13}H_8$); $^{13}$C{$^1$H} $\delta$ = 7.07 (SiMe), 17.46 ($SiCH_2$), 33.00 ($^t$Bu), 63.40 ($^t$Bu), 116.70, 119.55, 124.26, 125.33, 129.15 ($C_{13}H_8$). Anal. Calc. for $C_{20}H_{25}Cl_2NSiTi$: C, 56.35; H, 5.91; N, 3.29. Found: C, 56.13; H, 5.97; N, 3.29.

### 2.3. [{($\eta^1$-$NCMe_3$)$Si(Me)_2CH_2$($\eta^5$-$C_{13}H_8$)}$ZrCl_2$] (4)

A solution of **1** (0.50 g, 1.29 mmol) in diethyl ether (20 ml) was treated with $^n$BuLi in hexane (0.8 ml of 1.6 M solution, 1.29 mmol) at 0°C. After 5 min, the solution was allowed to warm up to room temperature and stirred for further 30 min. The reaction mixture was then added dropwise to $ZrCl_4$ (0.30 g, 1.29 mmol) in $Et_2O$ (15 ml) at −78°C. The color of the solution changed from red to brown. The reaction system was allowed to warm up to room temperature and stirred overnight. The volatiles were removed under reduced pressure. The resulting solid was taken up in toluene, the solution was filtered and the filtrate was concentrated. Addition of hexane followed by cooling to −25°C afforded dark yellow crystals of **4** in 75% yield. m.p. 245–248°C. $^1$H $\delta$ = 0.40 (s, 6H, SiMe), 1.26 (s, 9H, $^t$Bu), 2.43 (s, 2H, $CH_2$), 7.14–7.75 (m, 8H, $C_{13}H_8$); $^{13}$C{$^1$H} $\delta$ = 7.51 (SiMe), 15.01 ($SiCH_2$), 32.91 ($^t$Bu), 56.69 ($^t$Bu), 103.32, 120.09, 121.41, 125.10, 125.64, 129.09 ($C_{13}H_8$). Anal. Calc. for $C_{20}H_{25}Cl_2NSiZr$: C, 51.15; H, 5.37; N, 2.98. Found: C, 51.09; H, 5.31; N, 2.82.

### 2.4. [{($\eta^1$-$NCMe_3$)$Si(Me)_2CH_2$($\eta^5$-$C_{13}H_8$)}$HfCl_2$] (5)

A solution of **1** (0.50 g, 1.29 mmol) in diethyl ether (20 ml) was treated with $^n$BuLi in hexane (0.8 ml of 1.6 M solution, 1.29 mmol) at 0°C. After 5 min, the solution was allowed to warm up to room temperature and stirred for further 30 min. The reaction mixture was then added dropwise to an $Et_2O$ (15 ml) solution of $HfCl_4$ (0.41 g, 1.29 mmol) at −78°C. The color of the solution changed from red to brown. The resulting mixture was then stirred overnight at room temperature. The volatiles were removed under reduced pressure. The resulting solid was taken up in toluene, the solution was filtered and the filtrate was concentrated. Addition of hexane followed by cooling to −25°C afforded dark yellow crystals of **5** in 81% yield. m.p. 225–228°C. $^1$H $\delta$ = 0.42 (s, 6H, SiMe), 1.25 (s, 9H, $^t$Bu), 2.47 (s, 2H, $CH_2$), 7.12–7.75 (m, 8H, $C_{13}H_8$); $^{13}$C{$^1$H} $\delta$ = 7.96

(SiMe), 14.61 ($SiCH_2$), 33.63 ($^tBu$), 55.95 ($^tBu$), 97.82, 118.78, 121.13, 124.58, 125.47, 128.96 ($C_{13}H_8$). Anal. Calc. for $C_{20}H_{25}Cl_2NSiHf$: C, 43.13; H, 4.52; N, 2.52. Found: C, 43.04; H, 4.67; N, 2.40.

### 2.5. X-ray structure determination of 1

X-ray quality crystals of **1** were obtained by slow crystallization from toluene–hexane at −25°C. A suitable crystal was selected and mounted under nitrogen in a Lindemann capillary on a goniometer head and transferred to the goniostat of an Enraf-Nonius CAD 4 diffractometer. The unit cell parameters were determined by least-squares refinement of 25 reflections. Data were collected at room temperature. Three standard reflections were measured at every 3600 s of exposure time to check for crystal deterioration and/or misalignment. No significant deterioration in intensity was observed. Data were corrected for Lorentz and polarization effects, but not for absorption. The structure was solved by direct methods (SHELX 86) [37]. Anisotropic refinement was carried out by full-matrix least-squares on $F$. All non-hydrogen atoms with the exception of the carbons in the 5-membered ring and Li were refined with anisotropic thermal parameters. The H on the nitrogen was located on the difference map, and the remaining hydrogen atoms were included in the model at calculated position ($U$(H) = 1.3 [$U$(C)]). Refinement converged at $R = 0.0546$, $Rw = 0.0526$ ($w = [0.04F^2 + (\sigma F)^2]^{-1}$) [38]. Further details of the crystal structure are provided in the supplementary material.

### 2.6. X-ray structure determination of 4

Crystals of **4** were obtained by slow crystallization from toluene–hexane at −25°C. A suitable crystal was selected and mounted under nitrogen in a Lindemann capillary on a goniometer head and transferred to the goniostat of an Enraf-Nonius CAD 4 diffractometer. The unit cell parameters were determined by least-squares refinement of 25 reflections. Data were collected at room temperature. Three standard reflections were measured at every 3600 s of exposure time to check for crystal deterioration and/or misalignment. No significant deterioration in intensity was observed. Data were corrected for Lorentz and polarization effects, and a Fourier absorption correction was applied. The structure was solved by Patterson methods. Anisotropic refinement was carried out by full-matrix least-squares for all the non-hydrogen atoms, and hydrogen atoms were included in the model at calculated position ($U$(H) = 1.3 [$U$(C)]). Refinement on $F$ converged at $R = 0.0268$, $Rw = 0.0317$ ($w = [0.04F^2 + (\sigma F)^2]^{-1}$) [38]. Further details of the crystal structure are available in the supplementary material.

### 2.7. X-ray structure determination of 5

Crystals of **5** were obtained by slow crystallization from toluene–hexane at −25°C. The crystals were removed from the Schlenk tube under nitrogen and immediately covered with a layer of hydrocarbon oil. A suitable crystal was selected and attached to a glass fiber and immediately placed in the low temperature nitrogen stream of the Siemens P4 diffractometer with a LT-2A device [39]. The unit cell parameters were determined by least-squares refinement of 50 reflections. Data were collected at −80°C. Three standard reflections were measured at every 97 data points to check for crystal deterioration and/or misalignment. No significant deterioration in intensity was observed. Data were corrected for Lorentz and polarization effects, and an empirical absorption correction was applied [40]. The structure was solved by direct methods. All the non-hydrogen atoms were refined anisotropically. The hydrogen atoms were included in the refinement at calculated position ($U$(H) = 1.2 [$U$(C)]). Refinement on $F$ converged at $R = 0.0212$, $Rw = 0.0212$; [$w = 1/\sigma^2(F)$]. All the software programs and the sources of scattering factors are contained in the SHELXTL PC (Version 4.2) software package provided by Siemens Analytical X-ray Instruments, Inc. [41]. Further details of the crystal structure are available in the supplementary material.

## 3. Results and discussion

The monolithium complex of the amido-fluorenyl ligand, [{$Me_3CN(H)Si(Me)_2CH_2$–$C_{13}H_8$}Li(THF)] (**1**) was prepared in 67% yield by the treatment of $Me_3CN(H)SiMe_2CH_2Cl$ with two equivalents of fluorenyllithium in THF (Scheme 1). This compound has been isolated as a red solid and characterized by $^1H$, $^{13}C$ NMR spectroscopy and elemental analysis. These data also show the presence of one molecule of THF for each Li atom in **1**. The $^1H$ NMR signals due to the THF appear as two multiplets around 1.01 and 2.48 ppm. This somewhat upfield shift may be due to the shielding effects of fluorenyl ring current [25]. Compound **1** could be stored under dry nitrogen (preferably at −25°C) without any apparent decomposition.

[{$Me_3CNSi(Me)_2CH_2$–$C_{13}H_8$}]$Li_2$ **2** was prepared by the addition of one equivalent of $^nBuLi$ to **1** in toluene and used directly in the preparation of Group 4 metal complexes (Scheme 1). The treatment of **2** with an equivalent of $TiCl_4(THF)_2$ at low temperature led to dark green, air and moisture sensitive crystals of [{($\eta^1$-$NCMe_3$)$Si(Me)_2CH_2$($\eta^5$-$C_{13}H_8$)}$TiCl_2$] (**3**). Compounds [{($\eta^1$-$NCMe_3$)$Si(Me)_2CH_2$($\eta^5$-$C_{13}H_8$)}$ZrCl_2$] (**4**) and [{($\eta^1$-$NCMe_3$)$Si(Me)_2CH_2$($\eta^5$-$C_{13}H_8$)}$HfCl_2$] (**5**) were prepared in $Et_2O$ by treating **2** with the

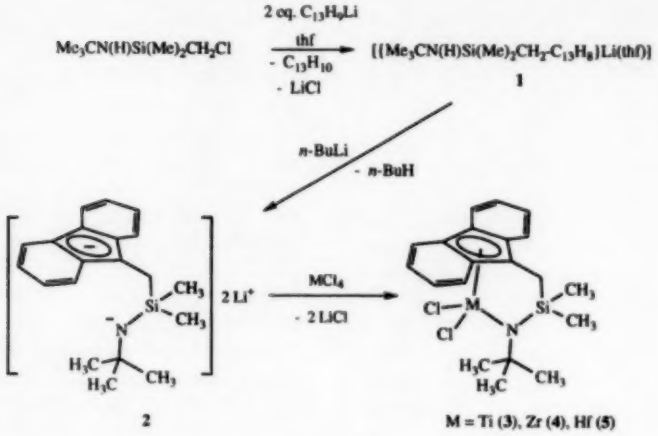


Scheme 1.

corresponding metal(IV) chloride, and isolated as dark yellow crystals in 75 and 81% yield respectively.

Compounds **3–5** were characterized by elemental analysis and $^1H$ and $^{13}C$ NMR spectroscopy. All three complexes show similar spectra with only minor differences in the chemical shift values, suggesting closely related structures in solution. However, the $^1H$ NMR chemical shift values of $^t$Bu and fluorenyl hydrogens of **3**, **4** and **5** show significant differences when compared to the corresponding signals of **1**. For example, the $^t$Bu hydrogens of **4** appear about 0.6 ppm downfield from that of **1**. The $^1H$ NMR signals due to the fluorenyl hydrogens of **4** are spread over a relatively narrow region of about 0.6 ppm, whereas in **1**, the spread is much wider (1.3 ppm).

The NMR and elemental analysis data of **3–5** show no evidence for the presence of solvent molecules or LiCl coordinated to the metal center. It is notable that the related alkoxy-fluorenyl Zr(IV) complexes, {($\eta^5$-$C_{13}H_8$)CHR–CHR–O}$ZrCl_2(THF)_2$ (**6**) (where CHR–CHR = cyclohexyl, cyclopentyl) have been isolated as bis-tetrahydrofuran adducts [21]. The attempted synthesis of THF free **6** using $CH_2Cl_2$ has resulted in products which contain one equivalent of LiCl or NaCl. The dimethylsilylene bridged amido-fluorenyl complex [{($\eta^1$-$NCMe_3$)$SiMe_2$($\eta^5$-$C_{13}H_8$)}$ZrCl_2$] (**7**) has been synthesized and characterized as its $Et_2O$ or THF coordinated species [25]. The loss of coordinated solvent from this compound results in the formation of oligomeric or polymeric solids which are insoluble even in hot THF. In contrast, compounds **3–5** show excellent solubility in $Et_2O$, THF, toluene or benzene. The relatively low coordination number in complexes **3**, **4** or **5** is probably an indication of increased crowding around the central metal ion. The increased bulk of the amido-fluorenyl ligand, $[\{(NCMe_3)Si(Me)_2CH_2(C_{13}H_8)\}]^{2-}$, may be due to a combination of effects of having a sterically demanding t-butylamido group and a relaxed ligand backbone.

### 3.1. Structural descriptions

Compound **1** crystallizes easily from toluene at −20°C. The structure of **1** has been confirmed by X-ray crystallography. A summary of crystal data, selected bond lengths and angles and atomic positional parameters are listed in Tables 1, 2 and 3 respectively.

Compound **1** adopts a monomeric structure (Fig. 1) in which the lithium atom is coordinated to the THF oxygen (Li–O distance of 1.85 (1) Å), nitrogen (Li–N distance of 2.16(1) Å) and to the fluorenyl group in a $\eta^2$-fashion (Li–C distances of 2.28(1) and 2.31(1) Å). The remaining Li–C(fluorenyl) distances are 2.62, 2.68 and 2.87 Å, and thus are not indicative of any interaction. The Li–O distance is relatively short, indicating a strong interaction between the two centers [42–44]. The amino nitrogen center is pyramidal as expected.

The X-ray crystal structures of **4** and **5** have been determined to examine the structural effects of the dimethylsilylmethylene ligand backbone. The ORTEP diagrams of **4** and **5** are shown in Figs. 2 and 3 respectively [45]. The Zr and the Hf compounds are essentially isostructural. The summary of crystal data for **4** and **5** are listed in Table 1, and selected bond lengths and angles and atomic parameters are listed in Tables 4 and 5.

In **4**, the Zr atom adopts a formal octahedral structure, being coordinated in an $\eta^5$-fashion to the fluorenyl ring (Zr to C distances range from 2.430(5) to 2.587(4) Å), the nitrogen and two chlorines [46,47]. The nitrogen atom adopts a planar geometry. The Zr–N bond distance is 2.060 (3) Å. This distance is slightly shorter

Table 1
Crystal data and summary of data collection and refinement

| Formula | $C_{24}H_{34}LiNOSi$ (1) | $C_{20}H_{25}Cl_2NSiZr$ (4) | $C_{20}H_{25}Cl_2NSiHf$ (5) |
|---|---|---|---|
| fw | 387.57 | 469.64 | 556.91 |
| Crystal color and habit | scarlet blocks | orange blocks | orange blocks |
| Cryst. dimensions (mm) | 0.25 × 0.32 × 0.35 | 0.50 × 0.62 × 0.68 | 0.26 × 0.30 × 0.40 |
| Crystal system | monoclinic | triclinic | triclinic |
| Space group | $P2_1/c$ | $P\bar{1}$ | $P\bar{1}$ |
| $a$ (Å) | 14.755(3) | 8.634(1) | 8.667(2) |
| $b$ (Å) | 11.494(2) | 9.6930(9) | 9.713(3) |
| $c$ (Å) | 14.836(3) | 14.346(2) | 14.463(4) |
| $\alpha$ (deg) | 90 | 82.964(9) | 82.62(2) |
| $\beta$ (deg) | 110.52(1) | 75.30(1) | 75.09(1) |
| $\gamma$ (deg) | 90 | 65.299(9) | 65.02(2) |
| $V$ (Å$^3$) | 2356.4(7) | 1054.9(2) | 1066.1(5) |
| $Z$ | 4 | 2 | 2 |
| $D_{calc}$ (g cm$^{-3}$) | 1.092 | 1.478 | 1.735 |
| abs. coeff. (cm$^{-1}$) | 1.08 | 8.27 | 52.02 |
| $F(000)$ | 848 | 480 | 544 |
| Scan method | $\theta$–$2\theta$ | $\theta$–$2\theta$ | $\theta$–$2\theta$ |
| Diffractometer | Enraf-Nonius CAD4 | Enraf-Nonius CAD4 | Siemens P4 |
| Radiation | Mo K$\alpha$ ($\lambda$ = 0.71073) | Mo K$\alpha$ ($\lambda$ = 0.71073) | Mo K$\alpha$ ($\lambda$ = 0.71073) |
| Monochromator | graphite | graphite | graphite |
| $T$ (K) | ambient | ambient | 193 |
| 2$\theta$ range | 2° to 44° | 2° to 44° | 3.5° to 50.0° |
| Scan rate (deg min$^{-1}$) | variable | variable | variable |
| Bckgd/scan time | 0.5 | 0.5 | 0.5 |
| No. of reflections measd | 3198 | 2584 | 4559 |
| No. of indep rflns | 3073 | 2584 | 3750 |
| No. of obsd rflns | 1563 [$F > 6\sigma(F)$] | 2330 [$F > 6\sigma(F)$] | 3578 [$F > 4\sigma(F)$] |
| Weighting scheme | $w = [0.04Ff^2 + (\sigma F)^2]^{-1}$ | $w = [0.04F^2 + (\sigma F)^2]^{-1}$ | $w = [\sigma^2(F)]^{-1}$ |
| $R$, $R_w$ | 0.0546, 0.0526 | 0.0268, 0.0317 | 0.0212, 0.0212[a,b] |
| Data : parameter ratio | 7.0 : 1 | 10.3 : 1 | 14.3 : 1 |

[a] $R = \Sigma(|F_o| - |F_c|)/\Sigma|F_o|$. [b] $R_w = [\Sigma w(|F_o| - |F_c|)^2/\Sigma w|F_o|^2]^{1/2}$.

than the Zr–N bond lengths observed for zirconocene complexes $[(\eta^5\text{-}C_5H_5)_2Zr(\eta^1\text{-}NC_4H_2Me_2)_2]$ (2.22(2) Å), $[\{Me_2Si(\eta^5\text{-}C_5H_4)(NPh)\}_2Zr]$ (2.137(2), 2.127(2) Å), and $[(\eta^5\text{-}C_5H_5)_2Zr(Cl)(Me_3CNSiMe_2H)]$ (2.139(3) Å) [23,48,49]. In fact, the Zr–N distance of **4** is very similar to the corresponding bond lengths found in closely related compounds, $[\{(\eta^1\text{-}NCMe_3)SiMe_2(\eta^5\text{-}C_{13}H_8)\}Zr(CH_2SiMe_3)_2]$ (**8**) (2.061(2) Å) and $[\{(\eta^1\text{-}NCMe_3)SiMe_2(\eta^5\text{-}C_{13}H_8)\}ZrCl_2]$ (2.056(6) Å) [25,50,51]. The Zr–Cl distances of 2.408(1) and 2.402(1) Å in **4** are shorter than the average distance of 2.44 Å observed for 16-electron complex $[(\eta^5\text{-}C_5H_5)_2ZrCl_2]$, and are much closer to the Zr–Cl(terminal) values in the formally 14-electron complex, $[\{(\eta^5\text{-}C_5Me_5)ZrCl_3\}_2]$ (av. 2.38 Å) [52,53]. For comparison, the Zr–Cl dis-

Table 2
Selected bond distances (Å) and bond angles (deg) for $[\{Me_3CN(H)\text{–}Si(Me)_2CH_2\text{–}C_{13}H_8\}Li(THF)]$ (**1**)

| | | | |
|---|---|---|---|
| Si–N | 1.748(4) | Si–C(14) | 1.864(7) |
| Si–C(15) | 1.845(8) | Si–C(16) | 1.853(8) |
| O–Li | 1.85(1) | N–C(17) | 1.495(6) |
| N–Li | 2.16(1) | C(1)–C(14) | 1.510(8) |
| C(1)–Li | 2.28(1) | C(13)–Li | 2.31(1) |
| N–Si–C(14) | 101.3(2) | N–Si–C(15) | 110.1(3) |
| N–Si–C(16) | 115.7(3) | C(14)–Si–C(15) | 109.5(3) |
| C(14)–Si–C(16) | 111.0(3) | C(15)–Si–C(16) | 108.9(4) |
| Si–N–C(17) | 127.9(4) | Si–N–Li | 100.2(3) |
| C(17)–N–Li | 117.6(4) | C(2)–C(1)–Li | 86.9(4) |
| C(13)–C(1)–Li | 73.4(4) | C(14)–C(1)–Li | 106.2(4) |

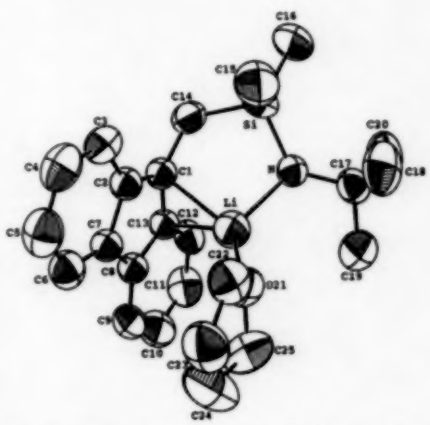


Fig. 1. Computer generated drawing of **1**. Hydrogen atoms omitted for clarity.

Table 3
Atomic coordinates ($\times 10^4$) for [{$Me_3CN(H)$–$Si(Me)_2CH_2$–$C_{13}H_8$}Li(THF)] (1)

| Atom | x | y | z |
|---|---|---|---|
| Si | 6643(1) | 1453(2) | 2289(1) |
| O | 7751(3) | −2028(3) | 3697(2) |
| N | 7693(3) | 1053(4) | 3235(3) |
| C(1) | 7325(3) | −306(4) | 1330(3) |
| C(2) | 6781(3) | −1343(5) | 1136(3) |
| C(3) | 5790(4) | −1573(6) | 764(4) |
| C(4) | 5453(4) | −2701(6) | 608(4) |
| C(5) | 6102(4) | −3638(6) | 812(4) |
| C(6) | 7072(4) | −3458(5) | 1169(4) |
| C(7) | 7439(3) | −2320(5) | 1322(3) |
| C(8) | 8390(3) | −1854(5) | 1653(3) |
| C(9) | 9301(4) | −2383(5) | 1934(4) |
| C(10) | 10116(4) | −1707(6) | 2218(4) |
| C(11) | 10042(4) | −510(6) | 2202(4) |
| C(12) | 9163(4) | 40(5) | 1923(4) |
| C(13) | 8303(3) | −619(4) | 1644(3) |
| C(14) | 6918(4) | 912(5) | 1228(4) |
| C(15) | 5591(4) | 660(7) | 2379(5) |
| C(16) | 6365(6) | 3030(6) | 2179(6) |
| C(17) | 7994(4) | 1404(5) | 4268(4) |
| C(18) | 7195(5) | 1164(7) | 4645(4) |
| C(19) | 8877(5) | 688(7) | 4826(5) |
| C(20) | 8275(6) | 2667(7) | 4410(5) |
| C(22) | 6924(4) | −2722(6) | 3622(4) |
| C(23) | 7246(5) | −3929(6) | 3823(5) |
| C(24) | 8281(5) | −3922(7) | 4047(6) |
| C(25) | 8597(5) | −2705(7) | 4186(5) |
| Li | 7758(7) | −773(9) | 2922(7) |

tance in 18-electron complex is much longer; e.g., the Zr–Cl in [{$Me_2C(\eta^5$-$C_5H_4)(\eta^3$-$C_{13}H_8)$}$Zr(\eta^5$-$C_5H_5)$Cl] is 2.560 (1) Å [54]. The Si–N distance of 1.765(4) Å in **4** is relatively long (e.g., 1.738(2) Å for **8**). The short Zr–Cl and Zr–N bonds and the trigonal planar nitrogen center in **4** possibly indicate the effects of increased metal Lewis acidity due to the replacement

Fig. 2. Computer generated drawing of **4**. Hydrogen atoms omitted for clarity.

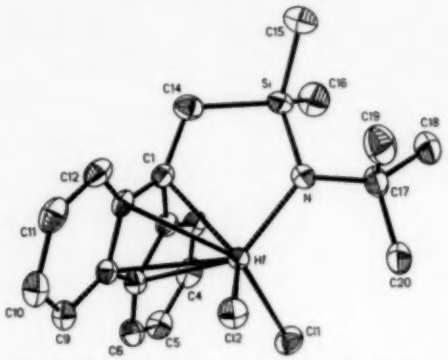


Fig. 3. Computer generated drawing of **5**. Hydrogen atoms omitted for clarity.

of 6-electron $\eta^5$-$C_5H_5^-$ donor with the 4 (or 2) electron donor amido group [19,31].

The effects of having an extra $-CH_2-$ moiety in the backbone is clearly evident from the X-ray data. For

Table 4
Selected bond distances (Å) and bond angles (deg) for [{$\eta^1$-$NCMe_3$}$Si(Me)_2CH_2(\eta^5$-$C_{13}H_8$)}$MCl_2$] (where M = Zr (**4**), Hf (**5**))

| | | | |
|---|---|---|---|
| Compound **4** | | | |
| Zr–Cl(1) | 2.408(1) | Zr–Cl(2) | 2.402(1) |
| Zr–N | 2.060(3) | Zr–C(1) | 2.430(5) |
| Zr–C(2) | 2.515(4) | Zr–C(7) | 2.587(4) |
| Zr–C(8) | 2.587(4) | Zr–C(13) | 2.508(5) |
| Si–N | 1.765(4) | Si–C(14) | 1.853(5) |
| Si–C(15) | 1.867(6) | Si–C(16) | 1.859(4) |
| N–C(17) | 1.503(6) | C(1)–C(14) | 1.493(5) |
| Cl(1)–Zr–Cl(2) | 103.20(4) | Cl(1)–Zr–N | 109.0(1) |
| Cl(1)–Zr–C(1) | 123.61(9) | Cl(1)–Zr–C(2) | 91.6(1) |
| Cl(1)–Zr–C(7) | 85.2(1) | Cl(1)–Zr–C(8) | 110.84(9) |
| Cl(1)–Zr–C(13) | 139.25(9) | Cl(2)–Zr–N | 110.47(9) |
| Cl(2)–Zr–C(1) | 126.01(9) | Cl(2)–Zr–C(2) | 138.97(8) |
| Cl(2)–Zr–C(7) | 110.02(7) | Cl(2)–Zr–C(8) | 85.31(8) |
| Cl(2)–Zr–C(13) | 93.05(9) | Zr–N–Si | 122.8(2) |
| Zr–C(1)–C(14) | 117.4(3) | N–Si–C(14) | 104.3(2) |
| C(1)–C(14)–Si | 112.2(3) | Zr–N–C(17) | 118.2(2) |
| Compound **5** | | | |
| Hf–Cl(1) | 2.396(1) | Hf–Cl(2) | 2.399(1) |
| Hf–N | 2.065(3) | Hf–C(1) | 2.430(5) |
| Hf–C(2) | 2.507(5) | Hf–C(7) | 2.607(5) |
| Hf–C(8) | 2.602(4) | Hf–C(13) | 2.521(5) |
| Si–N | 1.778(4) | Si–C(14) | 1.891(5) |
| Si–C(15) | 1.878(5) | Si–C(16) | 1.889(6) |
| N–C(17) | 1.534(7) | C(1)–C(14) | 1.509(5) |
| Cl(1)–Hf–Cl(2) | 102.7(1) | Cl(1)–Hf–N | 109.0(1) |
| Cl(1)–Hf–C(1) | 126.8(1) | Cl(1)–Hf–C(2) | 93.8(1) |
| Cl(1)–Hf–C(7) | 85.6(1) | Cl(1)–Hf–C(8) | 110.5(1) |
| Cl(1)–Hf–C(13) | 139.8(1) | Cl(2)–Hf–N | 107.6(1) |
| Cl(2)–Hf–C(1) | 123.8(1) | Cl(2)–Hf–C(2) | 140.1(1) |
| Cl(2)–Hf–C(7) | 111.9(1) | Cl(2)–Hf–C(8) | 85.8(1) |
| Cl(2)–Hf–C(13) | 91.7(1) | Hf–N–Si | 121.7(2) |
| Hf–C(1)–C(14) | 116.6(3) | N–Si–C(14) | 104.4(2) |
| C(1)–C(14)–Si | 112.1(4) | Hf–N–C(17) | 120.1(3) |

example, a comparison of the X-ray structural data between **4** and **8** shows that the Zr–N–$CMe_3$ (118.2(2)°) and Zr–N–Si (122.8(2)°) angles in **4** are significantly different from the corresponding values of 130.1(2)° and 103.1(1)° for **8**. These data are indicative of a relatively unstrained ligand backbone in **4**. The structure of **4** also shows that the $^t$Bu group is directed more towards the open face of the metal complex, providing increased protection to the Zr center.

Table 5
Atomic coordinates ($\times 10^4$) for [{($\eta^1$-$NCMe_3$)$Si(Me)_2CH_2$($\eta^5$-$C_{13}H_8$)}$MCl_2$] (where M = Zr (**4**), Hf (**5**))

| Atom | x | y | z |
|---|---|---|---|
| Compound **4** | | | |
| Zr | 1425.9(4) | 1108.1(4) | 2133.7(3) |
| Cl(1) | 2723(1) | 2868(1) | 1421(5) |
| Cl(2) | 3673(1) | −828(1) | 2831(8) |
| Si | −2778(1) | 2074(1) | 3294(7) |
| N | −756(4) | 2194(3) | 3192(2) |
| C(1) | −768(4) | 749(4) | 1533(3) |
| C(2) | 20(5) | 1453(4) | 738(3) |
| C(3) | −639(5) | 2928(4) | 303(3) |
| C(4) | 419(6) | 294(4) | −467(3) |
| C(5) | 2148(5) | 2287(5) | −836(3) |
| C(6) | 2852(5) | 883(4) | −431(3) |
| C(7) | 1799(4) | 445(4) | 375(3) |
| C(8) | 2115(4) | −944(4) | 917(3) |
| C(9) | 3574(5) | −2372(4) | 836(3) |
| C(10) | 3445(6) | −3526(5) | 1445(3) |
| C(11) | 1914(6) | −3334(4) | 2150(3) |
| C(12) | 470(5) | −2007(4) | 2253(3) |
| C(13) | 517(5) | −770(4) | 1620(3) |
| C(14) | −2613(5) | 1411(5) | 2101(3) |
| C(15) | −3155(6) | 655(6) | 4225(4) |
| C(16) | −4747(6) | 3892(6) | 3525(4) |
| C(17) | −597(5) | 3096(5) | 3915(3) |
| C(18) | −1352(7) | 4786(5) | 3642(4) |
| C(19) | −1518(6) | 2822(6) | 4936(3) |
| C(20) | 1310(6) | 2608(5) | 3941(3) |
| Compound **5** | | | |
| Hf | 3588(1) | 3911(1) | 2886(1) |
| Cl(1) | 1353(2) | 5825(1) | 2179(1) |
| Cl(2) | 2308(1) | 2148(1) | 3576(1) |
| N | 5732(4) | 2812(4) | 1815(2) |
| Si | 7770(2) | 2920(1) | 1701(1) |
| C(1) | 5775(5) | 4254(4) | 3485(3) |
| C(2) | 4499(5) | 5778(4) | 3389(3) |
| C(3) | 4550(6) | 7026(5) | 2743(3) |
| C(4) | 3094(7) | 8373(5) | 2832(3) |
| C(5) | 1549(6) | 8582(5) | 3541(3) |
| C(6) | 1417(6) | 7418(5) | 4161(3) |
| C(7) | 2881(5) | 5995(4) | 4088(3) |
| C(8) | 3193(5) | 4577(4) | 4642(3) |
| C(9) | 2112(6) | 4138(5) | 5447(3) |
| C(10) | 2811(6) | 2723(5) | 5859(3) |
| C(11) | 4575(6) | 1688(5) | 5488(3) |
| C(12) | 5650(6) | 2045(5) | 4715(3) |
| C(13) | 4976(5) | 3548(4) | 4282(3) |
| C(14) | 7635(6) | 3558(5) | 2912(3) |
| C(15) | 9759(7) | 1085(6) | 1449(4) |
| C(16) | 8135(8) | 4374(7) | 772(4) |
| C(17) | 5581(6) | 1906(5) | 1074(3) |
| C(18) | 6524(7) | 2199(7) | 52(3) |
| C(19) | 6346(7) | 206(6) | 1344(4) |
| C(20) | 3652(6) | 2387(7) | 1052(3) |

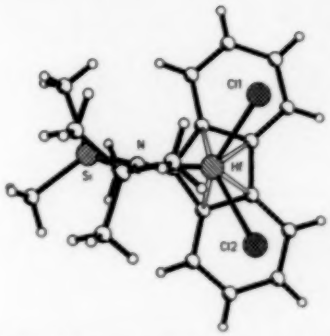


Fig. 4. View of **5** perpendicular to the flourene ring plane.

The cell dimensions and the structural features of [{($\eta^1$-$NCMe_3$)$Si(Me)_2CH_2$($\eta^5$-$C_{13}H_8$)}$HfCl_2$] (**5**) are very similar to those of the zirconium analog, **4**. Such close similarities between the zirconium and hafnium species have been observed previously [55,56]. As in **4**, compound **5** exists as discrete molecules in the solid state. Fig. 4 shows the orientation of the t-butyl group on nitrogen with respect to the two chlorine atoms.

The bond distances between the Hf to carbons of the five membered ring in the fluorene group (2.430(5) to 2.607(5) Å) suggest $\eta^5$-coordination [55,57]. The Hf–N distance 2.065(3) is somewhat longer than that found in [($\eta^5$-$C_5Me_5$)Hf(H)NHMe] (2.027(8) Å) but much closer to the distances found in [($\eta^5$-$C_5Me_5$)Hf[NH(2,6-$^i Pr_2C_6H_3$)]$_3$] (2.041(4), 2.048(4), and 2.065(3) Å) or [HfCl{$N(SiMe_3)_2$}$_3$] (2.040(10) Å) [58–60]. The Hf–Cl distances (2.396(1), 2.399(1) Å) may be compared with the values of 2.510(1) Å in [$Me_2C(\eta^5$-$C_5H_4)_2Hf(\eta^5$-$C_5H_5)Cl$], 2.42 Å in [$(CH_2)_3(\eta^5$-$C_5H_4)_2HfCl_2$] and 2.436(5) Å in [HfCl{$N(SiMe_3)_2$}$_3$] [56,60,61].

In conclusion, we have reported the synthesis of an amido-fluorenyl ligand system and its utility in the synthesis and isolation of solvent free, monomeric Group 4 metal dichloro complexes. The longer –$CH_2Si(Me)_2$– bridge increases the effectiveness of the protection offered by the ligand to the metal ion. The X-ray structures of **4** and **5** also represent rare examples of mono(fluorenyl) complexes of Group 4 metal ions [25]. The Group 4 metal complexes based on this amido-fluorenyl ligand could be useful as catalyst precursors in the olefin polymerization reactions [26–30]. We are currently studying the chemistry of **3–5**, and the reactions of **2** with various other metal ions. We are also currently investigating the chemistry of [{(N-$^i$Pr)$Si(Me)_2$-$CH_2(C_{13}H_8)$}]$^{2-}$ ligand [62].

## Acknowledgments

Financial support received from The University of Texas at Arlington, The Robert A. Welch Foundation and the UNT Research Office is gratefully acknowledged. We also thank The University of Texas at Arlington for providing funds to purchase the Siemens P4 single crystal X-ray diffractometer. The technical assistance of Wiechang Jin in obtaining the NMR data is greatly appreciated.

## References and notes

[1] W. Kaminsky, K. Kulper, H.H. Brintzinger and F.R.W.P. Wild, *Angew. Chem., Int. Ed. Engl., 24* (1985) 507.
[2] W. Kaminsky, R. Engehausen, K. Zoumis, W. Spalek and J. Rohrmann, *Makromol. Chem., 193* (1992) 1643.
[3] J.A. Ewen, *J. Am. Chem. Soc., 106* (1984) 6355.
[4] J.A. Ewen, R.L. Jones, A. Razavi and J.D. Ferrara, *J. Am. Chem. Soc., 110* (1988) 6255.
[5] J.A. Ewen, M.J. Elder, R.L. Jones, I. Haspeslagh, J.L. Atwood, S.G. Bott and K. Robinson, *Makromol. Chem., Macromol. Symp., 48/49* (1991) 253.
[6] J.A. Ewen and M.J. Elder, *Makromol. Chem., Macromol. Symp., 66* (1993) 179.
[7] W. Spaleck, M. Antberg, J. Rohrmann, A. Winter, B. Bachmann, P. Kiprof, J. Behm and W.A. Herrmann, *Angew. Chem., Int. Ed. Engl., 31* (1992) 1347.
[8] R.L. Halterman, *Chem. Rev., 92* (1992) 965.
[9] S. Rodewald and R.F. Jorden, *J. Am. Chem. Soc., 116* (1994) 4491.
[10] A. Razavi and J. Ferrara, *J. Organomet. Chem., 435* (1992) 299.
[11] M. Bochmann and S.J. Lancaster, *Organometallics, 12* (1993) 633.
[12] G.W. Parshall and S.D. Ittel, *Homogeneous Catalysis*, Wiley, New York, 2nd edn., 1992.
[13] G.W. Coates and R.M. Waymouth, *J. Am. Chem. Soc., 113* (1991) 6270.
[14] M. Bochmann and S.J. Lancaster, *Angew. Chem., Int. Ed. Engl., 33* (1994) 1634.
[15] R. Waymouth and P. Pino, *J. Am. Chem. Soc., 112* (1990) 4911.
[16] S.L. Colleti and R.L. Halterman, *Tetrahedron Lett., 33* (1992) 1005.
[17] P.J. Shapiro, E. Bunel, W.P. Schaefer and J.E. Bercaw, *Organometallics, 9* (1990) 867.
[18] W.E. Piers, P.J. Shapiro, E.E. Bunel and J.E. Bercaw, *Synlett, 2* (1990) 74.
[19] P.J. Shapiro, W.D. Cotter, W.P. Schaefer, J.A. Labinger and J.E. Bercaw, *J. Am. Chem. Soc., 116* (1994) 4623.
[20] J. Okuda, *Angew. Chem. Int. Ed. Engl., 31* (1992) 47.
[21] B. Rieger, *J. Organomet. Chem., 420* (1991) C17.
[22] A.K. Hughes, A. Meetsma and J.H. Teuben, *Organometallics, 12* (1993) 1936.
[23] W.A. Herrman, M.J. A. Morawietz and T. Priermeier, *Angew. Chem. Int. Ed. Engl., 33* (1994) 1946.
[24] U. Bohme and K.-H. Thiele, *J. Organomet. Chem., 472* (1994) 39.
[25] J. Okuda, F.J. Schattenmann, S. Wocadlo and W. Massa, *Organometallics, 14* (1995) 789.
[26] J.A.M. Canich, Eur. Patent 420 436, 1991.
[27] J.C. Stevens, F.J. Timmers, D.R. Wilson, G.F. Schmidt, P.N. Nickias, R.K. Rosen, G.W. Knight and S.Y. Lai, Eur. Patent 416 815, 1991.
[28] H.W. Turner, G.G. Hlatky and J.A.M. Canich, *PCT Int. Appl. WO 9319103* (1993).
[29] J.A.M. Canich, US Patent 5 026 798, 1991.
[30] J.A.M. Canich, US Patent 5 096 867, 1992.
[31] J.P. Collman, L.S. Hegedus, J.R. Norton and R.G. Finke, *Principles and Applications of Organotransition Metal Chemistry*, University Science Books, California, 1987.
[32] Part of this work was presented at the American Chemical Society, Southwest Regional meeting, November 1994, No. 102.
[33] D.D. Perrin, W.L.F. Armarego and D.R. Perrin, *Purification of Laboratory Chemicals*, Pergamon, New York, 1985.
[34] L.E. Manzer, J. Deaton, P. Sharp and R.R. Schrock, *Inorg. Synth., 21* (1982) 135.
[35] C.H. Yoder, C.M. Ryan, G.F. Martin and P.S. Ho, *J. Organomet. Chem., 190* (1980) 1.
[36] This product, $ClCH_2Si(Me)_2N(H)CMe_3$, decomposes in air, NMR data (in $C_6D_6$): $^1H$ $\delta = 0.10$ (s, 6H, SiMe) 1.09 (s, 9H, $^tBu$) 2.57 (s, 2H, $CH_2$); $^{13}C\{^1H\}$ $\delta = -1.08$ (SiMe) 32.33 ($SiCH_2$) 33.70 ($^tBu$) 49.37 ($^tBu$).
[37] G.M. Sheldrick, in G.M. Sheldrick, C. Kruger and R. Goddard (eds.), *Crystallographic Computing*, Oxford University Press, 1985, p. 184.
[38] *MolEN, An Interactive Structure Solution Program*, Enraf-Nonius, Delft, The Netherlands, 1990.
[39] H. Hope, in A.L. Wayda and M.Y. Darensbourg (eds.), *Experimental Organometallic Chemistry; ACS Symposium Series, No. 357*, American Chemical Society, Washington, DC, 1987, p. 257.
[40] G.M. Sheldrick, SHELXA, Göttingen, Germany, 1993.
[41] *Siemens* SHELXTL (PC version 4.2), Siemens Industrial Automation, Madison, WI, USA.
[42] L. Matilainen, M. Klinga and M. Leskela, *Polyhedron, 14* (1995) 635.
[43] R.A. Bartlett, H.V.R. Dias and P.P. Power, *J. Organomet. Chem., 341* (1988) 1.
[44] H.V.R. Dias, M.M. Olmstead, K. Ruhlandt-Senge and P.P. Power, *J. Organomet. Chem., 462* (1993) 1.
[45] C.K. Johnson, ORTEP II, Report ORNL-5138, Oak Ridge National Laboratory, Oak Ridge, TN, 1976.
[46] A. Razavi and J.L. Atwood, *J. Am. Chem. Soc., 115* (1993) 7529.
[47] C. Kowala, P.C. Wailes, H. Weigold and J.A. Wunderlich, *J. Chem. Soc., Chem. Commun.* (1974) 993.
[48] R.V. Bynum, H.M. Zhang, W.E. Hunter and J.L. Atwood, *Can. J. Chem., 64* (1986) 1304.
[49] L.J. Procopio, P.J. Carroll and D.H. Berry, *J. Am. Chem. Soc., 116* (1994) 177.
[50] J.C. Stevens, *Metcon 93*, May 26–28, 1993, Houston, p. 157.
[51] T.K. Woo, L. Fan and T. Ziegler, *Organometallics, 13* (1994) 2252.
[52] K. Prout, T.S. Cameron, R.A. Forder, S.R. Critchley, B. Denton and G.V. Rees, *Acta. Crystallogr., B30* (1974) 2290.
[53] A. Martin, M. Mena and F. Palacios, *J. Organomet. Chem., 480* (1994) C10.
[54] G.M. Diamond, M.L.H. Green, P. Mountford, N.A. Popham and A.N. Chernega, *J. Chem. Soc., Chem. Commun.* (1994) 103.
[55] A. Razavi and J.L. Atwood, *J. Organomet. Chem., 459* (1993) 117.
[56] G.M. Diamond, M.L.H. Green, N.A. Popham and A.N. Chernega, *J. Chem. Soc., Dalton Trans.* (1993) 2535.
[57] A. Razavi and J. Ferrara, *J. Organomet. Chem., 435* (1992) 299.

[58] Y. Bai, H.W. Roesky, M. Noltemeyer and M. Witt, *Chem. Ber.*, *125* (1992) 825.
[59] G.L. Hillhouse, A.R. Bulls, B.D. Santarsiero and J.E. Bercaw, *Organometallics*, *7* (1988) 1309.
[60] C. Airoldi, D.C. Bradley, H. Chudzynska, M.B. Hursthouse, K.M. Abdul Malik and P.R. Raithby, *J. Chem. Soc., Dalton Trans.* (1980) 2010.
[61] C.H. Saldarriaga-Molina, A. Clearfield and I. Bernal, *Inorg. Chem.*, *13* (1974) 2880.
[62] H.V.R. Dias, Z. Wang, unpublished results.

ELSEVIER

Journal of Organometallic Chemistry 508 (1996) 101–108

Journal of Organometallic Chemistry

# Mechanism of oxidative allyl transfer from allylic ammonium cations to palladium(0) α-diimine complexes

Luciano Canovese [a], Fabiano Visentin [a], Paolo Uguagliati [a,*], Francesca Di Bianca [b], Alberta Fontana [b], Bruno Crociani [c]

[a] *Dipartimento di Chimica, Università di Venezia, Venezia, Italy*
[b] *Dipartimento di Chimica Inorganica, Università di Palermo, Palermo, Italy*
[c] *Dipartimento di Scienze e Tecnologie Chimiche, Università di Roma 'Tor Vergata', Rome, Italy*

Received 20 April 1995

**Abstract**

The palladium(0) complex [Pd($\eta^2$-fn)(N—N′)] (**1**, fn = fumaronitrile; N—N′ = $C_5H_4$N-2-CH=N$C_6H_4$OMe-4) reacts slowly and reversibly with $\overset{+}{A}$—$CH_2$—CH=$CH_2$ (**2a**, A = $NEt_3$; **2b**, A = $C_5H_5N$) to yield the cationic $\eta^3$-allylpalladium(II) derivative [Pd($\eta^3$-$C_3H_5$)(N—N′)]$^+$ (**3**) the free amine A and fn. The equilibrium constant $K_e$ is $(2.6 \pm 0.1) \times 10^{-3}$ for **2a** and $1.0 \pm 0.4$ for **2b**. Kinetic studies of these oxidative allyl-transfer reactions show that the rates increase with increasing concentration of **2** and with decreasing concentration of fn. A stepwise mechanism is proposed which involves slow and reversible displacement of fn by **2** to give a labile intermediate [Pd($\eta^2$-$CH_2$=CH—$CH_2$—$\overset{+}{A}$)(N—N′)]. This undergoes slow and reversible intramolecular allyl transfer through nucleophilic attack by the palladium(0) metal centre on the nitrogen-bound allyl carbon. The kinetic parameters evaluated by a steady-state treatment satisfactorily generate the observed equilibrium constant $K_e$. The rate of formation of the intermediate and the relative rate of its decay to the starting reactants and final products are virtually independent of the nature of the amine A.

*Keywords:* Palladium; Allyl transfer; Kinetic studies

## 1. Introduction

Oxidative addition of an electrophilic allyl halide, sulphide, carboxylate, sulphonate or carbonate to a palladium(0) substrate is a key step in the palladium-catalyzed nucleophilic substitution of allylic compounds (Scheme 1) [1].

The stereochemistry of these catalytic reactions is a subject of much current interest. In respect of the oxidative addition, special attention has been given to the elucidation of the factors that favour retention vs. inversion of configuration at the allylic carbon bearing the leaving group X [2]. In all cases, prior coordination of the C=C double bond of the allylic electrophile to the metal seems to be an essential feature of the mechanism, and evidence for it has been reported [2b].

When the ligating properties of L are better than those of the leaving group X, the reaction of $PdL_n$ with $CH_2$=CH—$CH_2$—X, leading to the cationic species [Pd($\eta^3$-all)$L_2$]$^+$, can be better viewed as an *oxidative transfer* of the allyl group to the metal. Such is the case for the reactions with (allyloxy)phosphonium, (allylthio)uronium and allylpyridinium salts [3]. A particular case of oxidative allyl transfer is also involved in the reactions of $\eta^3$-allylpalladium(II) complexes with palladium(0) [4] and platinum(0) [5] derivatives (*redox transmetallation*).

Following on recent study of the mechanism of nucleophilic attack by triethylamine or pyridine on [Pd($\eta^3$-all)(N—N′)]$^+$ substrates (N—N′ = α-diimine)

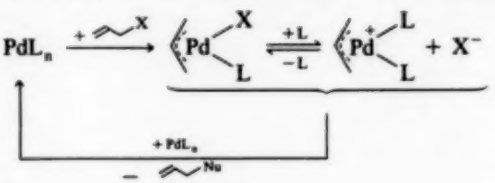


Scheme 1.

* Corresponding author.

0022-328X/96/$15.00 © 1996 Elsevier Science S.A. All rights reserved
*SSDI* 0022-328X(95)05780-3

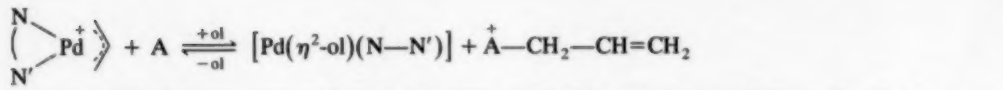

N—N′ = $C_5H_4N$-2-CH=N$C_6H_4$OMe-4; A = $NEt_3$ or $C_5H_5N$; ol = fumaronitrile or dimethyl fumarate

Scheme 2.

in the presence of fumaronitrile or dimethyl fumarate (Scheme 2), we reported some preliminary data for the influence of the activated olefin on the reverse reaction, i.e. the oxidative transfer of the allyl group from the ammonium cation $\overset{+}{A}—CH_2—CH=CH_2$ to the species [Pd($\eta^2$-ol) (N—N′)] [6]. We now report the results of a novel equilibrium and kinetic investigation of the latter reaction in the presence of fumaronitrile (fn). One aim of this study was to provide further evidence for prior coordination of the C=C double bond of the allylic electrophile to palladium by oxidative transfer of an allylic substrate to palladium(0).

## 2. Results and discussion

### 2.1. Equilibria of oxidative allyl transfer

When the palladium(0) complex **1** is treated with (prop-2-enyl)triethylammonium (**2a**) or 1-(prop-2-enyl) pyridinium (**2b**) perchlorate in chloroform at 25°C, an equilibrium is slowly established involving the $\eta^3$-allylpalladium(II) complex **3**, the free amine A ($NEt_3$ or $C_5H_5N$) and fumaronitrile [Eq. (1)].

No reaction was observed when **1** was treated with (2-methylprop-2-enyl) triethylammonium perchlorate. Equilibrium (1) was studied by UV–vis spectrophotometry by recording the spectral changes in the presence of a known excess of both A and fn over the palladium substrate **1** after sufficient time had elapsed following mixing of the reactants to ensure the attainment of equilibrium. Initial concentrations were: $[\mathbf{1}]_0 = 1 \times 10^{-4}$ mol $l^{-1}$, $[A]_0 = 1 \times 10^{-3}$ mol $l^{-1}$, $[fn]_0$ in the range $1 \times 10^{-3}$ to $5 \times 10^{-3}$ mol $l^{-1}$, $[\mathbf{2}]_0$ in the range $2 \times 10^{-5}$ to $2 \times 10^{-3}$ mol $l^{-1}$. The concentration of A was such that no appreciable $\alpha$-diimine displacement by A took place in **3**, the corresponding equilibrium $\mathbf{3} + 2A \rightleftharpoons [Pd(C_3H_5)\ (A)_2]^+ + N—N'$ being shifted completely to the left under these conditions [6]. Abstract-factor analysis of the observed UV–vis spectral changes indicated that only two independently absorbing species were present in the range 300–540 nm, i.e. complexes **1** and **3** [7].

Non-linear regression analysis of the dependence of the absorbance on the concentration of **2**, in terms of the model described in Experimental details, gave the following $K_e$ values: $(2.6 \pm 0.1) \times 10^{-3}$ for **2a** and $1.0 \pm 0.4$ for **2b**. These findings can be explained in terms of the much higher basicity of triethylamine than of pyridine in so far as this governs the stability of the $C_{allyl}$—N bond in **2**. An example of the spectral changes along with the least-squares fit is shown in Fig. 1.

### 2.2. Kinetics of oxidative allyl transfer

A kinetic study of reaction (1) was also carried out in chloroform at 25°C in the presence of an excess of **2**, A and fn relative to the palladium(0) substrate **1** in order to ensure effective constancy of their concentrations. The progress of the reaction with time was monitored by UV–vis spectroscopy in the range 280–540 nm. Under these conditions the extent of reaction, evaluated

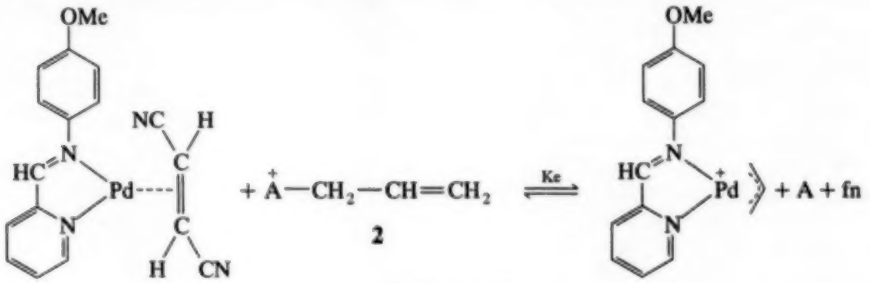

**1** + $\overset{+}{A}—CH_2—CH=CH_2$ (**2**) $\rightleftharpoons$ (**3**) + A + fn (1)

(**a**): A = $NEt_3$

(**b**): A = $C_5H_5N$

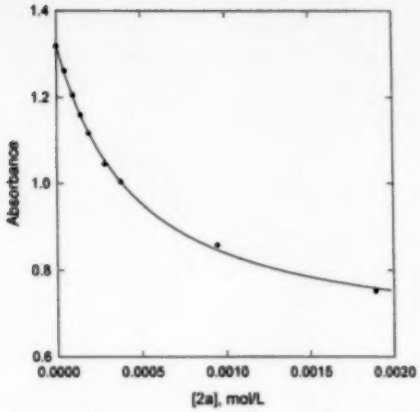


Fig. 1. Fit of the absorbance at 340 nm to [**2a**] for equilibrium (1) ($[Pd]_0 = 1\times10^{-4}$ mol $l^{-1}$, $[NEt_3] = 1\times10^{-3}$ mol $l^{-1}$, $[fn] = 1\times10^{-3}$ mol $l^{-1}$).

from the above equilibrium constants, was $> 60\%$. In all cases the reactions were monitored for up to six to seven half-lives. Again, abstract-factor analysis showed the presence of only two absorbing species, i.e. **1** and **3**, as confirmed by the observed two well-defined isosbestic points. The optical density changes were found to obey the mono-exponential law $D_t = D_\infty + (D_0 - D_\infty)\exp(-k_{obs}t)$, where $k_{obs}$ is the pseudo-first order rate constant for the process.

The $k_{obs}$ values are listed in Tables 1 and 2 for the reactions of **2a** and **2b**, respectively.

In general, the rates appear to increase with increasing concentrations of **2a** and with decreasing concentrations of fn, but are not affected by the concentration of A. For runs carried out at various concentrations of **2** but with a fixed amine A and fumaronitrile concentrations, the $k_{obs}$ values increase linearly with [**2**] (Fig. 2), according to the relationship:

$$k_{obs} = In + Sl[\mathbf{2}] \quad (2)$$

The slopes *Sl* of the straight lines generated by use of relationship [2] for a series of experiments at varying fn concentrations (Table 3) decrease with the concentration of fn according to Eq. (3) (Fig. 3):

$$Sl = \alpha/(1 + \beta[\mathrm{fn}]) \quad (3)$$

Table 1
Rate data for the reaction of **1** with **2a** in $CHCl_3$ at 25°C [a]

| $10^3[Et_3\overset{+}{N}–CH_2–CH=CH_2]$ (**2a**) (mol $l^{-1}$) | $10^3$[fn] (mol $l^{-1}$) | $10^3[NEt_3]$ (mol $l^{-1}$) | $10^4 k_{obs}$ ($s^{-1}$) |
|---|---|---|---|
| 2.37 | 0.5 | 1.0 | 2.56 ± 0.05 [b] |
| 4.74 | 0.5 | 1.0 | 5.11 ± 0.01 [b] |
| 9.47 | 0.5 | 1.0 | 9.81 ± 0.03 [b] |
| 18.90 | 0.5 | 1.0 | 19.42 ± 0.05 [b] |
| 2.37 | 1.0 | 1.0 | 1.81 ± 0.02 |
| 4.74 | 1.0 | 1.0 | 3.20 ± 0.03 |
| 9.47 | 1.0 | 1.0 | 6.21 ± 0.04 |
| 18.90 | 1.0 | 1.0 | 12.01 ± 0.02 |
| 2.37 | 1.0 | 2.0 | 1.90 ± 0.02 |
| 4.74 | 1.0 | 2.0 | 3.25 ± 0.03 |
| 9.47 | 1.0 | 2.0 | 6.28 ± 0.08 |
| 18.90 | 1.0 | 2.0 | 12.20 ± 0.02 |
| 2.37 | 1.5 | 1.0 | 1.40 ± 0.02 |
| 4.74 | 1.5 | 1.0 | 2.45 ± 0.03 |
| 9.47 | 1.5 | 1.0 | 4.70 ± 0.05 |
| 18.90 | 1.5 | 1.0 | 9.41 ± 0.08 |
| 2.37 | 2.5 | 1.0 | 0.99 ± 0.02 |
| 4.74 | 2.5 | 1.0 | 1.73 ± 0.03 |
| 9.47 | 2.5 | 1.0 | 3.41 ± 0.05 |
| 18.90 | 2.5 | 1.0 | 6.71 ± 0.07 |
| 2.37 | 5.0 | 1.0 | 0.61 ± 0.08 |
| 4.74 | 5.0 | 1.0 | 1.15 ± 0.02 |
| 9.47 | 5.0 | 1.0 | 1.91 ± 0.03 |
| 18.90 | 5.0 | 1.0 | 3.45 ± 0.07 |

[a] $[\mathbf{1}]_0 = 1.0\times10^{-4}$ mol $l^{-1}$, unless otherwise stated.
[b] $[\mathbf{1}]_0 = 5.0\times10^{-5}$ mol $l^{-1}$.

Table 2
Rate data for the reaction of **1** with **2b** in $CHCl_3$ at 25°C [a]

| $10^3[C_5H_5\overset{+}{N}–CH_2–CH=CH_2]$ (**2b**) (mol $l^{-1}$) | $10^3$[fn] (mol $l^{-1}$) | $10^3[C_5H_5N]$ (mol $l^{-1}$) | $10^4 k_{obs}$ ($s^{-1}$) |
|---|---|---|---|
| 0.83 | 0.21 | 0.2 | 1.53 ± 0.01 [b] |
| 1.67 | 0.21 | 0.2 | 2.90 ± 0.02 [b] |
| 2.50 | 0.21 | 0.2 | 4.33 ± 0.02 [b] |
| 3.34 | 0.21 | 0.2 | 5.73 ± 0.05 [b] |
| 0.83 | 0.41 | 0.4 | 1.20 ± 0.01 [b] |
| 1.67 | 0.41 | 0.4 | 2.41 ± 0.03 [b] |
| 2.50 | 0.41 | 0.4 | 3.46 ± 0.03 [b] |
| 3.34 | 0.41 | 0.4 | 4.85 ± 0.03 [b] |
| 0.83 | 0.84 | 0.4 | 0.72 ± 0.01 [b] |
| 1.67 | 0.84 | 0.4 | 1.42 ± 0.02 [b] |
| 2.50 | 0.84 | 0.4 | 2.0 ± 0.1 [b] |
| 3.34 | 0.84 | 0.4 | 2.6 ± 0.2 [b] |
| 0.83 | 1.73 | 1.0 | 0.40 ± 0.01 |
| 1.67 | 1.73 | 1.0 | 0.75 ± 0.01 |
| 2.50 | 1.73 | 1.0 | 1.20 ± 0.01 |
| 3.34 | 1.73 | 1.0 | 1.59 ± 0.01 |
| 0.83 | 4.84 | 1.0 | 0.19 ± 0.01 |
| 1.67 | 4.84 | 1.0 | 0.35 ± 0.01 |
| 2.50 | 4.84 | 1.0 | 0.49 ± 0.01 |
| 3.34 | 4.84 | 1.0 | 0.69 ± 0.01 |

[a] $[1]_0 = 1.0 \times 10^{-4}$ mol $l^{-1}$, unless otherwise stated.
[b] $[1]_0 = 2 \times 10^{-5}$ mol $l^{-1}$.

with $\alpha = 0.22 \pm 0.02$ ($NEt_3$), $0.27 \pm 0.04$ ($C_5H_5N$) $mol^{-1} l\ s^{-1}$, and $\beta = 2420 \pm 400$ ($NEt_3$), $2600 \pm 750$ ($C_5H_5N$) $mol^{-1}$ l. The slopes *Sl* are virtually independent of the concentration of A in the ranges examined ($5 \times 10^{-4}$ to $2 \times 10^{-3}$ mol $l^{-1}$ for [$NEt_3$] and $2 \times 10^{-4}$ to $1 \times 10^{-3}$ mol $l^{-1}$ for [$C_5H_5N$]).

These findings can be interpreted in terms of the following stepwise mechanism (Scheme 3):

The step $k_1$ corresponds to substitution of the $\eta^2$-bound fumaronitrile in **1** by **2** to give the labile palladium(0) intermediate **I** containing the $\eta^2$-coordinated allyl cation. This may either revert to the starting species **1** by re-entry of fn ($k_{-1}$) or undergo intramolecular oxidative rearrangement to the $\eta^3$-allyl palladium(II) product **3** with release of the free amine A through heterolytic breaking of the carbon–quaternary nitrogen bond under nucleophilic attack by the palladium(0) metal centre ($k_2$). The reverse step, $k_{-2}$, represents the first stage of the reductive amination of **3**, which was previously studied in detail [6,8]. Formation of the intermediate **I**, with accompanying reversible dissocia-

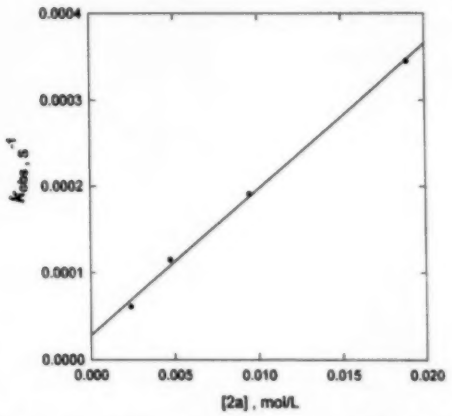


Fig. 2. Linear dependence of $k_{obs}$ on [**2a**] for reaction (1) ([$NEt_3$] = $1 \times 10^{-3}$ mol $l^{-1}$, [fn] = $5 \times 10^{-3}$ mol $l^{-1}$).

Table 3
Slopes (*Sl*) of plots of $k_{obs}$ versus [**2**]

| $\overset{+}{A}–CH_2–CH=CH_2$ (**2**) | $10^3$[A] (mol $l^{-1}$) | $10^3$[fn] (mol $l^{-1}$) | $10^2 Sl$ ($mol^{-1}$ l $s^{-1}$) |
|---|---|---|---|
| **2a**: A = $NEt_3$ | 1.0 | 0.5 | 10.16 ± 0.06 |
| | 1.0 | 1.0 | 6.18 ± 0.04 |
| | 2.0 | 1.0 | 6.20 ± 0.05 |
| | 1.0 | 1.5 | 4.86 ± 0.07 |
| | 1.0 | 2.5 | 3.48 ± 0.03 |
| | 1.0 | 5.0 | 1.69 ± 0.06 |
| **2b**: A = $C_5H_5N$ | 0.2 | 0.21 | 16.8 ± 0.1 |
| | 0.4 | 0.41 | 14.3 ± 0.1 |
| | 0.4 | 0.84 | 7.4 ± 0.2 |
| | 1.0 | 1.73 | 4.8 ± 0.2 |
| | 1.0 | 4.84 | 1.9 ± 0.1 |

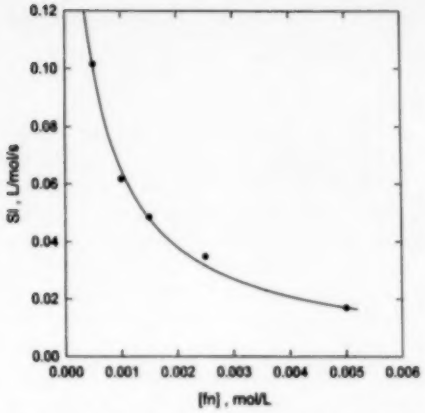


Fig. 3. Fit of slopes *Sl* to [fn] [Eq. (3)] for reaction (1) ([$NEt_3$] = $1 \times 10^{-3}$ mol $l^{-1}$).

tion of fn, is reasonable in the light of the retarding effect of added fn on the rates [Eq. (3)] and in line with earlier reports on the mechanism of (i) olefin substitution in palladium(0) complexes with rigid $\alpha$-diimino ligands [9] and (ii) oxidative addition of allylic halides to palladium(0) olefin complexes [2b], for which prior coordination of the C=C part of the entering ligand was proposed. The intermediate **I**, although kinetically significant, must be present in only very low concentration since it escaped detection by UV–vis (vide infra) and $^1$H NMR spectroscopy ($CDCl_3$ at 25°C). In the NMR spectra, only the typical proton resonances of the reactants **1** and **2**, and of the products **3**, fn, and **A**, were observed throughout the reaction (Experimental details) [6]. On the other hand, for the unreactive system **1**/(2-methylprop-2-enyl)triethylammonium perchlorate (1:5 molar ratio) in $CDCl_3$ at 25°C, only a slight broadening of the AB pattern at $\delta$ 2.98 ppm for the coordinated fn protons was observed, possibly due to a fast olefin exchange between **1** and trace amounts of a type **I** species. Therefore, by applying the steady-state approximation on [**I**] to Scheme 3, it can be shown (Experimental details) that, with the assumption $k_1[2] \ll k_2 + k_{-1}$ [fn], the decay of **1** and formation of **3** follow a simple first-order differential law of the type $-d[1]/dt = d[3]/dt = \varphi - k_{obs}$ [**3**], where $\varphi$ is a constant and $k_{obs}$ is given by Eq. (4):

$$k_{obs} = \frac{k_{-2}[A][fn]}{k_2/k_{-1} + [fn]} + \frac{k_1[2]}{1 + (k_{-1}/k_2)[fn]} \qquad (4)$$

To the extent that the above approximation is valid, Eq. (4) is equivalent to the experimental rate law (2), where

$$In = \frac{k_{-2}[A][fn]}{k_2/k_{-1} + [fn]} \text{ and } Sl = \frac{k_1}{1 + (k_{-1}/k_2)[fn]}$$

Moreover, comparison of the expression for *Sl* with the experimental rate law (3) yields $\alpha = k_1$ and $\beta = k_{-1}/k_2$.

The assumption $k_1[2] \ll k_2 + k_{-1}$[fn] {$k_1$[**2a**] in the range $(0.5–4.2) \times 10^{-3}$; $k_1$[**2b**] in the range $(2.2–9.0) \times 10^{-4}$ $s^{-1}$} is reasonable in the light of a steady-state approximation, for which the overall rate of decay of the intermediate **I** should be much higher than the rate of its formation. This is also in agreement with our failure to detect intermediate **I**.

The slopes *Sl* of Eq. (2) can be measured with good accuracy (Table 3) from plots of the type shown in Fig. 2, and exhibit the inverse dependence on [fn] shown in Eq. (3) (Fig. 3). In contrast, the extrapolated intercept values *In* are very uncertain, and show erratic features that preclude any correlation with [A] and/or [fn] data, thereby preventing any independent evaluation of the parameters $k_{-2}$ and $k_2/k_{-1}$ according to the relationship $In = k_{-2}[A][fn]/(k_2/k_{-1} + [fn])$.

The equilibrium constants $K_e$ for reaction (1) can also be calculated from the rate constants for the mechanism in Scheme 3 as $K_e = k_1k_2/k_{-1}k_{-2}$. The resulting values based on the appropriate $k_{-2}$ values from Ref. [6] [$K_e = (3.8 \pm 2) \times 10^{-3}$ for A = $NEt_3$; $0.5 \pm 0.3$ for A = $C_5H_5N$] are in satisfactory agreement with those obtained from direct equilibrium measurements [$(2.6 \pm 0.1) \times 10^{-3}$ and $1.0 \pm 0.4$, respectively]. This lends further support to the proposed mechanism and shows the internal consistency of the independently determined parameters.

The $k_1$ and $k_{-1}/k_2$ terms for A = $NEt_3$ are very close to those for A = $C_5H_5N$, indicating that the rate

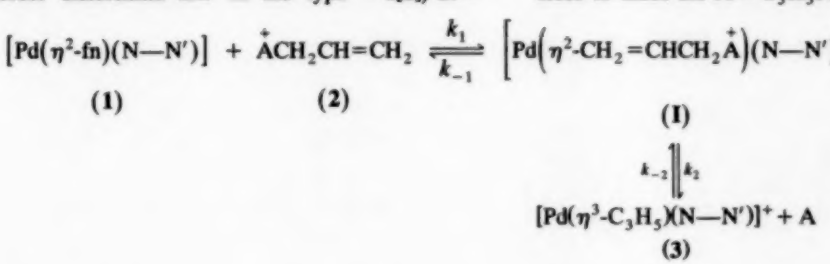


Scheme 3.

of formation of **I** and the relative rates of the reactions by which it disappears are virtually independent of the nature of the amine A. Therefore, the large differences in the equilibrium constants $K_e$ observed for reaction (1) are essentially due to the large difference in the $k_{-2}$ terms for the reverse amination reaction [6]. Whereas the reactivities of the two allylammonium cations **2** are rather similar, a large fall occurs upon replacement of the 2-allyl proton by a methyl group. The unreactivity of the (2-methylprop-2-enyl)triethylammonium cation may arise either from lack of formation of a type **I** intermediate or from its inertness toward oxidative allyl transfer caused by unfavourable electronic and steric properties of the methyl group. This is in line with the adverse role played by methyl substituents at the C=C carbons on the rates of oxidative addition of allyl halides to low-valent metal complexes.

## 3. Experimental details

The complexes $[Pd(\eta^2\text{-fn})(N—N')]$ [10a], $[Pd(\eta^3\text{-}C_3H_5)(N—N')]ClO_4$ [10b] and the allyl ammonium salts $[Et_3N—CH_2—CH=CH_2]ClO_4$ and $[C_5H_5N—CH_2—CH=CH_2]ClO_4$ [6] were prepared by published methods. Triethylamine and pyridine were distilled under nitrogen from anhydrous $K_2CO_3$ and KOH, respectively. Freshly distilled $CHCl_3$ was used for all kinetic runs. All other chemicals and solvents were reagent grade and were used without purification.

### 3.1. Preparation of $Et_3\overset{+}{N}—CH_2—C(Me)=CH_2$ as the perchlorate salt

A two-fold excess of freshly distilled 2-methylprop-2-enyl chloride (5.43 g, 60.0 mmol) was added to a methanol solution of $NEt_3$ (3.04 g, 30.0 mmol in 100 ml). The mixture was heated under reflux for 24 h. After addition of $NaClO_4 \cdot H_2O$(8.41 g, 60.0 mmol), the mixture was worked-up as previously described for the preparation of $[Et_3N—CH_2—CH=CH_2]ClO_4$ [6] to give the white product $[Et_3N—CH_2—CH=CH_2]ClO_4$ (7.30 g, 95.1%).

Molar conductivity: 110.9 S $cm^2$ $mol^{-1}$ for a $10^{-3}$ mol $l^{-1}$ MeOH solution at 25°C; IR spectrum (KBr pellet) ($cm^{-1}$): $\nu$(Cl—O) 1091, $\delta$(Cl—O) 631; $^1H$ NMR spectrum (in $CDCl_3$): allyl protons: $\delta$ 5.54 (1H,s,C$H_2$=C); 5.37 (1H,s,C$H_2$=C); 3.84 [2H,s,C(CH$_3$)—C$H_2$]; 2.00 [3H,C(C$H_3$)—CH$_2$] ppm; ethyl protons: $\delta$ 3.35 (6H, q, J = 7.3 Hz, $CH_2$); 1.40 (9H, t, $CH_3$) ppm.

### 3.2. Reactions of 1 with a 1:6 molar excess of allyl ammonium cations

*Method a*

The salt $[Et_3N—CH_2—CH=CH_2]ClO_4$ (0.09 mmol, 21.8 mg) was added to 3 ml of a $5 \times 10^{-3}$ mol $l^{-1}$ $CDCl_3$ solution of **1**. The progress of the reaction was monitored by $^1H$ NMR spectroscopy at 25°C. The initial spectrum showed the typical signals of **1** at virtually the same chemical shifts as those for the complex alone (with the amino proton as a singlet at $\delta$ 8.70 ppm and the $H^6$ pyridine proton as a multiplet at $\delta$ 8.90 ppm). The only significant difference was in the change of the $\eta^2$-coordinated fn proton signal from an AB system to a broad singlet at ca. $\delta$ 3.0 ppm. The signals of **1** decreased progressively with time with concomitant increase in those of **3** [imino proton as a singlet at $\delta$ 8.86 ppm, the $H^6$ pyridine proton as a multiplet at $\delta$ 8.80 ppm, the *syn*-allyl protons as a doublet at $\delta$ 4.20 ppm ($J$ = 7.0 Hz) and the *anti*-allyl protons as a doublet at $\delta$ 3.55 ppm ($J$ = 12.2 Hz)] and of $NEt_3$ ($CH_2$ protons as a quartet at $\delta$ 2.70 ppm and $CH_3$ protons as a triplet at $\delta$ 1.10 ppm). The olefin proton signal of free fumaronitrile could not be detected because of the fast exchange (on the NMR time scale) with the $\eta^2$-bound olefin in **1**. No other species was observed in the mixture. In the course of the reaction, some precipitation of product **3** took place.

Similar results were obtained for the reaction of **1** with $[C_5H_5N—CH_2—CH=CH_2]ClO_4$ under the same conditions.

*Method b*

The salt $[Et_3N—CH_2—C(Me)=CH_2]ClO_4$ (0.09 mmol, 23.0 mg) was added to 3 ml of a $5 \times 10^{-3}$ mol $l^{-1}$ $CDCl_3$ solution of **1**. The $^1H$ NMR spectra showed that no reaction took place at 25°C even after prolonged time and further addition of the allyl cation.

### 3.3. Physical measurements and instrumentation

The conductivity was measured with a CDM83 conductivity meter. The $^1H$ NMR spectra were run on Bruker AM-400 and AC-200 spectrometers at 25°C using tetramethylsilane as internal standard. Equilibrium and kinetic measurements were carried out on a Perkin-Elmer Lambda 5 spectrophotometer using 1-cm quartz cells. The IR spectra were recorded in the range 4000–200 $cm^{-1}$ on a Perkin-Elmer 983G instrument fitted with CsI windows.

### 3.4. Determination of equilibrium constants

Equilibrium constants in Eq. (1) were determined spectrophotometrically by adding known amounts of

chloroform solutions of **2** of known concentration to a solution of substrate **1** containing a known excess of fumaronitrile and base A over palladium in the thermostatted cell compartment of the spectrophotometer. Sufficient time was allowed for the establishment of the slow equilibrium. Spectral changes upon addition of **2** were monitored in the range 300–600 nm, in which only **1** and **3** show appreciable absorptions. The optical density data $D_\lambda$ were fitted by non-linear least-squares [11] using the following model:

$$\mathbf{1} + \mathbf{2} \rightleftharpoons \mathbf{3} + \text{fn} + \text{A} \quad (5)$$

$$K_e = [\mathbf{3}][\text{A}][\text{fn}]/[\mathbf{1}][\mathbf{2}] \quad (6)$$

$$[\text{Pd}]_0 = [\mathbf{1}] + [\mathbf{3}] \quad (7)$$

$$[\mathbf{2}]_0 = [\mathbf{2}] + [\mathbf{3}] \quad (8)$$

$$[\text{fn}], [\text{A}] \text{ constant (excess)} \quad (9)$$

$$D_\lambda = \varepsilon_1[\mathbf{1}] + \varepsilon_3[\mathbf{3}] \quad (10)$$

The function minimized was $\psi = \Sigma(D_{obs} - D_{calc})^2$. The optimized parameters were $K_e$ and the extinction coefficients. During each iterative cycle of the refining process the concentrations of all species involved were determined by solving the equilibrium and mass-balance equation system analytically (it reduces to a quadratic equation in [**3**]). The uncertainties quoted refer to the standard deviation.

### 3.5. Spectrophotometric kinetic measurements

The kinetics of reaction (1) were studied by adding known aliquots of chloroform solutions of **2** to freshly prepared solutions of **1** in the presence of an excess of both fn and A relative to the metal. The concentration of **2** was also much higher than that of palladium (Tables 1 and 2). Spectral changes at 25°C were monitored in the range 280–540 nm. The kinetic system in Scheme 3 can be described by the following system of equations ([**2**], [fn], [A] are constant):

$$d[\mathbf{3}]/dt = k_2[\mathbf{I}] - k_{-2}[\mathbf{3}][\text{A}] \quad (11)$$

$$[\text{Pd}]_0 = [\mathbf{1}] + [\mathbf{I}] + [\mathbf{3}] \quad (12)$$

$$d[\mathbf{I}]/dt = k_1[\mathbf{1}][\mathbf{2}] + k_{-2}[\mathbf{3}][\text{A}] - k_{-1}[\mathbf{I}][\text{fn}] - k_2[\mathbf{I}] \quad (13)$$

Under the hypothesis of steady-state for [**I**] ($d[\mathbf{I}]/dt \sim 0$, $[\mathbf{I}] \sim 0$) and using the approximation $k_1[\mathbf{2}] \ll k_2 + k_{-1}[\text{fn}]$, combination of these equations will yield:

$$d[\mathbf{3}]/dt = \varphi - k_{obs}[\mathbf{3}] \quad (14)$$

where

$$\varphi = \frac{k_1[\text{Pd}]_0[\mathbf{2}]}{1 + (k_{-1}/k_2)[\text{fn}]}$$

$$k_{obs} = \frac{k_{-2}[\text{A}][\text{fn}]}{k_2/k_{-1} + [\text{fn}]} + \frac{k_1[\mathbf{2}]}{1 + (k_{-1}/k_2)[\text{fn}]}$$

The first-order differential equation (14) can be integrated to give the customary mono-exponential rate law as the dependence of optical density $D_t$ on $t$, i.e. $D_t = D_\infty + (D_0 - D_\infty)\exp(-k_{obs}t)$, since $[\mathbf{3}] = (\varphi/k_{obs})[1 - \exp(-k_{obs}t)]$ (by integration), $[\mathbf{1}] \sim [\text{Pd}]_0 - [\mathbf{3}]$ [from Eq. (12) and the hypothesis $[\mathbf{I}] \sim 0$], $D_0 = \epsilon_1[\text{Pd}]_0$, $D_t = \epsilon_1[\mathbf{1}] + \epsilon_3[\mathbf{3}] = D_0 + (\epsilon_3 - \epsilon_1)[\mathbf{3}]$ and $D_\infty = D_0 + (\varphi/k_{obs})(\epsilon_3 - \epsilon_1)$. Values of $k_{obs}$ were obtained by non-linear regression [11] of the $D_t$ versus time data.

### 3.6. Data reduction and analysis

Mathematical and statistical analysis of equilibrium and kinetic data was carried out on a personal computer equipped with an INTEL 486 66 MHz central processor by the use of a locally adapted version of Marquardt's algorithm written in TURBOBASIC™ (Borland). Abstract factor analysis was carried out in the MATLAB™ (Mathworks) environment.

## Acknowledgment

Financial support by the Italian Ministero per l'Università e la Ricerca Scientifica e Tecnologica (Research Funds 40 and 60%) is gratefully acknowledged.

## References

[1] (a) B.M. Trost, and T.R. Verhoeven, in G. Wilkinson (ed.), *Comprehensive Organometallic Chemistry*, Pergamon, Oxford, UK, 1982, Vol. 8; (b) B.M. Trost, *Angew. Chem., Int. Ed. Engl., 28* (1989) 1173; (c) C.G. Frost, J. Howarth and J.M.J. Williams, *Tetrahedron: Asym., 3* (1992) 1089; (d) J. Tsuji, *Organic Synthesis with Palladium Compounds*, Springer Verlag, Heidelberg, 1980.

[2] (a) A. Vitagliano, B. Åkermark and S. Hansson, *Organometallics, 10* (1991) 2592; (b) H. Kurosawa, H. Kajimaru, S. Ogoshi, H. Yoneda, K. Miki, N. Kasai, S. Murai and I. Ikeda, *J. Am. Chem. Soc., 114* (1992) 8417, and references contained therein.

[3] P. Grenouillet, D. Neibecker and I. Tkatchenko, *Inorg. Chem., 19* (1980) 3189; R. Malet, M. Moreno-Manas and R. Pleixats, *Organometallics, 13* (1994) 397.

[4] K.L. Granberg and J.E. Bäckvall, *J. Am. Chem. Soc., 114* (1992) 6858.

[5] S. Ogoshi and H. Kurosawa, *Organometallics, 12* (1993) 2869.

[6] L. Canovese, F. Visentin, P. Uguagliati, F. Di Bianca, S. Antonaroli and B. Crociani, *J. Chem. Soc., Dalton Trans.*, (1994) 3113.

[7] P. Uguagliati, A. Benedetti, S. Enzo and L. Schiffini, *Comput. Chem., 8* (1984) 161.

[8] B. Crociani, S. Antonaroli, F. Di Bianca, L. Canovese, F. Visentin and P. Uguagliati, *J. Chem. Soc., Dalton Trans.*, (1994) 1145.

[9] R. van Asselt, C.J. Elsevier, W.J.J. Smeets and A.L. Spek, *Inorg. Chem., 33* (1994) 1521.

[10] (a) B. Crociani, F. Di Bianca, P. Uguagliati, L. Canovese and A. Berton, *J. Chem. Soc., Dalton Trans.*, (1991) 71; (b) B. Crociani, F. Di Bianca, A. Giovenco and T. Boschi, *Inorg. Chim. Acta, 127* (1987) 169.

[11] D.W. Marquardt, *SIAM J. Appl. Math., 11* (1963) 431.

ELSEVIER

Journal of Organometallic Chemistry 508 (1996) 109–120

Journal of Organometallic Chemistry

# Insertion reactions involving palladium complexes with nitrogen ligands I. Reactivity towards carbon monoxide of methylpalladium(II) complexes containing bidentate α-diimine ligands: crystal structures of four methylpalladium(II) and acylpalladium(II) complexes

R.E. Rülke [a], J.G.P. Delis [a], A.M. Groot [a], C.J. Elsevier [a], P.W.N.M. van Leeuwen [a], K. Vrieze [a,*], K. Goubitz [b], H. Schenk [b]

[a] *Anorganisch Chemisch Laboratorium, J.H. van't Hoff Research Institute, Universiteit van Amsterdam, Nieuwe Achtergracht 166, NL 1018 WV Amsterdam, Netherlands*

[b] *Laboratorium voor Kristallografie, Amsterdam Institute for Molecular Studies, Universiteit van Amsterdam, Nieuwe Achtergracht 166, NL 1018 WV Amsterdam, Netherlands*

Received 26 April 1995

**Abstract**

Neutral compounds of the type (2,2′-bipyridine)Pd($CH_3$)(Cl) and (6-R′-$C_5H_3$N-2-C(H)=N-R)Pd($CH_3$)(Cl) (R = $^i$Pr; R′ = H: $^i$Pr–PyCa) (R = $^t$Bu; R′ = H: $^t$Bu-PyCa) (R = $^i$Pr; R′ = $CH_3$: $^i$Pr-6-Me–PyCa) (R = $CH_2CH_2C_6H_5$; R′ = H: Phe–PyCa) (R = $^t$Bu; R′ = $CH_3$: $^t$Bu-6-Me–PyCa) (R = $^i$Pr; R′ = C(H)O: $^i$Pr–IPA) have been synthesized starting from (1,5-cyclooctadiene)Pd($CH_3$)(Cl) and ionic compounds of the type [(N-N)Pd($CH_3$)]$BF_4$ (N–N = bipy, $^i$Pr–PyCa, $^t$Bu–PyCa or $^i$Pr-6-Me–PyCa) by treatment of the methyl(chloro)palladium compounds with silver tetrafluoroborate. All products have been characterized by spectroscopic methods. Reaction of the compounds with carbon monoxide gives the neutral acyl compounds (N–N)Pd(C(O)$CH_3$)(Cl) and ionic acyl compounds [(N–N)Pd(C(O)$CH_3$)]$BF_4$ (N–N = bipy, $^i$Pr–PyCa, $^t$Bu–PyCa, $^i$Pr-6-Me–PyCa or Phe–PyCa). The crystal structures of ($^i$Pr-6-Me–PyCa)Pd($CH_3$)(Cl), ($^i$Pr–IPA)Pd($CH_3$)(Cl), (bipy)Pd(C(O)$CH_3$)(Cl) and ($^i$Pr–PyCa)Pd(C(O)$CH_3$)(Cl), have been determined. Comparison of data for the Pd–N=C–$C_5H_4$N moieties of the complexes concerned show that the geometries are almost identical, the largest r.m.s. deviation (between ($^i$Pr-6-Me–PyCa)Pd($CH_3$)(Cl) and (bipy)Pd(C(O)$CH_3$)(Cl)) being 0.2 Å. The Pd–C bond distances in the two acetylpalladium complexes are 0.05 Å shorter than those in the two methylpalladium complexes. The Pd–N bond distances for the nitrogen atoms situated *trans* to the organic group are shorter by 0.11 Å in the case of acetyl ligands.

An unprecedented influence of the steric properties of the ligands on the half-life for the CO insertion is observed; substituents adjacent to the nitrogen donor atoms cause strongly acceleration.

*Keywords:* Palladium; Imine; Carbon monoxide; Catalysis; Crystal structure; Late transition metals

## 1. Introduction

In many reactions catalyzed by late transition metals, in particular rhodium and palladium, the metal is stabilized by ligands having phosphorus donor atoms. Since late transition metals are soft Lewis acids, the soft Lewis-base phosphorus ligands stabilize a wide variety of oxidation states, thus providing very robust metal complexes, suitable for catalytic reactions under extreme conditions [1].

The number of late transition metal complexes used in catalytic processes bearing the harder nitrogen donor ligands is limited, although most processes involving catalysts containing phosphine ligands can also be carried out with those containing nitrogen ligands [2–5]. Examples are C–C cross-coupling reaction, allylic alkylation, hydrogenation and the Heck reaction, in which nitrogen-based catalysts perform better than phosphine-based catalysts [1,4], but in most cases the phosphine complexes are better, especially in industrial applications. It is known for example that, in the palladium-catalyzed terpolymerization of carbon monoxide, ethene and maleic anhydride, use of bipyridine and phenanthro-

* Corresponding author.

0022-328X/96/$15.00 © 1996 Elsevier Science S.A. All rights reserved
*SSDI* 0022-328X(95)05825-7

line ligands gives a considerably higher ethene : MA ratio but a much lower average molecular weight of the terpolymer than does that of diphosphine ligands [3].

In recent years we [6–8] and others [2,5] have shown in model studies of the separate steps of the alternating copolymerization of CO with alkenes that palladium complexes with nitrogen donor ligands are significantly more reactive than analogous palladium phosphine complexes, but they have the major disadvantage of being less stable under catalytic conditions, particularly in respect of their tendency to dissociate from the metal center. For example, the reaction of a palladium complex containing a bidentate α-diimine ligand with an olefin may lead to the dissociation of one nitrogen atom [9], and this under certain conditions may lead to formation of α-diimine-bridged binuclear species [10].

In order to study the steric and electronic effects of nitrogen ligands in carbonylation reactions, we have synthesized a series of neutral and ionic methylpalladium complexes containing bidentate nitrogen ligands 2,2′-bipyridine (bipy)(**1**), 2-(*N*-2-propanecarbaldimino)pyridine ($^i$Pr–PyCa)(**2**),2-(*N*-2-(2-methyl)propanecarbaldimino)-pyridine ($^t$Bu–PyCa)(**3**), 2-(*N*-2-propanecarbaldimino)-6-(methyl)pyridine ($^i$Pr-6-Me–PyCa)(**4**), 2-(*N*-(2-phenyl)ethanecarbaldimino)pyridine (Phe–PyCa)(**5**),2-(*N*-2-(2-methyl)propanecarbaldimino)-(methyl)pyridine ($^t$Bu-6-Me–PyCa)(**6**) and 2-(*N*-propanecarbaldimino)-6-(carbaldimino)pyridine ($^i$Pr-IPA)(**7**). Some palladium and platinum complexes containing some of these ligands have been used in the past by Vitagliano and coworkers [11a,12] in studies of alkene-stabilized five-coordinated palladium and platinum complexes. We have examined the reactivities of the methylpalladium complexes containing the ligands **1–7** towards carbon monoxide (Fig. 1) and also investi-

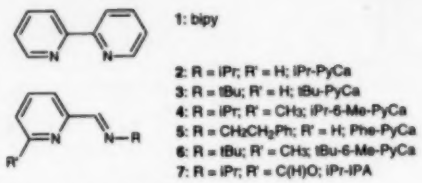
1: bipy
2: R = iPr; R' = H; iPr-PyCa
3: R = tBu; R' = H; tBu-PyCa
4: R = iPr; R' = CH3; iPr-6-Me-PyCa
5: R = CH2CH2Ph; R' = H; Phe-PyCa
6: R = tBu; R' = CH3; tBu-6-Me-PyCa
7: R = iPr; R' = C(H)O; iPr-IPA

Fig. 1. Structure and numbering of the ligands.

Table 1
Selected $^1$H NMR data for **2–14b** [a].

| Compound [b] | δ(Pd–R) (ppm) | δ(H$^a$) (ppm) | δ(H$^3$) (ppm) | δ(H$^6$ or 6-R) (ppm) | δ(H$^7$) (ppm) |
|---|---|---|---|---|---|
| **2** | — | 3.44 | 7.81 | 8.42 | 8.21 |
| **3** | — | — | 7.96 | 8.59 | 8.33 |
| **4** | — | 3.16 | 7.81 | 2.57 (Me) | 8.35 |
| **5** | — | 3.02 | 7.99 | 8.60 | 8.28 |
| **6** | — | — | 7.86 | 2.60 (Me) | 8.35 |
| **7** | — | 3.59 | ≈ 7.8 | 10.10 | 8.47 |
| **1a** | 1.03 | — | 8.09, 8.14 | 8.87, 9.19 | — |
| **2a$^c$** | 1.01 | 4.31 | 7.68 | 9.12 | 8.37 |
| **2a$^t$** | 1.11 | 4.43 | 7.68 | 8.64 | 8.27 |
| **3a** | 1.20 | — | 7.73 | 8.61 | 8.20 |
| **4a** | 1.17 | 4.21 | 7.50 | 3.00 (Me) | 8.38 |
| **5a$^c$** | 1.09 | 3.08 | 7.46 | 9.05 | 7.77 |
| **5a$^t$** | 1.07 | 3.25 | 7.52 | 8.62 | 7.77 |
| **6a** | 1.22 | — | 7.46 | 2.92 (Me) | 8.36 |
| **7a** | 1.05 | 4.21 | ≈ 8.10 | 10.99 | 8.68 |
| **11a** | 1.11 | — | 8.42 | 8.65, 8.71 | — |
| **12a$^c$** | 1.13 | 4.12 | 8.01 | 8.61 | 8.57 |
| **12a$^t$** | 1.01 | 4.20 | 8.06 | 8.68 | 8.67 |
| **13a** | 1.25 | — | 8.07 | 8.65 | 8.53 |
| **14a** | 1.21 | 4.19 | 7.86 | 2.77 (Me) | 8.65 |
| **1b** | 2.67 | — | — | 8.50, 9.02 | — |
| **2b$^c$** | 2.65 | 4.18 | 7.63 | 8.97 | 8.29 |
| **2b$^t$** | 2.65 | 4.16 | ≈ 7.6 | 8.42 | 8.19 |
| **3b** | 2.56 | — | — | 8.41 | 8.13 |
| **4b** | 2.66 | 4.00 | 4.00 | 2.90 (Me) | 8.28 |
| **5b$^c$** | 2.69 | 2.91 | 3.95 | 8.78 | 7.87 |
| **5b$^t$** | 2.64 | 3.18 | 3.98 | 8.39 | 7.78 |
| **11b** | 2.32 | — | 8.30 | 8.76, 8.82 | — |
| **12b** | 2.68 | 4.03 | 4.03 | 8.40 | 8.52 |
| **13b** | 2.70 | — | — | 8.31 | 8.43 |
| **14b** | 2.71 | 3.89 | 3.89 | 2.72 (Me) | 8.55 |

[a] In $CDCl_3$ at 293 K, except for the ionic complexes which were examined in $CD_3CN$ at 293 K.
[b] Superscript **t** indicates a *trans* configuration, and superscript **c** a *cis* configuration of the methyl and the imino-nitrogen.

gated the stability and the molecular structures by means of NMR techniques and single-crystal structure analyses. The ligands have in common an α-diimine chelating moiety which has both σ-donating and π-accepting properties [9]. The R–PyCa ligands are non-symmetric and thus can give rise to geometric isomers when coordinated to methyl(chloro)palladium moieties. α-Diimine ligands are known to coordinate in a bidentate fashion [13] but since they are quite flexible, they can if required also adopt a monodentate coordination mode. This was observed even in the case of *cis*-fixed ligands such as phenanthroline, although the non-coordinated nitrogen of the phenanthroline remains in the vicinity of the metal [9].

## 2. Results

In previous work we showed that (COD)Pd($CH_3$)(Cl) readily undergoes substitution by bidentate phosphorus or potentially terdentate nitrogen ligands [7,14]. Although other starting complexes are known, such as [Pd($CH_3$)($SMe_2$)μ-Cl]$_2$ [15] and (tmeda)Pd($CH_3$)(Cl) [2a], use of (COD)Pd($CH_3$)Cl proved to be an excellent method for the synthesis of neutral methyl(chloro)palladium complexes containing bidentate and terdentate nitrogen ligands.

The methyl(chloro)palladium complexes **1a–7a**, the methylpalladium tetrafluoroborate complexes **11a–14a**, the acetyl(chloro)palladium complexes **1b–5b** and the acetylpalladium tetrafluoroborate complexes **11b–14b** were isolated with high yields. Compounds **2a–4a** and **2b–4b** gave satisfactory elemental analysis. Compounds **5a**, **6a**, **11a–14a** and **11b–14b** were only stable for a few hours, in precluding elemental analysis. From **7a**, only a very small amount of product was isolated and this was not sufficient for elemental analysis. The structural features of **1a** and **1b** and the elemental analysis data were reported recently [2]. The complexes have been fully characterized by $^1$H and $^{13}$C NMR spectroscopy, and in the case of the acetylpalladium complexes **1b–14b** also by IR spectroscopy. For **4a**, **7a**, **1b** and **2b**, single-crystal structure analyses were carried out. Selected $^1$H NMR data are presented in Table 1.

### 2.1. Synthesis and properties of methylpalladium compounds 1a–14a

Substitution of COD in (COD)Pd($CH_3$)(Cl) by the appropriate nitrogen ligand in dichloromethane resulted in the rapid formation of complexes of the type (N-N)Pd($CH_3$)(Cl), numbered **1a–6a**. The colourless methyl(chloro)palladium complex **7a** was prepared in the same fashion but was isolated by a different procedure (see Section 5). The ionic complexes of the type [(N–N)Pd($CH_3$)(acetonitrile)]$BF_4$ (**11a–14a**) were obtained by reaction of the methylpalladium compounds with silver tetrafluoroborate in acetonitrile. The structure and numbering of the complexes is shown in Fig. 2. For clarity the neutral compounds are numbered **1a**, **1b**, **2a** etc. and the corresponding ionic compounds **11a**, **11b**, **12a** etc.

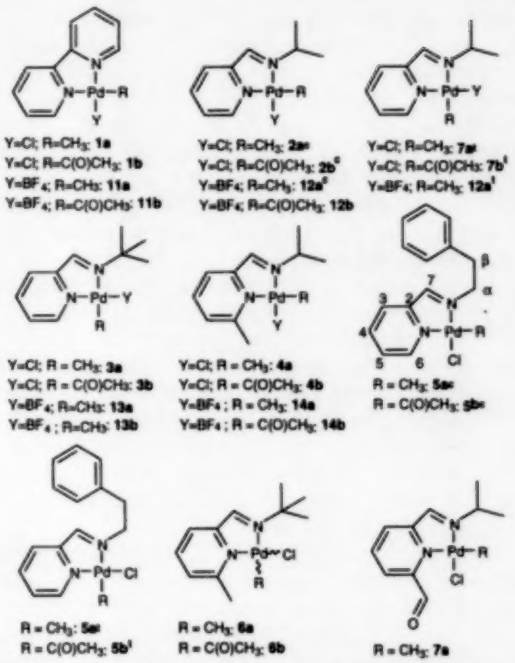


Fig. 2. Structure and numbering of the methyl-and acetylpalladium compounds **1a–14a** and **1b–14b**. The adopted numbering scheme of the R-PyCa ligands **2–7** is shown only for **5**. The superscript t indicates a *trans* configuration, and the superscript c a *cis* configuration of the methyl and the imino nitrogen.

Since the R–PyCa ligands **2–7** are asymmetric, coordination to methyl(chloro)palladium compounds can lead to the formation of two isomeric forms, which are *cis* and *trans* in respect of the relative positions of the methyl ligand and the imino nitrogen of the R–PyCa ligand on the palladium atom. This is the case for ($^i$Pr–PyCa)Pd($CH_3$)(Cl)(**2a**), (Phe–PyCa)Pd($CH_3$)(Cl)-(**5a**), [($^i$Pr-PyCa)Pd($CH_3$)]$BF_4$(**12a**) and the acetylpalladium analogues **2b** and **5b**, as can be concluded from the two sets of resonances in the NMR spectra.

The most sensitive resonances for the assignment of this isomerism are for $H^6$ and the α-protons of the imino substituents (Table 1). In the *cis* isomers, $H^6$ has a large chemical shift, owing to the strong deshielding effect of the chloride ligand, which is situated *cis* to the pyridyl group (Fig. 2), whereas the *trans* isomers have the $H^6$ resonances at a considerably lower chemical shift. For example, the $H^6$ signal for **2a** appears at 9.12 ppm, and for **2a$^t$** at 8.64 ppm. The methyl compounds

**2a**, **5a** and **12a** exist in *cis*:*trans* ratios of 1:0.79, 1:0.30 and 1:0.27 respectively and the acetylpalladium compounds **2b** and **5b** in 1:0.56 and a 1:0.25 ratios respectively, as indicated by the $^1$H NMR integrals. Interestingly, in the case of **2b**, only the *cis* isomer **2b**(*cis*) was present in the crystal. The $^1$H and $^{13}$C NMR spectra of the complexes of **2** and **5** have sharp resonances indicating that no dynamic processes, such as *cis–trans* isomerization are observed by these complexes on the NMR time scales.

For the palladium complexes **4a**, **14a**, **4b**, **14b** and **7a** containing the 6-substituted ligands $^i$Pr-6-Me–PyCa and $^i$Pr–IPA, only the *cis* isomers were observed, whereas the palladium complexes **3a**, **13a**, **3b** and **13b** containing $^t$Bu–PyCa occur exclusively in the *trans* configuration. The $^1$H NMR signals from all the R–PyCa palladium compounds are very sharp, except in the case of **6a**, vide infra, indicating that no fluxional processes such as methyl-chloro *cis–trans* isomerization, take place on the NMR time scale.

Surprisingly, the composition of **6a**, containing the sterically demanding ligand **6** proved to be very complex. Adding one equivalent of **6** to (COD)Pd($CH_3$)(Cl) led to very poor yields of **6a** (14%). Use of a five fold excess of **6** yielded after washing an aggregate containing **6a** and **6** in a 1:1 ratio. Further washing resulted in formation of Pd black and the recovery of the 1:1 aggregate. The $^1$H NMR spectrum of this aggregate shows a set of sharp signals of free **6** and a set of broadened signals of coordinated **6**. The structure of **6a** could be analyzed only with difficulty, since the usual indicator protons, $H^6$ and $H^\alpha$, are absent. The chemical shift for the methyl ligand in **6a** is close to that in **13a** and suggests a *cis* configuration. The chemical shift of the methyl group, however, may be affected by severe distortions of the methyl and the chloride ligands with respect to the coordination plane. Some nuclear Overhauser effect experiments performed to help to elucidate the configuration of **6a** revealed a chemical exchange of coordinated and free ligand, indicating that **6** is only weakly bonded to Pd(II). This is confirmed by the rapid substitution of **6** to give **4a** when an equimolar amount of **4** was added to **6a**.

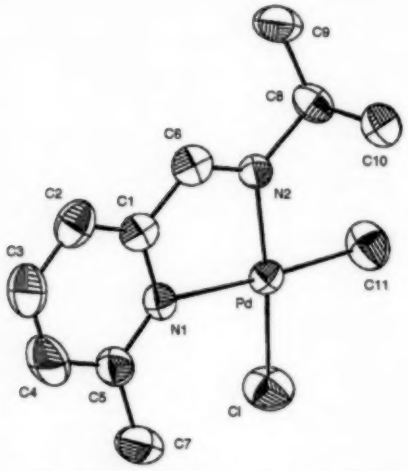


Fig. 3. ORTEP plot (drawn at the 50% probability level) of the molecular structure of [2-(*N*-2-propanecarbaldimino)-6-(methyl) pyridyl]methyl(chloro)palladium(II) (**4a**).

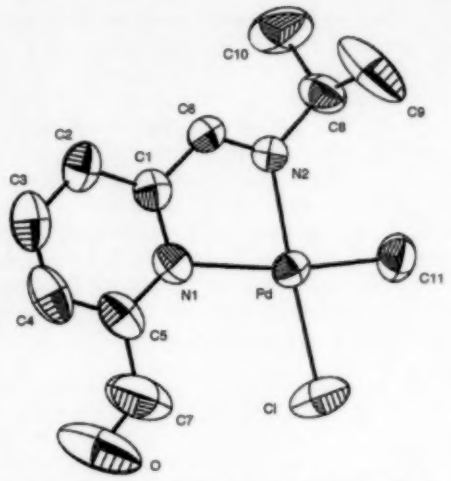


Fig. 4. ORTEP plot (drawn at the 50% probability level) of the molecular structure of 2-(*N*-propanecarbaldimino)-6-(carbaldimino) pyridyl]methyl(chloro)palladium(II) (**7a**).

## 2.2. Crystallographic section

Crystals suitable for X-ray determination were obtained for **4a**, **7a**, **1b** and **2b** by slow diffusion of diethyl ether into a dichloromethane solution of **4a**, **7a** and **1b**, or by slow evaporation of the solvent from an acetonitrile solution of **2b**. The molecular structures of **4a**, **7a**, **1b** and **2b** are presented in Figs. 3, 4, 5 and 6 respectively. Tables 2 and 3 list the bond distances and selected bond angles respectively, for the non-hydrogen atoms, and Table 5 later gives selected crystal data and refinement details.

The complexes **4a**, **7a**, **1b** and **2b** all have the expected square planar arrangement of the ligands around the palladium metal. The organic group R in **4a**, **7a** and **2b** is *trans* with respect to N(1) and *cis* to N(2), i.e. the *cis* isomers are formed. It is interesting to note that, for **4a**, only the *cis* isomer was found in the crystal, whereas in solution both isomers are present. The α-diimine ligands have bite angles of 77.8(4)–78.5(2)°, which are normal values for these types of ligands [2]. From Fig. 4 it can be seen that the formyl group has turned away from the palladium and does not

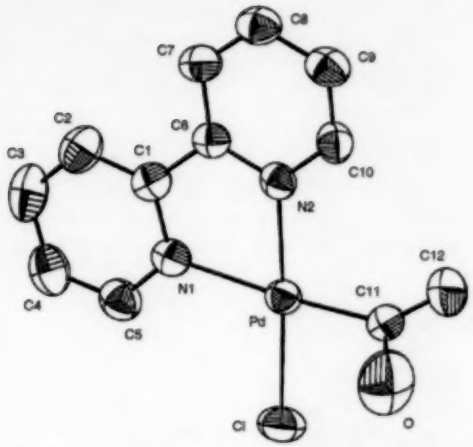


Fig. 5. ORTEP plot (drawn at the 50% probability level) of the molecular structure of (bipyridyl)methyl(chloro)palladium(II) (**1b**).

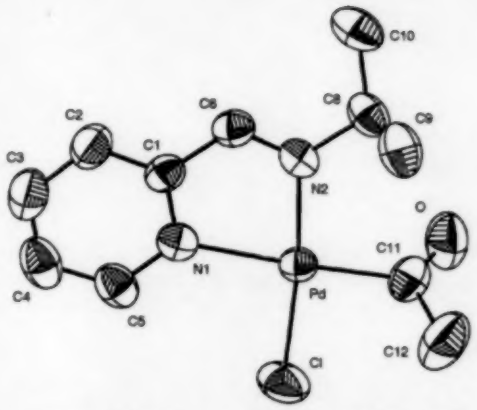


Fig. 6. ORTEP plot of (drawn at the 50% probability level) the molecular structure of [2-(*N*-2-propanecarbaldimino)pyridyl] methyl(chloro)palladium(II) (**2b**).

Table 2
Bond distances (with estimated standard deviations in parentheses) for the non-hydrogen atoms of **4a**, **7a**, **1b**, and **2b**

| | Bond distance (Å) | | | |
|---|---|---|---|---|
| | **4a** | **7a** | **1b** | **2b** |
| Pd–Cl | 2.307(2) | 2.312(2) | 2.32(1) | 2.319(1) |
| Pd–C(11) | 2.009(9) | 2.012(8) | 1.94(1) | 1.964(5) |
| Pd–N(1) | 2.260(5) | 2.253(5) | 2.16(1) | 2.170(4) |
| Pd–N(2) | 2.070(5) | 2.060(4) | 2.07(1) | 2.063(3) |
| C(1)–C(2) | 1.37(1) | 1.397(10) | 1.36(2) | 1.392(7) |
| C(1)–C(6) | 1.450(9) | 1.456(7) | 1.47(2) | 1.465(6) |
| C(1)–N(1) | 1.363(7) | 1.341(7) | 1.37(1) | 1.343(5) |
| C(2)–C(3) | 1.40(1) | 1.390(10) | 1.38(2) | 1.400(7) |
| C(3)–C(4) | 1.36(1) | 1.34(1) | 1.39(2) | 1.347(9) |
| C(4)–C(5) | 1.38(1) | 1.39(1) | 1.35(2) | 1.389(8) |
| C(5)–C(7) | 1.48(1) | 1.47(1) | — | — |
| C(5)–N(1) | 1.347(8) | 1.357(7) | 1.33(2) | 1.331(6) |
| C(6)–N(2) | 1.272(8) | 1.283(8) | 1.36(1) | 1.285(6) |
| C(8)–C(9) | 1.51(1) | 1.50(1) | 1.38(1) | 1.516(8) |
| C(8)–C(10) | 1.50(1) | 1.51(1) | — | 1.523(7) |
| C(8)–N(2) | 1.495(8) | 1.488(8) | — | 1.490(6) |
| C(11)–C(12) | — | — | 1.52(2) | 1.509(9) |
| C(11)–O | — | — | 1.20(2) | 1.174(7) |
| C(7)–C(8) | — | — | 1.39(2) | — |
| C(6)–C(7) | — | — | 1.39(2) | — |
| C(9)–C(10) | — | — | 1.36(2) | — |
| C(10)–N(2) | — | — | 1.36(2) | — |
| C(7)–O | — | 1.20(1) | — | — |

Table 3
Selected bond angles (with estimated standard deviations in parentheses) for the non-hydrogen atoms of **4a**, **7a**, **1b** and **2b**

| | Bond angle (°) | | | |
|---|---|---|---|---|
| | **4a** | **7a** | **1b** | **2b** |
| Cl–Pd–C(11) | 85.9(2) | 86.6(2) | 88.3(4) | 88.1(1) |
| Cl–Pd–N(1) | 101.6(1) | 102.0(1) | 97.2(6) | 96.1(1) |
| C(11)–Pd–N(2) | 94.5(3) | 92.9(3) | 96.7(7) | 97.7(2) |
| N(1)–Pd–N(2) | 78.4(2) | 78.5(2) | 77.8(4) | 78.1(1) |
| Pd–C(11)–C(12) | — | — | 117(1) | 115.4(5) |
| Pd–C(11)–O | — | — | 123.0(8) | 122.1(4) |
| C(12)–C(11)–O | — | — | 120(1) | 122.5(5) |

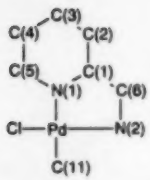


Fig. 7.

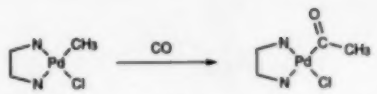


Scheme 1.

coordinate to the metal center. In **1b** and **2b**, the acetyl ligand lies in perpendicular position to the palladium coordination plane, in keeping with earlier reports [2a,16].

Comparison of the data for the corresponding compounds Pd, Cl, N(1), N(2), C(1), C(2), C(3), C(4), C(5), C(6) and C(11) (Fig. 7) in structures **4a–2b** led to the following results. Taking **4a** as reference the matching led to the following r.m.s. values: **4a–7a** r.m.s., 0.08 Å; **4a–1b** r.m.s., 0.20 Å; **4a–2b** r.m.s., 0.16 Å. The greatest variation in distances are for those involving the chloride atoms of the compounds, with r.m.s. values of 0.15, 0.39 and 0.34 Å respectively.

### *2.3. Carbonylation reactions of methylpalladium compounds 1a–14a*

The methyl(chloro)palladium compounds **1a–5a** (Scheme 1) and the methylpalladium tetrafluoroborate compounds **11a–14a** were treated with CO in order to investigate their reactivity in CO insertion.

For preparative purposes, Schlenk vessels containing a solution of **1a–5a** in dichloromethane or **11a–14a** in acetonitrile were evacuated, flushed twice with CO and then filled with CO, and the mixture was stirred for 30 min, during which a little palladium black was formed. Filtration gives the pure acetyl compounds **1b–14b**.

The half-lives for CO insertion were obtained by measuring the CO uptake with a gas buret (Table 4). Although use of high pressure $^1$H NMR spectroscopy for the determination of CO insertion half-lives was successful in the case of diphosphine palladium complexes [6a,17], this method was unsuitable for most compounds containing nitrogen ligands, because insertion half-lives are too short for reliable measurement.

## 3. Discussion

Several features in the $^1$H NMR data are note worthy. Whereas for the free ligands the resonances of the pyridine protons appear in the sequence $H^5$, $H^4$, $H^3$, $H^6$, those for the R–PyCa complexes normally appear in the sequence $H^5$, $H^3$, $H^4$, $H^6$. The negative coordination-induced shift (CIS) of $H^3$ can be attributed to the *E-trans* conformation of the free ligand. In this conformation, the nitrogen of the imino group points towards $H^3$ and the interaction between the hydrogen and the lone pair of the imine induces a low field shift for $H^3$. The CIS of $H^6$ depends strongly on the arrangement of the ligands around the palladium center. If the complex has a *cis* configuration, the chloride ligand is close to $H^6$ and the strong deshielding effect of the chloride ligand increases the chemical shift for $H^6$.

The *cis* configuration is apparently the most favourable configuration for methyl(chloro)palladium complexes with non-symmetric R–PyCa ligands, in keeping with previous reports [11a,12]. The differences between the energies of the *cis* and the *trans* configurations are clearly small, since minor changes on either side of the ligand can affect the configuration. Apparently, a very delicate balance is reached in the case of the configurations of **2a**, **2b**, **5a** and **5b** for which both isomers occur, while the steric requirement of the acetyl ligand compared with that of the methyl ligand changes the *cis* : *trans* ratio in favour of the *cis* configuration. This is also clear for the ionic isomer **12a**, in which the

Table 4
Half-lives for the carbonylation of **1a–14a**, and IR data for **1b–14b** [a] and related compounds taken from the literature

| Compound | Half-life (min:s) | ($\nu$(CO) cm$^{-1}$) |
|---|---|---|
| ($^i$Pr-6-Me–PyCa)Pd($CH_3$)(Cl) (**4a**) | 4:15 (±0:30) | 1697 |
| [($^i$Pr-6-Me–PyCa)Pd($CH_3$)]$BF_4$ (**14a**) | 8:00 (±0:30) | 1705 |
| [(bipy)Pd($CH_3$)]$BF_4$, (**11a**) | 8:30 (±0:30) | 1690 |
| [($^t$Bu-PyCa)Pd($CH_3$)]$BF_4$ (**13a**) | 12:00 (±0:30) | 1700 |
| ($^t$Bu-PyCa)Pd($CH_3$)(Cl) (**3a**) | 12:30 (±0:30) | 1692 |
| [($^i$Pr-PyCa)Pd($CH_3$)]$BF_4$ (**12a$^c$** and **12a$^t$**) | 14:00 (±0:30) | 1703 |
| ($^i$Pr-PyCa)Pd($CH_3$)(Cl) (**2a$^c$** and **2a$^t$**) | 19:00 (±0:30) | 1695 |
| (Phe–PyCa)Pd($CH_3$)(Cl) (**5a$^c$** and **5a$^t$**) | 23:45 (±0:30) | 1694 |
| (bipy)Pd($CH_3$)(Cl) (**1a**) | 28:30 (±0:30) | 1690 |
| ($^t$Bu–PyCa)Pd($CH_3$)(Cl)–$^t$Bu–PyCa (**6a**) | instantaneous Pd blackening | — |

[a] [Pd] = 40 mM; $P$(CO) = 2 bar; $T$ = 293 K.

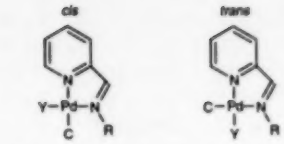


| | | | |
|---|---|---|---|
| 12b: | 1 | 0 | R=iPr; C=C(O)CH$_3$; Y=CH$_3$CN/BF$_4$. |
| 5b: | 1 | 0.25 | R=Phe; C=C(O)CH$_3$; Y=Cl. |
| 12a: | 1 | 0.27 | R=iPr; C=CH$_3$; Y=CH$_3$CN/BF$_4$. |
| 5a: | 1 | 0.30 | R=Phe; C=CH$_3$; Y=Cl. |
| 2b: | 1 | 0.56 | R=iPr; C=C(O)CH$_3$; Y=Cl. |
| 2a: | 1 | 0.79 | R=iPr; C=CH$_3$; Y=Cl. |

Fig. 8. *cis* : *trans* ratios of **2a**, **2b**, **5a**, **5b**, **12a** and **12b**.

chloride ligand has been replaced by an acetonitrile molecule. The preference for the *cis* configuration increases in the order **12b** > **5b** > **12a** > **5a** > **2b** > **2a** (Fig. 8).

The fact that the acetylpalladium compounds have a larger preference for the *cis* configuration can be attributed to the perpendicular position of the acetyl group with respect to the coordination plane. In this conformation the acetyl group is less bulky than the methyl group and is sterically less constrained by the bulk of the substituent on the imino-nitrogen. The *trans* influence of the acetyl group, which is larger than that of the methyl group [18], also increases the preference for the *cis* configuration. The effect of acetonitrile on the stereochemistry can also be attributed to the lower steric hindrance.

The higher *trans* influence of the methyl and the acetyl ligand than of the chloride ligand [18] is reflected in the longer Pd–N(1) distance (by 0.19 Å for the methylpalladium compounds and by 0.09–0.11 Å for the acetylpalladium compounds) with respect to the Pd–N(2) distance. The shorter Pd–C(11) distances in the acetylpalladium complexes **1b** and **2b** than in the methylpalladium complexes **4a** and **7a** (by about 0.05 Å) can be attributed to the shorter bonds found for $sp^2$-hybridized carbon atoms in general. An intriguing discrepancy, however, is found for the Pd–N(1) bond distances, which are severely affected by the nature of the organic ligand in the *trans* position. These Pd–N(1) distances in **1b** and **2b** are about 0.11 Å shorter than those in **4a** and **7a**, while the Pd–Cl and Pd–N(2) bond distances are not affected, and this must be due to the differences between the *trans* influences of the methyl and the acetyl ligands.

The acetyl ligand is known to have a larger *trans* influence than the methyl ligand [18] and this would be expected to lead to longer Pd–N(1) distances owing to σ-bond destabilization of the Pd–N bond. However, shorter bonds are, in fact, found in **1b** and **2b**. Since the R–PyCa and bipy ligands have suitable $p\pi_*$ orbitals for π back donation, the *trans* influence of the acetyl ligand causes an increased $d_{xz} \rightarrow p\pi_*$ back donation from the palladium to the pyridyl moiety. Hence, a push–pull process is present which causes the Pd–N(1) distances in **1b** and **2b** to be shorter than in the methylpalladium complexes **4a** and **7a**.

The half-lives of the CO insertion for the neutral compounds **1a–3a** are only slightly longer than those for the ionic methylpalladium analogues **11a–13a**, and that for the neutral compound **4a** is even shorter than that for the ionic compound **14a**. However, different solvents were used for the neutral and the ionic compounds and so the half-lives cannot be compared, since not only are the solubilities of CO in the two solvents different, but also different mechanistic routes may apply, vide infra. Nevertheless, it is expected that the presence of acetonitrile will lower the rate of CO insertion since it acts as a competing ligand.

The large differences in the half-lives between the various methylpalladium compounds are unexpected. The half-life clearly decreases with increasing steric hindrance on either side of the ligand. This surprising accelerating effect of a substituent adjacent to one nitrogen donor atom was very recently also observed for complexes with trinitrogen ligands [19]. The accelerating effect of a bulky group close to the N-donor function, however, reaches a limit. For example, when **6a** is treated with CO in dichloromethane, instantaneous formation of Pd-black is observed, and this is understandable since too much steric hindrance will cause inefficient bonding of the bidentate nitrogen ligand to the palladium atom, vide supra.

We showed previously that compounds (P–P)-Pd($CH_3$)(Y) (Y = $Cl^-$, $CF_3SO_3^-$ or $BF_4^-$) containing flexible diphosphine ligands P–P with large bite angles show short half-lives for CO insertion, since the transition state energy is when the CO and $CH_3$ groups will be forced closer together in the intermediate (P–P)Pd($CH_3$)(CO) [6a]. Therefore, we were rather surprised to find that methylpalladium compounds containing these flexible bidentate nitrogen ligands **1–5** with small bite angles (76–80°) underwent much faster CO insertion than those containing diphosphines [7]. We observed similar fast insertion of CO into the Pd–C bond recently also for methylpalladium complexes with rigid bidentate nitrogen ligands that have comparable small bite angles.

When we look at our earlier results [6,7] and those reported here in the light of other work [9a,20] we note that Natile and coworkers found that bidentate nitrogen ligands containing bulky groups adjacent to the N-donor functions cause deviations from planarity, as for example in (dmphen)Pd($CH_3$)(Cl) (dmphen = 2,9-dimethyl-1,10-phenanthroline) [20], and these ligands also show a greater tendency to form five-coordinated complexes with alkenes [9b,11,20]. Strikingly, dmphen can, depending on the donor and acceptor properties of the ligand, bond in the *trans* position as a bidentate ligand

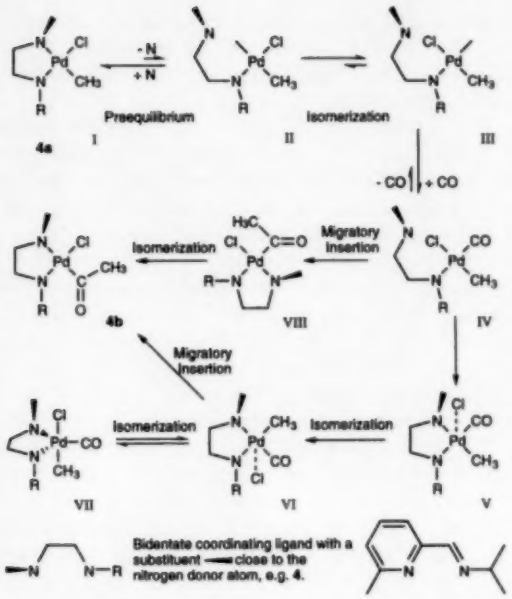


Scheme 2. Mechanism accounting for the accelerating effect of substituents adjacent to the nitrogen donor in the insertion reactions of CO with the complexes (N–N)Pd($CH_3$)(Cl).

(acceptor in the *trans* position) or as a monodentate ligand (donor in the *trans* position) and can even adopt a coordination mode in between monodentate and bidentate [9b].

In a recent article on the rigid bidentate nitrogen ligand Ar-BIAN (Ar-BIAN = bis(arylimino)acenaphtene) we have tentatively proposed a mechanism involving dissociation of $Cl^-$ to allow CO coordination, while the rigid N–N ligand remains bonded as a bidentate throughout the CO insertion [7a,b]. However, in the light of the previous discussion one might also propose for compounds (N–N)Pd($CH_3$)(Cl) the mechanism outlined in Scheme 2 for the carbonylation of **4a**, which is partly based on results reported by Natile and coworkers [9a].

According to Natile and coworkers, the first step involves (partial) dissociation of the nitrogen donor containing the bulky substituent. The resulting T-shaped intermediate II then isomerizes to the more stable T-shaped intermediate III with $CH_3$ *trans* to Cl. Addition of CO gives intermediate IV; such species with CO *cis* to the $CH_3$ group have recently been observed [8].

A conceivable alternative pathway would involve an initial migratory insertion to give the product **4b** via intermediate VIII. This is less likely, since $CH_3$ migration would not be expected to occur for $CH_3$ *trans* to Cl. The more likely pathway involves the dissociation of Cl *trans* to $CH_3$ to give V, in which has a strong *trans* influence, so favoring isomerization to VI. Depending on the solvent, this intermediate could be present as an ion pair, with a cationic palladium moiety and $Cl^-$, or as separated ions. Migratory insertion might now occur in the (N–N)Pd($CH_3$)(CO) plane to give, after reassociation of $Cl^-$, the final product **4b**. It is also possible that V isomerizes to the TBP-shaped intermediate VII. Since migratory insertion from VII is unlikely [21], this five-coordinated intermediate will be an unreactive species. This mechanism is attractive since it accounts for the rate-enhancing effect of bulky substituents on the nitrogen and is in line with the observation that both flexible and rigid bidentate nitrogen ligands may be in a monodentate bonding [9a,b,10]. The possibility cannot be excluded, however, that intermediate V is formed directly from intermediate I by association of CO, facilitated by distortion from planarity induced by the substituent close to one N-donor function.

Enhancement of the rate of CO insertion was also observed in acetonitrile for the compounds [(N–N)Pd($CH_3$)($NCCH_3$)]Y containing weakly coordinating groups Y such as OTf or $BF_4$. A similar mechanism may be proposed but with acetonitrile taking the coordination position occupied by $Cl^-$ in the neutral compounds. It may well be, however, that in the case of weakly coordinating groups there is a direct substitution by CO, while the N⌒N ligand remains bonded in a bidentate fashion. The rate-enhancing effect of steric bulk close to one of the N-donor atoms is then less easily explained.

It remains likely that the mechanisms of CO insertion will differ for bidentate phosphine and nitrogen ligands. They may differ not only in terms of the dissociation of ligands and anions but also in respect of the sequence in which such processes take place, and different mechanisms could even operate simultaneously.

## 4. Conclusions

The methyl(chloro)palladium compounds discussed undergo a very interesting isomerism, caused by the steric interactions of the substituents on the ligand. These interactions also have a large influence on the rate of CO insertion. The exact reason for this acceleration is not yet clear, and only a tentative but plausible mechanism can at present be put forward.

## 5. Experimental details

### 5.1. Materials and apparatus

All manipulations were carried out under purified dry nitrogen by use of standard Schlenk techniques. Sol-

vents were dried and stored under nitrogen. Starting chemicals from Aldrich Chemicals, and carbon monoxide 2.5 grade from HoekLoos were used without further purification except where otherwise indicated explicitly. The complex (COD)Pd($CH_3$)(Cl) was made from (COD)$PdCl_2$ by published methods [14,22].

Elemental analyses were carried out by the Elemental Analyses Section of ITC–TNO, Zeist, The Netherlands. $^1$H and $^{13}$C NMR spectra were recorded on Bruker AC 100 and AMX 300 spectrometers, and IR spectra on a Perkin–Elmer PE 283 spectrometer.

### 5.2. Compounds

#### 5.2.1. Synthesis of 2-(N-R-carbaldimino)-6-(R')-pyridine

Compounds **2–6** were made by the procedure described by Lavery and Nelson [23] from pyridine-2-carboxaldehyde, 6-methylpyridine-2-carboxaldehyde or 2,6-pyridinedicarboxaldehyde. Ligands **2**, **3** and **6** were vacuum distilled and all ligands were purified over activated basic alumina prior to use. Ligand **7** was obtained as a side product from the trinitrogen analogue 2,6-bis(isopropylcarbaldimino)pyridine [24] and was not purified, vide infra.

**2**: green oil. $^1$H NMR ($CDCl_3$): δ 1.09 (d, 6H, $^i$Pr), 3.44 (septet, $^i$Pr), 7.08 (dd, $H^5$), 7.51 (t, $H^4$), 7.81 (d, $H^3$), 8.21 (s, $H^7$), 8.42 (d, $H^6$) ppm.

**3**: pale-yellow oil. $^1$H NMR ($CDCl_3$): δ 1.28 (d, 9H, $^t$Bu), 7.23 (dd, $H^5$), 7.68 (t, $H^4$), 7.96 (d, $H^3$), 8.33 (s, $H^7$), 8.59 (d, $H^6$) ppm.

**4**: orange oil. $^1$H NMR ($CDCl_3$): δ 1.25 (d, 6H, $^i$Pr), 2.57 (s, 6-Me), 3.16 (septet, $^i$Pr), 7.18 (d, $H^5$), 7.59 (t, $H^4$), 7.81 (d, $H^3$), 8.35 (s, $H^7$) ppm.

**5**: orange oil. $^1$H NMR ($CDCl_3$): δ 3.02 (t, 2H, $H^\alpha$), 3.91 (t, 2H, $H^\beta$), 7.22 (m, 6H, $H^5$ + phenyl), 7.67 (t, $H^4$), 7.96 (d, $H^3$), 8.28 (s, $H^7$), 8.60 (d, $H^6$) ppm.

**6**: yellow oil. $^1$H NMR ($CDCl_3$): δ 1.31 (s, 9H, $^t$Bu), 2.60 (s, 3H, 6-Me), 7.17 (d, $H^5$), 7.62 (t, $H^4$), 7.86 (d, $H^3$), 8.35 (s, $H^7$) ppm.

**7**: $^1$H NMR ($CDCl_3$): δ 1.25 (d, 6H, $^i$Pr), 3.59 (septet, $^i$Pr), approximately 7.8 (m, 3H, $H^3$, $H^4$ and $H^5$), 8.47 (s, $H^7$), 10.10 (s, −C*H*O) ppm.

#### 5.2.2. Synthesis of methyl(chloro)palladium compounds 1a–5a

Compounds **1a–7a** have been synthesized by substitution of COD in (COD)Pd($CH_3$)(Cl) in dichloromethane as reported recently [14].

**1a**: pale-yellow microcrystals; yield, 85%. $^1$H NMR ($CDCl_3$): δ 1.03, (s, 3H, Pd–Me) 7.51 (t, $H^{5'}$), 7.54 (t, $H^{5''}$), 7.96 (t, $H^{4'}$), 8.06 (t, $H^4$), 8.09 (d, $H^3$), 8.14 (d, $H^{3'}$), 8.87 (d, $H^{6'}$), 9.19 (d, $H^6$) ppm.

**2a**: yellow microcrystals; yield, 96%. $^1$H NMR ($CDCl_3$): **2a**$^c$ δ 1.01 (s, 3H, Pd–Me), 1.44 (d, 6H, $^i$Pr), 4.31 (septet, $^i$Pr), 7.62 (dd, $H^5$), 7.68 (d, $H^3$), 7.98 (t, $H^4$), 8.37 (s, $H^7$), 9.12 (d, $H^6$); **2a**$^t$ δ 1.11 (s, 3H, Pd–Me), 1.48 (d, 6H, $^i$Pr), 4.43 (septet, $^i$Pr), 7.58 (dd, $H^5$), 7.68 (d, $H^3$), 8.37 (t, $H^4$), 8.27 (s, $H^7$), 8.64 (d, $H^6$) ppm. Anal. Found: C, 39.39; H, 4.89; N, 9.04. $C_{10}H_{15}ClN_2Pd$ calc.: C, 39.37; H, 4.96; N, 9.18%.

**3a**: yellow microcrystals; yield, 97%. $^1$H NMR ($CDCl_3$): δ 1.20 (s, 3H, Pd–Me), 1.57 (d, 9H, $^t$Bu), 7.58 (dd, $H^5$), 7.73 (d, $H^3$), 8.08 (t, $H^4$), 8.20 (s, $H^7$), 8.61 (d, $H^6$) ppm. Anal. Found: C, 41.27; H, 5.23; N, 8.66. $C_{11}H_{17}ClN_2Pd$ calc.: C, 41.40; H, 5.37; N, 8.78%.

**4a**: pale-yellow microcrystals; yield, 94%. $^1$H NMR ($CDCl_3$): δ 1.17 (s, 3H, Pd–Me), 1.38 (d, 6H, $^i$Pr), 3.00 (s, 6-Me), 4.21 (septet, $^i$Pr), 7.38 (d, $H^5$), 7.80 (t, $H^4$), 7.50 (d, $H^3$), 8.38 (s, $H^7$). Anal. Found: C, 41.43; H, 5.51; N, 8.76. $C_{11}H_{17}ClN_2Pd$ calc.: C, 41.40; H, 5.37; N, 8.78%.

**5a**: orange microcrystals; yield, 89%. $^1$H NMR ($CDCl_3$): **5a** (*cis*) δ 1.09 (s, 3H, Pd–Me), 3.08 (t, 2H, $H^\alpha$), 4.01 (t, 2H, $H^\beta$), 7.20 (m, phenyl), 7.46 (d, $H^3$), 7.60 (ddd, $H^5$), 7.77 (s, $H^7$), 7.91 (dt, $H^4$), 9.05 (d, $H^6$); **5a** (*trans*) δ 1.07 (s, 3H, P–Me), 3.25 (t, 2H, $H^\alpha$), 4.09 (t, 2H, $H^\beta$), 7.20 (m, phenyl), 7.52 (d, $H^3$), 7.59 (ddd, $H^5$), 7.77 (s, $H^7$), 8.01 (dt, $H^4$), 8.62 (d, $H^6$) ppm.

#### 5.2.3. Synthesis of [2-(N-2-(2-methyl)propanecarbaldimino)-6-methylpyridyl]methyl(chloro)palladium(II) (6a)

To a solution of 1.11 g (4.20 mmol) (COD)Pd($CH_3$)(Cl) in 50 ml of $CH_2Cl_2$ were added 3.6 ml (19.8 mmol; 4.7 equivalents) $^t$Bu-6-Me–PyCa(**6**). The mixture was stirred for 1 h, the solvent then removed in vacuo, and the resulting green oil washed with 3 × 30 ml of hexane and dried to constant weight. According to $^1$H NMR spectrum, the orange product **6a** contains approximately 1 equivalent of the free ligand. $^1$H NMR ($CDCl_3$): δ 1.22 (s, Me), 1.55 (s, 9H, $^t$Bu), 2.92 (s, 3H, 6-Me), 7.39 (d, $H^5$), 7.46 (d, $H^3$), 7.82 (t, $H^4$), 8.36 (s, $H^7$) ppm.

#### 5.2.4. Synthesis of 2-(N-propanecarbaldimino)-6-(carbaldimino)pyridine 7 and 2-(N-propanecarbaldimino)-6-(carbaldimino)pyridyl]methyl(chloro)palladium(II) (7a)

A solution of 279.6 mg (2.1 mmol) of 2,6-pyridinedicarboxaldehyde and 176 μl (121 mg, 2.1 mmol, 1.0 equivalent) of isopropylamine in 35 ml of dry diethyl ether was stirred over 3Å molecular sieves for 4 days. After filtration and evaporation of the solvent, 195 mg of a mixture of the unsubstituted, monosubstituted and bis-substituted ligands in a 3:1:3 ratio was obtained.

Without separation of the products 26.5 mg (0.1 mmol) of (COD)Pd($CH_3$)(Cl) in 5 ml of acetonitrile was treated with 25 μl of the mixture containing 13% of **7**. The products were precipitated by the addition of 5 ml of diethyl ether. The precipitate was isolated by

decantation washed with 3 ml of diethyl ether and dried in vacuo. This precipitate consists of 17% of **7a** and 83% of (2,6-bis(isopropylcarbaldimino)pyridyl)Pd-($CH_3$)(Cl) [24] as indicated by $^1$H NMR spectroscopy. Selective crystallization from acetonitrile yielded colourless cubic crystals of **7a** with about 15% yield and the red crystals of (NNN)Pd($CH_3$)(Cl) with about 80% yield.

**7a**: $^1$H NMR ($CDCl_3$): $\delta$ 1.05 (s, 3H, Pd–Me), 1.39 (d, 6H, $^i$Pr), 4.21 (septet, $^i$Pr), approximately 8.10 (m, 3H, $H^3$, $H^4$ and $H^5$), 8.68 (d, $H^7$), 10.99 (s, $-CHO$) ppm.

### 5.2.5. Synthesis of ionic methylpalladium tetrafluoroborate complexes 11a–14a

To a stirred solution of 0.05 mmol of **1a–4a** in 3 ml of dry acetonitrile was added 0.05 mmol of silver tetrafluoroborate. The immediately formed white precipitate was filtered off and the ionic methylpalladium complexes **11a–14a** were precipitated by addition of 5 ml of diethyl ether. The precipitate was isolated by decantation, washed with 2 ml of diethyl ether and 2 ml of pentane and dried in vacuo.

**11a**: pale-yellow microcrystals; yield, 95%. $^1$H NMR ($CD_3CN$): $\delta$ 1.11 (s, 3H, Pd–Me), 7.78 (m, 2H, $H^5$ and $H^{5'}$), 8.31 (m, 2H, $H^4$ and $H^{4'}$), 8.42 (m, $H^3$ and $H^{3'}$), 8.65 (d, $H^{6'}$), 8.71 ($H^6$) ppm.

**12a**: yellow microcrystals; yield, 73%. $^1$H NMR ($CD_3CN$): **12a**$^c$ $\delta$ 1.13 (s, 3H, Pd–Me), 1.44 (d, 6H, $^i$Pr), 4.12 (septet, $^i$Pr), 7.19 (dd, $H^5$), 8.01 (d, $H^3$), 8.31 (t, $H^4$), 8.57 (s, $H^7$), 8.61 (d, $H^6$); **12a**$^t$ $\delta$ 1.01 (s, 3H, Pd–Me), 1.45 (d, 6H, $^i$Pr), 4.20 (septet, $^i$Pr), 7.87 (dd, $H^5$), 8.06 (d, $H^3$), 8.67 (s $H^7$), 8.68 (d, $H^6$), ($H^4$ concealed) ppm.

**13a**: orange microcrystals; yield, 78%. $^1$H NMR ($CD_3CN$): $\delta$ 1.25 (s, 3H, Pd–Me), 1.53 (s, 9H, $^t$Bu), 7.82 (dd, $H^5$), 8.07 (d, $H^3$), 8.33 (t, $H^4$), 8.53 (s, $H^7$), 8.65 (d, $H^6$) ppm.

**14a**: yellow microcrystals; yield, 81%. $^1$H NMR ($CD_3CN$); $\delta$ 1.21 (s, 3H, Pd–Me), 1.48 (d, 6H, $^i$Pr), 2.77 (s, 3H, 6-Me), 4.19 (septet, $^i$Pr), 7.72 (d, $H^5$), 7.86 (d, $H^3$), 8.14 (t, $H^4$), 8.65 (s, $H^7$) ppm.

### 5.3. Carbonylation reactions

### 5.3.1. Synthesis of acetylpalladium compounds 1b–4b and 11b–14b

Synthesis on a preparative scale was carried out by keeping an evacuated Schlenk vessel containing a dichloromethane solution of about 20 mg of the methylpalladium compound filled with CO at 1 bar for 45 min [6,7]. The solution was filtered and the solvent removed in vacuo.

**1b**: yellow crystals; yield, 82%. $^1$H NMR ($CDCl_3$): $\delta$ 2.67 (s, 3H, C(O)Me), 7.50 (t, $H^5$ and $H^{5'}$), 7.99 (t, $H^4$ and $H^{4'}$), 8.07 (d, $H^{3'}$), 8.15 (d, $H^3$), 8.50 (d, $H^{6'}$), 9.02 (d, $H^6$) ppm.

**2b**: orange crystals; yield, 97%. $^1$H NMR ($CDCl_3$): **2b**$^c$ $\delta$ 1.36 (d, 6H, $^i$Pr), 2.65 (s, C(O)Me), 4.18 (septet, $^i$Pr), 7.59 (dd, $H^5$), 7.63 (d, H3), 7.97 (t, $H^4$), 8.29 (s, $H^7$), 8.97 (d, $H^6$); **2b**$^t$ $\delta$ 1.44 (d, 6H, $^i$Pr), 2.65 (s, C(O)Me), 4.16 (septet, $^i$Pr), approximately 7.6 (concealed, $H^5$ and $H^3$), 8.05 (t, $H^4$), 8.19 (s, $H^7$), 8.42 (d, $H^6$) ppm. Anal. Found: C, 39.61; H, 4.57; N, 8.31. $C_{11}H_{15}ClN_2OPd$ calc.: C, 39.66; H, 4.54; N, 8.41%.

**3b**: pale-yellow microcrystals; yield, 87%. $^1$H NMR ($CDCl_3$): $\delta$ 1.50 (s, 9H, $^t$Bu), 2.56 (s, 3H, C(O)Me), 7.55–8.05 (m, 3H, $H^3$, $H^4$, $H^5$), 8.13 (s, $H^7$), 8.41 (d, $H^6$) ppm. Anal. Found: C, 40.44; H, 4.85; N, 7.78. $C_{12}H_{17}ClN_2OPd$ calc.: C, 41.52; H, 4.94; N, 8.07%.

**4b**: orange microcrystals; yield, 80%. $^1$H NMR ($CDCl_3$): $\delta$ 1.35 (d, 6H, $^i$Pr), 2.66 (s, 3H, C(O)Me), 2.90 (s, 3H, 6-$CH_3$), 4.00 (septet, $^i$Pr), 7.36 (d, $H^5$), 7.44 (d, $H^3$), 7.81 (t, $H^4$), 8.28 (s, $H^7$) ppm. Anal. Found: C, 40.58; H, 4.72; N, 7.67. $C_{12}H_{17}ClN_2OPd$ calc.: C, 41.52; H, 4.94; N, 8.07%.

**5b**: orange microcrystals: yield, 77%. $^1$H NMR ($CDCl_3$): **5b**$^c$ $\delta$ 2.69 (s, 3H, C(O)Me), 2.91 (t, 2H, $H^\alpha$), 3.95 (t, 2H, $H^\beta$), 7.2 (m, 5H, phenyl), 7.54 (m, $H^3$), 7.87 (s, $H^7$), 7.91 (dt, $H^4$), 8.78 (d, $H^6$); **5b**$^t$ $\delta$ 2.64 (s, 3H, C(O)Me), 3.18 (t, 2H, $H^\alpha$), 3.98 (t, 2H, $H^\beta$), 7.2 (m, 5H, phenyl), 7.54 $H^3$), 7.78 (s, $H^7$), 8.01 (t, $H^4$), 8.39 (d, $H^6$) ppm.

**11b**: pale-yellow microcrystals; yield, 96%. $^1$H NMR ($CD_3CN$): $\delta$ 2.32 (s, 3H, C(O)Me), 7.78 (m, 2H, $H^5$ and $H^{5'}$), 8.30 m (2H, $H^3$ and $H^{3'}$), 8.41 (t, 2H, $H^4$ and $H^{4'}$), 8.76 (d, $H^6$), 8.82 (d, $H^{6'}$) ppm.

**12b**: yellow microcrystals; yield, 67%. $^1$H NMR ($CD_3CN$): $\delta$ 1.42 (d, 6H, $^i$Pr), 2.68 (s, 3H, C(O)Me), 4.03 (septet, $^i$Pr), 7.82 (dd, $H^5$), 7.98 (d, $H^3$), 8.29 (t, $H^4$), 8.40 (d, $H^6$), 8.52 (s, $H^7$) ppm.

**13b**: orange microcrystals; yield, 69%. $^1$H NMR ($CD_3CN$): $\delta$ 1.49 (s, 9H, $^t$Bu), 2.70 (s, 3H, C(O)Me), 7.9 (dd, $H^5$), 8.01 (d, $H^3$), 8.31 (m, 2H, $H^4$ and $H^6$), 8.43 (s, $H^7$) ppm.

**14b**: yellow microcrystals; yield, 73%. $^1$H NMR ($CD_3CN$): $\delta$ 1.41 (d, 6H, $^i$Pr), 2.71 (s, 3H, C(O)Me), 2.72 (s, 3H, 6-Me), 3.89 (septet, $^i$Pr), 7.67 (d, $H^5$), 7.80 (d, $H^3$), 8.10 (t, $H^4$), 8.55 (s, $H^7$) ppm.

### 5.3.2. Determination of the half-life for insertion of CO

The half-lives were determined at 293 K by use of a home-made gas buret. In a typical experiment, a 12 ml vessel was filled under nitrogen with 5 ml of a 0.4 mM solution of the methylpalladium complex (see Table VII for the solvent) and the solution was stirred. The vessel was carefully evacuated three times and connected to the CO-filled gas buret. The measurement was started by opening the valve betwen the CO and the vigorously stirred solution of the methylpalladium compound. When the equilibrium was reached, the time for take-up of

every 0.25 ml of CO was recorded until the CO uptake had stopped (i.e. at least three half-lives) and the half-life was calculated. Blank experiments in several solvents showed that the time for diffusion of CO was about 20 s.

*5.3.3. X-ray data collection and structure refinement*

Data for all four crystals were collected on a Enraf–Nonius CAD-4 diffractometer using graphite monochromated radiation, Cu Kα for **1b** and **2b** and Mo Kα for **4a** and **7a**, and $\omega$–$2\theta$ scan. The number of reflections measured was 3909 of which 2834 were treated as observed (significance level of 2.5 $\sigma(I)$) in the range $0 \leqslant h \leqslant 35$, $0 \leqslant k \leqslant 35$, $0 \leqslant l \leqslant 11$, maximum $(\sin\theta)/\lambda = 0.70$ for **4a**, 5630/3225, $-13 \leqslant h \leqslant 13$, $0 \leqslant k \leqslant 18$, $0 \leqslant l \leqslant 21$, $(\sin\theta)/\lambda = 0.80$ for **7a**, 1318/1272, $-9 \leqslant h \leqslant 0$, $-13 \leqslant k \leqslant 0$, $0 \leqslant l \leqslant 18$, $(\sin\theta)/\lambda = 0.63$ for **1b** and 2626/2476, $-9 \leqslant h \leqslant 0$, $-9 \leqslant k \leqslant 9$, $-14 \leqslant l \leqslant 14$, $(\sin\theta)/\lambda = 0.63$ for **2b**. All structures were solved by direct methods.

The positions of the hydrogen atoms were calculated. Full-matrix least-squares refinement on $F$ anisotropic for the non-hydrogen atoms and isotropic for the hydrogen atoms, with the latter restrained in such a way that the distance to their carrier remained constant at approximately 1.09 Å, converged to the values tabulated in Table V. The weighting scheme used was $w^{-1} = (A + F_{obs} + BF_{obs}^2)^{-1}$. An empirical absorption correction was applied [26]. The anomalous scattering of Pd and Cl was taken into account. Scattering factors were taken from the litterature [27]. All calculations were performed with XTAL [28] unless stated otherwise. For **1b**, which has chiral overall packing, the absolute structure was determined by additional refinement of the inverted structure (Table 5).

Tables of thermal parameters and H atom coordinates, and complete lists of bond lengths and angles have been deposited at the Cambridge Crystallographic Data Centre.

## Acknowledgements

The authors wish to thank D. Heijdenrijk and J. Fraanje for collecting the X-ray data and L.P. Häming and K. Erikson for solving and refining the crystal structures.

## References and note

[1] E. Drent, *Pure Appl. Chem., 62* (1990) 661.
[2] (a) B.A. Markies, P. Wijkens, J. Boersma, A.L. Spek and G. van Koten, *Recl. Trav. Chim. Pays-Bas, 110* (1991) 133; (b)

Table 5
Crystal and refinement data for **4a**, **7a**, **1b** and **2b**

| | **4a** | **7a** | **1b** | **2b** |
|---|---|---|---|---|
| Chemical formula | $C_{11}H_{17}ClN_2Pd$ | $C_{11}H_{15}ClN_2OPd$ | $C_{12}H_{11}ClN_2OPd$ | $C_{11}H_{15}ClN_2OPd$ |
| Formula weight | 319.1 | 333.1 | 341.1 | 333.1 |
| $a$ (Å) | 25.644(2) | 8.683(1) | 7.5083(8) | 7.3003(4) |
| $b$ (Å) | — | 11.475(4) | 10.840(1) | 7.8791(5) |
| $c$ (Å) | 7.907(1) | 13.339(5) | 15.173(1) | 11.603(1) |
| $\alpha$ (°) | — | — | — | 87.525(9) |
| $\beta$ (°) | — | 104.09(4) | — | 86.286(6) |
| $\gamma$ (°) | — | — | — | 74.272(6) |
| $V$ (Å$^3$) | 5199.8(9) | 1289.1(8) | 1234.9(2) | 640.85(9) |
| $T$ (K) | 293 | 293 | 293 | 293 |
| Crystal size (mm) | 0.25 × 0.38 × 0.5 | 0.2 × 0.5 × 0.5 | 0.15 × 0.4 × 0.4 | 0.15 × 0.25 × 0.4 |
| $\lambda$ (Å) | 0.71069 | 0.71069 | 1.5418 | 1.5418 |
| Crystal class | Tetragonal | Monoclinic | Orthorhombic | Triclinic |
| Space group | $I4_1/a$ | $P2_1/c$ | $Pna2_1$ | P1 |
| $Z$ | 16 | 4 | 4 | 2 |
| $d_x$ (g cm$^{-3}$) | 1.54 | 1.72 | 1.84 | 1.72 |
| $\mu$ (cm$^{-1}$) | 15.9 | 22.32 | 134.42 | 137.72 |
| $R$ | 0.041 | 0.045 | 0.033; 0.037 [a] | 0.034 |
| $R_w$ | 0.084 | 0.061 | 0.044; 0.050 [a] | 0.047 |
| Weights (A, B) | 6.8, 0.013 | 6.0, 0.115 | 8.1, 0.006 | 2.6, 0.005 |
| Extinction [25] | 0.08(6) | — | — | 0.006(2) |
| Absorption | 0.81–1.18 | 0.67–1.28 | 0.74–1.44 | 0.67–1.47 |
| Residual electron density (electrons) | −0.7–0.6 | −1.1–0.7 | −0.5–0.7 | −0.8–0.7 |

[a] Value for inverted structure

B.A. Markies, A.L. Spek, J. Boersma and G. van Koten, *J. Chem. Soc., Chem. Commun.*, (1993) 1317; (c) B.A. Markies, D. Kruis, M.H.P. Rietveld, K.A.N. Verkerk, J. Boersma, H. Kooijman, M.T. Lakin, A.L. Spek and G. van Koten, *J. Am. Chem. Soc., 117* (1995) 5253.

[3] Concerning CO–alkene copolymerization and terpolymerization: (a) E. Drent, *Eur. Pat. Appl. 121865*, 1954; *Chem. Abstr., 102* (1985) 46423; (b) E. Drent, J.A.M. van Broekhoven and M.J. Doyle, *J. Organomet. Chem., 417* (1991) 235; (c) A. Sen and Z. Jiang, *Macromolecules, 26* (1993) 911; (d) A. Sommazzi, F. Garbassi, G. Mestroni and B. Milani, *US Pat. 5310871*, 1994; *Chem. Abstr. 121* (1994) 301585; (e) B. Milani, E. Alessio, G. Mestroni, A. Sommazzi, F. Garbassi, E. Zangrando, N. Bresciani-Pahor and L. Randaccio, *J. Chem. Soc., Dalton Trans., 13* (1994) 1903.

[4] (a) C. Bolm, *Angew. Chem., Int. Edn. Engl. 30* (1991) 542; (b) G. Helmchen, A. Krotz, K.-T. Ganz and D. Hansen, *Synlett*, (1991) 257; (c) U. Leutenegger, G. Umbricht, C. Fahrni, P. von Matt and A. Pfaltz, *Tetrahedron, 48* (1992) 2143; (d) W. Cabri, I. Candiani, A. Bedeschi and R. Santi, *J. Org. Chem., 58* (1993) 7421; (e) R. van Asselt and C.J. Elsevier, *Tetrahedron, 50* (1994) 323; (f) A. Togni and L.M. Venanzi, *Angew. Chem., Int. Edn. Engl., 33* (1994) 497.

[5] (a) M. Brookhart, F.C. Rix, J.M. De Simone and J.C. Barborak, *J. Am. Chem. Soc., 114* (1992) 5894; (b) F.C. Rix and M. Brookhart, *J. Am. Chem. Soc., 117* (1995) 1137.

[6] (a) G.P.C.M. Dekker, C.J. Elsevier, K. Vrieze, C.F. Roobeek and P.W.N.M. van Leeuwen, *J. Organomet. Chem., 430* (1992) 357; (b) G.P.C.M. Dekker, C.J. Elsevier, K. Vrieze and P.W.N.M. van Leeuwen, *Organometallics, 11* (1992) 1598; (c) G.P.C.M. Dekker, A. Buijs, C.J. Elsevier, W.J.J. Smeets, A.L. Spek, Y-F. Wang, C.H. Stam, K. Vrieze and P.W.N.M. van Leeuwen, *Organometallics, 11* (1992) 1937.

[7] (a) R. van Asselt, E.E.C.G. Gielens, R.E. Rülke and C.J. Elsevier, *J. Chem. Soc., Chem. Commun.* (1993) 1203; (b) R. van Asselt, E.E.C.G. Gielens, R.E. Rülke, K. Vrieze and C.J. Elsevier, *J. Am. Chem. Soc., 116* (1994) 976; (c) R.E. Rülke, D. Kliphuis, J. Fraanje, K. Goubitz, C.J. Elsevier, P.W.N.M. van Leeuwen and K. Vrieze, *J. Chem. Soc., Chem. Commun.*, (1994) 1817; (d) P. Wehman, R.E. Rülke, V.E. Kaasjager, P.C.J. Kamer, H. Kooijman, A.L. Spek, K. Vrieze and P.W.N.M. van Leeuwen, *J. Chem. Soc., Chem. Commun.*, (1995) 331.

[8] I. Tóth and C.J. Elsevier, *J. Am. Chem. Soc., 115* (1993) 10388.

[9] (a) F.P. Fanizzi, F.P. Intini, L. Maresca, G. Natile, M. Lanfranchi and A. Tiripicchio, *J. Chem. Soc., Dalton Trans.*, (1991) 1007; (b) F.P. Fanizzi, L. Maresca, G. Natile, M. Lafranchi, A. Tiripicchio and G. Pacchioni, *J. Chem. Soc., Chem. Commun.*, (1992) 333; (c) F.P. Fanizzi, M. Lafranchi, G. Natile and A. Tiripicchio, *Inorg. Chem., 33* (1994) 3331; (d) H. van der Poel and G. van Koten, *J. Organomet. Chem., 187* (1980) C17.

[10] (a) V.G. Albano, F. Demartin, A. De Renzi, G. Morelli and A. Saporito, *Inorg. Chem., 24* (1985) 2032; (b) V. De Felice, P. Ganis, A. Vitagliano and G. Valle, *Inorg. Chim. Acta, 144* (1988) 57; (c) H. van der Poel, G. van Koten, K. Vrieze, M. Kokkes and C.H. Stam, *J. Organomet. Chem., 175* (1979) C21; (d) H. van der Poel, G. van Koten and K. Vrieze, *Inorg. Chem., 19* (1980) 1145; (e) H. van der Poel and G. van Koten, *J. Organomet. Chem., 217* (1981) 129.

[11] (a) V.G. Albano, C. Castellari, M.E. Cucciolito, A. Panunzi and A. Vitagliano, *Organometallics, 9* (1990) 1269; (b) V.G. Albano, G. Natile and A. Panunzi, *Coord. Chem. Rev., 133* (1994) 67.

[12] (a) V.G. Albano, D. Braga, V. De Felice, A. Panunzi and A. Vitagliano, *Organometallics, 6* (1987) 517; (b) M.E. Cucciolito, V. De Felice, A. Panunzi and A. Vitagliano, *Organometallics, 8* (1989) 1180.

[13] K. Vrieze and G. van Koten, *Inorg. Chim. Acta, 100* (1985) 79.

[14] R.E. Rülke, J.M. Ernsting, A.L. Spek, C.J. Elsevier, P.W.N.M. van Leeuwen and K. Vrieze, *Inorg. Chem., 32* (1993) 5769.

[15] P.K. Byers, A.J. Canty, L.M. Engelhardt and A. White, *J. Chem. Soc., Dalton Trans.*, (1986) 1731.

[16] (a) R. Bardi, A. del Pra, A.M. Piazzesi and L. Toniolo, *Inorg. Chim. Acta, 35* (1979) L345; (b) R. Bardi, A.M. Piazzesi, G. Cavinato, P. Cavoli and L. Toniolo, *J. Organomet. Chem., 224* (1982) 407; (c) R. Bardi, A.M. Piazzesi, A. del Pra, G. Cavinato and L. Toniolo, *Inorg. Chim. Acta, 102* (1985) 99.

[17] C.J. Elsevier, *J. Mol. Catal., 92* (1994) 285.

[18] T.G. Appleton, H.C. Clark and L.E. Manzer, *Coord. Chem. Rev., 10* (1973) 335.

[19] Part 2: R.E. Rülke, V.E. Kaasjager, D. Kliphuis, C.J. Elsevier, P.W.N.M. van Leeuwen and K. Vrieze, *Organometallics*, in press.

[20] V. de Felice, V.G. Albano, C. Castellari, M.E Cucciolito and A. de Renzi, *J. Organomet. Chem., 403* (1991) 269.

[21] V. De Felice, A. De Renzi, D. Tesauro and A. Vitagliano, *Organometallics, 11* (1992) 3669.

[22] P.W.N.M. van Leeuwen and C.F. Roobeek, *Eur. Pat. Appl. 380162*, 1990; *Chem. Abstr., 114* (1991) 62975.

[23] A. Lavery and S.M. Nelson, *J. Chem. Soc., Dalton Trans.*, (1984) 615.

[24] R.E. Rülke, I.M. Han, C.J. Elsevier, C.F. Roobeek, M.C. Zoutberg, Y.-F. Wang, C.H. Stam, P.W.N.M. van Leeuwen and K. Vrieze, *Inorg. Chim. Acta, 169* (1990) 5.

[25] (a) A.C. Larson, in F.R. Ahmed, S.R. Hall and C.P. Huber (eds.), *Refinement of Crystal Structures. Crystallographic Computing, The Inclusion of Secondary Extinction in Least-squares* Munksgaard, Copenhagen, 1969, p. 158; (b) W.H. Zachariasen, *Acta Crystallogr. Sect. A, 39* (1967) 558.

[26] N. Walker and D. Stuart, *Acta Crystallogr., Sect. A 39* (1983) 158.

[27] (a) D.T. Cromer and J.B. Mann, *Acta Crystallogr., Sect. A, 24* (1974) 321; (b) *International Tables for X-ray Crystallography 1974*, Vol. 4, Kynoch, Birmingham, 1975.

[28] S.R. Hall, H.D. Flack and J.M. Stewart (eds.), *XTAL3.2 Reference Manual*, University of Western Australia, Perth, University of Geneva, Geneva, Switzerland, University of Maryland, College Park, MD, 1992.

ELSEVIER

Journal of Organometallic Chemistry 508 (1996) 121–127

Journal of Organometallic Chemistry

# Synthetic studies of permethylcyclopentadienyl ruthenium(II) complexes involving dppf, (±)-BINAP and (±)-DIOP ligands

Masaru Sato *, Manabu Asai

*Chemical Analysis Center, Saitama University, Urawa, Saitama 338, Japan*

Received 27 April 1995; in revised form 8 June 1995

**Abstract**

1,1'-Bis(diphenylphosphino)ferrocene (dppf) reacted with $RuCl(Ph_3P)_2Cp^*$ to give $RuCl(dppf)Cp^*$ in good yield. The complex reacted with $AgBF_4$ in acetonitrile to give $[Ru(CH_3CN)(dppf)Cp^*]BF_4$ quantitatively and in acetone to give $[Ru(\eta^2\text{-}O_2)(dppf)Cp^*]BF_4$ in good yield. The structure of the latter was determined by X-ray analysis. (±)-BINAP and (±)-DIOP were reacted with $[RuCl_2Cp^*]_n/Zn$ to give RuCl[(±)-BINAP]Cp* and RuCl[(±)-DIOP]Cp*, respectively, in moderate yields. They reacted with phenylacetylene in the presence of $NH_4PF_6$ to afford the corresponding $Ru^{II}$ phenylacetylide complexes. The asymmetric condensation of phenylacetylene with allyl alcohol in the presence of these diphosphine complexes was unsuccessful.

*Keywords:* Iron; Ruthenium

## 1. Introduction

Ruthenium complexes are versatile and capable of catalyzing a variety of organic reactions, and for this reason have been investigated from many viewpoints [1,2]. Ruthenium complexes of the half-sandwich type having a cyclopentadienyl (Cp) ligand are stable and their structure and reactivity have been fully investigated [3]. Recently, various types of ruthenium complexes containing a permethylcyclopentadienyl ($Cp^*$) ligand, which can stabilize metal complexes by its steric and electronic effect [4], have been reported [5–12]. In addition, quite a number of ruthenium complexes containing phosphines as an additional ligand have been prepared [13–20]. Of these complexes, a considerable number are stable despite containing a coordinatively unsaturated Ru atom as a result of the steric effect of the bulky ligand [17a]. The possibility that the arrangement of coordinatively unsaturated Ru atom in the proximity of ferrocene may result in a dative Fe—Ru bond is interesting because such a dative bond has been recently reported in Ru cluster complexes [21]. Also, it is known that the optically active Ru–phosphine complex is an effective asymmetric catalyst [22]. We report here the synthesis and some properties of $Cp^*Ru$ complexes involving dppf, (±)-BINAP and (±)-DIOP ligands.

## 2. Results and discussion

The reaction of $RuCl(PPh_3)_2Cp^*$ (**1**) [13,16,23] with 1,1'-bis(diphenylphosphino)ferrocene (dppf) in refluxing benzene gave $RuCl(dppf)Cp^*$ (**2**) in excellent yield. The $^1H$ NMR spectrum of **2** showed the proton signal of the $Cp^*$ ligand at $\delta$ 1.02 ppm and those of the ferrocene rings at $\delta$ 3.87, 4.06, 4.16 and 5.14 ppm, respectively. Such an asymmetric pattern for the proton signals of the ferrocenyl ring seems to indicate a stepped conformation [24] for **2**.

Reaction of **1** with (+)- and (−)-2,2'-bis(diphenylphosphino)binaphthalenyl [(+)- and (−)-BINAP] or (+)- and (−)-2,3-O-isopropylidene-2,3-dihydroxy-1,4-bis(diphenylphosphino)butane [(+)- and (−)-DIOP] in refluxing benzene was unsuccessful. Hence, the method using a coordinatively unsaturated complex $[Cp^*Ru(\mu_3\text{-}Cl)]_4$ [10a,25] was employed. (+)- and (−)-BINAP were reacted with $[Cp^*RuCl_2]_n$ in the presence of zinc powder to give $Cp^*$[(+)-BINAP]RuCl and $Cp^*$[(−)-BINAP]RuCl (**3** and **4**), respectively, in moderate yields. Similarly, the reaction of $[Cp^*RuCl_2]_2$

* Corresponding author.

0022-328X/96/$15.00 © 1996 Elsevier Science S.A. All rights reserved
*SSDI* 0022-328X(95)05782-X

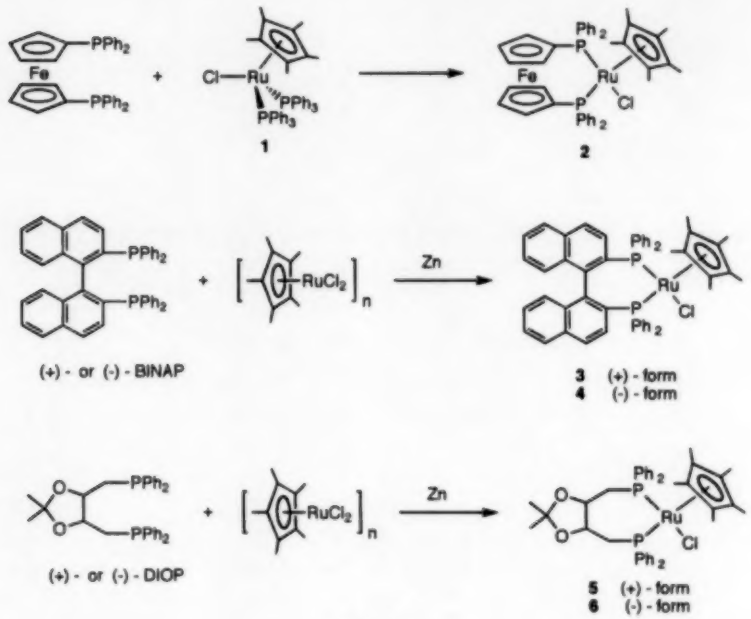


Scheme 1.

with (+)- and (−)-DIOP in the presence of zinc afforded $Cp^*$[(+)-DIOP]RuCl or $Cp^*$[(−)-DIOP]RuCl (**5** and **6**), respectively, in good yield (see Scheme 1).

The structures of **3**–**6** were confirmed from their $^1$H NMR spectra and by elemental analyses. The $^1$H NMR spectrum of **3** showed the methyl protons of the $Cp^*$ ligand at $\delta$ 1.10 ppm and the aromatic protons at $\delta$ 6.06–7.70 ppm in a pattern which was similar to that of the starting (+)-BINAP. In the $^1$H NMR spectrum of **5**, the protons of the $Cp^*$ ligand resonated at $\delta$ 1.08 ppm, the unequivalent methyl protons at $\delta$ 1.19 and 1.22 ppm, the methyne protons at $\delta$ 3.49 and 4.09 ppm, and the methylene protons at $\delta$ 2.04, 2.68, 3.10 and 3.70 ppm, respectively. The assignment of the methyne and methylene signals was accomplished by 2D H,H- and C,H-COSY experiments. The optical rotation of **3** and **4** indicates that the optical activity of the ligand is maintained in these complexes.

Reaction of **1** with $AgBF_4$ in acetonitrile gave the cation complex **7**, in which acetonitrile coordinated to the metal as yellow crystals in good yield. Its structure was determined on the basis of the IR and $^1$H NMR spectra, and from elemental analysis. The IR spectrum of **7** showed the C≡N stretching vibration of the coordinating acetonitrile at 2260 $cm^{-1}$ and the absorption band characteristic of a $BF_4$ anion at 1134 $cm^{-1}$. In the $^1$H NMR spectrum of **7** the proton signal of the coordinating acetonitrile was observed at $\delta$ 2.94 ppm and that of the $Cp^*$ ligand at $\delta$ 1.06 ppm. The ring protons of the ferrocene moiety resonated at $\delta$ 4.04, 4.19, 4.33 and 4.34 ppm, respectively. The unusual deshielding ($\Delta \sim$ 1.0 ppm) of the methyl protons of the coordinating acetonitrile may be caused by steric forcing of these protons into the deshielding zone of the ferrocene molecule.

On the other hand, reaction of **1** with 1 equiv. of $AgBF_4$ in acetone gave the oxidized complex **8** as dark brown crystals (see Scheme 2). Complex **8** exhibited the $BF_4$ group absorption at 1154 $cm^{-1}$ but no carbonyl absorption. In the $^1$H NMR spectrum of **8**, the proton signals of the ferrocenyl ring resonated at $\delta$ 4.28, 4.51, 4.59 and 5.15 ppm, and the methyl proton of the $Cp^*$

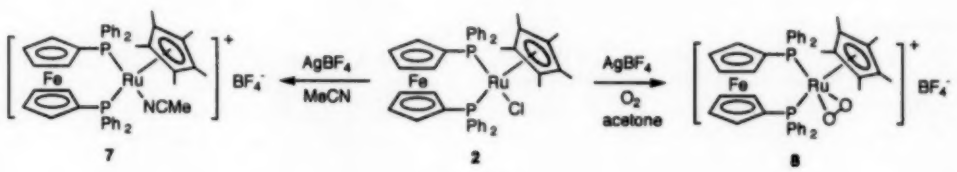


Scheme 2.

ligand at $\delta$ 1.25 ppm. No signal was observed for the coordinating acetone. Hence, because of its similarity with the reaction product of RuCl(dppe)Cp* and $AgBF_4$ [26], complex **8** is assigned as $[Ru(\eta^2\text{-}O_2)(dppf)Cp^*]BF_4$. The observation of the O–O stretching vibration at 840 $cm^{-1}$ supports this assignment (the O–O stretching vibration is normally observed at 800–900 $cm^{-1}$) [27].

An X-ray single-crystal analysis has established the structure of **8**. The corresponding crystallographic parameters are collected in Table 1, the ORTEP view of **8** is shown in Fig. 1 and selected bond distances and bond angles are given in Table 2. The O(1)—O(2) distance is 1.381(11) Å which is similar to that in $[Ru(\eta^2\text{-}O_2)(dppe)Cp^*]BF_4$ [1.398(5) Å] [26] and $[RuH(\eta^2\text{-}O_2)(dippe)_2]BPh_4$ [1.360(10) Å] [28] and $[Ru(\eta^2\text{-}O_2)(P\sim O)Cp^*]BPh_4$ [1.394(9) Å] [29]. The O—O distance is approximately intermediate between the reported peroxide (1.49 Å in $H_2O_2$) [30] and superoxide distances (1.28 Å in $KO_2$) [27], suggesting that complex **8** should formally be considered as an $Ru^{IV}$ complex. This suggestion is supported by the observation that the ring-carbon resonance of the Cp* ligand in the $^{13}C$ NMR spectrum ($\delta$ 108.71 ppm) appeared in the down-field region similar to that in the $Ru^{IV}$ complex, $[RuBr(Cp)Cp^*]^+$ ($\delta$ 112.4 ppm), in contrast to the corresponding carbon resonance of the $Ru^{II}$ complex, RuCl(dppf)Cp* ($\delta$ 88.57 ppm). The Ru—O distances, 2.035(8) and 2.029(8) Å, are similar to those in $[Ru(\eta^2\text{-}O_2)(dppe)Cp^*]BF_4$ [2.040(3) and 2.023(3) Å] [26] and $[RuH(\eta^2\text{-}O_2)(dippe)_2]BPh_4$ [2.04(1) and 2.00(1) Å] [28].

Table 1
Crystal and intensity collection data for **8**

| | |
|---|---|
| Molecular formula | $C_{44}H_{43}BF_4O_2P_2FeRu$ |
| Molecular weight | 909.50 |
| Crystal system | monoclinic |
| Space group | $P21/a$ (No. 14) |
| $a$ (Å) | 15.193(6) |
| $b$ (Å) | 25.08(1) |
| $c$ (Å) | 11.010(6) |
| $\beta$ (°) | 109.69(4) |
| $V$ (Å$^3$) | 3951(3) |
| $Z$ | 4 |
| $D_{cal}$ (g $cm^{-3}$) | 1.53 |
| Crystal dimensions (mm) | 0.22×0.24×0.12 |
| Linear absorption coefficient ($cm^{-1}$) | 8.761 |
| Radiation ($\lambda$, Å) | Mo K$\alpha$ (0.71073) |
| Reflection limits ($hkl$) | $19 < h < 18$, $-7 < k < 32$, $0 < l < 13$ |
| Total no. of reflections measured | 8965 |
| No. of unique reflections | 8029 |
| No. of reflections used in least squares | 4821 |
| Least-squares parameters | 600 |
| $R$ | 0.075 |
| $R_w$ | 0.078 |
| Max. peak in final Fourier map, e Å$^{-3}$ | 1.21 |
| Min. peak in final Fourier map, e Å$^{-3}$ | −1.23 |

The results described above seem to suggest that the

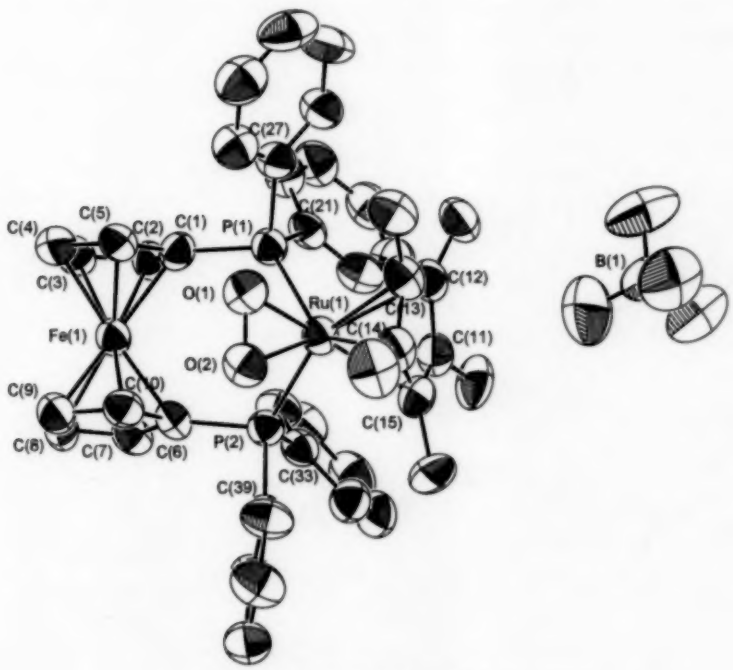


Fig. 1. ORTEP view of complex **8**.

Table 2
Selected bond distances (Å) and bond angles (°) for **8**

| | | | |
|---|---|---|---|
| *Bond distances* | | | |
| Ru–P(1) | 2.408(3) | Ru–P(2) | 2.390(3) |
| Ru–O(1) | 2.036(8) | Ru–O(2) | 2.029(8) |
| Ru–C(11) | 2.289(11) | Ru–C(12) | 2.339(11) |
| Ru–C(13) | 2.301(10) | Ru–C(14) | 2.234(12) |
| Ru–C(15) | 2.266(11) | P(1)–C(1) | 1.812(11) |
| P(2)–C(6) | 1.790(11) | O(1)–O(2) | 1.381(11) |
| *Bond angles* | | | |
| P(1)–Ru–P(2) | 91.6(1) | P(1)–Ru–O(1) | 77.6(3) |
| P(1)–Ru–O(2) | 106.9(3) | P(2)–Ru–O(1) | 107.1(3) |
| P(2)–Ru–O(2) | 80.0(3) | O(1)–Ru–O(2) | 39.7(4) |
| Ru–P(1)–C(1) | 119.8(4) | Ru–P(1)–C(21) | 119.2(4) |
| Ru–P(1)–C(27) | 109.0(4) | Ru–P(2)–C(6) | 116.5(4) |
| Ru–P(2)–C(33) | 117.8(4) | Ru–P(2)–C(39) | 114.4(4) |

reaction between **1** and an $Ag^+$ ion in acetone initially yields a coordinatively unsaturated Ru complex, which may be weakly coordinated by acetone. The complex then absorbs oxygen from the atmosphere to give the dioxygen complex **8**. A partial electronic interaction between the Fe atom of the ferrocene moiety and the Ru site may be anticipated in **8**, because ferrocene is an electron-rich system and the Ru atom is in the electron-deficient $Ru^{IV}$ state. However, upon refluxing a solution of **8** in acetonitrile, no removal of the $\eta$-$O_2$ ligand was observed as in the similar reaction of Ru($\eta$-$O_2$)(dppe)Cp* [26]. Hence, there is little, if any, electron donation from the Fe atom to Ru atom in complex **8**.

Complexes **3–6** reacted with phenylacetylene in the presence of $NH_4PF_6$, and following treatment with base gave the $Ru^{II}$ phenylacetylide complexes **9–12**, respectively, in moderate yield (see Scheme 3). The structures of complexes **9–12** have been confirmed by elemental analysis, and by IR and $^1H$ NMR spectroscopy. Thus, for example, the C≡C stretching vibration appeared at 2072 $cm^{-1}$ in the IR spectrum of **11**, while in the $^1H$ NMR spectrum this complex the isopropyl protons resonated at $\delta$ 1.02 and 1.20 ppm, the methyl proton of the Cp* ligand at $\delta$ 1.21 ppm, the methyne protons at $\delta$ 3.47 and 4.38 ppm, and the methylene protons at $\delta$ 1.96, 2.79, 3.04 and 4.03 ppm, respectively. Signal assignment has been based on the similarity to the spectrum of the starting complex **5**. It has been reported recently that the reaction of phenylacetylene with allyl alcohols proceeds catalytically in the presence of $Cp(Ph_3P)_2RuCl$ and $NH_4PF_6$ [31]. For this reason, a similar catalytic reaction of phenylacetylene with allyl alcohol in the presence of complexes **3–6** and $NH_4PF_6$ was attempted. However, the desired reaction was not observed. This lack of success may probably be attributed to steric hindrance caused by the bulky Cp* ligand in complexes **3–6**.

## 3. Experimental details

### 3.1. General

$[Cp^*RuCl_2]_n$ [10a] and $Cp^*(Ph_3P)_2RuCl$ (**1**) [23] were prepared by literature methods. All the other chemicals were reagent grade and were used as received from common commercial sources. Solvents were dried by standard procedures. IR spectra were recorded as KBr pellets on a Hitachi 270-50 spectrophotometer. $^1H$ and $^{13}C$ NMR spectra were recorded on a Bruker AM-400 instrument using TMS as internal standard. $^{31}P$ NMR signals were referred to external 85% $H_3PO_4$ as standard.

### 3.2. Preparation of Cp*(dppf)RuCl (2)

A suspension of **1** (0.41 g, 0.52 mmol) and dppf (0.29 g, 0.52 mmol) in benzene (25 ml) was heated at reflux for 2 h under dinitrogen. The resulting yellow powder was filtered and dried. Yield, 0.39 g (90%). Recrystallization from toluene gave an analytical sample. M.p. 205°C. Analysis: found: C, 65.70; H, 5.44%. $C_{44}H_{43}ClPFeRu \cdot 1/2C_6H_5CH_3$ requires: C, 65.41; H, 5.43%. $^1H$ NMR ($CDCl_3$) $\delta$: 1.02 (s, 15H); 3.87, 4.06, 4.16, 5.14 (s × 4, 8H); 7.31–7.67 (m, 20H) ppm. $^{13}C$ NMR ($CDCl_3$) $\delta$: 8.79 ($C_5Me_5$); 88.57 ($C_5Me_5$); 126.3–134.7 (m, Ph) ppm.

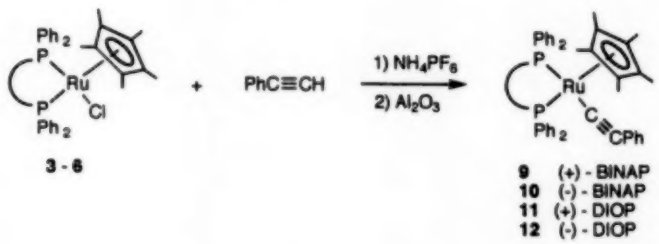


Scheme 3.

### 3.3. Preparation of Cp*[(+)-BINAP]RuCl (3)

A mixture of $[Cp^*RuCl_2]_n$ (92 mg, 0.3 mmol), (+)-BINAP (187 mg, 0.3 mmol) and Zn powder (92 mg, 1.4 mmol) in benzene (10 ml) was stirred under dinitrogen bubbling for 6 h at room temperature. After addition of hexane (10 ml), the reaction mixture was filtered. On cooling the filtrate, orange crystals of **3** precipitated. Yield, 80 mg (30%). M.p. 287°C. Analysis: Found: C, 72.31; H, 5.41%. $C_{54}H_{47}P_2ClRu$ requires: C, 72.51; H, 5.30%. $^1$H NMR ($CDCl_3$) $\delta$: 1.10 (s, 15H, Me—Cp); 6.04–7.70 (m, 32H, Ph) ppm. $^{31}$P NMR ($CDCl_3$) $\delta$: 40.76 (d, $J$ = 51 Hz); 49.34 (d, $J$ = 51 Hz) ppm. $[\alpha]_D$ = 1091°.

Cp*[(−)-BINAP]RuCl (**4**) was prepared in a similar manner. Yield, 80 mg (30%). M.p. 285°C. Analysis: Found: C, 72.78; H, 5.44%. $C_{54}H_{47}P_2ClRu$ requires: C, 72.51; H, 5.30%. $^1$H NMR ($CDCl_3$) $\delta$: 1.10 (s, 15H, Me—Cp); 6.04–7.70 (m, 32H, Ph) ppm. $[\alpha]_D$ = −1026°.

### 3.4. Preparation of Cp*[(+)-DIOP]RuCl (5)

A mixture of $[Cp^*RuCl_2]_n$ (92 mg, 0.3 mmol), (+)-DIOP (147 mg, 0.3 mmol) and Zn powder (92 mg, 1.4 mmol) in benzene (10 ml) was stirred under dinitrogen bubbling for 6 h at room temperature. After evaporation, the oily residue was dissolved in acetonitrile (1 ml) and the solution was then cooled on an ice bath to give **5** as orange crystals (120 mg, 52%). M.p. 264°C. Analysis: Found: C, 64.20; H, 6.15%. $C_{41}H_{47}ClO_2P_2Ru$ requires: C, 63.93; H, 6.15%. $^1$H NMR ($CDCl_3$) $\delta$: 1.08 (s, 15H; Me—Cp); 1.19, 1.22 (s, 3H, Me); 2.04, 2.68, 3.10, 3.70 (m, 1H, $CH_2$); 3.49, 4.09 (m, 1H, CH); 7.05–7.67 (m, 20H, Ph) ppm. $^{13}$C NMR ($CDCl_3$) $\delta$: 9.06 (s, $C_5Me_5$); 26.89, 27.18 (s, Me); 29.70 (d, $J$ = 21.3 Hz, $CH_2$); 36.48 (dd, $J$ = 24.0, 5.6 Hz, $CH_2$); 74.68 (d, $J$ = 12.2 Hz, CH); 80.12 (d, $J$ = 7.7 Hz, CH); 107.95 (s, C); 127.3–142.2 (m, Ph) ppm. $^{31}$P NMR ($CDCl_3$) $\delta$: 30.79 (d, $J$ = 38 Hz); 34.47 (d, $J$ = 38 Hz) ppm. $[\alpha]_D$ = 65°.

Cp*[(−)-DIOP]RuCl (**6**) was prepared in a similar manner. Yield, 120 mg (52%). M.p. 262°C. Analysis: Found: C, 64.03; H, 6.17; N, 0.88%. $C_{41}H_{47}ClO_2P_2Ru \cdot 1/2CH_3CN$ requires: C, 63.78; H, 6.18; N, 0.68%. $^1$H NMR ($CDCl_3$) $\delta$: 1.08 (s, 15H, Me—Cp); 1.19, 1.22 (s, 3H, Me); 2.04, 2.68, 3.10, 3.70 (m, 1H, $CH_2$); 3.49, 4.09 (m, 1H, CH); 7.05–7.67 (m, 20H, Ph) ppm. $[\alpha]_D$ = −62°.

### 3.5. Preparation of [Ru(CH$_3$CN)(dppf)Cp*]BF$_4$ (7)

To a suspension of **2** (42 mg, 0.05 mmol) in anhydrous acetone (5 ml) was added $AgBF_4$ (10 mg, 0.05 mmol). The mixture was stirred for 2 h under a dinitrogen atmosphere. The reaction mixture was evaporated and the residue dissolved in $CH_2Cl_2$ (5 ml). After the mixture had been filtered and the solvent evaporated, the residue was dissolved in $CH_3CN$ (2 ml) and the solution diluted with anhydrous ether (7 ml). On storing the solution in a refrigerator overnight, yellow crystals (36 mg, 76%) were obtained. M.p. 210°C. Analysis: Found: C, 60.33; H, 5.34; N, 2.65%. $C_{46}H_{46}BF_4NP_2FeRu \cdot CH_3CN$ requires: C, 60.07; H, 5.14; N, 2.91%. $^1$H NMR ($CDCl_3$) $\delta$: 1.06 (s, 3H, Me—Cp); 2.94 (s, 3H, $CH_3CN$); 4.04, 4.19, 4.33, 4.34 (bs, 2H, Fc); 7.41–7.72 (m, 20H, Ph) ppm. $^{31}$P NMR ($CDCl_3$) $\delta$: 44.67 ppm. IR (KBr) (cm$^{-1}$): 2260 (C≡N); 1134 ($BF_4$).

### 3.6. Preparation of [Ru(η-O$_2$)(dppf)Cp*]BF$_4$ (8)

To a suspension of **2** (42 mg, 0.05 mmol) in anhydrous acetone (5 ml) was added $AgBF_4$ (10 mg, 0.05 mmol). The mixture was stirred for 2 h in air. After the reaction mixture had been filtered, the filtrate was diluted with anhydrous ether (5 ml). On storing the solution in a refrigerator overnight, brown crystals (31 mg, 70%) were obtained. M.p. 172°C. Analysis: Found: C, 57.97; H, 5.09%. $C_{44}H_{43}BF_4O_2P_2FeRu$ requires: C, 58.11; H, 4.93%. $^1$H NMR (acetone-$d_6$) $\delta$: 1.25 (s, 3H, $C_5Me_5$); 4.28 (bs, 2H, Fc-$\beta$); 4.51 (bs, 2H, Fc-$\alpha$); 4.59 (bs, 2H, Fc-$\beta$); 5.15 (bs, 2H, Fc-$\alpha$); 7.46–7.85 (m, 20H, Ph) ppm. $^{13}$C NMR (acetone-$d_6$) $\delta$: 9.43 (Me—Cp); 70.76 (Fc-$\beta$); 74.86 (Fc-$\alpha$); 75.44 (Fc-$\beta$); 76.09 (Fc-$\alpha$); 87.08 (Fc-*ipso*); 108.71 ($C_5Me_5$); 128.30 (Ph-*ipso*); 129.14, 129.41 (Ph-*m*); 132.17, 133.56 (Ph-*p*); 134.69, 136.82 (Ph-*o*); 135.76 (Ph-*ipso*) ppm. $^{31}$P NMR ($CDCl_3$) $\delta$: 38.57 ppm. IR (KBr) (cm$^{-1}$): 1154 ($BF_4$); 840 (O—O).

### 3.7. Reaction of 3–6 with PhC≡CH

A mixture of **3** (55 mg, 0.06 mmol), PhC≡CH (2 drops) and $NH_4PF_6$ (10 mg, 0.06 mmol) in MeOH (5 ml) was stirred under dinitrogen for 2 h at room temperature. After evaporation, the residue was chromatographed on $Al_2O_3$ by elution with $CH_2Cl_2$ to give **9** as orange crystals (24 mg, 42%). Recrystallization from $MeOH/CH_2Cl_2$ gave an analytical sample. M.p. 205°C (dec.). Analysis: Found: C, 72.26; H, 5.23%. $C_{54}H_{48}P_2Ru \cdot 1/2CH_2Cl_2$ requires: C, 72.53; H, 5.47%. IR (KBr) (cm$^{-1}$): 2077 (C≡C). $^1$H NMR ($CDCl_3$) $\delta$: 1.27 (s, 15H, Me); 6.09–7.95 (m, 37H, Ph + Naph) ppm. $^{13}$C NMR ($CDCl_3$) $\delta$: 9.77 ($C_5Me_5$); 94.04 ($C_5Me_5$); 111.95 (≡*C*Ph); 122–141.5 (m, Ph + Naph + Ru*C*≡) ppm.

Complex **10** was prepared in a similar manner. M.p. 205°C. Analysis: Found: C, 72.26; H, 5.29%. $C_{54}H_{48}P_2Ru \cdot 1/2CH_2Cl_2$ requires: C, 72.53; H, 5.47%. IR (KBr) (cm$^{-1}$): 2076 (C≡C). $^1$H NMR ($CDCl_3$) $\delta$: 1.27 (s, 15H, Me); 6.09–7.95 (m, 37H, Ph + Naph) ppm. $^{13}$C NMR ($CDCl_3$) $\delta$: 9.77 ($C_5Me_5$);

94.04 ($C_5Me_5$); 111.95 (=*C*Ph); 122–141.5 (m, Ph + Naph + Ru*C*=) ppm.

To a solution of **5** (59 mg, 0.08 mmol) in MeOH (2 ml) and $CH_2Cl_2$ (5 ml) were added PhC≡CH (2 drops) and $NH_4PF_6$ (13 mg, 0.08 mmol). The mixture was stirred under dinitrogen for 2 hr at room temperature. After evaporation, the residue was chromatographed on $Al_2O_3$ by elution with $CH_2Cl_2$ to give **11** as yellow crystals (35 mg, 52%). Recrystallization from cyclohexane/$CH_2Cl_2$ gave an analytical sample. M.p. 220°C. Analysis: Found: C, 70.49; H, 6.37%. $C_{49}H_{52}O_2P_2Ru$ requires: C, 70.40; H, 6.27%. $^1$H NMR ($CDCl_3$) $\delta$: 1.02 (s, 3H, Me); 1.19 (s, 3H, Me); 1.21 (s, 15H, Me—Cp); 1.96, 2.79, 3.05, 4.03 (m, 1H, $CH_2$); 3.47, 4.39 (m, 1H, CH); 6.93–8.08 (m, 15H, Ph) ppm. IR (KBr) ($cm^{-1}$): 2072 (C≡C).

Complex **12** was prepared in a similar manner. M.p. 220°C. Analysis: Found: C, 70.53; H, 6.23%. $C_{49}H_{52}O_2P_2Ru$ requires: C, 70.40; H, 6.27%. $^1$H NMR ($CDCl_3$) $\delta$: 1.02 (s, 3H, Me); 1.19 (s, 3H, Me); 1.21 (s, 15H, Me—Cp); 1.96, 2.79, 3.05, 4.03 (m, 1H, $CH_2$); 3.47, 4.39 (m, 1H, CH); 6.93–8.08 (m, 15H, Ph) ppm. $^{13}$C NMR ($CDCl_3$) $\delta$: 9.35 ($C_5Me_5$); 26.63, 27.24 (Me); 31.91 (d, $J$ = 28.0 Hz, $CH_2$); 37.43 (dd, $J$ = 23.9, 5.6 Hz, $CH_2$); 74.70 (d, $J$ = 11.4 Hz, CH); 80.16 (dd, $J$ = 7.8, 1.6 Hz, CH); 92.90 ($C_5Me_5$); 107.95 ($CMe_2$); 111.80 (=*C*Ph); 122.7–141.4 (Ph + Ru*C*=) ppm. IR (KBr) ($cm^{-1}$): 2071 (C≡C).

### 3.8. Catalytic reaction of PhC≡CH with allyl alcohol

A mixture of PhC≡CH (0.1 ml, 1 mmol), allyl alcohol (4 ml), Cp*[(+)-BINAP]RuCl (54 mg, 0.06 mmol)$_4$ and $NH_4PF_6$ (16 mg, 0.1 mmol) was heated at 100°C in a sealed tube for 10 h. After evaporation of the allyl alcohol, the residue was chromatographed on $SiO_2$. Only a trace amount of $PhCH_2COCHCHCH_3$ was isolated however. $^1$H NMR ($CDCl_3$) $\delta$: 1.87 (dd, $J$ = 7.2, 1.8 Hz, 3H, Me); 3.81 (s, 2H, $CH_2$); 6.16, 6.92 (m, 1H, CH); 7.24 (m, 5H, Ph) ppm.

### 3.9. Structure determination

Crystal data for **8**: $C_{44}H_{43}BF_4O_2P_2FeRu$, FW = 909.50; monoclinic, $P21/a$; $a$ = 15.193(6), $b$ = 25.08(1), $c$ = 11.010(6) Å; $\beta$ = 109.69(4)°; $V$ = 3951(3) Å$^3$; $Z$ = 4; $D_{calc}$ = 1.53 g cm$^{-3}$; $\mu$(Mo K$\alpha$) = 8.761 $cm^{-1}$; $T$ = 298 K; crystal size 0.22 × 0.24 × 0.12 mm.

Data collection was performed at room temperature on a Mac Science MXC18K diffractrometer with graphite monochromated Mo K$\alpha$ radiation and a 18-kW rotating anode generator. Of 8965 reflections collected, 8029 reflections were unique, of which 8606 reflections with $I > 3.00\ \sigma\ (I)$ were used for refinement. The structure was solved using the Dirdif–Patty method with CRYSTAN-G (software package for structure determination) and refined by a full-matrix least-squares procedure. Absorption correction with the $\psi$-scan method and anisotropical refinements for non-hydrogen atoms were carried out; $R$ = 0.075 and $Rw$ = 0.078.

## References


[1] M.A. Benett and T.W. Matheson, in G. Wilkinson, F.G.A. Stone and E.W. Abel (eds.), *Comprehensive Organometallic Chemistry*, Pergamon, Oxford, UK, 1982, Vol. 4, p. 931.

[2] P. Kalck, Y. Peres and J. Jenck, *Adv. Organomet. Chem., 32* (1991) 121.

[3] G. Consiglio and F. Morandini, *Chem. Rev., 87* (1987) 761.

[4] J.M. Manriquez, P.J. Fagan, L.D. Schertz and T.J. Marks, *Inorg. Synth., 28* (1990) 317.

[5] (a) N. Oshima, H. Suzuki and Y. Moro-oka, *Chem. Lett.*, (1984) 1161; (b) T. Kakigano, H. Suzuki, M. Igarashi and Y. Moro-oka, *Organometallics, 9* (1990) 2192; (c) H. Suzuki, T. Kakigano, M. Igarashi, M. Tanaka and Y. Moro-oka, *J. Chem. Soc., Chem. Commun.*, (1992) 283.

[6] T.D. Tilley, R.H. Grubbs and J.E. Bercaw, *Organometallics, 3* (1984) 274.

[7] J.L. Schrenk, A.M. McNair, F.B. McCormick and K.R. Mann, *Inorg. Chem., 25* (1986) 3501.

[8] (a) U. Koelle and J. Kossakowski, *J. Organomet. Chem., 362* (1989) 383; (b) U. Koelle, B.-S. Kang, T.P. Spanniol and U. Engiert, *Organometallics, 11* (1992) 249.

[9] (a) S. Dev, K. Imagawa, Y. Mizobe, G. Cheng, Y. Wakatsuki, H. Yamazaki and M. Hidai, *Organometallics, 8* (1989) 1232; (b) S. Dev, Y. Mizobe and M. Hidai, *Inorg. Chem., 29* (1990) 4797.

[10] (a) P.J. Fagan, M.D. Ward and J.C. Calabrese, *J. Am. Chem. Soc., 111* (1989) 1698; (b) P.J. Fagan, W.S. Mahoney, J.C. Calabrese and I.D. Williams, *Organometallics, 9* (1990) 1843.

[11] (a) X.D. He, B. Chaudret, F. Dahan and Y.-S. Huang, *Organometallics, 10* (1991) 970; (b) Y.-S. Huang, S. Sabo-Etienne, X.-D. He and B. Chaudret, *ibid., 11* (1992) 3031.

[12] W.J. Kelly and W.E. Parthun, *Organometallics, 11* (1992) 4348.

[13] P.M. Treichel, D.A. Komar and P.J. Vincenti, *React. Inorg. Met.-Org. Chem., 14* (1984) 383.

[14] F.M. Conroy-Lewis and S.J. Simpson, *J. Organomet. Chem., 322* (1987) 221.

[15] J. Chang and R.G. Bergman, *J. Am. Chem. Soc., 109* (1987) 4298.

[16] H. Lehmkuhl, M. Bellenbaum, J. Grundke, H. Mauermann and C. Krügen, *Chem. Ber., 121* (1988) 1719.

[17] (a) B.K. Campion, R.H. Heyn and T.D. Tilley, *J. Chem. Soc., Chem. Commun.*, (1988) 278; (b) B.K. Campion, R.H. Heyn and T.D. Tilley, *ibid.*, (1992) 1201.

[18] H.E. Bryndza, P.J. Domaille, R.A. Paciello and J.E. Bercaw, *Organometallics, 8* (1989) 379.

[19] M.S. Chinn and D.M. Heinekey, *J. Am. Chem. Soc., 112* (1990) 5166.

[20] G. Jia, A.J. Lough and R.H. Morris, *Organometallics, 11* (1992) 151.

[21] M.I. Bruce, P.A. Humphrey, O.B. Shawkataly, M.R. Show, E.R.T. Tiekink and W.R. Cullen, *Organometallics, 9* (1990) 2910; W.R. Cullen, S.J. Rettig and T.C. Zheng, *ibid., 11* (1992) 853.

[22] R. Noyori and H. Takaya, *Acc. Chem. Res., 23* (1990) 345.

[23] M.S. Tin and M. Heinekey, *J. Am. Chem. Soc., 112* (1990) 5166.

[24] J.J. Bishop and A. Davison, *Inorg. Chem., 10* (1971) 826.

[25] G. Jia and H. Morris, *J. Am. Chem. Soc., 113* (1991) 875.

[26] K. Kirchner, K. Mauthner, K. Mereiter and R. Schmid, *J. Chem. Soc., Chem. Commun.*, (1993) 892.
[27] J.S. Valentine, *Chem. Rev., 73* (1973) 235.
[28] M. Jimenez-Tenorio, M.C. Puerta and P. Valerga, *J. Am. Chem. Soc., 115* (1993) 9794; *idem, Inorg. Chem., 33* (1994) 3515.
[29] E. Lindner, M. Haustein, R. Fawzi, M. Steimann and P. Wegner, *Organometallics, 13* (1994) 5021.
[30] J.-M. Savariault and M.S. Lehmann, *J. Am. Chem. Soc., 102* (1980) 1298.
[31] B.M. Trost, G. Dyker and R.J. Kulawiek, *J. Am. Chem. Soc., 112* (1990) 7809; B.M. Trost and R.J. Kulawiek, *ibid., 114* (1992) 5579.

ELSEVIER

Journal of Organometallic Chemistry 508 (1996) 129–136

Journal of Organometallic Chemistry

# $^{55}$Mn and $^{187}$Re NQR spectral studies of modulation effects of mutual motions of electrons and atomic nuclei in cyclopentadienyl tricarbonyl manganese and rhenium complexes

G.K. Semin *, S.I. Kuznetsov, E.V. Bryukhova, T.L. Khotsyanova

*Institute of Organo-Element Compounds, Academy of Sciences of Russia, 28 Vavilov Street, Moscow 117813, Russia*

Received 3 May 1995

**Abstract**

The $^{55}$Mn and $^{187}$Re NQR spectral parameters for cyclopentadienyl tricarbonyl complexes of these metals at 77 K are presented. An analytical dependence between $e^2Qq_{zz}$ and $\eta$ has been shown to exist. Such dependence may be associated with slow mutual electron–nuclear motions in these complexes.

*Keywords:* Manganese; Rhenium; Carbonyls; Nuclear Quadrupole Resonance; Electron–nuclear motions

## 1. Introduction

The mechanism of bond formation between the cyclopentadienyl ring and a metal atom is a problem that has not yet been resolved. The basic reason for this situation is that methods usually employed for studying the problem are incapable of elucidating the role of dynamic effects during such types of bond formation. In addition, if several configurational distributions exist for the electron density in a coordination complex or molecular system, and, if dynamic transitions occur between these configurational states due to the electron tunnelling, splitting the electron energy levels will result; such splittings are usually called tunnel or inversion splittings. They are caused by phase changes in the wave packets upon tunnelling from one energy well to another on the potential energy curve [1] and lead to additional differences in the electron distribution configurations. The above differences may be observed (or remain unnoticed) when the mutual positions of the atomic nuclei in a molecule or complex change and depend on the ratio of the lifetimes of the nuclei in the configurational states as well as on the ratio, $\tau$, of the total electron-transfer times for tunnelling to the characteristic times for the motion of atomic nuclei. An essential feature of this model is that changes occur in the ratio of the characteristic times for electron motions to those for the motion of atomic nuclei.

The characteristic times for electron motions are usually assumed to be some 5–10 orders of magnitude less than those for the motions of atomic nuclei. This assumption provides the basis for the well-known Born–Oppenheimer limitation [2], according to which quantum interactions between electrons and atomic nuclei can be neglected because of enormous difference between the characteristic times for their motions.

However, the probability of passing through a potential barrier upon electron tunnelling is $10^{-5}$ to $10^{-10}$ in typical cases [1], resulting in an increase in the correlation time $\tau$ for total electron transfer from one potential well to another one. The only exception to this situation is resonance tunnelling [1]. On the basis of the close values of the above estimates, it is possible to assume that times for total electron transfer upon tunnelling might, in several cases, be close to or coincide with the characteristic times for the motion of atomic nuclei. This means that the Born–Oppenheimer limitation [2] will no longer be valid in this region, and that hybrid electron–nuclear states will be generated [3].

Theoretical studies of the effect described above

* Corresponding author.

0022-328X/96/$15.00 © 1996 Elsevier Science S.A. All rights reserved
*SSDI* 0022-328X(95)05794-3

Table 1
$^{55}$Mn NQR spectral parameters at 77 K in the $(CO)_3MnC_5H_{5-n}R_n$ series

| No. | $R_n$ | $e^2Qq_{zz}$ (MHz) | $\eta$(%) | No. | $R_n$ | $e^2Qq_{zz}$ (MHz) | $\eta$(%) |
|---|---|---|---|---|---|---|---|
| 1 | $C_{17}H_{21}OSi$ [a] | 64.670 | (−)10.6 | 24 | $Sn(n-C_4H_9)_3$ | 63.58 | 2.0 |
| 2 | $C_2H_5$ | 64.708 | (−)9.1 | 25 | CH=NOH | 62.909 | 3.5 |
| 3 | $(CH_2I)_2$ | 64.689 | (−)7.45 | 26 | HgCl phase 1 | 62.30 | 4.8 |
| 4 | $CH_2Cl$ | 64.950 | (−)5.1 | 27 | | 65.41 | 10.2 |
| 5 | $CH_3$ | 64.860 | (−)4.4 | 28 | HgCl phase 2 | 64.20 | (−)10.3 |
| 6 | H | 65.20 | 1.9 | 29 | | 65.17 | 2.0 |
| 7 | $SO_3Na$ | 65.81 | 2.9 | 30 | HgBr | 63.99 | (−)3.2 |
| 8 | $(CH_3)_3$ | 65.919 | 3.35 | 31 | | 65.97 | 9.6 |
| 9 | I | 67.014 | 5.1 | 32 | HgI | 63.199 | 3.45 |
| 10 | Br | 67.44 | 5.3 | 33 | | 65.139 | 12.6 |
| 11 | Cl | 67.65 | 5.4 | 34 | $(CO)_3MnC_5H_4Hg$ | 63.525 | 9.9 |
| 12 | $(CH_3)_4$ | 68.782 | 5.7 | 35 | | 64.070 | (−)3.0 |
| 13 | $(CH_3)_5$ | 69.337 | 5.8 | 36 | $COOCH_3$ | 61.200 | 5.6 |
| 14 | $(C_2H_5)_5$ | 71.152 | 5.95 | 37 | $COCH_3$ | 61.630 | 6.8 |
| 15 | $Cl_5$ | 78.922 | 6.2 | 38 | COH | 61.378 | 9.0 |
| 16 | | 77.388 | 7.2 | 39 | COCl | 59.940 | 10.3 |
| 17 | $SO_2CH_3$ | 63.424 | 6.63 | 40 | $COCH_2Br$ | 60.700 | 10.6 |
| 18 | $SO_2NH_2$ | 63.56 | 6.64 | 41 | $COCH_2Cl$ | 60.740 | 10.65 |
| 19 | $SO_2C_2H_5$ | 64.396 | 6.70 | 42 | $COC_6H_5$ | 62.422 | 12.4 |
| 20 | $(CH_2Cl)_2$ | 65.234 | 6.76 | 43 | $COCF_3$ | 59.350 | 13.9 |
| 21 | $(CH_2Br)_2$ | 65.099 | 6.75 | 44 | $C_6H_9O_3S$ [b] | 62.25 | 7.5 |
| 22 | $SO_2Cl$ | 61.74 | 8.3 | 45 | COOH | 62.27 | 0 |
| 23 | $Sn(C_6H_5)_3$ | 63.90 | (−)3.5 | | | | |

[a] $C(OH)(C_6H_5)CH_2C_6H_4Si(CH_3)_3$ – 4,4'.
[b] $C(O)CH_2\underline{CHCH_2CH_2SO_2}CH_2$.

have encountered computing problems which were difficult to overcome because the adiabatic approach is no longer valid. This is why experimental evidence for this process becomes so important.

Nuclear quadrupole resonance (NQR) is associated with the existence of gradient electric fields on atomic nuclei. The method is the most appropriate for studying the problem because of its high accuracy and, hence, of its high level of information. An important point is that NQR frequencies are proportional to the second derivative of the electrostatic potential, whose changes are much more pronounced than those of the function itself.

The main spectral characteristics obtained from NQR spectra are: the quadrupole coupling constant (QCC), i.e. $e^2Qq_{zz}$, where $eQ$ is the electric quadrupole moment of the atomic nucleus (the nuclear constant), $eq_{zz}$ is the maximum diagonal component of the electric field gradient (EFG) tensor at the atomic nucleus, ($eq_{zz} = \partial^2U/\partial z^2$ is the second derivative of the electrostatic potential at the atomic nucleus), and the EFG asymmetry parameter

$$\eta = |(q_{xx} - q_{yy})/q_{zz}| \quad (1)$$

where $q_{xx}$, $q_{yy}$, $q_{zz}$ are the principal diagonal components of the EFG tensor

$$|q_{xx}| < |q_{yy}| < |q_{zz}| \quad (2)$$

In accordance with the Laplace condition, at the nucleus

$$q_{xx} + q_{yy} + q_{zz} = 0 \quad (3)$$

Changes in the QCC and $\eta$ with temperature arise from periodic and fast changes in the mutual orientation of the EFG tensor and the nuclear quadrupole moment tensor during the free thermal vibrations of the molecules (in the limiting case these are hindered reorientations).

Another source of temperature changes in the QCC and $\eta$ is modulation of the EFG caused by thermal translational motions of neighbouring molecules. It is the mechanism of EFG averaging by the comparatively slow mutual intramolecular motions of electrons and atomic nuclei which has not been considered earlier by other authors.

In the present work an attempt has been made to consider changes in the EFG at a fixed temperature (77 K) caused by configurational instability due to interconfigurational electron tunnelling. With this aim in mind, we have chosen the molecular system $(CO)_3Mn(Re)C_5H_{5-n}R_n$, since the resonant atom, $^{55}Mn(^{187}Re)$, is in the centre of the molecule and most affected by the configurational electron instability.

## 2. Experimental details

All measurements of $^{55}$Mn and $^{187}$Re NQR spectra were carried out at 77 K on the NQR spectrometer/relaxometer ISSh-2-13 developed and produced by SKB-IRE AN SSSR [4].

All known quadrupole coupling constants ($e^2Qq_{zz}$)

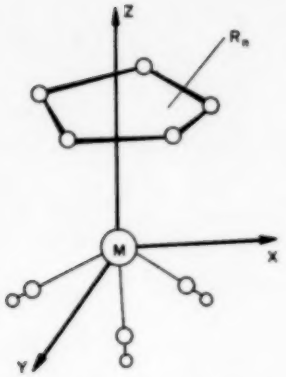


Fig. 1. Position of the EFG axes for molecules in the $(CO)_3MnC_5H_{5-n}R_n$ series.

and asymmetry parameters ($\eta$) in the series $(CO)_3MnC_5H_{5-n}R_n$ (Nos. 1–35) and $(CO)_3Mn$-$C_5H_4COX$ (Nos. 36–45) [5] are listed in Table 1. Apart from literature data, some of the listed spectra were studied for the first time, some were refined. As is shown by the spectra for compounds with $R_n = Cl_5$, HgBr, HgI and $HgH_4C_5Mn(CO)_3$, their molecules occupy two crystallographically non-equivalent positions. For $(CO)_3MnC_5H_4HgCl$ both crystalline phases were studied (at 77 K). In our subsequent calculations, data for different crystallographically non-equivalent positions were not averaged, but used separately for each position. Hence we used the common numbering given in Table 1. Formal changes in the asymmetry parameters signs indicating changes in the positions of $x$- and $y$-components will be explained below in the text.

Table 2 lists the numerical values of $e^2Qq_{zz}$ and $\eta$ from the $^{187}$Re NQR spectra of the $(CO)_3ReC_5H_{5-n}R_n$ series [5]. The meaning of the column with the $\tau$ values will be explained below in the text.

## 3. Results and discussion

As can be seen from the scheme in Fig. 1, the EFG on the $^{55}$Mn nucleus as observed by the NQR method is the difference between the contributions to the EFG from different parts of the $\pi$-cyclopentadienyl tricarbonyl manganese molecule, i.e. (1) from the three CO groups and (2) from the cyclopentadienyl ring and its substituents.

The charge separation between the manganese atom and the cyclopentadienyl ligand increases upon the addition of electron-donor substituents to the cyclopentadienyl ring, which results in an increase in the quadrupole coupling constant $e^2Qq_{zz}$ for $^{55}$Mn. In contrast, the addition of electron-acceptor substituents decreases the value of $e^2Qq_{zz}$ on the manganese atom (see Tables 1 and 2).

The redistribution of charge leads to a change in the characteristics of the interconfigurational transitions as well as in $e^2Qq_{zz}$ and $\eta$. The process of searching for a minimum in the energy system involving such configurational transitions is accompanied by mutually related fluctuations in the energy and in the shape of the electron distribution, whose measure in NQR spectroscopy is provided by the asymmetry parameters. By comparing the changes in $e^2Qq_{zz}$ and $\eta$, it is possible to observe the dynamics of these transitions. In this case, changes in the dimensionless quantity $\eta$ will characterize changes in the energy characteristics of the electron configuration, while changes in $e^2Qq_{zz}$ define the intrabonding charge distribution in $(CO)_3Mn$-$C_5H_{5-n}R_n$, including the 'recharge' process associated with the change in the direction of the 'induced' bond dipole [7].

For convenience in analyzing experimental data, we can divide the observed EFG tensor with components $e^2Qq_{xx}$, $e^2qQ_{yy}$, $e^2Qq_{zz}$ and $\eta = |(q_{xx} - q_{xx})/q_{zz}|$ [Eq. (1)] into two parts: the unchanged EFG tensor (at a given temperature) with components $eqQ_{xx0}$, $eqQ_{yy0}$, $eQq_{zz0}$ and

$$\eta_0 = |(q_{xx0} - q_{yy0})/q_{zz0}| \quad (4)$$

and the 'induced' EFG tensor with components $(e^2Qq_{xx} - e^2Qq_{xx0})$, $(e^2Qq_{yy} - e^2Qq_{yy0})$, $(e^2Qq_{zz} - e^2Qq_{zz0})$ and

$$\eta_{ind} = |[(q_{xx} - q_{xx0}) - (q_{yy} - q_{yy0})]/(q_{zz} - q_{zz0})| \quad (5)$$

Table 2
$^{187}$Re NQR spectral parameters at 77 K in the $(CO)_3ReC_5H_{5-n}R_n$ series

| No. | $R_n$ | $e^2Qq_{zz}$ (MHz) | $\eta$(%) | $\tau$ ($10^{-14}$s) | No. | $R_n$ | $e^2Qq_{zz}$ (MHz) | $\eta$(%) | $\tau$ ($10^{-14}$s) |
|---|---|---|---|---|---|---|---|---|---|
| 1 | $(CH_3)_5$ | 721.83 | (−)23.3 | 46.41 | 8 | $Sn(C_6H_5)_3$ | 539.10 | (−)15.0 | 26.73 |
| 2 | $(CH_3)_4$ | 691.03 | (−)16.3 | 28.65 | 9 | $COCH_3$ | 548.47 | 30.5 | 39.45 |
| 3 | $(CH_3)_3$ | 652.74 | (−)3.9 | 15.61 | 10 | COOH | 528.44 | 23.4 | |
| 4 | $(CH_3)_2$ | 633.27 | 6.1 | 8.79 | 11 | $COOCH_3$ | 496.61 | 8.95 | |
| 5 | $CH_3$ | 610.53 | 17.1 | 1.89 | 12 | COCl | 478.25 | 39.1 | 4.70 |
| 6 | I | 601.90 | 17.1 | 1.89 | 13 | $COC_6H_5$ | 464.66 | 41.8 | 1.97 |
| 7 | H | 586.64 | 8.7 | 7.15 | | | | | |

From Eqs. (1), (4) and (5) under condition (3) for all three sets of EFG components, we can derive an equation relating $e^2Qq_{zz}$, $\eta$, $\eta_{ind}$, $\eta_0$ and $e^2Qq_{zz0}$, i.e.

$$\frac{e^2Qq_{zz}}{e^2Qq_{zz0}} = \frac{\eta_0 - \eta_{ind}}{\eta - \eta_{ind}} \tag{6}$$

If in a series of compounds of the same type the difference between two transversal EFG components $(e^2Qq_{xx} - e^2Qq_{yy})$ depends on the change in the longitudinal component $(e^2Qq_{zz})$, i.e. $(e^2Qq_{xx} - e^2Qq_{yy}) = f(e^2Qq_{zz})$, the increment of the function $\eta(e^2Qq_{zz})$ and of the argument $(e^2Qq_{zz})$ must be related by an approximate equality $\delta\eta = \delta q_{zz} \cdot d\eta/dq_{zz}$, as is known. Taking into account that according to Eq. (1) the signs of $q_{zz}$ and $d\eta/dq_{zz}$ are different, at $\delta\eta = (\eta - \eta_0)$ and $\delta q_{zz} = (q_{zz} - q_{zz0})$ we get

$$\frac{d\eta}{\eta_0 - \eta} = \frac{dq_{zz}}{q_{zz} - q_{zz0}} \tag{7}$$

After solving Eq. (7) as a differential equation with separated variables, simple transformations lead to the relationship:

$$(e^2Qq_{zz} - e^2Qq_{zz0})(\eta_0 - \eta) = B \cdot \delta \tag{8}$$

where $B$ is a constant for a given series and $\delta = \pm 1$ [6]. From Eqs. (6) and (8) one can see that

$$\eta_{ind} = \eta - \delta \cdot \frac{e^2Qq_{zz0}}{B}(\eta_0 - \eta)^2 \tag{9}$$

In fact, Eq. (8) describes the picture observed experimentally quite well [6,7] except in the close vicinity of $\eta_0$.

It is interesting to note that the form of Eq. (8) coincides with that of the $e^2Qq_{zz}(I)$ dependence for $Cl_5Sb \cdot L_0$ complexes [7], where $L_0$ is an oxygen-containing ligand, with $I$ being the ionization potential for the lone pair electron of the oxygen atom. This confirms the above-mentioned considerations that energy changes and fluctuations must result in configurations whose measure are changes in $\eta$, i.e. $\delta I \sim \delta\eta$ [7].

Departures from dependence (8) in the vicinity of $\eta_0$ can be understood, if it is assumed the EFG fluctuations occur with an average modulation depth $\Delta\eta$ in the vicinity of $(\eta_0, e^2Qq_{zz0})$. If such EFG fluctuations are of a stochastic nature due to the multiplicity of the vibration processes, one can use the basic relationships of the theory of stochastic dynamics of non-linear vibration systems [8]. This theory predicts the appearance of a nearly rectangular spectrum for comparatively low frequency vibrations. In this case one can carry out a simple integrated averaging of Eq. (8) to take account of the mutual modulation motions of electrons and atomic nuclei when computing the observed $e^2Qq_{zz}$ values

$$e^2Qq_{zz} = \frac{1}{2\Delta\eta}\int_{\eta-\Delta\eta}^{\eta+\Delta\eta}\left[e^2Qq_{zz0} + \frac{B \cdot \delta}{(\eta_0 - \eta)}\right] d\eta$$

$$= e^2Qq_{zz0} + \frac{B \cdot \delta}{2\Delta\eta}\ln\left|\frac{\eta - (\eta_0 + \Delta\eta)}{\eta - (\eta_0 - \Delta\eta)}\right| \tag{10}$$

or in the interval $(\eta_0 \pm \Delta\eta)$

$$\left|\frac{\eta - \eta_0}{\Delta\eta}\right| = \text{th}\left|\frac{\Delta\eta}{B}(e^2Qq_{zz} - e^2Qq_{zz0})\right| \tag{11}$$

At $|(\eta - \eta_0)/\Delta\eta| = 2.5$–$3$ and above, the descriptive power of Eqs. (8) and (10) is almost equal.

A similar averaging can be obtained for $\eta_{ind}$ using Eq. (9)

$$\bar{\eta}_{ind} = \frac{1}{2\Delta\eta}\int_{\eta-\Delta\eta}^{\eta+\Delta\eta}\left[\eta - \delta \cdot \frac{e^2Qq_{zz0}}{B}(\eta - \eta_0)^2\right] d\eta$$

$$= \eta - \delta \cdot \frac{e^2Qq_{zz0}}{B}\left[(\eta - \eta_0)^2 + \frac{\Delta\eta^2}{3}\right] \tag{12}$$

### *3.1. Estimation of the total interconfigurational tunnel electron-transfer times ($\tau$)*

For a rough estimate of the total interconfigurational tunnel electron transfer, one can use the results reported in Ref. [9] where various aspects of the dipole instability have been considered. Let us consider two or more configurations of the electron distribution with different magnitudes and directions for their dipole moments undergoing the effect of local microscopic fields with the field strength $\varepsilon$. For a Boltzmann's distribution and $p_0\varepsilon \ll \delta E$, where $p_0$ is the absolute value of the dipole moment for an equilibrium configuration, and $\delta E$ is the inversion (tunnel) splitting, the average dipole moment appears to be

$$\bar{P} = \frac{P_0^2\varepsilon}{3\delta E}\ \text{th}|\,\delta E/kT\,| \tag{13}$$

However, if the dipole generated in the case of the orientational polarization of 'hard' dipoles is written as

$$\bar{P}' = \frac{P_0^2\varepsilon}{3kT} \tag{14}$$

the $\bar{P}/\bar{P}'$ ratio will be

$$\frac{\bar{P}}{\bar{P}'} = \frac{kT}{\delta E}\ \text{th}\left|\frac{\delta E}{kT}\right| \tag{15}$$

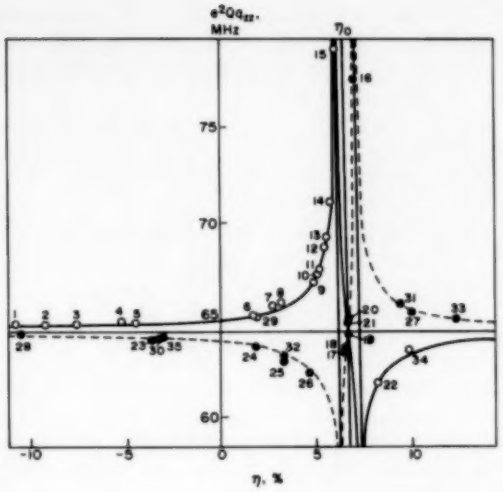


Fig. 2. Dependence of $e^2Qq_{zz}$ on $\eta$ for molecules in the $(CO)_3MnC_5H_{5-n}R_n$ series (see Nos. 1–35 in Table 1) as derived from Eq. (10): solid lines correspond to $\delta = +1$ (open points); dashed lines correspond to $\delta = -1$ (filled points).

Since the sources of changes in the asymmetry parameter $\eta$ have the same origin, then setting

$$\bar{P}/\bar{P}' \sim (\eta - \eta_0)/\Delta\eta \tag{16}$$

and using expression (11) one can obtain an approximate equation

$$\left|\frac{\eta - \eta_0}{\Delta\eta}\right| = \frac{kT}{\delta E}\,\mathrm{th}\left|\frac{\delta E}{kT}\right| \tag{17}$$

Eq. (17) allows one to estimate $\delta E$ at a fixed temperature using the parameters of Eq. (10) and experimental values for $e^2Qq_{zz}$. Values of $\tau$ and $\delta E$ are known to be related [1] by a simple dependence

$$\tau = \pi\hbar/\delta E \tag{18}$$

Tables 2 and 4 list the $\tau$-values for experimental points lying in the range $(\eta_0 \pm \Delta\eta)$. From a rough estimation it is seen that the $\tau$-values generally lie in the interval $8 \times 10^{-13}$ into $3 \times 10^{-15}$ s, i.e. within the range of characteristic times for nuclear motions. The direction of decrease in $\tau$ is $\eta_0 \pm \Delta\eta \rightarrow \eta_0$ and hence points corresponding to $(\eta_0 \pm \Delta\eta)$ are associated with the appearance of a slow tunnelling effect, while the point at $\eta_0$ corresponds to the most rapid electron tunnelling (see Fig. 2).

In all cases $\tau$ is smaller than the NQR characteristic times ($10^{-6}$–$10^{-9}$ s), i.e. the observed EFG values are always averaged. The only factor which changes is the efficiency of averaging by interconfigurational electron tunnelling.

### 3.2. Manganese-55 NQR data for $(CO)_3MnC_5H_{5-n}R_n$ at 77 K

We can use data from Table 1 for the $(CO)_3MnC_5H_{5-n}R_n$ series (Nos.1–35 in Table 1) and for the $(CO)_3MnC_5H_4COX$ series (Nos. 36–44 in Table 1) to check the validity of relation (10). Both sets of experimental data are described by Eq. (10) with a high degree of accuracy (see Table 3 and Figs. 2 and 3). When the parameters of Eq. (10) are used for molecules in the $(CO)_3MnC_5H_4COX$ series (Table 3, line 2), the origin of the resulting curve is shifted with respect to the corresponding curve for molecules in the $(CO)_3MnC_5H_{5-n}R_n$ series (Table 3, line 1) in such a way along the $e^2Qq_{zz0}$ and $\eta$ axes that $e^2Qq_{zz0}$ (1)

Table 3
Parameters of Eq. (10) for the $(CO)_3MnC_5H_{5-n}R_n$ series (series 1) and the $(CO)_3MnC_5H_4COX$ series (series 2) (from $^{55}$Mn NQR spectroscopy at 77 K) [a]

| Series No. | No. in Table 1 | $e^2Qq_{zz0}$ (MHz) | $B$ (MHz %) | $\eta_0$ (%) | $\Delta\eta$ (%) | $\pm\delta e^2Qq_{zz}$ (MHz) | $n$ | $r$ |
|---|---|---|---|---|---|---|---|---|
| 1 = $R_n$ | 1–35 | 64.451 | 4.018 | 6.7055 | 0.5285 | 0.09 | 35 | 0.999 |
| 2 = COX | 36–44 | 60.272 | 3.588 | 10.0245 | 1.9943 | 0.08 | 9 | 0.996 |

[a] Where $n$ is the number of experimental points used in calculating the parameters of Eq. (10) and $r$ is the correlation coefficient between the calculated values from Eq. (10) and the experimental $e^2Qq_{zz}$ values.

Table 4
Values of $\tau$ in the interval $(\eta_0 \pm \Delta\eta)$ for the $(CO)_3MnC_5H_{5-n}R_n$ series [a]

| No. in Table 1 | $\tau(10^{-14}$s) | No. in Table 1 | $\tau(10^{-14}$s) | No. in Table 1 | $\tau(10^{-14}$s) |
|---|---|---|---|---|---|
| 15 | 83.99 | 19 | 0.32 | 38 | 16.82 |
| 16 | 68.11 | 20 | 3.21 | 39 | 4.30 |
| 17 | 4.45 | 21 | 2.62 | 40 | 9.00 |
| 18 | 3.86 | | | 41 | 9.82 |

[a] Calculated via Eqs. (17) and (18).

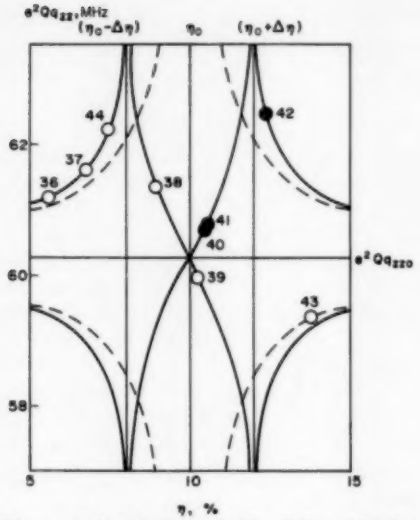


Fig. 3. The same dependence as in Fig. 2 for molecules in the $(CO)_3MnC_5H_4COX$ series (see Nos. 36–44 in Table 1). Solid lines relate to Eq. (10); dashed lines relate to Eq. (8). Notation the same as in Fig. 2.

$> e^2Qq_{zz}$ (2) and $\eta_0(1) < \eta_0(2)$. The specific nature of the effect of COX substituents has been described earlier [5].

One can see from Fig. 2 and Table 1 that most $\pi$-donor organic substituents and halogen atoms lie on the curve derived from Eq. (10) with $\delta = +1$. Organoelement and organometallic substituents, most of which are $\pi$-acceptors, lie on the branch of the curve derived from Eq. (10) with $\delta = -1$.

A graphic solution of Eq. (10) for molecules of the $(CO)_3MnC_5H_4COX$ series with $\delta = \pm 1$ is depicted by solid lines in Fig. 3 while that of Eq. (8) with $\delta = \pm 1$ is depicted by dashed lines.

The overlap between the experimental points demonstrates the comparative descriptive power of Eqs. (8) and (10) as well as differences between them [the only exception to Eq. (10) is point No. 45 (R = COOH), which might be due to the uncertainty caused by complex formation by water molecules during hydration].

A solution of Eq. (10) ($\delta = \pm 1$) using the coordinates $e^2Qq_{zz}$ and $e^2Qq_{ii}$, where $i = x, y$, for molecules in the $(CO)_3MnC_5H_{5-n}R_n$ series (Nos. 1–35 in Table 1) is shown in Fig. 4. Open points correspond to $\delta = +1$ while filled points correspond to $\delta = -1$. The values of $e^2Qq_{xx}$ and $e^2Qq_{yy}$ were determined using Eqs. (1) and (3) with module values of $\eta$ as expressed by:

$$e^2Qq_{xx} = -0.5(1-\eta)e^2Qq_{zz};$$

$$e^2Qq_{yy} = -0.5(1+\eta)e^2Qq_{zz} \qquad (19)$$

Intersection of the straight line corresponding to $\eta = 0$ by the curves $e^2Qq_{xx}(e^2Qq_{zz})$ and $e^2Qq_{yy}(e^2Qq_{zz})$ is clearly demonstrated in Fig. 4. It means that the $X$- and

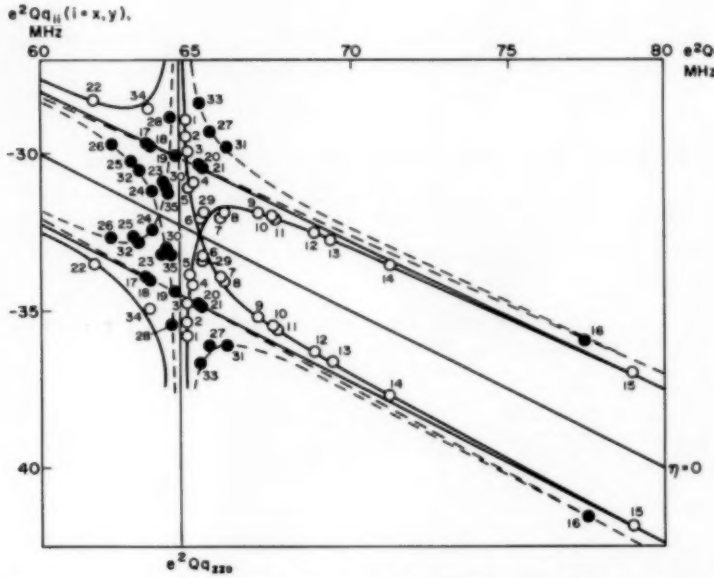


Fig. 4. Graphic solution of Eq. (10) for the $(CO)_3MnC_5H_{5-n}R_n$ series employing $e^2Qq_{zz}$ and $e^2Qq_{ii}$ coordinates, where $i = x, y$. Notation the same as in Fig. 2.

Table 5
Parameters of Eq. (10) for the $(CO)_3ReC_5H_{5-n}R_n$ series (series 1) and the $(CO)_3ReC_5H_4$ COX series (series 2) (from $^{187}$Re NQR spectroscopy at 77 K) [a]

| Series No. | No. in Table 2 | $e^2Qq_{zz0}$ (MHz) | $B$ (MHz %) | $\eta_0$ (%) | $\Delta\eta$ (%) | $\pm\delta e^2Qq_{zz}$ (MHz) | $n$ | $r$ |
|---|---|---|---|---|---|---|---|---|
| 1 = $R_n$ | 1–8 | 608.783 | 4185.888 | 20.117 | 49.755 | 2.0 | 8 | 0.999 |
| 2 = COX | 9–13 | 468.889 | 834.343 | 41.002 | 12.595 | 0.3 | 5 | 0.999 |

[a] Where $n$ is the number of the experimental points used in calculating the parameters of Eq. (10) and $r$ is the correlation coefficient between the calculated values from Eq. (10) and the experimental $e^2Qq_{zz}$ values.

$Y$-components in sequence expressed in Eq. (2) change places (for $\delta = +1$ such a point lies between No. 5 and No. 6, and for $\delta = -1$ between No. 24 and No. 30). The formal change in the sign of $\eta$ is tantamount to a change in the $e^2Qq_{xx}$ and $e^2Qq_{yy}$ direction [10] (see Table 1, Fig. 2 and Eq. (10)).

From Figs. 2 and 3 it can be seen that several experimental points lie in the interval $(\eta_0 \pm \Delta\eta)$. Using relations (17) and (18), $\eta_0$ and $\Delta\eta$ values from Table 3, it is possible to estimate the correlation times for total electron transfer as a consequence of tunnel interconfigurational transitions [Eq. (18)] (see Table 4). In accordance with our estimates, $\tau$-values computed from the experimental data lie in the interval $8.4 \times 10^{-13}$ to $3 \times 10^{-15}$ s, i.e. despite the fact that they are only rough estimates they are within the range of characteristic motion times for atomic nuclei ($10^{-10}$–$10^{-14}$ s).

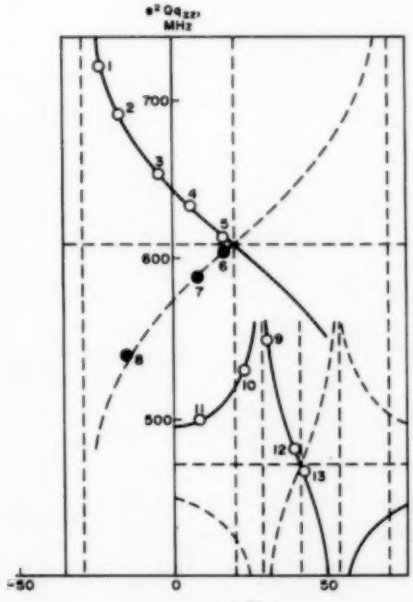


Fig. 5. Dependence of $e^2Qq_{zz}$ on $\eta$ for (a) molecules in the $(CO)_3ReC_5H_{5-n}R_n$ series (see Nos. 1–8 in Table 2) and (b) molecules in the $(CO)_3ReC_5H_4COX$ series (see Nos. 9–13 in Table 2).

### 3.3. Rhenium-187 NQR data for $(CO)_3ReC_5H_{5-n}R_n$ at 77 K

Further evidence for the reality of the processes described using the suggested model of interconfigurational tunnel transitions may be obtained from a comparison between the $\eta(e^2Qq_{zz})$ values for $^{187}$Re at 77 K and those for manganese compounds similar to those in the $(CO)_3ReC_5H_{5-n}R_n$ series (see Table 2). Despite the much narrower experimental basis relative to the manganese analogues, it was possible to obtain parameters via Eq. (10) for both the $(CO)_3ReC_5H_{5-n}R_n$ series (Nos. 1–8) (series 1) and $(CO)_3ReC_5H_4COX$ series (Nos. 9–13) (series 2) (see Table 5 and Fig. 5). The relationships obtained appear to be: $\Delta\eta_{Mn}(1) \ll \Delta\eta_{Re}(1)$ and $\Delta\eta_{Mn}(2) \ll \Delta\eta_{Re}(2)$. The shift of relation (10) for both series is similar to that for the manganese analogues, with only the relationship $\Delta\eta_{Mn}(1) < \Delta\eta_{Mn}(2)$ changing while $\Delta\eta_{Re}(1) > \Delta\eta_{Re}(2)$ remains valid.

Estimates of $\tau$-values for the experimental data in the interval $(\eta_0 \pm \Delta\eta)$ in the last column of Table 2 lie within the limits $5 \times 10^{-13}$ to $2 \times 10^{-14}$ s, i.e. also within the range of characteristic motion times for atomic nuclei.

## 4. Conclusions

From the highly descriptive power of Eq. (10) associated with estimates of electron motion times obtained from Eqs. (17) and (18), and the characteristic times of motion of atomic nuclei it is possible to demonstrate the existence of a real process, i.e. EFG averaging by comparatively slow mutual motions of electrons and atomic nuclei during tunnel interconfigurational transitions in $(CO)_3MC_5H_{5-n}R_n$ (M = Mn, Re) compounds.

The similarity between the theoretical curves derived from Eq. (10) (see Figs. 2, 3 and 5) and the dispersion curves suggests that the observed effect may be designate 'dispersion of electron nuclear motions' (DENM).

Consideration of DENM phenomena is important for understanding the nature of bonding of the $\pi$-cyclopentadienyl ring to a metal atom, since only via this phenomenon is it possible to understand the mechanism of the charge distribution in the so-called 'recharge' region.

It is that the development of low-frequency dynamics by electron systems in the DENM region will result in important changes in the reactivity and catalytic activity of compounds in the solid state as well as in anomalies in the electromagnetic properties of their crystals.

## References

[1] E.O. Kane, in *Tunneling Phenomena in Solids*, Plenum Press, New York, 1969, pp. 9–24.
[2] M. Born and R. Oppenheimer, *Ann. Phys., 84* (1927) 457.
[3] B.S. Tsukerblat and M.I. Belinskii, *Magnetochemistry and Radiospectroscopy of Exchange Clusters*, Kiev, 1983, pp. 219–249 (in Russian).
[4] B.N. Pavlov, in *Pribory i oborudovanie dlya nauchnykh issledovaniy*, Moscow, 1983, pp. 6–15 (in Russian).
[5] G.K. Semin, T.A. Babushkina and G.G. Yakobson, *NQR in Chemistry*. John Wiley & Sons, New York/Toronto, 1975.
[6] G.K. Semin, S.I. Kuznetsov, E.V. Bryukhova and S.I. Gushin, *Abs. XIth Int. Symp. NQR Spectrosc.*, London, UK, 1991, p. 11:35; G.K. Semin, S.I. Kuznetsov, A.M. Raevsky and E.V. Bryukhova, *Z. Naturforsch., Teil A, 49* (1994) 630.
[7] G.K. Semin, *Abs. Xth Int. Symp. NQR Spectrosc.*, Takayama, Japan, 1989, v P27; *Abs. XIth Int. Symp. NQR Spectrosc.*, London, UK, 1991, p. 11:32.
[8] B.V. Chirikov, *Phys. Rep., 52* (1978) 263.
[9] I.B. Bersuker, *Teor. Eksp. Khim., 5* (1969) 293 (in Russian).
[10] G.K. Semin, S.I. Gushchin, E.V. Bryukhova et al., *Dokl. Akad. Nauk SSSR, 282* (1985) 1126 (in Russian).

ELSEVIER

Journal of Organometallic Chemistry 508 (1996) 137–145

Journal of Organometallic Chemistry

# The reactions of tricobalt alkylidyne complexes $[Co_3(\mu_3\text{-}CR)(CO)_9]$ (R = Me, $CO_2Me$) with the vinyl phosphine ligands $PPh_2CH{=}CH_2$ and *cis*-$Ph_2PCH{=}CHPPh_2$; crystal structure of $[Co_3(\mu_3\text{-}CCO_2Me)(\mu\text{-}Ph_2PCH{=}CHPPh_2)(CO)_7]$

Gillian A. Acum, Martin J. Mays *, Paul R. Raithby, Gregory A. Solan

*University Chemical Laboratory, Lensfield Road, Cambridge CB2 1EW, UK*

Received 9 May 1995

**Abstract**

The alkylidyne-capped complexes $[Co_3(\mu_3\text{-}CR)(CO)_9]$ (R = Me **1a**, $CO_2Me$ **1b**) react with $PPh_2CH{=}CH_2$ in heptane at 308 K to give the phosphine-substituted complexes $[Co_3(\mu_3\text{-}CR)(CO)_8(PPh_2CH{=}CH_2)]$ (R = Me **2a**, $CO_2Me$ **2b**), $[Co_3(\mu_3\text{-}CR)(CO)_7(PPh_2CH{=}CH_2)_2]$ (R = Me **3a**, $CO_2Me$ **3b**) and, in the case of R = $CO_2Me$, the *tris*-substituted complex $[Co_3(\mu_3\text{-}CCO_2Me)(CO)_6(PPh_2CH{=}CH_2)_3]$ **4**. Heating of complexes **2a** and **2b** at 343 K results in loss of a CO group and coordination of the vinyl moiety of the $PPh_2CH{=}CH_2$ ligand to afford $[Co_3(\mu_3\text{-}CR)(\mu\text{-}PPh_2CH{=}CH_2)(CO)_7]$ (R = Me **5a**, $CO_2Me$ **5b**). In contrast, reaction of $[Co_3(\mu_3\text{-}CR)(CO)_9]$ (R = Me **1a**, $CO_2Me$ **1b**) with *cis*-$Ph_2PCH{=}CHPPh_2$ (dppee) gives $[Co_3(\mu_3\text{-}CR)(\mu\text{-}Ph_2PCH{=}CHPPh_2)(CO)_7]$ (R = Me **6a**, $CO_2Me$ **6b**) in which the dppee ligand bridges two adjacent cobalt atoms *via* both phosphino moieties. Nuclear magnetic resonance studies on **5a** and **5b** indicate that two isomeric structures in a ratio of 7 : 3 are present in solution at 293 K. Conversion of $[Co_3(\mu_3\text{-}CR)(\mu\text{-}PPh_2CH{=}CH_2)(CO)_7]$ **5a** and **5b** back to $[Co_3(\mu_3\text{-}CR)(CO)_8(PPh_2CH{=}CH_2)]$ **2a** and **2b** can be achieved by purging with CO at 293 K while further purging at 343 K results in conversion to $[Co_3(\mu_3\text{-}CR)(CO)_9]$ **1a** and **1b**. The structure of $[Co_3(\mu_3\text{-}CCO_2Me)(\mu\text{-}Ph_2PCH{=}CHPPh_2)(CO)_7]$ **6b** was determined by single-crystal X-ray diffraction. All the complexes have been characterized spectroscopically and by elemental analysis.

*Keywords:* Tricobalt; Alkylidyne; Vinylphosphine; Crystal structure; Carbonyl; Vinyl

## 1. Introduction

The use of the vinyl phosphines $[PR^1_2(CR^2{=}CR^3R^4)]$ (R = H, alkyl, aryl) as ligands in organometallic transition metal complexes continues to be the focus of a series of reports [1]. In such complexes the ligand has the potential to act as a four-electron donor via the vinyl and phosphino groups. Introduction of a further two-electron donor group, e.g. $R^4 = PPh_2$, on the β-carbon of the vinyl phosphine results in a ligand capable of coordination to one or more metal centres via up to three separate donor sites [2].

In recent years the cobalt clusters $[Co_3(\mu_3\text{-}CR)(CO)_9]$ and in particular the diphosphine-bridged complexes $[Co_3(\mu_3\text{-}CR)(\mu\text{-}L{-}L)(CO)_7]$ (L–L = diphosphine) have received much attention since the diphosphine ligand can stabilize and activate the cluster as a hydroformylation catalyst [3,4]. Our interest in this type of tricobalt system, $Co_3C$, stems from an investigation of the isolobal dimetallic system $Co_2C_2$ [5,6] in complexes of the type $[Co_2(\mu\text{-}C_2R_2)(CO)_6]$ towards multifunctional phosphine ligands [7–10].

In this work we describe the reactions of two tricobalt alkylidyne complexes $[Co_3(\mu_3\text{-}CR)(CO)_9]$ (R = Me **1a**, $CO_2Me$ **1b**) with the vinyl phosphines $PPh_2CH{=}CH_2$ and *cis*-$Ph_2PCH{=}CHPPh_2$ (dppee). In our dicobalt work we have found that the nature of the R groups on the bridging fragment, μ-RCCR, can influence the outcome of reactions [7,8,10]. As a consequence, in this investigation, we have chosen an electron donating (R = Me **1a**) and an electron withdrawing (R = $CO_2Me$ **1b**) R group in the cobalt clusters **1**.

* Corresponding author.

0022-328X/96/$15.00 © 1996 Elsevier Science S.A. All rights reserved
*SSDI* 0022-328X(95)05774-9

## 2. Results and discussion

### 2.1. Reactions of $[Co_3(\mu_3\text{-}CR)(CO)_9]$ (R = Me 1a, $CO_2$Me 1b) with $PPh_2CH{=}CH_2$

The complexes $[Co_3(\mu_3\text{-}CR)(CO)_9]$ (R = Me **1a**, $CO_2$Me **1b**) were heated together with the ligand in heptane at 308 K for 20 h to afford a range of vinyl phosphine substituted complexes, the degree of substitution being influenced by the nature of the R groups. When $[Co_3(\mu_3\text{-}CMe)(CO)_9]$ **1a** was reacted with $PPh_2CH{=}CH_2$ in an approximately 1:1 molar ratio, the products, in order of elution, were $[Co_3(\mu_3\text{-}CMe)(CO)_8(PPh_2CH{=}CH_2)]$ **2a** (37% yield) and $[Co_3(\mu_3\text{-}CR)(CO)_7(PPh_2CH{=}CH_2)_2]$ **3a** (33% yield). On the contrary, reaction of $[Co_3(\mu_3\text{-}CCO_2Me)(CO)_9]$ **1b** with $PPh_2CH{=}CH_2$ in similar proportions gave $[Co_3(\mu_3\text{-}CCO_2Me)(CO)_8(PPh_2CH{=}CH_2)]$ **2b** (5% yield), $[Co_3(\mu_3\text{-}CCO_2Me)(CO)_7(PPh_2CH{=}CH_2)_2]$ **3b** (55% yield) and $[Co_3(\mu_3\text{-}CCO_2Me)(CO)_6(PPh_2CH{=}CH_2)_3]$ **4** (27% yield) (Scheme 1).

All the complexes **2a**, **2b**, **3a**, **3b** and **4** have been characterized by mass spectrometry and by IR, $^1$H, $^{31}$P and $^{13}$C nuclear magnetic resonance (NMR) spectroscopy (Table 1 and Section 4). The mass spectra of complexes **2a**, **2b**, **3a**, **3b** and **4** all exhibit molecular ion peaks and/or peaks corresponding to fragmentation of the molecular ions. The IR spectra in the $\upsilon_{CO}$ region for complexes **2a**, **2b**, **3a**, **3b** and **4** exhibit absorption bands with a similar pattern to those reported for other *mono-*, *bis-* and *tris*-substituted phosphine derivatives of $[Co_3(\mu_3\text{-}CR)(CO)_9]$ **1** [11–14].

The $^1$H NMR spectra at 293 K for the *mono*-substituted **2a** and **2b**, *bis*-substituted **3a** and **3b** and the *tris*-substituted complex **4** display, in addition to phenyl resonances and resonances for the capping groups, three sets of doublets of doublets of doublets (ddd) for the three vinyl protons $H_A$, $H_B$ and $H_C$ (Scheme 1) in the expected 1:1:1 relative intensity ratios. The furthest downfield ddd resonance is attributed to $H_A$, the more upfield signal to $H_B$ and the most upfield signal to $H_C$. The $^{31}$P($^1$H) NMR spectra of **2a**, **2b**, **3a**, **3b** and **4** consist of broad singlet resonances in the range $\delta = -103.1$ to $-117.3$ ppm (relative to $P(OMe)_3$ at 0.0 ppm); these chemical shifts are consistent with phosphine ligands bonded terminally to tricobalt centres [11–15].

On the basis of the above data the structures shown in Scheme 1 are proposed for complexes **2a**, **2b**, **3a**, **3b** and **4**. Note that $H_C$ is *trans* to $H_A$.

### 2.2. Thermolysis of $[Co_3(\mu_3\text{-}CR)(CO)_8(PPh_2CH{=}CH_2)]$ (R = Me 2a, $CO_2$Me 2b)

When the complexes $[Co_3(\mu_3\text{-}CR)(CO)_8(PPh_2CH{=}CH_2)]$ (R = Me **2a**, $CO_2$Me **2b**) are heated in heptane

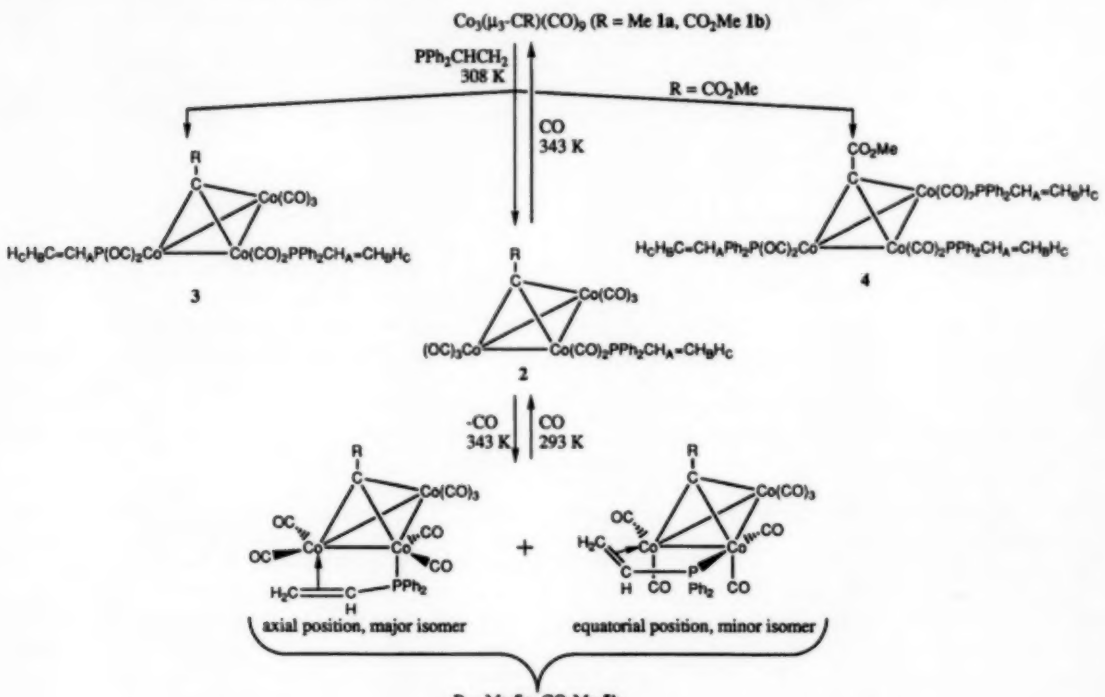


Scheme 1. Products from the reactions of $[Co_3(\mu_3\text{-}CR)(CO)_9]$ (R = Me **1a**, $CO_2$Me **1b**) with $PPh_2CH{=}CH_2$.

at 343 K there is no evidence for P–C bond cleavage within the diphosphine ligand as observed in related complexes [2]. Instead the main products are $[Co_3(\mu_3\text{-}CR)(\mu\text{-}PPh_2CH=CH_2)(CO)_7]$ (R = Me **5a**, $CO_2Me$ **5b**) in yields of 78%–84%. Similar heating of **3a**, **3b** and **4** did not have any effect but in refluxing toluene (384 K) cluster decomposition occurred. Complexes **5a** and **5b** have been characterized by mass spectrometry, IR, $^1H$, $^{31}P$ and $^{13}C$ NMR spectroscopy (Table 1 and Section 4).

The $^1H$ NMR spectra of **5a** and **5b** show clearly that the vinyl group of the phosphine ligand is coordinated

Table 1
IR $^1H$ nuclear magnetic resonance and $^{31}P$ nuclear magnetic resonance data for the complexes

| Compound | $\nu$ (CO) ($cm^{-1}$) [a] | $^1H$ NMR: $\delta$ (ppm) [b] | $^{31}P$ NMR: $\delta$ (ppm) [c] |
|---|---|---|---|
| **2a** | 2076s, 2031vs, 2020vs, 2011vs, 1986m, 1968m, 1878w, 1856w | 7.7–7.2 (m, 10H, Ph), 6.67, (ddd, $^2J(H_AP)$ = 24.3, $^3J(H_AH_C)$ = 17.8 Hz $^3J(H_AH_B)$ = 12.0 Hz, 1H, PC$H_A$=$CH_2$), 6.00 (ddd, $^3J(H_BP)$ = 37.0 Hz, $^2J(H_BH_C)$ = 1.2 Hz 1H, PCH=C$H_B$H), 5.30 (ddd, $^3J$(HCP) = 19.1 Hz, 1H, PCH=CH$H_C$), 3.25 (d, $^4J$(HP) = 0.4 Hz, 3H, Me) | −117.3 (s, $PPh_2CH=CH_2$) |
| **2b** | 2086m, 2047s, 2033s, 2025s, 1981w, 1682w | 7.7–7.3 (m, 10H, Ph), 6.62 (ddd, $^2J(H_AP)$ = 24.8 Hz, $^3J(H_AH_C)$ = 17.7 Hz, $^3J(H_AH_B)$ = 12.0 Hz, 1H, PC$H_A$=$CH_2$), 6.01 (ddd, $^3J(H_BP)$ = 37.6 Hz, $^2J(H_BH_C)$ = 1.2 Hz, 1H, PCH=C$H_B$H), 534 (ddd, $^3J(H_CP)$ = 19.2 Hz, 1H, PCH=CH$H_C$), 3.76 (s, 3H, Me) | −101.6 (s, $PPh_2CH=CH_2$) |
| **3a** | 2049s, 1994vs, 1981s, 1958m, 1944w, 1850w | 7.8–7.2 (m, 20H, Ph), 6.67 (ddd, $^2J(H_AP)$ = 24.5 Hz. $^3J(H_AH_C)$ = 18.0Hz, $^3J(H_AH_B)$ = 12.0 Hz, 2H, PC$H_A$=$CH_2$), 5.94 (ddd, $^3J(H_BP)$ = 35.7 Hz, $^2J(H_BH_C)$ = 1.2 Hz, 2H, PCH=C$H_B$H), 5.24 (ddd, $^3J(H_CP)$ = 19.2 Hz, 2H, PCH=CH$H_C$), 2.70 (t, $^4J$(HP) = 3.2 Hz, 3H, Me) | −104.0 (s, $PPh_2CH=CH_2$) |
| **3b** | 2060s, 2025s, 2012vs, 2001s, 1972m, 1671w | 7.7–7.3 (m, 20H, Ph), 6.64 (ddd, $^2J(H_AP)$ = 25.0 Hz, $^3J(H_AH_C)$ = 17.8 Hz, $^3J(H_AH_B)$ = 12.0 Hz, 2H, PC$H_A$=$CH_2$), 5.93 (ddd, $^3J$(HBP) = 36.4 Hz, $^2J(H_BH_C)$ = 1.3 Hz, 2H, PCH=C$H_B$H), 5.25 (ddd, $^3J$(HCP) = 18.0 Hz, 2H, PCH=CH$H_C$), 3.59 (s, 3H, Me) | −104.0 (s, $PPh_2CH=CH_2$) |
| **4b** | 2045m, 2022m, 2012s, 1988vs, 1967s, 1827w, 1817w | 7.7–7.3 (m, 30H, Ph), 6.71 (ddd, $^2J(H_AP)$ = 24 Hz, $^3J(H_AH_C)$ = 18 Hz, $^3J(H_AH_B)$ = 12 Hz, 3H, PC$H_A$=$CH_2$), 5.89 (ddd, $^3J(H_BP)$ = 36 Hz, $^2J(H_BH_C)$ = 0.8 Hz, 3H, PCH=C$H_B$H), 5.21 (td, $^3J(H_CP)$ = 18 Hz, 3H, PCH=CH$H_C$), 3.18 (s, 3H, Me) | −103.1 (s, $PPh_2CH=CH_2$) |
| **5a** | 2069s, 2016vs, 2003s, 1981m, 1970m | 8.0–7.3 (m, 10H, Ph), 4.3–2.0 (m, 3H, PCH=$CH_2$), 3.50 (s, 3H, Me–minor isomer), 2.89 (d, $^4J$(HP) = 0.9 Hz, 3H, Me–major isomer) | −110.1 (s, $\mu$-$PPh_2CH=CH_2$) |
| **5b** | 2078s, 2034vs, 2014s, 2003m, 1991m, 1679m | 7.9–7.3 (m, 10H, Ph), 4.3–2.8 (m, 3H, PC$H$=$CH_2$), 3.53 (s, 3H, Me–major isomer), 3.46 (s, 3H, Me–minor isomer) | −107.8 (s, $\mu$-$PPh_2CH=CH_2$) |
| **6a** | 2059s, 2020s, 2010vs, 2008vs, 1992s, 1976m, 1970m, 1954w, 1870w, 1828w | 7.8–7.0 (m, 20H, Ph), 2.87 (t, $^4J$(HP) = 2.7 Hz, 3H, Me), olefinic protons masked by phenyl signals | −86.9 (s, $\mu$-$PPh_2CH=CHPPh_2$) |
| **6b** | 2070vs, 2027vs, 2018vs, 2005m, 1992w, 1982m, 1965w, 1671w | 7.6–7.0 (m, 20H, Ph), 3.59 (s, 3H, Me), olefinic protons masked by phenyl signals | −100.1 (s, $\mu$-$PPh_2CH=CHPPh_2$) |

[a] Recorded in *n*-hexane solution.
[b] Chemical shifts $\delta$ relative to $SiMe_4$ (0.0 ppm), coupling constants in $CDCl_3$ at 293 K.
[c] $^{31}P$ chemical shifts relative to external $P(OMe)_3$ (0.0 ppm) (upfield shifts negative), $^1H$ gated decoupled, measured in $CDCl_3$ at 293 K.

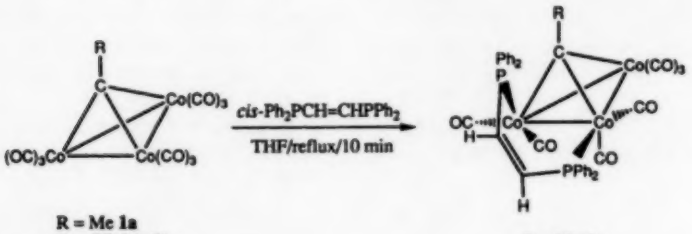


R = Me **1a**
R = $CO_2Me$ **1b**

R = Me **6a**
R = $CO_2Me$ **6b**

Scheme 2. Reactions of complexes **1a** and **1b** with *cis*-$Ph_2PCH{=}CHPPh_2$ (dppee).

rather than free in each case. The vinyl signals, which in the uncoordinated species (**2a**, **2b**, **3a**, **3b** and **4**) appear in the region $\delta = 5$ to 7 ppm, are now shifted upfield to the range $\delta = 2$–4 ppm. Furthermore, two inseparable isomers exist for each complex giving rise in total to six overlapping sets of ddd. There are also phenyl resonances and, for **5a**, a doublet at $\delta = 2.89$ ppm ($^4J$(HP) = 0.9 Hz) due to the methyl protons of the major isomer and a singlet at $\delta = 3.50$ ppm due to the methyl protons of the minor isomer. For **5b** the methyl protons of the major and minor isomers give rise to singlets at $\delta = 3.53$ ppm and $\delta = 3.46$ ppm respectively.

The $^{31}P\{^1H\}$ NMR spectra of complexes **5a** and **5b** both consist of broad singlet resonances at $\delta = -110.1$ ppm (**5a**) and $\delta = -107.8$ ppm (**5b**). The peaks probably consist in each case of overlapping signals arising from the presence of the two isomers.

The $^{13}C\{^1H\}$ NMR spectra at 293 K of **5a** and **5b** reveal the presence of two isomers (in a ratio of 7:3 in each case) most distinctly. For **5a**, the carbonyl ligands of both isomers give rise to only one broad signal while for **5b** two carbonyl resonances are seen. Every other resonance for **5a** and **5b** is observed to consist of two signals owing to the major and minor isomers. As is the case with the proton NMR spectrum, coordination of the vinyl group shifts the vinyl carbon peaks upfield.

On the basis of the above data proposed structures for the two isomers of complexes **5a** and **5b** are shown in Scheme 1. These differ in that in one the coordinated vinyl ligand occupies two equatorial positions whereas in the other it occupies two axial positions. The $^1H$ NMR spectrum of the major isomer of **5a** exhibits a doublet resonance ($^4J$(HP) = 0.9 Hz) for the methyl group on the capping carbon atom, whereas the corre-

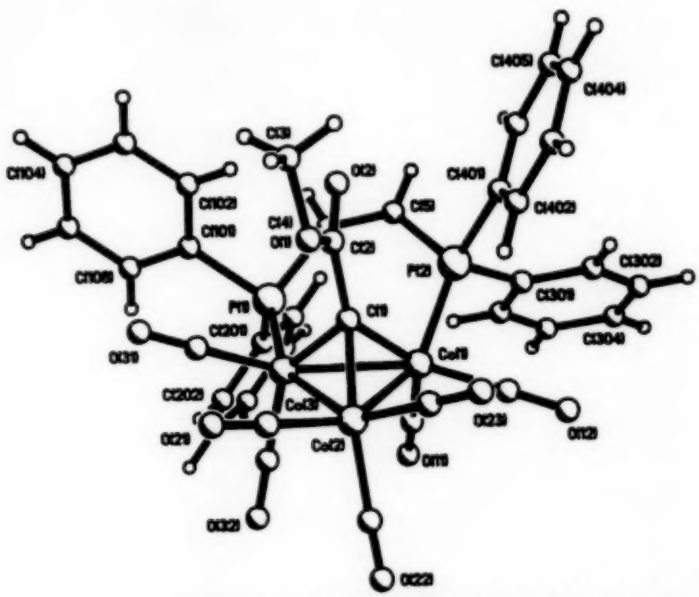


Fig. 1. Molecular structure of $[Co_3(\mu_3\text{-}CCO_2Me)(\mu\text{-}Ph_2PCH{=}CHPPh_2)(CO)_7]$ **6b** including the atom numbering scheme.

Table 2
Bond lengths (ångströms) for the complex $[Co_3(\mu_3\text{-}CCO_2Me)(\mu\text{-}Ph_2PCH{=}CHPPh_2)(CO)_7]$ **6b** with estimated standard deviations in parentheses

| | | | |
|---|---|---|---|
| Co(1)–Co(2) | 2.481(1) | Co(1)–Co(3) | 2.464(1) |
| Co(1)–C(1) | 1.892(6) | Co(1)–C(11) | 1.796(6) |
| Co(1)–C(12) | 1.759(7) | Co(1)–P(2) | 2.166(2) |
| Co(2)–Co(3) | 2.492(1) | Co(2)–C(1) | 1.918(6) |
| Co(2)–C(21) | 1.797(8) | Co(2)–C(22) | 1.809(7) |
| Co(2)–C(23) | 1.793(6) | Co(3)–C(1) | 1.903(5) |
| Co(3)–C(31) | 1.775(7) | Co(3)–C(32) | 1.796(6) |
| Co(3)–P(1) | 2.222(2) | C(1)–C(2) | 1.464(8) |
| C(2)–O(1) | 1.340(7) | C(2)–O(2) | 1.205(8) |
| O(1)–C(3) | 1.453(10) | C(11)–O(11) | 1.141(8) |
| C(12)–O(12) | 1.152(9) | C(21)–O(21) | 1.144(10) |
| C(22)–O(22) | 1.128(10) | C(23)–O(23) | 1.132(7) |
| C(31)–O(31) | 1.144(9) | C(32)–O(32) | 1.128(8) |
| P(1)–C(4) | 1.824(6) | P(1)–C(101) | 1.822(5) |
| P(1)–C(201) | 1.844(4) | C(4)–C(5) | 1.329(8) |
| C(5)–P(2) | 1.810(6) | P(2)–C(301) | 1.841(4) |
| P(2)–C(401) | 1.837(3) | | |

sponding resonance for the minor isomer is a singlet. This suggests that the major isomer is that in which the vinyl phosphine ligand occupies equatorial positions, since similar sized coupling constants of *ca.* 1 Hz have been observed for the methyl resonances of related $[Co_3(\mu_3\text{-}CMe)(\mu\text{-diphosphine})(CO)_7]$ species in which the diphosphine occupies equatorial sites [17].

The vinyl coordination in **5a** and **5b** can be released by purging with CO at 293 K to give **2a** and **2b** respectively. Prolonged heating at 343 K in an atmosphere of CO results in displacement of the $PPh_2CH{=}CH_2$ ligand entirely to give $[Co_3(\mu_3\text{-}CR)(CO)_9]$ (R = Me **1a**, $CO_2Me$ **1b**).

### 2.3. Reaction of $[Co_3(\mu_3\text{-}CR)(CO)_9]$ (R = Me 1a, $CO_2$Me 1b) with *cis*-$Ph_2PCH{=}CHPPh_2$

In order to compare its reactivity with that of the vinyl phosphine $PPh_2CH{=}CH_2$, the ligand *cis*-

Table 3
Bond angles (degrees) for complex $[CO_3(\mu_3\text{-}CCO_2Me)(\mu\text{-}Ph_2PCH{=}CHPPh_2)(CO)_7]$ **6b** with estimated standard deviations in parentheses

| | | | |
|---|---|---|---|
| Co(2)–Co(1)–Co(3) | 60.5(1) | Co(2)–Co(1)–C(1) | 49.8(2) |
| Co(3)–Co(1)–Co(1)–C(1) | 49.7(1) | Co(2)–Co(1)–C(11) | 111.5(2) |
| Co(3)–Co(1)–C(11) | 85.0(2) | C(1)–Co(1)–C(11) | 134.8(3) |
| Co(2)–Co(1)–C(12) | 92.6(2) | Co(3)–Co(1)–C(12) | 152.1(2) |
| C(1)–Co(1)–C(12) | 119.7(3) | C(11)–Co(1)–C(12) | 99.4(3) |
| Co(2)–Co(1)–P(2) | 143.0(1) | Co(3)–Co(1)–P(2) | 111.2(1) |
| C(1)–Co(1)–P(2) | 95.9(2) | C(11)–Co(1)–P(2) | 102.9(2) |
| C(12)–Co(1)–P(2) | 94.7(2) | Co(1)–Co(2)–Co(3) | 59.4(1) |
| Co(1)–Co(2)–C(1) | 48.9(2) | Co(3)–Co(2)–C(1) | 49.0(1) |
| Co(1)–Co(2)–C(21) | 150.5(2) | Co(3)–Co(2)–C(21) | 95.3(2) |
| C(1)–Co(2)–C(21) | 103.8(3) | Co(1)–Co(2)–C(22) | 94.9(2) |
| Co(3)–Co(2)–C(22) | 101.4(2) | C(1)–Co(2)–C(22) | 139.9(3) |
| C(21)–Co(2)–C(22) | 105.7(3) | Co(1)–Co(2)–C(23) | 97.3(2) |
| Co(3)–Co(2)–C(23) | 147.5(2) | C(1)–Co(2)–C(23) | 98.9(3) |
| C(21)–Co(2)–C(23) | 98.5(3) | C(22)–Co(2)–C(23) | 103.0(3) |
| Co(1)–Co(3)–Co(2) | 60.1(1) | Co(1)–Co(3)–C(1) | 49.3(2) |
| Co(2)–Co(3)–C(1) | 49.5(2) | Co(1)–Co(3)–C(31) | 147.1(2) |
| Co(2)–Co(3)–C(31) | 98.3(2) | C(1)–Co(3)–C(31) | 97.9(3) |
| Co(1)–Co(3)–C(32) | 103.1(2) | Co(2)–Co(3)–C(32) | 94.2(2) |
| C(1)–Co(3)–C(32) | 140.6(3) | C(31)–Co(3)–C(32) | 102.9(3) |
| Co(1)–Co(3)–P(1) | 97.6(1) | Co(2)–Co(3)–P(1) | 154.6(1) |
| C(1)–Co(3)–P(1) | 107.5(2) | C(31)–Co(3)–P(1) | 95.6(2) |
| C(32)–Co(3)–P(1) | 103.4(2) | Co(1)–C(1)–Co(2) | 81.2(2) |
| Co(1)–C(1)–Co(3) | 80.9(2) | Co(2)–C(1)–Co(3) | 81.4(2) |
| Co(1)–C(1)–C(2) | 137.1(4) | Co(2)–C(1)–C(2) | 132.6(4) |
| Co(3)–C(1)–C(2) | 123.3(4) | C(1)–C(2)–O(1) | 112.7(5) |
| C(1)–C(2)–O(2) | 126.1(5) | O(1)–C(2)–O(2) | 121.2(5) |
| C(2)–O(1)–C(3) | 114.4(6) | Co(1)–C(11)–O(11) | 177.6(7) |
| Co(1)–C(12)–O(12) | 179.2(6) | Co(2)–C(21)–O(21) | 177.0(6) |
| Co(2)–C(22)–O(22) | 177.7(7) | Co(2)–C(23)–O(23) | 178.3(6) |
| Co(3)–C(31)–O(31) | 179.0(6) | Co(3)–C(32)–O(32) | 174.5(6) |
| Co(3)–P(1)–C(4) | 122.5(2) | Co(3)–P(1)–C(101) | 111.1(1) |
| C(4)–P(1)–C(101) | 97.7(2) | Co(3)–P(1)–C(201) | 117.5(2) |
| C(4)–P(1)–C(201) | 101.4(2) | C(101)–P(1)–C(201) | 103.4(2) |
| P(1)–C(4)–C(5) | 132.3(5) | C(4)–C(5)–P(2) | 128.4(5) |
| Co(1)–P(2)–C(5) | 119.2(2) | Co(1)–P(2)–C(301) | 111.3(1) |
| C(5)–P(2)–C(301) | 100.1(2) | Co(1)–P(2)–C(401) | 118.6(1) |
| C(5)–P(2)–C(401) | 102.8(2) | C(301)–P(2)–C(401) | 102.0(2) |
| P(1)–C(101)–C(102) | 117.3(1) | P(1)–C(101)–C(106) | 122.6(1) |
| P(1)–C(201)–C(202) | 118.2(1) | P(1)–C(201)–C(206) | 121.8(1) |
| P(2)–C(301)–C(302) | 121.2(1) | P(2)–C(301)–C(306) | 118.7(1) |
| P(2)–C(401)–C(402) | 119.9(1) | P(2)–C(401)–C(406) | 120.1(1) |

$Ph_2PCH{=}CH_2PPh_2$ (dppee) was studied. This ligand differs from the vinyl phosphine in that a *cis*-β-hydrogen has been replaced by a phosphino group.

The complexes $[Co_3(\mu_3\text{-}CR)(CO)_9]$ (R = Me **1a**, $CO_2Me$ **1b**) were refluxed for 15 min in THF with one equivalent of dppee to afford $[Co_3(\mu_3\text{-}CR)(\mu\text{-}Ph_2PCH{=}CHPPh_2)(CO)_7]$ (R = Me **6a**, $CO_2Me$ **6b**) in yields of 85%–93% (Scheme 2). Complexes **6a** and **6b** have been characterized by mass spectrometry, microanalysis, IR, $^1H$, $^{31}P$ and $^{13}C$ NMR spectroscopy (Table 1 and Section 4). In addition, complex **6b** has been the subject of a single-crystal X-ray structure determination.

Suitable crystals of **6b** for single-crystal X-ray diffraction analysis were grown by cooling a concentrated pentane solution at 273 K. The molecular structure of $[Co_3(\mu_3\text{-}CCO_2Me)(\mu\text{-dppee})(CO)_7]$ **6b** is depicted in Fig. 1; Tables 2 and 3 list bond lengths and angles respectively and fractional atomic coordinates are given in Table 4. Complex **6b** exists as discrete molecules in the unit cell with no unusually short inter- or intramolecular contacts.

The structure of complex **6b** resembles that of the recently reported $[Co_3(\mu_3\text{-}CPh)(\mu\text{-dppee})(CO)_7]$ in which the capping group is CPh while in **6b** it is $CCO_2Me$ [18]. The structural features of the two complexes are essentially the same with a face-bridging CR group, an edge-bridging *cis*-dppee ligand and terminally bonded carbonyl groups, but there are some noticeable differences. The Co–$\mu_3$-C bond lengths are similar to within 0.026 Å in **6b** while in $[Co_3(\mu_3CPh)(\mu\text{-dppee})(CO)_7]$ a variation of 0.06 Å is observed. The mean value for the non-bridged Co–Co distances in **6b** of 2.487 Å is closely similar to the corresponding value of 2.485 Å in $[Co_3(CPh)(dppee)(CO)_7]$ but longer than the mean value of the Co–Co distances of 2.467 Å in the parent complex $[Co_3(\mu_3\text{-}CMe)(CO)_9]$ **1a** [17]. On the contrary, the shorter bridged Co–Co distance of 2.464(1) Å in **6b** is similar to the mean value for the Co–Co distances for **1a** while slightly shorter than that for the bridged distance in $[Co_3(\mu_3\text{-}CPh)(\mu\text{-dppee})(CO)_7]$ (2.473(2) Å).

Unlike the structure of $[Co_3(\mu_3\text{-}CPh)(\mu\text{-dppee})(CO)_7]$ in which the dppee ligand bridges equatorial sites, some twisting of the dppee ligand in **6b** is observed on its coordination to the Co(1)–Co(3) edge. The phosphorus atom (P(1)) of the ligand and C(31)O(31) bond equatorially to Co(3) while the remaining carbonyl group on Co(3) occupies an axial position. At Co(1), however, all three ligands are twisted round so that P(2) bonds to Co(1) in a nearly axial position from above the $Co_3$ plane (towards the capping group instead of away from it). The two carbonyl groups adopt pseudoequatorial positions but point slightly beneath the $Co_3$ plane instead of slightly above it as is the case at the other two Co atoms. This is most clearly exemplified by the angle Co(1)–Co(3)–P(1) of 97.6(1)° whereas Co(3)–Co(1)–P(2) is 111.2(1)°. Also C(1)–Co(3)–P(1) is 107.5(2)° whilst C(1)–Co(1)–P(2) is 95.9(2)°.

The dppee ligand itself only rarely bridges two metal atoms [18–22]. It is more usual for it to chelate a single metal atom [19,21,22a,23]. The bond lengths within the

Table 4
Atomic coordinates and equivalent isotropic displacement coefficients

| | $x(\times10^4)$ | $y(\times10^4)$ | $z(\times10^4)$ | $U$(eq) ($\times10^3$ Å$^2$) |
|---|---|---|---|---|
| Co(1) | 2616(1) | 7528(1) | 8166(1) | 33(1) |
| Co(2) | 3762(1) | 8207(1) | 6643(1) | 37(1) |
| Co(3) | 1435(1) | 8450(1) | 6747(1) | 35(1) |
| C(1) | 2701(5) | 7173(4) | 6753(4) | 34(2) |
| C(2) | 2678(5) | 6223(4) | 6152(4) | 37(2) |
| O(1) | 3499(5) | 6114(4) | 5316(3) | 69(2) |
| C(3) | 3471(9) | 5203(7) | 4675(6) | 90(4) |
| O(2) | 2013(4) | 5584(3) | 6350(3) | 57(2) |
| C(11) | 1736(6) | 8610(5) | 8949(5) | 52(2) |
| O(11) | 1148(5) | 9275(4) | 9456(4) | 82(2) |
| C(12) | 3971(6) | 7200(5) | 8848(5) | 48(2) |
| O(12) | 4855(5) | 6997(5) | 9300(4) | 80(2) |
| C(21) | 3931(6) | 8488(6) | 5278(6) | 59(3) |
| O(21) | 4070(6) | 8624(6) | 4405(5) | 100(3) |
| C(22) | 3952(6) | 9410(5) | 7269(6) | 55(3) |
| O(22) | 4056(6) | 10146(4) | 7689(5) | 100(3) |
| C(23) | 5243(6) | 7310(5) | 6760(5) | 45(2) |
| O(23) | 6164(5) | 6727(4) | 6850(4) | 69(2) |
| C(31) | 1235(6) | 8515(6) | 5402(6) | 55(3) |
| O(31) | 1093(6) | 8550(6) | 4538(4) | 99(3) |
| C(32) | 1166(6) | 9843(5) | 7090(6) | 53(3) |
| O(32) | 1085(5) | 10721(4) | 7262(6) | 98(3) |
| P(1) | −386(1) | 7990(1) | 7221(1) | 34(1) |
| C(4) | −491(5) | 6725(4) | 7894(5) | 41(2) |
| C(5) | 310(5) | 6045(4) | 8439(4) | 37(2) |
| P(2) | 1860(1) | 6158(1) | 8751(1) | 33(1) |
| C(102) | −789(4) | 6826(3) | 5571(3) | 59(2) |
| C(103) | −1336 | 6646 | 4676 | 78(2) |
| C(104) | −2296 | 7431 | 4309 | 83(2) |
| C(105) | −2710 | 8396 | 4837 | 79(2) |
| C(106) | −2163 | 8575 | 5732 | 55(2) |
| C(101) | −1202 | 7790 | 6098 | 44(1) |
| C(202) | −1743(4) | 10044(3) | 7718(3) | 52(2) |
| C(203) | −2654 | 10799 | 8265 | 64(2) |
| C(204) | −3386 | 10466 | 9094 | 68(2) |
| C(205) | −3208 | 9380 | 9377 | 76(2) |
| C(206) | −2297 | 8625 | 8830 | 58(2) |
| C(201) | −1564 | 8958 | 8000 | 38(1) |
| C(302) | 2467(3) | 5465(3) | 10772(3) | 48(2) |
| C(303) | 2320 | 5525 | 11848 | 63(2) |
| C(304) | 1343 | 6278 | 12325 | 65(2) |
| C(305) | 512 | 6970 | 11727 | 64(2) |
| C(306) | 659 | 6909 | 10651 | 51(2) |
| C(301) | 1637 | 6157 | 10173 | 38(1) |
| C(402) | 3993(3) | 4668(2) | 8005(3) | 53(2) |
| C(403) | 4687 | 3638 | 7788 | 59(2) |
| C(404) | 4178 | 2739 | 8063 | 52(2) |
| C(405) | 2974 | 2869 | 8556 | 51(2) |
| C(406) | 2280 | 3900 | 8774 | 48(2) |
| C(401) | 2790 | 4799 | 8499 | 34(1) |

Equivalent isotropic $U$ defined as one-third of the trace of the orthogonalized $U_{ij}$ tensor

bridging ligand in **6b** are comparable with other examples; thus the C(4)–C(5) double-bond length (1.329(8) Å) is in very good agreement with the value of 1.31(1) observed for $[Co_3(\mu_3\text{-}CPh)(\mu\text{-}dppee)(CO)_7]$ [18].

In the $^1H$ NMR spectra of **6a** and **6b**, in addition to phenyl resonances, signals for the methyl groups are observed at $\delta = 2.87$ ppm (t, $^4J(HP) = 2.7$ Hz) (**6a**) and $\delta = 3.59$ ppm(s) (**6b**). The olefinic resonances of the bridging dppee ligands are not seen but may be masked by the broad phenyl region. In the $^{13}C\{^1H\}$ NMR of **6a** and **6b** at 293 K, triplet resonances are seen for the olefinic carbons of the dppee ligand at $\delta = 146.6$ ppm ($^1J(CP) = {}^2J(CP) = 26$ Hz) and at $\delta = 145.6$ ppm ($^1J(CP) = {}^2J(CP) = 22$ Hz) respectively. Because of the close similarity of the spectroscopic data for **6a** and **6b** it may be assumed that **6a** possesses a similar structure to that of **6b**.

## 3. Conclusions

The outcome of the reactions of the tricobalt alkylidyne complexes $[Co_3(\mu_3\text{-}CR)(CO)_9]$ (R = Me **1a**, $CO_2Me$ **1b**) with the vinylphosphine ligands $PPh_2CH{=}CHL$ (L = H, $PPh_2$) is influenced both by the nature of the R group on the cluster and by the substituent L on the vinyl phosphine. Thus tris substitution of a $Ph_2PCH{=}CH_2$ ligand can be induced only in the case of **1b**. The ligand $Ph_2PCH{=}CH_2$ can bridge two cobalt atoms of the cobalt alkylidyne unit by making use of the vinyl moiety; in principle the *cis*-$Ph_2PCH{=}CHPPh_2$ could also bridge two cobalt atoms in this way but in practice coordination through the second phosphorus atom is more favourable.

## 4. Experimental details

All reactions were carried out under nitrogen using standard Schlenk techniques. Solvents were distilled under nitrogen from appropriate drying agents and degassed prior to use. Preparative thin layer chromatography (TLC) was carried out on commercial Merck plates with a 0.25 mm layer of silica, or on 1 mm silica plates prepared at the University Chemical Laboratory, Cambridge. Column chromatography was performed on Kieselgel 60 (70–230 mesh) or (230–400 mesh). Products are given in order of decreasing $R_f$ values.

The instrumentation used to obtain spectroscopic data has been described previously [24]. All NMR spectra were recorded at 293 K. Unless otherwise stated all reagents were obtained from commercial suppliers and used without further purification. The compounds $[Co_3(\mu_3\text{-}CR)(CO)_9]$ (R = Me **1a**, $CO_2Me$ **1b**) [25,26] were prepared by published methods.

### 4.1. Reaction of $[Co_3(\mu_3\text{-}CR)(CO)_9]$ (R = Me 1a, $CO_2Me$ 1b) with $PPh_2CH{=}CH_2$

(a) The complex $[Co_3(\mu_3\text{-}CMe)(CO)_9]$ **1a** (0.200 g, 0.44 mmol) was dissolved in heptane (50 ml) and $PPh_2CH{=}CH_2$ (0.10 ml, 0.50 mmol) was added. The mixture was stirred at 308 K for 20 h and the solvent then removed under reduced pressure. The residue was dissolved in the minimum quantity of $CH_2Cl_2$ and applied to the base of TLC plates. Elution with hexane–acetone (17 : 3) gave purple $[Co_3(\mu_3\text{-}CMe)(CO)_8(PPh_2CH{=}CH_2)]$ **2a** (0.105 g, 37%), $[Co_3(\mu_3\text{-}CMe)(CO)_7(PPh_2CH{=}CH_2)_2]$ **3a** (0.120 g, 33%) and a trace of an uncharacterized brown complex. Complex **2a**: fast atom bombardment (FAB) mass spectrum, $m/z = 640$ ($M^+$) and $M^+$-$n$CO ($n = 2$–8). NMR ($CDCl_3$): $^{13}C\{^1H\}$ composite pulse decoupled), $\delta =$ 199.7 (s, 8CO), 129.3–123.9 (m, Ph), 124.9 (s, $PC{=}CH_2$) and 39.2 (s, Me) ppm. Complex **3a**: FAB mass spectrum, $m/z = 824$ ($M^+$) and $M^+$-$n$CO($n = 2$–7). NMR ($CDCl_3$): $^{13}C\{^1H\}$ composite pulse decoupled), $\delta = 211.8$ (s, 7CO), 134.3–128.4 (m, Ph), 131.6 (d, $^1J(CP) = 59$ Hz, $PC{=}CH_2$), 128.8 (s, $PCH{=}CH_2$) and 42.2 (s, Me).

(b) The complex $[Co_3(\mu_3\text{-}CCO_2Me)(CO)_9]$ **1b** (0.300 g, 0.60 mmol) and $PPh_2CH{=}CH_2$ (0.14 ml, 0.70 mmol) were treated as in (a) to yield green $[Co_3(\mu_3\text{-}CCO_2Me)(CO)_8(PPh_2CH{=}CH_2)]$ **2b** (0.020 g, 5%), green $[Co_3(\mu_3\text{-}CCO_2Me)(CO)_7(PPh_2CH{=}CH_2)_2]$ **3b** (0.286 g, 55%) and green $[Co_3(\mu_3\text{-}CCO_2Me)(CO)_6(PPh_2CH{=}CH_2)_3]$ **4** (0.173 g, 27%). Complex **2b**: FAB mass spectrum, $m/z = 684$ ($M^+$) and $M^+$-$n$CO ($n = 1$–8). NMR ($CDCl_3$): $^{13}C\{^1H\}$ composite pulse decoupled), $\delta = 201.7$ (s, 8CO), 182.9 (s, $CO_2Me$), 133.9–128.6 (m, Ph), 132.8 (d, $^1J(CP) = 40$ Hz, $PCH{=}CH_2$), 129.9 (s, $PCH{=}CH_2$) and 52.2 (s, Me) ppm. Complex **3b**: FAB mass spectrum, $m/z = 868$ ($M^+$) and $M^+$-$n$CO ($n = 1$–3, 5). NMR ($CDCl_3$): $^{13}C\{^1H\}$ composite pulse decoupled), $\delta = 283.0$ (s, $\mu$-$CCO_2Me$), 205.6 (s, 7CO), 182.4 (s, $CO_2Me$), 134.2–128.3 (m, Ph), 133.3 (m, $PCH{=}CH_2$), 128.8 (s, $PCH{=}CH_2$) and 51.4 (s, Me) ppm. Complex **4**: FAB mass spectrum, $m/z = 1052$ ($M^+$) and $M^+$-$n$CO ($n =$ 1–6). NMR ($CDCl_3$): $^{13}C\{^1H\}$ composite pulse decoupled), $\delta = 272.0$ (s, $\mu$-$CCO_2Me$), 213.2 (s, 6CO), 182.5 (s, $CO_2Me$), 134.3–128.1 (m, Ph), 132.9 (m, $PCH{=}CH_2$), 127.9 (s, $PCH{=}CH_2$) and 50.8 (s, Me) ppm.

### 4.2. Reaction of $[Co_3(\mu_3\text{-}CR)(CO)_9]$ (R = Me 1a, $CO_2Me$ 1b) with dppee

(a) The complex $[Co_3(\mu_3\text{-}CMe)(CO)_9]$ **1a** (0.340 g, 0.75 mmol) was dissolved in THF (50 ml) and *cis*-$Ph_2PCH{=}CHPPh_2$ (0.326 mg, 0.83 mmol) was added.

The mixture was refluxed for 10 min and the solvent then removed under reduced pressure. The residue was then dissolved in the minimum amount of $CH_2Cl_2$ and applied to the base of TLC plates. Elution with hexane–acetone (3 : 2) gave red $[Co_3(\mu_3\text{-}CMe)(\mu\text{-}Ph_2PCH{=}CHPPh_2)(CO)_7]$ **6a** (0.550 g, 93%). Complex **6a** (found: C, 52.74%; H, 3.11%; P, 7.79%. $C_{35}H_{25}Co_3O_7P_2$ requires C, 52.78%; H, 3.16%; P, 7.78%): FAB mass spectrum, $m/z = 796$ ($M^+$) and $M^+$-$n$CO ($n = 1$–7). NMR ($CDCl_3$): $^{13}C$ ($^1H$ composite pulse decoupled), $\delta = 208.9$ (s, 7CO), 146.6 (t, $^1J(CP) = {}^2J(CP)$ 26 Hz, $Ph_2PCH$), 135.5–128.6 (m, Ph) and 43.4 (s, Me) ppm.

(b) The complex $[Co_3(\mu_3\text{-}CCO_2Me)(CO)_9]$ **1b** (0.102 g, 0.20 mmol) and *cis*-$Ph_2PCH{=}CHPPh_2$ (0.087 g, 0.22 mmol) were treated as in (a) to yield dark red $[Co_3(\mu_3\text{-}CCO_2Me)(\mu\text{-}Ph_2PCH{=}CHPPh_2)(CO)_7]$ **6b** (0.146 g, 85%). Complex **6b** (found: C, 51.62%; H, 3.05%; P, 6.83%. $C_{36}H_{25}Co_3O_9P_2$ requires C, 51.44%, H, 3.00%, P, 7.38%): FAB mass spectrum, $m/z = 840$ ($M^+$) and $M^+$-$n$CO ($n = 1$–7). NMR ($CDCl_3$): $^{13}C$ ($^1H$ composite pulse decoupled), $\delta = 204.3$ (s, 7CO), 182.0 (s, $CO_2Me$), 145.3 (t, $^1J(CP) = {}^2J(CP)$ 25 Hz, $Ph_2PCH$), 136.7–128.5 (m, Ph) and 51.4 (s, Me) ppm.

### 4.3. Thermolysis of $[Co_3(\mu_3\text{-}CR)(CO)_8(PPh_2CH{=}CH_2)]$ (R = Me 2a, $CO_2Me$ 2b), $[Co_3(\mu_3\text{-}CR)(CO)_7(PPh_2CH{=}CH_2)_2]$ (R = Me 3a, $CO_2Me$ 3b) and $[Co_3(\mu_3\text{-}CCO_2Me)(CO)_6(PPh_2CH{=}CH_2)_3]$ 4

(a) A solution of the complex $[Co_3(\mu_3\text{-}CMe)(CO)_8(PPh_2CH{=}CH_2)]$ **2a** (0.250 g, 0.39 mmol) in heptane (70 ml) was heated at 343 K for 2 h and the solvent then removed under reduced pressure.

The residue was dissolved in $CH_2Cl_2$ was applied to the base of TLC plates. Elution with hexane–acetone (17 : 3) gave black $[Co_3(\mu_3\text{-}CMe)(\mu\text{-}PPh_2CH{=}CH_2)(CO)_7]$ **5a** (0.187 g, 78%). Complex **5a**: FAB mass spectrum, $m/z = 612$ ($M^+$) and $M^+$-$n$CO ($n = 1$–7). NMR ($CDCl_3$): $^{13}C$ ($^1H$ composite pulse decoupled), $\delta = 204.4$ (s, 7CO), 136.0–128.4 (m, Ph) ppm, minor isomer: 56.2 (d, $^2J(CP) = 6$ Hz, $PCH{=}CH_2$), 44.5 (s, Me) and 35.6 (d, $^1J(CP) = 45$ Hz, $PCH{=}CH_2$) ppm, major isomer: 55.4 (d, $^2J(CP) = 7$ Hz, $PCH{=}CH_2$), 42.0 (s, Me) and 37.2 (d, $^1J(CP) = 43$ Hz, $PCH{=}CH_2$) ppm.

(b) Complex $[Co_3(\mu_3\text{-}CCO_2Me)(CO)_8(PPh_2CH{=}CH_2)]$ **2b** (0.250 g, 0.37 mmol) was treated as in (a) to yield green $[Co_3(\mu_3\text{-}CCO_2Me)(\mu\text{-}PPh_2CH{=}CH_2)(CO)_7]$ **5b** (0.202 g, 84%). Complex **5b**: FAB mass spectrum, $m/z = 656$ ($M^+$) and $M^+$-$n$CO ($n = 1$–7). NMR ($CDCl_3$): $^{13}C$ ($^1H$ composite pulse decoupled), major isomer: $\delta = 204.6$ (s, 7CO), 136.9–128.2 (m, Ph), 180.6 (s, $CO_2Me$), 57.1 (d, $^2J(CP) = 6$ Hz, $PCH{=}CH_2$), 51.7 (s, Me) and 41.8 (d, $^1J(CP) = 42$ Hz, $PCH{=}CH_2$) ppm, minor isomer: $\delta = 201.1$ (s, 7CO), 136.9–128.2 (m, Ph), 181.5 (s, $CO_2Me$), 58.2 (d, $^2J(CP) = 6$ Hz, $PC{=}CH_2$), 51.9 (s, Me) and 42.3 (d, $^1J(CP) = 51$ Hz, $PCH{=}CH_2$) ppm.

(c) Complex $[Co_3(\mu_3\text{-}CMe)(CO)_7(PPh_2CH{=}CH_2)_2]$ **3a** (0.120 g, 0.15 mmol) was treated as in (a) then redissolved in toluene (50 ml) and heated to 383 K but no change was observed.

(d) Complex $[Co_3(\mu_3\text{-}CCO_2Me)(CO)_7(PPh_2CH{=}CH_2)_2]$ **3b** (0.075 g, 0.09 mmol) was treated as in (c) but no change was observed.

(e) Complex $[Co_3(\mu_3\text{-}CCO_2Me)(CO)_6(PPh_2CH{=}CH_2)_3]$ **4** (0.045 g, 0.04 mmol) was treated as in (c) but no change was observed.

### 4.4. Reaction of $[Co_3(\mu_3\text{-}CR)(CO)_8(PPh_2CH{=}CH_2)]$ (R = Me 2a, $CO_2Me$ 2b) with CO

(a) A solution of the complex $[Co_3(\mu_3\text{-}CMe)(CO)_8(PPh_2CH{=}CH_2)]$ **2a** (0.125 g, 0.19 mmol) in heptane (50 ml) was heated to 343 K at 2 h, while CO was bubbled through. Separation by TLC using hexane–acetone (17 : 3) as eluent gave unchanged **2a** and $[Co_3(\mu_3\text{-}CMe)(CO)_9]$ **1a** (0.075 g, 87%).

(b) Complex $[Co_3(\mu_3\text{-}CCO_2Me)(CO)_8(PPh_2CH{=}CH_2)]$ **2b** (0.095 g, 0.14 mmol) was treated as in (a) to yield a trace of **2b** and $[Co_3(\mu_3\text{-}CCO_2Me)(CO)_9]$ (0.052 g, 74%).

### 4.5. Reaction of $[Co_3(\mu_3\text{-}CR)(\mu\text{-}PPh_2CH{=}CH_2)(CO)_7]$ (R = Me 5a, $CO_2Me$ 5b) with CO

(a) A solution of complex $[Co_3(\mu_3\text{-}CMe)(\mu\text{-}PPh_2CH{=}CH_2)(CO)_7]$ **5a** (0.115 g, 0.19 mmol) in heptane (50 ml) was stirred at 293 K for 7 h while CO was bubbled through. Separation by TLC using hexane–acetone (17 : 3) gave $[Co_3(\mu_3\text{-}CMe)(CO)_8(PPh_2CH{=}CH_2)]$ **2a** (0.109 g, 90%) and a trace of $[Co_3(\mu_3\text{-}CMe)(CO)_9]$ **1a**.

(b) Complex $[Co_3(\mu_3\text{-}CCO_2Me)(\mu\text{-}PPh_2CH{=}CH_2)(CO)_7]$ **5b** (0.130 g, 0.20 mmol) was treated as in (a) to yield $[Co_3(\mu_3\text{-}CCO_2Me)(CO)_8(PPh_2CH{=}CH_2)]$ **2b** (0.098 g, 72%) and $[Co_3(\mu_3\text{-}CCO_2Me)(CO)_9]$ **1b** (0.012 g, 12%).

### 4.6. X-ray crystal structure determination of 6b

Suitable crystals of $[Co_3(\mu_3\text{-}CCO_2Me)(\mu\text{-}Ph_2PCH{=}CHPPh_2)(CO)_7]$ **6b** were grown by keeping a concentrated pentane solution at 273 K. A single crystal was mounted on a goniometer head using epoxy resin and transferred to a Siemens R3m/V diffractometer.

*Crystal data*

$C_{36}H_{25}Co_3O_9P_2$, $M = 840.3$, triclinic, space group $P\bar{1}$, $a = 10.936(4)$ Å, $b = 12.699(3)$ Å, $c = 12.979(5)$ Å, $\alpha = 88.20(3)°$, $\beta = 85.22(3)°$, $\gamma = 78.12(2)°$, $U =$

1757.5(10) Å$^3$, $Z = 2$, $D_c = 1.588$ g cm$^{-3}$, $F(000) = 848$, $\mu$(Mo Ka) = 15.39 cm$^{-1}$, $T = 290$ K.

A dark red prism with approximate dimensions 0.20 mm × 0.31 mm × 0.41 mm was used. Accurate cell dimensions were obtained from 25 reflections in the range $20° \leqslant 2\theta \leqslant 25°$. Intensity data were recorded using graphite-monochromated Mo K$\alpha$ radiation ($\lambda$ = 0.71069 Å), and an $\omega$–$2\theta$ scan mode to a maximum $2\theta$ value of 45°. Three standard reflections were monitored every 97 reflections throughout the data collection and showed no significant variation in intensity.

A total of 4723 intensities were measured within the range $-11 \leqslant h \leqslant 11$, $-13 \leqslant k \leqslant 0$, $-13 \leqslant l \leqslant 13$ and averaged to give 4344 unique reflections ($R_{int} = 0.02$) of which 3584 were judged as significant using the criterion $F_{obs} > 4s(F_{obs})$. Corrections for Lorentz and polarization effects were applied. A semiempirical absorption correction based on 323 $\psi$ scan data was applied; minimum and maximum transmission, 0.2553–0.3079. The structure was solved by a combination of direct methods and Fourier difference techniques. The structure was refined by full-matrix least squares with all non-hydrogen atoms assigned anisotropic displacement parameters [27]. Hydrogen atoms were placed in idealized positions and allowed to ride on the relevant carbon atom with a C–H distance of 0.96 Å; each type of H atom was refined with a common isotropic displacement parameter. In the final cycles of refinement a weighting scheme of the form $w^{-1} = s^2(F) + 0.0014F^2$ which gave satisfactory agreement analysis was introduced. The refinement converged to $R = 0.048$ and $R_w = 0.053$; goodness of fit, 1.47. Final atomic coordinates and equivalent isotropic displacement parameters for the non-hydrogen atoms are listed in Table 4.

Additional crystallographic data including hydrogen-atom coordinates, displacement parameters and full lists of bond parameters have been deposited with the Cambridge Crystallographic Data Centre.

## Acknowledgement

We thank the EPSRC (G.A.A. and G.A.S.) for financial support.

## References

[1] (a) X. Morise, M.L.H. Green, P.C. McGowan and S.J. Simpson, *J. Chem. Soc., Dalton Trans.*, (1994) 871. (b) K. Henrick, M. McPartlin, J.A. Iggo, A.C. Kemball, M.J. Mays and P.R. Raithby, *J. Chem. Soc., Dalton Trans.*, (1987) 2669. (c) K. Henrick, J.A. Iggo, M.J. Mays and P.R. Raithby, *J. Chem. Soc., Chem. Commun.*, (1984) 209. (d) W.L. Wilson, J.H. Nelson and N.W. Alcock, *Organometallics, 9* (1990) 1699.

[2] M.I. Bruce, M.L. Williams and A.H. White, *J. Organomet. Chem., 306* (1986) 113. H. Werner and R. Zolk, *Chem. Ber.*, (1987) 1003. K. Yang, J.M. Smith, S.G. Bott and M.G. Richmond, *Organometallics, 12* (1993) 4779.

[3] G. Balavoine, J. Collin, J.J. Bonnet and G. Lavigne, *J. Organomet. Chem., 280* (1985) 429.

[4] J. Collin, C. Jossart and G. Balavoine, *Organometallics, 5* (1986) 203.

[5] F.G.A. Stone, *Angew. Chem., Int. Edn. Engl., 23* (1984) 89.

[6] C. Elschenbroich and A. Salzer, *Organometallics*, VCH, Weinheim, 1989, p. 399.

[7] A.J.M. Caffyn, M.J. Mays, G.A. Solan, D. Braga, P. Sabatino, G. Conole, M. McPartlin and H.R. Powell, *J. Chem. Soc., Dalton Trans.*, (1991) 3103.

[8] A.J.M. Caffyn, M.J. Mays, G.A. Solan, G. Conole and A. Tiripicchio, *J. Chem. Soc., Dalton Trans.*, (1993) 2345.

[9] A.J. Edwards, A. Martí, M.J. Mays, P.R. Raithby and G.A. Solan, *J. Chem. Soc., Chem. Commun.*, (1992), 1416.

[10] M.J. Mays and G.A. Solan, unpublished results.

[11] P.A. Dawson, B.H. Robinson and J. Simpson, *J. Chem. Soc., Dalton Trans.*, (1979) 1762.

[12] K. Hinkelmann, J. Heinze, H.T. Schacht, J.S. Field and H. Vahrenkamp, *J. Am. Chem. Soc., 111* (1989) 5078.

[13] B.H. Robinson and W.S. Tham, *J. Organomet. Chem., 16* (1969) 45.

[14] T.W. Matheson, B.H. Robinson and W.S. Tham, *J. Chem. Soc. A*, (1971) 1457.

[15] A.J. Edwards, A. Martín, M.J. Mays, D. Nazar, P.R. Raithby and G.A. Solan, *J. Chem. Soc., Dalton Trans.*, (1993) 355.

[16] G.A. Acum, M.J. Mays, H.R. Powell, P.R. Raithby and G.A. Solan, *J. Chem. Soc., Dalton Commun.*, (1995), submitted for publication.

[17] P.W. Sutton and L.F. Dahl, *J. Am. Chem. Soc., 89* (1967) 261.

[18] K. Yang, S.G. Bott and M.G. Richmond, *J. Organomet. Chem., 454* (1993) 273.

[19] V.G. Albano, D. Braga, R. Ros and A. Scrivanti, *J. Chem. Soc., Chem. Commun.*, (1985) 866.

[20] M.I. Bruce, O. bin Shawkataly, M.R. Snow and E.R.T. Tiekink, *Aust. J. Chem., 39* (1986) 1109.

[21] M. Bakir, F.A. Cotton, L.R. Falvello, K. Vidyasagar and R.A. Walton, *Inorg. Chem., 27* (1988) 2460.

[21] M. Bakir, F.A. Cotton, L.R. Falvello, C.Q. Simpson and R.A. Walton, *Inorg. Chem., 27* (1988) 4197.

[22] (a) M.G. Richmond and J.K. Kochi, *Organometallics, 6* (1987) 254. (b) M.G. Richmond and J.K. Kochi, *Inorg. Chem.*, (1993) 3682. (c) F.G.A. Stone, *Polyhedron, 8* (1989) 695.

[23] (a) T. Tanase, K. Kawahara, H. Ukaji, K. Kobayashi, H. Yamazaki and Y. Yamamoto, *Inorg. Chem., 32* (1993) 3682. (b) S.A. Brew, J.C. Jeffrey and F.G.A. Stone, *Polyhedron, 8* (1989) 695.

[24] D. Seyferth, J.E. Hallgren and P.L.K. Hung, *J. Organomet. Chem., 50* (1973) 265.

[25] J.J. Eisch and R.B. King (ed.), *Organometallic Syntheses*, Vol. 1, Academic Press, London, 1965.

[26] *Siemens SHELXTL-PLUS Crystallographic System*, release 4.21, Siemens Analytical X-Ray Instruments, Madison, WI, 1991.

ELSEVIER

Journal of Organometallic Chemistry 508 (1996) 147–152

Journal of Organometallic Chemistry

# Katalytische Hydrierung von Halogenmonosilanen mit Tributylzinnhydrid

U. Pätzold, G. Roewer *, U. Herzog

*Institut für Anorganische Chemie, Fakultät für Chemie und Physik, Technische Universität Bergakademie Freiberg, Leipziger Straße 29, D-09596 Freiberg / Sa., Deutschland*

Eingegangen den 18. Mai 1995

**Abstract**

$Bu_3SnH$ is an effective reagent for partial conversion of Si–Cl into Si–H groups. The presented hydrogenation mechanism postulates the coordination of the catalyst (Lewis bases) or the solvent to silicon, giving an intermediate with higher coordinated silicon atom in the first step, followed by the attack of tributyltin hydride by a single electron transfer. This mechanism implies that the intermediate having a hypervalent silicon atom reacts more rapidly than the starting tetracoordinated silane.

**Zusammenfassung**

$Bu_3SnH$ ist effektives Hydriermittel zur partiellen Umwandlung von Si–Cl- in Si–H-Gruppen. Der vorgestellte Hydriermechanismus erfordert die Koordination eines Katalysators (Lewis-Base) oder des Lösungsmittels unter Bildung eines Intermediates mit höher koordiniertem Siliciumatom in einem ersten Schritt. Dieser wird gefolgt von dem Angriff des Tributylzinnhydrids über einen Einelektronen-Transfer-Schritt. Der Mechanismus setzt voraus, daß das Intermediat mit hypervalentem Si-Atom schneller als das Ausgangssilan mit tetravalentem Si-Atom reagiert.

*Keywords:* Silicon; Halogenosilanes; Catalysis; Hydrogenation; Tributylstannane

## 1. Einleitung

Die Umsetzung von Halogensilanen $R_{4-x}SiCl_x$ ($x$ = 1–4; R = Alkyl oder Vinyl) mit salzartigen oder komplexen Hydriden führt in der Regel zu vollständig hydrierten Verbindungen $R_{4-x}SiH_x$. So entsteht bei der Hydrierung von $SiCl_4$ mit $LiAlH_4$ in polaren Lösungsmitteln, wie Tetrahydrofuran (THF) oder Diglyme, ausschließlich $SiH_4$ als Reaktionsprodukt. Auch bei Verwendung eines Unterschusses an Hydriermittel werden keine partiell hydrierten Produkte erhalten.

Eine solche Zielstellung sollte sich durch die Anwendung milderer Reduktionsmittel, wie Organozinnhydride, die seit langem als effektive Hydriermittel in der organischen Chemie bekannt sind, verwirklichen lassen.

D'Errico und Sharp [1–3] beschrieben die Möglichkeiten zur selektiven und schrittweisen Hydrierung von Halogensilanen mit Trimethylstannan in der Gasphase. In den untersuchten Halogensilanen und -disilanen wurden Si–Cl- und Si–Br-Bindungen in Si–H-Funktionen umgewandelt, die Si–Si- und Si–F-Bindungen in den untersuchten Halogendisilanen wurden dagegen nicht angegriffen. Für diese Reaktionen wurde ein unpolarer Vierzentren-Übergangszustand postuliert. Ein Radikalkettenmechanismus wurde ausgeschlossen, da der Reaktionsverlauf nicht durch zugesetzte Radikalfänger beeinflußt wird.

Eigene Untersuchungen an Halogenmono- und -disilanen ergaben, daß deren Hydrierung mit Tributylstannan durch Lewis-Basen katalysiert werden kann [4,5]. In einer einstufigen Synthese sind auf diesem Weg auch partiell hydrierte Silane erhältlich. Effektivität und Selektivität der Hydrierreaktion

$$R_{4-x}SiCl_x + yBu_3SnH \longrightarrow R_{4-x}SiH_yCl_{x-y} + yBu_3SnCl \quad (1)$$

* Corresponding author.

0022-328X/96/$15.00 © 1996 Elsevier Science S.A. All rights reserved
*SSDI* 0022-328X(95)05847-8

lassen sich durch Auswahl von Lösungsmittel und Katalysator (Lewis-Base) gezielt beeinflussen. Im folgenden sollen charakteristische Hydrierergebnisse und aufgefundene Zusammenhänge zu den gewählten Reaktionsbedingungen vorgestellt werden.

## 2. Ergebnisse und Diskussion

### 2.1. Hydrierung von Siliciumtetrachlorid

#### 2.1.1. Einfluß des Lösungsmittels.

Bei der lösungsmittelfreien Reaktion von $SiCl_4$ mit $Bu_3SnH$ ist eine mit geringer Effektivität ablaufende Trichlorsilanbildung zu beobachten. Sie verläuft offensichtlich auf einem radikalischen Reaktionsweg, der durch aus dem homolytischen Zerfall von $Bu_3SnH$ resultierende Radikale initiiert wird.

In unpolaren Lösungsmitteln, wie Aromaten und Kohlenwasserstoffen, findet keine Hydrierreaktion statt bezeihungsweise sie springt nicht an. Wahrscheinlich werden Käfigeffekte wirksam und/oder Startradikale abgefangen. Der Hydrierprozeß läßt sich in den genannten Lösungsmitteln aber mit Radikalstartern (AIBN oder Dibenzoylperoxid) initiieren. Hauptsächlich entsteht jeweils das monohydrierte Produkt $SiHCl_3$. Die Menge der erhaltenen Hydrierprodukte ist von der Reaktionstemperatur und von der Art und der Konzentration der Startradikale abhängig. Ein ähnlicher Reaktionsverlauf war in wenig polaren Ethern, z.B. 1,4-Dioxan, Anisol und Dibenzylether, die aber im Vergleich zu aliphatischen Kohlenwasserstoffen oder Toluen leichter mit Radikalen unter H-Abstraktion reagieren sollten, zu registrieren.

Im Gegensatz zu den ionischen oder komplexen Hydriden sind Organozinnhydride in den meisten organischen Lösungsmitteln sehr gut löslich beziehungsweise mit ihnen vollständig mischbar. Dies ermöglicht die Untersuchung des Einflusses von Solventien, die sich in ihren Eigenschaften sehr stark voneinander unterscheiden. Bezüglich ihrer Wirkung auf die Hydrierung von $SiCl_4$ mit $Bu_3SnH$ lassen sich die untersuchten Lösungsmittel in vier Gruppen einteilen (Tabelle 1). Unpolare Lösungsmittel mit geringen H-Donor-Eigenschaften sind grundsätzlich inaktiv. Radikalisch verlaufende Prozesse, die bei der $SiCl_4$-Hydrierung Trichlorsilan als Hauptprodukt liefern, sollten in einer Gruppe wenig polarer Ether zu finden sein.

Einen grundsätzlich anderen Verlauf nimmt die Hydrierung in polaren Lösungsmitteln, z.B. THF, Polyether, Nitrile oder Hexamethylphosphorsäueretriamid (HMPT). Der Reaktionsmechanismus sollte in diesen Fällen durch die Beteiligung ionischer Species und/oder Elektronenübertragungsschritte bestimmt sein, da der zeitliche Reaktionsverlauf dem der Hydrierung mit $LiAlH_4$ (in THF oder Diglyme) analog ist. Die Verwendung von polaren Lösungsmitteln führt zu einem Gemisch von Hydrierprodukten. Mit steigender Polarität und Donorstärke des Lösungsmittels wird $SiH_4$ immer mehr zum bevorzugten Hydrierprodukt. Durch einen Überschuß an $Bu_3SnH$ kann $SiH_4$ selektiv erhalten werden.

Tabelle 1
Lösungsmitteleinfluß auf die Hydrierung von $SiCl_4$ mit $Bu_3SnH$

| LM-Gruppe | DN [a] | AN [b] | $\mu$ (D) | DK |
|---|---|---|---|---|
| keine Hydrierung | 0–3 [c] | 0–3 | 0–1.2 | 1.9–3.1 |
| bevorzugt $SiHCl_3$ | 3–15 | 8–11 | 0.4–1.6 | 2.2–5.6 |
| alle Hydrierprodukte | 12–39 | 8–19 | 1.7–5.6 | 5.8–35.9 |
| alle Hydrierprodukte, Addukte | ≈ 30 | 2–19 | 1.0–4.0 | 2.4–23.6 |

[a] Donorzahl nach Gutmann [6] und Reichhardt [7].
[b] Akzeptorzahl nach Gutmann [6] und Reichhardt [7].
[c] Ausnahmen sind die Lösungsmittel Dibutyl- und Dibenzylether (DN, 18 beziehungsweise 19), für die die Donorzahlen allerdings nicht kalorimetrisch bestimmt, sondern berechnet wurden.

Lösungsmittel mit großer Donorstärke, aber geringerer Polarität (z.B. tert-Amine), bilden feste Addukte mit $SiCl_4$, woraus aber keine nachteiligen Wirkungen auf den Hydrierprozeß resultieren.

Im Falle der Verwendung von Acetonitril als Lösungsmittel entsteht ein zweiphasiges System ($Bu_3SnH$–MeCN + $SiCl_4$), in dem die Hydrierreaktion an der Phasengrenze stattfindet. Als bevorzugtes Hydrierprodukt wurde Trichlorsilan (neben Dichlorsilan) erhalten.

#### 2.1.2. Lewis-Basen als Katalysatoren der Hydrierung von Chlorsilanen.

Der Zusatz von quaternären Ammonium- und Phosphoniumhalogeniden als Katalysatoren zu einer $SiCl_4$–Tributylstannan-Lösung in einem inaktiven Lösungsmittel, wie Toluen, führt zur bevorzugten Bildung von $SiH_4$. Die katalytische Aktivität dieser Salze hängt generell nicht von der Art der organischen Reste am N- oder P-Atom ab. Die Verbindung $[(Ph_3P)_2N]^+Cl^-$ erbrachte beispielsweise die gleichen katalytischen Effekte wie Tetraalkylammoniumhalogenide. Dies bestätigte die Vermutung, daß die Halogenidionen die eigentlich katalytisch wirksamen Species sind. Die Ergebnisse korrelieren mit den bekannten Donorzahlen für die Halogenidionen [8]. Die angegebenen Werte für $Cl^-$, $Br^-$ und $I^-$ (DN, 36.2, 33.7 und 28.9) liegen in der selben Größenordnung wie für starke Donorlösungsmittel, in denen die Hydrierung bevorzugt zum vollständig hydrierten Produkt $SiH_4$ verläuft.

Verschiedene Stickstoff- und Phosphorverbindungen, wie Amine, Stickstoffheterocyclen, 1,4-Diaza-buta-1,3-diene (DAD), Phosphane und Phosphite, zeigen in Korrelation zu ihren elektronischen Strukturen eine abgestufte Katalysatorwirkung.

### 2.2. Stickstoff-Verbindungen

Mit steigender Basizität der Liganden erhöht sich prinzipiell die Reaktionsgeschwindigkeit, und $SiH_4$ wird immer mehr zum bevorzugten Hydrierprodukt. Die Basizität der Liganden kann zum Abschätzen der katalytischen Wirksamkeit dieser Verbindungen herangezogen werden. Allerdings läßt sich der Vergleich der Katalysatoren nicht durchgängig über die verschiedenen Verbindungsklassen hinweg führen. Beispielsweise zeigen Pyrazin und Diphenylamin, trotz ähnlicher Basizität ($pK_a = 0.61$ und 0.79), eine unterschiedliche katalytische Aktivität (Tabelle 2). Neben der Basizität müssen deshalb weitere elektronische und sterische Eigenschaften der Katalysatoren zur Beschreibung ihrer Effekte herangezogen werden.

Die Hydrierung von $SiCl_4$ wird auch durch DAD katalysiert. In allen Fällen wurde ein Gemisch von Hydrierprodukten erhalten. Über die Variation der organischen Reste ($R_1$ und $R_2$) gelingt die Veränderung der katalytischen Aktivität dieser Verbindungen. Gruppen mit einem +I-Effekt (Cyclohexyl oder tert-Butyl), die eine hohe Elektronendichte an den Stickstoffatomen erzeugen, ergeben auch einen hocheffektiven Katalysator für die $SiH_4$-Bildung (Abb. 1). Dagegen entsteht beim Einsatz der phenylsubstituierten Verbindung selektiv $SiHCl_3$.

Interessant erscheint auch ein Vergleich ein- und zweizähniger Stickstoffliganden. Gemessen an den Basizitätskonstanten von α,α'-Bipyridyl (bipy) und 1.10-Phenanthrolin (phen) ($pK_a = 4.50$ und 4.98 [9]) wäre eine mit Chinolin vergleichbare katalytische Aktivität

1.4-Diaza-buta-1.3-diene

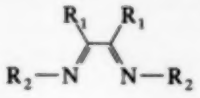


Verringerung der katalytischen Aktivität →

$R_1$ = H; $R_2$ = Cyh; $^t$Bu; $^s$Bu; Ph
$R_1$ = Me; $R_2$ = $^n$Pr; Bz; Ph
$R_2$ = Ph; $R_1$ = H; Me; Ph

Abb. 1. Katalytische Aktivität der DAD.

zu erwarten. Die beobachtete Aktivität ist im Falle der zweizähnigen Liganden aber wesentlich niedriger. Diese Effekte können durch die Bildung der oktaedrischen Komplexe $SiCl_4^*$ bipy und $SiCl_4^*$ phen hervorgerufen werden. Während Verbindungen mit pentakoordiniertem Si-Atom in jedem Falle sehr viel reaktiver als die entsprechenden tetrakoordinierten sind, ist das Verhalten von Species, in denen das Si-Atom die Koordinationszahl 6 aufweist, uneinheitlich [10]. Generell sollten für nukleophile $S_N2$-Reaktionen, die über Übergangszustände mit einem heptakoordinierten Si-Atom verlaufen, die sterischen Verhältnisse eine wichtige Rolle spielen.

### 2.3. Phosphor-Verbindungen

Für Phosphor(III)-liganden erweist sich der von Tolman [11] für die Charakterisierung der Donor- und Akzeptoreigenschaften eingeführte elektronische Parameter $\chi$ als eine geeignete Leitgröße zur Abschätzung der katalytischen Aktivität der Phosphorliganden [12,13]. Eine eindeutige Korrelation der Donoreigenschaften mit den katalytischen Effekten wurde beobachtet, d.h. mit

Tabelle 2
Wirkung von N-Lewis-Basen auf die $SiCl_4$-Hydrierung in Toluen

| Amine | $pK_a$ | *N*-Heterocyclen | $pK_a$ | Hydrierergebnis |
|---|---|---|---|---|
| Tributylamin | 10.89 | | | bevorzugt $SiH_4$ und $SiHCl_3$, Adduktbildung |
| TMEDA | 9.14 | | | bevorzugt $SiH_4$ und $SiHCl_3$, Adduktbildung |
| DABCO | 8.77 | *N*-Methylimidazol | 7.13 | bevorzugt $SiH_4$ und $SiHCl_3$, Adduktbildung |
| *N,N*-Dimethylanilin | 5.10 | Pyridin | 5.25 | bevorzugt $SiH_4$ und $SiHCl_3$, Adduktbildung |
| | | Chinolin | 4.94 | bevorzugt $SiH_4$ und $SiHCl_3$, Adduktbildung |
| | | Pyrimidin | 2.33 | $SiHCl_3$ und $SiH_2Cl_2$ (15%) |
| | | Pyridazin | 1.55 | selektiv $SiHCl_3$ |
| | | Pyrazin | 0.61 | selektiv $SiHCl_3$ |
| Diphenylamin | 0.79 | | | keine Hydrierung |
| Triphenylamin | < 0 | | | keine Hydrierung |

Tabelle 3
Wirkung von P-Lewis-Basen auf die $SiCl_4$-Hydrierung

| P-Ligand | elektronische Parameter $\chi$ nach Tolman | Basizität ($pK_a$) | Hydrierprodukte (in Toluen, $Bu_3SnH : SiCl_4 = 1:1$) |
|---|---|---|---|
| $PCyh_3$ | 1.40 | 9.70 | Hauptprodukt $SiH_4$, wenig $SiHCl_3$ |
| $PBu_3$ | 5.25 | 8.43 | Hauptprodukt $SiH_4$, wenig $SiHCl_3$ |
| $P(O^iPr)_3$ | 6.35 | 4.10 | Hauptprodukte $SiH_4$ und $SiHCl_3$, wenig $SiH_2Cl_2$ |
| $PMe_2Ph$ | 10.60 | 6.50 | Hauptprodukte $SiH_4$ und $SiHCl_3$, wenig $SiH_2Cl_2$ |
| $PPh_3$ | 13.25 | 2.73 | Hauptprodukt $SiHCl_3$, wenig $SiH_4$ und $SiH_2Cl_2$ |
| $P(OMe)_3$ | 24.10 | 2.60 | Hauptprodukt $SiHCl_3$, wenig $SiH_2Cl_2$, Spur $SiH_3Cl$ |
| $P(OPh)_3$ | 30.20 | −2.0 | Hauptprodukt $SiHCl_3$, wenig $SiH_2Cl_2$ |

Erhöhung der Donorstärke der Katalysatoren wird $SiH_4$ immer mehr zum Hauptprodukt (Tabelle 3). Die Darstellung partiell hydrierter Silane gelingt nur bei Verwendung schwach basischer Phosphane oder von Phosphiten.

### 2.4. Hydrierung von Methylchlorsilanen

Neben der Basizität der Katalysatoren bestimmt die Akzeptorstärke der Chlorsilane den Verlauf der Hydrierung. Die Reaktivität der Chlorsilane gegenüber Tributylstannan nimmt in der Reihe $SiCl_4 > MeSiCl_3 > Me_2SiCl_2 > Me_3SiCl$ ab. Diese Tendenz steht in Übereinstimmung mit der abnehmenden Akzeptorstärke der Methylchlorsilane. Nur starke Lewis-Basen, wie *N*-Methylimidazol (NMI), HMPT oder die Halogenidionen katalysieren beispielsweise die Hydrierung von $Me_3SiCl$. Die schwächeren Wechselwirkungen der Methylchlorsilane mit den Katalysatorbasen im Vergleich zu $SiCl_4$ werden auch dadurch dokumentiert, daß nur selten feste Addukte Methylchlorsilan–Katalysator entstehen. Die Tabelle 4 zeigt einen Vergleich der Hydrierergebnisse der Methylchlorsilane sowie des $SiCl_4$ bei Einsatz verschiedener Katalysatoren. Die gefundene Abstufung der Aktivität der Lewis-Basen als Hydrierkatalysatoren ist vergleichbar mit der Effektivität als Silylierungsreagenzien ($Me_3SiCl$–Lewis-Base) [14].

Auch Vinyltrichlorsilan ließ sich nach Zugabe von Lewis-Basen leicht hydrieren. Dabei wurden die gewünschten Produkte $ViSiH_xCl_{3-x}$ erhalten. Nebenreaktionen, wie die Hydrierung der Vinylgruppe oder eine Polymerisation, wurden nicht beobachtet.

### 2.5. Reaktionsmechanismus

Durch Radikalstarter kann prinzipiell eine $SiCl_4$-Hydrierreaktion zu $SiHCl_3$ initiiert werden, wie die eigenen Untersuchungen mit AIBN- oder DBPO-Zusatz gezeigt haben. Die Lewis-Base-katalysierte Reaktion der Chlorsilane mit $Bu_3SnH$ sollte aber weder über den von D'Errico und Sharp [1] postulierten unpolaren Vierzentrenübergangszustand noch über radikalische Schritte verlaufen.

Die eigenen Ergebnisse stehen im Einklang mit einem Hydriermechanismus, der durch folgende wesentliche Schritte geprägt wird:

$$D: + SiCl_4 \longrightarrow D{-}SiCl_4 \quad (2)$$

$$D{-}SiCl_4 + Bu_3SnH \longrightarrow [D{-}SiCl_4^-, Bu_3SnH^+] \quad (3)$$

$$[D{-}SiCl_4^-, Bu_3SnH^+] \longrightarrow D{-}SiHCl_3 + Bu_3SnCl \quad (4)$$

Die Katalysator–Lewis-Base koordiniert zunächst am Si-Atom im Chlorsilan über eine Donor–Akzeptor-Wechselwirkung, denn das Tributylzinnhydrid hat im Vergleich mit den Chlorsilanen wesentlich schwächer ausgeprägte Elektronenpaar-Akzeptor-Eigenschaften (Gl. (2)). Das heißt eine primäre Aktivierung der Sn–H-Bindung, die eine Verstärkung des hydridischen Charakters des Wasserstoffatoms zur Folge hätte, kann unter den eingestellten Reaktionsbedingungen ausgeschlossen werden.

Die Stärke der Wechselwirkungen zwischen dem Chlorsilan und der Lewis-Base variiert in Abhängigkeit von der Donorstärke der Katalysatoren und der Akzeptorstärke der Chlorsilane über einen weiten Bereich. Die Base-Addukte können in Lösung entweder weitgehend dissoziiert oder molekular vorliegen. In den Addukten sind die Si–Cl-Bindungen gegenüber den freien Chlorsilanen aufgeweitet. Die Neigung zur Bildung des Donor–Akzeptor-Komplexes ist in erster Linie von der σ-Donizität der Lewis-Basen, deren sterischen Eigenschaften, unter anderem der Möglichkeit zur Chelatbildung, sowie von der Akzeptorstärke des Chlorsilans abhängig. Im Einklang damit können der elektronische Ligandenparameter $\chi$ für Phosphor(III)-Verbindungen, die Basenstärke von *N*-Donor-Verbindungen und die Donorzahl der Lösungsmittel als Kriterien für die Abschätzung der katalytischen Aktivität verwendet werden. Die Koordination der Liganden führt zur Bildung von Verbindungen, in denen das Si-Atom penta- oder hexakoordiniert vorliegt. Eine wesentliche Voraussetzung für die Hydrierung besteht damit in der Aktivierung der Si–Cl-Bindung durch die Donor–Akzeptor-Wechselwirkung des Katalysators mit dem Chlorsilan, in die auch das Lösungsmittel einbezogen werden kann.

Tabelle 4
Ausgewählte Hydrierergebnisse an Methylchlorsilanen

| Katalysator | $SiCl_4$ | $MeSiCl_3$ | $Me_2SiCl_2$ | $Me_3SiCl$ |
|---|---|---|---|---|
| $PPh_3$ | Hauptprodukt $SiHCl_3$ | keine Reaktion | keine Reaktion | keine Reaktion |
| $PCyh_3$ | Hauptprodukt $SiH_4$ | alle Hydrierprodukte | alle Hydrierprodukte | keine Reaktion |
| $P(NEt_2)_3$ | Hauptprodukt $SiH_4$, Adduktbildung | alle Hydrierprodukte, Adduktbildung | alle Hydrierprodukte, Adduktbildung | keine Hydrierung, Adduktbildung |
| $Ph_4PBr$ | Hauptprodukt $SiH_4$ | Hauptprodukt $MeSiH_3$ | Hauptprodukt $Me_2SiH_2$ | $Me_3SiH$ (Spur) |
| HMPT | Hauptprodukt $SiH_4$ | Hauptprodukt $MeSiH_3$ | Hauptprodukt $Me_2SiH_2$ | $Me_3SiH$ |
| NMI | Hauptprodukt $SiH_4$, Adduktbildung | Hauptprodukt $MeSiH_3$, Adduktbildung | Hauptprodukt $Me_2SiH_2$, Adduktbildung | $Me_3SiH$, Adduktbildung |

Die eigentliche Hydrierreaktion erfolgt an den Species mit hypervalentem Si-Atom (Gl. (3)). Für den Cl–H-Austausch kann generell sowohl ein Elektronentransfer- als auch ein Hydridtransfer-Mechanismus diskutiert werden. Da aber die Hydrierung auch in unpolaren Medien durch bestimmte Katalysatoren zur Bildung der vollständig hydrierten Produkte stimuliert wird, müssen Prozesse, die über die Bildung von freien Ionen verlaufen, als wenig wahrscheinlich angesehen werden. Damit in Übereinstimmung sind auch die für die Hydrierung von $Me_3SiCl$ und $ClMe_2Si–SiMe_2Cl$ [5] mit $Bu_3SnH$–$Bu_3SnD$ ermittelten kinetische Isotopieeffekte $k_H/k_D$ mit einem Wert von ungefähr 1. Bei einem direkten Hydridtransfer sollte ein stark von 1 abweichender Wert auftreten.

Kochi hat an einer Reihe von Substitutionsreaktionen die Möglichkeit eines von Organozinnhydriden ausgehenden Elektronentransfers aufgezeigt [15]. Die Fähigkeit zur Aufnahme eines Elektrons wird wesentlich durch das Reduktionspotential bzw. die energetische Lage des "lowest unoccupied molecular orbital" (LUMO) im Donor–Akzeptor-Komplex bestimmt. Von Bedeutung ist weiterhin, wie stark das vom Stannan übertragenen Elektron im entstandenen Anionenradikal $D–SiCl_4^-$ delokalisiert werden kann. Wie *ab-initio*-Berechnungen zeigten [16], wird durch die Komplexbildung die Energie des LUMO gegenüber dem freien Chlorsilan deutlich abgesenkt ($E_{LUMO}(SiCl_4) = 3.55$ eV bzw. $E_{LUMO}(SiCl_4^{\bullet}DAD) = -0.46$ eV). Als Ligand wurde für die Berechnungen Glyoxaldiimin HN=CH–CH=NH ausgewählt.

Außerdem ist das Anionenradikal $SiCl_4^{\bullet}DAD^-$ stabiler also $SiCl_4^-$, d.h. die Species mit höher koordiniertem Si-atom dürften leichter reduzierbar sein als die Moleküle mit tetravalentem Si-Atom. Die katalytische Wirkung der Lewis-Base dokumentiert sich außer der Aktivierung der Si–Cl-Bindung in einer Begünstigung der Elektronenaufnahme und in der Stabilisierung der Anionenradikale.

Im, durch den Elektronentransfer vom Alkylstannan zum Katalysator–Silan-Komplex, gebildeten Radikalionenpaar ist das Radikalanion vermutlich durch die Katalysator–Lewis-Base stabilisiert (Gl. (4)). Das Radikalionenpaar reagiert in einem Lösungsmittelkäfig weiter zum Hydrierprodukt und $Bu_3SnCl$. Die Art der entstehenden Hydrierprodukte wird sowohl von der Donorstärke des Katalysators als auch der Akzeptorstärke des Chlorsilans bestimmt. Da die Akzeptorstärke in der Reihe $SiCl_4 \cdots SiH_4$ abnimmt, sind die Wechselwirkungen der Lewis-Base mit den Hydrierprodukten jeweils schwächer, als mit dem Start-Chlorsilan. Mit stark basischen Katalysatoren sind auch die Addukte bzw. Übergangszustände wasserstoffhaltiger Chlorsilane lange genug stabil. Da der Angriff des Alkylstannans bevorzugt an den Species mit hypervalentem Si-Atom erfolgt, können in einer schnellen Folge von Reaktionen mit $Bu_3SnH$ mehrfach hydrierte Produkte entstehen. Die Addukte mit schwächeren Katalysator–Lewis-Basen zerfallen dagegen schon nach dem ersten Hydrierschritt. So wird beispielsweise $SiHCl_3$ zum bevorzugten Produkt der $SiCl_4$-Hydrierung.

Die Hydrierung mit $Bu_3SnH$ läßt sich auch an $Si_2Cl_6$ und Methylchlordisilanen durchführen. Dabei ist zu beachten, daß Silylsubstituenten die Akzeptorstärke von Si-Atomen beträchtlich erhöhen. Dies ermöglicht die Katalyse der Hydrierung auch mit schwachen Lewis-Basen. Mit den katalytisch am stärksten wirksamen Basen tritt hier in Konkurrenz zur Hydrierung eine Disproportionierung des Disilans auf [17].

Die Hydrierung von Chlorsilanen mit $Bu_3SnH$ erwies sich als ein flexibler Zugangsweg zu teilhydrierten Produkten. Durch Auswahl geeigneter Lösungsmittel oder Katalysatoren kann die Reaktion auf die gewünschten Produkte hin optimiert werden. Verbindungen, die mehrere funktionelle Gruppen enthalten ($ViSiCl_3$), können selektiv mit $Bu_3SnH$ hydriert werden. Die durchgeführten Untersuchungen zeigten, daß $Bu_3SnH$ durch komplexe Hydride ($LiAlH_4$), aber unter bestimmten Bedingungen auch durch NaH, und katalytische Mengen $Bu_3SnCl$ ersetzt werden kann. Solche Systeme führen prinzipiell zu den gleichen Hydrierergebnissen. Das bei der Hydrierung gebildete $Bu_3SnCl$ ist auch über eine Umsetzung mit NaH in Polyethern wieder in $Bu_3SnH$ überführbar, so daß prinzipiell das Stannan im Kreislauf geführt werden kann [18].

## 3. Experimentelles

Chemikalien und Lösungsmittel waren handelsübliche Produkte meist der Fa. Merck. $Bu_3SnH$ wurde ohne vorherige Reinigung verwendet (das enthaltene $Bu_6Sn_2$ hatte keinen Einfluß auf die Reaktion). Die Lösungsmittel und Katalysatoren wurden vor dem Einsatz gereinigt und getrocknet. Die Diazadiene wurden durch Umsetzung der entsprechenden Amine mit α-Dicarbonyl-Verbindungen synthetisiert.

### *3.1. Hydrierversuche*

Die Versuche wurden unter anaeroben Bindingungen durchgeführt. Jeweils 6.6 mmol $Bu_3SnH$ wurden im betreffenden Lösungsmittel vorgelegt (ungefähr 25%ige Lösung). Das Molverhältnis Stannan: Chlorsilan betrug, wenn nicht anders angegeben, immer 1:1. Im Falle der $SiCl_4$-Hydrierung entspricht dies einem H:Cl-Verhältnis von 1:4. Die eingesetzte Katalysatormenge betrug gewöhnlich 1/50 der Molzahl des eingesetzten Chlorsilans. Durch die Reaktionsmischung wurde ein konstanter Wasserstoffstrom geleitet, der die entstandenen Reaktionsprodukte zum on-line gekoppelten Gaschromatografen (Chromatron GCFH 18.3, gepackte Säule,

Porolith mit 15% FS16 (Trifluorpropylsilicon)) spülte. Über eine Gasprobenschleife wurde in zeitlichen Intervallen von 3–5 min die Zusammensetzung der Gasphase über der Reaktionsmischung bestimmt. Auf diese Weise war es möglich, den zeitlichen Verlauf der Hydrierreaktion zu erfassen.

### 3.2. Analytik

Die Produktanalyse erfolgte weiterhin mittels $^{1}H$-, $^{13}C$-, $^{29}Si$, $^{31}P$- und $^{119}Sn$-NMR an einem Bruker MSL 300. Entstandene feste Addukte wurden mittels IR-Spektroskopie an einem Nicolet-FT-IR-Spektrometer oder Röntgendiffraktometrie an einem TuR M62-Gerät der Fa. Philips charakterisiert.

## Literatur

[1] J.J. D'Errico und K.G. Sharp, *Inorg. Chem., 28* (1989) 2177.
[2] J.J. D'Errico und K.G. Sharp, *Inorg. Chem., 28* (1989) 2886.
[3] J.J. D'Errico und K.G. Sharp, *US Pat. 4798713*, 1989.
[4] U. Pätzold, *BA Dissertation*, Freiberg 1995.
[5] U. Herzog, G. Roewer und U. Pätzold, *J. Organomet. Chem., 494* (1995) 143.
[6] V. Gutmann, *Angew. Chem., 82* (1970) 858.
[7] C. Reichhardt, *Solvent and Solvent Effects in Organic Chemistry*, VCH, Weinheim 1990, 17ff.
[8] W. Linert, R.F. Jameson und A. Taha, *J. Chem. Soc., Dalton Trans.*, (1993) 3181.
[9] P. Thomas, M. Benedix und H. Hennig, *Z. Chem., 17* (1977) 115.
[10] C. Chuit, R.J.P. Corriu, C. Reye und J.C. Young, *Chem. Rev., 93* (1993) 1371.
[11] C.A. Tolman, *Chem. Rev., 77* (1977) 313.
[12] M. Rahman, H. Liu, K. Eriks, A. Prock und W.P. Giering, *Organometallics, 8* (1989) 1.
[13] T. Bartik und T. Himmler, *J. Organomet. Chem., 293* (1985) 343.
[14] A.R. Bassindale und T. Stout, *Tetrahedron Lett., 26* (1985) 3403.
[15] R.J. Klingler, K. Mochida und J.J. Kochi, *J. Am. Chem. Soc., 101* (1979) 6626.
[16] U. Boehme, Programm GAMESS, Basissatz: 3-21G(*), vollständige Geometrieoptimierung, *unveröffentliche Mitteilung*.
[17] U. Herzog, R. Richter, E. Brendler und G. Roewer, *J. Organomet. Chem.*, (1995) im Druck.
[18] E. Hengge, F. Uhlig, C. Grogger, G. Roewer, U. Herzog und U. Pätzold, *Monatsh. Chem., 126* (1995) 549.

ELSEVIER

Journal of Organometallic Chemistry 508 (1996) 153–157

Journal of Organometallic Chemistry

# General valence force fields of the free and the coordinated cyclopentadienyl anion

T. Polzer, W. Kiefer *

*Institut für Physikalische Chemie der Universität Würzburg, Marcusstraße 9-11, D-97070 Würzburg, Germany*

Received 18 May 1995

**Abstract**

The modified general valence force field (GVFF) of the free cyclopentadienyl (Cp) anion was developed with internal coordinates to perform the normal coordinate analysis (NCA). Further it is shown that it is possible to transfer the GVFF of the free ring to the coordinated form. The NCA and the GVFF of (Cp)Tl with inclusion of the ring ligand is presented for the first time. Good agreement between observed and calculated wavenumbers has been achieved for both model calculations, the (Cp)K and the (Cp)Tl. The force fields together with force constants and potential energy distribution are given.

## 1. Introduction

Recently, we have studied the vibrational spectra of ferriosilanes of the type $(Cp)(OC)_2Fe(SiR_3)$ (Cp = $C_5H_5$; $SiR_3 = SiH_3$, $SiMe_3$, $Si(Cl)Me_2$, $Si(Cl)_2Me$ or $SiCl_3$) [1,2]. These molecules are photochemically active and therefore are of general interest for model studies of hydrosilylation. In these papers we focused our interest on the determination of the metal–ligand vibrations. In a first step towards the development of the valence force field of a complete ferriosilane molecule we carried out the normal coordinate analysis (NCA) of the trihydridosilane of the type $(Cp)(OC)_2Fe(SiH_3)$ where the ring ligand was treated as a point mass [3]. For inclusion of the complete ring ligand into the force field instead of the point mass approximation it is necessary to develop first the NCA of the free ring ligand, the cyclopentadienyl (Cp) anion.

In this paper we present the general valence force field (GVFF) of the Cp anion. The NCA was performed with the use of internal coordinates instead of possible symmetry-adapted coordinates for better transferability of the force field to the ferriosilanes which have lower symmetry. This principle was successfully used in our investigations concerning the development of the NCA of a complete osmium(II) half-sandwich molecule [4–6]. We have proven the validity of the force field performed for the free Cp for the coordinated state of the ring by application of the force field on the simpliest form of a $\eta^5$-coordinated Cp, the molecule (Cp)Tl. Therefore we have also developed the general valence force field for (Cp)Tl. For both the free and the Tl-coordinated Cp anion, we used the vibrational data given in the literature.

## 2. Group symmetry considerations

The cyclopentadienyl anion has $D_{5h}$ symmetry, and the 24 vibrational degrees of freedom are distributed amongst the symmetry species as

$$2A'_1(\mathrm{Ra}) + A'_2(\mathrm{n.a.}) + A''_2(\mathrm{IR}) + 3E_1(\mathrm{IR}) + E''_1(\mathrm{Ra}) + 4E'_2(\mathrm{Ra}) + 2E''_2(\mathrm{n.a.})$$

Therefore the ring has 14 bands with four of A-type symmetry and ten of E-type symmetry. Three bands are inactive and their band positions have to be calculated without available experimental data.

In the case of $\eta^5$ coordination on the thallium atom the symmetry of the molecule is lowered to $C_{5v}$. The former inactive modes of type $E''_2$ now transform as $E_2$ and are Raman active. The group-theoretical treatment

* Corresponding author.

0022-328X/96/$15.00 © 1996 Elsevier Science S.A. All rights reserved
*SSDI* 0022-328X(95)05844-3

yields 27 normal modes which are distributed as follows:

$$4A_1(\text{Ra, IR}) + A_2(\text{n.a.}) + 5E_1(\text{Ra, IR}) + 6E_2(\text{Ra})$$

There are three additional normal modes compared with the free ring. One is the symmetric ring–metal stretch vibration of symmetry type $A_1$ and two are degenerated with symmetry type $E_1$ and form the corresponding antisymmetric ring–metal stretch vibration. The symmetric C–H out-of-plane deformation mode $\delta_s(\text{C–H})_{oop}$ of symmetry type $A''_2$ now has $A_1$ symmetry, whereas the two inactive out-of-plane deformations of $E''_2$-type symmetry are now of $E_2$ symmetry and Raman active.

## 3. Normal coordinate analysis

### 3.1. Structure parameters

Regular pentagons for the rings were assumed. The bond lengths were taken from the literature [7,8] as follows: C–C bond, 1.417 Å; C–H bond, 1.110 Å; Tl–C bond, 2.680 Å; C–C–C angle, 108°; C–Tl–C angle, 55°.

### 3.2. Vibrational data

The first step of performing a NCA is the determination of the vibrational wavenumbers of the chosen compound. In contrast with benzene and its derivatives the Cp anion exists only as a salt with a counter-ion. The compound with predominently ionic character of the metal–ring bond is (Cp)K whose vibrational data we will use as those of a "free" Cp anion in this paper. There are several studies concerning the vibrational spectra of alkali metal cyclopentadienides [9–12]. However, some of the band positions of the normal modes of (Cp)K are still uncertain. The bands with $A''_2$- and $E''_2$-type symmetry are not IR active and not Raman active. Whereas a band at about 1260 $cm^{-1}$ was derived from solid state studies for the $\delta_s(\text{C–H})_{ip}$ vibration, there exist only calculated wavenumbers for the $E''_2$-type symmetry bands [13]. For one of these, the $\delta_{as}(\text{C–C})_{oop}$ band, a wavenumber of about 600 $cm^{-1}$ has been calculated. This value seems to be too large because the comparable normal mode of benzene is at about 400 $cm^{-1}$. The antisymmetric C–H stretch vibration of $E'_2$-type symmetry has been assumed in Refs. [12,13] to be at about 3060 $cm^{-1}$. Since in all other cyclopentadienides the wavenumber value of this band was determined to be about 5–15 $cm^{-1}$ below the corresponding antisymmetric C–H stretch vibration of $E'_1$-type symmetry, we estimated a value of 3050 $cm^{-1}$ in our calculations. Observed and calculated wavenumbers for the Cp anion in (Cp)K are compiled in Table 1 together with the assignments and the potential energy distribution (PED).

For the NCA of the $\eta^5$-coordinated Cp anion on

Table 1
Observed and calculated wavenumbers of the Cp anion in (Cp)K with assignments and potential energy distributions

| Symmetry ($D_{5h}$) | Assignment | Observed wavenumber [a] ($cm^{-1}$) | Calculated wavenumber ($cm^{-1}$) | PED [b] (%) |
|---|---|---|---|---|
| $A'_1$ | $\nu_s(\text{C–H})$ | 3088 | 3088 | $99s_2$ |
| | $\nu_s(\text{C–C})$ | 1119 | 1119 | $98s_1$ |
| $A'_2$ | $\delta_s(\text{C–H})_{ip}$ | — [c] | 1260 | $100\beta$ |
| $A''_2$ | $\delta_s(\text{C–H})_{oop}$ | 700 | 700 | $100\kappa$ |
| $E'_1$ | $\nu_{as}(\text{C–H})$ | 3061 | 3061 | $99s_2$ |
| | $\nu_{as}(\text{C–C})$ | 1440 | 1440 | $46\beta + 44s_1 + 9\alpha$ |
| | $\delta_{as}(\text{C–H})_{ip}$ | 1008 | 1008 | $64\beta + 30s_1 + 6\alpha$ |
| $E''_1$ | $\delta_{as}(\text{C–H})_{oop}$ | 719 | 719 | $55\tau + 44\kappa$ |
| $E'_2$ | $\nu_{as}(\text{C–H})$ | (≈ 3050) [d] | 3050 | $99s_2$ |
| | $\delta_{as}(\text{C–C})_{ip}$ | 1346 | 1346 | $56s_1 + 23\alpha + 21\beta$ |
| | $\delta_{as}(\text{C–H})_{ip}$ | 1070 | 1070 | $86\beta + 6s_1 + 6\alpha$ |
| | $\delta_{as}(\text{C–C})_{ip}$ | 854 | 854 | $54s_1 + 39s_2 + 6\beta$ |
| $E''_2$ | $\delta_{as}(\text{C–H})_{oop}$ | — [c] | 841 | $63\tau + 37\kappa$ |
| | $\delta_{as}(\text{C–C})_{oop}$ | — [c] | 334 | $64\tau + 36\kappa$ |

[a] [9–11].
[b] PED values below 3% are omitted.
[c] Not Raman active nor IR active.
[d] Estimated value (see text).

Table 2
Observed and calculated wavenumbers of the $\eta^5$-coordinated Cp anion (Cp)Tl with assignments and potential energy distributions

| Symmetry ($C_{5v}$) | Assignment [a] | Observed wavenumber [b] ($cm^{-1}$) | Calculated wavenumber ($cm^{-1}$) | PED [c] (%) |
|---|---|---|---|---|
| $A_1$ | $\nu_s$(C–H) | 3096 | 3096 | $99s_2$ |
| | $\nu_s$(C–C) | 1120 | 1120 | $96s_1$ |
| | $\delta_s$(C–H)$_{oop}$ | 727 | 727 | $98\kappa$ |
| | $\nu_s$(Tl–Cp) | 160 | 160 | $100s_3$ |
| $A_2$ | $\delta_s$(C–H)$_{ip}$ | 1255 | 1255 | $100\beta$ |
| $E_1$ | $\nu_{as}$(C–H) | 3070 | 3070 | $99s_2$ |
| | $\nu_{as}$(C–C) | 1425 | 1425 | $49\beta + 44s_1 + 6\alpha$ |
| | $\delta_{as}$(C–H)$_{ip}$ | 1008 | 1008 | $66\beta + 29s_1 + 4\alpha$ |
| | $\delta_{as}$(C–H)$_{oop}$ | 754 | 754 | $67\kappa + 31\tau$ |
| | $\nu_{as}$(Tl–Cp) | 290 | 290 | $94s_3 + 4\kappa$ |
| $E_2$ | $\nu_{as}$(C–H) | 3065 | 3065 | $99s_2$ |
| | $\delta_{as}$(C–C)$_{ip}$ | 1350 | 1350 | $59s_1 + 22\beta + 18\alpha$ |
| | $\delta_{as}$(C–H)$_{ip}$ | 1060 | 1060 | $93\beta + 6\alpha$ |
| | $\delta_{as}$(C–C)$_{ip}$ | 843 | 843 | $73s_1 + 18\alpha + 7\beta$ |
| | $\delta_{as}$(C–H)$_{oop}$ | 804 | 804 | $69\kappa + 27\tau + 4s_3$ |
| | $\delta_{as}$(C–C)$_{oop}$ | — [d] | 361 | $40s_3 + 33\tau + 26\kappa$ |

[a] The assignments of the ring vibrations are those of the free ring for better comprehension.
[b] [12–14].
[c] PED values below 3% are omitted.
[d] Band position uncertain (see text).

thallium we used the vibrational data reported in the literature. The wavenumbers of the ring vibrations were derived from solid state Raman and IR spectroscopy [14,15], whereas the metal–ring stretch vibrations were detected by microwave spectroscopy [16]. Table 2 summarizes the observed and calculated values similar to those of Table 1. As can be recognized, most of the vibrations of the ring in (Cp)Tl have only slightly changed band positions of up to 35 $cm^{-1}$ when compared with the free ring vibrations.

### 3.3. Vibrational force fields

The internal coordinates are defined in Figs. 1 and 2 for (Cp)K and for (Cp)Tl respectively; $s$ denotes the stretch coordinates, $\alpha$ and $\beta$ denote the in-plane deformation coordinates, and $\kappa$ and $\tau$ denote the out-of-plane coordinates.

The free Cp anion can be described by a force field with 35 diagonal elements including ten stretch, 15 in-plane bend, five out-of-plane bend and five torsion coordinates. In the case of the (Cp)Tl the internal coordinates are the same as used for the free ring with addition of the metal–ring stretch coordinates. To perform the NCA of (Cp)Tl, the optimized GVFF of the free Cp anion was expanded with the Tl–C stretch coordinates and necessary interaction force constants. The force field was then refined by use of the assignments and band positions of (Cp)Tl as stated above.

The normal coordinate calculations were performed by use of the FG matrix method of Wilson et al. [17] and of a modified version of QCMP-067 [18] and VIA [19]. The calculations were carried out on a SPARC/2 workstation and on a personal computer.

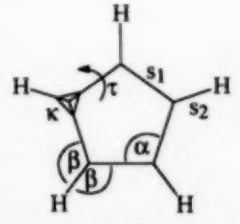


Fig. 1. Defined internal coordinates for the free cyclopentadienyl anion: $s_1$, C–C stretch; $s_2$, C–H stretch; $\alpha$, C–C–C bend in plane; $\beta$, C–C–H bend in plane; $\kappa$, C–H bend out of plane; $\tau$, C–C torsion.

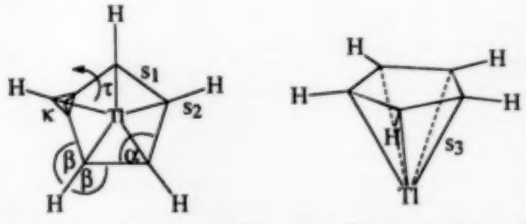


Fig. 2. Defined internal coordinates for the $\eta^5$-coordinated cyclopentadienyl anion: $s_1$, C–C stretch; $s_2$, C–H stretch; $s_3$, Tl–C stretch; $\alpha$, C–C–C bend in plane; $\beta$, C–C–H in plane; $\kappa$, C–H bend out of plane; $\tau$, C–C torsion.

## 4. Results and discussion

As already mentioned above, the wavenumbers calculated for (Cp)K and (Cp)Tl are compiled in Tables 1 and 2 respectively and compared with their observed values. The corresponding potential energy distribution of each normal mode is also given. The resulting force constants and their definitions are compiled in Table 3.

Good agreement between the calculated and observed wavenumbers for both the free and the coordinated Cp anion was obtained. The wavenumbers of the 24 normal modes of (Cp)K and of the 27 normal modes of (Cp)Tl were calculated with deviations smaller than 1 $cm^{-1}$ in all cases. For the (Cp)K we used a force field with 35 diagonal elements and 150 off-diagonal elements represented by 26 different force constants. The force field of (Cp)Tl was performed by means of 40 diagonal and 195 off-diagonal elements and the number of different force constants is increased to 35.

The small deviations of the band positions between free and coordinated ring lead also to small changes in the PEDs. Most of the force constants also differ only by small amounts. Larger changes were observed only for the diagonal force constant of the torsion coordinate $\tau$ which decreases from 0.595 mdyn $Å^{-1}$ for (Cp)K to 0.153 mdyn $Å^{-1}$ for (Cp)Tl. This is caused through the coupling with the Tl–C stretch coordinate because the displacements of both coordinates coincide. Likewise

Table 3
Internal coordinates and calculated force constants of the free and the $\eta^5$-coordinated Cp anion (for definitions see Figs. 1 and 2)

| Internal coordinate | Definition | $[(Cp)^-](D_{5h})$ value [a] | $[(Cp)Tl](C_{5v})$ value [a] |
|---|---|---|---|
| *Diagonal* | | | |
| C–C stretch | $s_1$ | 5.311 | 5.136 |
| C–H stretch | $s_2$ | 5.047 | 5.080 |
| Tl–C stretch | $s_3$ | — | 0.690 |
| C–C–C bend in plane | $\alpha$ | 1.583 | 1.013 |
| C–C–H bend in plane | $\beta$ | 0.460 | 0.466 |
| C–H bend out of plane | $\kappa$ | 0.245 | 0.213 |
| C–C torsion | $\tau$ | 0.595 | 0.153 |
| *Stretch–stretch interaction* | | | |
| C–C stretch–C–C stretch (adjacent) | $s_1 s_1'$ | 0.859 | 0.949 |
| C–C stretch–C–C stretch (1 adjacent) | $s_1 s_1''$ | −0.002 | −0.009 |
| C–C stretch–C–H stretch | $s_1 s_2$ | 0.007 | 0.009 |
| C–C stretch–Tl–C stretch (adjacent) | $s_1 s_3'$ | — | 0.015 |
| C–C stretch–Tl–C stretch (1 adjacent) | $s_1 s_3''$ | — | −0.021 |
| C–H stretch–C–H stretch (adjacent) | $s_2 s_2'$ | 0.030 | 0.027 |
| C–H stretch–C–H stretch (1 adjacent) | $s_2 s_2''$ | 0.007 | 0.009 |
| C–H stretch–Tl–C stretch | $s_2 s_3$ | — | 0.013 |
| Tl–C stretch–Tl–C stretch (adjacent) | $s_3 s_3'$ | — | −0.108 |
| Tl–C stretch–Tl–C stretch (1 adjacent) | $s_3 s_3''$ | — | −0.143 |
| *Stretch–Bend interaction* | | | |
| C–C stretch–C–C–C bend in plane | $s_1 \alpha$ | −0.032 | −0.116 |
| C–C stretch–C–C–C bend in plane (adjacent) | $s_1 \alpha'$ | −0.110 | −0.150 |
| C–C stretch–C–C–H bend in plane | $s_1 \beta$ | 0.098 | 0.172 |
| C–C stretch–C–C–H bend in plane (adjacent) | $s_1 \beta'$ | −0.062 | 0.062 |
| C–H stretch–C–C–H bend in plane | $s_2 \beta$ | 0.018 | 0.001 |
| Tl–C stretch–C–C–C bend in plane (adjacent) | $s_3 \alpha'$ | — | −0.014 |
| Tl–C stretch–C–C–C bend in plane (1 adjacent) | $s_3 \alpha''$ | — | −0.005 |
| Tl–C stretch–C–C–H bend in plane | $s_3 \beta$ | — | 0.001 |
| *Bend–bend interaction* | | | |
| C–C–C bend in plane–C–C–C bend in plane (adjacent) | $\alpha\alpha'$ | −0.124 | −0.568 |
| C–C–C bend in plane–C–C–C bend in plane (1 adjacent) | $\alpha\alpha''$ | 0.090 | 0.086 |
| C–C–C bend in plane–C–C–H bend in plane | $\alpha\beta$ | 0.032 | 0.002 |
| C–C–C bend in plane–C–C–H bend in plane (adjacent) | $\alpha\beta'$ | 0.057 | 0.022 |
| C–C–H bend in plane–C–C–H bend in plane | $\beta\beta$ | 0.039 | 0.053 |
| C–C–H bend in plane–C–C–H bend in plane (adjacent) | $\beta\beta'$ | 0.051 | 0.086 |
| C–C–H bend in plane–C–C–H bend in plane (1 adjacent) | $\beta\beta''$ | 0.028 | 0.052 |
| C–H bend out of plane–C–H bend out of plane | $\kappa\kappa$ | 0.036 | 0.064 |
| C–H bend out of plane–C–C torsion | $\kappa\tau$ | 0.166 | 0.212 |
| C–C torsion–C–C torsion | $\tau\tau$ | 0.206 | 0.001 |

[a] Values for stretches and their interactions are in millidynes per ångström, for bendings, waggings and torsions and all interactions thereoff in millidyne ångströms per square radian and for interactions of stretches with bendings, waggings and torsions in millidynes per radian.

the interaction force constant $\tau\tau$ is lowered from 0.206 to 0.001 mdyn Å $rad^{-2}$.

The antisymmetric C–C deformation modes $\delta_{as}(C–C)_{ip}$ of $E_2$ symmetry were found at 1346 $cm^{-1}$ and 854 $cm^{-1}$ in (Cp)K. Owing to coordination, the first is raised to 1350 $cm^{-1}$ and the other is lowered to 843 $cm^{-1}$. These small changes in the band positions cause a decrease in the interaction force constant $\alpha\alpha'$ in the force field which is lowered from −0.124 to −0.568 mdyn Å $rad^{-2}$.

The three inactive modes of the Cp anion with $A_2'$- and $E_2''$-type symmetry were calculated to be at 1260 $cm^{-1}$, 841 $cm^{-1}$ and 334 $cm^{-1}$ for the $\delta_s(C–H)_{ip}$, $\delta_{as}(C–H)_{oop}$ and $\delta_{as}(C–C)_{oop}$ bands respectively. For the latter a value of 361 $cm^{-1}$ (Cp)/Tl was evaluated. The high value of $\tau$ in the PED is lowered to 33% owing to the strong coupling with $s_3$ which participated with 40%.

The Tl–Cp vibrations which are described by $s_3$ are almost completely uncoupled with other coordinates. Only the PED of the metal-ring "tilt" vibration $\nu_{as}$(Tl–Cp) contains a small amount of an out-of-plane deformation coordinate. For the Tl–C stretch coordinate $s_3$ a value of 0.690 mdyn $Å^{-1}$ was evaluated. This shows the strength of the ring–metal bond of a system with $\eta^5$-coordinated Cp. If the ring ligand had been treated as a point mass at the center of the ring, the molecule (Cp)Tl could then be reduced to a two-mass oscillator. In this case, a force constant of 2.443 mdyn $Å^{-1}$ is obtained. Related to a single Tl–C bond this would be 0.498 mdyn $Å^{-1}$, which means a difference of about 30% compared with the result of the complete NCA. Therefore, the results of the NCA performed with point mass approximations in these cases have to be considered as questionable.

## Acknowledgments

We gratefully acknowledge support from the Deutsche Forschungsgemeinschaft (Sonderforschungsbereich 347, Teilprojekt C-2) as well as from the Fonds der Chemischen Industrie. Fruitful collaboration with Professor W. Malisch (Sonderforschungsbereich 347, Teilprojekt B-2) is also highly acknowledged.

## References

[1] T. Polzer, U. Posset, C. Engert, V. Deckert and W. Kiefer, in H. Werner, A.G. Griesbeck, W. Adam, G. Bringmann and W. Kiefer (eds.), *Selective Reactions of Metal Activated Molecules*, Vieweg, Braunschweig, 1992, p. 225.
[2] T. Polzer, D. Gernet and W. Kiefer, in W. Kiefer, M. Cardona, G. Schaack, F.W. Schneider and H.W. Schrötter (eds.), *Proc. 13th Int. Conf. on Raman Spectroscopy*, Wiley, Chichester, 1992, p. 730.
[3] T. Polzer and W. Kiefer, in preparation.
[4] T. Polzer, A. Ellebracht, W. Kiefer, U. Wecker and H. Werner, *J. Organomet. Chem., 438* (1992) 319.
[5] T. Polzer and W. Kiefer, *Asian J. Phys., 4* (1995) 4.
[6] T. Polzer and W. Kiefer, *J. Organomet. Chem., 472* (1994) 303.
[7] M.J.S. Dewar and R.C. Haddon, *J. Am. Chem. Soc., 95* (1973) 5836.
[8] E. Frasson, F. Menegus and C. Panattoni, *Nature, 199* (1963) 1087.
[9] (a) H.P. Fritz and L. Schäfer, *Chem. Ber., 97* (1964) 1829; (b) H.P. Fritz, *Adv. Organomet. Chem., 1* (1964) 239.
[10] V.T. Aleksanyan and B.V. Lokshin, *J. Organomet. Chem., 131* (1977) 113.
[11] V.T. Aleksanyan, in J.R. Durig (ed.), *Vibrational Spectra and Structure*, Vol. 11, Elsevier, Amsterdam, 1982, p. 115.
[12] I.A. Garbuzova, O.G. Garkusha, B.V. Lokshin, G.K. Borisov and T.S. Morozova, *J. Organomet. Chem., 279* (1985) 327.
[13] O.G. Garkusha, I.A. Garbuzova, B.V. Lokshin and J. Mink, *J. Mol. Struct., 175* (1988) 165.
[14] R.T. Bailey and A.H. Curran, *J. Mol. Struct., 6* (1970) 391.
[15] O.G. Garkusha, B.V. Lokshin, R.B. Materikova, L.M. Golubinskaya, V.I. Bregadze and A.P. Kurbakova, *J. Organomet. Chem., 342* (1992) 281.
[16] C. Roberts, A.P. Cox and M.J. Whittle, *J. Mol. Spectrosc., 35* (1970) 476.
[17] E.B. Wilson, Jr., J.C. Decius and P. Cross, *Molecular Vibrations*, Dover Publications, New York 1980.
[18] D.F. McIntosh and M.R. Peterson, *QCPE 342*, 1991.
[19] H.C. Fleischhauer, *Ph.D. Thesis*, University of Düsseldorf, 1991.

ELSEVIER

Journal of Organometallic Chemistry 508 (1996) 159–167

Journal of Organometallic Chemistry

# Preparation and some properties of Pt(II) ruthenocenylacetylide complexes

Masaru Sato *, Emiko Mogi

*Chemical Analysis Center, Saitama University, Urawa, Saitama 338, Japan*

Received 25 May 1995; in revised form 21 June 1995

**Abstract**

Ruthenocenylacetylene reacted with *trans*-PtI(C$_6$H$_4$X-*p*)(PPh$_3$)$_2$ (X = H, Me, OMe, Cl or CO$_2$Me) in the presence of CuI in diethylamine–CH$_2$Cl$_2$ to give the Pt(II) ruthenocenylacetylide complexes, *trans*-Pt(C≡CRc)(C$_6$H$_4$X-*p*)(PPh$_3$)$_2$ with a good yield. Similarly, *cis*-Pt(C≡CRc)(C$_6$H$_4$OMe-*p*)(dppe) was prepared. The structure of *trans*-Pt(C≡CRc)(C$_6$H$_4$CO$_2$Et-*p*)(PPh$_3$)$_2$ was determined by single-crystal X-ray diffraction. No reaction of the *trans* isomers with DDQ or AgBF$_4$ took place, while the *cis* isomer was oxidized with AgBF$_4$ to give the coupling products RcC≡CC$_6$H$_5$OMe-*p* with a low yield. The oxidation of the *cis* isomer with iodine occurred on the Pt atom to afford *p*-MeOC$_6$H$_4$I and PtI$_2$(dppe) as the main products.

*Keywords:* Ruthenocene; Oxidation; Acetylide complex; Platinum complex

## 1. Introduction

From the viewpoint of developing a new functionalized material, the chemistry of ferrocenylacetylene has been recently revived. Ferrocenylacetylene reacted with ruthenium dodecacarbonyl to give a new type of trinuclear complex [1]. B [2], Ru(II) [3], Fe(II) [4], Ni(II) [5], Pd(II) [5] and Pt(II) ferrocenylacetylide complexes [6] were reported. The reaction of Re(I) phenylacetylide and ferrocenylacetylene was also reported [7]. The Mn(I) ferrocenylacetylides were reported to have potential non-linear optics [8]. We recently reported the synthesis and oxidation of *trans*- and *cis*-Pt(II) ferrocenylacetylides [9,10]. However, the chemistry of ruthenocenylacetylene has been rarely investigated. It is well known that ruthenocene is a stable metallocene similar to ferrocene but shows different electrochemical properties. We here report the synthesis and oxidation of *trans*- and *cis*-Pt(II) ruthenocenylacetylides.

## 2. Results and discussion

Ruthenocenylacetylene (**1**) [11] was allowed to react with *trans*-PtI(PPh$_3$)$_2$C$_6$H$_4$OMe-*p* (**2a**), which was prepared from the reaction of Pt(PPh$_3$)$_4$ with *p*-MeOC$_6$H$_4$I [12], in diethylamine–CH$_2$Cl$_2$ in the presence of a catalytic amount of CuI at room temperature to give *trans*-Pt(C≡CRc)(C$_6$H$_4$OMe-*p*)(PPh$_3$)$_2$ (**3a**) with 78% yield (Scheme 1), Similarly, **3b** (X = Me), **3c** (X = H), **3d** (X = Cl) and **3e** (X = CO$_2$Et) were prepared with good yields. The structures of **3a–3e** were assigned by IR, $^1$H, $^{13}$C, $^{31}$P NMR spectra and elemental analysis. For example, the $^1$H NMR spectrum of **3b** showed the methyl protons of the tolyl group at $\delta$ = 1.94 ppm, the ring protons of the ruthenocenyl moiety at $\delta$ = 3.80 (2H), 4.13 (2H), and 4.16 (5H) ppm, the aryl protons as doublets at $\delta$ = 6.09 and 6.42 ppm, and the phenyl protons of PPh$_3$ as multiplets at $\delta$ = 7.19–7.56 ppm. In the $^{13}$C NMR spectrum of **3b**, the signals of the acetylenic carbon atoms were observed at $\delta$ = 109.00 and 109.70 ppm and the former signal was split by the coupling with the phosphorus atoms coordinated to the Pt atom ($J$ = 15.9 Hz). The $^{31}$P NMR spectrum of **3b** showed only one signal at 21.15 ppm accompanied by a satellite ($J$ = 3008 Hz) by coupling with the $^{195}$Pt atom, indicating the *trans* configuration of the PPh$_3$ ligands on the Pt atom in **3b**. In the IR spectrum of **3b**, the C≡C stretching vibration appeared at 2120 cm$^{-1}$. The spectral data of **3a–3e** are summarized in Table 1. In similar conditions, the reaction of ruthenocenylacetylene (**1**) with the Pd analog, PdI(C$_6$H$_4$OMe-*p*)(PPh$_3$)$_2$, gave no Pd complex, *trans*-Pd(C≡CRc)(C$_6$H$_4$OMe-*p*)-

* Corresponding author.

0022-328X/96/$15.00 © 1996 Elsevier Science S.A. All rights reserved
*SSDI* 0022-328X(95)05815-X

$(PPh_3)_2$, but the coupling product, $RcC{\equiv}CC_6H_4OMe$-*p* (**4**), with good yield. The IR spectrum of **4** showed the C≡C stretching vibration at 2225 $cm^{-1}$. In the $^{13}C$ NMR spectrum of **4**, the acetylenic carbon atoms appeared at $\delta = 85.43$ and 85.49 ppm as singlets. The $^1H$ NMR spectrum of **4** showed only doublets at $\delta = 6.82$ and 7.36 ppm in the phenyl proton region. These spectral data and elemental analysis confirmed the structure of **4**. When the *trans* isomer **3a** was allowed to react with 1,2-bis(diphenylphosphino)ethane (dppe) in $CH_2Cl_2$ at room temperature, the *cis* isomer, *cis*-$Pt(C{\equiv}CRc)(C_6H_4OMe$-*p*$)$(dppe) (**5**), was obtained with 84% yield (Scheme 2). It is a remarkable that both the acetylenic carbon atoms showed coupling with the phosphorus atoms coordinated to the Pt atom in the $^{13}C$ NMR spectrum of **5**. The acetylenic carbon atom connected directly to the Pt atom resonated at 108.76 ppm as a double doublet ($J = 148.0$ and 15.6 Hz) and the other acetylenic carbon atom at 105.77 ppm as a double doublet ($J = 33.4$ and 2.1 Hz), in which the phosphorus atom *trans* to the acetylide ligand is responsible for the larger coupling constant. Also, the methylene carbon atoms were observed at 26.72 and 30.43 ppm as double doublets owing to the coupling with the phosphorus atoms. In the $^{31}P$ NMR spectrum of **5**, two signals accompanied by the Pt satellite appeared at 43.65 ppm ($J = 2540$ Hz) and 38.23 ppm ($J = 1544$ Hz). From the comparison with the complex reported previously [13], the former is assigned to the phosphorous atom *trans* to the acetylide ligand.

Single-crystal X-ray diffraction was carried out to confirm the structure of **3e**. The ORTEP view of **3e** was shown in Fig. 1. The crystallographic data was summarized in Table 2 and the selected bond distances and angles are collected in Table 3. The bond angles around the Pt atom are nearly 90° and the stereochemical geometry around the Pt atom is a distorted square-planar in **3e**. The ruthenocenylacelylide ligand is coordinated trans to the aryl ligand on the Pt atom (C(1)–Pt–C(13), 175.7(3)°). The Pt–P distances (2.307(2) and 2.314(2) Å) are similar to those of the ferrocene analog, *trans*-$Pt(C{\equiv}CFc)(C_6H_5CO_2Et$-p$)(PPh_3)_2$ (2.296(2) and 2.305(2) Å) [10], *cis*-$Pt(C{\equiv}CFc)_2(PPh_3)_2$ (2.310(3) and 2.314(3) Å) [6a]. The Pt–C(1) distance is 2.067(8) Å, which is similar to that of *trans*-$Pt(C{\equiv}CFc)(C_6H_5CO_2$-Et-*p*$)(PPh_3)_2$ (2.034(7) Å) [10], somewhat shorter than that of *trans*-$Pt(C{\equiv}CFc)(H)(PPh_3)_2$ (2.137(10) Å), and somewhat longer than that of *cis*-$Pt(C{\equiv}CFc)_2(PPh_3)_2$ (1.991(10) Å) [6b]. The substituted cyclopentadienyl ring of ruthenocenyl moiety in **3e** is rotated by 70° from the plane of the square-planar around the Pt atom, contrary to the fact that the planes of the substituted cyclopentadienyl ring of the ferrocenyl moiety and the square-planar around the Pt atom are nearly coplanar to each other in *trans*-$Pt(C{\equiv}CFc)(C_6H_5CO_2Et$-*p*$)(PPh_3)_2$ [10]. It is note worthy that each one of the phenyl ring of the two $PPh_3$ ligands is nearly parallel to the benzene ring of the aryl ligand (17.3 and 19.3°). These are probably due to the intramolecular steric effect or the packing effect of the molecule in the crystal.

The cyclic voltammograms of **3a–3e** and the related complexes, *p*-$MeOC_6H_4C{\equiv}CRc$ (**4**) and *trans*-(*p*-$MeOC_6H_4)(Ph_3P)_2PtC{\equiv}CPh$ (**6**), were measured in a solution of 0.1 M *n*-$Bu_4NClO_4$ in $CH_2Cl_2$ at a Pt electrode and a sweep rate of 0.1 V $s^{-1}$ (Fig. 2). The redox potential was corrected to the potential of FcH–$FcH^+$. Complexes **3a–3e** showed successive three anodic waves at 0.2–0.7 V. The assignment of these waves is difficult, because the reference compounds **4** and **6** also afforded the waves in a similar region

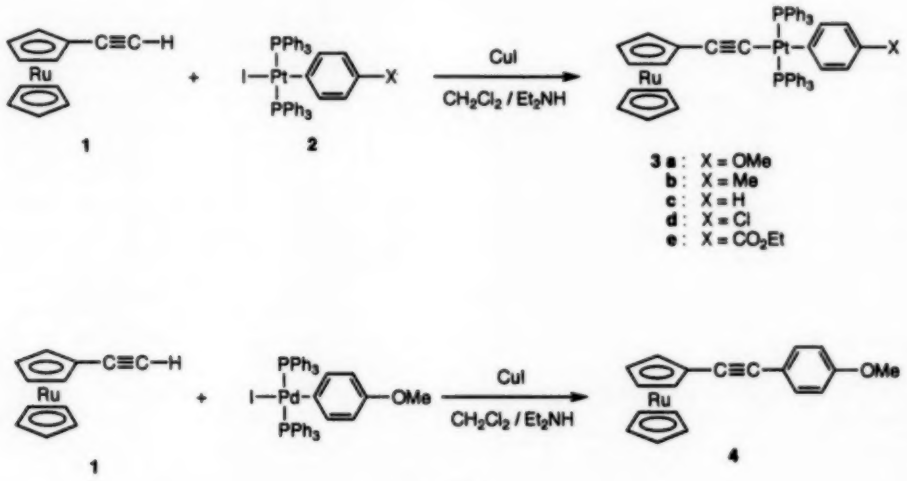


Scheme 1.

Table 1
NMR and IR data for **3a–3e**

| Complex | $^1$H NMR, $\delta$ (ppm) | $^{13}$C NMR, $\delta$ (ppm) | $^{31}$P NMR, $\delta$ (ppm) | IR ($cm^{-1}$) |
|---|---|---|---|---|
| **3a** | 3.52 (s, 3H, $OCH_3$)<br>3.81 (t, $J$ = 1.7 Hz, 2H, Cp-β),<br>4.13 (t, $J$ = 1.7 Hz, 2H, Cp-α),<br>4.15 (s, 5H, Cp-*ipso*),<br>5.94 (d, $J$ = 8.5 Hz, 2H, $C_6H_4$),<br>6.42 (d, $J$ = 8.5 Hz, 2H, $C_6H_4$),<br>7.21–7.58 (m, 30H, $PPh_3$) | 55.51 (s, $OCH_3$), 68.46 (s, Cp-β),<br>70.73 (s, Cp-unsub), 72.52 (s, Cp-α),<br>76.55 (s, Cp-*ipso*),<br>108.34 (t, $J$ = 15.6 Hz, C≡C), 109.75 (s, C≡C),<br>113.51 (s, $C_6H_4$), 127.43 (t, $J$ = 5.0 Hz, $PPh_3$),<br>129.60 (s, $PPh_3$), 131.61 (t, $J$ = 27.7 Hz, $PPh_3$),<br>134.85 (t, $J$ = 6.0 Hz, $PPh_3$),<br>139.02 (s, $C_6H_4$), 146.79 (t, $J$ = 10.1 Hz, $C_6H_4$),<br>154.86 (s, $C_6H_4$) | 21.39<br>($J_{PtP}$ = 2990 Hz) | 2117 |
| **3b** | 1.94 (s, 3H, $CH_3$),<br>3.80 (t, $J$ = 1.7 Hz, 2H, Cp-β),<br>4.13 (t, $J$ = 1.7 Hz, 2H, Cp-α),<br>4.16 (s, 5H, Cp-unsub),<br>6.09 (d, $J$ = 7.7 Hz, 2H, $C_6H_4$),<br>6.42 (d, $J$ = 7.7 Hz, 2H, $C_6H_4$),<br>7.19–7.56 (m, 30H, $PPh_3$) | 20.40 (s, $CH_3$), 68.44 (s, Cp-β)<br>70.73 (s, Cp-unsub), 72.54 (s, Cp-α),<br>74.47 (s, Cp-*ipso*), 109.70 (s, C≡C),<br>109.00 (t, $J$ = 15.9 Hz, C≡C),<br>127.38 (t, $J$ = 5.4 Hz, $PPh_3$),<br>127.88 (s, $C_6H_4$), 129.10 (s, $C_6H_4$),<br>129.52 (s, $PPh_3$), 131.68 (t, $J$ = 28.1 Hz, $PPh_3$),<br>134.87 (t, $J$ = 6.2 Hz, $PPh_3$), 139.06 (s, $C_6H_4$),<br>151.55 (t, $J$ = 10.1 Hz, $C_6H_4$-*ipso*) | 21.15<br>($J_{PtP}$ = 3008 Hz) | 2120 |
| **3c** | 3.80 (t, $J$ = 1.7 Hz, 2H, Cp-β),<br>3.72 (t, $J$ = 1.7 Hz, 2H, Cp-α),<br>4.14 (s, 5H, Cp-unsub),<br>6.01–6.33 (m, 3H, $C_6H_5$),<br>6.59 (d, $J$ = 7.6 Hz, 2H, $C_6H_5$),<br>7.20–7.57 (m, 30H, $PPh_3$) | 68.44 (s, Cp-β), 70.72 (s, Cp-unsub),<br>72.52 (s, Cp-α), 76.54 (s, Cp-*ipso*),<br>108.09 (t, $J$ = 16.1 Hz, C≡C), 109.93 (s, C≡C),<br>120.30 (s, $C_6H_5$), 126.87 (s, $C_6H_5$),<br>127.45 (t, $J$ = 5.2 Hz, $PPh_3$), 129.59 (s, $PPh_3$),<br>131.64 (t, $J$ = 28.2 Hz, $PPh_3$),<br>134.84 (t, $J$ = 6.1 Hz, $PPh_3$), 139.54 (s, $C_6H_5$),<br>157.65 (t, $J$ = 9.8 Hz, $C_6H_5$) | 21.63<br>($J_{PtP}$ = 3000 Hz) | 2121 |
| **3d** | 3.81 (bs, 2H, Cp-β)<br>4.14 (bs, 7H, Cp-α + Cp-unsub),<br>6.20 (d, $J$ = 8.1 Hz, 2H, $C_6H_4$),<br>6.49 (d, $J$ = 8.1 Hz, 2H, $C_6H_4$),<br>7.22–7.58 (m, 30H, $PPh_3$) | 68.44 (s, Cp-β), 70.72 (s, Cp-unsub),<br>72.50 (s, Cp-α), 76.27 (s, Cp-*ipso*),<br>106.63 (t, $J$ = 15.9 Hz, C≡C),<br>110.31 (s, C≡C), 126.55 (s, $C_6H_4$),<br>127.54 (t, $J$ = 5.2 Hz, $PPh_3$),<br>130.00 (s, $C_6H_4$), 131.30 (t, $J$ = 28.3 Hz, $PPh_3$),<br>134.81 (t, $J$ = 6.1 Hz, $PPh_3$), 140.00 (s, $C_6H_4$),<br>156.06 (t, $J$ = 10.0 Hz, $C_6H_4$) | 21.17<br>($J_{PtP}$ = 2956 Hz) | 2125 |
| **3e** | 1.30 (t, $J$ = 7.1 Hz, 3H, $CH_3$),<br>3.80 (t, $J$ = 1.7 Hz, 2H, Cp-β),<br>4.13 (t, $J$ = 1.7 Hz, 2H, Cp-α),<br>4.14 (s, 5H, Cp-unsub),<br>4.22 (q, $J$ = 7.1 Hz, 2H, $CH_2$),<br>6.72 (d, $J$ = 8.2 Hz, 2H, $C_6H_4$),<br>6.86 (d, $J$ = 8.2 Hz, 2H, $C_6H_4$),<br>7.20–7.58 (m, 30H, $PPh_3$) | 14.39 (s, $CH_3$), 59.72 (s, $CH_2$),<br>68.52 (s, Cp-β), 70.73 (s, Cp-unsub),<br>72.49 (s, Cp-α), 76.17 (s, Cp-*ipso*),<br>106.16 (t, $J$ = 16.6 Hz, C≡C), 110.69 (s, C≡C),<br>122.31 (s, $C_6H_4$), 126.98 ($C_6H_4$),<br>127.54 (t, $J$ = 5.0 Hz, $PPh_3$), 129.85 (s, $PPh_3$),<br>131.16 (t, $J$ = 28.7 Hz, $PPh_3$),<br>134.76 (t, $J$ = 6.0 Hz, $PPh_3$), 139.09 (s, $C_6H_4$),<br>168.48 (s, $C_6H_4$), 170.42 (t, $J$ = 9.6 Hz, $C_6H_4$) | 21.20<br>($J_{PtP}$ = 2953 Hz) | 2117 |

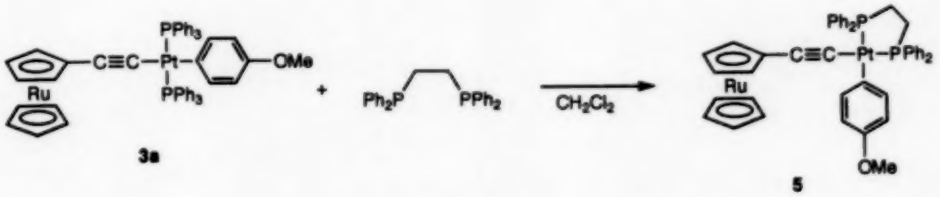


Scheme 2.

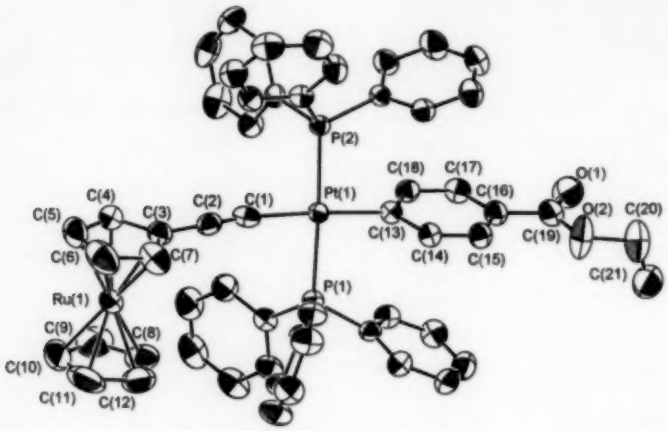


Fig. 1. ORTEP view of **3e**.

($E_{pa}$ = +0.50 and +0.52 V respectively) and the potential of each wave in **3a–3e** was not influenced systematically by the substituent on the aryl ligand. Ruthenocene undergoes an irreversible two-electron oxidation in $CH_2Cl_2$ [14] but shows a reversible one-electron redox wave if the supporting salt has an extremely weak coordination ability [15]. Also, [3] ruthenocenophanes and [4] ruthenocenophanes exhibit a behavior similar to that of ruthenocene in $CH_3CN$ [16]. However, decamethylruthenocene, in which the high oxidation state is expected to be stabilized by the $Cp^*$ ligand, gives a reversible redox wave both in $CH_2Cl_2$ and $CH_3CN$ [17]. These results indicate that the electrochemical behavior of ruthenocene derivatives is influenced by the kind of ligands, the solvent, the supporting salt and so on. Recently, the chemical or electrochemical oxidation of permethyl[3]ruthenocenophane in $CH_3CN$ was reported to result in the dicationic Ru(IV) complex coordinated by $CH_3CN$ [18]. Then, the cyclic voltammetry of **3a–3e** was also carried out in $CH_3CN$ but the cyclic voltammogram similar to that in $CH_2Cl_2$ was observed, suggesting that no stable complex coordi-

Table 2
Crystal and intensity collection data for **3e**

| | |
|---|---|
| Molecular formula | $C_{57}H_{48}O_2P_2RuPt$ |
| Molecular weight | 1123.12 |
| Crystal system | Triclinic |
| Space group | $P\bar{1}$ (No. 2) |
| $a$ (Å) | 11.910(5) |
| $b$ (Å) | 13.871(3) |
| $c$ (Å) | 16.718(2) |
| $\alpha$ (°) | 87.09(2) |
| $\beta$ (°) | 68.16(2) |
| $\gamma$ (°) | 65.38(1) |
| $V$ (Å$^3$) | 2312.5(10) |
| $Z$ | 2 |
| $D_{calc}$ (g cm$^{-3}$) | 1.61 |
| Crystal dimensions (mm) | 0.10 × 0.28 × 0.10 |
| Linear absorption coefficient (cm$^{-1}$) | 34.826 |
| Radiation ($\lambda$ (Å)) | Mo K$\alpha$ (0.71073) |
| Reflection ($hkl$) limits | $0 < h < 16$, $-17 < k < 19$, $21 < l < 23$ |
| Total number of reflections measured | 16185 |
| Number of unique reflections | 11246 |
| Number of reflections used in least-squares method | 9202 |
| Least squares parameters | 740 |
| $R$ | 0.0440 |
| $R_w$ | 0.0525 |
| Maximum peak in final Fourier map (electrons Å$^{-3}$) | 1.46 |
| Minimum peak in final Fourier map (electrons Å$^{-3}$) | −2.81 |

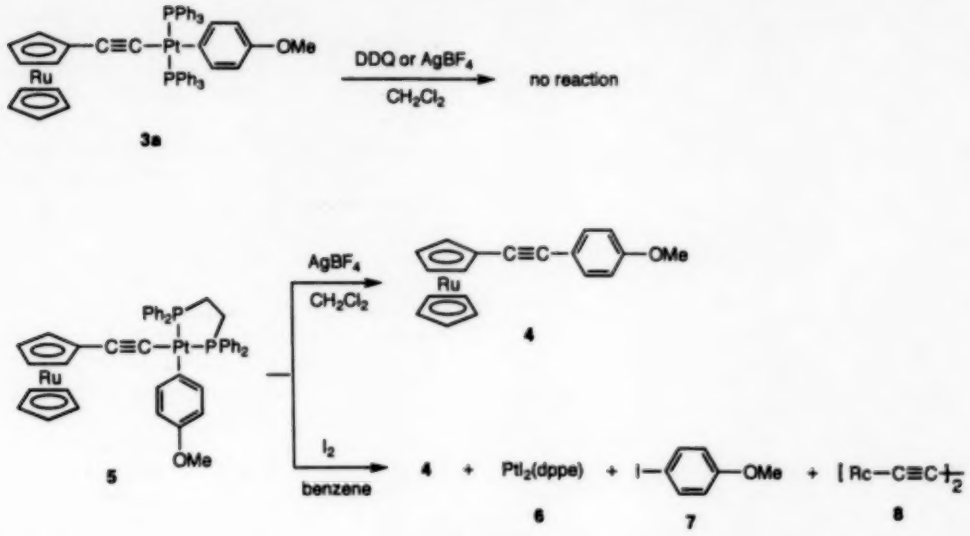


Scheme 3.

nating $CH_3CN$ to the Ru atom forms in the Pt(II) ruthenocenylacetylides. In contrast with the *trans* isomers, the *cis* isomer **5** in $CH_2Cl_2$ showed two distinct anodic waves at 0.22 and 0.48 V, as well as a small wave at 0.70 V, in the cyclic voltammogram. The large anodic waves seem to correspond to that of the reference compounds **4** and **6** but the precise assignment is impossible because of the similar anodic potentials of **4** and **6**. Similar to the *trans* isomers **3a–3e**, the first anodic potential of **5** is shifted to a lower level by about 0.3 V than the anodic potential of the reference complexes. This is probably caused by the increased electron density on the Ru atom due to the greater anionic character in the acetylide than the acetylene structure or the increased electron density on Pt atom due to the electron-donating ruthenocenyl group.

The oxidation of the *trans* isomer **3a** with dichlorodicyanobenzoquinone (DDQ) or $AgBF_4$ in $CH_2Cl_2$ was

Table 3
Selected bond distances (Å) and angles (°) for **3e**

| | | | |
|---|---|---|---|
| *Bond distances* | | | |
| Pt(1)–P(1) | 2.307(2) | Pt(1)–P(2) | 2.314(2) |
| Pt(1)–C(1) | 2.067(8) | Pt(1)–C(13) | 2.045(6) |
| Ru(1)–C(3) | 2.202(7) | Ru(1)–C(4) | 2.187(10) |
| Ru(1)–C(5) | 2.162(10) | Ru(1)–C(6) | 2.211(13) |
| Ru(1)–C(7) | 2.186(9) | Ru(1)–C(8) | 2.198(11) |
| Ru(1)–C(9) | 2.214(15) | Ru(1)–C(10) | 2.180(14) |
| Ru(1)–C(11) | 2.164(11) | Ru(1)–C(12) | 2.181(12) |
| P(1)–C(22) | 1.811(7) | P(1)–C(28) | 1.823(7) |
| P(1)–C(34) | 1.849(8) | P(2)–C(40) | 1.832(8) |
| P(2)–C(46) | 1.828(7) | P(2)–C(52) | 1.824(6) |
| C(1)–C(2) | 1.112(11) | C(2)–C(3) | 1.502(11) |
| *Bond angles* | | | |
| P(1)–Pt(1)–C(1) | 87.1(2) | P(1)–Pt(1)–C(13) | 90.5(2) |
| P(2)–Pt(1)–C(1) | 91.7(2) | P(2)–Pt(1)–C(13) | 90.9(2) |
| P(1)–Pt(1)–P(2) | 175.7(1) | C(1)–Pt(1)–C(13) | 175.7(3) |
| Pt(1)–C(1)–C(2) | 172.5(7) | C(1)–C(2)–C(3) | 177.2(9) |
| Pt(1)–P(1)–C(22) | 115.9(3) | Pt(1)–P(1)–C(28) | 115.1(3) |
| Pt(1)–P(1)–C(34) | 112.3(3) | C(22)–P(1)–C(28) | 102.8(4) |
| C(28)–P(1)–C(34) | 107.1(4) | C(22)–P(1)–C(34) | 102.5(4) |
| Pt(1)–P(2)–C(40) | 119.7(3) | Pt(1)–P(2)–C(46) | 110.4(3) |
| Pt(1)–P(2)–C(52) | 114.9(3) | C(40)–P(2)–C(46) | 101.2(4) |
| C(40)–P(2)–C(52) | 104.6(4) | C(46)–P(2)–C(52) | 104.2(4) |

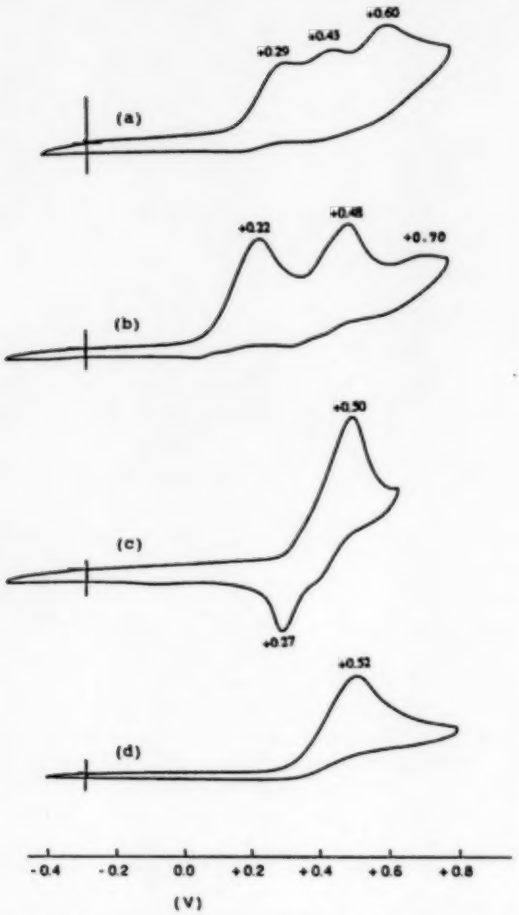


Fig. 2. The cyclic voltammograms of (a) **3a**, (b) **5**, (c) **4** and (d) **6** in 0.1 M $n$-$Bu_4NClO_4$ in $CH_2Cl_2$ at 0.1 V $s^{-1}$.

carried out but the starting material was recovered quantitatively. This is contrary to the case in the ferrocene analog in which the stable one-electron oxidized species was isolated with a good yield under similar conditions [10]. This may be because the first anodic potential of **3a** (0.29 V) is considerably higher than that of the ferrocene analogs (−0.16 V). In the mononuclear ruthenocene derivatives, only the oxidized species isolated stably is $[Cp_2RuX]^+$ which involves formally a Ru(IV) atom oxidized chemically by halogen [19]. So, the oxidation of **3a** with iodine in $CH_2Cl_2$ was attempted. A small amount of brown solid was isolated but the structure determination was impossible because of its instability in solution.

The *cis* isomer **5** was not oxidized with 1.1 equivalent of DDQ in $CH_2Cl_2$, similarly to the *trans* isomer **3a**. However, the reaction of **5** with a stronger oxidant, $AgBF_4$, afforded the coupling product, RcC≡$CC_6H_4$O-Me-*p* (**4**), with 37% yield. A similar coupling reaction was observed in the *cis* isomer of the ferrocene analogs [9]. It proves from this result that the oxidation of the ruthenocene analog **5** also induces the reductive elimination on the Pt atom to produce the C–C coupling product. The moderate yield of the coupling product in the oxidation of **5** with $AgBF_4$ is considered to be probably because the ruthenocene analog has a higher first anodic potential than the ferrocene analog and then the requirement of a stronger oxidant makes the reaction more complex. It is not clear whether the Ru or Pt atom in **5** is oxidized first, because the anodic potentials of both sites are close to each other. The oxidation of **5** with iodine in benzene gave $p$-$MeOC_6H_4I$ (**7**) (75%) and $PtI_2$(dppe) (**8**) (65%), together with a trace amount of **4** and RcC≡CC≡CRc (Scheme 3). The result can be explained as follows: the oxidative addition of iodine takes place on the Pt(II) atom, and not on the Ru atom in **5**, followed by the formation of short-lived Pt(IV) species and the reductive elimination from the intermediate. Probably, the reductive elimination from the Pt(IV) intermediate produces **7**, RcC≡CI and Pt(dppe). The Pt(0) species, Pt(dppe), immediately reacts with excess of iodine to give **8**. RcC≡CI does not seem to be isolated because of its instability but only a part of it is isolated as the coupling product, RcC≡CC≡CRc. Thus the difference of the oxidant seems to control the path of the oxidatively induced reductive elimination.

In summary, some novel Pt(II) ruthenocenylacetylide complexes, *trans*-Pt(C≡CRc)($C_6H_4X$-*p*)$(PPh_3)_2$ (X = OMe, Me, H, Cl or $CO_2Et$) and *cis*-Pt(C≡CRc)($C_6H_4$OMe-*p*)(dppe), were prepared. As expected, the waves in the cyclic voltammograms were irreversible and their anodic potentials were very high. As a result, the oxidation of the *trans* isomers with DDQ or $AgBF_4$ did not occur at all, while the *cis* isomer was oxidized only with $AgBF_4$ to afford the coupling product RcC≡$CC_6H_4$OMe-*p* with a moderate yield. It was not clear whether the formation of the coupling product proceeded through the first oxidation on the Ru atom and the successive electron transfer from the Pt atom or the direct oxidation on the Pt atom, followed by the reductive elimination from the Pt(III) species. On the contrary, the reaction of the *cis* isomer with iodine was initiated by the oxidative addition of iodine to the Pt atom and followed by the reductive elimination from the resulting Pt(IV) species.

## 3. Experimental details

### 3.1. General comments

Visible and near-IR spectra were recorded on a Shimadzu 365 spectrometer and IR spectra on a Perkin–Elmer System 2000 spectrometer. The $^1H$ NMR, $^{13}C$

NMR and $^{31}P$ NMR spectra were measured on a Bruker AM400, ARX400 or AC200 spectrometer. In the measurement of the $^{31}P$ NMR spectrum, 85% $H_3PO_4$ was used as the external reference. Electrochemical measurements were made by cyclic voltammetry in a solution of 0.1 M ($n$-Bu)$_4$NClO$_4$ in $CH_2Cl_2$ or acetonitrile under nitrogen at 25°C, using a standard three-electrode cell on a BAS CV-27 analyzer. All potentials were measured vs. an $Ag/AgNO_3$ (0.05 M) electrode and the scan rate was 100 mV $s^{-1}$. Ruthenocenylacetylene [11] and *trans*-PtI(PPh$_3$)$_2$C$_6$H$_4$OMe [12] were prepared according to the methods described in the literature. All experiments were undertaken in a nitrogen-saturated solvent under nitrogen.

### 3.2. Procedure

#### 3.2.1. *trans*-Pt(C≡CRc)(PPh$_3$)$_2$C$_6$H$_4$OMe-*p* (3a).

To a solution of ruthenocenylacetylene (102 mg, 0.4 mmol) and *trans*-PtI(PPh$_3$)$_2$C$_6$H$_4$OMe (381 mg, 0.4 mmol) in $CH_2Cl_2$ (15 ml) and diethylamine (15 ml) was added copper(I) iodide (80 mg, 0.04 mmol). The mixture was stirred for 20 min at room temperature and then the solvent was evaporated under reduced pressure. The residue was chromatographed on alumina by elution of hexane: $CH_2Cl_2$ (1:1) to give **3a** as pale-yellow crystals (338 mg (78.2%)) (recrystallized from hexane–$CH_2Cl_2$) (melting point (m.p.), about 171°C (decomposition)). Anal. Found: C, 59.68; H, 4.17%. $C_{55}H_{46}OP_2RuPt \cdot \frac{1}{2}CH_2Cl_2$ calc.: C, 59.33; H, 4.22%.

Other *trans* isomers were prepared in a similar manner.

#### 3.2.2. *trans*-Pt(C≡CRc)(PPh$_3$)$_2$C$_6$H$_4$Me-*p* (3b).

Pale-yellow crystals (yield, 71.0%, m.p., about 169°C (decomposition)). Anal. Found: C, 62.06; H, 4.24. $C_{55}H_{46}P_2RuPt$ calc.: C, 62.20; H, 4.35%.

#### 3.2.3. *trans*-Pt(C≡CRc)(PPh$_3$)$_2$C$_6$H$_5$ (3c).

Pale-yellow crystals (yield, 59.8%; m.p., about 170°C (decomposition)). Anal. Found: C, 61.22; H, 4.21. $C_{54}H_{44}P_2RuPt$ calc.: C, 61.70; H, 4.21%.

#### 3.2.4. *trans*-Pt(C≡CRc)(PPh$_3$)$_2$C$_6$H$_4$Cl-*p* (3d).

Pale-yellow crystals (yield, 81.6%; m.p., about 202°C (decomposition)). Anal. Found: C, 59.61; H, 3.92. $C_{54}H_{43}ClP_2RuPt$ calc.: C, 59.75; H, 3.99%.

#### 3.2.5. *trans*-Pt(C≡CRc)(PPh$_3$)$_2$C$_6$H$_4$CO$_2$Et-*p* (3e).

Pale-yellow crystals (yield, 77.2%; m.p., about 170°C (decomposition)). Anal. Found: C, 60.82; H, 4.28. $C_{57}H_{48}O_2P_2RuPt$ calc.: C, 60.95; H, 4.35%. IR (KBr): $\nu$(C≡C) 2117; $\nu$(C=O) 1702 $cm^{-1}$.

#### 3.2.6. RcC≡CC$_6$H$_4$OMe-*p* (4).

To a solution of ruthenocenylacetylene (51 mg, 0.2 mmol) and *trans*-PdI(PPh$_3$)$_2$C$_6$H$_4$OMe-*p* (173 mg, 0.2 mmol) in $CH_2Cl_2$ (10 ml) and diethylamine (10 ml) was added copper(I) iodide (40 mg, 0.02 mmol). After the mixture was stirred for 20 min at room temperature, the solvent was evaporated under reduced pressure. The residue was chromatographed on alumina by elution of hexane: $CH_2Cl_2$ (2:1) to give **4** as yellow crystals (46 mg (63%)) (recrystallized from hexane–$CH_2Cl_2$) (m.p., 122–123°C). Anal. Found: C, 63.30; H, 4.47. $C_{19}H_{16}ORu$ calc.: C, 63.15; H, 4.46%. IR (KBr): $\nu$(C≡C) 2225 $cm^{-1}$. $^1H$ NMR ($CDCl_3$): $\delta$ 3.80 (s, 3H, $OCH_3$), 4.57 (t, $J$ = 1.7 Hz, 2H, Cp-β), 4.62 (s, 5H, Cp-unsub.), 4.88 (t, $J$ = 1.7 Hz, 2H, Cp-α), 6.82 (d, $J$ = 8.9 Hz, 2H, $C_6H_4$), and 7.36 (d, $J$ = 8.9 Hz, 2H, $C_6H_4$) ppm. $^{13}C$ NMR ($CDCl_3$): $\delta$ 55.25 ($OCH_3$), 69.19 (Cp-*ipso*), 70.49 (Cp-β), 71.72 (Cp-unsub.), 73.48 (Cp-α), 85.43 (Rc–C≡), 85.49 (Ar–C≡), 113.86 ($C_6H_4$), 115.97 ($C_6H_4$), 132.76 ($C_6H_4$), 159.20 ($C_6H_4$) ppm.

#### 3.2.7. *cis*-Pt(C≡CRc)(C$_6$H$_4$OMe-*p*)(dppe) (5).

To a solution of *trans*-Pt(C≡CRc) (PPh$_3$)$_2$-C$_6$H$_4$OMe-*p* (**3a**) (195 mg, 0.18 mmol) in dichloroethane (10 ml) was added dppe (144 mg, 0.36 mmol). After the solution was stirred for 20 min at room temperature, the solvent was evaporated under reduced pressure. The residue was chromatographed on alumina by elution of hexane: $CH_2Cl_2$ (1:2) to give yellow oil and the crystallization from hexane–$CH_2Cl_2$ yielded **4** as pale-yellow crystals (144 mg (83.5%)) (m.p., about 168°C (decomposition)). Anal. Found: C, 56.65; H, 4.16. $C_{45}H_{40}OP_2RuPt$ calc.: C, 56.60; H, 4.22%. IR (KBr): $\nu$(C≡C) 2122 $cm^{-1}$. $^1H$ NMR ($CDCl_3$): $\delta$ 2.19–2.44 (m, 4H, $PCH_2$), 3.64 (s, 3H, $OCH_3$), 4.24 (s, 5H, Cp-unsub.), 4.33 (t, $J$ = 1.7 Hz, 2H, Cp-β), 4.59 (t, $J$ = 1.6 Hz, 2H, Cp-α), 6.46 (dd, $J$ = 9.2 and 1.3 Hz, 2H, $C_6H_4$), 7.22–8.01 (m, 22H, $C_6H_4$ + PPh) ppm. $^{13}C$ NMR ($CDCl_3$): $\delta$ 26.72 (dd, $J$ = 31.8 and 12.2 Hz, $PCH_2$), 30.43 (d, $J$ = 35.6 and 16.7 Hz, $PCH_2$), 54.97 ($OCH_3$), 68.89 (Cp-β), 70.93 (Cp-unsub.), 73.28 (Cp-α), 75.84 (Cp-*ipso*), 105.77 (dd, $J$ = 33.4 and 2.1 Hz, Rc–C≡), 109.04 ($J$ = 148.0 and 15.6 Hz, Pt–C≡), 113.01 ($C_6H_4$), 128.4–128.7 (m, $PPh_2$), 129.60 (d, $J$ = 8.0 Hz, $PPh_2$), 130.6–130.9 (m, $PPh_2$), 132.08 (d, $J$ = 45.5 Hz, $PPh_2$), 133.4–133.8 (m, $PPh_2$), 139.14 (t, $J$ = 1.9 Hz, $C_6H_4$), 142.57 (dd, $J$ = 115.3 and 8.5 Hz, $C_6H_4$), 155.66 (s, $C_6H_4$) ppm. $^{31}P$ NMR ($CDCl_3$): 38.23 (s, $J_{Pt-P}$ = 1544 Hz, *trans* to Ar) and 43.65 (s, $J_{Pt-P}$ = 2540 Hz, *trans* to C≡CRc).

#### 3.2.8. Reaction of 5 with iodine.

A solution of **5** (32.9 mg, 0.04 mmol) in $CH_2Cl_2$ (2 ml) and benzene (5 ml) was chilled on an ice bath. To the solution was dropwise added a solution of iodine (28 mg, 0.04 mmol) in benzene (5 ml). After evaporation of the solvent, the residue was chromatographed on silica gel to give $PtI_2$(dppe) (25.6 mg (75%)) and

Table 4
Position parameters and $U_{iso}$ for **3e**

| Atom | x | y | z | $U_{iso}$ (Å$^2$) |
|---|---|---|---|---|
| Pt(1) | 0.10879(3) | 0.10633(2) | 0.17220(2) | 0.032 |
| Ru(1) | −0.22574(7) | 0.48192(5) | 0.47116(4) | 0.051 |
| P(1) | 0.06676(18) | 0.27028(13) | 0.12110(11) | 0.034 |
| P(2) | 0.16232(18) | −0.05632(13) | 0.22673(11) | 0.034 |
| O(1) | 0.5045(7) | −0.1893(5) | −0.2513(4) | 0.070 |
| O(2) | 0.2951(7) | −0.1094(7) | −0.2492(4) | 0.087 |
| C(1) | −0.0015(8) | 0.1890(5) | 0.2958(5) | 0.044 |
| C(2) | −0.0694(8) | 0.2414(6) | 0.3584(5) | 0.050 |
| C(3) | −0.1659(8) | 0.3103(6) | 0.4433(5) | 0.050 |
| C(4) | −0.1317(11) | 0.3271(7) | 0.5130(6) | 0.071 |
| C(5) | −0.2549(13) | 0.3953(8) | 0.5826(6) | 0.079 |
| C(6) | −0.3679(13) | 0.4205(9) | 0.5558(8) | 0.089 |
| C(7) | −0.3084(9) | 0.3687(7) | 0.4678(7) | 0.064 |
| C(8) | −0.1276(11) | 0.5476(8) | 0.3582(7) | 0.075 |
| C(9) | −0.0910(15) | 0.5624(10) | 0.4254(9) | 0.112 |
| C(10) | −0.215(2) | 0.629(1) | 0.499(1) | 0.146 |
| C(11) | −0.3256(17) | 0.6524(8) | 0.4694(9) | 0.117 |
| C(12) | −0.2691(12) | 0.6000(8) | 0.3826(7) | 0.084 |
| C(13) | 0.2055(6) | 0.0308(5) | 0.0478(4) | 0.032 |
| C(14) | 0.1311(7) | 0.0389(5) | −0.0026(5) | 0.040 |
| C(15) | 0.1888(8) | −0.0114(6) | −0.0864(5) | 0.045 |
| C(16) | 0.3245(8) | −0.0741(6) | −0.1250(5) | 0.046 |
| C(17) | 0.4043(7) | −0.0829(6) | −0.0774(5) | 0.043 |
| C(18) | 0.3457(7) | −0.0312(5) | 0.0054(5) | 0.043 |
| C(19) | 0.3855(10) | −0.1299(6) | −0.2143(5) | 0.059 |
| C(20) | 0.3390(15) | −0.1569(12) | −0.3383(8) | 0.099 |
| C(21) | 0.3998(14) | −0.0984(11) | −0.4004(8) | 0.091 |
| C(22) | 0.1230(7) | 0.2678(5) | 0.0042(4) | 0.039 |
| C(23) | 0.0389(8) | 0.3040(6) | −0.0401(5) | 0.044 |
| C(24) | 0.0895(10) | 0.2886(7) | −0.1309(5) | 0.060 |
| C(25) | 0.2264(9) | 0.2358(7) | −0.1779(5) | 0.059 |
| C(26) | 0.3116(9) | 0.2006(7) | −0.1344(5) | 0.049 |
| C(27) | 0.2631(8) | 0.2171(6) | −0.0448(5) | 0.045 |
| C(28) | 0.1437(7) | 0.3454(5) | 0.1497(5) | 0.038 |
| C(29) | 0.1829(8) | 0.3239(7) | 0.2197(6) | 0.058 |
| C(30) | 0.2450(9) | 0.3823(8) | 0.2382(7) | 0.075 |
| C(31) | 0.2591(9) | 0.4635(8) | 0.1914(7) | 0.072 |
| C(32) | 0.2216(9) | 0.4853(7) | 0.1211(7) | 0.065 |
| C(33) | 0.1628(8) | 0.4267(6) | 0.1007(6) | 0.051 |
| C(34) | −0.1145(7) | 0.3583(5) | 0.1582(4) | 0.039 |
| C(35) | −0.2015(8) | 0.3120(6) | 0.1821(6) | 0.051 |
| C(36) | −0.3396(9) | 0.3754(7) | 0.2041(7) | 0.066 |
| C(37) | −0.3862(9) | 0.4839(7) | 0.2017(6) | 0.062 |
| C(38) | −0.2991(9) | 0.5313(7) | 0.1790(7) | 0.066 |
| C(39) | −0.1629(8) | 0.4683(6) | 0.1574(6) | 0.055 |
| C(40) | 0.0302(7) | −0.0826(5) | 0.3104(5) | 0.038 |
| C(41) | −0.0060(9) | −0.1618(7) | 0.2958(6) | 0.058 |
| C(42) | −0.0997(11) | −0.1835(8) | 0.3634(7) | 0.073 |
| C(43) | −0.1572(9) | −0.1291(8) | 0.4454(6) | 0.061 |
| C(44) | −0.1222(9) | −0.0500(7) | 0.4609(6) | 0.057 |
| C(45) | −0.0301(8) | −0.0262(6) | 0.3936(5) | 0.050 |
| C(46) | 0.2748(7) | −0.0737(5) | 0.2822(4) | 0.038 |
| C(47) | 0.3067(8) | −0.1597(6) | 0.3293(5) | 0.053 |
| C(48) | 0.3964(9) | −0.1766(7) | 0.3686(5) | 0.058 |
| C(49) | 0.4523(9) | −0.1045(9) | 0.3618(6) | 0.067 |
| C(50) | 0.4183(9) | −0.0191(9) | 0.3174(6) | 0.070 |
| C(51) | 0.3305(8) | −0.0025(6) | 0.2763(5) | 0.052 |
| C(52) | 0.2525(7) | −0.1731(5) | 0.1450(4) | 0.036 |
| C(53) | 0.3830(8) | −0.2466(6) | 0.1287(5) | 0.051 |
| C(54) | 0.4544(9) | −0.3275(7) | 0.0589(6) | 0.061 |

Table 4 (continued)

| Atom | x | y | z | $U_{iso}$ (Å$^2$) |
|---|---|---|---|---|
| C(55) | 0.3928(10) | −0.3360(7) | 0.0054(6) | 0.065 |
| C(56) | 0.2611(8) | −0.2641(6) | 0.0219(5) | 0.053 |
| C(57) | 0.1924(8) | −0.1837(6) | 0.0904(5) | 0.044 |

*p*-$MeOC_6H_4I$ (6.1 mg (65%)). Additionally, a trace amount of RcC≡$CC_6H_4$OMe-*p* and RcC≡CC≡CRc was isolated and confirmed by the $^1$H NMR spectra.

**$PtI_2$(dppe)**. M.p. greater than 250°C. Anal. Found: C, 36.95; H, 2.82. $C_{26}H_{24}P_2I_2Pt$ calc.: C, 36.85; H, 2.85%. $^1$H NMR ($CDCl_3$): δ 2.11 (m, 2H, $PCH_2$), 2.30 (m, 2H, $PCH_2$), 7.50 (m, 12H, Ph), and 7.83 (m, 8H, Ph) ppm. $^{13}$C NMR ($CDCl_3$): δ 29.20 (t, $J$ = 10 Hz, $PCH_2$), 30.20 (t, $J$ = 10 Hz, $PCH_2$), 128.3 (m, Ph), 131.85 (s, Ph), 133.7 (m, Ph) ppm. $^{31}$P NMR ($CDCl_3$): 45.88 ($J_{Pt-P}$ = 3369 Hz) ppm.

**RcC≡CC≡CRc**. M.p., 207°C (decomposition) (230–232°C) [20]. $^1$H NMR ($CDCl_3$): δ 4.56 (t, $J$ = 1.7 Hz, 4H, Cp-β), 4.62 (s, 10H, Cp-unsub.), 4.86 (t, $J$ = 1.7 Hz, 4H, Cp-α) ppm. $^{13}$C NMR ($CDCl_3$): δ 67.15 (≡C), 70.94 (Cp-β), 72.00 (Cp-unsub.), 74.14 (Cp-α), 78.11 (≡C) ppm.

### 3.3. Single-crystal X-ray diffraction of 3e

Data collection was performed at ambient temperature on a Mac Science DIP3000 image processor with graphite-monochromated Mo Kα radiation and an 18 kW rotating-anode generator. A total of 16 185 reflections were collected using the Weisenberg method in the range $2° < 2q < 60°$ ($0 < h < 16, -17 < k < 19, -21 < l < 23$). Of 11 246 unique reflections measured, only 9202 for which $I > 3\sigma(I)$ were used in the structure analysis. The structure was solved with the Dirdif–Patty method in CRYSTAN G (software-package for structure determination) and refined finally by the full-matrix least-squares procedure. Anisotropic refinement for non-hydrogen atoms was carried out. All the hydrogen atoms, partially located from difference Fourier maps, were isotopically refined. $R$ = 0.044 and $R_w$ = 0.053. The crystallographic data and the position parameters are listed in Tables 2 and 4 respectively.

## References


[1] A.A. Koridze, A.I. Yanovsky and Yu.T. Struchkov, *J. Organomet. Chem., 441* (1992) 277.
[2] Z. Yuan, N.J. Taylor, Y. Sun, T.B. Marder, I.D. Williams and L.-T. Cheng, *J. Organomet. Chem., 449* (1993), 27.
[3] (a) M. Sato, H. Shintate, Y. Kawata, M. Sekino, M. Katada and S. Kawata, *Organometallics, 13* (1994) 1956; (b) M.C.B. Colbert, S.L. Ingham, J. Lewis, N.J. Long and P.R. Raithby, *J. Chem. Soc. Dalton Trans.*, (1994) 2215.
[4] M. Sato, Y. Hayashi, H. Shintate, M. Katada and S. Kawata, *J. Organomet. Chem., 471* (1994) 179.
[5] K. Onitsuka, X.-Q. Tao and K. Sonogashira, *Bull. Chem. Soc. Jpn., 67* (1994) 2661.
[6] (a) W. Weigand and C. Robl, *Chem. Ber., 126* (1993) 1807; (b) M.V. Russo, A. Furlani, S. Licoccia, R. Paolesse, A.C. Villa and C. Guastini, *J. Organomet. Chem., 469* (1994) 245.
[7] A.A. Koridze, V.I. Zdanovich, O.A. Kizas, A.I. Yanovsky and Yu.T. Struchkov, *J. Organomet. Chem., 464* (1994) 197.
[8] M.C.B. Colbert, A.J. Edwards, J. Lewis, N.J. Long, N.A. Page, D.G. Parker and P.R. Raithby, *J. Chem. Soc., Dalton Trans.*, (1994) 2589.
[9] M. Sato, E. Mogi and S. Kumakura, *Organometallics, 14* (1995) 3157.
[10] M. Sato, E. Mogi and M. Katada, *Organometallics, 14* (1995) 4837.
[11] M.D. Rausch and A. Siegel, *J. Org. Chem., 43* (1969) 1974.
[12] N. Suguta, J.V. MinkieWicz and R.F. Heck, *Inorg. Chem., 17* (1978) 2809.
[13] T.G. Appleton and M.A. Bennett, *Inorg. Chem., 17* (1978) 738.
[14] T. Kuwana, D.E. Bublitz and G. Hoh, *J. Am. Chem. Soc., 82* (1960) 5811.
[15] M.G. Hill, W.M. Lamanna and K.R. Mann, *Inorg. Chem., 30* (1991) 4687.
[16] S. Kamiyama, T. Ikeshoji, A. Kasahara, T. Matsue and T. Oda, *Denkikagaku Oyobi Kougyoubuturikagaku*, (1986) 608.
[17] U. Koelle and A. Salzer, *J. Organomet. Chem., 243* (1983) C27.
[18] K. Hashizume, H. Tobita and H. Ogino, *Organometallics, 14* (1995) 1187.
[19] D.N. Hendrickson, Y.S. Sohn, W.H. Morrison, Jr. and H.B. Gray, *Inorg. Chem., 11* (1972) 808.
[20] O. Hofer and K. Schlögl, *J. Organomet. Chem., 13* (1968) 443.

ELSEVIER

Journal of Organometallic Chemistry 508 (1996) 169–181

Journal of Organometallic Chemistry

# Ring slippage in indenyl derivatives of molybdenum and tungsten

José R. Ascenso [b], Isabel S. Gonçalves [a], Eberhardt Herdtweck [c], Carlos C. Romão [a,*]

[a] *Instituto de Tecnologia Química e Biológica, R. da Quinta Grande 6, 2780 Oeiras, Portugal*
[b] *Centro de Química Estrutural, Instituto Superior Técnico, 1096 Lisboa Codex, Portugal*
[c] *Anorganisch-chemisches Institut, Technische Universität München, D-85478 Garching, Germany*

Received 25 May 1995

**Abstract**

Ring slippage of the indenyl occurs upon dissolution of the complexes $[\eta^5\text{-IndM(CO)}_2\text{L}_2]\text{BF}_4$ (M = Mo or W; L = NCMe or dimethylformamide) in an excess of L, to give $[(\eta^3\text{-Ind})\text{M(CO)}_2\text{L}_3]\text{BF}_4$. Other ring-slipped complexes synthesized are $[(\eta^3\text{-Ind})\text{Mo(CO)}_2\text{L}_3]\text{BF}_4$ ($\text{L}_3$ = $\text{HC(pz)}_3$, $[\text{HB(pz)}_3]^-$, $\text{Me}_3$tacn or {en(NCMe)}). Addition of NCMe or an excess of L failed to give ring slippage in $[\eta^5\text{-IndMo(CO)}_2\text{L}_2]\text{BF}_4$ ($\text{L}_2$ = bipy, dppe, $(\text{PMe}_3)_2$, $\{\text{P(OMe)}_3\}_2$ or triphos). NMR and X-ray studies reveal a large folding of the $\eta^3$-indenyl ring.

The structure complex $[(\eta^3\text{-Ind})\text{W(CO)}_2(\text{NCMe})_3]\text{BF}_4$ (**5**) was determined by X-ray analysis.

*Keywords:* Molybdenum; Tungsten; Indenyl complexes; Ring slippage; X-ray structure

## 1. Introduction

The attempt to achieve better control of the reactivity of transition-metal organometallic complexes has raised the interest in indenyl as a substitute for cyclopentadienyl. In fact, the higher rates of substitution reactions of complexes of indenyl when compared with their cyclopentadienyl congeners has long been recognized under the name of "indenyl effect" [1]. The accepted interpretation of this kinetic effect rests on the easy "ring slippage" of the indenyl from $\eta^5$ to $\eta^3$ coordination. As the electron count at the metal is reduced by this ring slippage, associative pathways for substitution reactions are favoured. However, under certain conditions, the intermediate trihapto-complexes may be stable enough to be isolated and fully characterized. Hence reaction of a two-electron donor L′ with a coordinatively saturated cation $[(\eta^5\text{-Ind})\text{M(CO)}_2\text{-L}_2]^+$ (M = Mo (**1**) or W (**2**)) may lead either to addition or to substitution, as exemplified by Eq. (1). In principle, the outcome of the reaction will depend on the stability of the trihapto complex which, in turn, will depend on the nature and number of the ancilliary ligands L. Substitution is the general result and, surprisingly, additions accompanied by $\eta^5 \rightarrow \eta^3$ "ring slippage" are relatively rare in spite of the many known examples of coordinatively saturated complexes with $\eta^3$-indenyl [2].

The first thoroughly characterized example was reported by Merola et al. [3] in 1986:

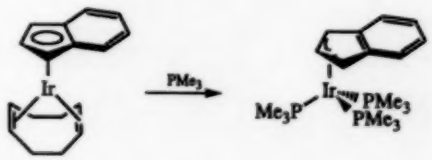


(2)

It follows the reports on the less expected $\eta^5 \rightarrow \eta^1$ ring slippages established earlier by Casey and O'Connor [4]

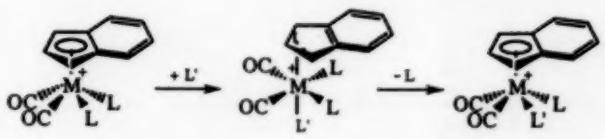


(1)

* Corresponding author.

Elsevier Science S.A.
*SSDI* 0022-328X(95)05859-1

in which all attempts to intercept the intermediate $\eta^3$-indenyl complex were unsuccessful:

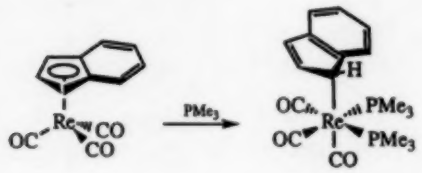


(3)

We have previously observed a facile ring slippage of the indenyl ligand in a tungsten complex by $^1$H NMR spectroscopy as described by [5]

$$[(\eta^5\text{-Ind})W(NCMe)_2(CO)_2]BF_4 \underset{CH_2Cl_2}{\overset{NCMe}{\rightleftharpoons}} [(\eta^3\text{-Ind})W(NCMe)_3(CO)_2]BF_4 \quad (4)$$

The present study reports the structural characterization of $[(\eta^3\text{-Ind})W(CO)_2(NCMe)_3]BF_4$ as well as describing a number of additions to the 18-electron cations $[(\eta^5\text{-Ind})M(CO)_2L_2]^+$ (M = Mo or W) in order to ascertain the conditions most favourable for "ring slippage".

## 2. Results and discussion

### 2.1. Chemical studies

The coordinatively saturated cations used in this work, $[(\eta^5\text{-Ind})M(CO)_2L_2]^+$ (M = Mo (**1**) or W (**2**)) are prepared as depicted in Scheme 1. The starting complexes $[(\eta^5\text{-Ind})M(\eta^3\text{-}C_3H_5)(CO)_2]$ (M = Mo or W) [6] are protonated with $HBF_4 \cdot OEt_2$, in $CH_2Cl_2$ at room temperature, and the resulting red solution treated with the desired L to give the products **1a–1i** (M = Mo) and **2**(M = W) with good isolated yields. This method has already been used by Cutler and coworkers [7] to prepare some cyclopentadienyl analogues $[CpMo(CO)_2L_2]BF_4$ and by us [5,6] to prepare a wide range of cyclopentadienyl and indenyl complexes with dienes, of general formula $[Cp'M(CO)_2(diene)]BF_4$ (Cp' = Cp, MeCp or Ind). The products are listed in Table 1, together with some selected $^1$H NMR data. Compounds **1a**, **1f** and **1h** are known but have been prepared by a different method [8a]. The acetonitrile derivative has been described in the literature as a useful promoter of diene transformations [8b,9].

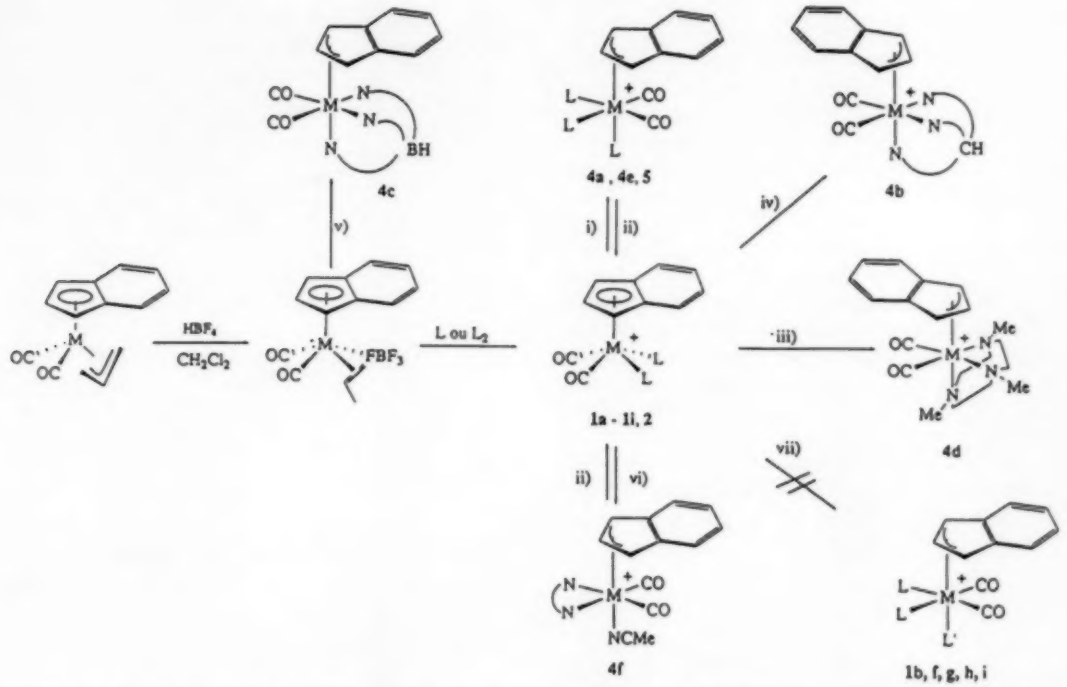


Scheme 1. (i) **1a**, **2** in NCMe or **1d** in dimethylformamide (DMF), at room temperature; (ii) **4a**, **4e** and **4f** in $CH_2Cl_2$; (iii) $Me_3tacn$ in $CH_2Cl_2$; (iv) **1c** dissolved in NCMe at 45°C; (v) $KHB(pz)_3$ in $CH_2Cl_2$; (vi) **1e** in NCMe, $L_2$ = en; (vii) **1b**, **1f**, **1g**, **1h** and **1i** with an excess of L or NCMe at reflux.

Table 1
List of $[(\eta^5\text{-Ind})M(CO)_2L_2]BF_4$ compounds prepared and selected $^1H$ NMR

| Compound | Ligand $L_2$ | $\eta^5$-indenyl resonances (room temperature), $\delta$ (ppm) | | |
|---|---|---|---|---|
| | | $H^{5/8}$ | $H^{1/3}$ | $H^2$ |
| *Mo* | | | | |
| **1a** | $(NCMe)_2$ | 7.60–7.54 m | 6.07 d | 5.02 t |
| **1b** | bipy | 6.95 m; 6.66 m | 6.47 d | 5.47 t |
| **1c** | tpm | – | – | – |
| **1d** | $(DMF)_2$ | 7.47 m; 7.39 m | 6.15 d | 4.98 t |
| **1e** | en | 7.84 m; 7.51 m | 6.23 d | 5.18 t |
| **1f** | $(P(OMe)_3)_2$ | 7.59 m; 7.30 m | 6.07 d | 5.60 t |
| **1g** | $(PMe_3)_2$ | 7.66 m; 7.28 m | 5.85 d | 5.54 t |
| **1h** | dppe | 7.08 m; 6.01 m | 5.59 d | 5.28 t |
| **1i** | triphos | 7.06 m; 6.58 m | 5.36 d | 5.71 t |
| *W* | | | | |
| **2** | $(NCMe)_2$ | 7.52 s | 6.16 d | 5.24 t |

pz = pyrazolyl, tpm = trispyrazolylmethane, dppe = 1,2-bis-(diphenylphosphino)ethane.
en = ethylenediamine; DMF = *N*,*N*-dimethylformamide, triphos = 1,1,1-tris(diphenylphosphinomethyl)ethane
The numbering scheme is as follows:

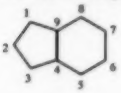


The characterization of most complexes in Table 1 is straightforward. The presence of a *cis*-$M(CO)_2$ unit is clear from the observed IR data which show, in all cases, two bands in the $\nu(CO)$ region. These values are, of course, dependent on the nature of L, they are higher for $P(OMe)_3$ and dppe but relatively invariant for all the other ligands.

All the $^1H$ NMR spectra show a similar pattern for the resonances of the $\eta^5$-indenyl, two sets of signals for the $C_6$ ring protons ($H^{5-8}$) at $\delta \approx 7.70$ and 7.30 ppm, a doublet at $\delta \approx 6.0$ ppm ($H^{1/3}$) and a triplet between $\delta \approx 5.00$ and 5.60 ppm ($H^2$) (see Table 1 for the numbering scheme). The exceptions are the $H^{5-8}$ resonances of the bipy, dppe and triphos complexes which are shifted to higher field by about 0.5 ppm. This pattern and chemical shift values are observed, for example, in the mixed-ring metallocene derivatives $[(\eta^5\text{-ind})(\eta^5\text{-Cp})ML_2]^{n+}$ [5,6]. The bidentate coordination of tris(pyrazolyl)methane in **1c** can only be assumed on the basis of several analogies. In fact, unlike

Table 2
Selected $^1H$ and $^{13}C$ NMR data of $[(\eta^3\text{-Ind})M(CO)_2L_3]BF_4$ and some related complexes

| Compound | Ligand $L_3$ | $^1H$ and $^{13}C$ $\eta$3-indenyl resonances, $\delta$ (ppm) [a] | | | |
|---|---|---|---|---|---|
| | | $H^2$ | $H^{5/8}$ | $H^{1/3}$ | $C^4/C^9$ |
| *Mo* | | | | | |
| **4a** | $(NCMe_3)$ [b] | 7.20 t | 6.47–6.37 m | 5.10 d | 146.73 |
| **4b** | tpm | 6.90 t | 6.70 m; 6.55 m | 5.55 d | 147.80 |
| **4c** | tpb | 6.63 t | 6.68 m; 6.50 m | 5.40 d | 148.56 |
| **4d** | $Me_3tacn$ | 6.94 t | 6.60 m; 6.47 m | 4.78 d | 147.03 |
| **4e** | $(DMF)_3$ [c] | 6.99 t | 6.47 m; 6.39 m | 5.08 d | 146.73 |
| **4f** | (en)(NCMe) | 7.07 t | 6.48 m; 6.41 m | 5.10 d | – |
| | $\eta^5$-Cp [d] | 6.75 t | 6.67 m; 6.43 m | 5.20 | 151.10 |
| *W* | | | | | |
| **5** | $(NCMe)_3$ | 6.46 t | 6.55–6.42 m | 5.02 d | 149.23 |
| | $\eta^5$-Cp [e] | 7.07 t | 6.66–6.47 m | 4.95 d | 152.03 |
| | $\eta^5$-Ind [f] | 3.4 | 6.6 m | 4.8 | – |

[a] All spectra in $CD_3CN$ at room temperature except otherwise indicated: see Table 1 for numbering.
[b] In $CD_3CN$ at −45°C.
[c] In DMF.
[d] Ref. [6].
[e] [5].
[f] [12]; tpb = hydrotrispyrazolylborato; $Me_3tacn$ = 1,4,7-*N*,*N'*,*N''*-trimethyltriazacyclononane.

all the other $[(\eta^5\text{-Ind})M(CO)_2L_2]BF_4$ cations reported here, **1c** precipitates instantaneously from the reaction mixture and its insolubility precludes NMR studies. The IR spectrum has two CO stretching vibrations at values rather similar to those of other similar $\eta^5$-indenyl complexes, such as **1a**, **1b** and **1g**, as expected on bidentate coordination of $HC(pz)_3$ (cf. **4b** below). Furthermore, this spectrum is very similar to that of $[CpMo\{\eta^2\text{-}HC(pz)_3\}(CO)_2]BF_4$ (**3**) which is readily prepared from $[CpMo(\eta^3\text{-}C_3H_5)(CO)_2]$ after protonation and reaction

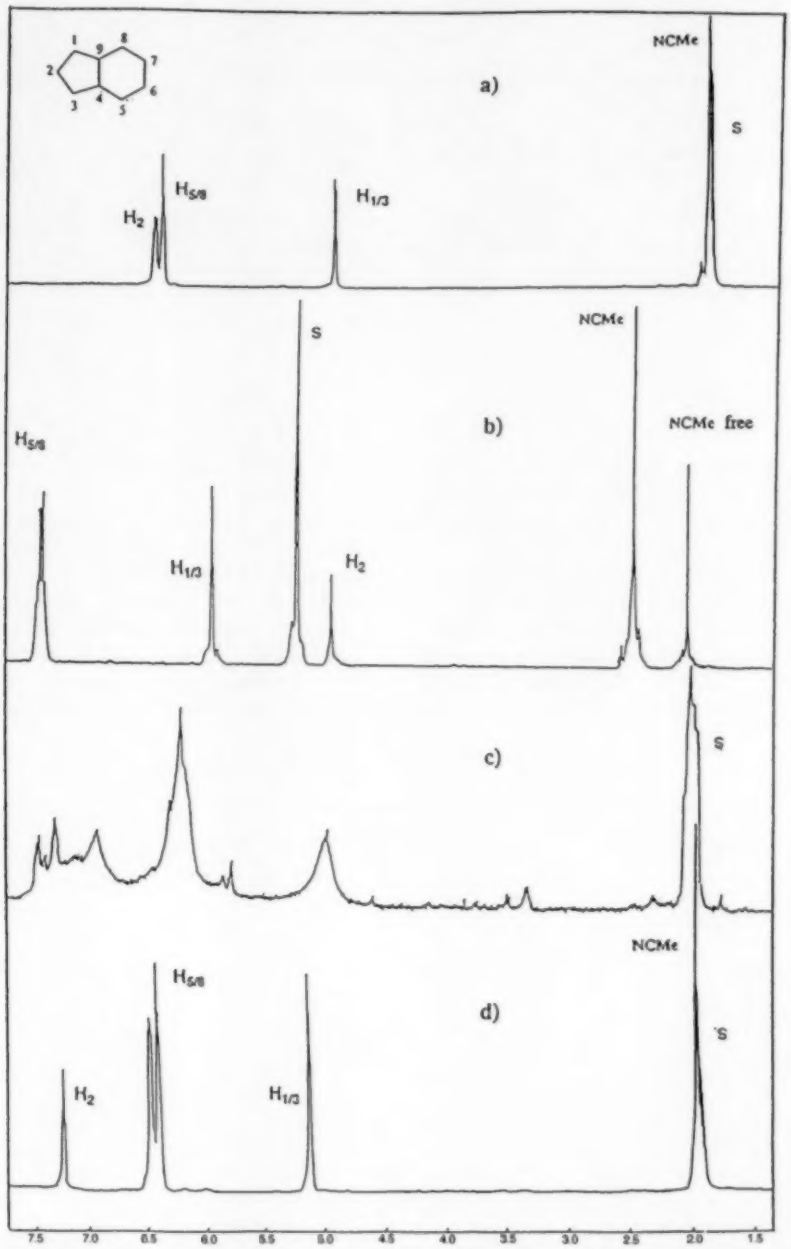


Fig. 1. $^1H$ NMR spectra (300 MHz) showing $\delta$ (ppm) of the complexes (S = solvent) (a) $[IndW(CO)_2(NCMe)_3]BF_4$ in NCMe (room temperature), (b) $[IndMo(CO)_2(NCMe)_3]BF_4$ in $CD_2Cl_2$, (c) $[IndMo(CO)_2(NCMe)_3]BF_4$ in NCMe (room temperature) and (d) $[IndMo(CO)_2(NCMe)_3]BF_4$ in NCMe (40°C).

with $HC(pz)_3$. Consistent with a bidentate coordination of $HC(pz)_3$, the $^1H$ NMR spectrum of **3** has two sets of pyrazolyl signals with relative intensities of 2.1, one of which appears at higher field and corresponds to the dangling pyrozolyl [10]. The insolubility of **1c** is paralleled in other $HC(pz)_3$ complexes, such as $[Mo\{HC(pz)_3\}(CO)_3]$ [11] and has been attributed to oligomerization or polymerization by means of M–pz–C–pz-M bridges. A similar situation is observed in **1i** where the triphos is bidentate with a dangling arm, as shown by $^1H$ NMR spectroscopy.

When **1a** or **2** are dissolved in NCMe, the colour darkens markedly. Addition of ether to the resulting solutions allows the isolation of crystalline $[(\eta^3\text{-Ind})M(CO)_2(NCMe)_3]BF_4$ (M = Mo (purple) (4a) or W (ruby-red) (**5**)). This change is faster when the solutions are at about 40°C. At room temperature, the $^1H$ NMR spectrum of **4a**, in NCMe-$d_3$, shows rather broad peaks, suggesting extensive dynamic structural interconversions (Fig. 1(c)). Upon cooling to −40°C the spectrum of **4a** becomes well resolved and sharp resonances are observed (Fig. 1(d)). Such a dynamic behaviour is absent in the spectrum of **1a** in $CD_2Cl_2$, which is sharp at room temperature (Fig. 1(b)). In fact, the $^1H$ NMR spectrum of **4a** in $CD_2Cl_2$ (Fig. 1(b)) corresponds to the spectrum of **1a** and 1 equivalent of free NCMe.

The pattern of the resonances for both **4a** at −40°C and **5** at room temperature, is best interpreted on the basis of the trihapto coordination of the indenyl. With regard to the Mo complexes, an upfield shift (about 1.1 ppm) of the benzenoid protons ($H^{5-8}$) and a remarkable downfield shift (about 2.2 ppm) of the *meso*-pseudoallylic $H^2$ signal are the most significant differences between **1a** and **4a** (Table 2).

Similar but slightly smaller variations in chemical shifts are observed for the pair of analogous W complexes **2** and **5**. These values are within the range of those measured in the trihapto-indenyl complexes $[(\eta^3\text{-Ind})CpM(CO)_2]$ (M = Mo or W) [5,6] (see also Table 2) and these reported for $[(\eta^3\text{-Ind})Ir(PMe_3)_3]$: $\delta$ = 7.09($H^2$), 6.55 ($H^{5-8}$) ppm [3]. In contrast with this pattern, the value of the chemical shift of $H^2$ observed

Table 3
Selected bond distances (pm) and angles (°) for $[\eta^3\text{-Ind}W(CO)_2(NCMe)_3]BF_4$ (**5**), where Cm(1) denotes the centre of gravity in C(6), C(7) and C(7)a, and Cm(2) denotes the centre of gravity in C(16), C(17) and C(17)a

| Molecule **A** | | Molecule **B** | |
|---|---|---|---|
| *Bond distances* | | | |
| W(1)–N(1) | 215.3(7) | W(2)–N(3) | 215.8(7) |
| W(1)–N(2) | 219.5(5) | W(2)–N(4) | 219.0(5) |
| W(1)–C(1) | 196.6(5) | W(2)–C(11) | 197.1(5) |
| W(1)–C(6) | 215.7(8) | W(2)–C(16) | 218.5(8) |
| W(1)–C(7) | 239.3(6) | W(2)–C(17) | 236.9(6) |
| W(1)–Cm(1) | 208.1 | W(2)–Cm(2) | 207.7 |
| O(1)–C(1) | 115.7(7) | O(2)–C(11) | 115.0(7) |
| N(1)–C(2) | 113.9(10) | N(3)–C(12) | 111.7(10) |
| N(2)–C(4) | 113.3(8) | N(4)–C(14) | 112.2(10) |
| C(2)–C(3) | 147.1(13) | C(12)–C(13) | 144.1(15) |
| C(4)–C(5) | 143.8(10) | C(14)–C(15) | 146.6(15) |
| C(6)–C(7) | 143.2(8) | C(16)–C(17) | 141.9(8) |
| C(7)–C(8) | 147.0(7) | C(17)–C(18) | 148.1(7) |
| C(8)–C(9) | 137.8(7) | C(18)–C(19) | 138.0(7) |
| C(8)–C(8)a | 142.0(6) | C(18)–C(18)a | 141.6(7) |
| C(9)–C(10) | 140.9(8) | C(19)–C(20) | 140.6(9) |
| C(10)–C(10)a | 135.9(10) | C(20)–C(20)a | 137.2(10) |
| *Bond angles* | | | |
| N(1)–W(1)–N(2) | 80.6(2) | N(3)–W(2)–N(4) | 80.8(2) |
| N(1)–W(1)–C(1) | 90.5(2) | N(3)–W(2)–C(11) | 90.3(2) |
| N(2)–W(1)–C(1) | 96.7(2) | N(4)–W(2)–C(11) | 96.8(2) |
| N(2)–W(1)–N(2)a | 83.3(2) | N(4)–W(2)–N(4)a | 83.4(2) |
| N(2)–W(1)–C(1)a | 171.0(2) | N(4)–W(2)–C(11)a | 170.9(2) |
| C(1)–W(1)–C(1)a | 81.9(2) | C(11)–W(2)–C(11)a | 81.6(2) |
| N(1)–W(1)–Cm(1) | 172.8 | N(3)–W(2)–Cm(2) | 173.3 |
| N(2)–W(1)–Cm(1) | 94.1 | N(4)–W(2)–Cm(2) | 94.2 |
| C(1)–W(1)–Cm(1) | 94.9 | C(11)–W(2)–Cm(2) | 94.8 |
| W(1)–N(1)–C(2) | 176.7(6) | W(2)–N(3)–C(12) | 176.5(6) |
| W(1)–N(2)–C(4) | 176.1(5) | W(2)–N(4)–C(14) | 178.2(6) |
| W(1)–C(1)–O(1) | 176.0(5) | W(2)–C(11)–O(2) | 177.2(5) |
| N(1)–C(2)–C(3) | 179.5(9) | N(3)–C(12)–C(13) | 180.0(6) |
| N(2)–C(4)–C(5) | 178.8(7) | N(4)–C(14)–C(15) | 178.6(9) |

in $[(\eta^5\text{-Ind})M(\eta^3\text{-Ind})(CO)_2]$ is abnormally low (Table 2). This exceptional situation is most certainly due to the influence of the ring current of the benzenoid ring of the ancilliary indenyl.

The values of the $\nu$(CO) stretching vibrations change little in each of the transformations **1a** → **4a** $\nu$(CO)(KBr), 1959, 1871 → 1964, 1869 $cm^{-1}$; $\nu$(CO) (Nujol), 1979, 1888 → 1962, 1890 $cm^{-1}$ and **2** → **5** ($\nu$(CO)(KBr), 1955, 1879 → 1948, 1874 $cm^{-1}$; $\nu$(CO) (Nujol), 1954, 1879 → 1952, 1881 $cm^{-1}$).

Further confirmation of the trihapto coordination of the indenyl ring in **4a** and **5** stems from the large downfield shift (deshielding) of the ring junction $C^4$ and $C^9$ carbon atoms in the $^{13}C$ NMR spectra (see Table 2). These types of values also indicate that the $\eta^3$-indenyl in **4a** and **5** is associated with a marked slip-fold distortion. Values of $\delta \approx 120$ ppm for these quaternary carbon atoms correspond to a typical $\eta^5$-indenyl with a fold angle ($\Omega$; see [13] for definition) close to 0°, i.e. planar. An appreciable degree of bending, $\Omega = 8.5°$, has already been found for $\delta \approx 127$ ppm [14b]. Strongly bent rings have $C^4$ and $C^9$ resonances at higher $\delta$ values as exemplified for $[(\eta^3\text{-Ind})Ir(PMe_3)_3]$ ($\Omega = 28°$; $\delta = 156.7$ ppm; $C^4$–$C^9$) [3] and $[CpMo(\eta^3\text{-Ind})(CO)_2]$ ($\Omega = 26°$; $\delta = 151.1$ ppm; $C^4$–$C^9$) [6a]. In the present case, the values of $\delta = 146.73$ and 149.23 ppm for **4a** and **5** imply a large $\Omega$, about 20°. A crystal structure determination of **5** confirms these assignments. The crystals of **5** are built up of discrete monomeric ions. Two crystallographically independent cations and anions are located on a mirror plane. The $BF_4^-$ anions are disordered on two equivalently occupied positions. Both cations (molecule **A** and molecule **B**) are identical in their three-dimensional assemblies within standards limits. Therefore only **A** will be discussed. In **5A** the molecular structure is best described as a slightly distorted octahedron around the tungsten atom with two acetonitrile ligands together with two carbonyl groups in the equatorial plane. The two remaining apices are occupied by an additional acetonitrile molecule and the indenyl group. A view of the molecule is shown in Fig. 2 with the appropriate numbering scheme. Relevant bond angles and distances are given in Table 3.

The metal atom W(1) and one acetonitrile group N(1), C(2), C(3) are located on the mirror plane which bisects the indenyl through C(6). As expected from the NMR measurements, the indenyl is clearly $\eta^3$ coordinated. Using the slip parameters of Faller et al. [13], the W(1) atom has slipped a distance $|S| = 130.7$ pm (**B** $|S| = 127.7$ pm) (!) away from the centroid of the five-membered ring. A key feature is the folding of the uncomplexed "ene fragment" (C(8), C(8)a in Fig. 2) (these atoms are numbered $C^4$ and $C^9$ in the NMR discussion above) of the benzonoid part of the indenyl ligand. The observed fold angle $\Omega$ is 24.1° (**B**, $\Omega$ = 27.4°). Table 4 compares all the slip parameters of **5** with those of other related and fully characterized $\eta^3$–$\eta^5$ indenyl complexes.

To the best of our knowledge, **5** is the first hexacoordinated tungsten complex with an indenyl at the apical

Table 4
Slip parameters (defined in [13,15]) for $[\eta^3\text{-IndW}(CO)_2(NCMe)_3]BF_4$ (**5**) and related compounds

| Compound | $\Delta = \|S\|$ (pm) | $\sigma$ (°) | $\Psi$ (°) | $\Delta$(M–C) (pm) | $\Omega$ (°) | References |
|---|---|---|---|---|---|---|
| $[IndW(CO)_2(NCMe)_3]^+$ | | | | | | This work |
| $\eta^3$-ind A | 130.7 | 0.0 | 33.0 | 93.5 | 24.1 | |
| $\eta^3$-ind B | 127.7 | 0.0 | 32.3 | 91.3 | 27.4 | |
| $[Ind_2V(CO)_2]^+$ | | | | | | [15] |
| $\eta^5$-ind 1 | 19.2 | 27.9 | 5.6 | 13 | No | |
| $\eta^5$-ind 2 | 19.7 | 17.7 | 5.8 | 15 | No | |
| $[Ind_2V(CO)_2]$ | | | | | | [16] |
| $\eta^5$-ind | 15.7 | 0.0 | 4.6 | 13 | No | |
| $\eta^3$-ind | 79.8 | 1.5 | 20.9 | 56 | 12.0 | |
| $[Cp_2W(CO)_2]$ | | | | | | [17] |
| $\eta^5$-Cp | 7.6 | 0 | 2.2 | 10 | 4.9 [a] | |
| $\eta^3$-Cp | 92.8 | 0 | 23.4 | 62 | 19.7 | |
| $[IndCpMo(NCME)]^{2+}$ | | | | | | [6b] |
| $\eta^5$-Cp | 6.5 | 9.7 | 1.9 | 4 | No | |
| $\eta^5$-Ind | 19.4 | 2.6 | 5.6 | 15 | 5.1 | |
| $[IndCpMo(CO)_2]$ | | | | | | [6a] |
| $\eta^5$-Cp | 12.0 | 0.6 | 3.4 | 9 | 2.1 | |
| $\eta^3$-ind | 94.7 | 6.0 | 24.1 | 65 | 21.4 | |

[a] Value may be incorrect.

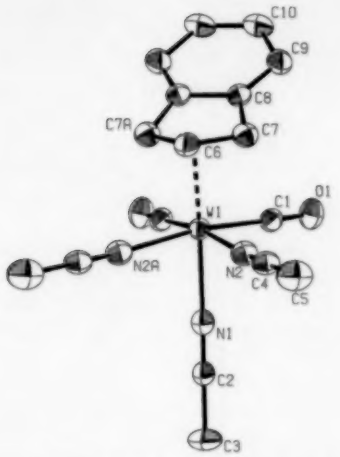


Fig. 2. Molecular structure of the cation **5** showing 50% probability ellipsoids and the atom-labelling scheme. Hydrogen atoms are omitted for clarity. A crystallographic mirror plane passes through C(3), C(2), N(1), W(1) and C(6). The operator for generating equivalent atoms is $(-x, y, z)$.

position, and up to now only three other similar tungsten η-allyl complexes have been structurally characterized: $[(\eta^3\text{-}C_3H_5)(CF_3COO)(CO)_2W(MeOCH_2CH_2OMe)]$ [19] $[(\eta^3\text{-}C_3H_5)Br(CO)_2W\text{-}(C_6H_{11}N{=}CH{-}CH{=}N\ C_6H_{11}\text{-}N,N')]$ [20] and $[N(Et)_4][\eta^3\text{-}(C_3H_5)Cl_2(CO)_2WP(C_6H_5)_3]$ [21]. All interatomic distances and angles are within the expected values for a hexacoordinated tungsten atom and fit those published in [19–21]. The conformation relative to the carbonyls of the indenyl in **5** is the same as observed in these η-allyl complexes and schematically represented in **a**; the open side of the coordinated allyl (or pseudo allylic) atoms is oriented towards the quadrant defined by the carbonyls. In other words, the directions defined between the central and terminal allylic (or pseudo allylic) carbons are projected over the M–CO directions in an eclipsed fashion. This conformation seems to be rather general for $[L_3M(CO)_2(\eta^3\text{-allyl})]^{n+}$ species (M = Mo or W) and is also observed in the crystal structure of $[Mo(\eta^3\text{-}C_3H_5)(CO)_2(CH_3CN)(bipy)]^+$. Molecular orbital (MO) calculations on this complex **a** at the extended Hückel level show it to be preferred over the rotated conformer [22]. Conformation **b** is present in the isoelectronic $[CpMo(\eta^3\text{-Ind})(CO)_2]$.

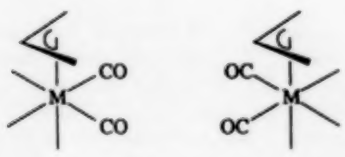


**a** **b**

As exemplified by the spectrum in Fig. 1(b) and later by product isolation, redissolution of **4a** and **5** in $CH_2Cl_2$ results in the expulsion of one coordinated NCMe and the inverse haptotropic shift, to form **1a** and **2** respectively Eq. (4) [5].

These mild reaction conditions show that ring slippage between **1a** and **4a** as well as between **2a** and **5** is very facile and prompted a study of similar reactions with other donors, which are also summarized in Scheme 1. Dissolution and recrystallization of the DMF complex $[(\eta^5\text{-Ind})Mo(CO)_2(DMF)_2]BF_4$ (**1d**) from DMF gives the ring-slipped adduct $[(\eta^3\text{-Ind})Mo(CO)_2(DMF)_3]BF_4$ (**4e**). In contrast with the structural flexibility of **4a** at room temperature, the $^1H$ NMR spectrum of **4e**, in DMF-$d_7$, is well resolved and compatible with the presence of a structurally rigid species **4e** with a well-defined $\eta^3$-Ind ($H^2$ at $\delta = 6.99$ ppm). This spectrum remains invariant at low temperatures showing that DMF is less labile than the NCMe in this systems. The low field chemical shifts of the $C^4$–$C^9$ junction atoms in the $^{13}C$ NMR spectrum suggests a high degree of folding. An intermediate behaviour is found for the ethylenediamine complex **1e**. At room temperature its $^1H$ NMR spectrum, NCMe-$d_3$, looks like that of **4a**, revealing dynamic interconversions. However, at −45°C, two species still remain clearly identifiable: **1e**, characterized by its $H^2$ at $\delta = 5.18$ ppm, and a trihapto-indenyl complex, $[(\eta^3\text{-Ind})Mo(CO)_2(en)(NCMe)]BF_4$ (**4f**), characterized by $H^2$ at $\delta = 7.07$ ppm. Under these circunstances, it is not surprising that **1e** readily rearranges, in warm acetonitrile, to give the ring-slipped complex $[(\eta^3\text{-Ind})Mo(CO)_2\{\eta^3\text{-}HC(pz)_3\}]BF_4$ (**4b**) in which the tpm becomes tridentate. The complex is now freely soluble in $CH_2Cl_2$ and the $^1H$ NMR and $^{13}C$ NMR spectra are consistent with this structural rearrangement. The *meso* $H^2$ of the indenyl appears at low field ($\delta = 6.90$ ppm), and the $C^4$–$C^9$ resonances at $\delta = 147.80$ ppm indicate a clearly folded $\eta^3$-indenyl. The two $\nu$(CO) bands appear now at 1946 and 1867 $cm^{-1}$ (Nujol mull) instead of 1958 and 1883 $cm^{-1}$ (KBr pellet). This set of data is similar to that observed for the neutral hydrotrispyrazolylborate analogue $[(\eta^3\text{-Ind})Mo(CO)_2\{\eta^3\text{-}HB(pz)_3\}]$ (**4c**) obtained from the reaction of **1a** with $K[HB(pz)_3]$. Likewise, reaction of **1a** with the triaza-macrocycle $Me_3tacn$ ($Me_3tacn$ = 1,4,7-*N*,*N*′,*N*″-trimethyltriazacyclononane) gives the ring-slipped complex $[(\eta^3\text{-Ind})Mo(CO)_2\{\eta^3\text{-}Me_3tacn\}]$ (**4d**). In both cases, no signs of an intermediate such as $[(\eta^5\text{-Ind})Mo(CO)_2\{\eta^2\text{-}HB(pz)_3\}]$ were detected although we believe that the transformations of **1c** into **4b** as well as the formation of **4c** and **4d** proceed by stepwise $\eta^5 \rightarrow \eta^3$ haptotropic shifts from initially formed complexes $[(\eta^5\text{-Ind})M(CO)_2L_2]^+$ where the nitrogen ligands are bidentate ($L_2 = CH(pz)_3$, $[HB(pz)_3]^-$ or $Me_3tacn$).

Table 5
Three examples of $\eta^5 \rightarrow \eta^3$ ring slippages in indenyl complexes

| $\eta^5$-Ind → $\eta^3$-Ind ring slippage reactions | Reference |
|---|---|
| $[(\eta^5\text{-Ind})\text{Ir(COD)}] + \text{PMe}_3$ (exc) → $[(\eta^3\text{-Ind})\text{Ir}(\text{PMe}_3)_2]$ | [3] |
| $[(\eta^5\text{-Ind})\text{Fe}(\text{CO})_2]^- + \text{CO}$ (1 atm) → $[(\eta^3\text{-Ind})\text{Fe}(\text{CO})_3]^-$ | [23] |
| $[(\eta^5\text{-Ind})_2\text{V}] + \text{CO}$ (1 atm) → $[(\eta^5\text{-Ind})(\eta^3\text{-Ind})\text{V}(\text{CO})_2]$ | [17] |

Formally, **4b–4d** are analogues of $[\text{Cp}'\text{Mo}(\eta^3\text{-ind})(\text{CO})_2]$ (Cp′ = Cp or Ind) reported elsewhere [5,6]. Complex **4d** is only accessible from the bis(acetonitrile) complex **1a** and not directly from species $[(\eta^5\text{-Ind})\text{Mo}(\text{CO})_2(\eta^2\text{-C}_3\text{H}_6)\text{FBF}_3]$ as noted in Scheme 1. Nitrogen bases such as $\text{Me}_3$tacn, $\text{NEt}_3$ or even aniline deprotonate the propene, as shown [22] by

$$[(\eta^5\text{-Ind})\text{Mo}(\eta^3\text{-C}_3\text{H}_5)(\text{CO})_2] \underset{\text{Me}_3\text{tacn}}{\overset{\text{HBF}_4}{\rightleftharpoons}} [(\eta^5\text{-Ind})\text{Mo}(\eta^2\text{-C}_3\text{H}_6)(\text{CO})_2\text{FBF}_3] \quad (5)$$

Having gathered all this evidence about ring-slippage reactions in $[(\eta^5\text{-Ind})\text{M}(\text{CO})_2\text{L}_2]^+$, we assumed that many other trihapto-indenyl complexes of general formula $[(\eta^3\text{-Ind})\text{M}(\text{CO})_2\text{L}_2\text{L}']^+$ could be obtained by addition of L or L′ to the bipyridyl, phosphine or phosphite complexes **1b**, **1f–1i** according to

$$[(\eta^5\text{-Ind})\text{M}(\text{CO})_2\text{L}_2]^+ + \text{L}' \longrightarrow [(\eta^3\text{-Ind})\text{M}(\text{CO})_2\text{L}_2\text{L}']^+ \quad (6)$$

Very much to our surprise, none of the reactions tried led to the expected addition or ring-slippage processes. In fact, the bipy, dppe and triphos derivatives, **1b**, **1h** and **1i**, remain unchanged after 12 h in refluxing NCMe. Preparative as well as in-situ $^1$H NMR experiments showed that the $\text{P(OMe)}_3$ and $\text{PMe}_3$ derivatives, **1f** and **1g**, also remain unchanged after prolonged reaction times (NCMe or $\text{CH}_2\text{Cl}_2$) in the presence of large excesses of $\text{P(OMe)}_3$ and $\text{PMe}_3$ respectively.

To the best of our knowledge, only three other examples of clear-cut $\eta^5 \rightarrow \eta^3$ ring slippages in indenyl complexes, promoted by donor addition, have been reported, as summarized in Table 5.

In the case of Ir-$d_8$, $\text{PMe}_3$ or $\text{PMe}_2\text{Ph}$ is necessary for the ring slippage to take place and CO is ineffective. In contrast, the very electron-rich iron and vanadium complexes undergo this slippage in the presence of CO at 1 atm. In the case of the three-legged piano-stool $d_6$ complex $[\text{IndRe}(\text{CO})_3]$, $\eta^5 \rightarrow \eta^1$ ring slippage is observed in the presence of $\text{PMe}_3$ and $\text{PBu}_3$, at room temperature, or with bipy at 54°C, but the kinetically required $\eta^3$ intermediate could not be detected chemically or spectroscopically (Eq. (3) [4]).

In view of these results and given the facility of many of the above-reported ring slippages, it is rather unexpected that the weakly coordinating labile NCMe is capable of inducing an $\eta^5 \rightarrow \eta^3$ haptotropic rearrangement, **1a** → **4a**, whereas the strong donor $\text{PMe}_3$ is not. As shown by Merola et al. [3] and Casey and O'Connor [4], bulky donors do not favour ring slippages which are otherwise facile with $\text{PMe}_3$. However, in our reactions, no important steric problems hindering ligand addition to any of the complexes **1b**, **1f–1h** are apparent. For instance, one would expect ready addition of NCMe to derivative $[(\eta^5\text{-Ind})\text{M}(\text{CO})_2\text{bipy}]^+$ (**1b**), where there are two N-donor ligands and bipy does not create steric problems if coordinated to the equatorial plane of the putative final octahedral product, $[\text{Mo}(\eta^3\text{-Ind})(\text{CO})_2\text{-(NCMe)(bipy)}]\text{BF}_4$. In fact, a crystal structure of $[\text{Mo}(\eta^3\text{-C}_3\text{H}_5)(\text{CO})_2\text{-(NCMe)(bipy)}]\text{BF}_4$ has the *fac*-{(NCMe)bipy} ligand arrangement and does not reveal any important intramolecular steric strain [24]. Clearly, ligands such as $\text{CH(pz)}_3$, $[\text{HB(pz)}_3]^-$ and $\text{Me}_3$tacn all possess a much larger steric bulk than the combined *fac*-{(NCMe)bipy} ligand arrangement. Nevertheless, they are capable of inducing or stabilizing indenyl slippage in the present system, whereas the *fac*-{(NCMe)bipy} ligand arrangement is not.

One may argue that ring slippage promoted by $\text{CH(pz)}_3$, $[\text{HB(pz)}_3]^-$ or $\text{Me}_3$tacn is favoured by the coordination geometry and the chelate effect of the tridentate ligands which overcome electronic barriers present in the *fac*-{(NCMe)bipy} ligand set. However, the reasons for the facile addition of NCMe or DMF to both **1a** and **2** must be almost entirely electronic as steric problems are obviously absent. The identification of these "electronic" factors or conditions should be important for understanding the reactivity enhancement of indenyl complexes and the "indenyl effect" and an independent MO study of these and related problems is under way.

## 3. Conclusions

Stable octahedral complexes of molybdenum and tungsten bearing the trihapto-indenyl ligand, $[(\eta^3\text{-Ind})\text{M}(\text{CO})_2\text{L}_2\text{L}']^+$, are easily accessible from four-legged piano-stool precursors, $[(\eta^5\text{-Ind})\text{M}(\text{CO})_2\text{L}_2]^+$, by addition of L′. This otherwise rare addition or ring-slippage reaction is facile for a series of *N*-donor ($\text{L}_2\text{L}' = (\text{NCMe})_3$, $\text{CH(pz)}_3$, $[\text{HB(pz)}_3]^-$ or $\text{Me}_3$tacn) and DMF but is not observed for the corresponding

complexes with $L_2$ = bipy, $(PMe_3)_2$, $(P(OMe)_3)_2$, dppe or triphos. The reasons for this unexpected behaviour seem to be essentially electronic in character and prompt theoretical and experimental studies with other ligands (N, P, S and O).

## 4. Experimental details

All preparations and manipulations were done with standard Schlenk techniques under argon. Solvents were dried by standard procedures (tetrahydrofuran and $Et_2O$ over Na–benzophenone ketyl; $CH_2Cl_2$, NCMe and NCEt over $CaH_2$) distilled under argon and kept over 4 Å molecular sieves (3 Å for NCMe).

Microanalyses were performed at the Instituto de Tecnologia Química e Biológica. NMR spectra were measured on a Bruker CXP 300, $^1H$ and $^{13}C$ chemical shifts are reported on the scale relative to $SiMe_4$ ($\delta = 0.0$ ppm) and the $^{31}P$ spectra are given relative to TMP–solvent [25]. IR spectra were obtained using a Unicam Mattson Model 7000 Fourier transform spectrometer. $[IndMo(NCMe)_2(CO)_2]BF_4$ (**1a**) [6a] and $[IndW(NCMe)_2(CO)_2]BF_4$ (**2**) [5] were prepared as published.

### 4.1. Preparation of $[IndMobipy(CO)_2]BF_4$ (1b)

A solution of $[IndMo(\eta^3\text{-}C_3H_5)(CO)_2]$ (0.22 g, 0.71 mmol) in $CH_2Cl_2$ (15 ml) was treated with $HBF_4 \cdot Et_2O$ (1 equivalent). After 10 min 2,2′-bipyridyl was added (0.13 g, 0.85 mmol) and the mixture left for 1 h. After concentration to about 5 ml and addition of ether, a pink–red complex precipitated. The mixture was filtered and the residue recrystallized from $CH_2Cl_2$–$Et_2O$ (yield, 98%). Anal. Found: C, 49.38; H, 3.05; N, 5.42. for $C_{21}H_{15}BF_4MoN_2O_2$ Calc.: C, 49.45; H, 2.96; N, 5.46%. Selected IR (KBr): $\nu$(CO) 1975, 1958, 1901, 1874 vs $cm^{-1}$ $^1H$ NMR (NCMe-$d_3$, 300MHz): $\delta$ 9.36 (d, 2H, bipy); 8.30 (d, 2H, bipy); 8.07 (t, 2H, bipy); 7.57 (t, 2H, bipy); 6.95 (m, 2H, $H^{5-8}$); 6.66 (m, 2H, $H^{5-8}$); 6.47 (d, 2H, $H^{1/3}$); 5.47 (t, 1H, $H^2$) ppm.

### 4.2. Preparation of $[IndMo(\eta^2\text{-}tpm)(CO)_2]BF_4$ (1c)

A solution of $[IndMo(NCMe)_2(CO)_2]BF_4$ (0.32 g, 0.73 mmol) in $CH_2Cl_2$ (20 ml) was treated with trispyrazolylmethane (0.16 g, 0.75 mmol) for 30 min. The pale-pink powder was filtered off and washed with ether (yield, 90%). Anal. Found: C, 44.53; H, 2.96; N, 14.62. $C_{21}H_{17}BF_4MoN_6O_2$ Calc.: C, 44.39; H, 2.99; N, 14.78%. Selected IR (KBr): $\nu$(CO) 1958, 1883 vs $cm^{-1}$.

### 4.3. Preparation of $[IndMo(DMF)_2(CO)_2]BF_4$ (1d)

A solution of $[IndMo(\eta^3\text{-}C_3H_5)(CO)_2]$ (0.10 g, 0.32 mmol) in $CH_2Cl_2$ (20 ml) was treated with $HBF_4 \cdot Et_2O$ (1 equivalent). After 10 min an excess of DMF (2 ml) was added and the mixture left for 1 h. The solvent was evaporated and the residue recrystallized from $CH_2Cl_2$–$Et_2O$ (yield, 88%). Selected IR (Nujol): $\nu$(CO) 1962, 1865 vs, $\nu$(C=O) 1657 vs $cm^{-1}$. $^1H$ NMR ($CH_2Cl_2$-$d_2$ 300 MHz): $\delta$ 8.04 (s, CH); 7.47 (m, 2H, $H^{5-8}$); 7.39 (m, 2H, $H^{5-8}$); 6.15 (d, 2H, $H^{1/3}$); 4.98 (t, 1H, $H^2$); 3.01 (s, 6H, $CH_3$); 2.72 (s, 6H, $CH_3$) ppm.

### 4.4. Preparation of $[IndMo(en)(CO)_2]BF_4$ (1e)

A solution of $[IndMo(\eta^3\text{-}C_3H_5)(CO)_2]$ (0.20 g, 0.65 mmol) in $CH_2Cl_2$ (20 ml) was treated with $HBF_4 \cdot Et_2O$ (1 equivalent). After 10 min, an excess of $H_2NCH_2$-$CH_2NH_2$ was added and the reaction left for 1 h. After concentration to about 5 ml and addition of ether, the orange precipitate was filtered off and washed with ether (yield, 92%). Anal. Found: C, 37.58; H, 3.59; N, 6.51. $C_{13}H_{15}BF_4MoO_2N_2$ Calc.: C, 37.71; H, 3.65 N, 6.77%. Selected IR. (KBr), $\nu$(CO) 1969, 1854 vs $cm^{-1}$. $^1H$ NMR ($Me_2CO$-$d_6$, 300 MHz): $\delta$ 7.84 (m, 2H, $H^{5-8}$); 7.51 (m, 2H, $H^{5-8}$); 6.23 (d, 2H, $H^{1/3}$); 5.18 (t, 1H, $H^2$); 5.41 (br, 2H, $NH_2$); 3.08 (br, 2H, $NH_2$); 2.33 (m, 2H, $CH_2$); 1.69 (m, 2H, $CH_2$) ppm.

### 4.5. Preparation of $[IndMo\{P(OMe)_3\}_2(CO)_2]BF_4$ (1f)

A solution of $[IndMo(\eta^3\text{-}C_3H_5)(CO)_2]$ (0.20 g, 0.65 mmol) in $CH_2Cl_2$ (15 ml) was treated with $HBF_4 \cdot Et_2O$ (1 equivalent). After 10 min, $P(OMe)_3$ was added (0.15 ml, 1.3 mmol) and the mixture left for 1 h. After concentration to about 8 ml and addition of ether, a microcrystalline yellow precipitate was filtered off and washed with ether (yield, 95%). Anal. Found: C, 34.07; H, 4.18. $C_{17}H_{25}BF_4MoO_8P_2$ Calc.: C, 33.91; H, 4.19%. Selected IR (KBr): $\nu$(CO) 1991, 1906 vs $cm^{-1}$. $^1H$ NMR (NCMe-$d_3$, 300 MHz): $\delta$ 7.59 (m, 2H, $H^{5-8}$); 7.30 (m, 2H, $H^{5-8}$); 6.07 (d, 2H, $H^{1/3}$); 5.60 (t, 1H, $H^2$); 3.75 (d, 18H, $J_{PH} = 11.2$ Hz, $OCH_3$) ppm. $^{31}P$ (NCMe-$d_3$, 121.49 MHz, 25°C): $\delta$ −58.93 (br, $P(OMe)_3$) ppm.

### 4.6. Preparation of $[IndMo(PMe_3)_2(CO)_2]BF_4$ (1g)

A solution of $[IndMo(\eta^3\text{-}C_3H_5)(CO)_2]$ (0.20 g, 0.65 mmol) in $CH_2Cl_2$ (15 ml) was treated with $HBF_4 \cdot Et_2O$ (1 equivalent). After 10 min, $PMe_3$ was added (0.13 ml, 1.3 mmol) and the mixture left for 1 h. After concentration to about 8 ml and addition of ether, a microcrystalline pale-yellow precipitate was filtered off and washed with ether (yield, 95%). Anal. Found: C, 40.13; H, 5.00, $C_{17}H_{25}BF_4MoO_2P_2$ Calc.: C, 40.35; H, 4.98%. Selected IR (KBr): $\nu$(CO) 1958, 1877 vs $cm^{-1}$. $^1H$ NMR (NCMe-$d_3$, 300 MHz): $\delta$ 7.66 (m, 2H, $H^{5-8}$); 7.28 (m, 2H, $H^{5-8}$); 5.85 (d, 2H, $H^{1/3}$); 5.54 (t, 1H, $H^2$); 1.66 (d, 18H, $J_{PH} = 8.7$ Hz, $CH_3$) ppm. $^{31}P$

(NCMe-$d_3$, 121.49 MHz, 25°C): δ 13.10 (s, $PMe_3$) ppm.

### 4.7. Preparation of [IndMo(dppe)(CO)$_2$]BF$_4$ (1h)

A solution of [IndMo($\eta^3$-$C_3H_5$)(CO)$_2$] (0.20 g, 0.65 mmol) in $CH_2Cl_2$ (15 ml) was treated with $HBF_4 \cdot Et_2O$ (1 equivalent). After 10 min, 1,2 bis(diphenylphosphino)ethane was added (0.30 g, 0.75 mmol) and the reaction mixture left for 1 h. After concentration to half the initial volume and addition of ether, the yellow precipitate was filtered off and washed with ether. It was then recrystallized from $CH_2Cl_2$–$Et_2O$ (yield, 94%). Anal. Found: C, 59.00; H, 4.00. $C_{37}H_{31}BF_4MoO_2P_2$ Calc.: C, 59.07; H, 4.15%. Selected IR (KBr): ν(CO) 1973, 1904 vs cm$^{-1}$. $^1$H NMR (NCMe-$d_3$, 300 MHz): δ 7.66–7.32 (m, 20H, Ph); 7.08 (m, 2H, $H^{5-8}$); 6.01 (m, 2H, $H^{5-8}$); 5.59 (d, 2H, $H^{1/3}$); 5.28 (t, 1H, $H^2$); 2.64 (br, 4H, $CH_2$) ppm. $^{31}$P NMR (NCMe-$d_3$, 121.49 MHz, 25°C): δ 35.86 (br, dppe); 15.08 (br, dppe) ppm.

### 4.8. Preparation of [IndMo(triphos)(CO)$_2$]BF$_4$ (1i)

A solution of [IndMo($\eta^3$-$C_3H_5$)(CO)$_2$] (0.20 g, 0.65 mmol) in $CH_2Cl_2$ (15 ml) was treated with $HBF_4$–$Et_2O$ (1 equivalent). After 10 min, triphos was added (0.40 g, 0.65 mmol) and the reaction mixture left for 2 h. After concentration to half the initial volume and addition of ether, the yellow precipitate was filtered off and washed with ether (yield, 94%). Selected IR (KBr): ν(CO) 1965, 1909 vs cm$^{-1}$. $^1$H NMR ($Me_2CO$-$d_6$, 300 MHz): δ 7.85–7.10 (m, 30H, Ph); 7.06 (m, 2H, $H^{5-8}$); 6.58 (m, 2H, $H^{5-8}$); 5.71 (t, 1H, $H^2$); 5.36 (d, 2H, $H^{1/3}$); 2.77 (m, 4H, $CH_2$); 2.55 (m, 2H, $CH_2$); 1.16 (m, 3H, $CH_3$) ppm.

### 4.9. Preparation of [CpMo{$\eta^2$-HC(pz)$_3$}(CO)$_2$]BF$_4$ (3)

A solution of [CpMo($\eta^3$-$C_3H_5$)(CO)$_2$] (0.25 g, 0.97 mmol) in $CH_2Cl_2$ (20 ml) was treated with $HBF_4$–$Et_2O$ (1 equivalent). After 10 min a slight excess of trispyrazolylmethane (0.21 g, 1.0 mmol) was added and stirring continued for 1 h. The reaction mixture was then concentrated and $Et_2O$ added to precipitate an orange product which was further recrystallized from $CH_2Cl_2$–$Et_2O$ (yield, 92%). Anal. Found: C, 39.25; H, 2.81; N, 16.26. $C_{17}H_{15}BF_4MoN_6O_2$ Calc.: C, 39.41; H, 2.92; N, 16.22%. Selected IR (KBr): ν(CO) 1983, 1912 vs cm$^{-1}$. $^1$H NMR (NCMe-$d_3$, 300 MHz, room temperature): δ 8.51 (s, 1H, CH), 8.47 (dd, 2H, $H^3$), 8.04 (dt, 2H, $H^5$), 7.50 (d, 1H, $H^5$), 6.77 (dd, 2H, $H^4$), 6.60 (d, 1H, $H^3$), 6.36 (dd, 1H, $H^4$), 5.80 (s, 5H, Cp) ppm. $^{13}$C NMR (NCMe-$d_3$, 75 MHz, room temperature); δ 253.29, CO; 154.62, 2$C^3$; 142.71, $C^3$; 141.10, 2$C^5$; 129.59, $C^5$; 110.87, 2$C^4$; 108.89, $C^4$; 99.32, Cp; 80.50, CH ppm.

### 4.10. Preparation of [IndMo(NCMe)$_3$(CO)$_2$]BF$_4$ (4a)

A solution of [IndMo(NCMe)$_2$(CO)$_2$]$BF_4$ (0.22 g, 0.50 mmol) in NCMe (20 ml) was warmed to 45°C for 30 min. The resulting dark-red solution was concentrated and addition of $Et_2O$ gave the crystalline product, which was further recrystallized from NCMe–$Et_2O$ (yield, 98%). Anal. Found: C, 42.75; H, 3.30; N, 8.75. $C_{17}H_{16}BF_4MoN_3O_2$ Calc.: C, 42.80; H, 3.38; N, 8.81%. Selected IR (Nujol): ν(N≡C) 2317, 2287 w; ν(CO) 1962, 1890 vs cm$^{-1}$. Selected IR (KBr): ν(CO) 1964, 1869 vs cm$^{-1}$. $^1$H NMR (NCMe-$d_3$, 300 MHz, −40°C): δ 7.20 (t, 1H, $H^2$), 6.47–6.37 (m, 4H, $H^{5-8}$), 5.10 (d, 2H, $H^{1/3}$), 1.95 (s, 9H, C$H_3$) ppm. $^{13}$C NMR (NCMe-$d_3$, 75 MHz, −40°C): δ 221.50, CO; 146.73, $C^{4/9}$; 125.03, $C^{5/8}$; 118.20, $C^{6/7}$; 118.16 (s, $NCCD_3$ and NCMe); 98.72, $C^2$; 75.40, $C^{1/3}$, 1.81–0.19 (m, $NCCD_3$ and NCMe) ppm.

### 4.11. Preparation of [($\eta^3$-Ind)Mo{$\eta^3$-HC(pz)$_3$}(CO)$_2$]BF$_4$ (4b)

A solution of [IndMo($\eta^2$-tpm)(CO)$_2$]$BF_4$ (0.20 g, 0.35 mmol) in NCMe (20 ml) was warmed to 45°C for 2 h. The solution was concentrated and addition of $Et_2O$ gave an orange product which was further recrystallized from NCMe–$Et_2O$ (−30°C) (yield, 98%). Anal. Found: C, 44.28; H, 3.00; N, 14.70. $C_{21}H_{17}BF_4MoN_6O_2$ Calc.: C, 44.39; H, 2.99; N, 14.78%. Selected IR (KBr) ν(CO) 1946, 1867 vs cm$^{-1}$. $^1$H NMR (NCME-$d_3$, 300 MHz, room temperature): δ 9.11 (d 1H, $H_5$), 8.55 (s, 1H, C$H$), 8.14 (d, 1H, $H_3$), 8.12 (d, 2H, $H_3$), 8.05 (d, 2H, $H_5$), 6.90 (t, 1H, $H^2$), 6.72–6.69 (m, 3H, $2H^{5-8} + H_4$), 6.59–6.51 (m, 4H, $2H^{5-8} + 2H_4$) 5.55 (d, 2H, $H^{1/3}$) ppm. $^{13}$C NMR (NCMe-$d_3$, 75 MHz, room temperature): 226.50, CO; 153.70, $C_3$; 147.80, $C^{4/9}$; 146.99, $2C_3$; 135.74, $2C_5$; 134.90, $C_5$; 125.63, $C^{5/8}$; 119.01, $C^{6/7}$; 110.67, $C_4$; 109.29, $2C_4$; 99.76, $C^2$; 76.07, $C^{1/3}$; 75.69, $C$H ppm.

### 4.12. Preparation of [($\eta^3$-Ind)Mo{$\eta^3$-HB(pz)$_3$}(CO)$_2$] (4c)

A solution of [IndMo(NCMe)$_2$(CO)$_2$][$BF_4$] (0.22 g, 0.50 mmol) in $CH_2Cl_2$ (20 ml) was treated with K[HB(pz)$_3$] (0.13 g, 0.52 mmol). After 2 h the solvent was removed under vacuum and the residue extracted with hexane. Ether was added and after concentration and evaporation the compound separated as brick-red microcrystals. Further recrystallization was from hexane–$Et_2O$ (yield, 86%). Anal. Found: C, 50.10; H, 3.55; N, 17.68. $C_{20}H_{17}BMoN_6O_2$ Calc.: C, 50.03; H, 3.57; N, 17.50%. Selected IR (KBr): ν(BH) 2475; ν(CO) 1939, 1848 vs cm$^{-1}$. $^1$H NMR (NCMe-$d_3$, 300 MHz, room temperature): δ 8.86 (d, 1H, $H_5$), 7.81 (d, 2H, $H_5$), 7.65 (d, 2H, $H_3$), 7.64 (d, 1H, $H_3$), 6.63 (t,

1H, $H^2$), 6.70–6.67 (m, 2H, $H^{5-8}$), 6.52–6.49 (m, 2H, $H^{5-8}$), 6.44 (t, 1H, $H_4$), 6.25 (d, 2H, $H_4$), 5.40 (d, 2H, $H^{1/3}$) ppm. $^{13}$C NMR (NCMe-$d_3$, 75 MHz, room temperature): $\delta$ 229.88, CO; 150.46, $C_3$; 148.56, $C^{4/9}$; 143.81, $2C_3$; 137.32, $2C_5$; 136.08, $C_5$; 124.83, $C^{5/8}$; 118.50, $C^{6/7}$; 108.35, $C_4$; 106.77, $2C_4$; 99.59, $C^2$; 75.05, $C^{1/3}$ ppm. Mass spectroscopy $m/z$ 424 ($M^+ - 2CO$); 308 ($M^+ - C_9H_7$).

### 4.13. Preparation of $[(\eta^3\text{-Ind})Mo\{\eta^3\text{-}Me_3tacn\}(CO)_2]BF_4$ (4d)

A solution of $[IndMo(NCMe)_2(CO)_2][BF_4]$ (0.25 g, 0.57 mmol) in $CH_2Cl_2$ (20 ml) was treated with an excess of 1,4,7-trimethyltriazocyclononan (0.40 ml). After 1 h the resulting dark-red solution was concentrated and addition of $Et_2O$ gave the product, which was further recrystallized from NCMe–$Et_2O$ (−30°C) (yield, 85%). Anal. Found: C, 45.59; H, 5.20; N, 8.01. $C_{20}H_{28}BF_4MoN_3O_2$ Calc.: C, 45.74; H, 5.37; N, 8.00%. Selected IR (KBr): $\nu$(CO) 1937, 1852 vs cm$^{-1}$. (NCMe-$d_3$, 300 MHz, room temperature): $\delta$ 6.94 (t, 1H, $H^2$), 6.60 (m, 2H, $H^{5-8}$); 6.47 (m, 2H, $H^{5-8}$), 4.78 (d, 2H, $H^{1/3}$), 3.99 (s, 3H, $CH_3$), 3.05 (m, 6H, $CH_2$), 2,72 (s, 6H, $CH_3$), 2.69 (m, 6H, $CH_2$) ppm. $^{13}$C NMR ($CH_2Cl_2$-$d_2$, 75 MHz, room temperature): $\delta$ 227.31, CO; 147.03, $C^{4/9}$; 125.56, $C^{5/8}$; 118.09, $C^{6/7}$; 93.80, $C^2$; 73.43, $C^{1/3}$; 59.53, 59.18, 57.65, $CH_2$ and $CH_3$ ppm.

Table 6
Summary of crystal data and details of intensity collection for **5**

| | |
|---|---|
| *Crystal data* | |
| Formula | $C_{17}H_{16}N_3O_2W$–$BF_4$ |
| Formula weight | 530.0 |
| Crystal system | Orthorhombic |
| Space group | $Cmc2_1$ (No. 36) |
| $a$ (pm) | 1048.8(1) |
| $b$ (pm) | 1350.4(2) |
| $c$ (pm) | 2765.3(4) |
| Cell volume ($10^6$ pm$^3$) | 3916.5(9) |
| $Z$; $d_{calc}$ g cm$^{-3}$ | 4; 1.916 |
| $F$(000) | 2160 |
| Crystal size (mm) | 0.38 × 0.25 × 0.386 |
| Crystal colour and habit | Red–brown prisms |
| *Data collection and data reduction* | |
| Diffractometer | Enraf–Nonius CAD4 |
| Radiation | Mo K$\alpha$ ($\lambda$ = 71.073 pm) |
| Temperature (K) | 193 ± 3 |
| Scan type | $\omega$ scan |
| Scan range (°) | 1.20 + 0.25 tan $\theta$ |
| Scan time (s) | Variable; maximum 90 |
| 2$\theta$ limits, (°); octants | 2.0–50.0; $+h$, $+k$, $\pm l$ |
| Number of reflections collected | 3811 |
| Number of reflections for $\psi$ scan | 9 |
| $m$ (Mo K$\alpha$) (cm$^{-1}$) | 59.5 |
| Transmission factor: maximum; minimum | 0.775 : 1.000 |
| Crystal decay (%) | No |
| Extinction parameter | $2.7 \times 10^{-7}$ |
| *Solution and refinement* | |
| Number of independent data | 3615 |
| Number of observed data | 3615 ($I > 0.00$) |
| Number of refined parameters | 370 |
| Weighting scheme: $w^{-1} = \sigma^2(F_o^2) + aP^2 + bP$ | $P = (F_o^2 + 2F_c^2)/3$<br>$a = 0.0202$; $b = 19.32$ |
| $R$ indices (all data) | |
| $R_1$ [a] | 0.018 |
| $wR_2$ [b] | 0.045 |
| Flack parameter | 0.05(1) |
| Goodness of fit [c] | 1.099 |
| Peak final difference map: maximum; minimum (electrons Å$^{-3}$) | 0.51; 0.52 |
| Maximum shift/error | < 0.001 |

[a] $R_1 = \Sigma \| F_o | - | F_c \| / \Sigma F_o$.
[b] $wR_2 = [\Sigma w(F_o^2 - F_c^2)^2 / \Sigma w(F_o^2)^2]^{1/2}$.
[c] Goodness of fit = $[\Sigma w(F_o^2 - F_c^2)^2 / (N_O - N_V)]^{1/2}$.

### 4.14. Preparation of $[IndMo(DMF)_3(CO)_2]BF_4$ (4e)

A solution of $[IndMo(\eta^3\text{-}C_3H_5)(CO)_2]$ (0.10 g, 0.32 mmol) in $CH_2Cl_2$ (20 ml) was treated with $HBF_4 \cdot Et_2O$ (1 equivalent). After 10 min an excess of DMF (5 ml) was added and the reaction mixture left for 1 h. The solvent was evaporated and the residue recrystallized from DMF–$Et_2O$ (yield, 91%). Selected IR (Nujol): $\nu$(CO) 1939, 1848 vs, $\nu$(C=O) 1649 $cm^{-1}$. $^1H$ NMR (DMF-$d_7$, 300 MHz, room temperature): $\delta$ 8.02 (s, CH); 6.99 (t, 1H, $H^2$); 6.47–6.39 (m, 4H, $H^{5-8}$); 5.08 (d, 2H, $H^{1/3}$); 2.95 (s, $CH_3$); 2.78 (s, $CH_3$) ppm. $^{13}C$ NMR (DMF-$d_7$, 75 MHz, room temperature): $\delta$ 229.94, CO; 162.8 (s, DMF); 146.73 $C^{4/9}$; 123.70, $C^{5/8}$; 117.20, $C^{6/7}$; 101.30, $C^2$; 74.53, $C^{1/3}$; 35.70 (s, DMF); 30.6 (s, DMF) ppm.

### 4.15. Preparation of $[IndW(CO)_2(NCMe)_3]BF_4$ (5)

A solution of $[IndW(CO)_2(NCMe)_2]BF_4$ (0.28 g; 0.49 mmol) in NCMe (20 ml) was warmed to 45°C for 30 min. The resulting dark-red solution was concentrated and addition of $Et_2O$ gave the crystalline product which was further recrystallized from NCMe–$Et_2O$ (yield, 96%), Anal. Found: C, 36.08; H, 2.99; N, 7.38. $C_{17}H_{16}BF_4O_2N_3W$ Calc.: C, 36.14; H, 2,85; N, 7.44%. Selected IR (Nujol): $\nu$(N=C) 2318, 2288 w; $\nu$(CO) 1952, 1881 vs $cm^{-1}$. Selected IR (KBr): $\nu$(CO) 1948,

Table 7
Final coordinates and equivalent isotropic thermal parameters of the non-hydrogen atoms for $[\eta^3\text{-}IndW(CO)_2(NCMe)_3]BF_4$ (5)

| Atom | x | y | z | $U_{eq}$ ($Å^2$) |
|---|---|---|---|---|
| W(1) | 0 | 0.09025(2) | 0.22198(1) | 0.0244(1) |
| O(1) | 0.1894(4) | 0.0167(3) | 0.3013(1) | 0.043(1) |
| N(1) | 0 | 0.2368(5) | 0.2526(2) | 0.030(2) |
| N(2) | 0.1391(5) | 0.1614(3) | 0.1739(2) | 0.034(1) |
| C(1) | 0.1229(5) | 0.0458(4) | 0.2711(2) | 0.030(2) |
| C(2) | 0 | 0.3161(6) | 0.2666(3) | 0.029(2) |
| C(3) | 0 | 0.4182(7) | 0.2851(4) | 0.047(3) |
| C(4) | 0.2089(6) | 0.1944(4) | 0.1471(2) | 0.034(2) |
| C(5) | 0.2997(8) | 0.2359(6) | 0.1138(3) | 0.054(2) |
| C(6) | 0 | −0.0210(6) | 0.1660(3) | 0.032(2) |
| C(7) | 0.1089(6) | −0.0536(4) | 0.1929(2) | 0.033(2) |
| C(8) | 0.0677(4) | −0.1386(3) | 0.2222(2) | 0.029(1) |
| C(9) | 0.1351(6) | −0.2105(4) | 0.2466(2) | 0.037(2) |
| C(10) | 0.0648(7) | −0.2865(4) | 0.2691(2) | 0.038(2) |
| W(2) | 0 | 0.119166(2) | 0.43481(1) | 0.0251(1) |
| O(2) | 0.1903(4) | 0.2638(3) | 0.3556(1) | 0.043(1) |
| N(3) | 0 | 0.0451(5) | 0.4037(2) | 0.032(2) |
| N(4) | 0.1389(5) | 0.1207(4) | 0.4827(2) | 0.039(1) |
| C(11) | 0.1228(5) | 0.2364(4) | 0.3855(2) | 0.031(2) |
| C(12) | 0 | −0.0326(6) | 0.3899(3) | 0.033(2) |
| C(13) | 0 | −0.1329(9) | 0.3721(4) | 0.048(3) |
| C(14) | 0.2075(8) | 0.0833(5) | 0.5079(3) | 0.053(2) |
| C(15) | 0.2960(14) | 0.0359(9) | 0.5418(4) | 0.103(5) |
| C(16) | 0 | 0.3054(5) | 0.4910(3) | 0.032(3) |
| C(17) | 0.1079(6) | 0.3342(4) | 0.4634(2) | 0.031(2) |
| C(18) | 0.0675(5) | 0.4196(3) | 0.4335(2) | 0.038(1) |
| C(19) | 0.1339(6) | 0.4931(4) | 0.4097(2) | 0.036(2) |
| C(20) | 0.0654(7) | 0.5688(5) | 0.3864(2) | 0.043(2) |
| F(1) | 0 | 0.5446(5) | 0.1076(2) | 0.072(3) |
| F(2) | 0.0863(15) | 0.4037(8) | 0.1378(5) | 0.108(6) [a] |
| F(3) | 0.1024(11) | 0.4544(16) | 0.1632(7) | 0.144(9) [a] |
| F(4) | 0.0731(16) | 0.5353(11) | 0.1830(4) | 0.127(7) [a] |
| B(1) | 0 | 0.4835(11) | 0.1486(4) | 0.064(4) |
| F(5) | 0 | 0.0971(9) | 0.0577(3) | 0.187(8) |
| F(6) | 0.0709(15) | 0.1278(10) | −0.0163(4) | 0.103(5) [a] |
| F(7) | 0.0723(20) | 0.2459(12) | 0.0361(8) | 0.160(10) [a] |
| F(8) | 0.1048(13) | 0.1912(21) | 0.0110(10) | 0.206(17) [a] |
| B(2) | 0 | 0.1642(11) | 0.0235(4) | 0.064(5) |

$U_{eq}$ is defined as a third of the trace of the orthogonalized $U_{ij}$ tensor.
[a] Atom sites have a population of 0.500.

1874 vs $cm^{-1}$. $^1H$ NMR (NCMe-$d_3$, 300 MHz, room temperature): $\delta$ 6.55–6.48 (m, 5H, $H^{5-8}$ and $H^2$); 5.02 (d, 2H, $H^{1/3}$); 1.96 (s, $CH_3$) ppm. $^{13}C$ NMR (NCMe-$d_3$; 75 MHz, room temperature): $\delta$ 213.93, CO; 149.23, $C^{4/9}$; 125.03, $C^{5/8}$; 119.04, $C^{6/7}$; 118.28 (s, $NCCD_3$ and NCMe); 91.72; $C^2$; 66.20, $C^{1/3}$; 2.09–0.48 (m, $NCCD_3$ and NCMe) ppm.

### 4.16. X-ray structure determination of 5

Details of data collection parameters, structure solution and refinement for **5** are presented in Table 6, and the final positional parameters in Table 7. A red–brown prism, coated with silicone grease in a glass capillary, was mounted on a CAD4 diffractometer equipped with a graphite monochromator. For determination of accurate cell dimensions the positional parameters of 25 reflection (each centred in four orientations; $\theta > 20.0°$) were refined by full-matrix least-squares methods. During data collection, the intensities of three standard reflections where monitored and showed no decay. Corrections for Lorentz–polarization effects, absorption and extinction were applied. From the original data set 196 reflections (20 with $I < 0.01$; 176 systematically absent) were rejected. The structure was solved by the heavy-atom method and subsequent difference Fourier synthesis and refined by full-matrix least-squares methods, with anisotropic thermal parameters for the non-hydrogen atoms. All H atoms were identified in difference maps and were refined with isotropic thermal parameters. Both of two $BF_4^-$ anions were found disordered in two positions. Scattering factors for neutral atoms and values for anomalous dispersion were taken from reference 26 and programs for solution and refinement [27] were run on a Micro VAX 3100.

Further details of the crystal structure investigation are available on request from the Fachinformationszentrum Karlsruhe, D-76344 Eggenstein-Leopoldshafen, on quoting the depository number CSD-401921, the names of the authors and the journal citation, or from one of the authors E.H.

## Acknowledgments

This work was financially supported by the Junta Nacional de Investigação Científica e Tecnológica (JNICT). ISG thanks JNICT for grants. We thank Professor W.A. Herrmann, Technische Universität Munich, for providing analytical facilities and mass spectra.

## References and note

[1] M.E. Rerek, L.-N. Ji and F. Basolo, *J. Chem. Soc., Chem. Commun.*, (1983) 1208–1209.

[2] (a) J.M. O'Connor and C.P. Casey, *Chem. Rev.*, *87* (1987) 307–318; (b) A.K. Kakkar, S.F. Jones, N.J. Taylor, S. Collins and T.B. Marder, *J. Chem. Soc., Chem. Commun.*, (1989) 1454–1456.

[3] J.S. Merola, R.T. Kacmarcyk and D. Van Engen, *J. Am. Chem. Soc.*, *108* (1986) 329–331.

[4] C.P. Casey and J.M. O'Connor, *Organometallics*, *4* (1985) 384–388.

[5] I.S. Gonçalves and C.C. Romão, *J. Organomet. Chem.*, *486* (1995) 155–161.

[6] (a) J.A. Ascenso, C.G. de Azevedo, I.S. Gonçalves, E. Herdtweck, D. Moreno, M. Pessanha and C.C. Romão, *Organometallics*, in press; (b) J.A. Ascenso, C.G. de Azevedo, I.S. Gonçalves, E. Herdtweck, D. Moreno, C.C. Romão and J. Zühlke, *Organometallics*, *13* (1994) 429–431.

[7] J. Markham, K. Menard and A. Cutler, *Inorg. Chem.*, *24* (1985) 1581–1587.

[8] (a) M. Botrill and M. Green, *J. Chem. Soc., Dalton Trans.*, (1977) 2365; (b) M. Green, S. Greenfield and M. Kersting, *J. Chem. Soc., Chem. Commun.*, (1985) 18–20.

[9] D.J. Norris, J.F. Corrigan, Y. Sun, N.J. Taylor and S. Collins, *Can. J. Chem.*, *71* (1993) 1029.

[10] A leading discussion of NMR spectra of $HC(pz)_3$ complexes may be found in: (a) M.A. Esteruelas, L.A. Oro, M.C. Apreda, C. Foces-Foces, F.H. Cano, R.M. Claramunt, C. Lopez, J. Elguero and M. Begtrup, *J. Organomet. Chem.*, *344* (1988) 93; (b) M.A. Esteruelas, L.A. Oro, R.M. Claramunt, C. Lopez, J.L. Lavandera and J. Elguero, *J. Organomet. Chem.*, *366* (1989) 245.

[11] Trofimenko, S., *J. Am. Chem. Soc.*, *92* (1970) 5118.

[12] A.N. Nesmeyanov, N.A. Ustynyuk, L.G. Makarova, V.G. Andrianov, Yu.T. Struchkov, S. Andrae, Yu.A. Ustynyuk and S.G. Malyugina, *J. Organomet. Chem.*, *159* (1978) 189–199.

[13] J.W. Faller, R.H. Crabtree and A. Habib, *Organometallics*, *4* (1985) 929.

[14] T.B. Marder, J.C. Calabrese, D.C. Roe and T.H. Tulip, *Organometallics*, *6* (1987) 2012; (b) R.T. Baker and T.H. Tulip, *Organometallics*, *5* (1986) 839.

[15] M.B. Honan, J.L. Atwood, I. Bernal, W.A. Herrmann, *J. Organomet. Chem.*, *179* (1979) 403.

[16] J.R. Bocarsly, C. Floriani, A. Chiesi-Villa and C. Guastini, *Inorg. Chem.*, *26* (1987) 1871.

[17] R.M. Kowalewski, A.L. Rheingold, W.C. Trogler and F. Basolo, *J. Am. Chem. Soc.*, *108* (1986) 2460–2461.

[18] G. Huttner, H.H. Brinzinger, L.G. Bell, P. Friedrich, V. Benjenke and D. Neugebauer, *J. Organomet. Chem.*, *145* (1978) 329.

[19] F. Dawans, J. Dewailly, J. Meunier-Piret and P. Piret, *J. Organomet. Chem.*, *76* (1974) 53.

[20] A.J. Graham, D. Akrigg and B. Sheldrick, *Cryst. Struct. Commun.*, *6* (1977) 253.

[21] M. Boyer, J.-C. Daran and Y. Jeannin, *J. Organomet. Chem.*, *190* (1980) 177.

[22] C.A. Gamelas, I.S. Gonçalves and C.C. Romão, unpublished results, 1995.

[23] T.C. Forschner, A.R. Cutler and R.K. Kullnig, *Organometallics*, *6* (1987) 889.

[24] A.M. Galvão, *Ph.D. Dissertation*, Technical University of Lisbon, 1993.

[25] L.A. Combs-Walker and C.L. Hill, *Inorg. Chem.*, *30* (1991) 4016–4026.

[26] A.J.C. Wilson (ed.), *International Tables for Crystallography*, Vol. C, Kluwer, Dordrecht 1992, Table 6.1.1.4 (pp. 500–502), Table 4.2.6.8 (pp. 219–222) and Table 4.2.4.2 (pp. 193–199).

[27] PLATON-92, PLUTON-92, SCHAKAL, SDP, SHELXL-93 and STRUX-V.

ELSEVIER

Journal of Organometallic Chemistry 508 (1996) 183–193

Journal of Organometallic Chemistry

# Diphenylphosphine derivatives of $Co(NO)(CO)_3$, $Fe(NO)_2(CO)_2$ and $Mn(NO)(CO)_4$

Jiann T. Lin [a,*], Shiow Y. Wang [b], Yung C. Chou [a], Ming L. Gong [a,c], Yui-May Shiow [a], Han-Mou Gau [c], Yuh S. Wen [a]

[a] *Institute of Chemistry, Academia Sinica, Taipei, Taiwan*
[b] *Private Chung Chou Junior College of Technology and Commerce, Chung Hua, Taiwan*
[c] *Department of Chemistry, National Chung-Hsin University, Taichung, Taiwan*

Received 2 June 1995; in revised form 19 July 1995

**Abstract**

The complexes $Co(NO)(CO)(Ph_2PH)_2$ (**1**), $Fe(NO)_2(Ph_2PH)_2$ (**2**) and $Mn(NO)(CO)_2(Ph_2PH)_2$ (**3**) are synthesized from $Co(NO)(CO)_3$, $Fe(NO)_2(CO)_2$ and $Mn(NO)(CO)_4$ respectively. Deprotonation of **1** with two equivalents of BuLi followed by subsequent addition of methyl iodide, allyl bromide and propargyl bromide provides $Co(NO)(CO)(Ph_2PMe)_2$ (**4**), $Co(NO)(CO)(Ph_2PCH_2CHCH_2)_2$ (**5**) and $Co(NO)(CO)(Ph_2PCH_2CCH)_2$ (**6**) respectively. X-ray crystal structure analyses for **1**, **3** and **4–6** were carried out to give data as followed. **1**: monoclinic; $C2/c$; $Z = 4$; $a = 17.130(5)$, $b = 9.894(2)$ and $c = 42.607(1)$ Å; $\beta = 93.29(2)°$; $V = 7210(2)$ Å$^3$; $R = 0.056$; $R_w = 0.058$. **3**: monoclinic; $C2/c$; $Z = 4$; $a = 15.231(5)$, $b = 10.247(2)$ and $c = 16.311(2)$ Å; $\beta = 102.29(2)°$; $V = 2488(1)$ Å$^3$; $R = 0.041$; $R_w = 0.042$. **4**: monoclinic; $C2/c$; $Z = 4$; $a = 15.556(3)$, $b = 12.072(1)$ and $c = 14.809(2)$ Å; $\beta$ 114.43(1)°; $V = 2532.0(7)$ Å$^3$; $R = 0.032$; $R_w = 0.031$. **5**: monoclinic; $P2_1/c$; $Z = 4$; $a = 15.427(2)$, $b = 10.118(2)$ and $c = 18.793(6)$ Å; $\beta = 102.56(1)°$; $V = 2863(1)$ Å$^3$; $R = 0.042$; $R_w = 0.046$. **6**: monoclinic; $P2_1/n$; $Z = 4$; $a = 9.3393(8)$, $b = 19.035(4)$ and $c = 16.007(1)$ Å; $\beta = 94.912(7)°$; $V = 2845.8(6)$ Å$^3$; $R = 0.052$; $R_w = 0.059$.

*Keywords:* Nitrosyl; Carbonyl; Manganese; Phosphine; Cobalt; Iron

## 1. Introduction

Coordinated NO ligands are usually much more resistant to ligand substitution than are CO groups [1]. Being a better $\pi$ acceptor than CO, a NO ligand frequently labilizes the CO ligands coordinated to the same metal atoms and sometimes causes ligand substitution to occur in rather mild conditions [2]. We are interested in dinuclear complexes with a phosphide bridge [3] since such a bridge normally is robust enough to prevent fragmentation of the dimer during reaction [4]. We therefore set out to synthesize the bis(diphenylphosphine) derivatives of $Co(NO)(CO)_3$, $Fe(NO)_2(CO)_2$, and $Mn(NO)(CO)_4$ since these metal nitrosyl carbonyls have been reported to react with various tertiary phosphines to form monosubstituted and disubstituted derivatives via carbonyl substitution [5], and deprotonation of $[M](R_2PH)$ has been one of the most frequently used methods to obtain phosphide-bridged complexes [6]. In this report we shall describe the syntheses of $[M](Ph_2PH)_2$ ($[M] = Co(NO)(CO)$ (**1**), $Fe(NO)_2$ (**2**) or $Mn(NO)(CO)_2$ (**3**)) from the aforementioned metal nitrosyl carbonyls. Such complexes could potentially form dinuclear complexes bridged by two diphenylphosphide [7], or phosphide-bridged trinuclear complexes. Some derivatives of **1** are also described.

## 2. Experimental section

### 2.1. General procedures

All reactions and manipulations were carried out under $N_2$ with use of standard inert-atmosphere and Schlenk techniques. Solvents were dried by standard procedures. All column chromatography was performed under $N_2$ with use of silica gel (230–400 mesh ASTM; Merck) as the stationary phase in a column 35 cm in length and 2.5 cm in diameter. The compounds

* Corresponding author.

0022-328X/96/$15.00 © 1996 Elsevier Science S.A. All rights reserved
*SSDI* 0022-328X(95)05841-9

[PPN][Fe(CO)$_3$(NO)] (PPN$^+$ = (Ph$_3$P)$_2$N$^+$) [8], Co(NO)(CO)$_3$ [9], Fe(NO)$_2$(CO)$_2$ [9] or Mn(NO)(CO)$_4$ [10]) were prepared by published procedures with modifications. IR measurements were measured on a Perkin–Elmer 880 spectrometer. The NMR spectra were measured using Bruker AMX500 ($^1$H and $^{31}$P), AC200 ($^1$H) and AC300 ($^1$H and $^{31}$P) spectrometers. Elementary analyses were performed on a Perkin–Elmer 2400 CHN analyzer.

## 2.2. Preparations

### 2.2.1. Co(NO)(CO)(Ph$_2$PH)$_2$ (1)

To a solution of 3.0 g of Co(NO)(CO)$_3$ (17.3 mmol) in 150 ml of CH$_3$CN pre-chilled to −20°C was added 2.01 equivalents of Ph$_2$PH (6.1 ml). The low temperature bath was then removed, and the solution was stirred at room temperature for 24 h and then at 40°C for 72 h. After removal of the solvent the residue was chromatographed. Elution with CH$_2$Cl$_2$ : hexane (1 : 10 by volume) gave the orange first band which was identified to be Co(NO)(CO)$_2$(Ph$_2$PH). The dark-red second band eluted from CH$_2$Cl$_2$/hexane (1 : 10 by vol) provided **1** (44%) after removal of the solvent. Anal. Found: C, 61.26; H, 4.39; N, 2.86. C$_{25}$H$_{22}$NO$_2$P$_2$Co calc.: C, 61.36; H, 4.53; N, 2.86.

### 2.2.2. Fe(NO)$_2$(Ph$_2$PH)$_2$ (2)

One equivalent of NO$^+$BF$_4^-$ (0.857 g, 7.34 mmol) was added all at once via a Schlenk tube into a vigorously stirred CH$_2$Cl$_2$ solution (30 ml) of [PPN][Fe(CO)$_3$(NO)] (5.00 g, 7.34 mmol) pre-chilled to −78°C. After 12 h at −78°C the solution was slowly warmed to room temperature. An acetonitrile solution (60 ml) of Ph$_2$PH (14.8 mmol, 2.60 ml) was then added and the solution was heated at 55°C for 48 h. The solvent was removed under reduced pressure and the residue was chromatographed. Elution with CH$_2$Cl$_2$ : hexane (1 : 5 by volume) gave the orange–red first band, from which trace amounts of Fe(NO)$_2$(CO)$_2$ was isolated. The dark-red second band eluted with CH$_2$Cl$_2$ : hexane (1 : 3 by volume) provided **2** with a yield of 2.11 g (59%). Anal. Found: C, 58.56; H, 4.15; N, 5.36. C$_{24}$H$_{22}$N$_2$O$_2$P$_2$Fe calc.: C, 59.04; H, 4.13; N, 5.36%.

Table 1
Crystal data for **1** and **3–6**

| | **1** | **3** | **4** | **5** | **6** |
|---|---|---|---|---|---|
| Formula | $C_{75}H_{60}Co_3N_3O_6P_6$ | $C_{26}H_{22}MnNO_3P_2$ | $C_{27}H_{26}CoNO_2P_2$ | $C_{31}H_{30}CoNO_2P_2$ | $C_{31}H_{26}CoNO_2P_2$ |
| Formula weight | 1461.96 | 513.35 | 517.39 | 569.46 | 565.43 |
| $a$ (Å) | 17.130(5) | 15.231(5) | 15.556(3) | 15.427(2) | 9.3393(8) |
| $b$ (Å) | 9.894(2) | 10.247(2) | 12.072(1) | 10.118(2) | 19.035(4) |
| $c$ (Å) | 42.607(1) | 16.311(2) | 14.809(2) | 18.793(6) | 16.007(1) |
| $\beta$ (°) | 93.29(2) | 102.29(2) | 114.43(1) | 102.56(1) | 94.912(7) |
| Crystal system | Monoclinic | Monoclinic | Monoclinic | Monoclinic | Monoclinic |
| Space group | $C2/c$ | $C2/c$ | $C2/c$ | $P2_1/c$ | $P2_1/n$ |
| $Z$ | 4 | 4 | 4 | 4 | 4 |
| $V$ (Å$^3$) | 7210(2) | 2488(1) | 2532.0(7) | 2863(1) | 2845.8(6) |
| $D_{calc}$ (g cm$^{-3}$) | 1.347 | 1.371 | 1.357 | 1.321 | 1.320 |
| Crystal size (mm) | 0.28 × 0.07 × 0.19 | 0.41 × 0.22 × 0.13 | 0.25 × 0.30 × 0.38 | 0.06 × 0.12 × 0.22 | 0.38 × 0.19 × 0.14 |
| Radiation | Cu Kα (λ = 1.5406 Å) | Mo Kα (λ = 0.7107 Å) | Same | Same | Same |
| $\mu$ (mm$^{-1}$) | 9.75 | 0.66 | 0.82 | 0.75 | 0.74 |
| Transmission factors (maximum–minimum) | 1.00–0.34 | 1.00–0.88 | 1.00–0.94 | 1.00–0.87 | 1.00–0.97 |
| 2$\theta$ range (°) | 2.0–130 | 2.0–5.0 | 2.0–50 | 2.0–45 | 2.0–45 |
| Octants | ±$h$(−20–20), +$k$(0–11), +$l$(0–50) | ±$h$(−18–18), +$k$(0–12), +$l$(0–19) | ±$h$(−18–18), +$k$(0–14), +$l$(0–17) | ±$h$(−16–16), +$k$(0–10), +$l$(0–20) | ±$h$(−10–10), +$k$(0–20), +$l$(0–17) |
| Number of unique reflections | 6135 | 2186 | 2234 | 3730 | 3700 |
| Number of reflections with $I > n\sigma$ | 2752 ($n$ = 2) | 1105 ($n$ = 2) | 1567 ($n$ = 2) | 1632 ($n$ = 2.5) | 2341 ($n$ = 2) |
| Number of variables | 421 | 155 | 150 | 334 | 335 |
| $R$, $R_w$ | 0.056, 0.058 | 0.041, 0.042 | 0.032, 0.031 | 0.042, 0.046 | 0.052, 0.059 |
| Goodness of fit | 2.06 | 1.68 | 2.04 | 1.45 | 2.46 |
| Maximum $\Delta/\sigma$ | 0.221 | 0.007 | 0.028 | 0.002 | 0.001 |

$R = \Sigma ||F_o| - |F_c|| / \Sigma |F_o|$. $R_w = [\Sigma w(|F_o| - |F_c|)^2 / \Sigma w |F_o|^2]^{1/2}$; $w = 1/[\sigma^2(F_o) + 0.0001F_o^2]$. For **1**, $k$ = 0.00015; for **3**, $k$ = 0.0001; for **4**, $k$ = 0.00002; for **5**, $k$ = 0.0001; for **6**, $k$ = 0.00005.

*2.2.3. $Mn(NO)(CO)_2(Ph_2PH)_2$ (3)*

The complex $Mn(NO)(CO)_4$ (0.745 g, 3.78 mmol) was vacuum transferred to a flask containing EtOH solution (50 ml) of $Ph_2PH$ (1.25 ml, 7.18 mmol). The flask containing the mixture was immersed in a cold bath at −20°C and an EtOH solution (20 ml) of $Me_3NO$ (0.292 g, 3.39 mmol) was added dropwise. When the addition of $Me_3NO$ was complete, the solution was slowly warmed to room temperature and stirred for 24 h, and then at 50°C for 48 h. After removal of the solvent the residue was chromatographed rapidly. The orange–red first band eluted with $CH_2Cl_2$ : hexane (1 : 3

Table 2
Atomic coordinates for **1**

| Atom | x | y | z | $B_{iso}$ (Å$^2$) |
|---|---|---|---|---|
| Co(1) | 0.16949(7) | 0.21127(12) | 0.57245(3) | 4.83(7) |
| Co(2) | 0.50000 | 0.97853(18) | 0.25000 | 5.79(11) |
| P(1) | 0.23524(11) | 0.03390(19) | 0.55837(5) | 4.11(10) |
| P(2) | 0.26141(11) | 0.33427(20) | 0.59679(5) | 4.36(10) |
| P(3) | 0.59358(12) | 0.83202(22) | 0.25997(5) | 4.99(11) |
| N | 0.1266(4) | 0.2825(7) | 0.5409(2) | 6.8(4) |
| O(1) | 0.0879(4) | 0.1258(9) | 0.6254(2) | 10.9(5) |
| O(2) | 0.0958(5) | 0.3280(6) | 0.5184(2) | 10.2(5) |
| O(3) | 0.5224(4) | 1.1357(8) | 0.1955(2) | 10.0(5) |
| C(1) | 0.1209(5) | 0.1590(9) | 0.6046(2) | 6.0(5) |
| C(N)(3) | 0.5152(5) | 1.0665(8) | 0.2167(2) | 6.5(5) |
| C(11) | 0.1800(4) | −0.1210(7) | 0.5506(2) | 4.0(4) |
| C(12) | 0.2144(4) | −0.2341(8) | 0.5382(2) | 4.5(4) |
| C(13) | 0.1693(5) | −0.3455(8) | 0.5295(2) | 5.0(4) |
| C(14) | 0.0896(5) | −0.3453(8) | 0.5332(2) | 5.4(4) |
| C(15) | 0.0560(4) | −0.2353(8) | 0.5456(2) | 5.5(5) |
| C(16) | 0.0998(4) | −0.1225(7) | 0.5546(2) | 4.7(4) |
| C(21) | 0.3212(4) | −0.0180(7) | 0.5826(2) | 4.3(4) |
| C(22) | 0.3143(5) | −0.0757(10) | 0.6112(2) | 6.6(5) |
| O(23) | 0.3805(7) | −0.1055(11) | 0.6305(2) | 8.0(6) |
| C(24) | 0.4531(6) | −0.0743(11) | 0.6213(2) | 7.1(6) |
| C(25) | 0.4596(5) | −0.0197(10) | 0.5930(3) | 7.6(6) |
| C(26) | 0.3950(5) | 0.0122(9) | 0.5737(2) | 6.3(4) |
| C(31) | 0.3257(4) | 0.4334(7) | 0.5731(2) | 3.7(3) |
| C(32) | 0.3335(4) | 0.3991(7) | 0.5419(2) | 4.3(4) |
| C(33) | 0.3824(5) | 0.4717(9) | 0.5240(2) | 5.0(4) |
| C(34) | 0.4232(4) | 0.5823(9) | 0.5365(2) | 5.2(4) |
| C(35) | 0.4150(5) | 0.6165(8) | 0.5674(2) | 5.3(4) |
| C(36) | 0.3670(4) | 0.5448(8) | 0.5854(2) | 4.7(4) |
| C(41) | 0.2255(4) | 0.4507(8) | 0.6252(2) | 4.2(4) |
| C(42) | 0.1784(5) | 0.5604(9) | 0.6147(2) | 5.5(5) |
| C(43) | 0.1436(5) | 0.6446(9) | 0.6356(2) | 6.1(5) |
| C(14) | 0.1537(6) | 0.6213(12) | 0.6667(2) | 8.0(6) |
| C(45) | 0.1989(7) | 0.5162(13) | 0.6775(2) | 9.9(7) |
| C(46) | 0.2347(5) | 0.4322(10) | 0.6570(2) | 7.1(5) |
| C(51) | 0.6890(5) | 0.8945(11) | 0.2753(2) | 6.1(5) |
| C(52) | 0.6931(6) | 1.0192(16) | 0.2884(3) | 12.1(9) |
| C(53) | 0.7640(9) | 1.0719(19) | 0.3029(3) | 15.7(12) |
| C(54) | 0.8220(12) | 0.9762(28) | 0.3024(5) | 17.0(20) |
| C(55) | 0.8325(15) | 0.8666(24) | 0.2877(7) | 21.1(21) |
| C(56) | 0.7538(8) | 0.8224(12) | 0.2757(4) | 14.0(10) |
| C(61) | 0.5753(4) | 0.6968(10) | 0.2878(2) | 5.5(5) |
| C(62) | 0.5528(5) | 0.7270(10) | 0.3171(2) | 6.7(5) |
| C(63) | 0.5383(6) | 0.6197(16) | 0.3373(3) | 9.5(8) |
| C(64) | 0.5461(8) | 0.4883(19) | 0.3284(4) | 10.5(10) |
| C(65) | 0.5691(8) | 0.4615(13) | 0.2995(4) | 11.3(9) |
| C(66) | 0.5832(6) | 0.5629(11) | 0.2784(2) | 8.2(6) |

Table 3
Atomic coordiantes for **3**

| Atom | x | y | z | $B_{iso}$ (Å$^2$) |
|---|---|---|---|---|
| Mn | 0.0 | 0.20155(12) | 0.25 | 4.45(6) |
| P | 0.13247(9) | 0.19233(14) | 0.21054(8) | 4.15(7) |
| N | 0.0 | 0.3708(7) | 0.25 | 5.5(4) |
| O(1) | −0.0751(3) | 0.0425(4) | 0.1018(2) | 7.3(2) |
| O(2) | 0.0 | 0.4852(6) | 0.25 | 7.7(4) |
| C(1) | −0.0458(3) | 0.1035(5) | 0.1598(3) | 4.3(3) |
| C(11) | 0.2325(4) | 0.2476(5) | 0.2840(3) | 4.3(2) |
| C(12) | 0.3171(4) | 0.2318(6) | 0.2673(3) | 5.9(3) |
| C(13) | 0.3927(4) | 0.2701(7) | 0.3238(4) | 6.7(4) |
| C(14) | 0.3850(4) | 0.3250(6) | 0.3988(4) | 5.7(3) |
| C(15) | 0.3028(4) | 0.3428(5) | 0.4168(3) | 4.9(3) |
| C(16) | 0.2259(3) | 0.3050(5) | 0.3600(3) | 4.4(2) |
| C(21) | 0.1354(3) | 0.2747(5) | 0.1127(3) | 4.2(3) |
| C(22) | 0.1384(5) | 0.4077(7) | 0.1084(4) | 8.3(5) |
| C(23) | 0.1335(6) | 0.4712(7) | 0.0335(5) | 10.1(6) |
| C(24) | 0.1273(5) | 0.3998(7) | −0.0384(4) | 6.7(4) |
| C(25) | 0.1262(4) | 0.2688(6) | −0.0353(3) | 6.2(4) |
| C(26) | 0.1307(4) | 0.2058(5) | 0.0403(3) | 5.1(3) |
| H | 0.162(2) | 0.069(3) | 0.196(2) | 2.4(8) |

Table 4
Atomic coordinates for **4**

| Atom | x | y | z | $B_{iso}$ (Å$^2$) |
|---|---|---|---|---|
| Co | 0.00000 | 0.19413(5) | 0.25000 | 4.60(3) |
| P | −0.00952(5) | 0.31213(7) | 0.13234(5) | 3.79(4) |
| C(N) | −0.1047(2) | 0.1277(2) | 0.2159(2) | 5.2(1) |
| C(1) | 0.1002(2) | 0.3815(3) | 0.1486(2) | 5.0(2) |
| C(2) | −0.0939(2) | 0.4242(2) | 0.1090(2) | 3.6(1) |
| C(3) | −0.0700(2) | 0.5351(2) | 0.1154(2) | 4.6(2) |
| C(4) | −0.1377(2) | 0.6167(3) | 0.0982(2) | 6.0(2) |
| C(5) | −0.2291(2) | 0.5891(3) | 0.0745(2) | 6.1(2) |
| C(6) | −0.2548(2) | 0.4792(3) | 0.0686(2) | 5.6(2) |
| C(7) | −0.1877(2) | 0.3983(2) | 0.0864(2) | 4.6(2) |
| C(8) | −0.0422(2) | 0.2519(2) | 0.0086(2) | 3.7(1) |
| C(9) | −0.1127(2) | 0.2958(2) | −0.0773(2) | 4.2(1) |
| C(10) | −0.1304(2) | 0.2491(3) | −0.1690(2) | 5.1(2) |
| C(11) | −0.0787(2) | 0.1595(3) | −0.1759(2) | 5.8(2) |
| C(12) | −0.0099(2) | 0.1153(3) | −0.0925(2) | 5.7(2) |
| C(13) | 0.0079(2) | 0.1609(2) | −0.0004(2) | 4.8(2) |
| O | −0.1751(2) | 0.0813(2) | 0.1955(2) | 9.4(2) |

Table 5
Atomic coordinates **5**

| Atom | x | y | z | $B_{iso}$ (Å$^2$) |
|---|---|---|---|---|
| Co | 0.76419(11) | 0.31464(18) | 0.10288(9) | 3.61(8) |
| P(1) | 0.65424(19) | 0.1712(3) | 0.08176(16) | 3.15(16) |
| P(2) | 0.87773(19) | 0.1898(4) | 0.15541(16) | 3.06(16) |
| N | 0.7419(7) | 0.4270(11) | 0.1640(6) | 5.2(6) |
| C(1) | 0.7802(7) | 0.4132(11) | −0.0341(5) | 7.9(7) |
| C(2) | 0.7234(8) | 0.5070(11) | 0.2034(6) | 8.1(7) |
| C(1) | 0.7767(7) | 0.3701(11) | 0.0216(6) | 3.1(6) |
| C(2) | 0.6580(8) | 0.0352(12) | 0.0164(6) | 4.0(7) |
| C(3) | 0.6905(11) | 0.0770(15) | −0.0511(8) | 6.6(10) |
| C(4) | 0.6509(11) | 0.0603(16) | −0.1166(9) | 8.1(11) |
| C(5) | 0.8926(7) | 0.1603(12) | 0.2546(6) | 3.9(7) |
| C(6) | 0.9104(8) | 0.2851(13) | 0.2985(7) | 4.4(7) |
| C(7) | 0.8660(9) | 0.3212(16) | 0.3462(7) | 6.3(8) |
| C(11) | 0.5463(8) | 0.2478(11) | 0.0405(6) | 3.4(6) |
| C(12) | 0.5393(8) | 0.3186(14) | −0.0246(7) | 4.6(7) |
| C(13) | 0.4590(10) | 0.3708(14) | −0.0591(7) | 5.6(8) |
| C(14) | 0.3849(9) | 0.3568(14) | −0.0297(8) | 5.5(8) |
| C(15) | 0.3898(9) | 0.2890(14) | 0.0337(8) | 5.2(8) |
| C(16) | 0.4713(9) | 0.2347(14) | 0.0688(7) | 4.7(8) |
| C(21) | 0.6320(7) | 0.0855(12) | 0.1603(7) | 3.3(6) |
| C(22) | 0.6336(10) | 0.1551(14) | 0.2231(8) | 6.2(9) |
| C(23) | 0.6139(11) | 0.0926(20) | 0.2833(9) | 7.9(11) |
| C(24) | 0.5984(11) | −0.0373(21) | 0.2836(9) | 7.0(11) |
| C(25) | 0.5998(11) | −0.1088(16) | 0.2240(11) | 7.5(11) |
| C(26) | 0.6163(9) | −0.0461(15) | 0.1612(7) | 5.1(8) |
| C(31) | 0.8793(7) | 0.0217(12) | 0.1214(6) | 3.0(6) |
| C(32) | 0.8515(8) | −0.0870(12) | 0.1568(7) | 3.7(7) |
| C(33) | 0.8460(8) | −0.2109(12) | 0.1244(8) | 4.3(7) |
| C(34) | 0.8700(9) | −0.2314(14) | 0.0586(8) | 5.2(8) |
| C(35) | 0.8986(9) | −0.1266(16) | 0.0233(7) | 5.3(8) |
| C(36) | 0.9042(8) | −0.0011(13) | 0.0551(7) | 4.2(7) |
| C(41) | 0.9869(7) | 0.2514(13) | 0.1483(6) | 3.0(6) |
| C(42) | 1.0649(8) | 0.1794(14) | 0.1784(6) | 4.1(7) |
| C(43) | 1.1458(8) | 0.2294(14) | 0.1717(7) | 4.7(8) |
| C(44) | 1.1505(8) | 0.3493(15) | 0.1365(7) | 4.9(8) |
| C(45) | 1.0754(9) | 0.4190(12) | 0.1081(7) | 4.3(7) |
| C(46) | 0.9943(8) | 0.3708(12) | 0.1145(6) | 3.7(6) |

by volume) provided 0.497 g (16.0%) of powdery **3**. Anal. Found: C, 60.44; H, 4.10; N, 2.51. $C_{26}H_{22}NO_3P_2Mn$ calc.: C, 60.83; H, 4.32; N, 2.73%.

### 2.2.4. $Co(NO)(CO)(Ph_2PMe)_2$ (4)

Two equivalents of BuLi (1.6 M in tetrahydrofuran (THF), 2.5 ml) was added dropwise to a THF solution (100 ml) of **1** (0.978 g, 2.00 mmol) pre-chilled to −78°C. After being stirred at −78°C for 1 h, to the solution was added 0.25 ml (4.00 mmol) of MeI. The solution was stirred at the same temperature for 30 min and then was slowly warmed to room temperature. After removal of the solvent the residue was chromatographed. Complex **4** was obtained (82%) from the reddish first band eluted with $Et_2O$:hexane (1:5 by volume). Anal. Found: C, 62.41; H, 4.95; N. 2.50. $C_{27}H_{26}NO_2P_2Co$ calc.: C, 62.68; H, 5.06; N, 2.71%.

### 2.2.5. $Co(NO)(CO)(Ph_2PCH_2CHCH_2)_2$ (5)

The procedure for the synthesis of **4** was followed, except that allyl bromide was used instead of methyl iodide, and the eluent for the chromatography was $CH_2Cl_2$:hexane (1:7 by volume). Complex **5** was obtained as reddish-brown powders (67%) Anal. Found: C, 65.07; H, 5.33; N, 2.38. $C_{31}H_{30}NO_2P_2Co$ calc.: C, 65.30; H, 5.31; N, 2.46%.

### 2.2.6. $Co(NO)(CO)(Ph_2PCH_2CCH)_2$ (6)

The procedure for the synthesis of **4** was followed except that propargyl bromide was used instead of methyl iodide. The first band eluted with $CH_2Cl_2$:hexane (1:7 by volume) was not characterized. The orange–red, second band eluted with $CH_2Cl_2$:hexane (1:4 by volume) provided **6** (31%) after removal of the

Table 6
Atomic coordinates for **6**

| Atom | $x$ | $y$ | $z$ | $B_{iso}$ (Å$^2$) |
|---|---|---|---|---|
| Co | 0.08324(11) | 0.33596(5) | 0.24096(6) | 3.70(5) |
| P(1) | −0.02023(21) | 0.41497(10) | 0.31605(11) | 3.33(9) |
| P(2) | 0.20179(20) | 0.40380(10) | 0.16039(11) | 3.13(8) |
| N | −0.0383(7) | 0.2863(3) | 0.1839(4) | 4.6(3) |
| O(1) | 0.2980(7) | 0.2668(3) | 0.3487(4) | 7.6(4) |
| O(2) | −0.1189(7) | 0.2486(3) | 0.1462(4) | 7.2(3) |
| C(1) | 0.2134(9) | 0.2961(3) | 0.3068(5) | 3.4(4) |
| C(2) | 0.0980(7) | 0.4610(4) | 0.3968(4) | 3.9(4) |
| C(3) | 0.1611(8) | 0.4133(4) | 0.4615(5) | 4.1(4) |
| C(4) | 0.2152(10) | 0.3764(5) | 0.5129(5) | 6.0(5) |
| C(5) | 0.0931(8) | 0.4464(4) | 0.0728(4) | 3.7(3) |
| C(6) | 0.0138(8) | 0.3939(4) | 0.0205(4) | 3.8(4) |
| C(7) | −0.0490(10) | 0.3518(5) | −0.0200(5) | 5.6(5) |
| C(11) | −0.1089(8) | 0.4887(4) | 0.2606(5) | 3.7(4) |
| C(12) | −0.2074(9) | 0.4744(4) | 0.1933(5) | 4.7(4) |
| C(13) | −0.2767(9) | 0.5273(5) | 0.1475(5) | 5.7(5) |
| C(14) | −0.2491(11) | 0.5955(5) | 0.1661(6) | 6.4(5) |
| C(15) | −0.1543(12) | 0.6114(5) | 0.2313(6) | 7.2(6) |
| C(16) | −0.0826(11) | 0.5591(4) | 0.2773(5) | 6.1(5) |
| C(21) | −0.1642(8) | 0.3812(4) | 0.3762(4) | 3.8(4) |
| C(22) | −0.2299(9) | 0.4238(4) | 0.4315(5) | 4.6(4) |
| C(23) | −0.3385(10) | 0.3990(5) | 0.4754(5) | 5.8(5) |
| C(24) | −0.3839(11) | 0.3327(6) | 0.4648(6) | 7.3(6) |
| C(25) | −0.3233(12) | 0.2902(5) | 0.4093(8) | 9.6(7) |
| C(26) | −0.2116(11) | 0.3140(5) | 0.3649(6) | 7.6(6) |
| C(31) | 0.3425(8) | 0.3624(4) | 0.1056(4) | 3.6(3) |
| C(32) | 0.4369(9) | 0.3998(4) | 0.0630(5) | 4.9(4) |
| C(33) | 0.5402(10) | 0.3681(6) | 0.0197(6) | 6.5(5) |
| C(34) | 0.5506(11) | 0.2965(6) | 0.0203(7) | 7.4(6) |
| C(35) | 0.4554(13) | 0.2580(5) | 0.0611(8) | 9.5(7) |
| C(36) | 0.3519(11) | 0.2906(5) | 0.1051(6) | 6.9(5) |
| C(41) | 0.2959(8) | 0.4790(4) | 0.2093(4) | 3.4(3) |
| C(42) | 0.2582(10) | 0.5470(4) | 0.1945(5) | 5.5(5) |
| C(43) | 0.3285(12) | 0.6023(4) | 0.2371(7) | 7.4(6) |
| C(44) | 0.4365(12) | 0.5879(6) | 0.2955(6) | 6.9(6) |
| C(45) | 0.4788(9) | 0.5212(6) | 0.3120(5) | 5.7(5) |
| C(46) | 0.4077(9) | 0.4661(4) | 0.2697(5) | 4.6(4) |

Table 7
Selected bond distances (Å) and angles (°) for **1** and **3–6**

| | 1 | 3 | 4 | 5 | 6 |
|---|---|---|---|---|---|
| *Bond distances* | | | | | |
| Co(1)–P(1) | 2.188(2) | | | | |
| Co(1)–P(2) | 2.202(2) | | | | |
| Co(1)–C(1) | 1.722(9) | | | | |
| Co(1)–N | 1.653(8) | | | | |
| Co(2)–P(3) or Co(2)–P(3a) | 2.185(2) | | | | |
| Co(2)–C/N(3) or Co(2)–C/N(3a) | 1.696(9) | | | | |
| Mn–P or Mn–Pa | | 2.246(2) | | | |
| Mn–N | | 1.734(8) | | | |
| Mn–C(1) or Mn–C(1a) | | 1.796(5) | | | |
| Co–P or Co–Pa | | | 2.2076(8) | | |
| Co–C/N or Co–C/N(a) | | | 1.694(3) | | |
| Co–P(1) | | | | 2.201(3) | 2.202(2) |
| Co–P(2) | | | | 2.212(3) | 2.194(2) |
| Co–N | | | | | 1.687(7) |
| Co–C(1) | | | | | 1.718(8) |
| Co–C/N(1) | | | | 1.70 (1) | |
| Co–C/N(2) | | | | 1.69 (1) | |
| N(1)–(1) | | | | | |
| C/N(3)–O(3) | 1.15(1) | | | | |
| N–O(2) | 1.16(1) | 1.17(1) | | | 1.170(9) |
| C/N–O | | | 154(4) | | |
| C(1)–O(1) | 1.13(1) | 1.142(6) | | | 1.14(1) |
| C(2)–O(2) | | | | | |
| C(3)–O(3) | | | | | |
| C/N(1)–O(1) | | | | 1.16(1) | |
| C/N(2)–O(2) | | | | 1.17(1) | |
| P(1)–C(2) | | | | 1.85(1) | 1.851(7) |
| P(2)–C(5) | | | | 1.841(9) | 1.851(7) |
| C(2)–C(3) | | | | 1.51(2) | 1.47(1) |
| C(3)–C(4) | | | | 1.26(2) | 1.16(1) |
| C(5)–C(6) | | | | 1.50(1) | 1.46(1) |
| C(6)–C(7) | | | | 1.28(2) | 1.16(1) |
| P–H | | 1.38(3) | | | |
| *Bond angles* | | | | | |
| P(1)–Co(1)–P(2) | 101.95(9) | | | | |
| P(1)–Co(1)–N | 109.3(3) | | | | |
| P(1)–Co(1)–C(1) | 104.9(3) | | | | |
| P(2)–Co(1)–N | 114.8(2) | | | | |
| P(2)–Co(1)–C(1) | 99.0(4) | | | | |
| N–Co(1)–C(1) | 124.2(4) | | | | |
| P(3)–Co(2)–P(3a) | 96.9(1) | | | | |
| P(3)–Co(2)–C/N(3) | 110.9(3) | | | | |
| P(3)–Co(2)–C/N(3a) | 108.9(3) | | | | |
| C/N(3)–Co(2)–C/N(3a) | 118.3(4) | | | | |
| P–Mn–Pa | | 175.18(8) | | | |
| P–Mn–N or Pa–Mn–N | | 92.41(5) | | | |
| P–Mn–C(1) or Pa–Mn–C(1a) | | 87.6(2) | | | |
| P–Mn–C(1a) or Pa–Mn–C(1) | | 89.7(2) | | | |
| N–Mn–C(1) or N–Mn–C(1a) | | 124.0(2) | | | |
| C(1)–Mn–C(1a) | | 111.9(2) | | | |
| P–Co–Pa | | | 99.63(4) | | |
| P–Co–C/N or Pa–Co–C/N(a) | | | 109.12(8) | | |
| P–Co–C/N(a) or Pa–Co–C/N | | | 106.4(1) | | |
| C/N–Co–C/N(a) | | | 123.5(1) | | |
| P(1)–Co–P(2) | | | | 102.0(1) | 100.87(8) |
| P(1)–Co–N | | | | | 112.0(2) |
| P(1)–Co–C(1) | | | | | 106.6(2) |
| P(2)–Co–N | | | | | 111.1(2) |
| P(2)–Co–C(1) | | | | | 104.9(2) |
| P(1)–Co–C/N(1) | | | | 106.9(3) | |
| P(1)–Co–C/N(2) | | | | 107.5(3) | |

Table 7 (continued)

| | 1 | 3 | 4 | 5 | 6 |
|---|---|---|---|---|---|
| *Bond angles* | | | | | |
| P(2)–Co–C/N(1) | | | | 111.1(3) | |
| P(2)–Co–C/N(2) | | | | 109.6(3) | |
| N–Co–C(1) | | | | | 119.6(3) |
| C/N(1)–Co–C/N(2) | | | | 118.2(4) | |
| P(1)–C(2)–C(3) | | | | 114.5(7) | 112.6(5) |
| C(2)–3–C(4) | | | | 127 (1) | 178.0(9) |
| P(2)–C(5)–C(6) | | | | 113.5(6) | 110.7(5) |
| C(5)–C(6)–C(7) | | | | 124 (1) | 179.1(8) |
| Co(1)–C(1)–O(1) | 178.8(8) | | | | |
| Co(1)–N–O(2) | 177.6(6) | | | | |
| Co(2)–C/N(3)–O(3) | 173.9(8) | | | | |
| Mn–N–O(2) | | 180.0 | | | |
| Mn–C(1)–O(1) or Mn–C(1a)–O(1a) | | 179.1(5) | | | |
| Co–C/N–O | | | 178.0(2) | | |
| Co–N–O(2) | | | | | 176.3(6) |
| Co–C(1)–O(1) | | | | | 176.9(6) |
| Co–C/N(1)–O(1) | | | | 175.2(8) | |
| Co–C/N(2)–O(2) | | | | 177.1(8) | |

solvent. Anal. Found: C, 65.64; H, 4.61; N, 2.48. $C_{31}H_{26}NO_2P_2Co$ calc.: C, 65.85; H, 4.64; N, 2.48%.

### 2.3. Crystallographic studies

Crystals of **1** were grown by cooling a concentrated solution of **1** in hexane at −5°C for several days, and crystals of **3–6** were grown by cooling a concentrated solution of relevant complexes in $CH_2Cl_2$ : hexane (1 : 5) at −5°C for several days. Crystals were mounted in thin-walled glass capillaries. Diffraction measurements were made on an Enraf–Nonious CAD4 diffractometer using graphite-monochromated Mo Kα radiation (λ =

Table 8
IR Spectra and $^1H$ and $^{31}P\{^1H\}$ NMR spectra of compounds

| Complex | ν(CO), ν(NO); ν(PH) [a] ($cm^{-1}$) | δ [b,c] (ppm) | δ [b,d] (ppm) |
|---|---|---|---|
| **1** | 1967s, 1723*s*; 2319vw, 2312vw | *Ph* (7.60–7.60, m, 20H); P*H* (6.20, d, 2H, $^1J$(P–H) = 340 Hz) | *P* (35.1, br) |
| **2** | 1724*m*, 1673*s*; 2313vw, 2287vw | *Ph* (7.53–7.26, m, 20H); PH (6.45, d, 2H, $^1J$(P–H) = 392 Hz) | *P* (37.4) |
| **3** | 1954m, 1867vs, 1660*s*; 2324vw, 2324vw | *Ph* (7.84–7.48, m, 20H); *PH* (7.38, d, 2H, $^1J$(P–H) = 362 Hz) | *P* (55.8) |
| **4** | 1939s, 1701*s* | *Ph* (7.49–7.37, m, 20 H); *Me* (1.49, d, 6H, $^2J$(R–H) = 6.6 Hz) | *P* (43.2, br) |
| **5** | 1943s, 1700*s* | *Ph* (7.46–7.34, m, 20H); CH=$CH_2$ (5.39, m, 2H); CH=C*Ha*Hb (4.78, d, 2H, $^3J$(H–H) = 6.8 Hz); CH = CHa*Hb* (4.61, d, 2H, $^3J$(H–H) = 11.2 Hz); PC*Ha*Hb (2.80, m, 2H); PCHa*Hb* (2.58, m, 2H) | *P* (52.5, br) |
| **6** | 1943s, 1700*s* | *Ph* (7.34–7.23, m, 20 H); PC*Ha*Hb (2.67, ddd, 2H, $^2J$(H–H) = 16.5, $^2J$(P–H) = 7.0 Hz, $^4J$(H–H) = 2.5 Hz), PCHaHb (2.65, ddd, 2H, $^2J$(H–H) = 16.5 Hz, $^2J$(P–H) = 7.0 Hz, $^4J$(H–H) = 2.5 Hz); CC*H* (1.87, m, 2H) | *P* (52.5, br) |
| **7** | 2041s, 1989vs, 1770*s*; 2284vw | | |
| **8** | 2013m, 1765*m*, 1720*s*; 2336vw | | |
| **9** | 2038s, 1975m, 1926s, 1715*s*; 2300vw | | |
| $Co(NO)(CO)_3$ | 2104m, 2034s, 1801*s* | | |
| $Fe(NO)_2(CO)_2$ | 2067s, 2018s, 1824*s*, 1764*s* | | |
| $Mn(NO)(CO)_4$ | 2101w, 2028vs, 1974vs, 1758*s* | | |

[a] Measured in $CH_2Cl_2$ (**3–6**, **8**), hexane (**1**, **7**, $Co(NO)(CO)_3$) or $CH_3CN$ (h2, **9**, $Fe(NO)_2(CO)_2$, $Mn(NO)(CO)_4$) solution.
[b] Measured in acetone-$d^6$ except for **6** ($CD_2Cl_2$).[c] Reported in parts per million relative to δ($Me_4Si$) 0 ppm.[d] Reported in parts per million relative to δ (85% $H_3PO_4$) 0 ppm. Abbreviations; s, singlet; d, doublet; t, triplet; m, multiplet.

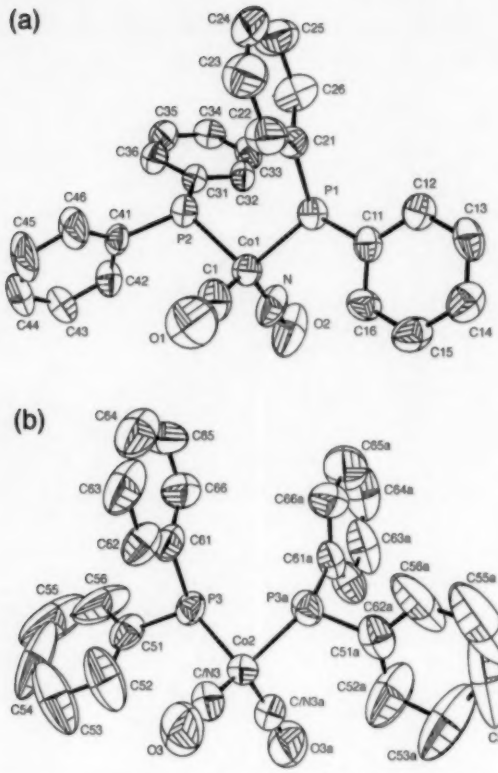


Fig. 1. ORTEP drawing of $Co(NO)(CO)(Ph_2PH)_2$ (1). Thermal ellipsoids are drawn with 30% probability boundaries.

0.7107 Å) or Cu K$\alpha$ radiation ($\lambda = 1.5406$ Å) with the $\theta$–$2\theta$ scan mode. Unit cells were determined by centering 25 reflections in the suitable $2\theta$ range. Other relevant experimental details are listed in Table 1. All data reduction and refinements were carried out on DecAlpha 3000/400 computer using NRCVAX programs [11]. Intensities were collected and corrected for decay, absorption (empirical and $\psi$ scan) and Lorentz–polarization effects. Each structure was solved by direct methods [12] and refined on $F$ using full-matrix least-squares techniques. An $E$ map from the starting set with the highest combined figure of merit revealed coordinates for metal atoms. The remaining non-H atoms were located from successive difference Fourier maps. All non-hydrogen atoms were refined anisotropically. All hydrogen atoms were included in the structure factor calculation in idealized positions with $d_{C-H} = 0.98$ Å. The final positional parameters are listed in Tables 2–6 and selected interatomic distances and bond angles are given in Table 7.

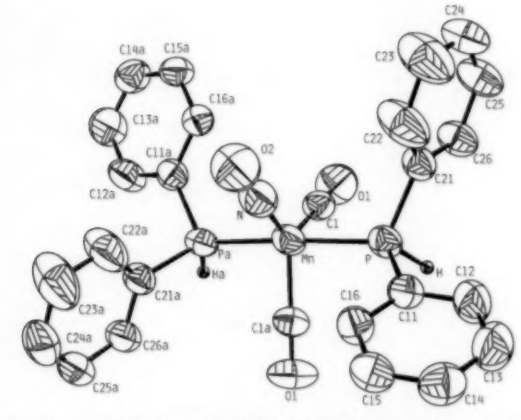


Fig. 2. ORTEP drawing of $Mn(NO)(CO)_2(Ph_2PH)_2$ (3). Thermal ellipsoids are drawn with 30% probability boundaries.

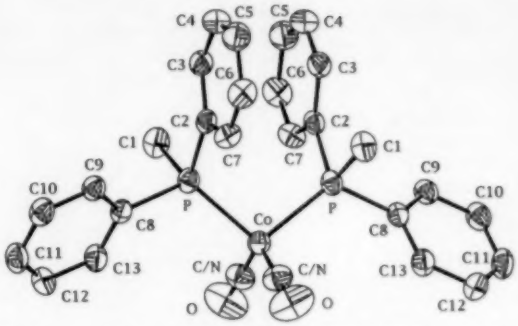


Fig. 3. ORTEP drawing of $Co(NO)(CO)(Ph_2PMe)_2$ (4). Thermal ellipsoids are drawn with 30% probability boundaries.

## 3. Results and discussion

Complexes $Co(NO)(CO)(Ph_2PH)_2$ (1), $Fe(NO)_2(Ph_2PH)_2$ (2) and $Mn(NO)(CO)_2(Ph_2PH)_2$ (3) were synthesized from ligand substitution of $Co(NO)(CO)_3$, $Fe(NO)_2(CO)_2$ and $Mn(NO)(CO)_4$ respectively as follows:

$$Co(NO)(CO)_3 \xrightarrow[24\ h]{Ph_2PH} Co(NO)(CO)_2(Ph_2PH)$$

$$\xrightarrow[72\ h]{Ph_2PH,\ 40°C} Co(NO)(CO)(Ph_2PH)_2 \quad (1)$$

**1**, 44%

$$Fe(NO)_2(CO)_2 \xrightarrow[48\ h]{Ph_2PH,\ 55°C} Fe(NO)_2(Ph_2PH)_2 \quad (2)$$

**2**, 59%

$$Mn(NO)(CO)_4 \xrightarrow[24\ h]{Ph_2PH–Me_3NO,\ -20°C\ to\ rt} Mn(NO)(CO)_3(Ph_2PH)$$

$$\xrightarrow[48\ h]{Ph_2PH,\ 50°C} Mn(NO)(CO)_2(Ph_2PH)_2 \quad (3)$$

**3**, 16%

The IR monitoring of the reactions suggested that $Co(NO)(CO)_2(Ph_2PH)$ (**7**), $Fe(NO)_2(CO)(Ph_2PH)$ (**8**) and $Mn(NO)(CO)_3(Ph_2PH)$ (**9**) formed as intermediates (Table 4), although they were not isolated pure. As expected, the ligation of the second phosphine requires more vigorous conditions than that of the first phosphine. The low yield for **3** is mainly due to its air sensitivity and extensive decomposition during chromatography.

The spectroscopic properties of **1–3** (Table 8) are consistent with their formulation. The presence of ligated $Ph_2PH$ is evident from the observation of two weak $\nu$(P–H) bands at about 2300 $cm^{-1}$ and a large one-bond P–H coupling (350–400 Hz) in both $^1H$ and $^{31}P$ NMR spectra. Both $\nu$(NO) and $\nu$(CO) decrease when an additional CO ligand is displaced by a phosphine ligand. According to the prediction of Rossi and Hoffmann [13] for a pentacoordinated metal atom with $d^8$ electronic configuration and trigonal bipyramidal geometry, the two better $\sigma$-donating ligands, $Ph_2PH$, should reside in the apical positions, whereas the better $\pi$-accepting ligands, CO and NO, prefer to be in the equatorial sites for **3**. Complex **3** indeed has a structure (vide infra) which is consistent with the postulate of Rossi and Hoffmann and, as expected, it has a medium and a strong CO stretchings in the IR spectra and two magnetically equivalent $Ph_2PH$ ligands in both $^1H$ and $^{31}P$ NMR spectra (Table 8).

The lithiated phosphine complex $[Co(NO)(CO)(Ph_2PLi)_2]$ is likely to be generated upon treating **1** with two equivalents of BuLi. Reactions of this thermally unstable anion with methyl iodide, allyl bromide and propargyl bromide provide the complexes $Co(NO)(CO)(Ph_2PMe)_2$ (**4**), $Co(NO)(CO)(Ph_2PCH_2CHCH_2)_2$ (**5**) and $Co(NO)(CO)(Ph_2PCH_2CCH)_2$ (**6**) respectively. The characteristic $\nu$(P–H) bands in IR absorption and one-bond P–H coupling in NMR spectra found in **1** disappeared in **4–6** (Table 8). Both $\nu$(CO) and $\nu$(NO) in **4–6** are significantly lower than those in **1**, implying that substitution of methyl, allyl and propargyl for hydrogen in $Ph_2PH$ significantly enhances the $\sigma$-donating ability, or suppresses the $\pi$-accepting ability of the phosphine ligand. The two methylene protons of the phosphine ligands in **5** and **6** appear to be diastereotopic since no plane of symmetry bisecting these groups is possible in both complexes. Complex **6** is likely to be useful for construction of polynuclear metal complexes such as $[Co(NO)(CO)(Ph_2PCH_2CCH)_2][Co_2(CO)_6]_2$ via ligation of the alkyne entities [14], or for synthesizing organometallic polymers via polymerization of the alkyne entities [15]. Use of the two available diphenylphosphine for heterodinuclear complexes bridged by two phosphide ligands and phosphide-bridged heterotrinuclear complexes will be pursued in future.

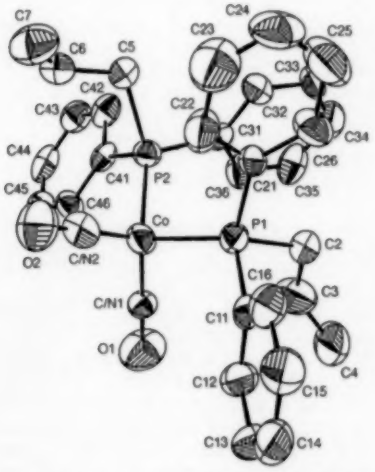


Fig. 4. ORTEP drawing of $Co(NO)(CO)(Ph_2PCH_2CHCH_2)_2$ (**5**). Thermal ellipsoids are drawn with 30% probability boundaries.

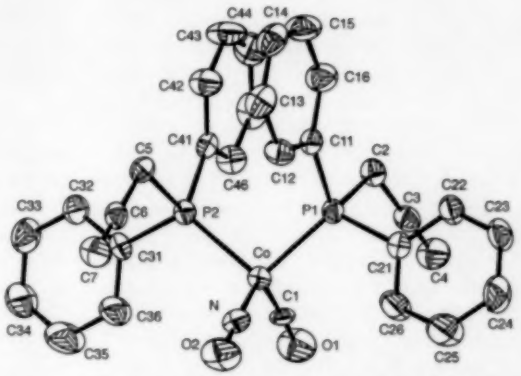


Fig. 5. ORTEP drawing of $Co(NO)(CO)(Ph_2PCH_2CCH)_2$ (**6**). Thermal ellipsoids are drawn with 30% probability boundaries.

### *3.1. Crystal structure of $Co(NO)(CO)(Ph_2PH)_2$ (1), $Mn(NO)(CO)_2(Ph_2PH)_2$ (3), $Co(NO)(CO)(Ph_2PMe)_2$ (4), $Co(NO)(CO)(Ph_2PCH_2CHCH_2)_2$ (5) and $Co(NO)(CO)(Ph_2PCH_2CCH)_2$ (6)*

The ORTEP drawings of **1**, **3**, **4**, **5** and **6** are shown in Figs. 1, 2, 3, 4 and 5 respectively. Important interatomic distances and angles are listed in Table 7. The coordination geometries of **1** and **4–6** are distorted tetrahedras about the cobalt center. There are two crystallographically independent molecules, A and B, for **1**. The two molecules have approximately similar structures except that the nitrosyl and the carbonyl ligands of molecule B are disordered owing to the presence of a twofold symmetry axis which passes the cobalt atom and bisects the angles P–Co–P and C–Co–N. Such a twofold axis also exists in **4** and renders the nitrosyl and the carbonyl

ligands disordered. In **5** the nitrogen atom of NO and the carbon atom of CO are disordered and both sites have 50% N and 50% C. The location of the NO ligand in other complexes was distinguished from that of the CO ligand by conspicuous discrepancies in the thermal parameters for the N and C atoms when incorrectly assigned [16]. Albano et al. [17] and Mingos and Ibers [18] suggested that, in tetrahedral Co, Pt and Ir complexes of general formula $ML_nL'_{4-n}$ (L = CO or NO; L' = tertiary phosphine), the good $\pi$-accepting abilities of NO and CO would result in non-bonding repulsions and cause the N–M–C angle to deviate significantly from the ideal value of 109.48°. Indeed, **1** (124.2(4)°; 18.3(4)°), **4** (123.5(1)°), **5** (118.2(4)°) and **6** (119.6(3)°) all have large N–Co–C angles, similar to that of $Co(NO)(CO)(PPh_3)_2$ (120.0(4)°) [17a]. The P–Co–P angles in $Co(NO)(CO)(PPh_3)_2$ (114.1(2)°) is larger than those in **1** (101.95(9)°; 96.9(1)°), **4** (99.63(4)°), **5** (102.0(1)°) and **6** (100.87(8)°), apparently owing to the greater steric crowdedness of $PPh_3$. The structure of **3** is similar to that of $Mn(NO)(CO)_2(PPh_3)_2$ [19] which has a trigonal bipyramidal geometry with apical phosphine ligands and with NO in an equatorial position. The two carbonyls and the two phosphines are symmetry related owing to the presence of a twofold axis which is on the equatorial plane and bisects the angle spanned by the two carbonyls. The two phosphine ligands are slightly bent away from the NO group with a P–Mn–Pa angle of 175.18(8)°. Other relevant crystal data for **1** and **3–6** appear to be normal. Neither carbonyl nor nitrosyl ligands deviate significantly from linearity. The metal–N distances lie in the range 1.57–2.03 Å reported for metal nitrosyls, and the N–O distances (1.154(4)–1.17(1) Å) compare well with other N–O distances ranging from 1.1 to 1.26 Å [20]. The $sp^2$ carbon–carbon distance (average, 1.27(1) Å) in the two allyl entities of **5** and the sp carbon–carbon distance (average, 1.16(1) Å) in the two propargyl entities of **6** are not abnormal. The average Co–P distances in **1** (2.19(1) Å), **4** (2.2076(8) Å), **5** (2.206(8) Å) and **6** (2.20(1) Å) are shorter than those in $Co((NO)(CO)_2(PPh_3)$ (2.224(3) Å) and $Co((NO)(CO)(PPh_3)_2$ (2.224(3) Å) [17a]. Complex **3** also appears to have a shorter Mn–P distance (2.246(2) Å) than $Mn(NO)(CO)_3(PPh_3)$ (2.305(4) Å) and $Mn(NO)(CO)_2(PPh_3)_2$ (2.278(1) Å) [21]. These observations could be attributed to the larger cone angle of $PPh_3$.

## 4. Supplementary materials available

All bond distances and angles (Table S1; **1**, 2 pages; **3**, 1 page; **4**, 1 page; **5**, 2 pages; **6**, 2 pages), anisotropic thermal parameters and isotropic thermal parameters (Table S2; **1**, 2 pages; **3**, 1 page; **4**, 1 page; **5**, 2 pages; **6**, 2 pages) and positional parameters for calculated hydrogen atoms (Table S3; **1**, 1 page; **3**, 1 page; **4**, 1 page; **5**, 1 page; **6**, 1 page), are available from the authors.

## Acknowledgment

This work was supported by the National Science Council under grant NSC-84-2113-M-001-018.

## References

[1] J.P. Collman, L.S. Hegedus, J.R. Norton and R.G. Finke, *Principles and Applications of Organotransition Metal Chemistry*, University Science Books, Mill Valley CA, 2nd edn., 1987, Chapter 3.

[2] See for example: (a) J.T. Lin, S.Y. Wang, A.C. Yeh, T.Y.R. Tsai and S.M. Peng, *Inorg. Chem., 33* (1994) 1948; (b) J.T. Lin, P.S. Huang, T.Y.R. Tsai, C.Y. Liao, L.H. Tseng, Y.S. Wen and F.K. Shi, *Inorg. Chem., 31* (1992) 4444; (c) Q.Z. Shi, T.G. Richmond, W.C. Trogler and F. Basolo, *Inorg. Chem., 23* (1984) 957.

[3] (a) J.T. Lin, Y.C. Chou, Y.E. Shih, F.E. Hong, Y.S. Wen, S.C. Lin and M.M. Chen, *J. Chem. Soc., Dalton Trans.*, (1995) 1791; (b) J.T. Lin, A.C. Yeh, Y.C. Chou, T.Y.R. Tsai and Y.S. Wen, *J. Organomet. Chem., 486* (1995) 147.

[4] (a) T. Blum, P. Braunstein, A. Tiripicchino and M.T. Camellini, *New J. Chem., 12* (1988) 539; (b) P. Braustein, in A.F. Williams, C. Floriani and A.E. Merbach (eds.), *Perspectives in Coordination Chemistry*, VCH, Weinheim, 1992, p. 76.

[5] (a) D.E. Morris and F. Basolo, *J. Am. Chem. Soc., 90* (1968) 2531; (b) E.M. Thorsteinson and F. Basolo, *J. Am. Chem. Soc., 88* (1966) 3929; (c) R.J. Mawby, D. Morris, E.M. Thorsteinson and F. Basolo, *Inorg. Chem., 5* (1966) 27; (d) H. Wawersik and F. Basolo, *J. Am. Chem. Soc., 89* (1967) 4626.

[6] D.A. Roberts and G.L. Geoffroy, in G. Wilkinson, F.G.A. Stone and E. Abel (eds.), *Comprehensive Organometallic Chemistry*, Pergamon, Oxford, 1992, Chapter 40.

[7] (a) J. Powell, C. Couture, M.R. Gregg and J.F. Sawyer, *Inorg. Chem., 28* (1989) 3437; (b) R.T. Baker, T.H. Tulip and S.S. Wreford, *Inorg. Chem., 24* (1985) 1379; (c) T.S. Targos, R.P. Rosen, R.R. Whittle and G.L. Geoffroy, *Inorg. Chem., 24* (1985) 1375; (d) E.D. Morrison, A.D. Harley, M.A. Marcelli, G.L. Geoffroy, A.L. Rheingold and W.C. Fultz, *Organometallics, 3* (1984) 1407.

[8] R.E. Stevens and W.L. Gladfelter, *Inorg. Chem., 22* (1983) 2034.

[9] J.J. Eisch and R.B. King, *Organometallic Syntheses*, Academic Press, New York, 1965, p. 161.

[10] P.M. Treichel, E. Pitcher, R.B. King and F.G.A. Stone, *J. Am. Chem. Soc., 83* (1961) 2593.

[11] E.J. Gabe, Y. LePage, J.P. Charland, F.L. Lee and P.S. White, *J. Appl. Crystallogr., 22* (1989) 384.

[12] P. Mai, S.J. Fiske, S.E. Hull, L. Lessinger, G. Germain, J.P. Declercq and M.M. Woolfson, *MULTAN82*.

[13] A.R. Rossi and R. Hoffmann, *Inorg. Chem., 14* (1975) 365.

[14] (a) M.R. Tirpark, C.A. Hollingsworth and J.H. Wotiz, *J. Org. Chem., 25* (1960) 687; (b) H. Greenfield, H.W. Sternberg. R.A. Friedel, J.H. Wotiz, R. Markby and I. Wender, *J. Am. Chem. Soc., 78* (1952) 120.

[15] (a) U.H.F. Bunz, V⟩ Enkelmann and J. Räder, *Organometallics,*

*12* (1993) 4745; (b) M. Zeldih, K. Wynne and H.R. Allcock, *Inorganic and Organometallic Polymers, Advances in Chemistry Series 224* American Chemical Society, Washington, DC, 1988.
[16] D.J. Hodgson and J.A. Ibers, *Inorg. Chem., 7* (1968) 2345.
[17] (a) V.G. Albano, P.L. Bellon and G. Ciani, *J. Organomet. Chem., 38* (1972) 155; (b) V.G. Albano, P.L. Bellon, G. Ciani and M. Manassero, *J. Chem. Soc., Dalton Trans., 35* (1972) 423.
[18] D.M.P. Mingos and J.A. Ibers, *Inorg. Chem., 10* (1971) 1479.
[19] J.H. Enemark and J.A. Ibers, *Inorg. Chem., 6* (1967) 1575.
[20] D.J. Hodgson and J.A. Ibers, *Inorg. Chem., 7* (1968) 2345.
[21] B.A. Frenz, J.H. Enemark and J.A. Ibers., *Inorg. Chem., 8* (1969) 1288.

ELSEVIER

Journal of Organometallic Chemistry 508 (1996) 195–208

Journal of Organometallic Chemistry

# Isomeric diphosphines of a heteroannularly bridged ferrocene: preparation, chromatographic separation and structure elucidation

Georg Kutschera [a], Christoph Kratky [b], Walter Weissensteiner [a], Michael Widhalm [a,*]

[a] *Institut für Organische Chemie, Universität Wien, Währingerstraße 38, A-1090 Wien, Austria*
[b] *Institut für Physikalische Chemie, Universität Graz, Heinrichstraße 28, A-8010 Graz, Austria*

Received 20 June 1995

**Abstract**

Twofold lithiation of the heteroannularly bridged aminophosphine **5** yielded a mixture of five isomeric aminodiphosphines **7a–7d** and **11**, which were separated by adsorption chromatography. Their substitution pattern was elucidated by X-ray structure analyses and chemical correlation. Corresponding diphosphines **10a–10d** were derived with moderate yields via acetates **8a–8d**. A search for stable conformers of **7a–7d** and **11** was conducted using empirical force field calculations. Calculated minimum-energy geometries were compared with crystal structures of **7a**, **7c** and **7d**.

*Keywords:* Iron; Heteroannularly-bridged ferrocene; Diphosphine; X-ray structure; Circular dichroism

## 1. Introduction

Following the successful use of ferrocene derivatives as catalysts in asymmetric cross-coupling reactions, attention has focused on structural variations of 1-diphenylphosphino-2-(1-*N*,*N*-dimethylaminoethyl)-ferrocene (**2**), which was originally employed by Kumada's group [1]. Subsequently a second phosphino group was introduced at the unsubstituted cyclopentadiene ring to yield **3** with an additional site for transition metal coordination. Moreover, the ethylamino group was transformed into ethyl, methoxyethyl on acetoxyethyl, or into more complex "side arms" with additional heteroatoms to support a stereoselective coordination of the substrate at the transition metal. So far more than 200 ferrocenyl-based ligands have been designed in the quest for chiral catalysts for a variety of asymmetric reactions, including hydrogenation, hydrosilylation, cross-coupling reactions and aldol condensation [2]. Most of these catalysts were synthesized from *N*,*N*-dimethyl-1-ferrocenylethylamine (**1**) as a key intermediate [3], which permitted a highly diastereoselective access to planar-chiral derivatives via ortho-lithiation. An additional advantage is the availability of a convenient procedure for optical resolution of **1** via diastereomeric tartrates, permitting the facile preparation of optically active derivatives [4].

As it is generally accepted that the catalyst's conformational stability favours high diastereoselectivity [5], we set out to synthesize homoannularly and heteroannularly bridged ferrocenes with phosphorus and nitrogen as coordination sites. Thus we recently prepared the homoannularly bridged compound **4** and tested its efficiency in asymmetric cross-coupling reactions [6]. In the preceding paper, we described the synthesis of aminomonophosphine **6**, derived from the heteroannularly bridged ferrocene **5** [7]. Here we report the synthesis and chromatographic separation of five isomeric aminodiphosphines **7a–7d** and **11** obtained by twofold lithiation of **5**, and the elucidation of their substitution pattern and molecular conformation by both chemical and physical methods.

## 2. Results and discussion

Ortho-lithiation of **5** with *n*-BuLi exhibited high diastereoselectivity, similar as observed for the non-bridged aminoferrocene **1**. In each case, quenching the reaction with electrophiles such as benzophenone [8] or chlorodiphenylphosphine [7] led to the predominant formation of a single diastereomer. Excess of *n*-BuLi–

* Corresponding author.

0022-328X/96/$15.00 © 1996 Elsevier Science S.A. All rights reserved
*SSDI* 0022-328X(95)05849-4

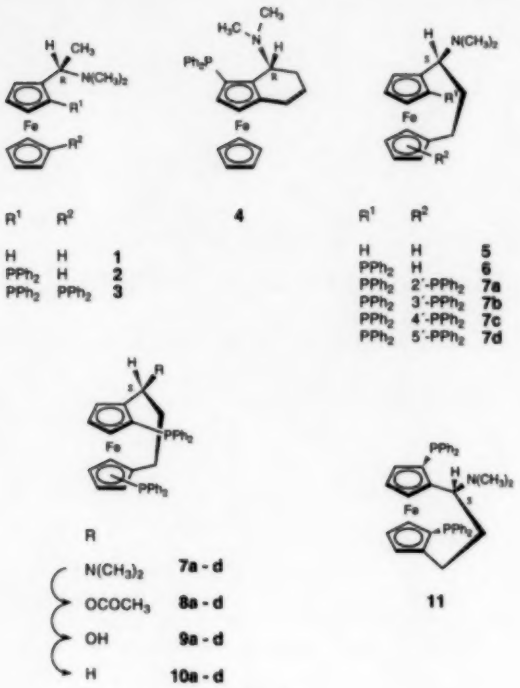


Scheme 1.

TMEDA introduced a second Li atom at the opposite cyclopentadiene ring, resulting in up to four isomers, as a consequence of the non-equivalence of positions 2'–5' (Scheme 1). Thin layer chromatography (TLC) analysis of the reaction mixture shows several well-separated spots, indicating that all four possible diastereomers are indeed produced and should be separable by chromatographic methods. Since the reaction products were observed to be stable towards oxidation, a conventional column chromatography on silica gel under gravity with ethylacetate–petroleum ether–triethylamine as eluent could be employed for preparative scale separation to yield the five diphosphine products in significant amounts. One diphosphine predominated and was isolated with 44% yield, well separated from four isomeric diphosphines which were obtained with low yields (2–7%). In addition some monophosphine **6** was also recovered from the reaction mixture to give a total yield of approximately 100%. Four of the isomers could be obtained as orange to brown crystals. All of them were characterized by spectroscopic methods ($^1$H, $^{13}$C, $^{31}$P NMR and mass spectroscopy (MS)).

In the preceding communication we demonstrated that the first lithiation step selectively forms the 2-lithio derivative [7], and there is undoubtful NMR evidence from homonuclear and heteronuclear shift correlation experiments that the second lithium atom is introduced into the opposite ring [9]. Thus four structures, **7a–7d**, had to be assigned to four of the five isomers obtained.

Contrary to benzoid compounds, the substitution pattern in ferrocenes cannot be deduced from the magnitude of the coupling constants $J_{HH}$ of ring protons since $J_{HH}$ is only 1–3 Hz and multiplets are not well resolved. We therefore carried out crystal structure analyses on those compounds that yielded suitable crystals. This permitted unambiguous assignment of configurations **7a**, **7c** and **7d** (see Figs. 3–5 later) to the diphosphines isolated from fractions 2, 3 and 1 respectively.

The decision as to which of the remaining two compounds (fractions 4 and 5) would be the isomer **7b** was based on a combination of chemical correlation and spectroscopy. Transformation of amines **7a–7d** into the corresponding hydrocarbons **10a–10d** was performed by a two- or three-step sequence (see Scheme 1). The diphosphine of fraction 4 yielded a $C_1$-symmetrical hydrocarbon, which is in agreement with structure **7b**, while deamination of **7a** (fraction 2) and diphosphine of fraction 5 afforded identical products (**10a**) as judged from $^{13}$C NMR spectroscopy. Consequently the aminodiphosphine of fraction 5 was identified as **11** obviously formed from the small amount of **5** lithiated at C(5). Characteristic properties relevant for the structural assignments are listed in Table 1.

Since the optically active ligands [10] are of interest in view of their projected application in asymmetric catalysis, we prepared (*S*)-**7a–7d** and **11** from (−)(*S*)-**5** and recorded their CD spectra (Fig. 1). The short-wavelength range (250–400 nm) was found to be largely congruent, but distinct differences were observed in the range of the "ferrocene band" between 400 and 600 nm. Compound, **7b–7d** show positive Cotton effects of similar strength ($\Delta\varepsilon = 2.1–3.1$); these were found to be diminished for **7a** and **11**. Moreover, for **7a** the sign was inverted [11]. $^{31}$P NMR spectra were recorded of all

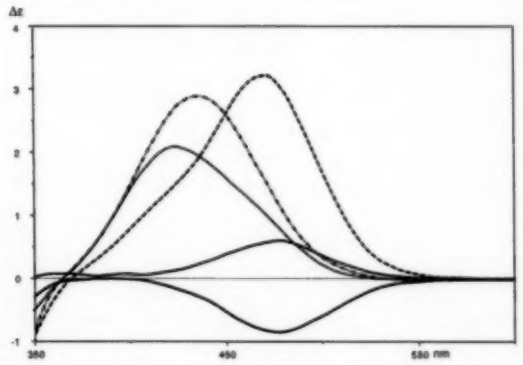


Fig. 1. CD spectra of **7a** (———), **7b** (– – – –), **7c** (–·–·–·–·–), **7d** (· · · · · ·), and **11** (———), derived from (*S*)-**5**.

Table 1
Characteristic properties relevant for the structural assignments

| Compound | Chromatographic fraction | $\delta$ ($^{31}$P) (ppm) | $J_{PP}$ (Hz) | CD, $\lambda_{max}$ ($\Delta\varepsilon$) (nm) | | | | | $\delta$ ($^{31}$P) (ppm) | Symmetry |
|---|---|---|---|---|---|---|---|---|---|---|
| **7a** | 2 | −24.30 (d), −24.77 (d) | 43.9 | 260 (−27.6) | | | 474 (−0.848) | → **10a** | −25.92 (s) | $C_s$ |
| **7b** | 4 | −20.10 (s), −21.70 (s) | 0.0 | 243 (−2.24) | 274 (+11.42) | 340 (−1.21) | 470 (+3.22) | → **10b** | −18.85 (s), −20.60 (s) | $C_1$ |
| **7c** | 3 | −16.68 (s), −21.61 (s) | 0.0 | 251 (−12.5) | | 332 (−2.30) | 436 (+2.98) | → **10c** | −15.84 (s), −21.19 (s) | $C_1$ |
| **7d** | 1 | −22.09 (s), −21.79 (s) | 0.0 | 257 (−18.1) | | | 424 (+2.07) | → **10d** | −21.11 (s) | $C_2$ |
| **11** | 5 | −25.01 (d), −26.48 (d) | 48.4 | 256 (+8.10) | 283 sh (+2.76) | | 475 (+0.572) | → **10a** | −25.92 (s) | $C_s$ |

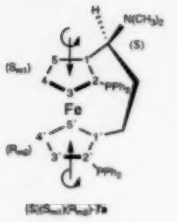

isomers and showed a marked dependence of shift values from the substitution pattern. For **7a** and **11** with direct opposition of diphenylphosphino groups an upfield shift of up to 9 ppm relative to **7b–7d** is observed. Similar P–P coupling constants were found for **7a** and **11**, but virtually no P–P coupling occurred in **7b–7d**. We attribute this behavior to the nearly eclipsed conformation of cyclopentadienyl (Cp) rings in **7** (see below) which results in a perfect arrangement of phosphorus atoms for interaction either through space or with involvement of the iron atom.

To expand the scope of this new class of ferrocenyldiphosphines we also prepared acetates and hydrocarbons of **7**. Acetates **8** were accessible with a good to excellent yield by refluxing the amines **7** with acetic anhydride. The hydrocarbons **10** were finally obtained with a moderate yield by reduction with $AlCl_3$–$LiAlH_4$.

Table 2
Atomic coordinates and equivalent isotropic displacement parameters for the non-hydrogen atoms in the crystal structure of **7a**, where $U$(eq) is defined as one third of the trace of the orthogonalized $U_{ij}$ tensor and the atomic numbering is defined in Fig. 2

| | $x/a$ ($\times 10^{-4}$) | $y/b$ ($\times 10^{-4}$) | $z/c$ ($\times 10^{-4}$) | $U_{eq}$ ($\times 10^{-3}$ Å$^2$) |
|---|---|---|---|---|
| Fe(1) | 8622(1) | 435(1) | 1797(1) | 17(1) |
| P(1) | 6924(1) | −221(1) | 164(1) | 18(1) |
| P(2) | 7769(1) | 2511(1) | 226(1) | 17(1) |
| N(1) | 8068(2) | −1108(3) | −1211(3) | 20(1) |
| C(1) | 8481(2) | −616(3) | 663(4) | 18(1) |
| C(2) | 7807(2) | −480(3) | 1045(3) | 18(1) |
| C(3) | 7968(2) | −652(3) | 2193(4) | 20(1) |
| C(4) | 8711(2) | −909(3) | 2526(4) | 19(1) |
| C(5) | 9027(2) | −903(3) | 1584(4) | 20(1) |
| C(11) | 9056(2) | 1431(3) | 965(4) | 18(1) |
| C(12) | 8414(2) | 1843(3) | 1255(4) | 17(1) |
| C(13) | 8516(2) | 1810(3) | 2429(4) | 18(1) |
| C(14) | 9215(2) | 1412(3) | 2851(4) | 21(1) |
| C(15) | 9553(2) | 1207(3) | 1960(4) | 22(1) |
| C(21) | 8606(2) | −495(3) | −483(3) | 19(1) |
| C(22) | 8577(2) | 565(3) | −873(4) | 20(1) |
| C(23) | 9157(2) | 1224(3) | −181(4) | 20(1) |
| C(31) | 8186(3) | −2119(3) | −894(4) | 24(1) |
| C(32) | 8089(3) | −1017(4) | −2371(4) | 29(1) |
| C(41) | 6359(2) | 19(3) | 1182(4) | 20(1) |
| C(42) | 6578(3) | 693(3) | 2020(4) | 23(1) |
| C(43) | 6115(3) | 958(4) | 2707(4) | 26(1) |
| C(44) | 5423(3) | 576(4) | 2548(4) | 27(1) |
| C(45) | 5192(3) | −86(4) | 1710(4) | 28(1) |
| C(46) | 5658(2) | −368(4) | 1033(4) | 22(1) |
| C(51) | 6632(2) | −1468(3) | −244(4) | 21(1) |
| C(52) | 6352(2) | −1655(4) | −1349(4) | 26(1) |
| C(53) | 6155(3) | −2599(4) | −1690(5) | 35(1) |
| C(54) | 6234(3) | −3352(4) | −951(5) | 38(1) |
| C(55) | 6496(3) | −3169(4) | 144(5) | 35(1) |
| C(56) | 6700(3) | −2235(3) | 505(4) | 26(1) |
| C(61) | 8241(2) | 3698(3) | 386(4) | 18(1) |
| C(62) | 8980(2) | 3805(3) | 853(4) | 22(1) |
| C(63) | 9311(3) | 4710(3) | 877(4) | 23(1) |
| C(64) | 8914(3) | 5520(3) | 465(4) | 24(1) |
| C(65) | 8179(3) | 5431(3) | 15(4) | 23(1) |
| C(66) | 7849(3) | 4526(3) | −33(4) | 22(1) |
| C(71) | 6991(2) | 2799(3) | 844(4) | 20(1) |
| C(72) | 6305(2) | 2510(3) | 284(4) | 21(1) |
| C(73) | 5688(3) | 2764(4) | 668(4) | 28(1) |
| C(74) | 5750(3) | 3303(4) | 1611(4) | 30(1) |
| C(75) | 6431(3) | 3590(3) | 2182(4) | 25(1) |
| C(76) | 7049(2) | 3336(3) | 1812(4) | 21(1) |

A one-step conversion of **8** to **10** succeeded in one case (**10b**), while **10a**, **10c** and **10d** were only accessible after isolation of the intermediate alcohols **9a**, **9c** and **9d** and subsequent treatment with $AlCl_3$–$LiAlH_4$. As expected, NMR spectroscopy revealed $C_1$ symmetry (**10b** and **10c**) for two of them, but $C_s$ or $C_2$ symmetry for **10a** and **10d** respectively.

### 2.1. Force field calculations and crystal structure determinations

In order to get insight into stability and minimum-energy conformations of aminodiphosphines, force field calculations were conducted for all aminophosphines using the program PCMODEL [12] and minimum geometries were compared with X-ray structural analyses of **7a**, **7c** and **7d** (Tables 2–5). All crystal structures show similar general shape with same conformation of the $C_3$ bridge (Figs. 2–5). Minor differences arising from different substitution pattern are listed in Table 6. Since the torsional angle of Cp rings is determined by the conformation of the $C_3$ bridge which is stabilized in the *out-of-plane* conformation (Fig. 6A) obviously caused by steric interaction with the $PPh_2$ group adjacent at Cp(1) in all cases similar torsional angles (5.3–6.2°) are found. The same is true for the tilt angle of the Cp

Table 3
Coordinates and displacement parameters for the crystal structure of **7c**

| | $x/a$ ($\times 10^{-4}$) | $y/b$ ($\times 10^{-4}$) | $z/c$ ($\times 10^{-4}$) | $U_{eq}$ ($\times 10^{-3}$ Å$^2$) |
|---|---|---|---|---|
| Fe(1) | 2763(1) | 4265(1) | 7621(1) | 18(1) |
| P(1) | 4266(1) | 1864(1) | 6600(1) | 19(1) |
| P(2) | −27(1) | 6821(1) | 7618(1) | 21(1) |
| N(1) | 6740(2) | 1675(2) | 7930(1) | 26(1) |
| C(1) | 4819(3) | 3518(2) | 7586(2) | 21(1) |
| C(2) | 4312(2) | 3390(2) | 6834(2) | 19(1) |
| C(3) | 3741(2) | 4686(2) | 6355(2) | 20(1) |
| C(4) | 3898(3) | 5596(3) | 6783(2) | 23(1) |
| C(5) | 4583(3) | 4884(2) | 7526(2) | 22(1) |
| C(11) | 2129(3) | 3201(3) | 8826(2) | 24(1) |
| C(12) | 1516(3) | 2920(3) | 8190(2) | 24(1) |
| C(13) | 732(3) | 4103(2) | 7718(2) | 23(1) |
| C(14) | 810(3) | 5144(2) | 8071(2) | 21(1) |
| C(15) | 1662(3) | 4569(3) | 8764(2) | 23(1) |
| C(21) | 5459(3) | 2439(2) | 8315(2) | 23(1) |
| C(22) | 4446(3) | 1545(3) | 8885(2) | 26(1) |
| C(23) | 3165(3) | 2252(3) | 9387(2) | 26(1) |
| C(31) | 7714(3) | 2541(3) | 7437(2) | 35(1) |
| C(32) | 7460(3) | 629(3) | 8588(2) | 37(1) |
| C(41) | 5923(3) | 1551(2) | 5896(2) | 21(1) |
| C(42) | 6726(3) | 2493(3) | 5450(2) | 23(1) |
| C(43) | 7917(3) | 2187(3) | 4880(2) | 27(1) |
| C(44) | 8322(3) | 941(3) | 4759(2) | 31(1) |
| C(45) | 7544(3) | −4(3) | 5208(2) | 36(1) |
| C(46) | 6339(3) | 299(3) | 5770(2) | 29(1) |
| C(51) | 3068(3) | 2532(2) | 5767(2) | 21(1) |
| C(52) | 3481(3) | 3079(3) | 4878(2) | 29(1) |
| C(53) | 2512(3) | 3626(3) | 4289(2) | 32(1) |
| C(54) | 1101(3) | 3635(3) | 4584(2) | 29(1) |
| C(55) | 674(3) | 3086(3) | 5459(2) | 28(1) |
| C(56) | 1647(3) | 2527(3) | 6044(2) | 24(1) |
| C(61) | 594(3) | 7689(2) | 8242(2) | 22(1) |
| C(62) | 1471(3) | 8557(2) | 7783(2) | 23(1) |
| C(63) | 1974(3) | 9252(3) | 8215(2) | 27(1) |
| C(64) | 1582(3) | 9092(3) | 9109(2) | 30(1) |
| C(65) | 702(3) | 8232(3) | 9573(2) | 28(1) |
| C(66) | 211(3) | 7527(3) | 9142(2) | 24(1) |
| C(71) | −1830(3) | 6801(3) | 8159(2) | 23(1) |
| C(72) | −2272(3) | 5721(3) | 8771(2) | 27(1) |
| C(73) | −3674(3) | 5773(3) | 9107(2) | 32(1) |
| C(74) | −4651(3) | 6902(3) | 8845(2) | 35(1) |
| C(75) | −4228(3) | 7973(3) | 8239(2) | 39(1) |
| C(76) | −2829(3) | 7927(3) | 7890(2) | 33(1) |

Table 4
Coordinates and displacement parameters for the crystal structure of **7d**

| | $x/a$ ($\times 10^{-4}$) | $y/b$ ($\times 10^{-4}$) | $z/c$ ($\times 10^{-4}$) | $U_{eq}$ ($\times 10^{-3}$ Å$^2$) |
|---|---|---|---|---|
| Fe(1) | 3571(1) | 7265(1) | 1296(1) | 19(1) |
| P(1) | 5118(1) | 6305(1) | 3606(1) | 21(1) |
| P(2) | 211(1) | 8367(1) | −125(1) | 22(1) |
| N(1) | 2243(3) | 8417(2) | 3863(2) | 25(1) |
| C(1) | 3162(3) | 8145(2) | 2280(2) | 20(1) |
| C(2) | 4688(3) | 7384(2) | 2473(2) | 20(1) |
| C(3) | 5626(3) | 7617(2) | 1602(2) | 22(1) |
| C(4) | 4725(3) | 8501(2) | 890(2) | 23(1) |
| C(5) | 3233(3) | 8829(2) | 1314(2) | 23(1) |
| C(11) | 1612(3) | 6701(2) | 1567(2) | 22(1) |
| C(12) | 2969(3) | 5826(2) | 1787(2) | 24(1) |
| C(13) | 3912(3) | 5838(2) | 920(2) | 24(1) |
| C(14) | 3130(3) | 6691(2) | 149(2) | 23(1) |
| C(15) | 1698(3) | 7229(2) | 534(2) | 22(1) |
| C(21) | 1748(3) | 8234(2) | 2958(2) | 23(1) |
| C(22) | 1019(3) | 7245(2) | 3186(2) | 26(1) |
| C(23) | 380(3) | 7061(2) | 2280(2) | 24(1) |
| C(31) | 2869(3) | 9383(2) | 3646(2) | 30(1) |
| C(32) | 960(4) | 8543(3) | 4573(2) | 39(1) |
| C(41) | 5718(3) | 6961(2) | 4456(2) | 22(1) |
| C(42) | 6637(3) | 7706(2) | 4192(2) | 26(1) |
| C(43) | 7020(3) | 8179(2) | 4881(2) | 31(1) |
| C(44) | 6530(3) | 7885(2) | 5841(2) | 35(1) |
| C(45) | 5649(4) | 7131(2) | 6118(2) | 35(1) |
| C(46) | 5224(3) | 6681(2) | 5428(2) | 30(1) |
| C(51) | 7041(3) | 5480(2) | 3340(2) | 22(1) |
| C(52) | 8198(3) | 5044(2) | 4067(2) | 28(1) |
| C(53) | 9596(3) | 4336(2) | 3912(2) | 30(1) |
| C(54) | 9868(3) | 4053(2) | 3026(2) | 32(1) |
| C(55) | 8713(3) | 4463(2) | 2306(2) | 32(1) |
| C(56) | 7313(3) | 5156(2) | 2470(2) | 28(1) |
| C(61) | 1302(3) | 8796(2) | −1264(2) | 24(1) |
| C(62) | 1471(3) | 8321(2) | −2042(2) | 30(1) |
| C(63) | 2384(3) | 8649(3) | −2853(2) | 37(1) |
| C(64) | 3160(3) | 9452(3) | −2897(2) | 37(1) |
| C(65) | 2998(3) | 9939(2) | −2128(2) | 34(1) |
| C(66) | 2073(3) | 9617(2) | −1326(2) | 29(1) |
| C(71) | −1086(3) | 7657(2) | −512(2) | 23(1) |
| C(72) | −2260(3) | 8261(2) | −1200(2) | 28(1) |
| C(73) | −3312(3) | 7778(2) | −1495(2) | 30(1) |
| C(74) | −3213(3) | 6699(2) | −1121(2) | 29(1) |
| C(75) | −2089(3) | 6096(2) | −422(2) | 29(1) |
| C(76) | −1031(3) | 6577(2) | −119(2) | 26(1) |

Table 5
Selected parameters from crystal structure analyses and calculated minimum geometries (in parentheses) [a]

| | 7a | 7c | 7d |
|---|---|---|---|
| P(1)–N (Å) | 3.249 (3.323) | 3.503 (3.425) | 3.365 (3.383) |
| P(1)–P(2) (Å) | 4.075 (3.741) | | |
| Cp(1)–Cp(2) torsional angle (°) | 6.1 (3.6) | 6.2 (4.5) | 5.3 (2.9) |
| Cp(1)–Cp(2) tilt angle (°) | 13.0 (19.1) | 9.4 (16.5) | 11.5 (15.9) |
| Deviation from best Cp plane [b] | | | |
| C(21)–Cp(1) (Å) | −0.044 | −0.070 | −0.020 |
| P(1)–Cp(1) (Å) | 0.148 | −0.093 | −0.089 |
| C(23)–Cp(2) (Å) | −0.157 | −0.164 | −0.135 |
| P(2)–Cp(2) (Å) | 0.429 | −0.066 | 0.047 |

[a] See [11]; labeling scheme as given in Fig. 2.
[b] Positive values refer to deviations distal to iron, while negative values refer to deviations proximal to iron.

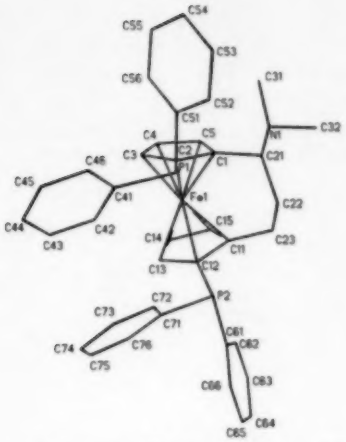


Fig. 2. The crystal structure of **7a**, together with the atom numbering used for the description of the crystal structures.

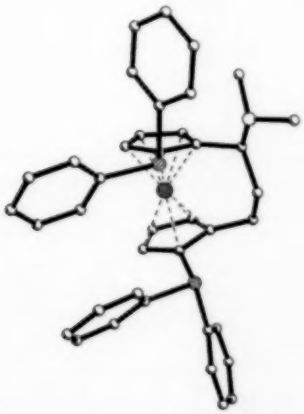

Fig. 3. Crystal structure of racemic **7a** (fraction 2; (*S*)-enantiomer shown). Hydrogen atoms have been omitted for clarity.

planes which range from 9.4 to 13.0°. Noticeable deviations from ideal geometry are observed for C(21) and C(23) which are shifted towards iron and for the phosphorus atoms in **7a** which are shifted to the distal side of the Cp planes.

Force field calculations were conducted for all aminodiphosphines in two conformations A and B which are interconvertible by a flip of the $C_3$ bridge (Fig. 6).

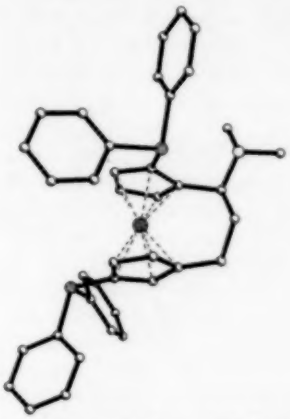

Fig. 4. Crystal structure of racemic **7c** (fraction 3)

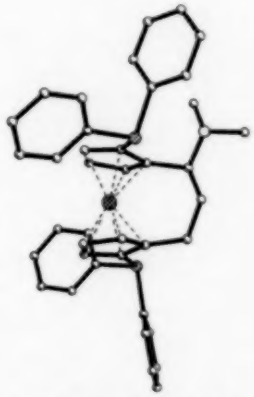

Fig. 5. Crystal structure of racemic **7d** (fraction 1).

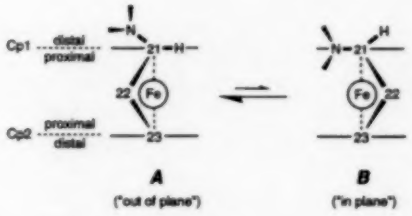


Fig. 6.

Table 6
MMX calculations for conformers of **7a–7d** and **11**

| | 7a | 7b | 7c | 7d | 11 |
|---|---|---|---|---|---|
| $\Delta E_{\text{in-out}}$ [a] (kJ) | 30.7 | 28.3 | 33.3 | 30.6 | 25.3 |
| $(E_{\text{7a out}})-(E_{\text{x out}})$ [b] (kJ) | 0 | 9.7 | 9.6 | 4.4 | 1.3 |

[a] Energy difference of conformers with dimethylamino substituent either in plane or out of plane of Cp(1); see Fig. 6.

[b] Energy differences arising from substitution pattern are calculated for the "out-of-plane" conformation (Fig. 6A); **7a** with highest energy was arbitrarily set equal to zero.

Energy differences between A and B are similar for **7a–7d** and **11** and high enough to exclude the population of B in detectable amounts. Only in the case of **11** was a somewhat smaller energy difference calculated which reflects a less pronounced steric interaction between $PPh_2$ and $N(CH_3)_2$. Energy differences arising from different substitution pattern are as expected for varying steric repulsions. So **7a** shows highest energy since it receives steric strain of two $PPh_2$ groups adjacent to the carbon bridge and directly opposed to each other. In contrast with this, **7b** and **7c** with a single $Ph_2P\cdot\cdot\cdot\cdot\cdot\cdot CHN(CH_3)_2$ contact show considerably lower energy. Good agreement with the crystal structures was found for torsional angles and tilt angles; in particular, trends are reproduced satisfactorily although tilt angles tend to be too large.

## 3. Conclusions

Our findings clearly demonstrate that dilithiation in ferrocenes takes place at the second Cp ring preferred opposite to the first Li atom. We believe that this arrangement is stabilized via lithium associates, possibly with participation of TMEDA since for the dilithio derivative of the non-bridged aminoferrocene **1** a corresponding structure was confirmed by X-ray analysis [13]. As a consequence of this, kinetic control favors the formation of **7a** despite of its significantly higher energy compared with isomers **7b–7d**. Compound **7a** is expected to function as a bidentate ligand in transition metal complexes, with either P–P or P–N coordination. The corresponding complexes will be tested for their efficiency in asymmetric catalysis.

## 4. Experimental part

The $^1H$, $^{13}C$ and $^{31}P$ NMR (proton-decoupled) spectra were recorded in $CDCl_3$ on a Bruker AM-400 spectrometer at 400, 100 and 162 MHz respectively. Chemical shifts $\delta$ are given relative to tetramethylsilane (TMS) as internal standard ($^1H$ and $^{13}C$ NMR) and relative to 85% $H_3PO_4$ ($^{31}P$ NMR). $^{13}C$ NMR spectra were recorded in a *J*-modulated mode; *J* refers to phosphorus–carbon coupling constants. In spectral areas with extensive signal overlapping, multiplets could not be identified; these signals of unclear relationship are underlined, ignoring probable multiplet structures. Mass spectra were recorded on a Varian MAT-CH7. Optical rotations were measured with a Perkin–Elmer polarimeter 241 in $CH_2Cl_2$ at 20°C (thermostated). CD spectra were recorded on a dichrograph CD 6 (Jobin–Yvon) ($CH_2Cl_2$ at 20°C) and UV spectra were recorded on a Perkin–Elmer Lambda 7 spectrometer ($CH_2Cl_2$). Melting points were determined on a Kofler melting-point apparatus and are uncorrected. Elemental analyses were carried out at Mikroanalytisches Laboratorium der Universität Wien (J. Theiner). Diethyl ether and benzene were distilled from $LiAlH_4$ prior to use; chlorodiphenylphosphine (Aldrich) was distilled and stored under Ar. All the other chemicals were of analytical grade and used as purchased.

### 4.1. (±)-1,1'-(1-N,N-Dimethylaminopropane-1,3-diyl)-ferrocene (5)

This was prepared according to literature procedures [14]. The optical resolution of **5** was performed via fractional crystallization of the diastereomeric tartrates [15].

### 4.2. Isomeric bis(diphenylphosphino)-1,1'-(1-N,N-dimethylaminopropane-1,3-diyl)ferrocenes (7a–7d and 11) and 2-diphenylphosphino-1,1'-(1-N,N-dimethylaminopropane-1,3-diyl)-ferrocene (6)

The reaction was carried out in 100 ml Schlenk tubes under Ar. 1.00 g (3.71 mmol) of **5** was dissolved in 25 ml of absolute diethyl ether. The solution was degassed and 2.7 ml of a 1.6 N solution of *n*-BuLi in hexane (4.32 mmol) was added dropwise. After stirring for 3 h at room temperature, 1.35 ml (9.0 mmol) of *N,N,N',N'*-tetramethylethylenediamine and 8.1 ml of *n*-BuLi in hexane (13.0 mmol) were added in portions. The mixture was stirred at room temperature for 20 h. The dark-red solution was cooled to −78°C, and 3.65 ml (19.8 mmol) of chlorodiphenylphosphine was added. After warming to room temperature the mixture was refluxed for 1 h. The reaction was quenched by careful addition of 10 ml of $Na_2CO_3$ solution (10%). The organic layer was separated and the aqueous layer was extracted twice with 10 ml of diethyl ether. The combined extracts were dried with $MgSO_4$ and the solvent was removed in vacuo to give 3.8 g of a red wax. The crude mixture was chromatographed on silica gel (40–63 μm; column, 3 × 90 cm) using petroleum ether : ethylacetate : triethylamine (75 : 24.5 : 0.5) for packing. Elution with a solvent gradient petroleum ether : ethylacetate : triethylamine (75 : 24.7 : 0.3 → 65 : 34.8 : 0.2) afforded the following fractions (in the order of elution).

#### 4.2.1. Fraction 1: (±)-2,5'-bis(diphenylphosphino)-1,1'-(1-N,N-dimethylaminopropane-1,3-diyl)-ferrocene (7d)

Yield, 161 mg (6.8%); melting point (m.p.), above 170°C (decomposition). $^1H$ NMR: $\delta$ 1.86 (6H, s), 2.35 (1H, br. t, $J$ = 12 Hz), 2.43 (2H, m), 2.67 (1H, br. d, $J$ = 10.6 Hz), 2.98 (1H, br. q, $J$ = 12 Hz), 3.34 (1H, s), 3.59 (1H, br.s), 3.75 (1H, m), 3.84 (1H, m), 4.43 (1H, br.s), 4.67 (1H, br.s), 7.15–7.36 (16H, m), 7.36–7.46 (4H, m) ppm. $^{13}C$ NMR: $\delta$ 23.63 ($CH_2$, d, $J$ = 11.7 Hz), 38.39 ($CH_2$, d, $J$ = 9.1 Hz), 44.34 ($CH_3$, s), 66.23

(CH, s), 69.89 (CH, s), 71.35 (CH, s), 71.91 (CH, d, $J = 4$ Hz), 73.93 (CH, d, $J = 4$ Hz), 74.88 (CH, m), 75.83 (C, d, $J = 12$ Hz), 78.28 (C, d, $J = 3$ Hz), 79.63 (CH, m), 92.18 (C, d, $J = 20.2$ Hz), 93.56 (C, d, $J = 22.1$ Hz), 127.57 (CH, d, $J = 7.5$ Hz), 127.72 (CH, d, $J = 6.8$ Hz), 127.76 (CH, s), 127.96 (CH, s), 128.06 (CH, d, $J = 7.6$ Hz), 128.20 (CH, d, $J = 7$ Hz), 128.23 (CH, s), 128.93 (CH, s), 132.26 (CH, d, $J = 18$ Hz), 133.42 (CH, d, $J = 20$ Hz), 134.30 (CH, d, $J = 20$ Hz), 134.59 (CH, d, $J = 20$ Hz), 137.00 (C, d, $J = 10$ Hz), 138.70 (C, d, $J = 12$ Hz), 139.21 (C, d, $J = 16$ Hz), 139.30 (C, d, $J = 17$ Hz) ppm. $^{31}$P NMR: $\delta$ −22.09 (s), −21.79 (s) ppm. MS (250°C): $m/z$ (relative %) 638 M + (100), 623 (49), 594 (23), 560 (12), 515 (5), 452 (25), 408 (34), 331 (44), 329 (25), 319 (52). UV ($c = 6.04 \times 10^{-2}$ and $1.2 \times 10^{-3}$ mol$^{-1}$): $\lambda_{max}(\varepsilon)$ 255 (22 100), 437 (257) nm. Anal. Found: C, 73.02; H, 5.85; N, 2.31; P, 9.52; $C_{39}H_{37}FeNP_2$ calc.: C, 73.48; H, 5.85; N, 2.20; P, 9.72%. When the reaction was carried out with (−)(*S*)-**5**, (−)($S_c$)($S_{m1}$)($S_{m2}$)-**7d** was obtained: $[\alpha]_D^{20} = -208°$ ($c = 0.385$).

#### 4.2.2. Fraction 2: (±)-2,2'-bis(diphenylphosphino)-1,1'-(1-N,N-dimethylaminopropane-1,3-diyl)ferrocene (7a)

Yield, 1034 mg (43.6%); m.p., above 172°C (decomposition). $^1$H NMR: $\delta$ 1.61 (6H, s), 1.74 (1H, br. t, $J = 14$ Hz), 1.93 (1H, br. d, $J = 14.9$ Hz), 2.22 (1H, br. d, $J = 13.5$ Hz), 2.33 (1H, br. d, $J = 11.1$ Hz), 3.37 (1H, br. q, $J = 13$ Hz), 4.07 (1H, br.s), 4.14 (2H, br.s), 4.22 (1H, t, $J = 2.5$ Hz), 4.26 (1H, t, $J = 2.5$ Hz), 4.28 (1H, br.s), 6.84 (2H, t, $J = 7.5$ Hz), 7.06 (3H, m), 7.21 (7H, m), 7.33 (2H, t, $J = 7.5$ Hz), 7.43 (6H, m) ppm. $^{13}$C NMR: $\delta$ 25.95 ($CH_2$, s), 38.76 ($CH_2$, t, $J = 8.2$ Hz), 43.95 ($CH_3$, s), 66.87 (CH, s), 67.51 (CH, s), 68.44 (CH, s), 73.13 (CH, d, $J = 5.4$ Hz), 73.73 (CH, br. d, $J = 3.1$ Hz), 73.85 (CH, s), 74.33 (CH, s), 78.05 (C, d, $J = 18.4$ Hz), 80.45 (C, d, $J = 12.7$ Hz), 91.73 (C, dd, $J = 8.2$, 1.9 Hz), 92.14 (C, dd, $J = 15.1$, 3.7 Hz), 126.36 (CH, s), 127.21 (CH, d, $J = 3.7$ Hz), 127.35 (CH, d, $J = 7.6$ Hz), 127.74 (CH, d, $J = 6.8$ Hz), 127.78 (CH, s), 128.11 (CH, d, $J = 7.6$ Hz), 128.24 (CH, s), 128.65 (CH, s), 133.08 (CH, dd, $J =$ 13.7, 3.8 Hz), 133.29 (CH, dd, $J = 19.8$, 2.3 Hz), 134.98 (CH, dd, $J = 19.9$, 3.0 Hz), 135.73 (CH, dd, $J = 20.6$, 2.3 Hz), 137.98 (C, d, $J = 11$ Hz), 139.99 (C, d, $J = 15$ Hz), 140.40 (C, d, $J = 12$ Hz), 140.67 (C, d, $J = 10$ Hz) ppm. $^{31}$P NMR: $\delta$ −24.30 (d, $J = 43.5$ Hz), −24.77 (d, $J = 43.9$ Hz) ppm. MS (200°C): $m/z$ (relative %) 638 M + (60), 595 (13), 560 (5), 517 (13), 453 (14), 409 (29), 408 (27), 331 (49). UV ($c = 1.72 \times 10^{-2}$ and $3.4 \times 10^{-4}$ mol$^{-1}$): $\lambda_{max}(\varepsilon)$ 255 sh (24 100), 447 (425) nm. Anal. Found: C, 73.02; H, 5.83; N, 2.13; P, 9.77. $C_{39}H_{37}FeNP_2$ Calc.: C, 73.48; H, 5.85; N, 2.20; P, 9.72%. When the reaction was carried out with (−)(*S*)-**5**, (−)($S_c$)($S_{m1}$)($R_{m2}$)-**7a** was obtained: $[\alpha]_D^{20} = -235°$ ($c = 0.109$).

#### 4.2.3. Fraction 3: (±)-2,4'-bis(diphenylphosphino)-1,1'-(1-N,N-dimethylaminopropane-1,3-diyl)ferrocene (7c)

Yield, 113 mg (4.8%); m.p., 194–198°C (decomposition). $^1$H NMR: $\delta$ 1.78 (6H, s), 1.85 (1H, br. t, $J = 14$ Hz), 2.38 (2H, br. d, $J = 9$ Hz), 2.63 (1H, br. d, $J = 15$ Hz), 2.91 (1H, br. q, $J = 13$ Hz), 3.53 (1H, br.s), 3.56 (1H, br.s), 4.11 (1H, t, $J = 1.5$ Hz), 4.13 (1H, m), 4.17 (1H, t, $J = 2.3$ Hz), 4.56 (1H, br.s), 7.14–7.38 (20H, m) ppm. $^{13}$C NMR: $\delta$ 25.55 ($CH_2$, s), 38.23 ($CH_2$, d, $J = 9.4$ Hz), 44.26 ($CH_3$, s), 66.31 (CH, d, $J = 2$ Hz), 73.00 (CH, d, $J = 2.9$ Hz), 74.56 (CH, dd, $J = 6.3$, 3 Hz), 74.84 (CH, d, $J = 4.8$ Hz), 74.99 (CH, d, $J = 4.5$ Hz), 75.08 (CH, d, $J = 10.3$ Hz), 76.00 (C, d, $J = 6.8$ Hz), 76.28 (C, d, $J = 14.3$ Hz), 76.40 (CH, d, $J = 19.5$ Hz), 91.50 (C, d, $J = 4.8$ Hz), 91.87 (C, m), 127.53 (CH, d, $J = 7.3$ Hz), 127.64 (CH, d, $J = 6.3$ Hz), 127.74 (CH, s), 127.84 (CH, d, $J = 6.7$ Hz), 128.07 (CH, d, $J = 6.8$ Hz), 128.12 (CH, s), 128.22 (CH, s), 128.33 (CH, s), 133.05 (CH, d, $J = 19$ Hz), 133.19 (CH, d, $J = 19$ Hz), 133.47 (CH, d, $J = 20$ Hz), 133.91 (CH, d, $J = 19$ Hz), 138.55 (C, d, $J = 11.4$ Hz), 138.65 (C, d, $J = 8$ Hz), 139.10 (C, d, $J = 9.8$ Hz), 139.27 (C, d, $J = 8.5$ Hz) ppm. $^{31}$P NMR: $\delta$ −16.68 (s), −21.61 (s) ppm. MS (240°C); $m/z$ (relative %) 638 M + (83), 594 (23), 593 (22), 409 (31), 408 (42), 407 (21), 331 (39). UV ($c = 1.81 \times 10^{-2}$ and $3.63 \times 10^{-4}$ moll$^{-1}$): $\lambda_{max}(\varepsilon)$ 253 (24 200), 437 (398) nm. Anal. Found: C, 73.16; H, 6.09; N, 2.04; P, 9.77. $C_{39}H_{37}FeNP_2$ Calc.: C, 73.48; H, 5.85; N, 2.20; P, 9.72%. When the reaction was carried out with (−)(*S*)-**5** the (−)($S_c$)($S_{m1}$)($S_{m2}$)-**7c** was obtained: $[\alpha]_D^{20} = -47°$ ($c = 0.116$).

#### 4.2.4. Fraction 4: (±)-2,3'-bis(diphenylphosphino)-1,1'-(1-N,N-dimethylaminopropane-1,3-diyl)ferrocene (7b)

Yield, 150 mg (6.3%); m.p., above 145°C (decomposition). $^1$H NMR: $\delta$ 1.79 (6H, s), 1.94 (1H, br. t, $J = 14$ Hz), 2.37 (1H, br. d, $J = 13$ Hz), 2.42 (1H, br. d, $J = 12$ Hz), 2.64 (1H, br. d, $J = 14$ Hz), 3.26 (1H, br. q, $J = 14$ Hz), 3.46 (1H, m), 3.76 (1H, t, $J = 2.5$ Hz), 3.85 (1H, br.s), 4.08 (1H, br.s), 4.23 (1H, br.s), 4.60 (1H, br.s), 7.03 (2H, m), 7.10 (2H, m), 7.18 (2H, m), 7.22 (7H, m), 7.28 (2H, m), 7.36 (1H, m), 7.44 (2H, br.t, $J = 7.5$ Hz), 7.65 (2H, br.t, $J = 7.5$ Hz) ppm. $^{13}$C NMR: $\delta$ 25.74 ($CH_2$, s), 38.64 ($CH_2$, d, $J = 13.6$ Hz), 44.26 ($CH_3$, s), 66.81 (CH, d, $J = 2$ Hz), 69.03 (CH, s), 69.74 (CH, d, $J = 5$ Hz), 74.37 (CH, d, $J = 4$ Hz), 74.65 (CH, s), 76.73 (CH, s), ~ 77.38 (CH), 78.48 (C, d, $J = 17$ Hz), 79.67 (C, d, $J = 15$ Hz), 90.56 (C, dd, J = 17.7, 2.5 Hz), 91.70 (C, d, $J = 9$ Hz), 127.45, 127.47, 127.51, 127.52, 127.58, 127.60 (4 × CH), 127.92 (CH, d, $J = 5.4$ Hz), 128.26 (CH, s), 128.36 (CH, s), 128.58 (CH, dd, $J = 7.0$, 2.4 Hz), 132.20 (CH, d, $J = 18$ Hz), 133.46 (CH, d, $J = 20$ Hz), 134.12 (CH, d, $J = 20$ Hz), 135.22 (CH, dd, $J = 20$, 4.5 Hz), 137.86 (C, d, $J = 9$ Hz), 138.67 (C, d, $J = 12$ Hz), 139.93 (C, d, $J = 8$ Hz), 140.80 (C, d, $J = 13$ Hz)

ppm. $^{31}$P NMR: δ −20.10 (s), −21.70 (s). MS (240°C): *m/z* (relative %) 638 M+ (100), 594 (28), 593 (31), 592 (30), 560 (4), 517 (7), 452 (7), 409 (27), 408 (25), 407 (14), 331 (20), UV ($c = 1.76 \times 10^{-2}$ and $3.51 \times 10^{-4}$ moll$^{-1}$): $\lambda_{max}(\varepsilon)$ 255 (23900), 453 (327) nm. Anal. Found: C, 73.18; H, 5.96; N, 1.97; P, 9.94. $C_{39}H_{37}FeNP_2$ Calc.: C, 73.48; H, 5.85; N, 2.20; P, 9.72%. When the reaction was carried out with (−)(*S*)-**5**, (+)($S_c$)($S_{m1}$)($R_{m2}$)-**7b** was obtained: $[\alpha]_D^{20} = +446°$ ($c = 0.0224$).

*4.2.5. Fraction 5: (±)-5,5'-bis(diphenylphosphino)-1,1'-(1-N,N-dimethylaminopropane-1,3-diyl)ferrocene (11)*

Yield, 50 mg (2.1%); oil. $^1$H NMR: δ 1.85 (6H, s), 2.03 (1H, m), 2.13 (1H, m), 2.16 (1H, m), 2.48 (1H, m), 3.18 (1H, br. s), 3.94 (1H, br.s), 4.13 (1H, br.s), 4.31 (1H, t, $J = 2.5$ Hz), 4.36 (1H, t, $J = 2.5$ Hz), 4.37 (1H, br.s), 4.54 (1H, br.s), 6.95 (2H, td, $J = 7$, 2 Hz), 7.00–7.61 (16H, m), 7.71 (2H, m) ppm. $^{13}$C NMR: δ 23.05 ($CH_2$, s), 38.82 ($CH_2$, s), 43.58 ($CH_3$, s), 60.96 (CH, d, $J = 7.2$ Hz), 69.12 (CH, s), 69.62 (CH, s), 70.88 (CH, s), 71.08 (CH, br.s), 72.58 (2 × CH, br.s), 79.37 (C, d, $J = 12$ Hz), 82.67 (C, d, $J = 10$ Hz), ~ 87.3 (C, m), 90.42 (C, d, $J = 15$ Hz), 127.50 (CH, d, $J = 7.4$ Hz), 127.60 (CH, s), 127.78 (CH, d, $J = 7.4$ Hz), 128.04, 128.11, 128.17, 128.41, 128.67 (5 × CH), 133.10 (CH, d, $J = 20$ Hz), 133.80 (CH, dd, $J = 17$, 2.5 Hz), 134.66 (CH, d, $J = 22$ Hz), 135.05 (CH, d, $J = 20$ Hz), 137.64 (C, m), 139.36 (C, d, $J = 13$ Hz), 140.17 (C, d, $J = 14$ Hz) ppm. $^{31}$P NMR: δ −25.01 (d, $J = 48.4$ Hz), −26.48 (d, $J = 48.4$ Hz) ppm. MS (200°C): *m/z* (relative %) 638 M+ (9), 623 (7), 560 (3), 452 (4), 386 (10), 331 (7). UV ($c = 1.59 \times 10^{-2}$ and $3.2 \times 10^{-4}$ moll$^{-1}$): [$\lambda_{max}(\varepsilon)$] 253 sh (19500), 451 (308) nm.

When the reaction was carried out with (−)(*S*)-**5**, (+) ($S_c$)($R_{m1}$)($S_{m2}$)-**11** was obtained: $[\alpha]_D^{20} = +60°$ ($c = 0.101$).

*4.2.6. Fraction 6: (±)-2-diphenylphosphino-1,1'-(1-N,N-dimethylaminopropane-1,3-diyl)ferrocene (6)*

Yield, 334 mg (19.8%); m.p., 168–172°C; spectral properties were found to be identical with those of an authentic sample.

*4.3. Bis(diphenylphosphino)-1,1'-(1-acetoxypropane-1,3-diyl)ferrocenes (8a–8d) from corresponding bis(diphenylphosphino)-1,1'-(1-N,N-dimethylaminopropane-1,3-diyl)-ferrocenes (7a–7d) (general procedure)*

The aminodiphosphine **7** and freshly distilled acetic anhydride were mixed in a small Schlenk tube, degassed and heated to about 100°C. During the course of the reaction, the amine dissolved. After completion of the reaction (TLC) the excess of anhydride was removed in vacuo and the residue was chromatographed on a short column (silica gel; 1 × 20 cm) with petroleum ether : ethylacetate (75 : 25). Different reaction conditions were applied to isomers **7a–7d** as specified below:

*4.3.1. (±)-2,2'-Bis(diphenylphosphino)-1,1'-(1-acetoxypropane-1,3-diyl)ferrocene (8a)*

450 mg (0.70 mmol) of **7a** were heated to 100°C for 2 h; yield, 430 mg (94%). $^1$H NMR: δ 1.06 (3H, s), 1.89 (2H, m), 2.01 (1H, m), 3.74 (1H, m), 3.94 (2H, br.s), 4.13 (1H, t, $J = 2$ Hz), 4.32 (1H, t, $J = 2.4$ Hz), 4.37 (1H, br.s), 4.51 (1H, br.s), 5.35 (1H, br.d, $J = 9.8$ Hz), 7.00 (2H, t, $J = 7.3$ Hz), 7.04–7.30 (14H, m), 7.38–7.49 (4H, m) ppm. $^{13}$C NMR: δ 19.73 ($CH_3$, s), 24.71 ($CH_2$, s), 40.58 ($CH_2$, dd, $J = 9.1$, 7.6 Hz), 67.36 (CH, s), 69.42 (CH, s), 73.47 (CH, s), 73.70 (CH, d, $J = 3.8$ Hz), 73.83 (CH, d, $J = 3.8$ Hz), ~ 74.11 (2 × CH, m), 80.33 (C, dd, $J = 18.3$, 2 Hz), 80.46 (C, d, $J = 13.8$ Hz), 84.09 (C, d, $J = 16.8$ Hz), 91.60 (C, d, $J = 11.4$ Hz), 127.76 (CH, d, $J = 6.9$ Hz), 127.77 (CH, s), 127.81 (CH, d, $J = 6.8$ Hz), 128.05 (CH, d, $J = 6.8$ Hz), 128.09 (CH, s), 128.22 (CH, s), 128.33 (CH, d, $J = 7.7$ Hz), 128.78 (CH, s), 132.95 (CH, d, $J = 19.9$ Hz), 133.98 (CH, d, $J = 22.1$ Hz), 134.30 (CH, d, $J = 19.8$ Hz), 134.83 (CH, dd, $J = 18.3$, 3.1 Hz), 137.59 (C, d, $J = 13$ Hz), 137.99 (C, d, $J = 14.5$ Hz), 138.53 (C, d, $J = 15.2$ Hz), 140.90 (C, d, $J = 12.2$ Hz), 170.75 (C, s) ppm. $^{31}$P NMR: δ −23.45 (d, $J = 41.0$ Hz), −26.59 (d, $J = 41.0$ Hz) ppm. MS (240°C): *m/z* (relative %) 653 M+ (100), 610 (11), 593 (5), 575 (15), 515 (11), 467 (15), 424 (18), 407 (41).

*4.3.2. (±)-2,3'-Bis(diphenylphosphino)-1,1'-(1-acetoxypropane-1,3-diyl)ferrocene (8b)*

245 mg (0.38 mmol) of **7b** were heated to 100°C for 2 h; yield, 187 mg (73%). $^1$H NMR: δ 1.14 (3H, s), 2.17 (2H, m), 2.63 (1H, br.d, $J = 14.7$ Hz), 3.56 (3H, m), 3.76 (1H, t, $J = 2.4$ Hz), 4.36 (2H, s), 4.75 (1H, s), 5.32 (1H, dd, $J = 11.3$, 2.9 Hz), 6.93 (2H, t, $J = 6.9$ Hz), 7.08–7.19 (6H, m), 7.20–7.30 (7H, m), 7.41–7.53 (3H, m), 7.60 (2H, td, $J = 7.9$, 1.5 Hz) ppm. $^{13}$C NMR: δ 19.87 ($CH_3$, s), 24.38 ($CH_2$, s), 40.17 ($CH_2$, d, $J = 13$ Hz), 69.79 (CH, s), 69.94 (CH, d, $J = 5.4$ Hz), 73.47 (CH, s), 73.82 (CH, d, $J = 3.8$ Hz), 74.54 (CH, s), 76.95 (CH, m), 78.39 (CH, dd, $J = 32.9$, 5 Hz), 79.36 (C, d, $J = 16$ Hz), 79.75 (C, d, $J = 14.5$ Hz), 84.41 (C, d, $J = 16.8$ Hz), 91.33 (C, d, $J = 6.9$ Hz), 127.47 (CH, s), 127.58 (CH, d, $J = 7.4$ Hz), 127.92 (CH, s), 127.94 (CH, d, $J = 5.3$ Hz), 128.07 (CH, d, $J = 6.9$ Hz), 128.47 (CH, s), 128.68 (CH, dd, $J = 7.6$, 2.2 Hz), 128.95 (CH, s), 131.98 (CH, d, $J = 17.6$ Hz), 132.75 (CH, d, $J = 19.8$ Hz), 134.21 (CH, d, $J = 20.6$ Hz), 135.70 (CH, dd, $J = 20.6$, 3.8 Hz), 136.29 (C, d, $J = 9.9$ Hz), 138.30 (C, d, $J = 10.4$ Hz), 140.00 (C, d, $J = 9.9$ Hz), 140.71 (C, d, $J = 13$ Hz), 170.19 (C, s) ppm. $^{31}$P NMR: δ −19.92 (s), −20.92 (s) ppm. MS

(240°C): *m/z* (relative %) 653 M+ (100), 610 (14), 595 (3), 576 (1), 515 (2), 467 (4), 424 (24), 407 (12).

#### 4.3.3. (±)-2,4'-Bis(diphenylphosphino)-1,1'-(1-acetoxypropane-1,3-diyl)ferrocene (8c)

122 mg (0.19 mmol) of **7c** were heated to 100°C for 2 h; yield, 85 mg (68%). $^1$H NMR: δ 1.14 (3H, s), 2.05 (1H, br. t, $J$ = 14 Hz), 2.23 (1H, m), 2.62 (1H, br. d, $J$ = 14.7 Hz), 3.27 (1H, br. q, $J$ = 13 Hz), 3.33 (1H, br.s), 3.70 (1H, br.s), 4.20 (2H, m), 4.40 (1H, m), 4.72 (1H, br.s), 5.27 (1H, dd, $J$ = 11.3, 3.3 Hz), 7.12–7.34 (20H, m) ppm. $^{13}$C NMR: δ 19.83 ($CH_3$, s), 24.34 ($CH_2$, s), 39.61 ($CH_2$, d, $J$ = 10.7 Hz), 73.22 (CH, s), 73.88 (CH, d, $J$ = 3.0 Hz), 74.64 (CH, d, $J$ = 3.8 Hz), 74.73 (CH, d, $J$ = 3.8 Hz), 75.02 (CH, d, $J$ = 12.2 Hz), 75.13 (CH, dd, $J$ = 7, 3 Hz), 76.38 (CH, d, $J$ = 18.2 Hz), 76.50 (C, d, $J$ = 7 Hz), 77.41 (C, d, $J$ = 13.7 Hz), 85.17 (C, d, $J$ = 18.2 Hz), 91.31 (C, d, $J$ = 4.6 Hz), 127.83 (CH, d, $J$ = 6.8 Hz), 127.93 (CH, d, $J$ = 6.8 Hz), 128.08 (CH, s), 128.11 (2 × CH, d, $J$ = 6.1 Hz), 128.25 (CH, s), 128.46 (CH, s), 128.77 (CH, s), 132.80 (CH, d, $J$ = 19.1 Hz), 132.94 (CH, d, $J$ = 19.1 Hz), 133.18 (CH, d, $J$ = 19.2 Hz), 134.06 (CH, d, $J$ = 19.1 Hz), 136.89 (C, d, $J$ = 9.9 Hz), 138.45 (C, d, $J$ = 9.1 Hz), 138.67 (C, d, $J$ = 9.9 Hz), 138.96 (C, d, $J$ = 9.9 Hz), 170.49 (C, s) ppm. $^{31}$P NMR: δ −17.06 (s), −20.66 (s) ppm. MS (240°C): *m/z* (relative %): 653 M+ (100), 610 (10), 595 (3), 576 (2), 515 (2), 467 (3), 424 (32), 407 (13).

#### 4.3.4. (±)-2,5'-Bis(diphenylphosphino)-1,1'-(1-acetoxypropane-1,3-diyl)ferrocene (8d)

129 mg (0.20 mmol) of **7d** were heated to 90°C for 2 h; yield, 97 mg (74%) of **8d** as a mixture of diastereoisomers (approximately 30:70). The crude product was used without further purification.

### 4.4. (±)-2,3'-Bis(diphenylphosphino)-1,1'-(propane-1,3-diyl)ferrocene (10b)

80 mg (0.60 mmol) of $AlCl_3$ and 200 mg (5.3 mmol) of $LiAlH_4$ were mixed with 2 ml of anhydrous diethyl ether. A solution from 80 mg (0.12 mmol) of **8b** in 4 ml of diethylether:benzene (1:1) was added to the $AlCl_3$–$LiAlH_4$ suspension with cooling. After stirring the mixture at room temperature for 100 h, the reaction was quenched by careful addition of water. The organic layer was separated and the aqueous layer was extracted with 3 × 10 ml of methylene chloride. The combined extracts were dried with $MgSO_4$ and evaporated. Chromatography on silica gel with petroleum ether:chloroform (50:50) afforded **10b** as an oil; yield, 12 mg (19%). $^1$H NMR: δ 1.93 (2H, m), 2.07 (1H, m), 2.22 (1H, m), 2.38 (1H, m), 3.42 (1H, br.s), 3.60 (1H, br.s), 3.67 (1H, t, $J$ = 2.5 Hz), 4.06 (1H, br.s), 4.11 (1H, br.s), 4.45 (1H, br.s), 7.04–7.11 (2H, m), 7.12–7.35 (14H, m), 7.37–7.50 (2H, m), 7.55–7.63 (2H, m) ppm. $^{13}$C NMR: δ 22.78 ($CH_2$, d, $J$ = 7.6 Hz), 24.21 ($CH_2$, s), 34.85 ($CH_2$, d, $J$ = 3.8 Hz), 69.16 (CH, s), 70.92 (CH, d, $J$ = 4.5 Hz), 71.44 (CH, s), 71.51 (CH, d, $J$ = 3.1 Hz), 74.87 (CH, s), 77.89 (C, d, $J$ = 12.2 Hz), 79.42 (C, d, $J$ = 6.1 Hz), 82.27 (CH, dd, $J$ = 36.6, 6.9 Hz), 88.77 (C, d, $J$ = 8.4 Hz), 90.05 (C, d, $J$ = 19.1 Hz), 127.40 (CH, s), 127.54 (CH, d, $J$ = 6.8 Hz), 127.93 (CH, d, $J$ = 5.5 Hz), 128.05 (CH, s), 128.18 (CH, d, $J$ = 6.2 Hz), 128.34 (CH, s), 128.52 (CH, dd, $J$ = 7.6, 1 Hz), 128.87 (CH, s), 132.06 (CH, d, $J$ = 17.6 Hz), 132.63 (CH, d, $J$ = 19.1 Hz), 134.30 (CH, d, $J$ = 20.5 Hz), 135.40 (CH, dd, $J$ = 20.6, 4.2 Hz), 136.38 (C, d, $J$ = 9.9 Hz), 138.86 (C, d, $J$ = 10.6 Hz), 139.26 (C, d, $J$ = 12.2 Hz), 141.09 (C, d, $J$ = 13 Hz) ppm. $^{31}$P NMR: δ −18.85 (s), −20.60 (s) ppm. MS (200°C): *m/z* (relative %) 595 M+ (62), 518 (9), 486 (2), 410 (100), 333 (25), 331 (26).

### 4.5. Hydroxy derivatives 9a, 9b and 9d (general procedure)

The acetate **8** was suspended in anhydrous diethyl ether and $LiAlH_4$ was added. After stirring at room temperature for 1 h, the mixture was quenched with excess of water. The organic layer was separated and the aqueous layer was extracted with three 10 ml portions of ether. The combined extracts were dried with $MgSO_4$ and chromatographed on silicagel with petroleum ether:ethyl acetate (75:25). The products isolated from the chromatography were used without further purification for the preparation of hydrocarbons **10**.

#### 4.5.1. (±)-2,2'-Bis(diphenylphosphino)-1,1'-(1-hydroxypropane-1,3-diyl)ferrocene (9a)

210 mg (0.32 mmol) of **8a** and 19 mg (0.50 mmol) of $LiAlH_4$ in 20 ml of ether yielded 181 mg (92%) of **9a**. $^1$H NMR: δ 1.93 (1H, m), 2.02 (1H, m), 2.15 (1H, m), 2.71 (1H, ddd, $J$ = 10.1, 5.5, 3.5 Hz), 3.83 (1H, m), 3.66 (1H, t, $J$ = 2 Hz), 4.06 (1H, m), 4.17 (1H, m), 4.19 (1H, t, $J$ = 2.5 Hz), 4.28 (1H, m), 4.32 (1H, t, $J$ = 2.5 Hz), 4.38 (1H, br. t, $J$ = 8 Hz), 6.97–7.07 (4H, m), 7.11–7.43 (14H, m) 7.63–7.72 (2H, m) ppm. $^{13}$C NMR: δ 19.05 ($CH_2$, d, $J$ = 6.4 Hz), 42.06 ($CH_2$, d, $J$ = 3 Hz), 67.47 (CH, s), 68.89 (CH, s), 69.23 (CH, s), 71.43, 71.65, 71.67, 71.69 (2 × CH), 73.72 (CH, d, $J$ = 2.3 Hz), 80.02 (C, d, $J$ = 7.9 Hz), 80.41 (C, d, $J$ = 17.6 Hz), 89.72 (C, d, $J$ = 10.7 Hz), 89.87 (C, d, $J$ = 16.8 Hz), 127.57 (CH, d, $J$ = 6.9 Hz), 127.60 (CH, s), 128.08 (CH, d, $J$ = 7.6 Hz), 128.17 (CH, s), 128.20 (CH, d, $J$ = 6.1 Hz), 128.29 (CH, d, $J$ = 6.9 Hz), 128.40 (CH, s), 128.95 (CH, s), 132.72 (CH, d, $J$ = 19.8 Hz), 133.49 (CH, d, $J$ = 20.6 Hz), 133.66 (CH, d, $J$ = 15.3 Hz), 135.91 (CH, dd, $J$ = 19.8, 2.2 Hz), 136.36 (C, d, $J$ = 9.9 Hz), 138.60 (C, d, $J$ = 16 Hz), 139.75

(C, d, $J = 13$ Hz), 139.83 (C, dd, $J = 12.2$, 1.5 Hz) ppm. $^{31}$P NMR: $\delta$ −23.11 (d, $J = 52.0$ Hz), −26.83 (d, $J = 52.0$ Hz) ppm. MS (240°C): $m/z$ (relative %) 611 M + (100), 533 (21), 425 (30), 409 (36), 348 (40).

*4.5.2. (±)-2,3'-Bis(diphenylphosphino)-1,1'-(1-hydroxypropane-1,3-diyl)ferrocene (9b)*

93 mg (0.14 mmol) of **8b** and 22 mg (0.57 mmol) of $LiAlH_4$ in 10 ml of diethyl ether yielded 68 mg (78%) of **9b**. $^1$H NMR: $\delta$ 2.12 (2H, br. m), 2.51 (1H, m), 3.25 (1H, br. q, $J = 10$ Hz), 3.51 (1H, br.s), 3.54 (1H, br.s), 3.71 (1H, t, $J = 2.5$ Hz), 4.16 (1H, s), 4.25 (1H, br.s), 4.33 (1H, m), 4.66 (1H, br.s), 6.97 (2H, t, $J = 7$ Hz), 7.07–7.16 (4H, m), 7.18–7.29 (9H, m), 7.39–7.51 (3H, m) 7.62 (2H, td, $J = 7.8$, 1.5 Hz) ppm. $^{13}$C NMR: $\delta$ 23.12 ($CH_2$, s), 43.19 ($CH_2$, d, $J = 9.8$ Hz), 69.71 (CH, s), 70.07 (CH, d, $J = 5.2$ Hz), 70.62 (CH, s), 72.72 (CH, d, $J = 3.6$ Hz), 73.62 (CH, s), 76.61 (CH, dd, $J = 2$, 2 Hz), 78.85 (C, d, $J = 14.4$ Hz), 79.23 (C, d, $J = 13.8$ Hz), 79.61 (CH, dd, $J = 36$, 5.7 Hz), 88.81 (C, d, $J = 15.3$ Hz), 91.44 (C, d, $J = 7.5$ Hz), 127.50 (CH, s), 127.58 (CH, d, $J = 7.2$ Hz), 127.96 (CH, d, $J = 5.4$ Hz), 128.38, 128.40, 128.43, 128.46 (3 × CH), 128.67 (CH, dd, $J = 7.6$, 1.3 Hz), 129.09 (CH, s), 132.05 (CH, d, $J = 17.9$ Hz), 132.76 (CH, d, $J = 19.2$ Hz), 134.21 (CH, d, $J = 20.5$ Hz), 135.66 (CH, dd, $J = 20.8$, 4.2 Hz), 136.23 (C, d, $J = 10.2$ Hz), 138.46 (C, d, $J = 11.5$ Hz), 140.19 (C, d, $J = 10.6$ Hz), 140.72 (C, d, $J = 12.9$ Hz) ppm. $^{31}$P NMR: $\delta$ −19.70 (s), −19.82 (br.s) ppm. MS (230°C): $m/z$ (relative %): 611 M + (100), 533 (11), 425 (24), 409 (33), 347 (16), 305 (6).

*4.5.3. (±)-2,5'-Bis(diphenylphosphino)-1,1'-(1-hydroxypropane-1,3-diyl)ferrocene (9d)*

100 mg (0.15 mmol) of **8d** (m.d.) and 26 mg (0.68 mmol) of $LiAlH_4$ in 30 ml of ether yielded 70 mg (76%) of **9d** as a mixture of diastereomers.

*4.5.4. (±)-2,4'-Bis(diphenylphosphino)-1,1'-(1-hydroxypropane-1,3-diyl)ferrocene (9c)*

80 mg (0.12 mmol) of **8c**, dissolved in 4 ml of a mixture of diethyl ether:benzene (50:50), was added under cooling to a suspension from 64 mg (0.48 mmol) of $AlCl_3$ and 200 mg (5.27 mmol) of $LiAlH_4$ in 2 ml of diethyl ether. After stirring at room temperature for 100 h, the reaction was quenched with water. The organic layer was separated and the aqueous layer was extracted with 3 × 10 ml of methylene chloride. The combined extracts were dried with $MgSO_4$ and evaporated. The crude product was chromatographed on silicagel with petroleum ether:chloroform (50:50) to give 55 mg (75%) of **9c**; no trace of the hydrocarbon **10c** could be observed. $^1$H NMR: $\delta$ 2.01 (1H, br. t, $J = 13$ Hz), 2.23 (1H, m), 2.52 (1H, ddd, $J = 15$, 5.9, 2.5 Hz), 3.06 (1H, br. q, $J = 12$ Hz), 3.40 (1H, m), 3.60 (1H, m), 4.15 (1H, m), 4.19 (1H, t, $J = 2.4$ Hz), 4.24 (1H, m), 4.33 (1H, dd, $J = 10$, 3 Hz), 4.61 (1H, br.s), 7.14–7.37 (20H, m) ppm. $^{13}$C NMR: $\delta$ 23.56 ($CH_2$, s), 43.05 ($CH_2$, d, $J = 8.6$ Hz), 70.81 (CH, s), 73.75 (CH, d, $J = 4.6$ Hz), 73.87 (CH, d, $J = 3.1$ Hz), 74.53 (CH, d, $J = 10.2$ Hz), 74.60 (CH, d, $J = 4.5$ Hz), 75.77 (CH, m), 75.91 (CH, d, $J = 19.1$ Hz), 76.38 (C, d, $J = 7.6$ Hz), 76.69 (C, d, $J = 13.0$ Hz), 89.48 (C, d, $J = 18.5$ Hz), 91.75 (C, d, $J = 4.5$ Hz), 127.85 (CH, d, $J = 6.8$ Hz), 127.99 (CH, d, $J = 6.8$ Hz), 128.10 (CH, d, $J = 6.1$ Hz), 128.22 (CH, s), 128.27 (CH, s), 128.30 (CH, d, $J = 6.1$ Hz), 128.40 (CH, s), 128.92 (CH, s), 132.54 (CH, d, $J = 18.3$ Hz), 133.05 (CH, d, $J = 19$ Hz), 133.14 (CH, d, $J = 19.1$ Hz), 134.22 (CH, d, $J = 20.5$ Hz), 136.84 (C, d, $J = 9.9$ Hz), 138.51 (C, d, $J = 9.9$ Hz), 138.83 (C, d, $J = 9.9$ Hz), 139.36 (C, d, $J = 8.9$ Hz) ppm. $^{31}$P NMR: $\delta$ −16.87 (s), −20.00 (br.s) ppm. MS (240°C): $m/z$ (relative %): 611 M + (100), 595 (21), 533 (3), 517 (3), 486 (1), 454 (6), 425 (12), 409 (21).

*4.6. Hydrocarbons 10a, 10c and 10d (general procedure)*

$AlCl_3$ and $LiAlH_4$ were added to a solution of alcohol **9** in diethyl ether–benzene. After stirring and heating the mixture as stated below, the reaction was quenched with an excess of water, the organic layer was separated and the aqueous layer was extracted with 3 × 10 ml of methylenechloride. The combined extracts were dried with $MgSO_4$ and chromatographed on silicagel with petroleum ether:chloroform (50:50).

*4.6.1. (±)-2,2'-Bis(diphenylphosphino)-1,1'-(propane-1,3-diyl)ferrocene (10a)*

52 mg (0.085 mmol) of **9a** 2 ml of ether, 2 ml of benzene, 210 mg (1.57 mmol) of $AlCl_3$, 50 mg (1.3 mmol) of $LiAlH_4$ for 100 h at room temperature yielded 24 mg (47%) of **10a**; oil; $^1$H NMR: $\delta$ 1.75 (3H, m), 1.88 (2H, m), 2.36 (1H, m), 3.80 (2H, m), 4.10 (2H, br.s), 4.14 (2H, t, $J = 2$ Hz), 7.00 (4H, t, $J = 7.4$ Hz), 7.11 (2H, t, $J = 7.4$ Hz), 7.17 (6H, m), 7.26 (8H, m) ppm. $^{13}$C NMR: $\delta$ 23.50 ($CH_2$, t, $J = 3.5$ Hz), 34.29 ($CH_2$, t, $J = 3$ Hz), 68.47 (CH, s), 71.43 (CH, s), 71.90 (CH, s), 81.07 (C, t, $J = 5$ Hz), 89.09 (C, t, $J = 8$ Hz), 127.77 (CH, t, J = 3.5 Hz), 128.07 (CH, s), 128.11 (CH, t, J = 3.8 Hz), 128.19 (CH, s), 133.45 (CH, t, J = 10.6 Hz), 134.57 (CH, t, $J = 10.5$ Hz), 137.89 (C, t, $J = 7$ Hz), 139.69 (C, t, $J = 6.7$ Hz) ppm. $^{31}$P NMR: $\delta$ −25.92 (s) ppm. MS (220°C): $m/z$ (relative %) 594 M + (80), 517 (44), 409 (44).

*4.6.2. (±)-2,4'-Bis(diphenylphosphino)-1,1'-(propane-1,3-diyl)ferrocene (10c)*

55 mg (0.09 mmol) of **9c**, 2 ml of ether, 2 ml of benzene, 124 mg (0.93 mmol) of $AlCl_3$, 92 mg (2.4

mmol) of $LiAlH_4$ was heated under reflux for 8 h to yield 12 mg (22%) of **10c**; oil. $^1$H NMR: $\delta$ 1.90 (2H, m), 2.07 (3H, m), 2.37 (1H, m), 3.36 (1H, s), 3.66 (1H, s), 3.98 (1H, s), 4.12 (1H, s), 4.15 (1H, s), 4.38 (1H, s), 7.15–7.37 (20H, m) ppm. $^{13}$C NMR: $\delta$ 22.77 ($CH_2$, d, $J$ = 6.9 Hz), 24.20 ($CH_2$, s), 34.85 ($CH_2$, d, $J$ = 4.5 Hz), 73.02, 73.05, 73.08 (2 × CH), 73.28 (CH, d, $J$ = 2.9 Hz), 73.61 (CH, d, $J$ = 13 Hz), 73.89 (CH, d, $J$ = 17.6 Hz), ≈ 76.4 (2 × C, m?), 78.05. (CH, dd, $J$ = 6.4, 2.6 Hz), 89.35 (C, d, $J$ = 4.5 Hz), 90.72 (C, d, $J$ = 21.9 Hz), 127.85 (CH, d, $J$ = 6.9 Hz), 128.00 (CH, d, $J$ = 7.7 Hz), 128.06 (CH, s), 128.09 (CH, d, $J$ = 6.1 Hz), 128.21 (CH, d, $J$ = 6.1 Hz), 128.24 (CH, s), 128.45 (CH, s), 128.75 (CH, s), 132.42 (CH, d, $J$ = 18.3 Hz), 133.04 (CH, d, $J$ = 18.3 Hz), 133.34 (CH, d, $J$ = 19.1 Hz), 134.10 (CH, d, $J$ = 19.8 Hz), 136.87 (C, d, $J$ = 9.1 Hz), 138.76–139.01 (3 × C, m?) ppm. $^{31}$P NMR: $\delta$ −15.84 (br.s), −21.19 (s) ppm. MS (160°C): $m/z$ (relative %) 594 M+ (100), 517 (15), 409 (23), 332 (21).

#### 4.6.3. (±)-2,5'-Bis(diphenylphosphino)-1,1'-(propane-1,3-diyl)ferrocene (10d)

70 mg (0.11 mmol) of **9d**, 4 ml of ether, 6 ml of benzene, 108 mg (0.8 mmol) of $AlCl_3$, 48 mg (1.2 mmol) of $LiAlH_4$ for 4 h, at 80°C yielded 21 mg (31%) of **10d**; oil, $^1$H NMR: $\delta$ 2.00 (2H, br.m), 2.09 (2H, br.m), 2.36 (2H, br. m), 3.30 (2H, m), 3.75 (2H, t, $J$ = 2 Hz), 4.37 (2H, d, $J$ = 1.5 Hz), 7.11–7.26 (16H, m), 7.26–7.35 (4H, m) ppm. $^{13}$C NMR: $\delta$ 23.03 ($CH_2$, d, $J$ = 6.8 Hz), 34.85 ($CH_2$, t, $J$ = 4.9 Hz), 69.92 (CH, s), 72.41 (CH, d, $J$ = 3.8 Hz), 76.63 (C, d, $J$ = 6.1 Hz). 77.84 (CH, dd, J = 7.6, 3.8 Hz). 91.26 (C, d, $J$ = 21.4 Hz), 128.00 (CH, s), 128.04 (CH, d, $J$ = 6.8 Hz), 128.22 (CH, d, $J$ = 6.1 Hz), 128.84 (CH, s), 132.37 (CH, d, $J$ = 18.3 Hz), 134.44 (CH, d, $J$ = 19.8 Hz), 137.19 (C, d, $J$ = 9.9 Hz), 139.11 (C, d, 10.7 Hz) ppm. $^{31}$P NMR: $\delta$ −21.11 (s) ppm. MS (250°C): $m/z$ (relative %): 596 (84), 595 M+ (100), 517 (14), 410 (21), 409 (67), 332 (31), 331 (18).

### 4.7. Crystal structure analyses [16]

#### 4.7.1. (±)-7a

Crystals of orange–red color were grown by slow evaporation from $CHCl_3$. A specimen of size 0.3 × 0.3 × 0.3 mm was used for diffraction experiments, which were performed at 84(2) K on a modified STOE diffractometer using Mo Kα radiation ($\lambda$ = 0.71073 Å). Unit-cell parameters were obtained by least-squares refinement against the setting angles of 23 reflections ($3° \leq \theta \leq 11°$). Crystals are monoclinic, of space group $P2_1/c$, with four molecules ($C_{39}H_{37}FeNP_2$; formula weight, 637.5) per unit cell: $a$ = 18.770(4) Å, $b$ = 13.763(3) Å and $c$ = 12.443(2) Å; $\beta$ = 101.98(3)°; $V$ = 3144.4(11) Å$^3$; $d_c$ = 1.347 g cm$^{-3}$ (calculated from the cell constants observed at 84(2) K); $F(000)$ = 1336.

Intensity data ($\omega$ scan; $\Delta\omega$ = 1.5°) were collected for two octants of reciprocal space ($0 \leq h \leq 22$; $-16 \leq k \leq 0$; $-15 \leq l \leq 14$, $3° \leq \theta \leq 26°$), yielding 5526 symmetry independent reflections, of which 3769 are significant ($I > 2\sigma(I)$). Lorentz–polarization correction and an empirical absorption correction (program DIFABS [17]) were applied to the data ($\mu$(Mo Kα) = 0.611 mm$^{-1}$; ratio of minimum to maximum transmission, 0.699). The structure was solved with direct methods and refined with least squares, using a full-matrix least-squares program (SHELXL93 [17]) which minimizes the quantity $\Sigma\omega(F_o^2 - F_c^2)^2$ with $\omega = 1/[\sigma^2(F_o^2) + (aP)^2 + bP]$, $P = (\max(F_o^2, 0) + 2F_c^2)/3$, $a$ = 0.05, b = 21, using all reflections. Anisotropic atomic displacement parameters (ADPs) were refined for all non-hydrogen atoms; H atoms were included at calculated positions ("riding"), an isotropic ADP, was refined for each H atom.

Refinement of 425 parameters against 5517 intensity data and 150 restraints converged at the following values for the reliability indices: $\omega R_2 = [\Sigma[\omega(F_o^2 - F_c^2)^2]/\Sigma[\omega(F_o^2)^2]]^{1/2}$ = 0.1477 (for all 5526 reflections), $R_1 = \Sigma \| F_o | - | F_c \| / \Sigma | F_o |$ = 0.0466 for 3769 significant reflections and 0.0941 for all 5526 data, Goodness of fit $S = [\Sigma[\omega[F_o^2 - F_c^2)^2]/(n-p)]^{1/2}$ = 0.852 (number $n$ of observations, 5517, number $p$ of parameters, 425). Features up to 0.352 electrons Å$^{-3}$ and down to −0.297 electrons Å$^{-3}$ were observed in a final difference electron density map.

Atomic coordinates and equivalent isotropic displacement parameters are given in table 2.

#### 4.7.2. (±)-7c.

Conditions and procedures analogous to the structure determination of **7a**, except where noted explicitly; yellow crystals were grown from $CH_2Cl_2$–methanol; crystal size, 0.4 × 0.4 × 0.4 mm; temperature, 86(2) K. Unit-cell parameters from 24 reflections with $4° \leq \theta \leq 10°$. Crystals are triclinic, of space group $P1$, two molecules ($C_{39}H_{37}FeNP_2$; formula weight, 637.5) per unit cell: $a$ = 9.958(2) Å, $b$ = 10.899(2) Å and $c$ = 16.150(3) Å; $\alpha$ = 72.49(3)°, $\beta$ = 78.80(3)° and $\gamma$ = 76.21(3)°; $V$ = 1609.1(5) Å$^3$; $d_c$ = 1.316 g cm$^{-3}$ (at 86(2) K); $F(000)$ = 668.

Intensity data ($\Delta\omega$ = 1.0°) were collected for four octants ($-11 \leq h \leq 11$, $-12 \leq k \leq 12$, $-1 \leq l \leq 19$; $3° \leq \theta \leq 25°$); 5663 symmetry-independent and 4898 significant reflections. DIFABS [17] absorbtion correction with $\mu$(Mo Kα) = 0.597 mm$^{-1}$. Refinement (425 parameters; 5655 observations; 150 restraints) converged at $\omega R_2$ = 0.1160 (all 5663 reflections), $R_1$ = 0.0413 (4898 significant reflections), $R_1$ = 0.0503 (all 5663 data), $S$ = 1.062 ($n$ = 5655; $p$ = 425). Maximum and minimum residual electron density: 0.451 electrons Å$^{-3}$

and down to −0.411 electrons Å$^{-3}$. Atomic coordinates are given in Table 3.

*4.7.3. (±)-7d*

Orange crystals were grown from $CHCl_3$; crystal size, 0.5 × 0.4 × 0.2 mm; temperature, 87(2) K. Unit-cell parameters from 34 reflections with $4° \leq \theta \leq 11°$. Crystals are triclinic, of space group $P1$, two molecules ($C_{39}H_{37}FeNP_2$; formula weight, 637.5) per unit cell: $a = 8.785(9)$ Å, $b = 13.297(10)$ Å, and $c = 14.134(9)$ Å; $\alpha = 74.33(6)°$, $\beta = 85.74(7)°$ and $\gamma = 75.74(6)°$, $V = 1540.7(22)$ Å$^3$, $d_c = 1.374$ g cm$^{-3}$ (at 87(2) K); $F(000) = 668$.

Intensity data ($\Delta\omega = 1.0°$) were collected for four octants ($-10 \leq h \leq 10$, $-14 \leq k \leq 15$, $0 \leq l \leq 16$, $3° \leq \theta \leq 25°$); 5420 symmetry independent and 4644 significant reflections. DIFABS [17] absorbtion correction with $\mu$(Mo K$\alpha$) = 0.623 mm$^{-1}$. Refinement (426 parameters; 5414 observations; 150 restraints) converged at $\omega R_2 = 0.1009$ (all 5420 reflections), $R_1 = 0.0373$ (4644 significant reflections with $F_o > 4\sigma(F_o)$), $R_1 = 0.0486$ (all 5420 data), $S = 1.078$ ($n = 5414$; $p = 426$). Maximum and minimum residual electron density: 0.351 electrons Å$^{-3}$ and down to −0.394 electrons Å$^{-3}$. Atomic coordinates are given in Table 4.

## Acknowledgments

Thanks are due to B. Jedlicka for assistance in performing the crystal structure determination of **7a** and to the Fonds zur Förderung der wissenschaftlichen Forschung (P-CHE8414 and P-CHE9859) for financial support.

## References and notes

[1] (a) T. Hayashi, K. Yamamoto and M. Kumada, *Tetrahedron Lett.*, (1974) 4405; (b) T. Hayashi, M. Tajika, K. Tamao and M. Kumada, *J. Am. Chem. Soc.*, *98* (1976) 3718.

[2] For an actual exhaustive compilation of ferrocene-based asymmetric catalysts refer to: H. Brunner and W. Zettelmeier, *Handbook of Enantioselective Catalysis with Transition Metal Compounds*, VCH, Weinheim, 1993; A. Togni and T. Hayashi (eds.), *Ferrocenes*, VCH, Weinheim, 1995.

[3] There are only a few exceptions of chiral ferrocenyl-phosphino ligands not being derived from the $C_1$-symmetrical base structure **1**: cf.: T. Hayshi, A. Yamamoto, M. Hojo and Y. Ito, *J. Chem. Soc., Chem. Commun.*, (1989) 495; N. Deus, D. Robles and R. Herrmann, *J. Organomet. Chem.*, *386* (1990) 253; M. Sawamura, A. Yamauchi, T. Takegawa and Y. Ito, *J. Chem. Soc., Chem. Commun.*, (1991) 874.

[4] D. Marquarding, H. Klusacek, G. Gokel, P. Hoffmann and I. Ugi, *J. Am. Chem. Soc.*, *92* (1970) 5389.

[5] Cf.: J. Halpern, in J.D. Mosher (ed.), *Asymmetric Synthesis*, Vol. 5, Academic Press, New York, 1985, pp. 41–69; K.E. Koenig, in J.D. Mosher (ed.), *Asymmetric Synthesis*, Vol. 5, Academic Press, New York, pp. 71–101.

[6] B. Jedlicka, C. Kratky, W. Weissensteiner and M. Widhalm, *J. Chem. Soc., Chem. Commun.*, (1993) 1329.

[7] A. Mernyi, C. Kratky, M. Widhalm and W. Weissensteiner, *J. Organomet. Chem.*, (1995).

[8] S. Hinterberger, unpublished, 1993.

[9] G. Kutschera, unpublished, 1993.

[10] For clarity, we have chosen a labeling scheme for the atoms of the cyclopentadiene rings which is not in accord with IUPAC rules. The stereochemical descriptors for the metallocene chirality, *S* or *R*, are indexed m1 or m2 if related to the upper or lower ring respectively. The viewing direction and the sequence of substituents with decreasing priority according to the CIP system is exemplified for 2,2′-bis(diphenylphosphino)-1,1′-(1-dimethylaminopropane-1,3-diyl) ferrocene (**7a**) which was derived from (*S*)-**5**. Compare with figure in section 2.

[11] This behavior can be rationalized if viewing **7a** and **11** as $C_s$-symmetrical diphosphinoferrocenes with a (small) chiral interference from the asymmetric α-carbon. The relationship between the two isomers resembles that between epimers, since the structural differences arise from the α-C with a proximal P–N arrangement in **7a** and distal P–N arrangement in **11**. Thus the observed small and reversed CD effects qualitatively agree with intuitive expectations.

[12] FCMODEL, *Molecular Modeling Software*, Serena Software, Bloomington, IN, 1992.

[13] I.R. Butler, W.R. Cullen, J. Reglinsky and S.J. Rettig, *J. Organomet. Chem.*, *249* (1983) 183.

[14] M. Rosenblum, A.K. Banerjee, N. Danieli, R.W. Fish and V. Schlatter, *J. Am. Chem. Soc.*, *85* (1963) 316; P. Dixneuf and R. Dabard, *Bull. Soc. Chim. Fr.*, *7* (1972) 2847.

[15] G. Tainturier, K. Chhor y Sok and B. Gautheron, *C.R. Acad. Sci., Sèr. C*, *277* (1973) 1269.

[16] Supplementary data (bond length, bond angles, torsional angles and structure factors) have been deposited at the Cambridge Crystallographic Data Centre.

[17] The following computer programs were used for the crystallographic work: SHELXTL PC, *Version 4.1*, Siemens Analytical Instruments, Inc., Madison, WI, 1990; SHELXL-93, *a Program for the Refinement of Crystal Structures from Diffraction Data*, G.M. Sheldrick, University of Göttingen, Göttingen 1993; DIFABS, N. Walker and D. Stuart, *Acta Crystallogr., Sect. A*, *39* (1983) 158.

ELSEVIER

Journal of Organometallic Chemistry 508 (1996) 209–218

Journal of Organometallic Chemistry

# Synthesis and molecular structure of enantiopure 1-(diphenylphosphino)-2,1′-[(1-*N*,*N*-dimethylamino)-1,3-propanediyl]-ferrocene and its palladium dichloride complex, a new ligand for enantioselective catalysts

Alexander Mernyi [a], Christoph Kratky [b], Walter Weissensteiner [a,*], Michael Widhalm [a]

[a] *Institut für Organische Chemie, Universität Wien, Währingerstraße 38, A-1090 Wien, Austria*
[b] *Institut für Physikalische Chemie, Universität Graz, Heinrichstraße 28, A-8010 Graz, Austria*

Received 20 June 1995

**Abstract**

The palladium dichloride complex of ($S_c$, $S_m$)-1-(diphenylphosphino)-2,1′-[(1-*N*,*N*-dimethylamino)-1,3-propanediyl]-ferrocene (**5**–$PdCl_2$) has been prepared from enantiopure (*S*)-1,1′-[(1-*N*,*N*-dimethylamino)-1,3-propanediyl]-ferrocene (**4**) via a highly stereoselective ortho-lithiation followed by reaction with chlorodiphenyl phosphine to give amino phosphine **5**, which on treatment with $(CH_3CN)_2PdCl_2$ gave the complex **5**–$PdCl_2$. The absolute configuration of the $(-)_{589}$-enantiomer of **4** was deduced from the X-ray structure of its tartrate confirming (*S*)-configuration at the stereogenic center. A conformational analysis including X-ray structure analysis of **5** and **5**–$PdCl_2$ as well as empirical force field calculations on **4** and **5** together with NMR data shows strong stereochemical similarities of **5** and **5**–$PdCl_2$ with the widely used ligand PPFA and its palladium dichloride complex PPFA–$PdCl_2$.

*Keywords:* Iron; Aminophosphines; Palladium complex; Ferrocenes; Crystal structure; Catalyst

## 1. Introduction

A variety of ferrocene derivatives has already been successfully identified as ligands for enantioselective homogeneous catalysts [1,2]. Most of these ligands are derived from (1-*N*,*N*-dimethylaminoethyl)ferrocene (**1**) as the starting material, which is easy to resolve into its enantiomers and can conveniently be transformed into a number of 1,2-disubstituted bidentate ligands via ortho-lithiation and subsequent reaction with electrophiles [3]. Thus the synthesis of the widely used PPFA ligand 2-(1-*N*,*N*-dimethylaminoethyl)-1-diphenylphosphino-ferrocene (**2**) was easily achieved by reaction of **1** with butyllithium and subsequent treatment of the reaction mixture with chlorodiphenylphosphine [3,4]. Further modification of the dimethylamino group led to a diversity of bidentate or potentially multidentate ferrocene ligands. Although a respectable number of highly enantioselective reactions have been reported with ferrocenyl modified transition metal catalysts [1,5], ligand development appears to be limited by the small number of easily accessible enantiomerically pure starting compounds. Therefore we set out to search for enantiopure amino ferrocenes other than **1** and to test their potential as starting material for new bidentate and multidentate ligands of homogeneous enantioselective catalysts. Recently, we reported on aminoalcohols and aminophosphines based on α-*N*,*N*-dimethylamino [1,2] tetramethyleneferrocene (**3**) and on their use in cross coupling and alkylation reactions [6–8].

In the present communication we describe synthesis and structural features of the heteroannularly bridged amine **4**, aminophosphine **5** and its palladium dichloride complex **5**–$PdCl_2$, which was found to be a potential Grignard cross-coupling catalyst precursor similar to the widely used PPFA–$PdCl_2$ complex (**2**–$PdCl_2$). Furthermore, structural features of **4**, **5** and **5**–$PdCl_2$ are compared with those of **1**, **2** and **2**–$PdCl_2$ both in the solid state and in solution.

* Corresponding author.

0022-328X/96/$15.00 © 1996 Elsevier Science S.A. All rights reserved
*SSDI* 0022-328X(95)05850-8

Fig. 1. Crystal structure of the (*R*, *R*) tartrate of (−)-($S_c$)-**4** (**4**-*T*). Hydrogen atoms have been omitted for clarity.

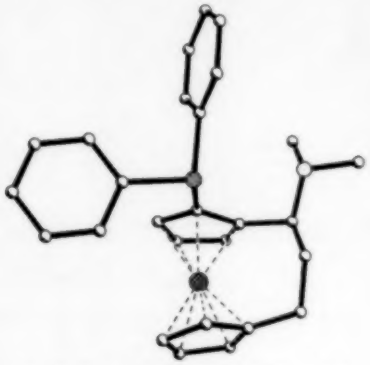

Fig. 2. Crystal structure of (−)-($S_c$, $S_m$)-**5**.

## 2. Results and discussion

Racemic amine **4** is readily accessible from ferrocene aldehyde via a published five-step synthesis [9,10]. Optical resolution of **4** can be achieved by fractional crystallization of its tartrates [11]. A single-crystal X-ray structure analysis of the less soluble salt reveals an (*S*)-configuration for the (−)-enantiomer of **4** (Fig. 1), thus confirming the original assignment based on chemical correlation [12]. Reaction of **4** with 1.2 equivalents of *n*-butyl lithium and subsequent treatment with chlorodiphenylphosphine gave aminophosphine **5**. As for (*S*)-**1** [3], the ortho-lithiation of (*S*)-**4** is highly stereoselective; however, it leads to products with reversed configuration at the ferrocene unit. Reaction of lithiated (*S*)-**1** with chlorodiphenylphosphine results in ($S_c$, $R_m$)-**2** [1] (Scheme 1), while (*S*)-**4** gives aminophosphine ($S_c$, $S_m$)-**5** (Scheme 1) as confirmed by X-ray structure analysis (Figs. 2 and 3). Treatment of **5** with $(CH_3CN)_2$ $PdCl_2$ in benzene gave the palladium dichloride complex **5**–$PdCl_2$ whose molecular structure was also determined by X-ray crystallography (Fig. 4).

### 2.1. X-ray structures of the tartrate of 4 (4-T), aminophosphine 5 and its palladium dichloride complex 5–$PdCl_2$

All diffraction data were collected at a low temperature (85(2) K); structures were solved with direct methods and refined with least squares as described in Section 3. For each structure analysis, the absolute structure was determined from the anomalous data [13] and agreed with the chemical evidence.

#### 2.1.1. 4.

The less soluble (*R*, *R*)-tartrate of **4** (**4**-*T*) crystallizes in the monoclinic space group $P2_1$, with two molecules in the unit cell. The molecular conformation of the ferrocene moiety of **4**-T is shown in Fig. 1; final atomic coordinates are listed in Table 1. Since the configuration of the tartrate monoanion is known to be (*R*, *R*), the assignment of (*S*)-configuration to carbon C(21) of **4**-*T*, and of the related $(-)_{589}$-enantiomer of **4** is straightforward. This is also corroborated by the anomalous dispersion data (see Section 3).

A discussion of general structural features of the ferrocenyl ammonium cation is given below. As expected [7], the tartrate monoanion shows almost identical C–O bond lengths in the carboxylate part (1.249(4) and 1.266(4) Å) whereas these bond distances differ

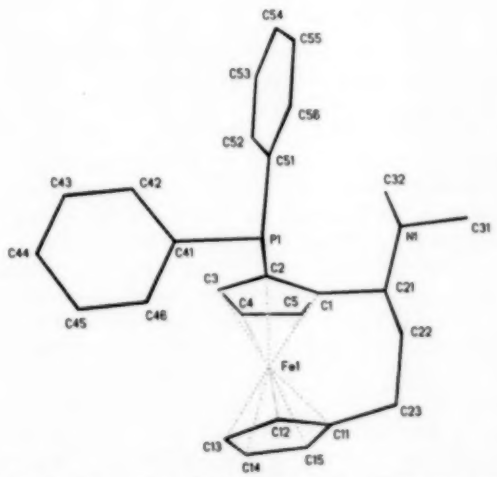


Fig. 3. Crystal structure of (−)-($S_c$, $S_m$)-**5**, showing the atom numbering. An analogous scheme was also employed for the crystal structure of **4**-*T* and **5**–$PdCl_2$.

[1] The subscript c denotes the stereogenic center at C(21) (see Fig. 3 later) while m refers to the metallocene unit.

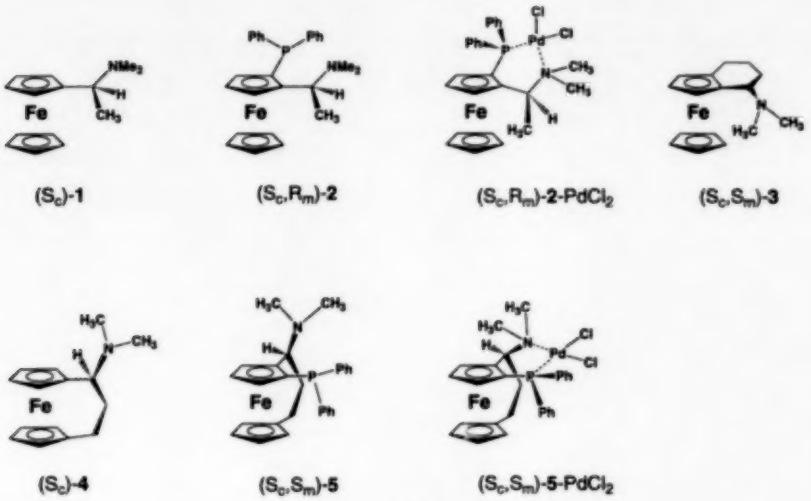


Scheme 1.

significantly in the hydroxycarbonyl group (C–OH, 1.313(4) Å C=O, 1.206(4) Å). The crystal packing is dominated by the formation of two intermolecular H bonds between translationally equivalent tartrate ions (H(O(6)) ··· O(2) $(1+x, y, z)$, 1.65 Å) and between the ammonium hydrogen atom H(N(1)) and one of the

Table 1
Atomic coordinates and equivalent isotropic displacement parameters for the non-hydrogen atoms in the crystal structure of **4**-*T*, where $U_{eq}$ is defined as one third of the trace of the orthogonalized $U_{ij}$ tensor, and the atomic numbering is analogous to that shown in Fig. 3

| | x/a ($\times 10^{-4}$) | y/b ($\times 10^{-4}$) | z/c ($\times 10^{-4}$) | $U_{eq}$ ($\times 10^{-3}$ Å$^2$) |
|---|---|---|---|---|
| Fe(1) | 3448(1) | 5034(1) | 9383(1) | 15(1) |
| C(1) | 4640(3) | 5037(5) | 8030(2) | 16(1) |
| C(2) | 5243(4) | 6242(4) | 8607(3) | 18(1) |
| C(3) | 6035(4) | 5723(4) | 9525(3) | 19(1) |
| C(4) | 5961(4) | 4185(4) | 9504(3) | 19(1) |
| C(5) | 5106(4) | 3733(4) | 8587(3) | 16(1) |
| C(11) | 908(3) | 5015(5) | 8908(2) | 18(1) |
| C(12) | 1239(5) | 6274(4) | 9509(3) | 20(1) |
| C(13) | 1810(5) | 5807(5) | 10501(3) | 24(1) |
| C(14) | 1825(5) | 4265(5) | 10512(3) | 22(1) |
| C(15) | 1259(5) | 3777(4) | 9530(3) | 20(1) |
| C(21) | 3530(3) | 5146(4) | 7084(2) | 16(1) |
| C(22) | 1805(4) | 4281(3) | 7107(2) | 19(1) |
| C(23) | 410(3) | 4989(6) | 7794(2) | 21(1) |
| N(1) | 4597(3) | 4754(3) | 6140(2) | 18(1) |
| C(31) | 6229(4) | 5647(4) | 6069(2) | 23(1) |
| C(32) | 5026(4) | 3177(4) | 6062(2) | 25(1) |
| C(81) | −1932(3) | 10260(3) | 6197(2) | 18(1) |
| O(1) | −2421(3) | 10705(3) | 5342(2) | 22(1) |
| O(2) | −2853(3) | 9579(3) | 6845(2) | 25(1) |
| C(82) | −37(4) | 10612(4) | 6518(2) | 18(1) |
| O(3) | 898(3) | 11302(3) | 5722(2) | 21(1) |
| C(83) | 948(4) | 9234(3) | 6833(2) | 18(1) |
| O(4) | 813(3) | 8146(3) | 6077(2) | 24(1) |
| C(84) | 2854(3) | 9659(3) | 7081(2) | 18(1) |
| O(5) | 3181(3) | 10496(3) | 7762(2) | 27(1) |
| O(6) | 4016(3) | 9045(3) | 6476(2) | 22(1) |

Table 2
Coordinates and displacement parameters for the crystal structure of 5, where the atomic numbering is defined in Fig. 3

| | $x/a\,(\times10^{-4})$ | $y/b\,(\times10^{-4})$ | $z/c\,(\times10^{-4})$ | $U_{eq}\,(\times10^{-3}\,Å^2)$ |
|---|---|---|---|---|
| Fe(11) | 1411(1) | −4773(2) | 2875(1) | 20(1) |
| P(11) | 3272(1) | −5460(4) | 3518(1) | 19(1) |
| N(11) | 3497(4) | −3252(10) | 1904(4) | 26(2) |
| C(11) | 2292(4) | −3360(11) | 2515(4) | 19(2) |
| C(21) | 2465(4) | −4017(12) | 3250(4) | 18(2) |
| C(31) | 1909(4) | −3272(11) | 3719(5) | 19(2) |
| C(41) | 1392(5) | −2192(12) | 3303(5) | 26(2) |
| C(51) | 1645(5) | −2225(11) | 2554(5) | 24(2) |
| C(111) | 1312(4) | −6569(12) | 2042(5) | 26(2) |
| C(121) | 1454(5) | −7506(11) | 2717(5) | 28(2) |
| C(131) | 872(5) | −7098(12) | 3211(6) | 33(2) |
| C(141) | 356(4) | −5941(14) | 2839(5) | 35(2) |
| C(151) | 613(4) | −5601(12) | 2119(5) | 33(2) |
| C(211) | 2709(5) | −3834(12) | 1804(5) | 21(2) |
| C(221) | 2654(5) | −5839(13) | 1583(5) | 25(2) |
| C(231) | 1849(5) | −6493(13) | 1401(5) | 28(2) |
| C(311) | 3952(5) | −3561(15) | 1255(5) | 33(2) |
| C(321) | 3545(5) | −1343(12) | 2103(5) | 26(2) |
| C(411) | 2948(5) | −6293(12) | 4416(4) | 23(2) |
| C(421) | 3036(4) | −5357(13) | 5086(4) | 25(2) |
| C(431) | 2791(5) | −6139(14) | 5741(5) | 33(2) |
| C(441) | 2439(6) | −7812(15) | 5719(5) | 41(3) |
| C(451) | 2346(6) | −8759(14) | 5069(5) | 39(3) |
| C(461) | 2589(5) | −7982(11) | 4420(5) | 26(2) |
| C(511) | 3946(4) | −3718(12) | 3828(5) | 24(2) |
| C(521) | 4707(4) | −4209(14) | 3870(4) | 26(2) |
| C(531) | 5266(5) | −2999(14) | 4114(5) | 35(2) |
| C(541) | 5067(5) | −1253(14) | 4305(5) | 35(2) |
| C(551) | 4313(4) | −747(13) | 4275(5) | 29(2) |
| C(561) | 3760(5) | −1967(12) | 4038(5) | 27(2) |
| Fe(12) | 8809(1) | −115(0) | 872(1) | 16(1) |
| P(12) | 7062(1) | −865(4) | 1701(1) | 18(1) |
| N(12) | 7895(4) | 2328(11) | 2824(4) | 23(2) |
| C(12) | 8340(4) | 1602(11) | 1581(4) | 15(2) |
| C(22) | 7752(4) | 561(10) | 1228(4) | 14(2) |
| C(32) | 7797(4) | 900(12) | 451(4) | 18(2) |
| C(42) | 8404(4) | 2121(12) | 319(5) | 20(2) |
| C(52) | 8717(4) | 2603(11) | 1033(5) | 16(2) |
| C(112) | 9533(4) | −1344(12) | 1586(4) | 20(2) |
| C(122) | 9018(5) | −2656(11) | 1270(5) | 22(2) |
| C(132) | 9109(5) | −2624(12) | 479(5) | 22(2) |
| C(142) | 9672(4) | −1356(12) | 308(5) | 23(2) |
| C(152) | 9944(4) | −564(13) | 981(4) | 27(2) |
| C(212) | 8562(4) | 1672(13) | 2405(4) | 20(2) |
| C(222) | 8841(4) | −155(14) | 2700(4) | 28(2) |
| C(232) | 9597(5) | −796(14) | 2380(4) | 28(2) |
| C(312) | 8091(6) | 2648(15) | 3611(5) | 33(3) |
| C(322) | 7648(5) | 4096(12) | 2539(5) | 25(2) |
| C(412) | 6614(4) | −2019(12) | 902(4) | 19(2) |
| C(422) | 5901(4) | −1598(11) | 603(5) | 20(2) |
| C(432) | 5603(4) | −2562(13) | 0(4) | 20(2) |
| C(442) | 5999(4) | −3965(12) | −308(4) | 22(2) |
| C(452) | 6721(4) | −4402(12) | −21(5) | 26(2) |
| C(462) | 7017(4) | −3468(12) | 578(5) | 22(2) |
| C(512) | 6331(4) | 809(11) | 1895(4) | 17(2) |
| C(522) | 6220(4) | 2371(11) | 1478(5) | 20(2) |
| C(532) | 5628(4) | 3565(12) | 1634(5) | 24(2) |
| C(542) | 5144(5) | 3188(12) | 2208(4) | 24(2) |
| C(552) | 5252(5) | 1623(13) | 2622(5) | 26(2) |
| C(562) | 5833(4) | 434(11) | 2469(4) | 20(2) |
| C(1X) | 9732(11) | 3356(34) | 4959(7) | 107(6) |
| C(2X) | 10300(11) | 4949(43) | 5174(8) | 138(6) |
| C(3X) | 9659(16) | 6603(36) | 4623(12) | 183(9) |

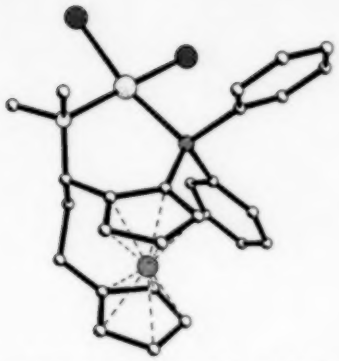

Fig. 4. Crystal structure of (+)-($S_c$, $S_m$)-**5**–$PdCl_2$.

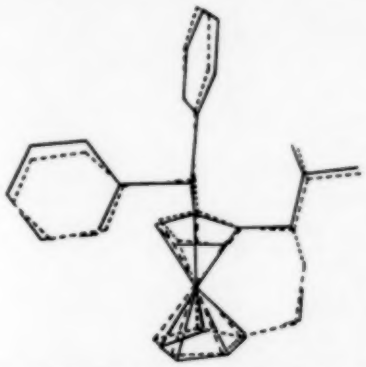

Fig. 5. Superposition of the two symmetry-independent molecules of the crystal structure of **5**.

tartrate carboxylate oxygen atoms (H(N(1)) ··· O(1) $(-x, -1/2+y, 1-z)$, 1.97 Å).

*2.1.2. 5.*

For the X-ray structure determination a crystal of the $(-)_{589}$-enantiomer was used. Crystals belong to the monoclinic space group $P2_1$, with four molecules in the unit cell, i.e. two non-equivalent molecules in the asymmetric unit. These two independent molecules have a very similar conformation as shown in their superposition in Fig. 5. The molecular conformations of one of the two molecules of **5** is shown in Fig. 2. Atomic

Table 3
Coordinates and displacement parameters for the crystal structure of **5**–$PdCl_2$, where the atomic numbering is analogous to that shown in Fig. 3

| | x/a (×10⁻⁴) | y/b (×10⁻⁴) | z/c (×10⁻⁴) | $U_{eq}$ (×10⁻³ Å²) |
|---|---|---|---|---|
| Pd(1) | 9839(1) | 7277(0) | 971(1) | 16(1) |
| Cl(1) | 11980(2) | 7187(1) | 3557(2) | 30(1) |
| Cl(2) | 9610(2) | 5936(1) | 973(2) | 21(1) |
| Fe(1) | 6625(1) | 8770(1) | −4034(1) | 17(1) |
| P(1) | 7550(1) | 7180(1) | −1295(1) | 14(1) |
| N(1) | 10072(5) | 8530(3) | 914(5) | 16(1) |
| C(1) | 7708(6) | 8832(3) | −1630(6) | 17(1) |
| C(2) | 6755(6) | 8130(2) | −2080(6) | 16(1) |
| C(3) | 5060(6) | 8341(3) | −3014(7) | 20(1) |
| C(4) | 4978(7) | 9179(3) | −3101(7) | 21(1) |
| C(5) | 6595(6) | 9482(3) | −2237(6) | 18(1) |
| C(11) | 8642(6) | 8899(3) | −4567(6) | 21(1) |
| C(12) | 7830(7) | 8176(3) | −5221(6) | 21(1) |
| C(13) | 6194(7) | 8342(3) | −6297(7) | 23(1) |
| C(14) | 5963(7) | 9177(3) | −6343(7) | 24(1) |
| C(15) | 7486(7) | 9519(3) | −5279(7) | 23(1) |
| C(21) | 9540(6) | 8888(3) | −750(6) | 17(1) |
| C(22) | 10532(6) | 8537(3) | −1694(6) | 20(1) |
| C(23) | 10312(6) | 8990(3) | −3243(6) | 22(1) |
| C(31) | 9031(7) | 8857(3) | 1745(6) | 23(1) |
| C(32) | 11788(7) | 8804(4) | 1887(7) | 26(1) |
| C(41) | 7661(6) | 6619(3) | −2959(5) | 16(1) |
| C(42) | 6218(6) | 6503(3) | −4335(6) | 21(1) |
| C(43) | 6307(8) | 6186(3) | −5718(7) | 26(1) |
| C(44) | 7826(9) | 5975(4) | −5752(8) | 30(1) |
| C(45) | 9254(8) | 6078(4) | −4383(8) | 28(1) |
| C(46) | 9173(6) | 6395(3) | −2980(6) | 21(1) |
| C(51) | 5886(6) | 6757(3) | −845(6) | 17(1) |
| C(52) | 5040(6) | 7228(4) | −153(6) | 21(1) |
| C(53) | 3778(7) | 6909(3) | 224(7) | 23(1) |
| C(54) | 3347(6) | 6132(3) | −97(6) | 20(1) |
| C(55) | 4191(7) | 5653(3) | −768(7) | 25(1) |
| C(56) | 5461(7) | 5972(3) | −1135(7) | 22(1) |

Table 4
Selected conformational parameters of **1**-*T*, **2**, **2**–$PdCl_2$, **4**-*T*, **5** and **5**–$PdCl_2$

| Parameter (units) | Value for following compounds | | | | | |
|---|---|---|---|---|---|---|
| | **1**–*T* [a] | **2** | **2**–$PdCl_2$ | **4**–*T* | **5** [a] | **5**–$PdCl_2$ |
| Tilt angle [b] $Cp^1$–$Cp^2$ (°) | 1.8<br>4.0 | 2.0 | 3.9 | 9.7 | 10.45<br>10.63 | 9.86 |
| Distance of atom from Cp plane (Å) | | | | | | |
| $Cp^1$–C(21) | 0.079<br>0.012 | −0.026 | 0.115 | 0.176 | 0.066<br>0.086 | 0.099 |
| $Cp^2$–C(23) | — | — | — | 0.102 | 0.147<br>0.111 | 0.163 |
| $Cp^1$–N(1) | −1.461<br>−1.533 | −1.314 | −1.037 | −1.127 | −1.103<br>−1.106 | −1.104 |
| $Cp^1$–P(1) | — | 0.064 | −0.284 | — | −0.055<br>−0.069 | −0.283 |
| $Cp^1$–Pd(1) | — | — | −1.383 | — | — | −1.207 |
| $Cp^1$–Cl(1) | — | — | −2.910 | — | — | −2.475 |
| $Cp^1$–Cl(2) | — | — | −1.599 | — | — | −1.255 |
| Distance P(1)–N(1) (Å) | — | 3.361 | 3.233 | — | 3.362<br>3.401 | 3.275 |

[a] Two molecules per asymmetric unit.
[b] $Cp^1$, $Cp^2$, least-squares planes defined by carbon atoms C(1)–C(5) ($Cp^1$) and C(11)–C(15) ($Cp^2$).

coordinates are given in Table 2. According to a force field study (see below), both conformations are calculated to represent minimum-energy conformations.

### 2.1.3. 5–$PdCl_2$.

Reaction of the $(-)_{589}$-enantiomer of **5** with $(CH_3CN)_2PdCl_2$ in benzene gave $(+)_{589}$-**5**–$PdCl_2$. A suitable crystal was used for X-ray structure analysis. Crystals belong to the monoclinic space group $P2_1$ with two molecules in the unit cell. Fig. 4 shows the molecular conformation of **5**-$PdCl_2$. Table 3 lists final atomic parameters.

As mentioned above, lithiation of (−)-(*S*)-**4**, and subsequent treatment with chlorodiphenylphosphine leads to ($S_c$, $S_m$)-**5** (Fig. 2) while the same reaction applied to (S)-**1** gives ($S_c$, $R_m$)-**2**. Although the relative configuration of **2** differs from that of **5**, it is certainly of interest to compare the molecular structures of **4**-*T*, **5** and **5**–$PdCl_2$ with those of the very popular and widely used compounds **1**-*T* [14], **2** [15] and **2**–$PdCl_2$ [16].

The general structural features of **4**-*T*, **5** and **5**–$PdCl_2$ are very similar. The cyclopentadienyl (Cp) rings are essentially planar but are forced by the three-carbon bridge into a tilted arrangement with a tilt angle of about 10° (Table 4). Steric strain induced by the bridging carbon atoms not only results into tilting of the Cp rings but also leads to significant out-of-plane deformations of the benzylic carbon atoms C(21) and C(23) towards the proximal Cp side (towards the iron-coordinated side of the Cp ring). Bond lengths and bond angles in the ferrocene unit are quite normal; the average Fe–Cp bond lengths are 2.03(2), 2.03(4) and 2.03(2) Å for **4**-T, **5** and **5**–$PdCl_2$; the average $C_{ar}$–$C_{ar}$ bond lengths are 1.43(1), 1.42(1) and 1.43(1) Å respectively.

While in **1**-T, **2** and **2**–$PdCl_2$ the distance of the amino nitrogen from the best plane of the $Cp^1$ ring (defined by carbon atoms C(1) to C(5)) is adjustable via rotation of the dimethylamino group and varies between 1.533 and 1.037 Å, it is fixed in the bridged compounds at about 1.13 Å (Table 4). Aminophosphines **2** and **5** show many similarities. In both cases the phosphorus atom is only slightly out of plane of the $Cp^1$ ring with the phosphorus lone pair pointing towards the proximal side (Fig. 2); the N–P distance is 3.361 Å in **2** and

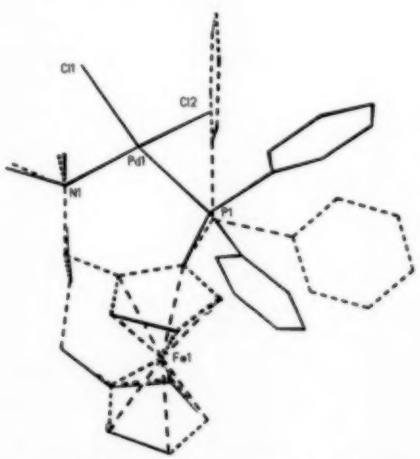


Fig. 6. Superposition of the asymmetric units of the crystal structures of 5 (----) and **5**–$PdCl_2$ (———).

3.362 and 3.401 Å in **5**. As for **2**, complexation of **5** to **5**–$PdCl_2$ results in pronounced structural changes as shown in the superposition of the crystal structures of **5**–$PdCl_2$ and **5** (Fig. 6). In order to allow for complexation, the diphenylphosphino group has to be rotated so that the lone pair points towards the distal Cp side, which puts one phenyl ring into close proximity to the $Cp^2$ proton H(12), at a distance of 2.59 Å in **2**–$PdCl_2$ and 2.47 Å in **5**. This structural change can also be seen by NMR spectroscopy (see below). In both complexes, the phosphorus atom is forced out of the Cp plane towards the distal side, by 0.284 Å in **2**–$PdCl_2$ and 0.283 Å in **5**–$PdCl_2$, resulting in shorter P–N distances compared with the free ligands (Table 4). Evidently, the non-coplanarity of phosphorus and Cp also relieves some of the strain caused by the proximity between phenyl ring and H(12).

In both structures (**2**–$PdCl_2$ and **5**–$PdCl_2$), the square planar arrangement of the palladium substituents is rather distorted, the Cl–Pd–Cl plane being tilted against the N–Pd–P plane by 9.9° in **2**–$PdCl_2$ and 7.8° in **5**–$PdCl_2$. The N–Pd–P bond angles are opened up to 96.1° and 96.4° respectively. According to previous reports [17] this might enhance the reactivity of such complexes in catalytic reactions.

The close conformational similarity between the crystal structures of **2**–$PdCl_2$ and **5**–$PdCl_2$ is evident from the superposition shown in Fig. 7.

### 2.2. Minimum-energy conformations of 4 and 5

To check the conformational possibilities of **4** and **5** an empirical force field study was carried out using the MMX force field implemented in the program PCMODEL [18]. In each case, minimum-energy conformations very similar to those found in the solid state could be located. A close comparison of calculated and experimental data shows that the force field program is well suited to model this type of ferrocene except that out-of-plane deformations are underestimated. While in the crystal C(21) and C(23) are pushed towards the proximal $Cp^1$ side, these atoms are calculated to essentially lie in the Cp planes. As a consequence the Cp rings are calculated to be much more tilted (**5A**, 24.4°; **5B**, 24.6°) than actually found in the solid state (10.5° and 10.6°; see Table 4).

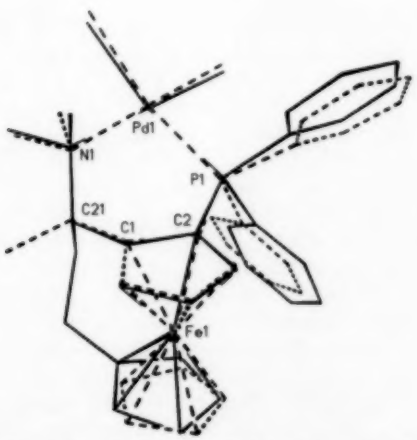


Fig. 7. Superposition (labelled atoms) of the asymmetric units of the crystal structures of **5**–$PdCl_2$ (———) and **2**–$PdCl_2$ (– – –).

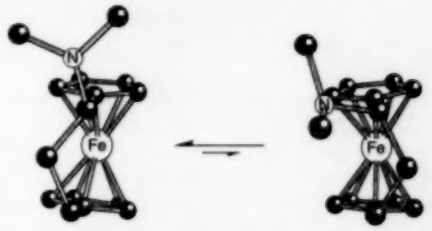


Fig. 8. Calculated molecular structures of **4** with an out-of-plane (left) and an in-plane (right) dimethylamino group.

When viewed along the bond N(1)–C(21) the dimethylamino group in **4**-*T* can be seen to be in a staggered conformation with bond C(21)–C(1) bisecting the angle C(31)–N(1)–C(32). In **5A** and **5B**, staggered conformations are also found for the dimethylamino group but now the bond H(21)–C(21) bisecting angle C(31)–N(1)–C(32). These side-chain features are again reproduced very well by the force field used. Hence, it was of interest to search for additional conformers which might also contribute to an equilibrium in solution.

As shown in Fig. 8, a flip of the carbon bridge will cause the out-of-plane dimethylamino group to adopt an in-plane position. Calculations show that these minimum energy conformations are of higher energy than the out-of-plane arrangements, the differences being 7.9 kJ $mol^{-1}$ for **4**, and 24.3 and 22.2 kJ $mol^{-1}$ for **5A** and **5B** respectively.

### 2.3. Conformation of 4, 5 and 5–$PdCl_2$ in solution

Straightforward analysis of the vicinal $^1H$–$^1H$ coupling constants shows conclusively that all compounds **4**, **5** and **5**-$PdCl_2$ are present in solution preferably in an out-of-plane conformation. The vicinal coupling constants measured for H(21) (10.3 and 2.8 Hz for **4**, 11.3 and 2.8 Hz for **5**, and 11 and 2 Hz for **5**–$PdCl_2$) are indicative for one *trans* and one *gauche* interaction, possible only in an out-of-plane arrangement of the dimethylamino group. In addition the complex **5**–$PdCl_2$ shows a very strong upfield shift of about 2 ppm for one $Cp^2$ proton (H(12)) compared with the remaining Cp protons caused by a close interaction with one phenyl ring of the diphenylphosphine unit (Fig. 4). According

to the force field calculations, such an arrangement cannot be expected for a complex with an in-plane dimethylamino group.

The NMR results together with the empirical force field calculations clearly indicate that **5**–$PdCl_2$ adopts in solution a preferred conformation with the dimethylamino group in an out-of-plane arrangement. Furthermore, comparison of the molecular conformations of **5** and **5**–$PdCl_2$ with PPFA and its palladium dichloride complex shows many structural similarities most pronounced in the $PdCl_2$ complexes. It is anticipated that, like PPFA, aminophosphine **5** should be a useful ligand in homogeneous catalysis.

## 3. Experimental part

$^1H$, $^{13}C$ and $^{31}P$ NMR (proton-decoupled) spectra were run in $CDCl_3$ on a Bruker AM-400 spectrometer at 400, 100 and 162 MHz respectively. $^{13}C$ NMR spectra were run in a *J*-modulated mode. Listed *J* values refer to phosphorus–carbon coupling constants. Chemical shifts $\delta$, are given relative to tetramethylsilane as internal standard ($^1H$ and $^{13}C$ NMR) and relative to 85% $H_3PO_4$ ($^{31}P$ NMR). Mass spectroscopy (MS) was carried out on a Varian MAT-CH7. Optical rotations were measured with a Perkin–Elmer polarimeter 241 in $CH_2Cl_2$ at 20°C ($d$ = 1dm). CD spectra were recorded on a dichrograph CD6 (Jobin–Yvon) in $CH_2Cl_2$. Melting points were determined on a Kofler melting-point apparatus and are uncorrected. Elemental analyses were carried out at Mikroanalytisches Laboratorium der Universität Wien (J. Theiner).

### *3.1. 1,1'-[1-(Dimethylamino)-1,3-propanediyl]-ferrocene (4)*

This was prepared according to modified literature procedures [9,10]. Optical resolution was performed via fractional crystallization of the diastereomeric tartrates [11].

### *3.2. 1-Diphenylphosphino-2,1'-[1-(N,N-dimethylamino)-1,3-propanediyl]-ferrocene I(−)($S_c$, $S_m$)-5*

In a 100 ml Schlenk tube, 720 mg (2.68 mmol) of **4** ($[\alpha]_D^{20} = -31°$, (c = 1; MeOH)) was dissolved under argon in 15 ml of absolute diethyl ether. To the degassed solution was added dropwise 2.0 ml (3.2 mmol) of *n*-butyllithium (1.6 M in hexane). After stirring for 4 h at room temperature an orange precipitate was formed. To this suspension, 0.58 ml (3.2 mmol) of chlorodiphenylphosphine was added dropwise at 0°C and the mixture was stirred for an additional 16 h at room temperature. The yellow reaction mixture was quenched at 0°C with 15 ml of saturated aqueous $NaHCO_3$ solution. The organic layer was separated and the aqueous layer was extracted with diethyl ether (4 × 15 ml). The combined organic layers were washed with 20 ml of water and dried with $MgSO_4$; the solvent was removed under reduced pressure to give 1.2 g of a yellow precipitate. The crude product was chromatographed on silica gel (40–63 $\mu$m; column, 3 × 50 cm) using a mixture of 0.4% triethylamine–20% methanol–79.6% chloroform as eluent, yielding 766 mg (1.69 mmol, 63%) of **5** ($R_f$ = 0.57). In addition, 265 mg (0.984 mmol) of the amine **4** ($R_f$ = 0.17) was recovered. Aminophosphine **5** (melting point (m.p.), 125–135°C) was used without further purification. An analytical sample of **5** (m.p., 138–140°C) was obtained by MPLC (silica gel; 25–40 $\mu$m; 40 × 4.3 cm) with MeOH : chloroform (5 : 95) as eluent.

$^1H$ NMR: $\delta$ 1.83 (6H, s), 1.90 (1H, m), 2.40 (1H, m), 2.46 (H21), dd, $J$ = 2.8, 11.3 Hz,), 2.62 (1H, ddd, $J$ = 2.5, 4.7, 14.7 Hz), 3.00 (1H, m), 3.71 (2H, m), 3.86 (1H, m), 4.08 (1H, m), 4.16 (1H, m), 4.19 (1H, m), 4.39 (1H, m), 7.29 (8H, m), 7.46 (2H, m) ppm. $^{13}C$ NMR: $\delta$ 25.60 (C(23)), 38.38 (C(22), d, $J$ = 10 Hz), 44.31 (C(31), C(32)), 66.70 (C(21)), 67.58 (Cp), 69.14 (Cp), 70.21 (Cp), 71.42 (Cp), 71.55 (Cp, d, $J$ = 5.3 Hz), 74.05 (Cp, d, $J$ = 5.2 Hz), 74.36 (Cp, d, $J$ = 4.6 Hz), 75.60 (Cp, d, $J$ = 20.1 Hz), 88.68 (Cp), 91.50 (Cp, d, $J$ = 18.4 Hz), 127.53 (2Ph, d, $J$ = 7.5 Hz), 127.71 (2Ph, d, $J$ = 6.6 Hz), 127.70 (Ph), 128.08 (Ph), 133.51 (2Ph, d, $J$ = 20.3 Hz), 134.19 (2Ph, d, $J$ = 19.3 Hz), 138.89 (Ph, d, $J$ = 11.8 Hz), 139.47 (Ph, d, $J$ = 8.6 Hz) ppm $^{31}P$ NMR: $\delta$ − 21.04 (s) ppm. MS: $m/e$ (relative%) 453 (100, $M^+$), 438 (38), 408 (70), 332 (32), 253 (27), 225 (33), 224 (96), 183 (27), 176 (18), 165 (24), 121 (19), 78 (12). $[\alpha]_\lambda^{20}$ (c = 1.024) −207.8 (589), −209.1 (578), −194.3 (546) °(nm). CD ($c = 2.3 \times 10^{-3}$–$2.3 \times 10^{-4}$ $moll^{-1}$): $\lambda$ ($\Delta\varepsilon$): 251 (−11.2), 276 sh (−8.36), 325 (−0.84), 418 (+1.31) nm.

### *3.3. 1-Diphenylphosphino-2,1'-[1-(N,N-dimethylamino)-1,3-propanediyl]-ferroceno-$PdCl_2$ [(+)-($S_c$, $S_m$)-5-$PdCl_2$]*

A 100 ml Schlenk tube was charged under argon with 269 mg (1.04 mmol) of $(CH_3CN)_2PdCl_2$ and 15 ml of dry benzene. A degassed solution of **5** (495 mg, 1.09 mmol) in 10 ml of dry benzene was added through a Teflon tube. After stirring for 12 h at room temperature a red–orange precipitate was formed. The supernatant solution was removed via a syringe and the remaining precipitate was washed twice with 10 ml of dry ether. The crude complex was dissolved in 15 ml of dry dichloromethane and to this solution was added carefully 10 ml of dry ethanol avoiding mixing of the two layers. After standing for 90 h in a slow stream of argon 479 mg (0.76 mmol, 76%) (m.p., 280°C (decomposition)), deep-red needles of **5**–$PdCl_2$ were formed.

$^1$H NMR: δ 1.85 (1H, m), 2.18 (1H, m), 2.44 (1H, m), 2.54 (H21, dd, $J$ = 2.0, 11.0 Hz), 2.65 (1H, m), 2.81 (3H, s), 2.90 (1H, m), 3.33 (3H, s), 3.68 (1H, m), 3.82 (1H, m), 4.07 (1H, m), 4.26 (1H, m), 4.37 (1H, m), 4.46 (1H, m), 7.31 (5H, m), 7.57 (3H, m), 8.27 (2H, m) ppm. $^{13}$C NMR: δ 24.48 (C(23)), 42.80 (C(22), d, $J$ = 4 Hz), 52.38 (N–$CH_3$), 56.81 (N–$CH_3$), 68.22 (Cp, d, $J$ = 45.6 Hz), 68.82 (C(21)), 70.54 (Cp, d, $J$ = 6.5 Hz), 71.68 (Cp), 72.00 (Cp, d, $J$ = 8.3 Hz), 72.10 (Cp, d, $J$ = 3.5 Hz), 72.13 (Cp), 72.93 (Cp), 75.15 (Cp), 88.25 (Cp), 88.40 (Cp, d, $J$ = 18.6 Hz), 127.85 (2Ph, d, $J$ = 11.7 Hz), 128.08 (2Ph, d, $J$ = 11.7 Hz), 130.49 (Ph, d, $J$ = 3.2 Hz), 131.63 (Ph, d, $J$ = 66.3 Hz), 133.67 (Ph, d, $J$ = 2.5 Hz), 133.15 (2Ph, d, $J$ = 9.6 Hz), 133.86 (Ph, d, $J$ = 65.3 Hz), 136.29 (2Ph, d, $J$ = 11.3 Hz) ppm. $^{31}$P NMR: δ 10.51 (s), ppm. $[\alpha]_\lambda^{20}$ ($c$ = 1.0034) +304.0 (589), +373.7 (578), +756.4 (546) °(nm). CD: λ(Δε) 244 (−17.8), 257 (+7.29), 276 (−6.77), 311 (+9.05), 344 (−3.47), 388 (−2.58), 452 (+8.04) nm.

### 3.4. Crystal structure analysis of 4-T

Crystals of yellow color were grown from methanol. A specimen of size 0.4 × 0.3 × 0.3 mm was used for diffraction experiments, which were performed at 85(2) K on a modified STOE diffractometer using Mo Kα radiation (λ = 0.710 73 Å). Unit-cell parameters were obtained by least-squares refinement against the setting angles of 70 reflections (3° ⩽ θ ⩽ 9°). Crystals are monoclinic, of space group $P2_1$, with two molecules ($C_{19}H_{25}FeNO_6$; formula weight, 419.3) per unit cell: $a$ = 7.559(2) Å, $b$ = 9.216(2) Å and $c$ = 13.119(3) Å; β = 90.16(3)°; $V$ = 913.9(4) Å; $d_c$ = 1.524 g cm$^{-3}$ (calculated from the cell constants observed at 85(2) K; $F$(000) = 440.

Intensity data (ω scan; Δω = 1.5°) were collected for two octants of reciprocal space (−10 ⩽ $h$ ⩽ 10; −1 ⩽ $k$ ⩽ 12; −1 ⩽ $l$ ⩽ 18; 3° ⩽ θ ⩽ 30°), yielding 2623 symmetry independent reflections, of which 2374 are significant ($I > 2\sigma(I)$). Lorentz–polarization correction and empirical adsorption correction (program DIFABS [19]) were applied to the data μ(Mo Kα) = 0.862 mm$^{-1}$; ratio of minimum to maximum transmission, 0.796.

The structure was solved with direct methods and refined with least squares, using a full-matrix least squares program (SHELXL93 [19]) which minimizes the quantity $\Sigma\omega(F_o^2 - F_c^2)^2$ with $\omega = 1/[\sigma^2(F_o^2) + (aP)^2 + bP]$, $P = (\max(F_o^2, 0) + 2F_c^2)/3$, $a$ = 0.038, $b$ = 0.56, using all reflections. Anisotropic atomic displacement parameters (ADP's) were refined for all non-hydrogen atoms; H atoms were included at calculated positions ("riding"); an isotropic ADP was refined for each H atom.

Refinement of 244 parameters against 2623 intensity data and 98 restraints converged at the following values for the reliability indices: $\omega R_2 = [\Sigma[\omega(F_o^2 - F_c^2)^2]/\Sigma[\omega(F_o^2)^2]]^{1/2}$ = 0.0829 (for all 2623 reflections); $R_1 = \Sigma \| F_o | - | F_c \| / \Sigma | F_o |$ = 0.0296 for 2374 significant reflections and 0.0362 for all 2623 data: goodness of fit $S = [\Sigma\omega(F_o^2 - F_c^2)^2/(n-p)]^{1/2}$ = 0.956 number $n$ of observations, 2623; number $P$ of parameters, 244). Features up to 0.336 electrons Å$^{-3}$ and down to −0.368 were observed in a final difference electron density map. The absolute structure parameters [13] converged to 0.00(2) (a value of 0 indicating the correct and a value of 1 the opposite enantiomer). Atomic coordinates and equivalent isotropic displacement parameters are given in Table 1.

### 3.5. Crystal structure analysis of 5

Conditions and procedures analogous to the structure determination of **4-T**, except where noted explicitly: orange crystals were grown from $CH_2Cl_2$–hexane; crystal size, 0.5 × 0.4 × 0.3 mm; temperature, 84(2) K. Unit-cell parameters from 47 reflections with 4° ⩽ θ ⩽ 7°. Crystals are monoclinic, of space group $P2_1$, with four molecules ($C_{27}H_{28}FeNP$; formula weight, 453.35) per unit cell: $a$ = 17.578(4) Å, $b$ = 7.3220(10) Å and $c$ = 18.040(4) Å; β = 91.42(3)°; $V$ = 2321.1(8) Å$^3$; $d_{calc}$ = 1.359 g cm$^{-3}$ (calculated from the 84(2) K cell constants, with four molecules **5** plus one molecule hexane per unit cell); $d_{obs}$ = 1.34 g cm$^{-3}$ (determined at room temperature by flotation in aqueous CsCl); $F$(000) = 1002.

Intensity data (Δω = 1.5°) were collected for two octants (−1 ⩽ $h$ ⩽ 22; −1 ⩽ $k$ ⩽ 9; −23 ⩽ $l$ ⩽ 23; 3° ⩽ θ ⩽ 27.5°), 6161 symmetry independent reflections and 3221 significant reflections. DIFABS [19] absorption correction with μ(Mo Kα) = 0.735 mm$^{-1}$ (ratio of minimum to maximum transmission, 0.623). Refinement (621 parameters; 6161 observations; 457 restraints) converged at $\omega R_2$ = 0.1423 (all 6161 reflections); $R_1$ = 0.0678 (3221 significant reflections); $R_1$ = 0.1404 (all 6161 data); $S$ = 0.934 ($n$ = 6161; $p$ = 621). Maximum and minimum residual electron densities 0.644 and −0.555 electrons Å$^{-3}$. Absolute-structure parameter [13], 0.03(3). Atomic coordinates are given in Table 2.

### 3.6. Crystal structure analysis of 5PdCl$_2$

Conditions and procedures analogous to the structure determination of **4-T**, except where noted explicitly: red crystals were grown from $CH_2Cl_2$–ethanol; crystal size, 0.3 × 0.2 × 0.2 mm; temperature, 85(2) K. Unit-cell parameters from 44 reflections with 3° ⩽ θ ⩽ 7°. Crystals are monoclinic, of space group $P2_1$, with two molecules ($C_{27}H_{28}Cl_2FeNPPd$; formula weight, 630.6) per unit cell: $a$ = 8.768(2) Å, $b$ = 17.065(3) Å and

$c = 8.978(2)$ Å; $\beta = 112.81(3)°$; $V = 1238.3(5)$ Å$^3$; $d_{calc} = 1.691$ g cm$^{-3}$ (at 85(2) K); $F(000) = 636$.

Intensity data ($\Delta\omega = 1.2°$) were collected for two octants ($-1 \leqslant h \leqslant 14$; $-1 \leqslant k \leqslant 27$; $-14 \leqslant l \leqslant 14$; $3° \leqslant \theta \leqslant 35°$), 5821 symmetry independent reflections and 4661 significant reflections. DIFABS [19] absorption correction with $\mu$(Mo K$\alpha$) = 1.609 mm$^{-1}$ (ratio of minimum to maximum transmission, 0.521). Refinement (297 parameters; 5821 observations; 129 restraints) converged at $\omega R_2 = 0.1293$ (all 5821 reflections); $R_1 = 0.0376$ (4661 significant reflections); $R_1 = 0.0548$ (all 5821 data); $S = 0.649$ ($n = 5821$; $p = 297$). Maximum and minimum residual electron densities, 1.091 and $-1328$ electron Å$^{-3}$. Absolute-structure parameter [13], $-0.04(3)$. Atomic coordinates are given in Table 3.

## Acknowledgment

This work was kindly supported by the Fonds zur Förderung der Wissenschaftlichen Forschung (P8414 and P9859).

## References and note

[1] A. Togni and T. Hayashi, (eds.), *Ferrocenes*, VCH, Weinheim, 1995.

[2] H. Brunner and W. Zettlmeier, *Handbook of Enantioselective Catalysis with Transition Metal Compounds*, VCH, Weinheim, 1993.

[3] D. Marquarding, H. Klusacek, G. Gokel, P. Hoffmann and I. Ugi, *J. Am. Chem. Soc., 92* (1970) 5389.

[4] T. Hayashi, T. Mise, M. Fukushima, M. Kagotani, N. Nagashima, Y. Hamada, A. Matsumoto, S. Kawakami, M. Konishi, K. Yamamoto and M. Kumada, *Bull. Chem. Soc. Jpn., 53* (1980) 1138.

[5] M. Sawamura and Y. Ito, *Chem. Rev. 92* (1992) 857.

[6] B. Jedlicka, Ch. Kratky, W. Weissensteiner and M. Widhalm, *J. Chem. Soc., Chem. Commun.*, (1993) 1329.

[7] H. Wally, Ch. Kratky, W. Weissensteiner, M. Widhalm and K. Schlögl, *J. Organomet. Chem., 450* (1993) 185.

[8] H. Wally, K. Schlögl, W. Weissensteiner and M. Widhalm, *Tetrahedron Asymm., 4* (1993) 285.

[9] M. Rosenblum, A.K. Banerjee, N. Danieli, R.W. Fish and V. Schlatter, *J. Am. Chem. Soc., 85* (1963) 316.

[10] P. Dixneuf and R. Dabard, *Bull. Soc. Chim. Fr., 7* (1972) 2847.

[11] G. Tainturier, K. Chhor y Sok and B. Gautheron, *C.R. Acad. Sci., Sér. C. 277* (1973) 1269.

[12] C.Y.S. Khay, G. Tainturier and B. Gautheron, *Tetrahedron Lett., 25* (1974) 2207.

[13] H.D. Flack, *Acta Crystallogr., Sect. A, 39* (1983) 876.

[14] Y.G. Luo, R.J. Barton and B.E. Robertson, *Can. J. Chem., 65* (1987) 2756.

[15] F.W.B. Einstein and A.C. Willis, *Acta Crystallogr., Sect. B, 36* (1980) 39.

[16] F.H. van der Steen and J.A. Kanters, *Acta Crystallogr., Sect. C, 42* (1986) 547.

[17] T. Hayashi, M. Konishi, Y. Kobori, M. Kumada, T. Higuchi and K. Hirotsu *J. Am. Chem. Soc., 106* (1984) 158.

[18] PCMODEL Serena Software, Bloomington, IN, 1992.

[19] The following computer programs were used for the crystallographic work: SHELXTL PC, *Version 4.1*, Siemens Analytical Instruments, Inc., Madizon, WI, 1990; G.M. Sheldrick, *SHELXL-93, a Program for Refinement of Crystal Structures from Diffraction Data*, University of Göttingen, 1993; DIFABS, N. Walker and D. Stuart, *Acta Crystallogr., Sect. A, 39* (1983) 158.

ELSEVIER

Journal of Organometallic Chemistry 508 (1996) 219–225

Journal of Organometallic Chemistry

# Optically active transition-metal complexes. III. Synthesis of optically active ($\eta^4$-aminodiolefin)tricarbonyl iron complexes. Kinetic resolution of a chiral amine by means of an optically active dienyl iron cation ☆

M. Käser, A. Salzer *

*Institut für Anorganische Chemie der RWTH Aachen, Prof.-Pirlet-Str. 1, D-52056 Aachen, Germany*

Received 20 June 1995

**Abstract**

The synthesis of optically active $\eta^4$-(aminodiolefin)tricarbonyl iron complexes by the nucleophilic addition of primary and secondary amines to the optically active tricarbonyl-(*1R*)-($\eta^5$-methyl-nopadienyl)iron(1 + ) cation (**4**) is described. Under either kinetic or thermodynamic control, the reaction leads to (*E,Z*)- or (*E,E*)-diolefin complexes with generation of a new chiral carbon centre. Racemic (*R/S*)-phenylethylamine was kinetically resolved (*de* = 38%) by treatment with **4** at −78°C.

*Keywords:* Optically active ligands; Iron; Carbonyl complexes; Kinetic resolution.

## 1. Introduction

There has been considerable recent interest in the synthesis and reactivity of $\eta^5$-tricarbonyl(pentadienyl)-iron(1 + ) complexes. Their utility as intermediates and reactands in organic synthesis with respect to highly diastereoselective addition reactions of various nucleophiles to $\eta^5$-tricarbonyl(dienyl)iron( + 1) cations is well documented [1]. The U-shaped cationic complex **II**, synthesized from the corresponding alcohol complex **I** (LG = H), reacts with a wide range of nucleophiles such as alcohols, amines, carbon nucleophiles, hydrides, phosphites and phosphines in a stereoselective but not always regioselective manner, giving rise to four possible regiochemical isomers **IV–VII**. The ratios of the kinetically controlled (*E,Z*)- and thermodynamically controlled (*E,E*)-complexes depend on the electronic and steric effects of $R^1$, $R^2$ and $R^3$ as well as the type of nucleophile employed [1e,1k,2]. Recently, several groups have reported on a regio- and stereospecific nucleophilic substitution via S-shaped cationic complexes such as **IIIb** to give (*E,E*)-complexes of the form **VI**. However, this route is limited to specific leaving groups LG, as well as carbon nucleophiles and phosphorus nucleophiles such as phosphites [3] (Scheme 1).

In all cases, however, the nucleophile invariably attacks trans to the tricarbonyl iron moiety [1–3]. We have recently prepared the optically active tricarbonyl-(*1R*)-($\eta^5$-methylnopadienyl)iron(1 + ) cation **4**, derived from the optically active natural product (*1R*)(-)-myrtenal via the ketone **1** [4] (Scheme 2).

The cation offers various advantages over the previously discussed pentadienyl complexes:

(a) Owing to the optical activity originating from the organic precursor and the planar chirality introduced by coordination of the $Fe(CO)_3$ moiety, nucleophilic reactions will generate a new chiral centre, whose enantiomeric purity is easily checked by NMR spectroscopy,

(b) Because of the ring structure, a nucleophile will only attack at C12 of the dienyl system, limiting the number of possible products to one pair of (*E,Z*)- and (*E,E*)-diastereomers. By careful kinetic or thermodynamic control of the reaction conditions, it should be possible to generate one single product with a well-defined new centre of chirality.

We have therefore investigated the reaction of complex **4** with a variety of amines and phosphines in order to synthesize optically active organometallic amines and

☆ For Part II, see Ref. [8].

* Corresponding author.

0022-328X/96/$15.00 © 1996 Elsevier Science S.A. All rights reserved
*SSDI* 0022-328X(95)05851-6

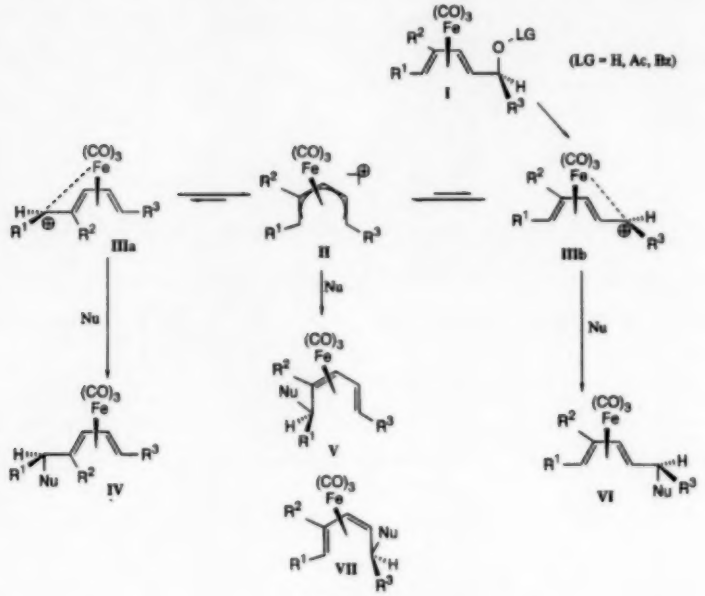

Scheme 1.

phosphines, which might themselves be useful as ligands in homogeneous catalysis or might be suitable as derivatizing agents in racemic resolutions.

## 2. Results and discussion

### 2.1. Reactions between 4 and primary and secondary amines

The (aminodiene)tricarbonyl iron complexes were prepared as outlined in Scheme 3. They were obtained in good to excellent yields (Table 1). We used two general methods:

(a) Addition of two equivalents of the primary or secondary amine to **4** at −78°C, and

(b) Addition of one equivalent of the amine at room temperature and deprotonation of the primarily formed ammonium salt with a non-nucleophilic base such as $NEt_3$.

Absolute configurations of the products were assigned in analogy to previous work by Maglio et al. [1o] as well as our own X-ray structure analysis of an addition product with a secondary phosphine [5]. (*E,Z*)- and (*E,E*)-diolefin complexes are easily distinguished by their typical chemical-shift values in $^1H$ and $^{13}C$ NMR. Typical values in the $^1H$ NMR for H11 in (*E,Z*)- and (*E,E*)-diolefin complexes are at 1.9–2.5 ppm and 0.6–1.1 ppm respectively [1o]. Table 1 shows that method (a) in most cases led to the kinetically controlled (*E,Z*)-diolefin complexes **A** only, while method

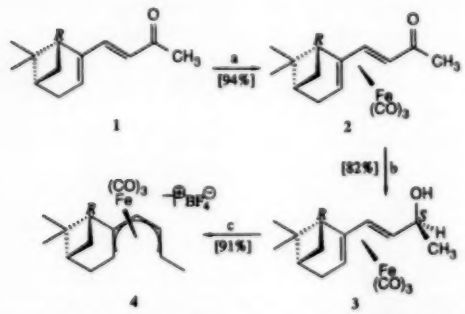

Scheme 2. (a) $Fe_2(CO)_9$ (1.5 eq), benzene 18 h, 80°C; (b) $NaBH_4$ (2.3 eq), MeOH, 1.5 h, 0°C; (c) $HBF_4$, propionic anhydride, 0.5 h, 0°C.

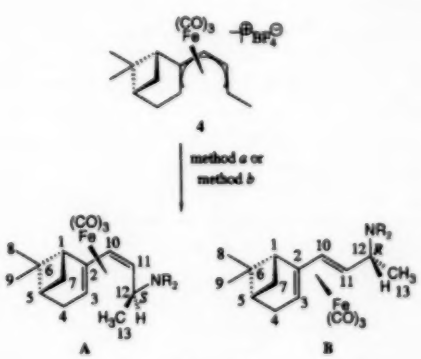

Scheme 3.

Table 1
The reaction between the optically active cation complex **4** and primary or secondary amines

| Amine | Product (method) | A [a] | B [a] | (%) | T (°C) | t (h) | eq |
|---|---|---|---|---|---|---|---|
| Dimethylamine | **5** (a) | 100 | – | 88 | −78 | 4 | 2.2 |
| Dimethylamine | **5** (b) | 90 | 10 | 80 | r.t. | 72 | 1.1 |
| Diethylamine | **6** (a) | 100 | – | 97 | −78 | 1.5 | 2.2 |
| Diethylamine | **6** (b) | – | 100 | 65 | r.t. | 84 | 1.1 |
| Piperidine | **7** (a) | 100 | – | 91 | −78 | 4 | 2.2 |
| Piperidine | **7** (b) | 89 | 11 | 79 | r.t. | 72 | 1.1 |
| Cyclohexylamine | **8** (b) | 12 | 88 | 51 | r.t. | 72 | 1.1 |
| Isopropylamine | **9** (b) | 11 | 89 | 46 | r.t. | 72 | 1.1 |
| Aniline | **10** (a) | – | 100 | 85 | −78 | 4 | 2.2 |
| *o*-Toluidine | **11** (a) | – | 100 | 70 | −78 | 13 | 2.2 |
| Benzylamine | **12** (b) | – | 100 | 88 | r.t. | 84 | 1.1 |

[a] The ratios **A**/**B** are determined by the integration of the $^1$H NMR spectra.

(b) predominantly gave the thermodynamically more stable (*E*,*E*)-complexes **B** (Scheme 3 and Table 1).

Further conclusions can be drawn from Table 1. The ratio **A**/**B** increases with the basicity of the respective amine on the addition of two equivalents of amine. This is probably due to the fact that the second amine rapidly deprotonates the primarily formed ammonium salt. This is the case for strongly basic amines such as dimethylamine, diethylamine and piperidine (Scheme 4).

The addition of the first amine is therefore irreversible ($k_2 \gg k_{-1}$, and $k_{-2}$ negligible) in these cases. For dimethylamine and piperidine, it was not possible under any conditions to generate exclusively the (*E*,*E*)-diolefin complex **B**. With the bulkier diethylamine, however, the reaction via method (b) gave full conversion to the (*E*,*E*)-diolefin **B**. This means that the U-shaped cation **II** and the S-shaped cation **IIIb** can still achieve equilibrium, so that the thermodynamically more stable (*E*,*E*)-diolefin product can be formed eventually. A reaction time of several days may be necessary in some cases to establish this equilibrium fully, with the exclusive formation of product **B**.

While the reactions in some cases led to almost quantitative yields, the yields decreased with longer reaction times and at ambient temperatures. This is due

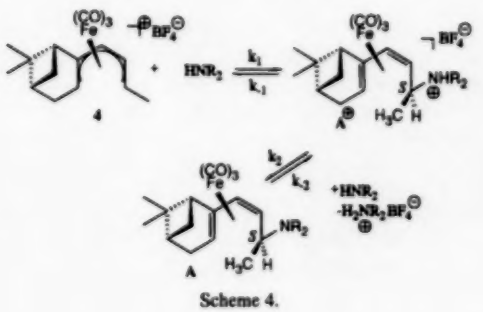

Scheme 4.

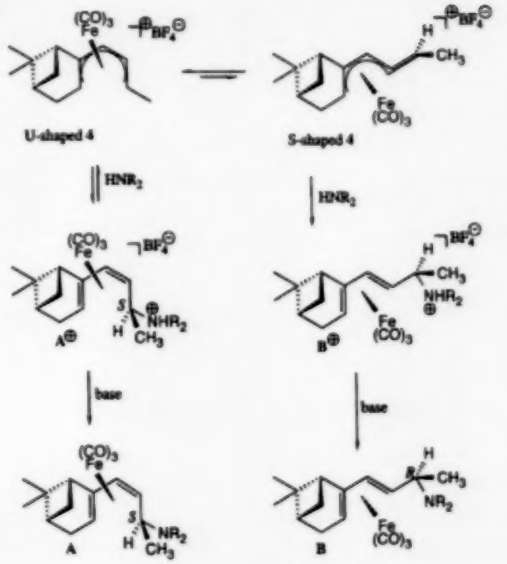

Scheme 5.

to some decomposition of the cationic precursors as well as competing elimination reactions of **4** with formation of a mixture of triolefin complexes (10–20% isolated yields). Based on the observed results, the detailed kinetic studies of nucleophilic addition reactions by Kane-Maguire and co-workers [6], and $^1$H NMR studies on the equilibria between U- and S-shaped dienyl cations by Sorensen and Jablonski [7], we propose the following reaction mechanism for the nucleophilic addition of primary and secondary amines to the optically active tricarbonyl($\eta^5$-methylnopadienyl)iron cation **4** (Scheme 5):

### 2.2. Kinetic resolution of (R,S)-phenylethylamine by reaction with 4

Reaction of **4** with either (*R*)- or (*S*)-phenylethylamine by method (c) (addition of **4** to one or two equivalents of amine at −78°C) gave rise to similar results to those discussed previously (Table 2).

Table 2
The reaction between the optically active cation complex **4** and phenylethylamine

| Amine | Product (method) | A | B | (%) | (T) (°C) | t (h) | eq |
|---|---|---|---|---|---|---|---|
| (*S*)-Phenylethylamine | **13** (b) | – | 100 | 94 | r.t. | 96 | 1.1 |
| (*S*)-Phenylethylamine | **13** (c) | 100 | – | 53 | −78 | 8 | 1.1 |
| (*R*)-Phenylethylamine | **14** (c) | 100 | – | 54 | −78 | 8 | 1.1 |
| (*R*/*S*)-Phenylethylamine [a] | **13**/**14** (b) | – | 100 | 90 | r.t. | 72 | 1.1 |
| (*R*/*S*)-Phenylethylamine | **13**/**14** (c) | 100 | – | 48 | −78 | 2.5 | 2.2 |

[a] The ratio **13**/**14** is determined by the integration of the $^1$H NMR spectra.

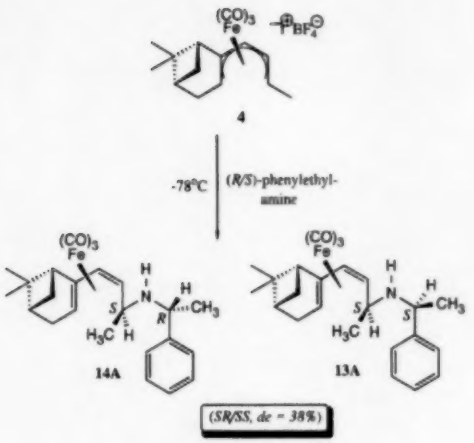


Scheme 6.

Reaction at low temperatures led to the (*E,Z*) product only, while reaction at ambient temperatures gave the rearranged (*E,E*) product. The pure (*E,Z*) product could only be isolated by strictly keeping the reaction mixture at −78°C and deprotonating the intermediate ammonium salt with the non-nucleophilic base $EtN(^iPr)_2$, as the rearranged product **B** begins to form at −50°C. Reaction of optically active **4** with racemic (*R,S*)-phenylethylamine by method (b) led to an equal mixture of the (*E,E*)-complexes **13B** and **14B**, differing only in the chirality of phenylethylamine. No kinetic resolution was therefore observed under these conditions. **13B** and **14B** could not be separated by chromatography. This changed when **4** was added at −78°C to two equivalents of (*R,S*)-phenylethylamine in methylene chloride. After deprotonation with $EtN(^iPr)_2$ at −78°C, the amines **13A** and **14A** were isolated and could be separated by chromatography. The ratio of **13A** to **14A** was determined as 1:2.2 (*de* = 38%). The optically active **4** had therefore preferentially reacted with (*R*)-phenylethylamine. This to our knowledge constitutes the first example of a kinetic resolution of a racemic amine with an optically active dienyl complex (Scheme 6).

The addition of (*R/S*)-phenylethylamine to the optically active **4** (method (a)), however, led to a considerable decrease in the diastereomeric excess (1:1.3; *de* = 13%).

We are currently examining whether optically pure (*R*)-phenylethylamine can be separated from the complex and the starting material **4** recovered, so that it can be used for repeated resolutions. We are also investigating whether other chiral amines can be resolved in a similar manner. Analogous reactions to those described in this paper can also be performed with secondary phosphines. These will be reported in a separate paper [5].

## 3. Experimental details

All experiments were carried out under an atmosphere of nitrogen using solvents purified under nitrogen by standard procedures. The starting optically active cation **4** was prepared as described in the literature [4]. Mass spectra were recorded on a Finnigan MAT 95 instrument. IR spectra were recorded on a Perkin–Elmer 1720 X infrared spectrophotometer and NMR spectra on Varian VXR 300 and Varian Unity 500 instruments. $^{13}C$ NMR spectra were assigned by use of APT and were decoupled. Tetramethylsilane was used as internal standard in the case of $C_6D_6$. In the case of $CDCl_3$, the chemical shifts are referred to the signal of solvent.

### *3.1. Preparation of the amine complexes*

#### *3.1.1. Method (a)*

The amine (2.2 eq) was added in one portion to a solution of the optically active cation **4** in methylene chloride (10–40 ml) at room temperature or −78°C. The reaction mixture was stirred for 1.5–48 h. The solvent was evaporated and the residue was purified by chromatography ($SiO_2$).

#### *3.1.2. Method (b)*

The amine (1.1 eq) was added in one portion to a solution of the optically active cation **4** in methylene chloride (10–30 ml) at room temperature. The reaction mixture was stirred for 84–96 h. The primarily formed ammonium salt was deprotonated with $NEt_3$ (1.1 eq) at room temperature. The solvent was evaporated and the residue was purified by chromatography ($SiO_2$).

#### *3.1.3. Method (c)*

The optically active cation **4** in methylene chloride (20.0 ml) was slowly added to phenylethylamine (1.1 or 2.2 eq) in methylene chloride (30.0 ml) at −78°C within 0.5 h. The reaction mixture was stirred for 2.5–8 h at −78°C. The primarily formed ammonium salt was deprotonated with $EtN(^iPr)_2$ (1.2 eq) at −78°C. The solvent was evaporated and the residue was purified by chromatography ($SiO_2$).

#### *3.2.1. Tricarbonyl[η⁴-4-[(1R)-6,6-dimethyl-bicyclo-[3.1.1]-hept-2-ene-2-yl]-(Z)-(2S)-2-N,N-dimethylamino-but-3-ene]iron (5A)*

Method (a); eluent, hexane/ether (3:1) to ether, yellow oil, yield 0.40 g (88%). $^1H$ NMR (500 MHz, $CDCl_3$): δ (ppm) = 0.93 (s, 3H, H9), 1.16 (d, *J* = 6.7 Hz, 3H, H13), 1.33 (s, 3H, H8), 1.43 (d, *J* = 10.1 Hz, 1H, H7), 1.80 (dd, *J* = 7.9 Hz, *J* = 10.4 Hz, 1H, H11), 2.05 (s, 6H, $2 \times CH_3(NMe_2)$), 1.94–2.08, 2.15–2.22, 2.50–2.60 (3m, 7H, H1, H3, H4, H5, H7, H12), 5.28 (d, *J* = 7.9 Hz, H10). $^{13}C$ NMR (125 MHz, $CDCl_3$): δ

(ppm) = 19.26 (C13), 21.23 (C9), 25.05 (C8), 29.12 (C4), 35.94 (C7), 38.95 (C6), 39.09 ($CH_3(NMe_2)$), 41.22, 46.92, 50.05, 52.80 (C1, C3, C5, C11), 56.60 (C12), 81.45 (C10), 125.03 (C2), 211.29 (CO). IR (hexane): $\nu$(C≡O) = 2038, 1974, 1962 $cm^{-1}$. Anal. Found: C, 60.10; H, 7.01; N, 3.54. $C_{18}H_{25}FeNO_3$ (359.25). Calc.: C, 60.02; H, 7.01; N, 3.89%.

### 3.2.2. *Tricarbonyl[η⁴-4-[(1R)-6,6-dimethyl-bicyclo-[3.1.1]-hept-2-ene-2-yl]-(Z)-(2S)-2-N,N-diethylamino-but-3-ene]iron (6A)*

Method (a); eluent, hexane/ether (1:1), orange oil, yield 0.39 g (97%). $^1$H NMR (500 MHz, $CDCl_3$): δ (ppm) = 0.93 (t, $J$ = 7 Hz, 6H, 2 × C$H_3$(NEt$_2$)), 1.02 (s, 3H, H9), 1.17 (d, $J$ = 5.8 Hz, 3H, H13), 1.41 (s, 3H, H8), 1.49 (d, $J$ = 9.7 Hz, 1H, H7), 1.97 (br t, 1H, H11), 2.01–2.09, 2.21–2.48, 2.56–2.64 (3m, 11H, H1, H3, H4, H5, H7, H12, 2 × C$H_2$(NEt$_2$)), 5.27 (d, $J$ = 7.9 Hz, H10). $^{13}$C NMR (125 MHz, $CDCl_3$): δ (ppm) = 15.01 ($CH_3$(NEt$_2$)), 19.22 (C13), 22.40 (C9), 26.13 (C8), 30.06 (C4), 37.05 (C7), 39.95 (C6), 43.54 ($CH_2$(NEt$_2$)), 42.21, 47.88, 53.79, 54.22, 54.84 (C1, C3, C5, C11, C12), 82.89 (C10), 126.19 (C2), 212.45 (CO). IR (hexane): $\nu$(C≡O) = 2038, 1972, 1961 $cm^{-1}$. Anal. Found: C, 61.66; H, 7.88; N, 3.21. $C_{20}H_{29}FeNO_3$ (387.30). Calc.: C, 62.00; H, 7.54; N, 3.61%.

### 3.2.3. *Tricarbonyl[η⁴-4-[(1R)-6,6-dimethyl-bicyclo-[3.1.1]-hept-2-ene-2-yl]-(E)-(2R)-2-N,N-diethylamino-but-3-ene]iron (6B)*

Method (b); eluent, hexane/ether (10:1) to ether, yellow oil, yield 0.30 g (65%). $^1$H NMR (300 MHz, $CDCl_3$): δ (ppm) = 0.46 (t, $J$ = 8.8 Hz, 1H, H11), 0.94 (s, 3H, H9), 1.02 (t, $J$ = 7.0 Hz, 6H, 2 × $CH_3$(NEt$_2$)), 1.15 (d, $J$ = 6.8 Hz, 3H, H13), 1.40 (s, 3H, H8), 1.42–1.50 (m, 2H, H7, H12), 1.59 (br d, 1H, H3), 1.96–2.08, 2.13–2.25, 2.44–2.65 (3m, 9H, H1, H4, H5, H7, 2 × $CH_2$(NEt$_2$)), 5.29 (d, $J$ = 8.8 Hz, H10). $^{13}$C NMR (75 MHz, $CDCl_3$): δ (ppm) = 14.47 ($CH_3$(NEt$_2$)), 17.61 (C13), 21.97 (C9), 26.07 (C8), 29.76 (C4), 37.05 (C7), 40.18 (C6), 43.73 ($CH_2$(NEt$_2$)), 42.50, 47.45, 53.92, 57.54, 58.23 (C1, C3, C5, C11, C12), 84.70 (C10), 116.49 (C2), 213.15 (CO). IR (hexane): $\nu$(C≡O) = 2037, 1972, 1960 $cm^{-1}$. Anal. Found: C, 60.27; H, 7.53; N, 3.01. $C_{20}H_{29}FeNO_3$ (387.30). Calc.: C, 62.00; H, 7.54; N, 3.61%.

### 3.2.4. *Tricarbonyl[η⁴-4-[(1R)-6,6-dimethyl-bicyclo-[3.1.1]-hept-2-ene-2-yl]-(Z)-(2S)-2-N-azacyclohexyl-but-3-ene]iron (7A)*

Method (a); eluent, hexane/ether (1:1), orange oil (0.89, 91%). $^1$H NMR (500 MHz, $CDCl_3$): δ (ppm) = 1.01 (s, 3H, H9), 1.22 (d, $J$ = 6.4 Hz, 3H, H13), 1.35–1.52 (m, 7H, H7, 3 × C$H_2$($C_5H_{10}$N)), 1.41 (s, 3H, H8), 1.91 (br dd, 1H, H11), 2.00–2.10, 2.11–2.29, 2.40–2.50, 2.55–2.65 (4m, 11H, H1, H3, H4, H5, H7, H12, 2 × C$H_2$($C_5H_{10}$N)), 5.33 (d, $J$ = 7.6 Hz, 1H, H10). $^{13}$C NMR (125 MHz, $CDCl_3$): δ (ppm) = 19.65 (C13), 22.46 (C9), 24.92 ($CH_2$($C_5H_{10}$N)), 26.08 (C8), 26.34 ($CH_2$($C_5H_{10}$N)), 30.14 (C4), 36.95 (C7), 39.98 (C6), 49.33 ($CH_2$($C_5H_{10}$N)), 42.25, 47.92, 52.77, 54.16, 58.81 (C1, C3, C5, C11, C12), 82.75 (C10), 125.85 (C2), 212.43 (CO). IR (hexane): $\nu$(C≡O) = 2038, 1973, 1961 $cm^{-1}$. Anal. Found: C, 62.21; H, 7.35; N, 3.01. $C_{21}H_{29}FeNO_3$ (399.31). Calc.: C, 63.16; H, 7.32; N, 3.50%.

### 3.2.5. *Tricarbonyl[η⁴-4-[(1R)-6,6-dimethyl-bicyclo-[3.1.1]-hept-2-ene-2-yl]-(E)-(2R)-2-N-phenylamino-but-3-ene]iron (10B)*

Method (a); eluent, $CH_2Cl_2$, yellow solid, yield 0.55 g (85%); $^1$H NMR (500 MHz, $CDCl_3$): δ (ppm) = 0.38 (t, $J$ = 8.4 Hz, 1H, H11), 0.91 (s, 3H, H9), 1.34 (d, $J$ = 6.1 Hz, 3H, H13), 1.37 (s, 3H, H8), 1.44 (d, $J$ = 10.4 Hz, 1H, H7), 1.66 (br d, 1H, H3), 1.98–2.06, 2.17–2.25, 2.49–2.62 (3m, 5H, H1, H4, H5, H7), 3.32 (dq, $J$ = 6.4 Hz, $J$ = 7.9 Hz, 1H, H12), 3.52 (s, 1H, N$H$), 5.29 (d, $J$ = 8.2 Hz, H10), 6.60 (d, $J$ = 7.9 Hz, 2H, 2 × C$H$(Ph)), 6.71 (t, $J$ = 7.3 Hz, 1H, C$H$(Ph)), 7.17 (dd, $J$ = 7.3 Hz, $J$ = 8.2 Hz, 2H, 2 × C$H$(Ph)). $^{13}$C NMR (125 MHz, $CDCl_3$): δ (ppm) = 22.11, 22.64 (C9, C13), 26.01 (C8), 29.79 (C4), 37.10 (C7), 40.10 (C6), 42.40, 47.35, 52.60, 54.40 (C1, C3, C5, C11), 58.97 (C12), 83.10 (C10), 113.86, 117.76 ($CH$(Ph)), 118.05 (C2), 129.35 ($CH$(Ph)), 146.95 ($C$(Ph)), 212.73 (CO). IR (hexane): $\nu$(C≡O) = 2040, 1975, 1963 $cm^{-1}$. Anal. Found: C, 64.92; H, 6.26; N, 3.33. $C_{22}H_{25}FeNO_3$ (407.28). Calc.: C, 64.87; H, 5.98; N, 3.43%. EI–MS ($m/z$ (rel. int.)): $M^+$ 407 (1.3), $M^+$-CO 379 (17.9), $M^+$-2CO 351 (0.9), $M^+$-3CO 323 (100), $M^+$-Fe(CO)$_3$ 267 (6.5).

### 3.2.6. *Tricarbonyl[η⁴-4-[(1R)-6,6-dimethyl-bicyclo-[3.1.1]-hept-2-ene-2-yl]-(E)-(2R)-2-N-o-tolylamino-but-3-ene]iron (11B)*

Method (a); eluent, $CH_2Cl_2$, yellow solid, yield 0.25 g (70%). $^1$H NMR (500 MHz, $CDCl_3$): δ (ppm) = 0.46 (t, $J$ = 8.4 Hz, 1H, H11), 0.92 (s, 3H, H9), 1.36 (d, $J$ = 6.6 Hz, 3H, H13), 1.38 (s, 3H, H8), 1.44 (d, $J$ = 10.1 Hz, 1H, H7), 1.67 (br d, 1H, H3), 2.11 (s, 3H, C$H_3$(Ph)), 2.00–2.07, 2.17–2.22, 2.49–2.62 (3m, 5H, H1, H4, H5, H7), 3.39 (m, 2H, H12, N$H$), 5.26 (d, $J$ = 8.2 Hz, H10), 6.64–6.67, 7.04–7.13 (2m, 4H, 4 × C$H$(Ph)). $^{13}$C NMR (125 MHz, $CDCl_3$): δ (ppm) = 17.69 (C13), 22.09, 22.74 (C9, $CH_3$C(Ph)), 26.00 (C8), 29.79 (C4), 37.10 (C7), 40.09 (C6), 42.41, 47.36, 52.52, 54.35 (C1, C3, C5, C11), 59.31 (C12), 83.05 (C10), 111.44, 117.35 ($CH$(Ph)), 117.90 (C2) 122.45 ($CH_3C$(Ph)), 127.14, 130.41 ($CH$(Ph)), 145.00 ($C$(Ph)), 212.70 (CO). IR (hexane): $\nu$(C≡O) = 2040, 1975, 1963 $cm^{-1}$. Anal. Found: C, 65.67; H, 7.19; N, 2.87. $C_{23}H_{27}FeNO_3$ (421.30). Calc.: C, 65.56; H, 6.49; N, 3.32%.

*3.2.7. Tricarbonyl[$\eta^4$-4-[(1R)-6,6-dimethyl-bicyclo-[3.1.1]-hept-2-ene-2-yl]-(E)-(2R)-2-N-benzylamino-but-3-ene]iron (**12B**)*

Method (b); eluent, hexane/ether (10:1) to ether, orange oil, yield 1.00 g (88%). $^1$H NMR (300 MHz, $C_6D_6$): δ (ppm) = 0.13 (t, $J$ = 8.7 Hz, 1H, H11), 0.73 (s, 3H, H9), 1.18 (s, 3H, H8), 1.23 (d, $J$ = 6.4 Hz, 4H, H13, this d obscures the signal of H7), 1.48 (d, $J$ = 10 Hz, 1H, H7), 1.74 (sept, 1H, H3), 1.80–1.88 (m, 2H, H4), 2.21 (br t, 1H, H1), 2.29–2.48 (m, 2H, H5, H12), 3.52 (d, $J$ = 12.8 Hz, 1H, C$H$HPh), 3.66, $J$ = 13.1 Hz, 1H, CH$H$Ph), 4.90 (dd, $J$ = 8.2 Hz, $J$ = 1 Hz, 1H, H10), 7.06–7.32 (m, 5H, 5 × C$H$(Ph)). $^{13}$C NMR (75 MHz, $C_6D_6$): δ (ppm) = 21.90 (C9), 23.94 (C13), 25.99 (C8), 29.76 (C4), 37.34 (C7), 40.05 (C6), 42.68, 47.51, 51.71, 54.46, 57.04, 60.98 (C1, C3, C5, C11, C12, C14), 84.14 (C10), 116.94 (C2), 127.13, 128.37, 128.56 (*C*H(Ph)), 141.29 (*C*(Ph)), 213.51 (CO). IR (hexane): ν(C≡O) = 2039, 1974, 1961 cm$^{-1}$. Anal. Found: C, 66.28; H, 6.87; N, 3.03. $C_{23}H_{27}FeNO_3$ (421.32). Calc.: C, 65.57; H, 6.46; N, 3.32. EI–MS (*m/z* (rel. int.)): $M^+$ 421 (0.07), $M^+$-CO 393 (1.2), $M^+$-2CO 365 (1.2), $M^+$-3CO 337.0 (100), $M^+$-Fe(CO)$_3$ 281.0 (2.4).

*3.2.8. Tricarbonyl[$\eta^4$-4-[(1R)-6,6-dimethyl-bicyclo-[3.1.1]-hept-2-ene-2-yl]-(E)-(2R)-2-N-(1S)-(1-phenyl-ethylamino)-but-3-ene]iron (**13B**)*

Method (b); eluent, hexane/ether (10:1) to ether, orange oil, yield 0.49 g (94%). $^1$H NMR (300 MHz, $C_6D_6$): δ (ppm) = 0.12 (t, $J$ = 9.5 Hz, 1H, H11), 0.72 (s, 3H, H9), 1.12–1.26 (m, 10H, H7, H8, H13, CH(C$H_3$)Ph), 1.44 (d, $J$ = 10 Hz, H7), 1.74 (sept, $J$ = 3 Hz, H3), 1.80–1.88 (m, 2H, H4), 2.15 (t, $J$ = 6 Hz, 1H, H1), 2.27–2.43 (m, 2H, H5, H12), 3.70 (q, $J$ = 6.5 Hz, 1H, C$H$(CH$_3$)Ph), 4.87 (dd, $J$ = 8.5 Hz, $J$ = 1 Hz, 1H, H10), 7.07 (tt, $J$ = 7 Hz, $J$ = 1 Hz, 1H, C$H$(Ph)), 7.14–7.26 (m, 4H, 4 × C$H$(Ph)). $^{13}$C NMR (75 MHz, $C_6D_6$): δ (ppm) = 21.98 (C9), 23.18 (C13), 24.82 (CH(*C*H$_3$)Ph), 25.99 (C8), 29.76 (C4), 37.41 (C7), 39.99 (C6), 42.62, 47.46, 54.06, 54.57, 55.77, 61.79 (C1, C3, C5, C11, C12, *C*H(CH$_3$)Ph), 84.1 (C10), 117.4 (C2), 126.9, 127.1, 128.6 (*C*H(Ph)), 146.7 (*C*(Ph)), 213.52 (CO). IR (hexane): ν(C≡O) = 2038, 1973, 1960 cm$^{-1}$. Anal. Found: C, 67.25; H, 7.11; N, 3.04. $C_{24}H_{29}FeNO_3$ (435.34). Calc.: C, 66.21; H, 6.71; N, 3.21%. EI–MS (*m/z* (rel. int.)): $M^+$ 435 (0.01), $M^+$-CO 407 (0.7), $M^+$-2CO 379 (0.6), $M^+$-3CO 351 (100), $M^+$-Fe(CO)$_3$ 295 (6.5).

*3.2.9. Tricarbonyl[$\eta^4$-4-[(1R)-6,6-dimethyl-bicyclo-[3.1.1]-hept-2-en-2-yl]-(Z)-(2S)-2-N-(1S)-(1-phenyleth-ylamino)-but-3-ene]iron (**13A**)*

Method (c); eluent, hexane/ether (10:1 to 3:1), yellow-orange oil, yield 0.47 g (53%). $^1$H NMR (300 MHz, $C_6D_6$): δ (ppm) = 0.66 (s, 3H, H9), 1.10–1.20 (2d, $J$ = 6.7 Hz, the second d is obscured by the s at 1.16, 9H, H8, H13, CH(C$H_3$)Ph), 1.46 (d, $J$ = 10.1 Hz, H7), 1.60–1.88, 1.96–2.10, 2.20–2.42 (3m, H1, H3, H4, H5, H7, H11, H12), 3.63 (q, $J$ = 6.2 Hz, C$H$(CH$_3$)Ph), 4.90 (d, $J$ = 7.7 Hz, H10), 7.00–7.35 (m, 5 × C$H$(Ph)). $^{13}$C NMR (75 MHz, $CDCl_3$): δ (ppm) = 22.21 (C9), 23.72 (C13), 25.07 (CH(*C*H$_3$)Ph), 25.98 (C8), 30.05 (C4), 36.91 (C7), 39.69 (C6), 42.10, 47.77, 50.95, 54.33, 54.83, 58.70 (C1, C3, C5, C11, C12, *C*H(CH$_3$)Ph), 81.08 (C10), 126.30, 126.52 (*C*H(Ph)), 126.74 (C2), 128.22 (*C*H(Ph)), 146.40 (*C*(Ph)), 212.05 (CO). IR (hexane): ν(C≡O) = 2038, 1974, 1962 cm$^{-1}$. Anal. Found: C, 66.86; H, 7.46; N, 3.01. $C_{24}H_{29}FeNO_3$ (435.34). Calc.: C, 66.21; H, 6.71; N, 3.21%. EI–MS (*m/z* (rel. int.)): $M^+$-CO 407 (0.2), $M^+$-2CO 379 (5.2), $M^+$-3CO 351 (80.4), $M^+$-Fe(CO)$_3$ 295 (14.2), $C_8H_{12}N$ 122 (17.2), $C_8H_9$ 105.0 (100).

*3.1.10. Tricarbonyl[$\eta^4$-4-[(1R)-6,6-dimethyl-bicyclo-[3.1.1]-hept-2-en-2-yl]-(Z)-(2S)-2-N-(1R)-(1-phenyleth-ylamino)-but-3-ene]iron (**14A**)*

Method (c); eluent, hexane/ether (10:1 to 3:1), yellow-orange oil, yield 0.39 g (54%). $^1$H NMR (300 MHz, $CDCl_3$): δ (ppm) = 1.02 (s, 3H, H9), 1.16 (d, $J$ = 5.4 Hz, 3H, H13), 1.24 (d, $J$ = 6.7 Hz, 3H, CH(C$H_3$)Ph), 1.42 (s, H8, obscures particularly the d of H7), 1.80–2.20, 2.35–2.45, 2.52–2.66 (3m, H1, H3, H4, H5, H7, H12), 3.74 (q, $J$ = 6.5 Hz, C$H$(CH$_3$)Ph), 5.14 (d, $J$ = 6.7 Hz, H10), 7.12–7.32 (m, 5H, 5 × C$H$(Ph)). $^{13}$C NMR (75 MHz, $CDCl_3$): δ (ppm) = 22.15, 22.42 (C9, C13), 23.99 (CH(*C*H$_3$)Ph)), 25.96 (C8), 29.94 (C4), 36.99 (C7), 39.55 (C6), 42.05, 47.81, 49.44, 54.38, 54.55, 58.67 (C1, C3, C5, C11, C12, *C*H(CH$_3$)Ph), 81.18 (C10), 126.30 (*C*H(Ph)), 126.78 (C2), 126.86, 128.34 (*C*H(Ph)), 145.06 (*C*(Ph)), 211.90 (CO). IR (hexane): ν(C≡O) = 2038, 1974, 1962 cm$^{-1}$. Anal. Found: C, 66.82; H, 7.69; N, 3.20. $C_{24}H_{29}FeNO_3$ (435.34). Calc.: C, 66.21; H, 6.71; N, 3.21%. EI–MS (*m/z* (rel. int.)): $M^+$-CO 407 (0.3), $M^+$-2CO 379 (6.8), $M^+$-3CO 351 (52.8), $M^+$-Fe(CO)$_3$ 295 (11.4), $C_8H_{12}N$ 122 (13.8), $C_8H_9$ 105.0 (100).

*3.3. Kinetic resolution of (R/S)-phenylethylamine by reaction with 4 at −78°C*

(R/S)-Phenylethylamine (0.50 g, 4.13 mmol, 0.53 ml, 2.2 eq) was dissolved in methylene chloride (50.0 ml) and the solution was cooled to −78°C. A solution of the optically active cation **4** (0.76 g, 1.88 mmol) in methylene chloride (20.0 ml) was added dropwise to the reaction mixture (0.5 h). After stirring for 2.5 h at −78°C, EtN($^i$Pr)$_2$ (0.29 g, 2.26 mmol, 1.2 eq) was added and the reaction mixture slowly warmed to room temperature. The solvent was evaporated in vacuo and the residue was purified by chromatography ($SiO_2$; eluent, hexane/ether (10:1) to ether). Two fractions, (*E,Z*)-**13A** (0.12 g, 15%) and (*E,Z*)-**14A** (0.27 g, 33%),

were obtained as orange oils. The $^{13}C$ NMR spectra are in accordance with those of (*E,Z*)-**13A** and (*E,Z*)-**14A**.

## Acknowledgements

We thank the Deutsche Forschungsgemeinschaft (SFB 380) and the Fonds der Chemischen Industrie for financial support, as well as BASF for a gift of pentacarbonyl iron.

## References

[1] (a) C. Quirosa-Guillou and J.-P. Lellouche, *J. Org. Chem., 59* (1994) 4693; (b) H.-J. Knölker, A.-A. El-Ahl and G. Weingärtner, *Synlett* (1994) 194; (c) W.A. Donaldson, L. Shang and R.D. Rogers, *Organometallics, 13* (1994) 6; (d) L. Tao and W.A. Donaldson, *J. Org. Chem., 58* (1993), 2134; (e) W.A. Donaldson, M.-J. Jin and P.T. Bell, *Organometallics, 12* (1993) 1174; (f) M.-C.P. Yeh, B.A. Sheu, H.W. Fu, S.-I. Tau and L.-W. Chuang, *J. Am. Chem. Soc., 115* (1993) 5941; (g) W.A. Donaldson and M.-J. Jin, *Tetrahedron, 49* (1993) 8787; (h) A.J. Pearson, S. Balasubramanian and K. Srinivasan, *Tetrahedron, 49* (1993) 5663; (i) H.-J. Knölker, M. Bauermeister, J.-B. Pannek, D. Bläser and R. Boese, *Tetrahedron, 49* (1993) 841; (j) A. Teniou, L. Toupet and R. Grée, *Synlett* (1991) 195; (k) W.A. Donaldson, *J. Organomet. Chem., 395* (1990) 187; (l) R. Grée, *Synthesis* (1989) 341 and references cited therein; (m) A. Salzer, in H. Werner and G. Erker (eds.), *Organometallics in Organic Syntheses, Vol. 2*, Springer, Berlin, 1989, p. 291; (n) A.J. Pearson, *Acc. Chem. Res., 13* (1980) 463; (o) G. Maglio, A. Musco, R. Palumbo and A. Sirigu, *J. Chem. Soc., Chem. Commun.* (1971) 100; (p) G. Maglio, A. Musco and R. Palumbo, *J. Organomet. Chem., 32* (1971) 127.

[2] (a) W.A. Donaldson, P.T. Bell and M.-J. Jin, *J. Organomet. Chem., 441* (1992) 449; (b) W.A. Donaldson and M. Ramaswamy, *Tetrahedron Lett., 30* (1989) 1339,1343 and references cited therein; (c) A. Hafner, W. v. Philipsborn and A. Salzer, *Helv. Chim. Acta, 69* (1986) 1757; (d) A.J. Pearson, T.R. Perrior and D.C. Rees, *J. Organomet. Chem., 226* (1982) C39; (e) R.S. Bayoud, E.R. Biehl and P.C. Reeves, *J. Organomet. Chem., 174* (1979) 297; (f) R.S. Bayoud, E.R. Biehl and P.C. Reeves, *J. Organomet. Chem., 150* (1978) 75.

[3] (a) W.R. Roush and C.K. Wada, *Tetrahedron Lett., 35* (1994) 7347; (b) W.R. Roush and C.K. Wada, *J. Am. Chem. Soc., 116* (1994) 2151; (c) E. Heßler, H.G. Schmalz and G. Dürner, *Tetrahedron Lett., 35* (1994) 4547; (d) P. Pinsard, J.-P. Lellouche, J.-P. Beaucourt, L. Toupet, L. Schio and R. Grée, *J. Organomet. Chem., 371* (1989) 219; (e) M. Uemura, T. Minami, Y. Yamashita, K.I. Hiyoshi and Y. Hayashi, *Tetrahedron Lett., 28* (1987) 641.

[4] A. Salzer, H. Schmalle, R. Stauber and S. Streiff, *J. Organomet. Chem., 408* (1991) 403.

[5] U. Englert, B. Hofmann, M. Käser, E. Klinkhammer, A. Salzer and T. Wagner, *Chem. Eur. J.*, submitted.

[6] (a) L.A.P. Kane-Maguire, R. Kanitz, P. Jones and P.A. Williams, *J. Organomet. Chem., 464* (1994) 203; (b) L.A.P. Kane-Maguire, E.D. Honig and D. Sweigart, *Chem. Rev., 84* (1984) 525; (c) L.A.P. Kane-Maguire, T.I. Odiaka, S. Turgoose and P.A. Williams, *J. Chem. Soc., Dalton Trans.* (1981) 2489.

[7] T.S. Sorensen and C.R. Jablonski, *J. Organomet. Chem., 25* (1970) C62.

[8] W.H. Bosch, U. Englert, B. Pfister, R. Stauber and A. Salzer, *J. Organomet. Chem., 506* (1995) 273.

ELSEVIER

Journal of Organometallic Chemistry 508 (1996) 227–230

Journal of Organometallic Chemistry

# Syntheses of tungsten-substituted oligosilanes

A. Zechmann, E. Hengge

*Institute of Inorganic Chemistry, University of Technology Graz, Stremayrgasse 16, A-8010 Graz, Austria*

Received 22 June 1995

**Abstract**

By way of alkali halide elimination, monotungsten- and ditungsten-substituted oligosilanes can be obtained. The polarity of the solvent used and the leaving groups at silicon have a strong influence on the syntheses. Heterogeneous reactions (apolar solvent) result in monotungsten compounds, whereas homogeneous conditions (mixture of solvents) shorten the reaction time and lead to $\alpha,\omega$-ditungstensilanes. Using this modified alkali halide elimination method, the new permethylated silicon–tungsten compounds Cl–$(SiMe_2)_n$–Wp and Wp–$(SiMe_2)_n$–Wp ($n = 3, 4$; Wp = $W(CO)_3cp$) were isolated. In addition, the synthesis of the first perhydrogenated $\alpha,\omega$-ditungsten oligosilanes Wp–$(SiH_2)_n$–Wp ($n = 2, 3$) is reported. Cyclic silanes with a tungsten substituent and further reactive groups in the molecule are obtained by selective reaction of the triflate group at silicon.

## 1. Introduction

The elimination of alkali halides is a very useful method to obtain transition metal–silicon compounds. Many applications of this reaction, in particular for earlier transition metals with low electron densities at the central atom, have been found [1–3]. Only a small number of compounds containing transition metal–oligosilane bonds are known, mainly with the late transition metals iron and cobalt [4,5]. The first compounds with tungsten substituents on disilanes were prepared by Malisch in 1972 [6] in the reaction of $Na[W(CO)_3cp]$ with permethylated halosilanes in apolar solvents (e.g. cyclohexane). In the reaction of $\alpha,\omega$-dihalosilanes with 2 eq. $[W(CO)_3cp]^-$, monosubstituted tungsten compounds were obtained only for thermodynamic reasons [7]. Recently, we reported the syntheses of perhydrogenated silicon complexes of iron and molybdenum [8], which could be suitable precursors in MOCVD processes [9] to deposit stoichiometric metal silicides. In this work, we attempted to apply these reactions to perhydrogenated silanes bearing tungsten substituents.

## 2. Syntheses

### 2.1. Permethylated species

Silicon–tungsten compounds are rather unstable towards temperature or light. To avoid decomposition of the substances, it is necessary to observe defined conditions such as the polarity of the solvent used. By reaction of $Na[W(CO)_3cp]$ with $\alpha,\omega$-dichlorosilanes ($n = 3, 4$) in methylcyclohexane, $\alpha$-chloro-$\omega$-tungstensilanes (**1**, **2**) were achieved, according to the results of Malisch [6] on disilanes.

$$Cl\text{–}(SiMe_2)_n\text{–}Cl + Na[W(CO)_3cp] \xrightarrow[\text{room temperature/14–20 days}]{\text{methylcyclohexane}} Cl\text{–}(SiMe_2)_n\text{–}W(CO)_3cp$$

**1** ($n = 3$, $cp = C_5H_5$)
**2** ($n = 4$, $cp = MeC_5H_4$)

The reaction is very slow because of the insolubility of the metal salt and the low reactivity of chlorosilanes. The flask was treated with ultrasound repeatedly to accelerate the reaction by better suspension of the undissolved reagents. Subsequent reaction with another eq. $Na[W(CO)_3cp]$ did not result in disubstitution, but led to the formation of the transmetallation product.

Thereby a large amount of Si–O derivatives was isolated. Oxygen in these siloxanes probably originated from the solvent or from decomposed CO ligands. However, there was a large amount of non-isolable polymers containing Si, O and W. A more effective way to obtain disubstitution was to modify the conditions of the reaction. Using the more soluble and therefore more nucleophilic salt $K[W(CO)_3cp']$ ($cp' \equiv MeC_5H_4$) and homogeneous conditions, it was possible to isolate $\alpha,\omega$-ditungsten compounds (**3**, **4**). To obtain a homoge-

0022-328X/96/$15.00 © 1996 Elsevier Science S.A. All rights reserved
*SSDI* 0022-328X(95)05846-X

$$Na[W(CO)_3cp] + Cl\text{–}(SiMe_2)_n\text{–}W(CO)_3cp \longrightarrow cp(CO)_3W\text{–}(SiMe_2)_n\text{–}W(CO)_3cp$$

$n = 3, 4$

$$\longrightarrow [W(CO)_3cp]_2 + \text{–}(Si\text{–}O)_n\text{–} + \text{polymer}$$

neous solution, the anion was dissolved in 1,2-dimethoxyethane (DME) and added to the silane compound dissolved in n-heptane at room temperature.

$[KW(CO)_3cp']$, $cp' \equiv MeC_5H_4$; DME; n-heptane; $Cl\text{–}(SiMe_2)_n\text{–}Cl$, $n = 3, 4$

$Cl\text{–}(SiMe_2)_n\text{–}W(CO)_3cp'$ + $cp'(CO)_3W\text{–}(SiMe_2)_n\text{–}W(CO)_3cp'$

**3** ($n = 3$)
**4** ($n = 4$)

The transformation was finished within 2 days, but the yields decreased because of the formation of byproducts and a small amount of transmetallation product. The monosubstituted byproducts (**1**, **2**) could be removed due to their different solubility in n-pentane.

### 2.2. Perhydrogenated species

So far, no perhydrogenated oligosilane compounds involving tungsten substituents have been prepared. In a similar manner to the synthesis of **3** and **4**, the preparation of the first $\alpha,\omega$-ditungsten-perhydrooligosilanes was undertaken. $\alpha,\omega$-Diphenylsilanes are liquids and stable at room temperature for longer periods. Phenyl groups are split off easily using trifluoromethanesulphonic acid to give bistriflic silanes. The triflate group is very useful for the synthesis of transition metal–silicon compounds, because transmetallation reactions are avoided. The use of freshly prepared $K[W(CO)_3cp']$ was necessary. The preparation of $K[W(CO)_3cp']$ from $[W(CO)_3cp']_2$ was performed as described in Ref. [10].

The hydrogenated complexes (**5**, **6**) were far more stable than the methylated complexes, as indicated by the increased yields. Compounds **5** and **6** could be suitable precursors for the deposition of stoichiometric thin metal silicide layers.

### 2.3. Cyclic systems

Cyclohexasilanes with transition metal substituents (Fe, Co, Mo) have been synthesized previously [11] by reaction of the cyclohexasilane derivatives $Si_6Me_{11}X$ ($X \equiv Cl, Br, I$) with the highly nucleophilic metallates $Na[Co(CO)_3(PPh_3)]$ and $Na[Fe(CO)_2cp]$. To act against the inclination of silicon–metal compounds to decompose, transformations were performed in apolar medium, but the halogen derivatives of cyclohexasilane showed poor reactivity in these solvents. To avoid long reaction times and higher temperatures, it was necessary to use more reactive sila compounds and solvents of lower polarity than pure tetrahydrofuran (THF). Silanes bearing a triflate group were more appropriate. Transmetallations could be avoided and side reactions were almost suppressed (**7**). The selectivity of the reaction of triflicsilanylesters with complex metal anions can be seen in the syntheses of **8** and **9**. Because of the higher reactivity, the triflic group reacted much faster than the halogen function.

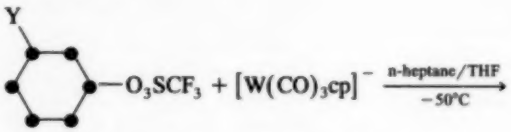


**7a** (Y = Me)
**8a** (Y = Cl)
**9a** (Y = Br)

$cp = MeC_5H_4$
● = $SiMe_{2-n}$ (n = 1,2)

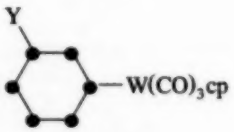


**7** *Y = Me*
**8** *Y = Cl*
**9** *Y = Br*

Despite the high reactivity of the bromo group in molecule **9a**, the main product of the reaction was **9**. Thus the selectivity of the triflate group in the reaction of 1,3-mixed substituted cyclohexasilanes offers a wide field of synthetic variations.

$[W(CO)_3cp']_2 \xrightarrow[THF]{Na/K} 2[W(CO)_3cp']^-$, $cp' \equiv MeC_5H_4$

$Ph\text{–}(SiH_2)_n\text{–}PH \xrightarrow[n\text{-heptane}]{CF_3SO_3H} Tf\text{–}(SiH_2)_n\text{–}TF$, $n = 2, 3$; $Tf \equiv CF_3SO_3$

$\xrightarrow{-50°C}$ $Wp\text{–}(SiH_2)_n\text{–}Wp$

**5** ($n = 2$)
**6** ($n = 3$)
$Wp \equiv W(CO)_3cp'$

## 3. Experimental section

### 3.1. General

All transformations involving air- or moisture-sensitive materials were carried out under dry nitrogen or argon using a modified Schlenk technique. Solvents were dried over Na/K alloy under nitrogen and distilled prior to use. Metallates [12,13] and silicon starting materials [14–17] were prepared according to literature methods. NMR spectra were recorded with a Bruker MSL 300 ($^1$H, 300.13 MHz; $^{13}$C, 75.47 MHz; $^{29}$Si, 59.627 MHz); the compounds were dissolved in $C_6D_6$ or spectra were obtained from the reaction solution with a capillary filled with $D_2O$ ($^{29}$Si spectra only). IR spectra were recorded with a Perkin–Elmer 883 IR spectrometer using an NaCl IR cuvette (0.05 mm). GC/MS analyses were performed on an HP 5890 Series II (capillary column HP-1, 15 m × 0.2 mm × 0.1 μm, MSD/HP 5971 A). Mass spectra were recorded with a Kratos profile spectrometer.

### 3.2. Synthesis of $Cp(CO)_3W$–$(SiMe_2)_n$–Cl (1: $n = 3$, $cp \equiv C_5H_5$; 2: $n = 4$; $cp \equiv MeC_5H_4$)

$Na[W(CO)_3cp$ (**1**, 1.0 g/2.8 mmol; **2**, 1.08 g/2.9 mmol) and $Cl(SiMe_2)_nCl$ (1 mmol) were suspended in 50 ml of dry methylcyclohexane and stirred for 14 ($n = 3$) and 20 ($n = 4$) days at room temperature. Because the product is sensitive to light, the flask was enveloped in aluminium foil. When the IR spectrum showed no further reaction, the salts were filtered off and the solvent was removed. The product was extracted with n-pentane (5 ×) from the brown residue and then recrystallized from n-pentane at −70°C.

1-Chloro-3-($\eta^5$-cyclopentadienyltricarbonyltungsten)hexamethyltrisilane (**1**): yield, less than 30%; $^{29}$Si NMR (ppm/TMS): 27.59, −7.67, −34.53, $^1J_{Si-W}$ = 22.3 Hz; $^1$H NMR (ppm/TMS): 4.61 (5H), 0.71 (6H), 0.50 (6H), 0.33 (6H); IR (cm$^{-1}$/n-pentane): 2026, 1937; $C_{14}H_{23}ClO_3Si_3W$, $M_R$ = 542.89.

1-Chloro-4-($\eta^5$-methylcyclopentadienyltricarbonyltungsten)octamethyltetrasilane (**2**): yield, 0.2 g (32.5%); $^{29}$Si NMR (ppm/TMS): 27.94, −5.26, −32.80, −42.75, $^1J_{Si-W}$ = 21.0 Hz; $^1$H NMR (ppm/TMS): 4.60 (q, 4H), 1.41 (s, 3H), 0.62–0.25 (m, 24H); IR (cm$^{-1}$/n-pentane): 2026, 1936; $C_{17}H_{31}ClO_3Si_4W$, $M_R$ = 615.08.

### 3.3. Synthesis of $cp'(CO)_3W$–$(SiMe_2)_n$–$W(CO)_3cp'$ (3, $n = 3$; 4, $n = 4$; $cp' \equiv MeC_5H_4$)

$Cl(SiMe_2)_nCl$ (1 mmol, $n = 3$, 4) was dissolved in 50 ml of dry n-pentane, and a solution of $K[W(CO)_3cp']$ (1 g/2.5 mmol) dissolved in 30 ml of dry 1,2-dimethoxyethane was added dropwise at room temperature with the exclusion of light. After stirring for 2 days at room temperature, no further reaction was detected by IR. All solids were separated by filtration and the solvent was removed. The brown residue was dissolved in 50 ml of dry n-pentane and filtered again. The solvents and unreacted starting materials were removed at room temperature in vacuo ($10^{-4}$ bar) in about 2 h. n-Pentane (15 ml) was added to the brown residue and the suspension was treated with ultrasound for 10 min to dissolve all the product. The product was crystallized at −70 °C.

1,3-Bis($\eta^5$-methylcyclopentadienyltricarbonyltungsten)hexamethyltrisilane (**3**): yield, 0.12 g (14%); $^{29}$Si NMR (ppm/TMS): −6.94, −39.82; IR (cm$^{-1}$/n-pentane): 2031, 1929; $C_{24}H_{32}O_6Si_3W_2$, $M_R$ = 868.47.

1,4-Bis($\eta^5$-methylcyclopentadienyltricarbonyltungsten)octamethyltetrasilane (**4**): yield, 0.08 g (9%); $^{29}$Si NMR (ppm/TMS): −4.07, −21.47; IR (cm$^{-1}$/n-pentane): 2021, 1931; $C_{26}H_{38}O_6Si_4W_2$, $M_R$ = 926.63; MS (selected, M/I): 897 (M−CO/21.5%), 73 ($SiMe_3$/100%), 263 (Wcp'/63.0%).

### 3.4. Synthesis of $cp'(CO)_3W$–$(SiH_2)_n$–$W(CO)_3cp'$ (5, $n = 2$, $cp' = MeC_5H_4$; 6, $n = 3$, $cp' = C_5H_5$)

$Ph(SiH_2)_nPh$ (1.8 mmol, $n = 2$, 3) was dissolved in 30 ml of dry n-heptane, cooled to −40 °C and treated with 4 mmol/0.6 g $CF_3SO_3H$. After 2 h, no $Ph(SiH_2)_nPh$ could be detected by GC/MS. The solution was decanted into a flask. In a parallel reaction, $[W(CO)_3cp']_2$ (0.62 g/0.9 mmol) was dissolved in dry THF and treated with 0.2 ml of Na/K alloy ($1 : 3/\rho \approx 0.9$) at room temperature. When the carbonyl stretching frequencies of the starting material disappeared from the IR spectrum, excess alloy was filtered off over celites (ROTH) and the solution was transferred into a dropping funnel. The solution was added dropwise to a stirred solution of Tf–$(SiH_2)_n$–Tf (Tf ≡ $CF_3SO_3$) at −60 °C. After the reaction had finished (observation with IR spectroscopy), the solvent was removed and the residue was suspended in dry n-pentane. After filtration from the formed salts, the solution was reduced to 10 ml. The product was crystallized at −70 °C.

1,2-Bis($\eta^5$-methylcyclopentadienyltricarbonyltungsten)disilane (**5**): yield, 0.7 g (55%); $^{29}$Si NMR (ppm/TMS): −65.78, $^1J_{Si-H}$ = 184 Hz, $^1J_{Si-W}$ = 22.3 Hz; $^1$H NMR (ppm/TMS): 4.65 (q, 4H), 4.22 (s, 4H), 0.88 (s, 3H); $^{13}$C NMR (ppm/TMS): 221.02, 215.17 (CO), 89.81, 88.56, 86.84 (Me–**cp**), 32.13 (**Me**–cp); IR (cm$^{-1}$/n-pentane): 2016, 1922; $C_{18}H_{18}O_6Si_2W_2$, $M_R$ = 754.21; MS (selected M/I): 726 (M–CO/8.5%), 722 (M–$SiH_4$/15.0%), 44 (100%), 302 (65.3%).

1,3-Bis($\eta^5$-cyclopentadienyltricarbonyltungsten)trisilane (**6**): yield, 0.25 g (45%); $^{29}$Si NMR (ppm/TMS): −74.06 (tt), −95.29 (pt), $^1J_{Si1-H1}$ = 185.85 Hz, $^1J_{Si2-H2}$ = 177.95 Hz, $^2J_{Si1-H2}$ = 4.2 Hz, $^2J_{Si2-H1}$ = 7.4

Hz, $^1J_{Si-W}$ = 24.1 Hz; $^1$H NMR (ppm/TMS): 4.68 (q, 4H), 4.02 (s, 6H), 3.82 (s, 1H); $^{13}$C NMR (ppm/TMS): 224.7, 219.0 (**CO**), 92.4 (**cp**); IR ($cm^{-1}$/THF–n-heptane): 2020, 2003, 1927; $C_{16}H_{16}O_6Si_3W_2$, $M_R$ = 756.26.

### 3.5. Synthesis of cp'(CO)$_3$W–Si$_6$Me$_{11}$ (7)

Tf–$Si_6Me_{11}$ (Tf ≡ $CF_3SO_3$) (1.0 mmol), freshly prepared from $PhSi_6Me_{11}$, was dissolved in n-heptane and cooled to −50 °C. A solution of K[W(CO)$_3$cp'] (0.5 g/1.3 mmol) in 50 ml 1,2-dimethoxyethane was added dropwise. After the addition, reaction was allowed at room temperature for 2 h. The solvent was removed and dry petrolether was added. After filtration, the solution was reduced to 15 ml. The product was crystallized at −70 °C.

($\eta^5$-Methylcyclopentadienyltricarbonyltungsten)undecamethylcyclohexasilane (**7**): yield, 0.4 g (58%); $^{29}$Si NMR (ppm/TMS): 7.02, −39.23, −42.21, −42.58, $^1J_{Si-W}$ = 34.92 Hz; $^{13}$C NMR (ppm/TMS): 217.67 (**CO**), 109.33 (Me–**C**$_1$), 88.82, 86.92 (Me–**cp**), 14.57 (**Me**–cp), −5.12 to −6.42 (Si–**Me**); IR ($cm^{-1}$/petrolether): 2018, 1989, 1924; $C_{20}H_{40}O_3Si_6W$, $M_R$ = 680.90; MS (selected M/l): 682 ($M^+$/23.4%), 73 ($SiMe_3$/100%), 264 (71.1%).

### 3.6. Synthesis of 1-X-3-(cp'(CO)$_3$W)Si$_6$Me$_{10}$ (8, X ≡ Cl; 9, X ≡ Br)

A solution of 2.88 mmol of freshly prepared $[W(CO)_3cp']^-$ in THF was added to a stirred solution of 1-Cl-3-($CF_3SO_3$)$Si_6Me_{10}$ (2.90 mmol) in n-heptane at −50 °C. To complete the transformation, the solution was stirred for 2 h at 0 °C. After the solvents had been removed at room temperature, 100 ml of dry n-pentane was added. The flask was treated with ultrasound for 15 min and the solids were removed by filtration. The yellow solution was reduced to 20 ml and the product was crystallized at −70 °C.

1-Chloro-3-($\eta^5$-methylcyclopentadienyltricarbonyltungsten)decamethylcyclohexasilane (**8**): yield, 1.1 g (59%); $^{29}$Si NMR (ppm/TMS): 15.37, −28.50, −30.44, −41.31, −41.40, −53.08, $^1J_{Si-W}$ = 23.51 Hz; $^{13}$C NMR (ppm/TMS): 220.06, 215.64, 215.35 (**CO**), 108.27 (Me–**C**$_1$), 91.14, 86.66 (Me–**cp**), 16.06 (**Me**–cp), 1.33 to −6.13 (**Me**); IR ($cm^{-1}$/n-pentane): 2021, 1916, 1895; $C_{19}H_{37}ClO_3Si_6W$, $M_R$ = 701.32.

1-Bromo-3-($\eta^5$-methylcyclopentadienyltricarbonyltungsten)decamethylcyclohexasilane (**9**): yield, 0.4 g (19%); $^{29}$Si NMR (ppm/TMS): 13.07, −27.99, −31.15, −40.37, −40.95, −52.69, $^1J_{Si-W}$ = 24.3 Hz; $^{13}$C NMR (ppm/TMS): 221.22, 216.37, 215.98 (**CO**), 110.20 (Me–**C**$_1$), 92.65, 88.73 (Me–**cp**); 18.30 (**Me**–cp); 2.54 to −5.86 (**Me**); IR ($cm^{-1}$/n-pentane): 2019, 1925, 1896; $C_{19}H_{37}BrO_3Si_6W$, $M_R$ = 745.78.

## Acknowledgements

The authors gratefully thank the Fonds zur Förderung der Wissenschaftlichen Forschung for financial support (project P-9860-CHE) and the Wacker-Chemie GmbH for gifts of several silane derivatives.

## References

[1] W. Malisch and M. Kuhn, *Chem. Ber. 107* (1974) 979.
[2] S. Sharma, R.N. Kapoor, F. Cervantes-Lee and K.H. Pannell, *Polyhedron, 107* (11) (1991) 1177.
[3] (a) T.D. Tilley, in S. Patai and Z. Rappaport (eds.), *The Chemistry of Organo–Silicon Compounds II*, Wiley, 1989, S.1415; (b) T.D. Tilley, in S. Patai and Z. Rappaport (eds.), *The Silicon–Heteroatom Bond*, Wiley, 1991, S.309; (c) U. Schubert, *Transition Met. Chem., 16* (1991) 136.
[4] R.B. King and K.H. Pannell, *Z. Naturforsch., Teil B, 24* (1969) 262.
[5] M. Eibl and E. Hengge, *Organometallics, 10* (1991) 3185.
[6] W. Malisch, *J. Organomet. Chem., 39* (1972) C28.
[7] W. Malisch, *J. Organomet. Chem., 82* (1974) 185.
[8] B. Stadelmann, P. Lassacher, H. Stüger and E. Hengge, *J. Organomet. Chem., 482* (1994) 201.
[9] R.A. Fischer, A. Miehr and M.M. Schulte, *Adv. Mater., 7* (1) (1995) 58.
[10] J.E. Ellis and A.A. Flom, *J. Organomet. Chem., 99* (1975) 263.
[11] E. Hengge, M. Eibl and F. Schrank, *J. Organomet. Chem., 369* (1989) C23.
[12] E.O. Fischer, W. Hafner and H.O. Stahl, *Z. Anorg. Allg. Chem., 282* (1955) 47.
[13] G. Wilkinson, *J. Am. Chem. Soc., 76* (1954) 209.
[14] H. Gilman and S. Inoue, *J. Org. Chem., 29* (1969) 3418.
[15] F. Feher, P. Plichta and R. Guillery, *Tetrahedron Lett.*, (1970) 2889.
[16] K. Hassler and U. Katzenbeißer, *J. Organomet. Chem., 421* (1991) 151.
[17] B.J. Helmer and R. West, *J. Organomet. Chem., 236* (1982) 21.

ELSEVIER

Journal of Organometallic Chemistry 508 (1996) 231–242

Journal of Organometallic Chemistry

# Multiply substituted cyclopentadienyl metal complexes: I. Solid-state and solution conformational studies on $(\eta^5\text{-}C_5Me_4R)Fe(CO)(L)I$ (R = H, $^t$Bu)

Karen E. du Plooy, Johan du Toit, Demetrius C. Levendis, Neil J. Coville *

*Department of Chemistry, University of the Witwatersrand, Johannesburg, P.O. WITS 2050, South Africa*

Received 22 June 1995

**Abstract**

A series of $(\eta^5\text{-}C_5Me_4R)Fe(CO)(L)I$ complexes (R = H, L = $P(OMe)_3$, $PMe_3$, $P(O^iPr)_3$, $PPh_3$, $P(O\text{-}o\text{-}tol)_3$, $PBz_3$; R = $^t$Bu, L = $P(OMe)_3$, $P(OPh)_3$, $PPh_3$) have been synthesized and characterized by spectroscopic techniques (IR, $^1$H and $^{13}$C NMR). NOE spectroscopy was used to ascertain that the L group resided, on average, away from the bulky ring substituents. Thus, for R = $^t$Bu, L was displaced away from the $^t$Bu group, while, for R = H, L resided close to the H group. Crystal structure determinations were performed on $(\eta^5\text{-}C_5Me_4H)Fe(CO)(PPh_3)I$ (**1**) and $(\eta^5\text{-}C_5Me_4^tBu)Fe(CO)[P(OPh)_3]I$ (**2**). Both structures showed expected bond angle and bond length trends. The arrangement of the ligand set (L, CO, I) below the cyclopentadienyl ring in the solid state was the same as that found in solution. These results again reveal the importance of the steric effects associated with the cyclopentadienyl ring substituents on the properties of cyclopentadienyl–metal complexes in both the solution and solid states.

*Keywords:* Iron; Cyclopentadienyl; Carbonyl; Crystal structure; Ring substituents; Steric effects; NMR

## 1. Introduction

Since the first synthesis of ferrocene in 1951 [1], the cyclopentadienyl ring has played an important part in the development of both high- [2] and low-oxidation-state [3] organometallic chemistry. This importance relates to the ease of synthesis of cyclopentadienyl complexes, as well as the variation in both steric and electronic properties that can be associated with the ring with the introduction of ring substituents [4,5].

In earlier studies we have shown that substitution of even one of the $C_5H_5$ ring protons can lead to discernible changes in the physical and chemical properties of cyclopentadienyl–metal complexes [3,6]. Further substitution to give di-, tri-, tetra- and penta-substituted cyclopentadienyl ligands should lead to even more significant changes in these properties [5,7]. For instance, penta-substituted cyclopentadienyl ligands have been used to great advantage in the synthesis of cyclopentadienyl lanthanide and actinide complexes [8–10]. On a practical note, substituted cyclopentadienyl metal complexes can have improved solubility [5] and stability [9,10] characteristics compared to the related unsubstituted cyclopentadienyl metal complexes [2].

To elaborate further on our earlier studies, we wished to assess the effect of $C_5Me_4R$ ligands on the properties of $(\eta^5\text{-}C_5Me_4R)Fe(CO)(L)I$ complexes. In particular, by using R groups which were both smaller and larger than the Me group, steric effects could be probed by the ligand set attached to iron. To achieve this end we have chosen to synthesize a range of $(\eta^5C_5Me_4R)Fe(CO)(L)I$ complexes with R = H, $^t$Bu and L = Group-15 donor ligands. These new complexes have been characterized both in solution (IR, NMR spectroscopy) and the solid state (X-ray crystallography; R = H, L = $PPh_3$; R = $^t$Bu, L = $P(OPh)_3$). The data have been compared with earlier studies reported on $(\eta^5\text{-}C_5H_4R)Fe(CO)(L)I$ (R = $^t$Bu) complexes [6].

It is to be noted that numerous transition-metal complexes containing the $C_5Me_4R$ ligand have been reported in the literature, e.g. R = menthyl [11], neomenthyl [11], C(H)(Ph)Et [12], bridging group (i.e. of type $(C_5Me_4)_2X$, [9,13,14]) $(CH_2)_2CH=CH_2$ [15], H

* Corresponding author.

0022-328X/96/$15.00 © 1996 Elsevier Science S.A. All rights reserved
*SSDI* 0022-328X(95)05865-6

[16], $CH_2X$ [17–20], $CH_3$ [21,22], etc. The $C_5Me_4R$ ligands have also been synthesized directly, by deprotonation of $(\eta^5\text{-}C_5Me_5)ML_x$ complexes and from organic fragments in which the metal acts as a template [23–25]. To our knowledge, this latter method is the only reported method for synthesizing the $C_5Me_4^tBu$ ligand [22e].

## 2. Experimental section

### 2.1. General procedures

All experimental procedures were carried out under a dry nitrogen atmosphere, in dry deoxygenated solvents. The solvents were distilled and dried by standard procedures. A 100-W Hanovia UV irradiation lamp was used for photochemical reactions. Chromatography was carried out on Merck silica gel 60 (particle size, 0.063–0.200 mm). The 2,3,4,5-tetramethylcyclopent-2-enone and $Mo(CO)_6$ were obtained from Fluka. The $Fe(CO)_5$, $Fe_2(CO)_9$ and $[(\eta^5\text{-}C_5H_5)Fe(CO)_2]_2$ were obtained from Strem Chemicals. The ligands were obtained from various sources. $C_5Me_4H_2$ was prepared according to a literature method [9].

Melting points were determined on a Koffler micro hot-stage apparatus and are uncorrected. Infrared spectra were recorded on a Bruker IFS 88 FT–IR spectrometer, using NaCl solution cells. NMR spectra were recorded on a Bruker AC 200 NMR spectrometer, as $C_6D_6$ solutions. The numbering system used is indicated in Fig. 1, with protons numbered in relation to the ring-carbon numbering system. Microanalyses were performed by the Division of Energy Technology, CSIR, Pretoria, South Africa.

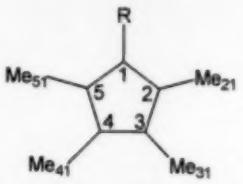


Fig. 1. Numbering scheme used for the $\eta^5\text{-}C_5Me_4R$ ligands.

### 2.2. Synthesis of $[(\eta^5\text{-}C_5Me_4H)Fe(CO)_2]_2$

$Fe_2(CO)_9$ (24.5 mmol, 8.93 g) was added to a solution of $C_5Me_4H_2$ (24.5 mmol, 3.00 g) in 100 ml benzene, and stirred at room temperature, under a nitrogen atmosphere. Further $Fe_2(CO)_9$ was added after 17 h (11.0 mmol, 4.00 g) and 24 h (13.5 mmol, 4.93 g). The mixture was stirred for another 24 h, after which it was filtered through celite. The solvent was removed and the product purified by partial dissolution of the material in hexane, and filtration through celite. The residue was extracted with benzene, and recrystallized from benzene to give $[(\eta^5\text{-}C_5Me_4H)Fe(CO)_2]_2$. Further product was obtained by recrystallization from the hexane fraction. (Total yield: 2.30 g, 40.3%). $[(\eta^5\text{-}C_5Me_4H)Fe(CO)_2]_2$ was obtained as a purple-brown to rust-brown solid. $^1H$ NMR: $\delta$ 1.59 (s, 6H, $H_{21,51}/H_{31,41}$), 1.73 (s, 6H, $H_{21,51}/H_{31,41}$), 3.75 (s, 1H, $H_1$). $^{13}C$ NMR: $\delta$ 8.81 (s, $C_{21,51}/C_{31,41}$), 10.48 (s, $C_{21,51}/C_{31,41}$), 87.60 (s, $C_1$), 99.24 (s, $C_{2,5}/C_{3,4}$), 99.69 (s, $C_{2,5}/C_{3,4}$), 245.51 (s, *C*O). See Table 1 for further analytical and spectroscopic data.

### 2.3. Synthesis of $(\eta^5\text{-}C_5Me_4H)Fe(CO)_2I$

$[(\eta^5\text{-}C_5Me_4H)Fe(CO)_2]_2$ (4.29 mmol, 2.00 g) was dissolved in 100 ml chloroform, in a 500 ml round-bot-

Table 1
Analytical and spectroscopic data for $(\eta^5\text{-}C_5Me_4R)$ complexes of iron

| Complex | M.P. (°C) | IR [a] $\bar{\nu}$(CO) ($cm^{-1}$) | Analysis [b] C (%) | H (%) |
|---|---|---|---|---|
| $[(\eta^5\text{-}C_5Me_4H)Fe(CO)_2]_2$ | 163 (dec) | 1929, 1753 | 56.59 (56.69) | 5.58 (5.62) |
| $(\eta^5\text{-}C_5Me_4H)Fe(CO)_2I$ | 68.5-69 | 2023, 1976 | 36.45 (36.70) | 3.51 (3.64) |
| $(\eta^5\text{-}C_5Me_4H)Fe(CO)(L)I$ | | | | |
| L = $PPh_3$ | 148–151 | 1932 | 56.06 (56.59) | 4.61 (4.75) |
| L = $P(OMe)_3$ | 124–126 | 1942 | 34.06 (34.24) | 4.81 (4.86) |
| L = $PBz_3$ | 112–115 | 1929 | – | |
| L = $P(O\text{-}o\text{-}Tol)_3$ | 109–111 | 1957 | 54.17 (54.41) | 4.92 (5.01) |
| L = $P(O\text{-}^iPr)_3$ | 76–78 | 1933 | 42.51 (42.25) | 6.43 (6.34) |
| L = $PMe_3$ | 125.5–127 | 1926 | – | |
| $[(\eta^5\text{-}C_5Me_4^tBu)Fe(CO)_2]_2$ | 180 (dec) | 1923, 1747 | – | – |
| $(\eta^5\text{-}C_5Me_4^tBu)Fe(CO)_2I$ | 163–164 | 2017, 1971 | 43.07 (43.30) | 5.05 (5.09) |
| $(\eta^5\text{-}C_5Me_4^tBu)Fe(CO)(L)I$ | | | | |
| L = $PPh_3$ | 145–148 | 1921 | – | – |
| L = $P(OMe)_3$ | 100.5–102.5 | 1934 | – | – |
| L = $P(OPh)_3$ | 112.5–115 | 1954 | 54.51 (55.04) | 5.01 (5.20) |

[a] Recorded in $CH_2Cl_2$. [b] Calculated values in parentheses.

Table 2
Experimental details for the reaction: $(\eta^5\text{-}C_5Me_4H)Fe(CO)_2I + L \rightarrow (\eta^5\text{-}C_5Me_4H)Fe(CO)(L)I + CO$

| | L = $PPh_3$ | $P(OMe)_3$ | $PBz_3$ | $P(O\text{-}o\text{-}Tol)_3$ | $P(O\text{-}^iPr)_3$ | $PMe_3$ |
|---|---|---|---|---|---|---|
| Catalyst [a] | 1 | 2 | 1 | 1 | 1 | 1 |
| Reaction time (h) | 18 | 2 | 17 | 1 | 1 | 4 |
| Yield (%) | 67 | 71 | 22 | 76 | 86 | 12 |
| Chromatography eluent | Hexane/ benzene | Hexane/ benzene | Hexane/ $CH_2Cl_2$ | Hexane/ benzene | Hexane/ benzene | Hexane/ benzene |
| Recrystallisation solvent | Hexane/ $CH_2Cl_2$ | Hexane | Hexane/ $CH_2Cl_2$ | Hexane | Hexane | Hexane |

[a] $1 = [(\eta^5\text{-}C_5H_5)Fe(CO)_2]_2$, $2 = [(\eta^5\text{-}C_5Me_4H)Fe(CO)_2]_2$

tom flask. $I_2$ (4.29 mmol, 1.09 g) was dissolved in 100 ml chloroform, and approximately 75 ml of the iodine solution was added to the solution, which was stirred at room temperature under a nitrogen atmosphere. The reaction was monitored by IR spectroscopy. On completion of the reaction, the solution was washed with a saturated sodium thiosulphate solution (to remove excess $I_2$) and water, and dried with anhydrous $MgSO_4$, and the solvent was removed to yield a black oil (3.22 g). The product was purified by column chromatography (silica gel, hexane, and 3:1 hexane:dichloromethane mixtures as eluents) and obtained as a brown-black solid (2.36 g, 76% yield). $^1$H NMR: $\delta$ 1.45 (s, 6H, $H_{21,51}/H_{31,41}$), 1.49 (s, 6H, $H_{21,51}/H_{31,41}$), 3.60 (s, 1H, $H_1$). $^{13}$C NMR: $\delta$ 10.12 (s, $C_{21,51}/C_{31,41}$), 11.72 (s, $C_{21,51}/C_{31,41}$), 80.91 (s, $C_1$), 96.26 (s, $C_{2,5}/C_{3,4}$), 98.47 (s, $C_{2,5}/C_{3,4}$), 216.03 (s, *CO*). See Table 1 for further analytical and spectroscopic data.

### 2.4. Synthesis of $(\eta^5\text{-}C_5Me_4H)Fe(CO)(L)I$

The compounds $(\eta^5\text{-}C_5Me_4H)Fe(CO)(L)I$, (L = $P(OMe)_3$, $PPh_3$, $PBz_3$, $PMe_3$, $P(O\text{-}^iPr)_3$ and $P(O\text{-}o\text{-}Tol)_3$) were all synthesized by approximately the same procedure, outlined below. $(\eta^5\text{-}C_5Me_4H)Fe(CO)_2I$ (0.5 mmol, 0.18 g), L (0.55 mmol) and approximately 15 mg catalyst ($[(\eta^5\text{-}C_5Me_4H)Fe(CO)_2]_2$ or $[(\eta^5\text{-}C_5H_5)Fe(CO)_2]_2$) were heated together under reflux in benzene (20 ml), for 1 to 24 h. The reactions were followed by thin-layer chromatography. The reaction solvent was removed on a rotary evaporator and the product purified by column chromatography (silica gel)

Table 3
$^1$H NMR data for $(\eta^5\text{-}C_5Me_4R)Fe(CO)(L)I$ (R = H, $^t$Bu) complexes of iron [a]

| L | $\delta H_1$ [b] | $\delta H_{21}$ [b] | $\delta H_{31}$ [b] | $\delta H_{41}$ [b] | $\delta H_{51}$ [b] |
|---|---|---|---|---|---|
| *R = H* | | | | | |
| $P(OMe)_3$ [c] | 4.00 (3.4) | 1.50 | 1.64 (1.5) | 1.87 (1.8) | 1.92 |
| $PMe_3$ [d] | 3.35 (6.7) | 1.19 (1.0) | 1.66 | 1.99 (1.0) | 1.89 |
| $P(O\text{-}^iPr)_3$ [e] | 4.19 (3.6) | 1.51 (1.1) | 1.67 (1.3) | 1.89 (2.2) | 2.05 |
| $PPh_3$ [f] | 2.97 (4.3) | 1.20 | 1.72 (1.1) | 2.10 | 1.51 |
| $P(O\text{-}o\text{-}Tol)_3$ [g] | 3.78 (5.3) | 1.18 | 1.62 (2.7) | 2.06 (1.8) | 1.78 |
| $PBz_3$ [h] | 2.70 (3.3) | 1.07 | 1.55 (0.8) | 1.95 | 1.61 |
| *R = $^t$Bu* | | | | | |
| $P(OMe)_3$ [i] | 1.43 | 1.66 | 1.60 (1.1) | 1.88 (0.5) | 2.26 (1.9) |
| $P(OPh)_3$ [j] | 1.40 | 1.68 | 1.71 (1.2) | 1.86 (0.4) | 2.25 (2.2) |
| $PPh_3$ [k] | 1.56 | 1.56 | 0.82 | 1.21 | 2.47 |

[a] Recorded in $C_6D_6$. $\delta$, in ppm, relative to $SiMe_4$.
[b] $J_{H\text{-}P}$, in Hz, given in parentheses.
[c] $P(OMe)_3$: 3.47 (d, 9H, $J_{P\text{-}H}$ = 10.8 Hz, $P(OCH_3)_3$)
[d] $PMe_3$: 1.16 (d, 9H, $J_{P\text{-}H}$ = 9.4 Hz, $P(CH_3)_3$)
[e] $P(O\text{-}^iPr)_3$: 1.21 (d, 9H, $J_{H\text{-}H}$ = 6.1 Hz, $P(OCH(CH_3)(CH_3))_3$), 1.23 (d, 9H, $J_{H\text{-}H}$ = 6.1 Hz, $P(OCH(CH_3)(CH_3))_3$), 4.84 (d of septets, 3H, $J_{P\text{-}H}$ = 8.6 Hz, $J_{H\text{-}H}$ = 6.1) $P(OCH(CH_3)(CH_3))_3$
[f] $PPh_3$: 6.99 (m, 9H, $H_{m,p}$ of Ph), 7.83 (m, 6H, $H_o$ of Ph)
[g] $P(O\text{-}o\text{-}Tol)_3$: 2.37 (s, 9H, $P(O\text{-}o\text{-}CH_3C_6H_4)$, 6.78 (m, 9H, $H_{m,p}$ of Ph), 7.58 (d, 3H, $J_{P\text{-}H}$ = 8.1 Hz, $H_o$ of Ph
[h] $PBz_3$: 3.39 (dd, 3H, $J_{P\text{-}H}$ = 9.8 Hz, $J_{H\text{-}H}$ = 14.7 Hz, $P(CH_aH_bC_6H_5)_3$), 3.60 (dd, 3H, $J_{P\text{-}H}$ = 6.4 Hz, $J_{H\text{-}H}$ = 14.6 Hz, $P(CH_aH_bC_6H_5)_3$), 7.05 (m, 15H, $P(CH_aH_bC_6H_5)_3$)
[i] $P(OMe)_3$: 3.46 (d, 9H, $J_{P\text{-}H}$ = 10.5 Hz, $P(OCH_3)_3$)
[j] $P(OPh)_3$: 6.79 (m, 3H, $H_p$ of Ph), 6.95 (m, 6H, $H_m$ of Ph), 7.36 (m, 6H, $H_o$ of Ph).
[k] $PPh_3$: 6.99 (m, 9H, $H_{m,p}$ of Ph), 7.85 (m, 6H, $H_o$ of Ph)

and recrystallization. For more details, see Table 2: also see Table 1 for the analytical and spectroscopic data, Table 3 for the $^1$H NMR data and Table 4 for the $^{13}$C NMR data of these new compounds.

### 2.5. Synthesis of tert-butyl-tetramethylcyclopentadiene ($C_5Me_4^tBuH$)

2,3,4,5-Cyclopent-2-enone (25.0 mmol, 3.46 g) and 20 ml dry diethyl ether were placed in a flame-dried 100 ml round-bottom flask, with a stirrer bar. The solution was cooled to −78°C, with stirring, and $^t$BuLi (27.5 mmol, 1.7 M, 16.2 ml) was added dropwise via a syringe. The reaction mixture was stirred at −78°C for 1 h, quenched by the addition of water (approximately 1 ml), and allowed to warm up to room temperature slowly (1 h). A few drops of concentrated $H_2SO_4$ were added, the reaction mixture stirred for a further 15 min, washed with concentrated sodium bicarbonate solution, and then twice by water. The organic layer was then dried with anhydrous $MgSO_4$, and the solvent was removed (crude yield, 3.91 g). The product was purified by column chromatography (silica gel, eluent hexane). The clear to light-yellow product eluted rapidly, as two bands, corresponding presumably to different isomers of the substituted cyclopentadiene (2.95 g, 66% yield). $C_5Me_4^tBuH$ (isomeric mixture). $^1$H NMR: δ 0.86–0.88 (singlets, $C_5Me_4^tBuH$), 0.94–1.57 (singlets, $C_5Me_4^tBu$-H), 1.9–2.6 (multiplets, $C_5Me_4^tBuH$).

### 2.6. Synthesis of $[(\eta^5\text{-}C_5Me_4^tBu)Fe(CO)_2]_2$

The dimer was obtained from the reaction between the cyclopentadienyl ligand and $Fe(CO)_5$. *Tert*-butyl-tetramethyl-cyclopentadiene (10 mmol, 1.78 g) and $Fe(CO)_5$ (30 mmol, 5.88 g) were heated together under reflux in octane (70 ml) for three days. The reaction mixture was cooled to room temperature, and filtered under a nitrogen atmosphere through a very thin layer of celite (about 1 cm thick and about 5 cm diameter), with benzene and dichloromethane as solvents. Red-purple crystals separated after partial removal of the solvent (0.44 g, 15% yield). $[(\eta^5\text{-}C_5Me_4^tBu)Fe(CO)_2]_2$. $^1$H NMR: δ 1.50 (s, 6H, $H_{21,51}$/ $H_{31,41}$), 1.56 (s, 9H, $^t$Bu), 1.83 (s, 6H, $H_{21,51}/H_{31,41}$). See Table 1 for further analytical and spectroscopic data.

### 2.7. Synthesis of $(\eta^5\text{-}C_5Me_4^tBu)Fe(CO)_2I$

The dimer, $[(\eta^5\text{-}C_5Me_4^tBu)Fe(CO)_2]_2$ (0.78 mmol, 0.45 g), was dissolved in 30 ml chloroform. $I_2$ (0.78 mmol, 0.20 g), in chloroform (40 ml), was added in small portions, over a period of 3.5 h. During this time, the mixture was stirred at room temperature under a

Table 4
$^{13}$C NMR data for $(\eta^5\text{-}C_5Me_4H)Fe(CO)(L)I$ [a]

| L | δ $C_{21}$ | δ $C_{31}$ | δ $C_{41}$ | δ $C_{51}$ | δ $C_1$ | δ $C_2$–$C_5$ [b] | δ CO [b] |
|---|---|---|---|---|---|---|---|
| *R* = *H* | | | | | | | |
| $P(OMe)_3$ [c] | 11.21 | 9.96 | 11.41 | 12.33 | 82.80 | 85.11, 95.83(3.6)<br>93.85, 98.27(4.7) | 221.95(44.2) |
| $PMe_3$ [d] | 11.30 | 10.18 | 12.41 | 12.71 | 84.25 | 77.92, 94.38(2.5)<br>91.24, 98.82(4.5) | 221.81(32.5) |
| $P(O\text{-}^iPr)_3$ [e] | 11.10 | 10.05 | 11.44 | 12.71 | 84.58 | 82.24, 96.26(3.4)<br>94.54, 97.01(5.6) | 222.56(45.5) |
| $PPh_3$ [f] | 11.08 | 10.53 | 12.68 | 11.80 | 80.21 | 86.70, 91.25(3.4)<br>95.32, 100.10(1.6) | 223.86(29.8) |
| $P(O\text{-}o\text{-}Tol)_3$ [g] | 10.80 | 9.79 | 12.71 | 11.98 | 79.34 | 86.41, 93.48(6.1)<br>94.22, 103.54(4.6) | 221.32(41.6) |
| *R* = *$^t$Bu* | | | | | | | |
| $P(OMe)_3$ [h] | 13.36 | 10.24 | 11.28 | 15.48 | [i] | 86.55, 93.30 | [i] |
| $P(OPh)_3$ [j] | 13.52 | 10.53 | 11.41 | 15.62 | 87.25 | 95.12, 95.87<br>[i], 99.38(4.5) | 221.23 |

[a] Recorded in $C_6D_6$. δ, in ppm, is relative to $C_6D_6$ (central peak at 128.03 ppm)
[b] $J_{C\text{-}P}$, in Hz, are given in parentheses.
[c] $P(OMe)_3$: 53.40 (d, $J_{C\text{-}P}$ = 5.9 Hz, $P(OCH_3)_3$)
[d] $PMe_3$: 20.54 (d, $J_{C\text{-}P}$ = 29.9 Hz, $P(CH_3)_3$)
[e] $P(O\text{-}^iPr)_3$: 24.22(d, $J_{C\text{-}P}$ = 2.9 Hz, $P\{OCH(CH_3)(CH_3)\}_3$), 24.26 (d, $J_{C\text{-}P}$ = 1.8 Hz, $P\{OCH(CH_3)(CH_3)\}_3$), 70.52 (d, $J_{C\text{-}P}$ = 6.8 Hz, $P\{OCH(CH_3)(CH_3)\}_3$)
[f] $PPh_3$: 128.14 (s, $C_m$ of Ph), 129.88 (s, $C_p$ of Ph), 134.70 (d, $J_{C\text{-}P}$ = 9.5 Hz, $C_o$ of Ph), 136.77 (d, $J_{C\text{-}P}$ = 40.0 Hz, $C_i$ of Ph).
[g] $P(O\text{-}o\text{-}Tol)_3$: 17.61 (s, $P(O\text{-}o\text{-}CH_3C_6H_4)$, 120.61 (d, $J_{C\text{-}P}$ = 3.7 $C_o$H of Ph), 124.50, 126.80, 131.74 (singlets, $C_{m,p}$ of Ph), 129.76 (d, $J_{C\text{-}P}$ = 5.4 Hz, $C_o$Me of Ph), 151.52 (d, $J_{C\text{-}P}$ = 12.7 Hz, $C_i$ of Ph)
[h] $P(OMe)_3$: 53.45 (d, $J_{C\text{-}P}$ = 6.6 Hz, $P(OCH_3)_3$); δ $C(CH_3)_3$ = 32.28, δ $C(CH_3)_3$ 33.70
[i] not observed
[j] $P(OPh)_3$; 121.71–129.63; δ $C(CH_3)_3$ = 32.23, δ $C(CH_3)_3$ 33.74. (m, $P(OPh)_3$: $C_{o,m,p}$), 152.74 (d, $J_{C\text{-}P}$ = 13.5 Hz, $P(OPh)_3$: $C_{ipso}$).

nitrogen atmosphere, and the reaction was monitored by IR spectroscopy. The appearance of the carbonyl stretching peaks for the iodo derivative ($\bar{\nu}$(CO) ($CH_2Cl_2$) = 2017, 1971 $cm^{-1}$), and the disappearance of the carbonyl peaks of the dimer ($\bar{\nu}$(CO) ($CH_2Cl_2$) = 1923, 1747 $cm^{-1}$) indicated the progress of the reaction. When all the dimer had reacted, the mixture was washed twice with concentrated sodium thiosulphate, and then twice with water. The chloroform layer was dried with anhydrous $MgSO_4$, and the solvent was evaporated off (crude yield 0.64 g). The product was purified by column chromatography (silica, hexane (100%) to hexane:dichlomethane mixtures (up to a ratio of 3:2), as eluents). The product recrystallized from the solvent as the solvent was partially removed on the rotary evaporator and the fine red-brown crystals were filtered off (0.56 g, 86% yield). ($\eta^5$-$C_5Me_4^tBu$)Fe ($CO)_2$I. $^1$H NMR: $\delta$ 1.12 (s, 9H, $^t$Bu), 1.61, 1.73 (s, 6H, $H_{21,51}$/ $H_{31,41}$). $^{13}$C NMR: $\delta$ 10.79 (s, $C_{21,51}$/ $C_{31,41}$), 13.73 (s, $C_{21,51}$/$C_{31,41}$), 32.16 (s, $C(CH_3)_3$), 33.26 (s, $C(CH_3)_3$), 97.52 (s, $C_1$/$C_{2,5}$/$C_{3,4}$), 98.67 (s, $C_1$/$C_{2,5}$/$C_{3,4}$), 101.10 (s, $C_1$/$C_{2,5}$/$C_{3,4}$), 216.83 (s, CO). See Table 1 for further analytical and spectroscopic data.

### 2.8. Synthesis of ($\eta^5$-$C_5Me_4^tBu$)Fe(CO)(L)I

#### 2.8.1. Catalytic procedure

($\eta^5$-$C_5Me_4^tBu$)Fe$(CO)_2$I (0.50 mmol, 0.21 g), L (0.55 mmol) and about 10 mg catalyst, [($\eta^5$-$C_5H_5$)Fe$(CO)_2]_2$, were heated under reflux in 25 ml benzene. The reactions were followed by thin-layer chromatography.

*2.8.1.1. L = P(OMe)$_3$.* All the starting material, ($\eta^5$-$C_5Me_4^tBu$)Fe$(CO)_2$I, was used up after 18 h, and the product, ($\eta^5$-$C_5Me_4^tBu$)Fe(CO){P$(OMe)_3$}I, was obtained as a dark brown solid (0.10 g, 39% yield) after purification by column chromatography (silica gel, hexane/benzene mixtures as eluent).

*2.8.1.2. L = PPh$_3$.* The desired product, ($\eta^5$-$C_5Me_4^tBu$)Fe(CO)($PPh_3$)I, could not be obtained in significant yield, even after two days reaction time. However, the "catalyst" formed a product, ($\eta^5$-$C_5H_5$) Fe(CO)($PPh_3$)I.

*2.8.1.3. L = P(OPh)$_3$.* The desired product was formed in very low yield, after a two-day reaction. The reaction mixture was purified by column chromatography (silica gel, hexane/ dichloromethane mixtures as eluent), which separated excess P$(OPh)_3$, unreacted starting material, ($\eta^5$-$C_5Me_4^tBu$)Fe$(CO)_2$I (0.03 g), product, ($\eta^5$-$C_5Me_4^tBu$)Fe(CO){P$(OPh)_3$}I (0.03 g), and "catalytic product", ($\eta^5$-$C_5H_5$)Fe(CO){P$(OPh)_3$}I (0.05 g).

#### 2.8.2. Photochemical reaction

($\eta^5$-$C_5Me_4^tBu$)Fe$(CO)_2$I (0.200 mmol, 0.0832 g) and L (0.240 mmol), dissolved in THF (40 ml), were irradiated with UV light. The reactions were followed by thin-layer chromatography, which indicated completion of reaction after 2.3 h (L = $PPh_3$) and 1.8 h (L = P$(OPh)_3$). The products were purified by column chromatography (silica gel, hexane:$CH_2Cl_2$ = 9:1 to 6:4 as eluent). ($\eta^5$-$C_5Me_4^tBu$)Fe(CO)($PPh_3$)I was obtained as a light brown solid by recrystallization from toluene at 0°C. ($\eta^5$-$C_5Me_4^tBu$)Fe(CO){P$(OPh)_3$}I was obtained as a green solid by recrystallization from $CH_2Cl_2$/hexane at room temperature. See Table 1 for the analytical and spectroscopic data, Table 3 for the $^1$H NMR data and Table 4 for the $^{13}$C NMR data of these ($\eta^5$-$C_5Me_4^tBu$)Fe(CO)(L)I compounds.

### 2.9. Crystal structure determination

Single crystals of ($\eta^5$-$C_5Me_4H$)Fe(CO)(I) ($PPh_3$) (**1**) and ($\eta^5$-$C_5Me_4^tBu$)Fe(CO)(I)[P$(OPh)_3$] (**2**) were obtained by recrystallization from $CH_2Cl_2$/hexane at 0°C and were mounted on glass fibres. Crystallographic analyses were based on room-temperature X-ray diffraction data collected with an Enraf–Nonius CAD4 four-circle single-crystal diffractometer, using graphite-monochromated Mo K$\alpha$ radiation. Cell constants were measured and refined from 25 accurately measured reflections in the range $15° \leq \theta \leq 20°$. Standard reflections were measured every hour of exposure time. Each data set was corrected for crystal decay and Lorentz-polarization effects. Data reduction was done using the

Table 5
Crystallographic data for **1** and **2**

| Chem. formula | $FeC_{28}H_{28}OPI$ | $FeC_{32}H_{36}O_4PI$ |
|---|---|---|
| F.W. | 594.254 | 698.361 |
| Cryst. systems | Monoclinic | Monoclinic |
| Space group | C 2/c | $P2_1$/c |
| $a$ (Å) | 23.863(3) | 20.695(2) |
| $b$ (Å) | 15.353(2) | 8.7436(6) |
| $c$ (Å) | 17.560(2) | 17.632(3) |
| $V$ (Å$^3$) | 5100.8(13) | 3132.71(63) |
| $\alpha$ (deg) | – | – |
| $\beta$ (deg) | 127.547(10) | 100.93(1) |
| $\gamma$ (deg) | – | – |
| $Z$ | 8 | 4 |
| $d_{calc}$ (g $cm^{-3}$) | 1.547 | 1.480 |
| $T$ (°C) | 23 ± 2 | 23 ± 2 |
| 2$\alpha$ range (deg) | 6–54 | 6–60 |
| No. of data colld. | 5768 | 5222 |
| No. of data observed | 3171 | 2476 |
| No. of variables | 264 | 250 |
| $R^a$ | 0.047 | 0.071 |
| $R_w$ [b] | 0.039 | 0.059 |

[a] $R = \Sigma||F_o| - |F_c|| / \Sigma|F_o|$ [b] $R_w = \Sigma(|w^{1/2}||F_o| - |F_c||)/\Sigma(|w^{1/2}||F_o|)$

XTAL suite of programs [26]. Analytical absorption corrections using the NRCVAX suite of programs [27] were applied to both data sets. Unit-cell parameters and details of the data collections are given in Table 5.

The structures of **1** and **2** were solved by Patterson methods, and subsequent Fourier synthesis revealed the remaining non-hydrogen atoms. Refinement was carried out using full-matrix least-squares calculations in which the hydrogen atoms (except the H1 cyclopentadienyl ring atom) were included at calculated positions. All the non-hydrogen atoms were refined anisotropically for structure **1**. For structure **2** the phenyl carbon atoms were not refined anisotropically, although the remaining non-hydrogen atoms were. The phenyl rings were refined as rigid bodies for both **1** and **2**. The $R$ values converged to 0.047 and 0.071 for structures **1** and **2** respectively. All calculations were performed using the SHELX set of programs [28].

Final positional parameters are found in Tables 6 and 7, and selected bond lengths and angles for **1** and **2** are given in Table 8. Figs. 2 and 3, obtained using ORTEP [29], show the structures of **1** and **2**.

Details of crystallographic parameters, a table of anisotropic thermal factors, and a complete list of bond distances and angles for each structure have been deposited at the Cambridge Crystallographic Data Centre.

Table 6
Fractional coordinates and isotropic displacement parameters of the non-hydrogen atoms of structure **1**

| Atom | $x$ | $y$ | $z$ | $U$ |
|---|---|---|---|---|
| I | 0.67146(2) | 0.51621(3) | 0.40714(3) | *0.0629(3) |
| FE | 0.68556(4) | 0.48866(5) | 0.27111(5) | *0.0383(4) |
| P | 0.80402(7) | 0.49549(9) | 0.3730(1) | *0.0354(7) |
| O | 0.6762(3) | 0.3077(3) | 0.2897(3) | *0.073(4) |
| C(1) | 0.6655(3) | 0.5090(5) | 0.1412(4) | *0.063(4) |
| C(2) | 0.6706(3) | 0.5919(4) | 0.1777(4) | *0.056(4) |
| C(3) | 0.6182(3) | 0.5979(4) | 0.1882(4) | *0.057(4) |
| C(4) | 0.5805(3) | 0.5171(5) | 0.1580(4) | *0.064(4) |
| C(5) | 0.6087(3) | 0.4637(4) | 0.1257(5) | *0.067(4) |
| C(6) | 0.7168(4) | 0.6655(5) | 0.1884(6) | *0.099(6) |
| C(7) | 0.6005(4) | 0.6783(5) | 0.2186(6) | *0.113(7) |
| C(8) | 0.5152(3) | 0.4959(7) | 0.1517(6) | *0.131(7) |
| C(9) | 0.5798(5) | 0.3753(6) | 0.0768(6) | *0.133(7) |
| C(10) | 0.6840(3) | 0.3738(5) | 0.2878(4) | *0.054(4) |
| C(11) | 0.8466(2) | 0.5866(2) | 0.4588(3) | *0.037(3) |
| C(12) | 0.9184(2) | 0.5844(2) | 0.5363(3) | *0.047(4) |
| C(13) | 0.9497(2) | 0.6551(2) | 0.5990(3) | *0.055(4) |
| C(14) | 0.9092(2) | 0.7279(2) | 0.5844(3) | *0.061(5) |
| C(15) | 0.8374(2) | 0.7301(2) | 0.5069(3) | *0.064(5) |
| C(16) | 0.8061(2) | 0.6594(2) | 0.4441(3) | *0.053(4) |
| C(17) | 0.8506(2) | 0.4015(3) | 0.4529(3) | *0.044(4) |
| C(18) | 0.9094(2) | 0.3653(3) | 0.4654(3) | *0.058(4) |
| C(19) | 0.9430(2) | 0.2930(3) | 0.5249(3) | *0.081(5) |
| C(20) | 0.9179(2) | 0.2568(3) | 0.5718(3) | *0.089(6) |
| C(21) | 0.8592(2) | 0.2931(3) | 0.5592(3) | *0.087(6) |
| C(22) | 0.8255(2) | 0.3654(3) | 0.4998(3) | *0.063(4) |
| C(23) | 0.8447(2) | 0.5013(2) | 0.3115(3) | *0.041(3) |
| C(24) | 0.8287(2) | 0.4352(2) | 0.2466(3) | *0.053(4) |
| C(25) | 0.8565(2) | 0.4379(2) | 0.1960(3) | *0.069(5) |
| C(26) | 0.9002(2) | 0.5066(2) | 0.2104(3) | *0.077(5) |
| C(27) | 0.9162(2) | 0.5727(2) | 0.2754(3) | *0.074(5) |
| C(28) | 0.8884(2) | 0.5701(2) | 0.3259(3) | *0.053(4) |

Table 7
Fractional coordinate and isotropic displacement parameters of the non-hydrogen atoms of structure **3**

| | $x$ | $y$ | $z$ | $U$ |
|---|---|---|---|---|
| FE | 0.1752(1) | 0.20317(9) | 0.1540(2) | *0.0381(6) |
| I | 0.21625(5) | 0.08862(5) | 0.29064(9) | *0.0632(4) |
| P | 0.2717(2) | 0.2857(2) | 0.1493(3) | *0.0367(9) |
| O(1) | 0.2697(5) | 0.4287(4) | 0.0895(7) | *0.050(2) |
| O(2) | 0.3248(4) | 0.3393(4) | 0.2223(7) | *0.045(2) |
| O(3) | 0.3195(5) | 0.1729(4) | 0.1168(7) | *0.057(2) |
| C(1) | 0.0756(7) | 0.1372(6) | 0.111(1) | *0.036(2) |
| C(2) | 0.1137(7) | 0.0006(6) | 0.125(1) | *0.039(2) |
| C(3) | 0.1657(7) | 0.0079(7) | 0.082(1) | *0.051(2) |
| C(4) | 0.1589(7) | 0.1417(7) | 0.037(1) | *0.059(2) |
| C(5) | 0.1056(7) | 0.2224(6) | 0.053(1) | *0.047(2) |
| C(6) | 0.0124(9) | 0.1633(7) | 0.137(1) | *0.074(2) |
| C(7) | −0.0216(8) | 0.3159(7) | 0.117(1) | *0.084(2) |
| C(8) | 0.0209(7) | 0.1546(7) | 0.227(1) | *0.071(2) |
| C(9) | −0.0401(9) | 0.0420(7) | 0.101(1) | *0.089(2) |
| C(10) | 0.1037(7) | −0.1400(6) | 0.171(1) | *0.057(2) |
| C(11) | 0.2178(7) | −0.1203(6) | 0.076(1) | *0.065(2) |
| C(12) | 0.1934(6) | 0.1785(6) | −0.028(1) | *0.059(2) |
| C(13) | 0.0833(7) | 0.3727(7) | 0.011(1) | *0.074(2) |
| C(14) | 0.1498(9) | 0.3780(6) | 0.193(1) | *0.072(2) |
| O(4) | 0.1320(7) | 0.4813(5) | 0.2140(8) | *0.092(2) |
| C(2b) | 0.3535(4) | 0.3892(3) | 0.3556(6) | 0.057(2) |
| C(3b) | 0.3516(4) | 0.4827(3) | 0.4193(6) | 0.091(3) |
| C(4b) | 0.3152(4) | 0.6180(3) | 0.4102(6) | 0.102(3) |
| C(5b) | 0.2807(4) | 0.6598(3) | 0.3373(6) | 0.089(3) |
| C(6b) | 0.2826(4) | 0.5664(3) | 0.2736(6) | 0.083(3) |
| C(1b) | 0.3189(4) | 0.4311(3) | 0.2828(6) | 0.049(2) |
| C(2a) | 0.3367(4) | 0.4487(3) | −0.0075(6) | 0.057(2) |
| C(3a) | 0.3904(4) | 0.5113(3) | −0.0340(6) | 0.074(3) |
| C(4a) | 0.4318(4) | 0.6147(3) | 0.0121(6) | 0.072(2) |
| C(5a) | 0.4195(4) | 0.6555(3) | 0.0845(6) | 0.075(3) |
| C(6a) | 0.3659(4) | 0.5930(3) | 0.1109(6) | 0.065(2) |
| C(1a) | 0.3244(4) | 0.4896(3) | 0.0649(6) | 0.039(2) |
| C(2c) | 0.4349(3) | 0.1453(3) | 0.1264(6) | 0.059(2) |
| C(3c) | 0.4944(3) | 0.0784(3) | 0.1608(6) | 0.084(3) |
| C(4c) | 0.4966(3) | −0.0232(3) | 0.2222(6) | 0.077(3) |
| C(5c) | 0.4391(3) | −0.0578(3) | 0.2492(6) | 0.085(3) |
| C(6c) | 0.3796(3) | 0.0091(3) | 0.2148(6) | 0.067(2) |
| C(1c) | 0.3775(3) | 0.1107(3) | 0.1534(6) | 0.051(2) |

## 3. Results and discussion

### 3.1. Synthesis

The reduction of 2,3,4,5-tetramethylcyclopent-2-enone by $LiAlH_4$, followed by acid-catalysed dehydration, yielded tetramethylcyclopentadiene [9]. This ligand was reacted with $Fe_2(CO)_9$ and produced $[(\eta^5\text{-}C_5Me_4H)Fe(CO)_2]_2$ as purple-brown crystals. The cleavage of this dimer with iodine gave a high yield of dark-brown crystals of $(\eta^5\text{-}C_5Me_4H)Fe(CO)_2I$. Reaction of $(\eta^5\text{-}C_5Me_4H)Fe(CO)_2I$, with L (L = $P(OMe)_3$,

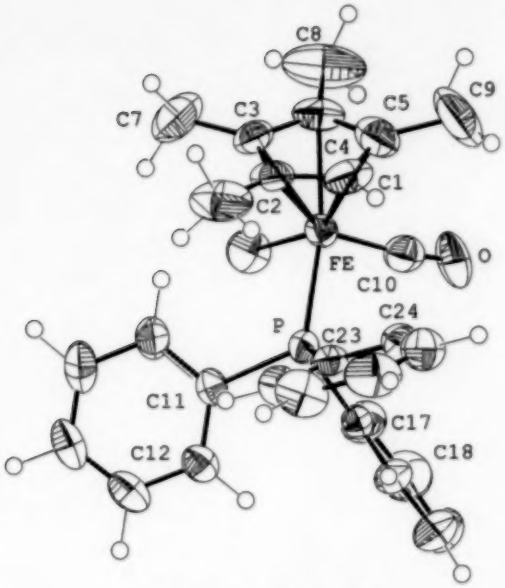


Fig. 2. ORTEP plot of **1** (side view).

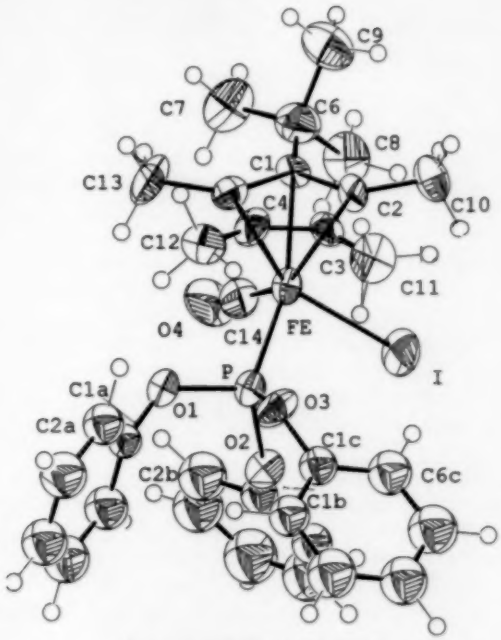


Fig. 3. ORTEP plot of **2** (side view).

$P(O^iPr)_3$) in the presence of $[(\eta^5\text{-}C_5Me_4H)Fe(CO)_2]_2$ as catalyst gave the required product (Table 2). The larger phosphite, $P(O\text{-}o\text{-}Tol)_3$, and the phosphines $PMe_3$, $PPh_3$ and $PBz_3$ required the more active catalyst, $[(\eta^5\text{-}C_5H_5)Fe(CO)_2]_2$, to produce the required substituted complex. No reaction between $(\eta^5\text{-}C_5Me_4H)Fe(CO)I$ and L was observed in the absence of catalyst under similar reaction conditions. Presumably electronic and steric arguments account for these observations.

When $[(\eta^5\text{-}C_5H_5)Fe(CO)_2]_2$ was used as the catalyst, both $(\eta^5\text{-}C_5H_5)Fe(CO)(L)I$ and the dimer $[(\eta^5\text{-}C_5Me_4H)Fe(CO)_2]_2$ were formed as side-products, as detected by NMR spectroscopy. The formation of these products from the catalyst, $[(\eta^5\text{-}C_5H_5)Fe(CO)_2]_2$, during thermal reaction between $(\eta^5\text{-}C_5Me_4H)Fe(CO)_2I$ and L, can be readily rationalized by a radical mechanism:

$$[CpFe(CO)_2]_2 \rightleftarrows [CpFe(CO)_2]\cdot$$

$$[CpFe(CO)_2]\cdot + L \rightarrow [CpFe(CO)(L)]\cdot + CO$$

$$[CpFe(CO)(L)]\cdot + [Cp'Fe(CO)_2I] \rightarrow [CpFe(CO)(L)I] + [Cp'Fe(CO)_2]\cdot$$

Table 8
Comparison between bond lengths and bond angles for **1**, **2** and **3**

| | 1 | 2 | 3 |
|---|---|---|---|
| Cp [a]: C–C (Å) | 1.37(1)–1.43(1) [b] | 1.38(2)–1.50(2) [c] | 1.385(8)–1.425(8) |
| Cp [a]: C–Me (Å) | 1.50(1)–1.53(1) | 1.49(2)–1.57(2) | – |
| Cp [a]: C–$^t$Bu (Å) | – | 1.50(2) | 1.522(7) |
| Fe–Cen (Å) | 1.737 | 1.741 | 1.731 |
| Fe–CO (Å) | 1.792(7) | 1.794(13) | 1.769(6) |
| C–O (Å) | 1.036(9) | 1.069(16) | 1.095(6) |
| Fe–I (Å) | 2.641(1) | 2.599(19) | 2.618(1) |
| Fe–P (Å) | 2.245(2) | 2.14(4) | 2.234(1) |
| Fe–C–O (deg) | 172.5(5) | 176.9(12) | 178.3(5) |
| Cen–Fe–CO (deg) | 121.2 | 122.1 | 127.2 |
| Cen–Fe–I (deg) | 121.6 | 122.1 | 120.0 |
| Cen–Fe–P (deg) | 128.3 | 125.9 | 123.1 |

[a] Cp = cyclopentadienyl
[b] C1–C2, 1.391(11); C2–C3, 1.374(13); C3–C4, 1.430(10); C4–C5, 1.383(11); C5–C1, 1.396(12).
[c] C1–C2, 1.427(15); C2–C3, 1.430(20); C3–C4, 1.409(15); C4–C5, 1.382(18); C5–C1, 1.504(17)

$2[Cp'Fe(CO)_2]\cdot \rightleftarrows [Cp'Fe(CO)_2]_2$, and

$[Cp'Fe(CO)_2]\cdot + L \rightarrow [Cp'Fe(CO)(L)]\cdot + CO$

etc., where $Cp = \eta^5\text{-}C_5H_5$ and $Cp' = \eta^5\text{-}C_5H_4Me$.

Successful synthesis of the *free tert*-butyltetramethylcyclopentadiene ligand was achieved in this study by the reduction of 2,3,4,5-tetramethylcyclopent-2-enone with $^t$BuLi at low temperature (−78°C), followed by hydration to the tertiary alcohol. Water was eliminated from this alcohol by acid-catalysed dehydration, to give the desired product. *Tert*-butyltetramethylcyclopentadiene was obtained as a light-yellow liquid after purification by column chromatography. Vacuum distillation led to decomposition of this material, with the formation of a very-high-boiling, darker residue over time.

$[(\eta^5\text{-}C_5Me_4^tBu)Fe(CO)_2]_2$ was obtained by the thermal reaction between $Fe(CO)_5$ and *tert*-butyltetramethylcyclopentadiene in octane. In contrast with the analogous tetramethylcyclopentadienyl dimer, $[(\eta^5\text{-}C_5Me_4{}^tBu)Fe(CO)_2]_2$ appeared to decompose very easily, especially in solution. Attempts to produce the dimer using $Fe_2(CO)_9$ at room temperature gave low yields of $[(\eta^5\text{-}C_5Me_4^tBu)Fe(CO)_2]_2$ together with large quantities of $Fe_3(CO)_{12}$ which proved difficult to remove from the dimer. The iodo derivative, $(\eta^5\text{-}C_5Me_4^tBu)Fe(CO)_2I$, was obtained from the dimer by standard procedures, as fluffy red-brown crystals, in high yield.

The ligand-substitution reaction, $(\eta^5\text{-}C_5Me_4^tBu)Fe(CO)_2I + L \rightarrow (\eta^5\text{-}C_5Me_4^tBu)Fe(CO)(L)I$ (L = $PPh_3$, $P(OMe)_3$ and $P(OPh)_3$), was attempted by the catalytic procedures described above for $(\eta^5\text{-}C_5Me_4H)Fe(CO)_2I$. This method only gave the required product for $L = P(OMe)_3$, and then only when the catalyst $[(\eta^5\text{-}C_5H_5)Fe(CO)_2]_2$ was used. The use of this catalyst in reactions with $L = PPh_3$ and $P(OPh)_3$ led mainly to the formation of $(\eta^5\text{-}C_5H_5)Fe(CO)(L)I$. However, the desired products of the carbonyl substitutions reactions, $(\eta^5\text{-}C_5Me_4^tBu)Fe(CO)(L)I$, were obtained successfully and cleanly when the reagents $(\eta^5\text{-}C_5Me_4{}^tBu)Fe(CO)_2I$ and L (L = $PPh_3$, $P(OMe)_3$ and $P(OPh)_3$) were reacted photochemically.

All the above complexes containing the $C_5Me_4H$ and $C_5Me_4^tBu$ rings were characterized by melting points, micro-analyses and IR and NMR spectroscopy. As expected, the carbonyl stretching frequencies in the infrared spectra of the complexes containing $C_5Me_4R$ rings occurred at higher wavenumbers for $C_5Me_4H$ than for $C_5Me_4^tBu$. X-Ray crystallographic studies on $[(\eta^5\text{-}C_5Me_4H)Fe(CO)(PPh_3)I$ and $(\eta^5\text{-}C_5Me^tBu)Fe(CO)(P(OPh)_3]I)]$ also confirmed the structures of the new complexes (see below).

NOE spectroscopy was also used to assign ring atoms (C and H) to specific resonances to enable conformational properties to be deduced.

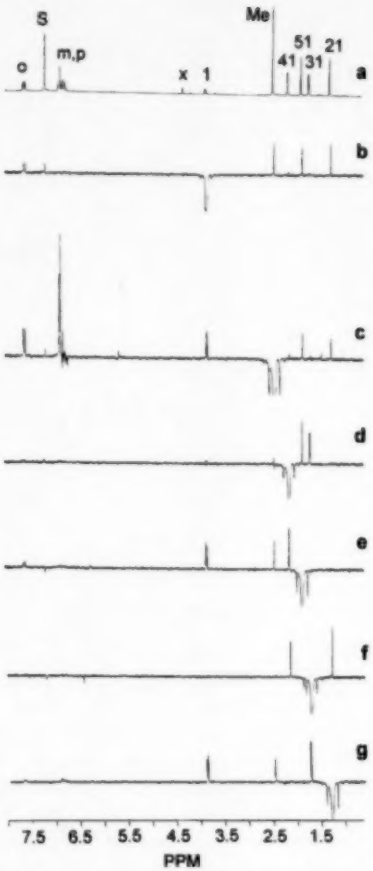


Fig. 4. NOE spectra for $(\eta^5\text{-}C_5Me_4H)Fe(CO)[P(O\text{-}o\text{-}Tol)_3]I$. Curve (a), non-irradiated spectrum: o, m, p, Me are the ortho-, meta-, para-hydrogen and methyl signals of $P(O\text{-}o\text{-}Tol)_3$, x is an impurity peak, S is the solvent (deuterated benzene) peak, 1, 21–51 are the cyclopentadienyl ring protons. Curves (b)–(g), irradiation of (b) $H_1$, (c) Me, (d) $H_{41}$, (e) $H_{51}$, (f) $H_{31}$, (g) $H_{21}$.

### 3.1.1. $(\eta^5\text{-}C_5Me_4H)Fe(CO)(L)I$

The $^1$H NMR spectra of the $(\eta^5\text{-}C_5Me_4H)Fe(CO)(L)I$ complexes (Table 3) show four separate resonances for the four methyl groups ($H_{21}$–$H_{51}$), and an additional absorption for $H_1$ (See Fig. 1 for cyclopentadienyl ring numbering scheme). A typical $^1$H NMR spectrum ($(\eta^5\text{-}C_5Me_4H)Fe(CO)[P(O\text{-}o\text{-}Tol)_3]I$) is shown in Fig. 4, curve (a). The four ring-methyl proton absorptions occur in the 1.0–2.1 ppm region, and are well separated, with up to three methyl groups coupled to phosphorus. Ring-methyl groups were assigned by means of NOE spectroscopy. For example, irradiation of the $H_1$ resonance led to the growth of two methyl group resonances only, and these can be assigned to the $H_{21}$ and $H_{51}$ protons (Fig. 4, curve (b)). The spectra of the complexes with $L = P(OMe)_3$, $PPh_3$, $P(O\text{-}o\text{-}Tol)_3$ and $PMe_3$

were also assigned by NOE spectroscopy, while, for $L = PBz_3$ and $P(O^iPr)_3$, assignments were made by comparison with the other spectra.

The chemical shift of $H_1$ reflects the electronic nature of L. When L is a phosphine, the chemical shift of $H_1$ occurs in the 2.70–3.35 ppm region, and, when L is a phosphite, $H_1$ is more deshielded, and its resonance occurs in the 3.78–4.19 ppm region.

Assignment of the four separate methyl-carbon resonances, $C_{21}$ to $C_{51}$ (Table 4), was achieved by the use of CH-correlated spectra. The ring carbons $C_1$ to $C_5$ appeared as five different resonance groups in the $^{13}C$ NMR spectra. The $C_1$ resonance could be recognized by its higher intensity relative to the other four resonances. However, since all four of the carbons $C_2$ to $C_5$ were attached to other carbon atoms ($C_{21}$ to $C_{51}$), CH-correlated spectra did not distinguish between the four different resonances. Hence definite assignment of $C_2$ to $C_5$ was not possible. Generally two of these resonances were coupled to the P atom of ligand, L, and two of them were not. Although it is tempting to use this coupling information to assign the $C_2$–$C_5$ resonances, the $^{13}C$ NMR data for the $(\eta^5\text{-}C_5H_4^tBu)Fe(CO)(L)I$ complexes has revealed that no simple correlation exists between phosphorus and the coupling of the cyclopentadienyl ring carbons [6].

We have shown previously that, for the $(\eta^5\text{-}C_5H_4^tBu)Fe(CO)(L)I$ series, a correlation exists between the size of L and the NMR parameter $\Delta(H_2\text{–}H_5)$. However, for both the $^1H$ and $^{13}C$ spectra of the $(\eta^5\text{-}C_5Me_4H)Fe(CO)(L)I$ complexes (Tables 3 and 4), no correlation could be obtained between the separation of the peaks and the steric size of the ligands L. This relates to the small spectral ranges in which their methyl resonances occur ($\delta$ 1.07–2.10 ppm for $H_{21}$–$H_{51}$ and $\delta$ 9.79–12.71 ppm for $C_{21}$–$C_{51}$). Similar observations were noted for related ruthenium complexes [30]. It is unfortunate that the resonances of $C_2$–$C_5$ could not be unequivocally assigned, since their proximity to L would make them much better at "sensing" the steric size of L. These resonances do indeed occur over a wide spectral range ($\delta$ 77.92–103.54 ppm).

### 3.1.2. $(\eta^5\text{-}C_5Me_4^tBu)Fe(CO)(L)I$

Assignments of the $^1H$ and $^{13}C$ NMR spectra for $(\eta^5\text{-}C_5Me_4^tBu)Fe(CO)(L)I$ were also deduced from NOE and CH-correlated spectra as outlined above. The $^1H$ NOE spectra for $(\eta^5\text{-}C_5Me_4^tBu)Fe(CO)\{P(OMe)_3\}I$ is discussed below. It is to be noted that in the non-irradiated $^1H$ NMR spectrum (Fig. 4, curve (a)) all four methyl resonances are distinct, again with coupling between only two of the methyl protons and the P atom of the ligand. The $^t$Bu group gives rise to a singlet in the same region as, and in some cases overlapping with, the methyl resonances. The methyl groups did not appear in a specific order in the spectra. Although the $H_{21}$–$H_{51}$ resonances of the complex with $L = PPh_3$ occurred over a larger range ($\delta$ 0.82–2.47 ppm), compared to the complexes with $L = P(OPh)_3$ and $P(OMe)_3$ ($\delta$ 1.60–2.26 ppm), the data set is too small to speculate about a correlation between the size of L and the separations between any of the ring resonances.

The chemical-shift positions of the $^t$Bu peaks of the $(\eta^5\text{-}C_5Me_4^tBu)Fe(CO)(L)I$ complexes can be compared to those of the $(\eta^5\text{-}C_5H_4^tBu)Fe(CO)(L)I$ complexes [6], for the same or very similar L. It was found that the $^t$Bu resonance in the $^1H$ NMR spectra appeared at higher chemical-shift positions for the $C_5Me_4^tBu$ complexes. The $^{13}C$ NMR resonances change in the same direction. This suggests that methyl substitution of the ring leads to *deshielding* of the $^t$Bu group, which is counter-intuitive. However, a possible explanation for this phenomenon is that the four electron-donating methyl groups on the cyclopentadienyl ring lead to increased $\pi$-bonding from the cyclopentadienyl ring to iron. Thus, electron density is withdrawn from the cyclopentadienyl ligand as a *whole*, including the attached $^t$Bu group.

## 3.2. Solution conformational studies

### 3.2.1. $(\eta^5\text{-}C_5Me_4H)Fe(CO)(L)I$

NOE spectroscopy was used to obtain the conformational preferences of these complexes. These were deduced from the relative growths of the $H_{21}$–$H_{51}$ absorptions when an L absorption was irradiated (Fig. 4, curve (c)), and the relative growths of the L peak when $H_{21}$ to $H_{51}$ were in turn irradiated (Fig. 4, curves (d)–(g)). It was found that L spent most of the time in the proximity of the smallest ring substituent, $H_1$ (percent enhancement = 8.0), and the Me groups adjacent to $H_1$ ($H_{21}$, percent enhancement = 1.0; $H_{51}$, percent enhancement = 1.4) (percent enhancements for $H_{31}$ and $H_{41}$ are 0.5 and 0.2 respectively). The NOE spectra of the other compounds ($L = PMe_3$, $P(OMe)_3$, $PPh_3$) showed that L was closest to $H_1$ and only *one* of the ring methyl groups, $H_{21}$. See Fig. 5(a) for the representation of the preferential conformer. Note that the protons on the methyl groups closest to the L group exhibit no coupling to P, whereas the "*trans*"-methyl protons ($H_{31}$, $H_{41}$) couple most strongly to P (Table 3).

### 3.2.2. $(\eta^5\text{-}C_5Me_4Bu')Fe(CO)(L)I$

The NOE spectra showed that the ligand set had definite conformational preferences with respect to orientation about the Fe-ring centroid axis. The spectra suggest that L spends most of its time away from the largest ring substituent, $^t$Bu. For example, Fig. 5(b) suggests that L is in the vicinity closest to $H_{31}$ and $H_{41}$ (percent enhancements, 2.0 each). The NOE experiments show that L is also close to $H_{51}$ (percent enhancement, 1.0), and that L lies away from $H_{21}$ and $^t$Bu (percent enhancements, 0.5 each). The NOE spectra of

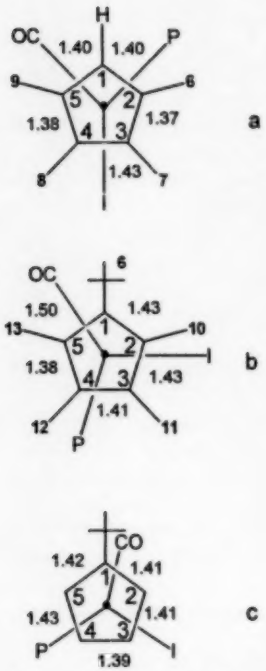


Fig. 5. Ligand conformational arrangement and crystal structural data for (a) **1**, (b) **2**, (c) **3** (C–C bond length data accuracy: see Table 8). The conformers shown correspond to those in Figs. 2–5 and Ref. [6], with the CO, P and L ligands *below* the ring plane.

the other compounds (L = $PPh_3$ and $P(OPh)_3$) also indicate conformations where L is closest to $H_{41}$ and away from $H_{21}$ and $^t$Bu. Fig. 5(b) represents this preferential conformer.

### *3.2.3. Comparison of the ($\eta^5$-$C_5H_4^tBu$)Fe(CO)(L)I, ($\eta^5$-$C_5Me_4H$)Fe(CO)(L)I and ($\eta^5$-$C_5Me_4^tBu$)Fe(CO)(L)I complexes*

The different electronic natures of the three different series of compounds are indicated by their IR spectra. For the same L groups, $\nu$(CO) decreases as more electron-donating groups are introduced onto the cyclopentadienyl ring, ($\eta^5$-$C_5H_4^tBu$)Fe(CO)(L)I > ($\eta^5$-$C_5Me_4H$)Fe(CO)(L)I > ($\eta^5$-$C_5Me_4^tBu$)Fe(CO)(L)I.

NMR spectra reveal that, in solution, all of the new complexes show conformations that reduce steric interactions between L and the ring atoms. The complexes containing the large $^t$Bu substituents on the cyclopentadienyl ring, ($\eta^5$-$C_5H_4^tBu$)Fe(CO)(L)I and ($\eta^5$-$C_5Me_4^tBu$)Fe(CO)(L)I, adopt conformations where the L group points away from this substituent. In the ($\eta^5$-$C_5Me_4H$)Fe(CO)(L)I complexes, the L group is found close to the H group, avoiding the four larger methyl groups on the cyclopentadienyl ring.

### *3.3. Solid-state structures and conformations*

Crystal structure determinations were carried out for ($\eta^5$-$C_5Me_4H$)Fe(CO)($PPh_3$)I (**1**) and ($\eta^5$-$C_5Me_4^tBu$)Fe(CO)[$P(OPh)_3$]I (**2**) to assess their solid-state conformations and to permit comparison with the known crystal structure of ($\eta^5$-$C_5H_4^tBu$)Fe(CO)($PPh_3$)I (**3**) [6]. The use of L = $PPh_3$ instead of L = $P(OPh)_3$ in **2** would have been preferable, and would have given a closer series of complexes Cp″Fe(CO)($PPh_3$)I (Cp″ = $\eta^5$-$C_5Me_4H$, $\eta^5$-$C_5Me_4^tBu$ and $\eta^5$-$C_5H_4^tBu$) for comparison. However, suitable crystals could not be obtained for ($\eta^5$-$C_5Me_4^tBu$)Fe(CO)($PPh_3$)I, and the crystal structure of ($\eta^5$-$C_5Me_4^tBu$)Fe(CO)[$P(OPh)_3$]I (**2**) was determined instead. The NMR spectra revealed similar solution conformers for ($\eta^5$-$C_5Me_4^tBu$)Fe(CO)(L)I (L = $PPh_3$ and $P(OPh)_3$), and thus the $P(OPh)_3$ complex should still provide the required information to compare the effects of variation of ring substituents on the solid-state conformers.

Comparisons between complexes **1** and **2** and a related complex ($\eta^5$-$C_5H_4^tBu$)Fe(CO)($PPh_3$)I (**3**) (Fig. 5) show that the magnitudes of various bond lengths and bond angles are comparable (see Table 8). Surprisingly, the electron-donating substituents had little effect on the observed Fe–Cen (Cen = cyclopentadienyl ring centroid) bond lengths, which are almost identical for **1**, **2** and **3**, and range from 1.731 to 1.737 to 1.741 Å. These values are comparable to Fe–Cen distances for other related complexes [31]. Similarly, the differences between C–O, Fe–CO and Fe–I bond lengths for **1**, **2** and **3** are small (C–O: 1.04(1), 1.07(2), 1.095(6) Å; Fe–CO: 1.792(7), 1.794(13), 1.769(6) Å; Fe–I: 2.642(1), 2.599(19), 2.618(1) Å. The Cen–Fe–L bond angles, where L = CO, I, $PPh_3$ or $P(OPh)_3$, did not change significantly with L in **1**, **2** and **3** (Cen–Fe–L bond angle range: 121.2, 122.1 and 127.2°).

As expected, the Fe–P bond length in **2** is shorter than that in **1** (Fe–P: **1**, 2.245(2) Å; **2**, 2.139(4) Å). This is related to the stronger metal-to-phosphorus backbonding in the $P(OPh)_3$ complex (**2**) compared to the $PPh_3$ complex (**1**).

The cyclopentadienyl C–C bond lengths show fairly significant deviations for both complexes **1** and **2**, indicating that cyclopentadienyl ring aromaticity has been disturbed (cyclopentadienyl C–C bond lengths: **1**, 1.37(1)–1.43(1); **2**, 1.38(2)–1.50(2)) (see Fig. 5).

In a recent publication [32] on $Cp^*Co(CO)_2$ complexes ($Cp^*$ = $\eta^5$-$C_5H_5$, $\eta^5$-$C_5Me_5$, $\eta^5$-$C_5Bz_5$), it was shown that the cyclopentadienyl C–C bonds which are eclipsed by carbonyl ligands (as viewed along the cyclopentadienyl centroid–metal axis) are longer, whereas the shortest bonds are those which are non-eclipsed [32]. Similarly, for **1**, **2** and **3**, the shortest cyclopentadienyl C–C bond lengths all pertain to bonds that are not eclipsed by any ligand and/or are adjacent to a bond

eclipsed by the phosphine or phosphite ligand (see Fig. 5).

The above discussion shows that there are no significant structural differences between **1**, **2** and **3** as reflected by bond length and angle data. Also, the bond length data (e.g. Fe–Cen distance) do not reflect any significant electronic differences between these complexes (see Table 8).

However, the different steric effects for these three complexes are reflected by the different arrangements of the ligand set relative to the cyclopentadienyl ring. In each case, the bulky $PPh_3$ or $P(OPh)_3$ ligand was positioned away from the largest cyclopentadienyl ring substituent(s). Hence in **1** the $PPh_3$ ligand is found close to the smallest cyclopentadienyl ring substituent, H. In **2** the $P(OPh)_3$ ligand is far from the largest cyclopentadienyl ring substituent $^t$Bu. A similar result was obtained for **3**, in which the $PPh_3$ ligand was positioned away from the large $^t$Bu substituent. This appears to be a very general phenomenon. Indeed a recent crystal structure determination of $(C_5Me_4H)_2TiCl_2$ also indicates that the smallest ring substituent occupies the least sterically hindered space [33]. The CO and I ligands did not adopt preferential positions.

Another possible indicator of the steric effects experienced by the cyclopentadienyl rings is the angle by which the cyclopentadienyl ring substituents (Me, $^t$Bu) deviate from the ring mean plane. In both **1** and **2** these angles are large [31] and in the direction away from the metal-ligand set (deviation angles: 3.2–9.7°).

In summary: the solution conformations are similar to those observed in the solid state.

## 4. Conclusions

As discussed above, NMR spectroscopy showed that $(\eta^5\text{-}C_5Me_4R)Fe(CO)(L)I$ (R = H, $^t$Bu) complexes displayed definite conformational preferences with regard to the position of the ligand set (CO, L and I) attached to iron, relative to the cyclopentadienyl ring substituents as viewed down the Fe-ring centroid axis. The conformational preferences were such that the relatively large phosphine and phosphite ligands on iron were positioned away from the largest substituents on the cyclopentadienyl ring. Thus for R = H, the L group was found close to R, while for R = $^t$Bu, the L group was found away from R. This can be rationalized in terms of steric interaction between L and the cyclopentadienyl ring substituents. The accommodation of the other ligands (CO and I) can be expected to lead to finer adjustments to the conformations. The molecular structures of $(\eta^5\text{-}C_5Me_4H)Fe(CO)(PPh_3)I$ and $(\eta^5\text{-}C_5Me_4\text{-}^tBu)Fe(CO)[P(OPh)_3]I$ were determined by X-ray crystallography. The conformations of these complexes in the solid state (with respect to the position of L) corresponded to those obtained in solution, showing that the preferred conformations are those where the L group is positioned in such a way as to avoid interaction with the larger cyclopentadienyl ring substituents.

## Acknowledgements

We wish to thank the University and the FRD for financial support.

## References

[1] (a) T.J. Kealy and P.L. Pauson, *Nature, 168* (1951) 1039; (b) S.A. Miller, J.A. Tebboth and J.F. Tremaine, *J. Chem. Soc.* (1952) 632.
[2] J. Okuda, E. Herdtweck and W.A. Herrmann, *Inorg. Chem., 27* (1988) 1254.
[3] N.J. Coville, K.E. du Plooy and W. Pickl, *Coord. Chem. Rev., 116* (1992) 1.
[4] R.B. King, in J.J. Eisch and R.B. King (eds.), *Organometallic Syntheses, Vol. I*, Academic Press, New York, 1965, pp. 94–95.
[5] (a) C. Janiak and H. Schumann, *Adv. Organomet. Chem., 33* (1991) 291; (b) R.B. King, *Coord. Chem. Rev., 20* (1976) 1554; (c) M.I. Bruce and A.H. White, *Aust. J. Chem., 43* (1990) 949; (d) J. Okuda, *Topics Curr. Chem., 160* (1992) 97; (e) R.L. Halterman, *Chem. Rev., 92* (1992) 965.
[6] K.E. du Plooy, C.F. Marais, L. Carlton, R. Hunter, J.C.A. Boeyens and N.J. Coville, *Inorg. Chem., 28* (1989) 3855.
[7] (a) C.H. Winter, X.-X. Zhou and M.J. Heeg, *Inorg. Chem., 31* (1992) 1808; (b) P. Jutzi, *Comments Inorg. Chem., 6* (1987) 123; (c) D.W. Slocum, M. Matusz, A. Clearfield, R. Peascoe and S.A. Duraj, *J. Macromol. Sci., Chem., A27* (1990) 1405.
[8] J.M. Manriquez, P.J. Fagan, L.D. Schertz and T.J. Marks, *Inorg. Synth., 28* (1990) 317.
[9] C.M. Fendrick, L.D. Schertz, V.W. Day and T.J. Marks, *Organometallics, 7* (1988) 1828.
[10] (a) H. van der Heijden, P. Pasman, E.J.M. de Boer, C.J. Schaverien and A.G. Orpen, *Organometallics, 8* (1989) 1459; (b) G. Jeske, L.E. Schock, P.N. Swepston, H. Schumann and T.J. Marks, *J. Am. Chem. Soc., 107* (1985) 8103; (c) A. Dormond, *J. Organomet. Chem., 256* (1983) 47; (d) E.A. Mintz, K.G. Moloy, T.J. Marks and V.W. Day, *J. Am. Chem. Soc., 104* (1982) 4692.
[11] P.A. Schofield, H. Adams, N.A. Bailey, E. Cesarotti and C. White, *J. Organomet. Chem., 412* (1991) 273.
[12] A. Dormond, A.E. Bouadili and C. Moise, *Tetrahedron Lett., 24* (1983) 3087.
[13] H.J. Scholtz and H. Werner, *J. Organomet. Chem., 303* (1986) C8.
[14] (a) J. Szymoniak, M.M. Kubicki, J. Besanson and C. Moise, *Inorg. Chim. Acta, 180* (1991) 153; (b) H. Tobita, H. Habazaki, M. Shimoi and H. Ogino, *Chem. Lett.* (1988) 1041.
[15] J. Okuda and K.H. Zimmermann, *Chem. Ber., 125* (1992) 637, and references cited therein.
[16] R.C. Hemond, R.P. Hughes and H.B. Locker, *Organometallics, 5* (1986) 2391.
[17] (a) A.N. Nesmeyanov, O.V. Nogina, G.I. Drogunova and B.V. Lokshin, *Izv. Akad. Nauk SSSR, Ser. Khim.*, (1973) 406; CA 79 (1973) 5433j; (b) O.V. Nogina, I.A. Uralets, G.I. Drogunova and N.S. Obezyuk, *Izv. Akad. Nauk SSSR, Ser. Khim.*, (1976) 150; CA 85 (1976) 21570f.

[18] J.A. Miguel-Garcia, H. Adams, N.A. Bailey and P.M. Maitlis, *J. Chem. Soc., Dalton Trans.* (1992) 131, and references cited therein.

[19] (a) D.S. Glueck and R.G. Bergman, *Organometallics, 9* (1990) 2862; (b) D.A. Straus, C. Zhang and T.D. Tilley, *J. Organomet. Chem., 369* (1989) C13; (c) H. Werner, G.T. Crisp, P.W. Jolly, H.-J. Kraus and C. Krüger, *Organometallics, 2* (1983) 1369, and references cited therein.

[20] (a) K. Mach, V. Varga, V. Hanuš and P. Sedmera, *J. Organomet. Chem., 415* (1991) 87; (b) L.J. Johnston and M.C. Baird, *J. Organomet. Chem., 358* (1988) 405.

[21] M.L.H. Green and R.B.A. Pardy, *J. Chem. Soc., Dalton Trans.* (1979) 355.

[22] (a) H. Schumann, H. Kucht, A. Dietrich and L. Esser, *Chem. Ber., 123* (1990) 1811; (b) D.M. Bensley and E.A. Mintz, *J. Organomet. Chem., 353* (1988) 93; (c) V.S. Kaganovich, A.R. Kudinov and M.I. Rubinskaya, *J. Organomet. Chem., 323* (1987) 111; (d) A.R. Bulls, J.E. Bercaw, J.M. Manriquez and M.E. Thompson, *Polyhedron, 7* (1988) 1409; (e) R.S. Threlkel and J.E. Bercaw, *J. Organomet. Chem., 136* (1977) 1; (f) C.P. Gibson, D.S. Bern, S.B. Falloon, T.K. Hitchens and J.E. Cortopassi, *Organometallics, 11* (1992) 1742.

[23] (a) J.F. Buzinkai and R.R. Schrock, *Inorg. Chem., 28* (1989) 2837, and references cited therein; (b) J.F. Buzinkai and R.R. Schrock, *Organometallics, 6* (1987) 1447, and references cited therein; (c) S.F. Pederson, R.R. Schrock, M.R. Churchill and H.J. Wasserman, *J. Am. Chem. Soc., 104* (1982) 6808.

[24] J. Okuda, R.C. Murray, J.C. Dewan and R.R. Schrock, *Organometallics, 5* (1986) 1681, and references cited therein.

[25] H. van der Heijden, A.W. Gal and P. Pasman, *Organometallics, 4* (1985) 1847.

[26] S.R. Hall, H.D. Flack and J.M. Stewart, XTAL 3.2 *Reference Manual*, Universities of Western Australia, Geneva and Maryland, 8th edn., 1992.

[27] E.J. Gabe, F.L. Lee and Y. Le Page, in G.M. Sheldrick, C. Kruger and R. Goddard (eds.), *Crystallographic Computing 3*, Clarendon, Oxford, UK, 1985.

[28] M. Sheldrick, in G.M. Sheldrick, C. Kruger and R. Goddard (eds.), *Crystallographic Computing 3*, Clarendon, Oxford, UK, 1985.

[29] C.K. Johnston, ORTEP, *Report ORNL-3794*, 1965 (Oak Ridge National Laboratory, Oak Ridge TN).

[30] M.S. Loonat, L. Carlton, J.C.A. Boeyens and N.J. Coville, *J. Chem. Soc., Dalton Trans.* (1989) 2407.

[31] N.J. Coville and K.E. du Plooy, *Inorg. Chim. Acta, 5* (1993) 209.

[32] M.Yu. Antipin, Yu.T. Struchkov, A.N. Chernega, M.F. Meidine and J.F. Nixon, *J. Organomet. Chem., 436* (1992) 60.

[33] S.I. Troganov, V.B. Rybakov, U. Thewalt, V. Varga and K. Mach, *J. Organomet. Chem., 447* (1993) 221.

ELSEVIER

Journal of Organometallic Chemistry 508 (1996) 243–248

Journal of Organometallic Chemistry

# Reactions of trimethylaluminium with aliphatic diols

W. Ziemkowska, S. Pasynkiewicz *

*Warsaw Technical University, Faculty of Chemistry, Koszykowa 75, 00-662 Warsaw, Poland*

Received 28 June 1995

**Abstract**

The reactions of trimethylaluminium with aliphatic diols, derivatives of 1,4-butandiol and 1,3-propandiol were studied. A mixtures of linear and cyclic organoaluminium compounds were the products of these reactions carried out for $AlMe_3$ : diol molar ratios of 3 : 2 or greater. One of the products isolated in all the studied reactions was a complex of a formula $Me_5Al_3[diol(-2H)]_2$ possessing one central five-coordinated aluminium atom and two terminal four-coordinated aluminium atoms. All the complexes were characterized by means of $^1H$, $^{13}C$ and $^{27}Al$ NMR spectra, elemental analysis and molecular weight determination.

*Keywords:* Aluminium; Aliphatic diols; Complexes; Spectroscopy; Isomers

## 1. Introduction

We have previously studied reactions of trimethylaluminium with *cis*-1,4-but-2-en-diol derivatives of a general formula **1** [1–3]:

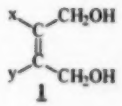

**1**

where x = y = H; x = $SiMe(OSiMe_3)_2$, y = H; x,y = –CH=CH–CH=CH–.

Complexes of the general formula **2** were one of the reaction products isolated and characterized by means of spectroscopic methods. These complexes possess one central five-coordinated aluminium and two terminal four-coordinated aluminium atoms.

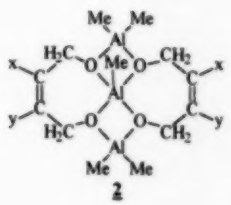

**2**

In this paper we present the results of our studies on the reactions of trimethylaluminium with saturated diols, derivatives of 1,4-butandiol and 1,3-propandiol. These diols do not possess a rigid C=C structure and can react with trimethylaluminium to form a mixture of linear and cyclic organoaluminium compounds. One of the products isolated in all of the studied reactions was a complex **3** of a structure analogues to the complex **2**.

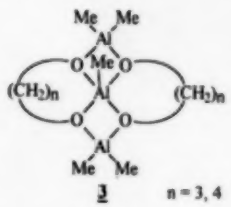

**3** n = 3, 4

## 2. Results

The reactions of trimethylaluminium with saturated diols were carried out at an $AlMe_3$ : diol molar ratio of 3 : 2, similarly to the previously studied reactions of trimethylaluminium with *cis*-1,4-but-2-en-diol derivatives.

Trimethylaluminium reacts with 1,4-butandiol to form a mixture of organoaluminium compound. The solid complex **4** was sublimed off from this mixture ($T$ = 100°C; $p = 1 \times 10^{-3}$ Torr; yield, 47%):

* Corresponding author.

0022-328X/96/$15.00 © 1996 Elsevier Science S.A. All rights reserved
*SSDI* 0022-328X(95)05856-7

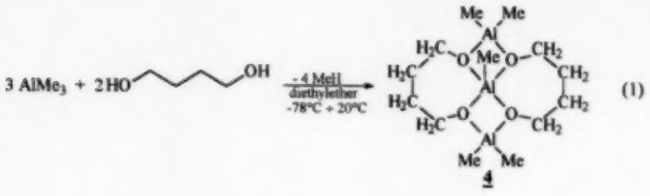


(1)

The $^{1}H$ NMR spectrum of **4** (Fig. 1) revealed two multiplets of $CH_2O$ and $CH_2$ protons and three singlets of the protons of methyl groups bonded to aluminium with a $-CH_2O-:-CH_2:CH_3Al$ integration ratio of 8:8:15 which was fully consistent with the structure **4**. The integration ratio of three singlets of methyl groups at −0.50, −0.56 and −0.57 ppm was 2:2:1. The first two of these signals were assigned to four methyl groups bonded to two four-coordinated aluminium atoms and a signal at −0.57 ppm corresponded to one methyl group bonded to the central five-coordinated aluminium atom.

The following signals were present in $^{13}C$ NMR spectrum: 62.42 ppm ($-CH_2O$), 30.61 ($-CH_2-$) and two broad signals at −10.83 ppm and −11.66 ppm $CH_3$ groups bonded to four- and five-coordinated aluminium atoms respectively. The presence of only one signal of $CH_2O$ carbon atoms and one signal of $CH_2$ carbon atoms is consistent with the proposed structure of **4**.

Two broad signals at 159.7 ppm and 74.0 ppm were present in the $^{27}Al$ NMR spectrum of **4**. The signal at 159.7 ppm appeared in the region characteristic for four-coordinated aluminium and the signal at 74.0 ppm in the region characteristic for five-coordinated aluminium.

The molecular weight of **4** determined cryoscopically was 335 (calculated, 332) which indicated an association degree equal to 1.0. Percentages of aluminium and methyl groups bonded to aluminium were very close to their theoretical values (see Section 4) which further confirmed the proposed structure of **4**.

Trimethylaluminium reacts with 1,3-propandiol to form **5** with a relatively low yield (8.5%):

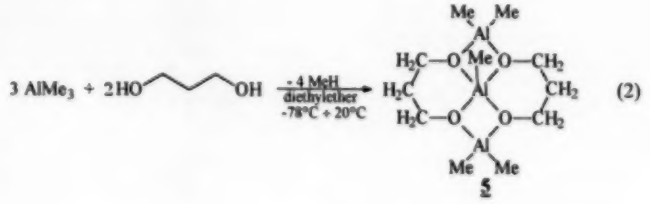


(2)

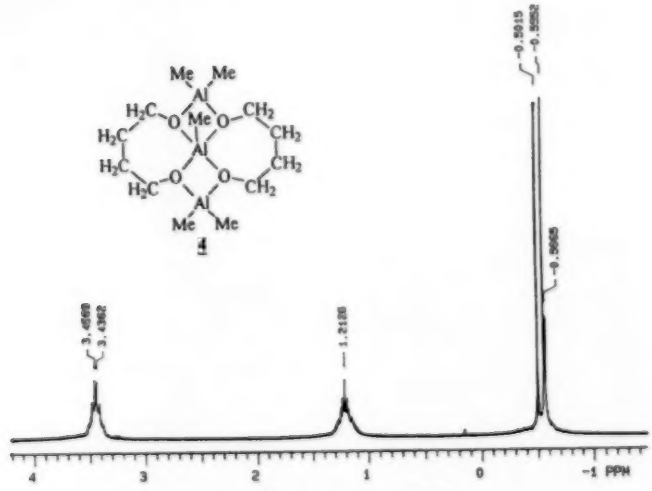


Fig. 1. $^{1}H$ NMR spectrum of **4**.

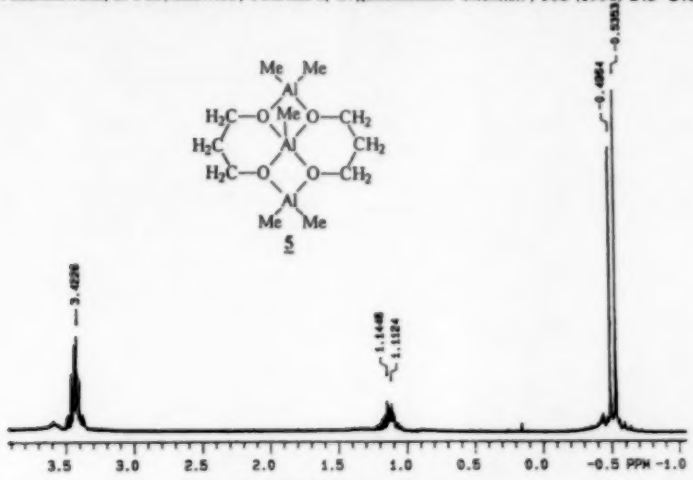


Fig. 2. $^1$H NMR spectrum of **5**.

The $^1$H NMR spectrum of **5** showed two multiplets of $CH_2O$ and $CH_2$ protons and two singlets (−0.50 and −0.54 ppm) of the protons of methyl groups bonded to aluminium with a $-CH_2O-:-CH_2-:CH_3Al$ integration ratio of 8:4:15 (Fig. 2) which was consistent with the proposed structure of **5**. The integration ratio of two singlets assigned to the protons of methyl groups was 2:3. The first signal at −0.50 ppm was assigned to the protons of two methyl groups bonded to the terminal four-coordinated aluminium and the second signal at −0.54 ppm was the result of overlapping of the signals of two methyl groups bonded to four-coordinated aluminium and of one methyl group bonded to five-coordinated aluminium. Two signals at 153.6 and 67.0 ppm were present in the $^{27}$Al NMR spectrum of **5** which confirmed the existence of two kinds of aluminium atoms (four- and five-coordinated). The association degree of **5** calculated on the basis of molecular weight measurements was 1.1.

The reaction of 2,2-dimethyl-1,3-propandiol with trimethylaluminium proceeds with the formation of a solid complex **6** with 7.2% yield:

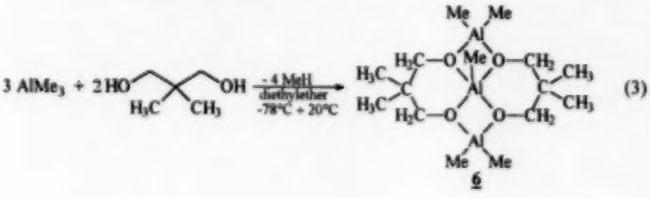


(3)

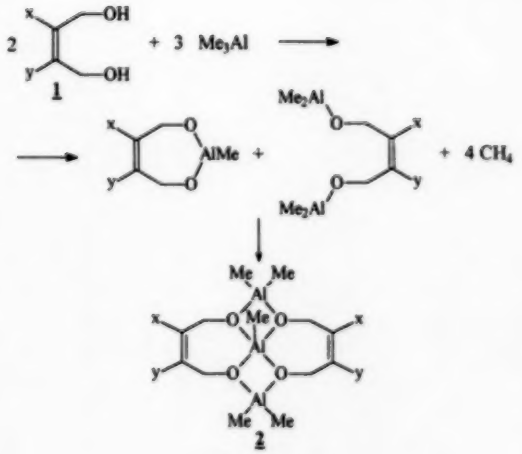


Scheme 1.

The complex **6** was isolated from the reaction mixture by sublimation ($T = 100$°C; $p = 1 \times 10^{-3}$ Torr) and was characterized by spectroscopic methods. The following signals were present in the $^1$H NMR spectrum of **6**: 3.34, 2.99 ppm (two doublets; $CH_2O$; $J = 10.4$ Hz), 0.91 ppm and 0.14 ppm (singlets, $CH_3$), −0.46, −0.52, −0.57 ppm (singlets, $CH_3Al$). The $-CH_2O-:CH_3:CH_3Al$ integration ratio was 8:12:15 which was fully consistent with the proposed structure of **6**. The signals of the protons of methyl groups bonded to aluminium were in the 2:2:1 ratio. The first two of them (−0.46 and −0.52 ppm) were assigned to four methyl groups bonded to four-coordinated terminal aluminium atoms and the third signal at −0.57 ppm was assigned to the methyl group bonded to the five-coordinated central aluminium atom.

Four sharp signals at 72.37 ppm ($CH_2O$), 34.43 ppm ($C(CH_3)_2$), 21.53 and 21.51 ppm ($CH_3$) and a very broad signal at −11.08 ppm ($AlCH_3$) were observed in the $^{13}C$ NMR spectrum of **6**. Similarly as for compounds **4** and **5** there were two broad signals at 156.0 and 68.6 ppm in the $^{27}Al$ NMR spectrum of **6**. They were assigned to four- and five-coordinated aluminium respectively. The compound **6** is monomeric in benzene as determined on the basis of molecular weight measurements.

1-Methyl-1,3-propandiol possesses a methyl group as a side chain and in the reaction with trimethylaluminium forms a mixture of six isomers of **7** with a total yield of 17.5%:

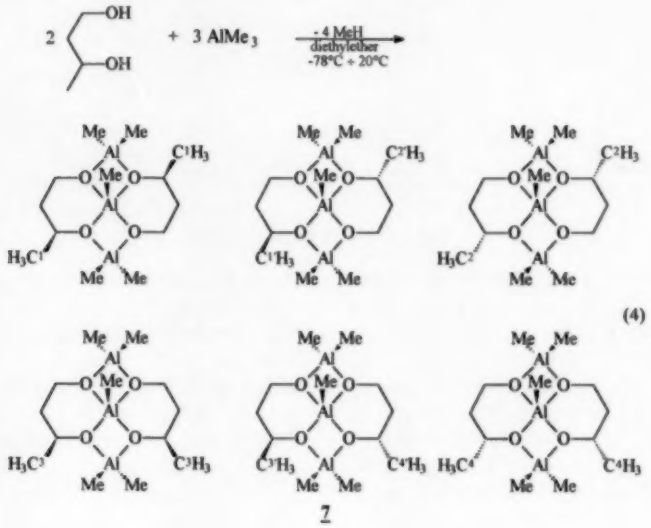


(4)

7

The mixture of isomers was isolated by distillation ($T = 100°C$; $p = 1 \times 10^{-3}$ Torr) as a colourless viscous liquid. An analysis of NMR spectra allowed us to propose the structure of the isomers. Most of the signals

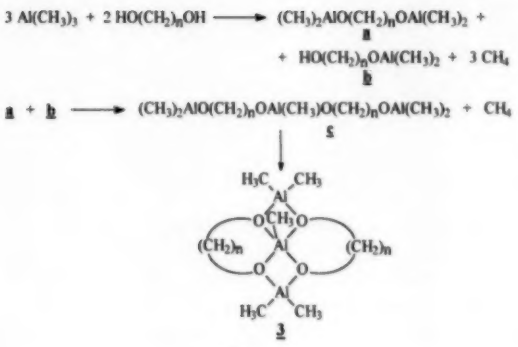


Scheme 2.

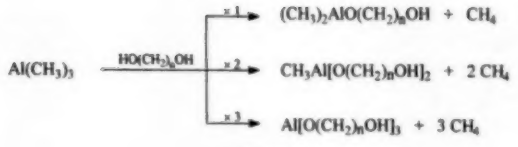


Scheme 3.

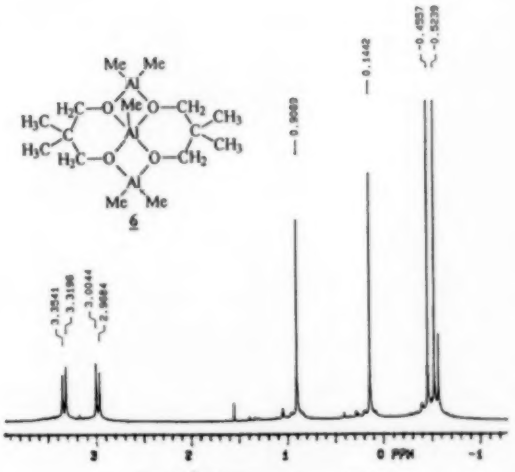


Fig. 3. $^1H$ NMR spectrum of **6**.

in the $^1$H NMR spectrum appeared as complex multiplets because of the number of isomers present in the mixture. Only protons of methyl groups $CH_3CH$ appeared as four doublets. The analysis of the structure of isomers indicated that they were eight different kinds of methyl group proton in the six isomers. It is very probable that chemical shifts of the protons of methyl groups numbered $C^1H_3$ and $C^{1\prime}H_3$, $C^2H_3$ and $C^{2\prime}H_3$, $C^3H_3$ and $C^{3\prime}H_3$, $C^4H_3$ and $C^{4\prime}H_3$ (Eq. (4)) are the same or very close to each other which causes overlapping of the signals and results in an appearance of only four doublets in the $^1$H NMR spectrum.

These methyl groups appear in the $^{13}$C NMR spectra as four signals at 38.39, 38.31, 36.92 and 36.76 ppm. The other carbon atoms in $CH_2$, HCO and $H_2CO$ show in $^{13}$C NMR four signals each. The carbon atoms of methyl groups bonded to aluminium appear as several overlapping signals which confirms the presence of the mixture of isomers of **7**.

There were two signals at 153.0 ppm and 67.2 ppm present in the $^{27}$Al NMR spectrum of **7** which indicated the presence of four- and five-coordinated aluminium in the molecule. Molecular weight determined cryoscopically in benzene indicated the monomeric structure of **7**.

## 3. Discussion

It appears from our previous studies [1–3] that trimethylaluminium reacts with *cis*-2-buten-1,4-diol derivatives of the general structure **1**, with an $AlMe_3$ : diol molar ratio of 3 : 2 or higher, to form complexes of the structure **2** with a high yield. All those diols possessed a double bond C=C with *cis* configuration of $CH_2OH$ groups, indicating a facile reaction with an excess of $AlMe_3$ according to Scheme 1.

In this work we have studied the reactions of trimethylaluminium with aliphatic diols possessing three and four carbon atoms. It was found that, besides oligomeric products, compounds of structure **3**, similar to structure **2**, were formed in these reactions. These compounds could be isolated by sublimation under reduced pressure. The results obtained suggest that aliphatic diols react with trimethylaluminium similarly as unsaturated diols to form analogues products (Scheme 2). The OH group of **b** reacts with **a** to form a linear compound **c** which stabilizes as **3** by the formation of acceptor–donor Al–O bonds.

The reactions of trimethylaluminium with aliphatic diols lead not only to the formation of **3** but also to the formation of oligomeric products, probably linear and cyclic. Trimethylaluminium can react with one, two or three molecules of aliphatic diols (Scheme 3). Products of these reactions can react further between themselves or with trimethylaluminium and diol, which leads to the formation of a mixture of oligomers.

## 4. Experimental details

All manipulations were carried out using standard Schlenk techniques in anhydrous solvents under an inert gas atmosphere.

$^1$H NMR spectra were recorded with a Varian VXR 300 spectrometer, at 299.9 MHz. Chemical shifts were referenced to the residual proton signal of $C_6D_6$ (7.15 ppm). $^{13}$C NMR spectra were run on the same instrument at 75.4 MHz (standard, benzene $^{13}CC_5D_6$, 128 ppm). $^{27}$Al spectra were run at 78.2 MHz (standard, $Al(acac)_3$, 0.0 ppm). The molecular weight of the complexes was determined by the cryoscopy in benzene.

### 4.1. Reaction of 1,4-butandiol with $AlMe_3$ (2 : 3)

1.260 g (14 mmol) of diol in 25 cm$^3$ of diethyl ether was placed in 250 cm$^3$ two-necked flask and cooled to −78°C. The solution of 1.548 g (21.5 mmol) of $AlMe_3$ in 20 cm$^3$ of diethyl ether was then added drop by drop within 0.5 h. The reaction mixture was allowed to warm to room temperature within 2 h. Evolution of gases was observed during the course of the reaction. The solvent was distilled off and the remaining white solid was sublimed ($T = 100$°C; $p = 1 \times 10^{-3}$ Torr) yielding 1.092 g (47%) of **4**.

$^1$H NMR (benzene-$d_6$): $\delta$ 3.45 (m, 8H, $CH_2O$), 1.21 (m, 8H, $CH_2$), −0.50 (s, 6H, $CH_3Al$), −0.56 (s, 6H, $CH_3Al$), −0.57 (s, 3H, $CH_3Al$) ppm. $^{13}$C NMR (benzene-$d_6$): $\delta$ 62.42($CH_2O$), 30.61 (–$CH_2$–), −10.83 ($CH_3Al$), −11.69 ($CH_3Al$) ppm. $^{27}$Al NMR (benzene-$d_6$): $\delta$ 159.7 (4-coord. Al), 74.0 (5-coord. Al) ppm. Molecular weight. Found: 335. Calc.: 332. Elemental anal. Found: Al, 24.50; hydrolysable methyl groups, 22.47. Calc.: Al, 24.40; Me, 22.59 wt.%.)

### 4.2. Reaction of 1,3-propandiol with $AlMe_3$ (2 : 3)

The reaction was carried out as described above using 1.216 g (16 mmol) of 1,3-propandiol and 1.764 g (24.5 mmol) of trimethylaluminium. 0.207 g (8.5%) of crystalline compound **3** was obtained by sublimation ($T = 95$°C; $p = 1 \times 10^{-3}$ Torr) from the post-reaction mixture.

$^1$H NMR (benzene-$d_6$): $\delta$ 3.43 (m, 8H, $CH_2O$), 1.13 (m, 4H, $CH_2$), −0.50(s, 6H, $CH_3Al$), −0.54(s, 9H, $CH_3Al$) ppm. $^{13}$C NMR (benzene-$d_6$): $\delta$ 63.08 (–$CH_2$–O), 31.24 (–$CH_2$–), −11.47 (Al–$CH_3$) ppm. $^{27}$Al NMR (benzene-$d_6$): $\delta$ 153.6 (4-coord. Al), 67.0 (5-coord. Al) ppm. Molecular weight. Found: 329. Calc.: 304. Elemental anal. Found: Al, 26.44; hydrolysable methyl groups, 25.20. Calc.: Al, 26.64; Me, 24.67 wt.%.

### 4.3. Reaction of 2,2-dimethyl-1,3-propandiol with $AlMe_3$ (2 : 3)

1.332 g (18.5 mmol) of trimethylaluminium in 25 cm$^3$ of diethyl ether was placed in 250 cm$^3$ two-necked

flask and cooled to −78°C. The solution of 1.248 g (12 mmol) of diol in 20 $cm^3$ of diethyl ether was then added drop by drop within 0.5 h. The reaction mixture was allowed to warm to room temperature within 2 h. Evolution of gases was observed during the course of the reaction. The solvent was distilled off and the remaining white solid was sublimed ($T = 100$°C; $p = 1 \times 10^{-3}$ Torr) to give 0.156 g (7.2%) of a solid compound **6**.

$^1$H NMR (benzene-$d_6$): δ 334 (d, $^2J = 10.4$ Hz, 4H, $CH_2O$), 2.99 (d, $^2J = 10.4$ Hz, 4H, $CH_2O$), 0.91 (s, 6H, $CH_3$), 0.14 (s, 6H, $CH_3C$), −0.46 (s, 6H, $CH_3Al$), −0.52 (s, 6H, $CH_3Al$), −0.57 (s, 3H, $CH_3Al$) ppm. $^{13}$C NMR (benzene-$d_6$): δ 72.37($CH_2O$), 34.43 ($C(CH_3)_2$), 21.53, 20.51 ($CH_3$), −11.08 ($CH_3Al$) ppm. $^{27}$Al NMR (benzene-$d_6$): δ 156.0 (4-coord. Al), 68.6 (5-coord. Al) ppm. Molecular weight. Found: 358. Calc.: 362.

### 4.4. Reaction of 1-methyl-1,3-propandiol with $AlMe_3$ (2:3)

The reaction was carried out as described in 4.1 using 1.080 g (12 mmol) of 1-methyl-1,3-propandiol and 1.332 g (18.5 mmol) of trimethylaluminium. 0.349 g (17.5%) of product **7** was distilled off ($T = 110$°C; $p = 1 \times 10^{-3}$ Torr) from the reaction mixture as a viscous colourless liquid.

$^1$H NMR (benzene-$d_6$): δ 3.75, (m, 2H, HCO), 3.44, (m, 4H, $CH_2O$), 1.39, 1.24, 0.95, 0.80 (four multiplets, 4H, $CH_2$), 1.002, 0.980, 0.965, 0.946 (four doublets, $^3J \approx 1.5$ Hz, 6H, $CH_3$), from −0.448 to −0.537 (several singlets, 15H, $CH_3Al$) ppm. $^{13}$C NMR (benzene-$d_6$): δ 70.67, 70.57, 70.38, 70.27 (HCO), 61.68, 61.50, 61.44, 61.22 ($H_2CO$), 30.39, 38.31, 36.92, 36.76($CH_3$), 24.17, 24.14, 23.72, 23.64 ($CH_2$) from −9.33 to −11.63 (several signals $CH_3Al$) ppm. $^{27}$Al NMR (benzene-$d_6$): δ 153.0 (4-coord. Al), 67.2 (5-coord. Al) ppm. Molecular weight. Found: 332. Calc.: 332. Elemental anal. Found: Al, 24.2; hydrolysable methyl groups, 22.1. Calc.: Al, 24.4; Me, 22.6 wt.%.

## Acknowledgement

The authors thank the State Committee for Scientific Research for financial support of this work (Grant 3 3413 92 03).

## References

[1] S. Pasynkiewicz and W. Ziemkowska, *J. Organomet. Chem., 423* (1992) 1.
[2] S. Pasynkiewicz and W. Ziemkowska, *J. Organomet. Chem., 437* (1992) 99.
[3] W. Ziemkowska, S. Pasynkiewicz and E. Kalbarczyk, *J. Organomet. Chem., 465* (1994) 93.

ELSEVIER

Journal of Organometallic Chemistry 508 (1996) 249–253

Journal of Organometallic Chemistry

# Synthesis, properties and crystal structure of bis(cyclopentadienyl)aluminium complex $[\eta^1\text{-}(C_5H_5)_2AlO\text{–}{}^iPr]_2$

A. Kunicki, R. Sadowski, J. Zachara

*Faculty of Chemistry, Warsaw Technical University, Koszykowa 75, 00-662 Warsaw, Poland*

Received 28 June 1995

**Abstract**

The reaction of $Cl_2AlO\text{–}{}^iPr$ with $C_5H_5Na$ affords the isopropoxy-bridged dimer $[\eta^1\text{-}(C_5H_5)_2AlO\text{–}{}^iPr]_2$. The compound has been characterized by NMR and its crystal structure determined by X-ray diffraction study.

*Keywords:* Aluminium; X-ray diffraction; Nuclear magnetic resonance; Cyclopentadienyl

## 1. Introduction

Cyclopentadienyl compounds of the main-group metals are of interest because of the variety of bonding modes that have been observed. Since the bonding modes influence the properties and reactions of the compounds, it is of importance to determine the nature of the interaction of the cyclopentadienyl groups with metal atoms.

Relatively few data have been given on structural characterisation of aluminium cyclopentadienyl complexes. Several dialkylaluminium and chloroalkylaluminium cyclopentadienyl complexes have only been studied by X-ray crystallography and electron diffraction [1–4]. The known monocyclopentadienylaluminium derivatives are highly fluxional and therefore no conclusive evidence can be drawn on their ground-state structure from IR and NMR spectra [4–7].

From X-ray analysis it has been established that dimethyl(cyclopentadienyl)aluminium in solid state consists of infinitive chains [1]. Dimethylaluminium units are bridged by cyclopentadienyl rings. The one length of the bridge bond anticipates for an electron deficient bond while the other is significantly longer. In the gas phase the compound has been found to be monomeric with cyclopentadienyl ring in $\eta^2$ fashion bonded to the aluminium atom [2]. The nature of the Cp–aluminium bond in hydrocarbon solutions of the compound is not clear. In benzene solution the degree of association of the compound is 1.4 [8]. An X-ray crystal structural study of chloro(pentamethylcyclopentadienyl)methylaluminium reveals dimeric units with Al–Cl bridge bonds [4]. The cyclopentadienyl groups are bonded to aluminium atoms in an $\eta^3$ manner.

To the best of our knowledge no structural information has been given on bis(cyclopentadienyl)aluminium derivatives. In this paper we describe the synthesis, characterization and a single-crystal X-ray diffraction analysis of the novel bis($\eta^1$-cyclopentadienyl)isopropoxide dimer $[\eta^1\text{-}(C_5H_5)_2AlO\text{–}{}^iPr]_2$.

## 2. Results and discussion

### 2.1. Synthesis, properties and NMR analysis

The title compound $[\eta^1\text{-}(C_5H_5)_2AlO\text{–}{}^iPr]_2$ **(I)** was obtained according to Eq. 1 at ambient temperature from the reaction of $Cl_2AlO\text{–}{}^iPr$ **(II)** with $C_5H_5Na$ **(III)** in toluene or a toluene-tetrahydrofuran (THF) mixture with a high yield.

$$2Cl_2AlO\text{–}{}^iPr + 4C_5H_5Na \rightarrow \underset{\textbf{(I)}}{\left[\eta^1\text{-}(C_5H_5)_2AlO\text{–}{}^iPr\right]_2} + 4NaCl \qquad (1)$$

The isopropoxyaluminium dichloride **(II)** was obtained from reaction of $MeAlCl_2$ with isopropoxy alcohol:

$$MeAlCl_2 + {}^iPrOH \rightarrow \underset{\textbf{(II)}}{Cl_2ArO\text{–}{}^iPr} + MeH \qquad (2)$$

0022-328X/96/$15.00 © 1996 Elsevier Science S.A. All rights reserved
*SSDI* 0022-328X(95)05857-5

The aluminium compound **II** formed in Eq. (2) was not isolated and used directly in the synthesis of bis(cyclopentadienyl)aluminium derivative **I**. $[\eta^1\text{-}(C_5H_5)_2AlO\text{–}{}^iPr]_2$ can be isolated as light-yellow crystals by recrystallization from a toluene–hexane mixture. As expected, **I** is quite air sensitive. In the presence of a slight amount of oxygen a brown solid is formed. An elemental analysis of the resulting compound confirms the formation of **I**. In benzene solution the compound was found to be a dimer ($n = 1.96$). The molecular weight was obtained cryometrically.

The $^1H$ and $^{13}C$ NMR spectra of **I** in deuterated benzene show signal pattern characteristic of the isopropoxy group in high field region and one signal of the cyclopentadienyl ligands in low one (see Section 3). The spectroscopic data are consistent with the proposed chemical formulation of the obtained compound; however, they did not permit us to determine the nature of the Cp bonding to the aluminium atom in a solution. Attempts to detect a static structure of **I** in toluene at $-70°C$ by $^1H$ NMR revealed no changes in signal pattern and no appreciable alteration in the ring proton atoms signal shape compared with the resonance signal width measured at room temperature. Similar dynamic behaviour has been reported for other cyclopentadienylaluminium compounds [4–7]. The equivalence of cyclopentadienyl proton atoms on the NMR time scale may results from rapid changes in aluminium atom-ring hapticity or rapid ring whizzing. The $^{27}Al$ NMR measurements of **I** showed a signal at 101.99 ppm.

No stable donor–acceptor complex was found to be formed in the reaction of **I** with excess of THF or diethyl ether in toluene. Reactions were carried out at room temperature. After removal of the solvents in vacuum the $^1H$ NMR spectra of crystalline residue showed no THF or $Et_2O$ signals but the signals of **I** only.

The reaction of **I** with $TiCl_4$ at room temperature in toluene afforded with a high yield $(C_5H_5)_2TiCl_2$ (**IV**):

$$2TiCl_4 + \left[\eta^1\text{-}(C_5H_5)_2AlO\text{–}{}^iPr\right]_2 \xrightarrow[(2)\ H_2O\text{–}HCl]{(1)\ \text{toluene}} \underset{\textbf{(IV)}}{2(C_5H_5)_2TiCl_2} \qquad (3)$$

The titanium compound **IV** was identified by $^1H$ NMR spectra and elemental analysis (see Section 3).

### 2.2. Crystal and molecular structure of $[\eta^1\text{-}(C_5H_5)_2\text{-}AlO\text{-}{}^iPr]_2$ (I)

A perspective view of the molecule with the atom numbering system is shown in Fig. 1.

The X-ray crystal structure analysis revealed the presence of isopropoxy-bridged dimers in a solid state (Fig. 1). The dimer is centrosymmetric and there are no short intermolecular contacts between dimers. Selected atomic bond distances and angles are presented in the Tables 1 and 2 respectively. The cyclopentadienyl groups are bonded to the Al atom in the $\eta^1$ manner. Examination of C–C distances in the cyclopentadienyl ring shows that are two shorter distances (C(12)–C(13), 1.347(4) Å; C(14)–C(15), 1.335(3) Å) with the remain-

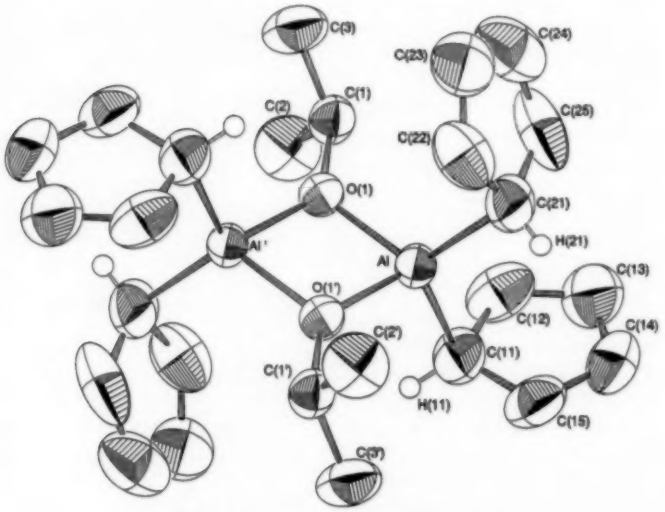


Fig. 1. Structure of **I** with the atom-numbering scheme.

Table 1
Selected bond lengths (Å) for $[\eta^1\text{-}(C_5H_5)_2AlO\text{–}^iPr]_2$

| | | | |
|---|---|---|---|
| Al–O(1) | 1.8212(11) | Al–O(1′) | 1.8370(11) |
| Al–C(21) | 2.003(2) | Al–C(11) | 2.022(2) |
| C(1)–C(2) | 1.493(6) | C(1)–C(3) | 1.508(5) |
| C(11)–C(15) | 1.429(3) | C(21)–C(22) | 1.434(3) |
| C(11)–C(12) | 1.441(3) | C(21)–C(25) | 1.444(4) |
| C(12)–C(13) | 1.347(4) | C(22)–C(23) | 1.342(4) |
| C(13)–C(14) | 1.386(4) | C(23)–C(24) | 1.378(4) |
| C(14)–C(15) | 1.335(3) | C(24)–C(25) | 1.310(4) |
| O(1)–C(1) | 1.473(2) | | |

Symmetry transformations used to generate equivalent atoms (designated by prime): $-x, -y, -z$.

ing distances as follows: C(11)–C(12), 1.441(3) Å; C(11)–C(15), 1.429(3) Å; C(13)–C(14), 1.386(4) Å. For the second cyclopentadienyl ring bonded to the same aluminium atom the distances are 1.342(4) Å, 1.310(4) Å, 1.434(3) Å, 1.444(4) Å and 1.378(4) Å respectively.

The cyclopentadienyl rings are almost flat; the rms deviations of the ring carbon atoms from mean least-square planes in both cases are 0.02 Å. A small fold of the rings along lines containing C(12), C(15) and C(22), C(25) respectively is observed. The dihedral angle between the C(12), C(11), C(15) plane and the C(12), C(13), C(14), C(15) plane is 5.2(2)° In the second ring the angle between the same sets of planes is 4.3(2)°. For both cyclopentadienyl rings there is one short aluminium atom–ring carbon atom distance: Al–C(11), 2.022(2) Å; Al–C(21), 2.003(2) Å. These distances fall within the range expected for Al–C bonding interaction in cyclopentadienyl aluminium compounds. The remaining aluminium–carbon ring distances are longer (e.g. Al–C(12), 2.693(2) Å; Al–C(15), 2.709(2) Å; Al–C(22), 2.802(2) Å; Al–C(25), 2.721(2) Å) compared with the accepted range of Al–C bonds and they are considered to be non-bonding distances. These data providing support for an $\eta^1$-$C_5H_5$–metal interaction. As mentioned earlier a cyclopentadienyl ligand is able to interact with aluminium atom in a different manner. It is likely that in **I** the bonding of Cp groups in $\eta^1$ fashion is derived from steric hindrance. In the dimeric structure of the studied compound **I**, each aluminium atom is surrounded by four bulky groups. The plane containing C(11), Al, C(21) is perpendicular to the plane of the four-membered $Al_2O_2$ ring. The $Al_2O_2$ four-membered ring is planar. The Al–O(1) and Al–O′(1′) bond lengths are 1.821(11) Å and 1.837(11) Å respectively. The bond angle of Al–O(1)–Al′ is 99.15(5)° and of O(1)–Al–O′(1′) is 80.85(5)°. The four-membered ring has been found to be a structural feature of the $Al_2(O\text{–}^tBu)_6$ [9].

## 3. Experimental details

### 3.1. General comments

All the reactions were carried out under dry argon using Schlenk techniques. Solvents were dried by standard methods. CpNa (**III**) was obtained from the reaction of freshly distilled CpH with NaH in THF and used directly in the synthesis of the aluminium compound. NMR spectra were run on Varian VXR-300 ($^1$H, $^{13}$C and $^{27}$Al).

### 3.2. Synthesis of $[\eta^1\text{-}(C_5H_5)_2AlO\text{–}^iPr]_2$

$^i$PrOH (6.42 ml, 84 mmol) was added slowly (0.5 h) to a stirred solution of $Cl_2AlMe$ (9.5 g, 84 mmol) in toluene (100 ml) cooled to −30°C. During the reaction, methane slowly evolved. The mixture was allowed to warm to ambient temperature (1 h) and then CpNa (15.0 g, 170 mmol) in THF (100 ml) added. The reaction mixture was stirred for 1 h; the solvent was removed in vacuo. A yellow residue was washed with pentane (30 ml) and dried in vacuo; extracted toluene (150 ml) was

Table 2
Selected bond angles (°) for $[\eta^1\text{-}(C_5H_5)_2AlO\text{–}^iPr]_2$

| | | | |
|---|---|---|---|
| O(1)–Al–O(1′) | 80.85(5) | Al–O(1)–Al′ | 99.15(5) |
| O(1)–Al–C(21) | 115.20(8) | O(1′)–Al–C(21) | 114.50(9) |
| O(1)–Al–C(11) | 111.96(8) | O(1′)–Al–C(11) | 109.63(8) |
| C(21)–Al–C(11) | 118.66(9) | C(2)–C(1)–C(3) | 112.5(5) |
| C(1)–O(1)–Al | 123.8(2) | C(1)–O(1)–Al′ | 137.0(2) |
| O(1)–C(1)–C(2) | 109.6(3) | O(1)–C(1)–C(3) | 109.2(3) |
| C(15)–C(11)–Al | 102.1(2) | C(25)–C(21)–Al | 103.0(2) |
| C(12)–C(11)–Al | 100.74(14) | C(22)–C(21)–Al | 108.07(14) |
| C(15)–C(11)–C(12) | 104.4(2) | C(22)–C(21)–C(25) | 103.4(2) |
| C(13)–C(12)–C(11) | 108.1(2) | C(23)–C(22)–C(21) | 108.1(3) |
| C(12)–C(13)–C(14) | 109.1(2) | C(22)–C(23)–C(24) | 109.6(3) |
| C(15)–C(14)–C(13) | 109.3(2) | C(25)–C(24)–C(23) | 109.2(3) |
| C(14)–C(15)–C(11) | 108.9(2) | C(24)–C(25)–C(21) | 109.5(3) |

Symmetry transformations used to generate equivalent atoms (designated by prime): $-x, -y, -z$.

Table 3
Crystal data and structure refinement for $[\eta^1\text{-}(C_5H_5)_2AlO\text{-}^iPr]_2$.

| | |
|---|---|
| Empirical formula | $C_{13}H_{17}AlO$ |
| Formula weight | 216.25 |
| Temperature (K) | 295(2) |
| Wavelength (Å) | 0.71073 |
| Crystal system | Monoclinic |
| Space group | $P2_1/n$ |
| Unit-cell dimensions | |
| $a$ (Å) | 8.710(2) |
| $b$ (Å) | 10.572(3) |
| $c$ (Å) | 13.193(3) |
| $\beta$ (Å) | 90.25(2) |
| Volume (Å$^3$) | 1214.9(5) |
| $Z$ | 4 |
| Density (calculated) (Mg m$^{-3}$) | 1.182 |
| Absorption coefficient (mm$^{-1}$) | 0.139 mm$^{-1}$ |
| $F(000)$ | 464 |
| Crystal size (mm) | 1.20×0.45×0.35 |
| $\theta$ range for data collection (°) | 2.5 to 25.0 |
| Index ranges | $0 \leqslant h \leqslant 10$, $0 \leqslant k \leqslant 12$, $-15 \leqslant l \leqslant 15$ |
| Number of reflections collected | 2282 |
| Number of independent reflections | 2134 ($R_{int}$ = 0.0135) |
| Refinement method | Full-matrix least-squares on $F^2$ |
| Number of data | 2117 |
| Number of restraints | 6 |
| Number of parameters | 224 |
| Goodness of fit on $F^2$ | 1.062 |
| Reflections with $I > 2\sigma(I)$ | 1845 |
| Final $R$ indices ($I > 2\sigma(I)$) | |
| $R_1$ | 0.0347 |
| $wR_2$ | 0.0965 |
| $R$ indices (all data) | |
| $R_1$ | 0.0409 |
| $wR_2$ | 0.1012 |
| Extinction coefficient | 0.004(2) |
| Largest difference peak and hole (electrons Å$^{-3}$) | 0.18 and −0.16 |

added. The toluene was evaporated in vacuo to give **I** as a light-yellow solid (yield, 14.7 g (81%)) which was crystallized from toluene–hexane.

Anal. found: C, 72.39; H, 7.98; Al, 12.33; $M_w$ (cryometrically in benzene) 423 ($n$ = 1.96). $C_{13}H_{17}OAl$ calc.: C, 72.22; H, 7.87; Al, 12.50%; $M_w$ = 216. $^1$H NMR ($C_6D_6$): $\delta$ 0.89 (d, $J$ = 6.3 Hz, 6H, $CH_3$), 3.68 (sep., $J$ = 6.3 Hz, 1H, CH), 6.11 (s, 10H, $C_5H_5$) ppm. $^{13}$C NMR ($C_6D_6$): $\delta$ 25.57 ($CH_3$), 70.19 (CH), 113.72 ($C_5H_5$) ppm. $^{27}$AlNMR ($C_6D_6$): $\delta$ 101.99 ppm.

### 3.3. Reaction of $[(\eta^1\text{-}C_5H_5)_2AlO\text{-}^iPr]_2$ (I) with $TiCl_4$

A solution of **I** (3.0 g, 13.8 mmol) in toluene (10 ml) was added to a stirred solution of $TiCl_4$ (2.64 g, 13.8 mmol) in toluene at room temperature. The red solution was stirred for 1 h and then a water–HCl mixture (20 ml) (5 : 1) added. More toluene was added, the toluene extract washed with water, dried, filtered and evaporated to dryness to give $(C_5H_5)_2TiCl_2$ as a red solid (yield, 2.61 g (76%)).

$^1$H NMR ($CDCl_3$): $\delta$ 6.57 (s, $C_5H_5$). Anal. Found: Cl, 28.11; Ti, 19.42. $C_{10}H_{10}Cl_2Ti$ calc.: Cl, 28.51; Ti, 19.27%.

### 3.4. X-ray structure determination

A transparent light-yellow well-shaped crystal of **I** was placed in a thin-walled capillary tube (Lindemann glass) in an inert atmosphere. The tube was plugged with grease, flame sealed and then mounted on the goniometer head of a four-circle P3 (Siemens AG) diffractometer. The crystallographic data, a summary of

Table 4
Atomic coordinates and equivalent isotropic displacement parameters for $[\eta^1\text{-}(C_5H_5)_2AlO\text{-}^iPr]_2$.

| | $x$ (×10$^{-4}$) | $y$ (×10$^{-4}$) | $z$ (×10$^{-4}$) | $U_{eq}$ (×10$^{-3}$ Å$^2$) | SOF |
|---|---|---|---|---|---|
| Al | 76(1) | 139(1) | 1049(1) | 45(1) | |
| O(1) | 840(1) | 876(1) | −91(1) | 45(1) | |
| C(1) | 1909(2) | 1955(2) | −79(3) | 51(1) | 0.890(11) |
| C(2) | 3451(5) | 1533(7) | −436(7) | 87(2) | 0.890(11) |
| C(3) | 1253(8) | 3008(4) | −718(6) | 83(2) | 0.890(11) |
| C(11) | 1696(3) | −857(2) | 1807(2) | 70(1) | |
| C(12) | 2662(3) | 151(2) | 2174(2) | 82(1) | |
| C(13) | 2316(4) | 358(3) | 3154(2) | 96(1) | |
| C(14) | 1224(3) | −515(2) | 3459(2) | 89(1) | |
| C(15) | 877(3) | −1273(2) | 2681(2) | 76(1) | |
| C(21) | −1387(3) | 1209(2) | 1843(2) | 79(1) | |
| C(22) | −2552(3) | 1661(3) | 1162(2) | 83(1) | |
| C(23) | −2263(3) | 2883(3) | 964(2) | 96(1) | |
| C(24) | −1010(4) | 3277(3) | 1521(3) | 103(1) | |
| C(25) | −495(3) | 2328(3) | 2064(2) | 99(1) | |
| C(1A) | 2001(20) | 1715(17) | −655(29) | 64(7) | 0.110(11) |
| C(2A) | 3546(23) | 1480(28) | −280(28) | 38(7) | 0.110(11) |
| C(3A) | 1473(39) | 3030(19) | −692(28) | 42(8) | 0.110(11) |

$U_{eq}$ is defined as one third of the trace of the orthogonalized $U_{ij}$ tensor.

data collection and the refinement procedure are presented in Table 3.

The crystal system, the orientation matrix and the unit-cell parameters were obtained from the least-squares refinement of the angular positions measured for 17 reflections randomly found in the $2\theta$ range between 15 and 31°. The intensities were collected up to $2\theta = 50°$ (maximum $(\sin\theta)/\lambda = 0.60$) in the $\theta$–$2\theta$ mode with the scan range 1.8° plus the $K\alpha_1$–$K\alpha_2$ separation at various scan speeds. Two check reflections $(31\bar{6})$ and $(22\bar{4})$, repeated every 70 reflections, showed a decay of 3.6%. The intensities were adjusted accordingly and corrected for the Lorentz–polarization effect. No absorption correction was applied. The phase problem was solved by direct methods using the SHELXS-86 program [10].

Positional and thermal parameters of the non-hydrogen atoms (first isotropic and then anisotropic) were adjusted by means of several rounds of full-matrix least-squares calculation [11]. The positions of the hydrogen atoms were determined on the subsequent difference Fourier map. We found disorder of isopropyl groups in the studied molecule. The low electron density maximum near the C(1) atom of the isopropyl group indicated that the group could flip between two positions. Because of this, further refinement was carried out for two isopropyl groups, assuming that the occupation factors of both groups added to unity. Owing to partial overlapping of the atoms of the disordered groups, geometrical restraints was introduced and only a secondary carbon atom of the second isopropyl group was refined anisotropically (site occupation factor was refined at a level of 11%). In the later iterations, hydrogen atoms of the second isopropyl group were incorporated at their calculated positions. An extinction correction was included as a variable in the final cycles. Final difference Fourier synthesis contained no unusual features. The structure was refined against $F^2$ with $w^{-1} = \delta^2(F_0^2) + (0.0601P)^2 + 0.1562P$ where $P = (F_0^2 + 2F_c^2)/3$. The $R$ values presented in Table 3 are defined as $wR_2 = (\sum w(F_0^2 - F_c^2)^2 / \sum wF_0^4)^{1/2}$ and $R1 = \sum ||F_0| - |F_c|| / \sum |F_0|$

Atomic coordinates and equivalent isotropic thermal parameters are listed in Table 4.

Tables of hydrogen atom coordinates and anisotropic thermal parameter and a complete list of bond lengths and angles have been deposited at the Cambridge Crystallographic Data Centre.

## Acknowledgements

The author thank the State Committee for Scientific Research for financial support of this work (Grant No 3 3413 92 03).

## References

[1] B. Teele, W.R. Corfield and J.P. Oliver, *Inorg. Chem., 21* (1982) 458.
[2] D. Drwa and A. Haaland, *Acta Chem. Scand., 27* (1973) 3735.
[3] P.R. Schonberg, R.T. Paine and C.F. Campana, *J. Am. Chem. Soc., 101* (1979) 7726.
[4] P.R. Schonberg, R.T. Paine, C.F. Campana and E.N. Duesler, *Organometallics, 1* (1982) 799.
[5] J. Stadelhofer, J. Weidlein and P. Fischer, *J. Organomet. Chem., 116* (1976) 55.
[6] J. Stadelhofer, J. Weidlein and A. Haaland, *J. Organomet. Chem., 84* (1975) C1.
[7] P. Fischer, J. Stadelhofer and J. Weidlein, *J. Organomet. Chem., 116* (1976) 65.
[8] A. Haaland and J. Weidlein, *J. Organomet. Chem., 40* (1972) 29.
[9] R.H. Cayton, M.H. Chisholm, E.R. Davidson, V.F. DiStasi, P. Du and J.C. Huffman, *Inorg. Chem., 30* (1991) 1020.
[10] G.M. Sheldrick, *Acta Crystallogr., Sect. A, 46* (1990) 467.
[11] G.M. Sheldrick, *SHELXL-93*, Universität Göttingen, Göttingen, 1993.

ELSEVIER

Journal of Organometallic Chemistry 508 (1996) 255–257

Journal of Organometallic Chemistry

# Palladium-catalyzed reaction of 1-aza-5-germa-5-organobicyclo[3.3.3]undecane with aryl bromide

Masanori Kosugi [a,*], Tadatoshi Tanji [a], Yukio Tanaka [a], Atsushi Yoshida [a], Keigo Fugami [a], Masayuki Kameyama [b], Toshihiko Migita [c]

[a] *Department of Chemistry, Gunma University, Kiryu, Gunma 376, Japan*
[b] *Oyama National College of Technology, Oyama, Tochigi 323, Japan*
[c] *School of High-Technology for Human Welfare, Tokai University, Numazu, Shizuoka 410-03, Japan*

Received 5 July 1995; in revised form 19 July 1995

**Abstract**

Successive treatment of triallylamine with zirconocene chloride hydride and germanium tetrachloride affords 1-aza-5-germa-5-chlorobicyclo[3.3.3]undecane, which is converted to the 5-organo derivatives by the reaction with Grignard or lithium reagents. The organo groups showed higher reactivities toward Stille-type coupling than the corresponding organotributylgermanes.

*Keywords:* Germanium; Cross-coupling; Palladium; Catalysis

Organostannane is one of the useful synthetic reagents for carbon–carbon bond formation. Transition-metal-catalyzed cross-coupling reaction of organostannane with organic halides or triflates is now widely utilized [1]. As for the organosilicon compounds, fluoride-ion-mediated palladium-catalyzed reactions have been recently developed [2]. Relatively few papers, however, have appeared for the palladium-catalyzed reactions of organogermanes [3]. To our knowledge, only the cross-coupling reaction of trimethylvinylgermane with aryl tetrafluoroborate is known [4]. From the observation of the silicon chemistry, the usual tetracoordinated organogermanium species are considered to be less reactive in the presence of a palladium catalyst. Therefore we intended to prepare 1-aza-5-germa-5-organobicyclo[3.3.3]undecane, expecting that reactivity of the organo group is enhanced by the transannular coordination of nitrogen to germanium. We now report the preparation of 1-aza-5-germa-5-organobicyclo-[3.3.3]undecane and the palladium-catalyzed reaction with aryl bromides. As the transmetalation of zirconium to germanium is known [5], we used a similar method to synthesize the corresponding tin compound reported by Vedejs et al. [6].

Thus hydrozirconation of triallylamine, followed by the transmetalation with germanium tetrachloride gave a novel 1-aza-5-germa-5-chlorobicyclo[3.3.3]undecane with 89% yield [7]. By the reaction with the corresponding Grignard or lithium reagents, it could be converted into the corresponding 5-organo compounds (yields; butyl, 74%; allyl, 82%; phenyl, 97%; vinyl, 98%; 1-ethoxyvinyl, 86%; phenylethynyl, 11%) [8].

First of all, the corresponding tributylgermanes were prepared and their palladium-catalyzed reaction with *p*-bromotoluene was investigated as a comparison with the reaction of the bicyclo germanium compounds. Most of the reactions did not give the cross-coupling products at all, except for the reaction of tributylvinylgermane, which afforded *p*-methylstyrene with 60% yield. The result can be explained from a similar palladium-catalyzed reaction of trimethylvinylsilane with aryl iodide [9].

Palladium-catalyzed reaction of 1-aza-5-germa-5-organobicyclo[3.3.3]undecanes thus prepared with aryl bromide was carried out as follows: a mixture of the germane (1 mmol) and the halide (1 mmol) in the presence of tris(dibenzylideneacetone)dipalladium chloroform (0.01 mmol) plus the phosphine (0.04 mmol) and tetrahydrofuran (1 ml) was sealed in vacuo in a glass ampoule and was heated in a thermobath at 120°C for 24 h. The product was analyzed by gas–liquid

* Corresponding author.

0022-328X/96/$15.00 © 1996 Elsevier Science S.A. All rights reserved
*SSDI* 0022-328X(95)05840-0

Table 1
Pd-catalyzed reaction of the bicyclogermane with *p*-bromotoluene

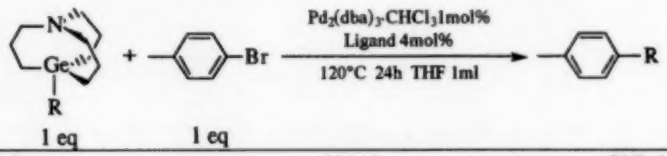


| Entry | R | Ligand | GLC yield [a] (%) |
|---|---|---|---|
| 1 | Butyl | $PPh(o\text{-tol})_2$ | 8 |
| 2 | Allyl [b] | $PPh_3$ | 88 (77) |
| 3 | Phenyl | $P(o\text{-tol})_3$ | 95 (85) |
| 4 | Vinyl | $P(o\text{-tol})_3$ | 82 |
| 5 | 1-Ethoxyvinyl [c] | $PPh(o\text{-tol})_2$ | 59 |
| 6 | Phenylethynyl | $PPh(o\text{-tol})_2$ | 67 |

[a] Isolated yield given in parentheses
[b] Bromobenzene was used as the aryl halide.
[c] The product was *p*-methylacetophenone.

chromatography (GLC) with *n*-dodecane as an internal standard. The product was isolated by silica gel chromatography, after aqueous work-up of the reaction mixture, followed by extraction with ether and dried over sodium sulfate. The results are shown in Table 1. As expected, cross-coupling products were obtained with moderate to good yield except for the butylation. It is interesting to note that generally the phosphine having the *o*-tolyl group gave products with a good yield. However, the allylation was the only exception, i.e. the use of triphenylphosphine gave a superior yield to that of tri(*o*-tolyl)phosphine. At present the reason for this is not known. Use of tri(2-furyl)phosphine or triphenylarsine, which are good ligands of palladium for the Stille-type coupling, [10] showed similar results when used triphenylphosphine.

Thus, we synthesized 1-aza-5-germa-5-organobucyclo[3.3.3]undecanes. In these compounds, a significant enhancement of reactivities of the organo groups toward Stille-type coupling was observed, in comparison with that of the corresponding organotributylgermanes, presumably owing to the transannular coordination of nitrogen to germanium, although the reactivity was not as great as that of the corresponding tributyltin compounds. Further work is in progress.

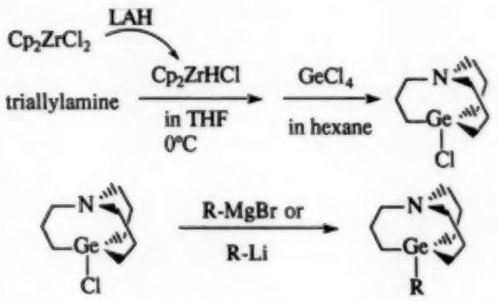


R = butyl, allyl, phenyl, vinyl, 1-ethoxyvinyl, phenylethynyl

## Acknowledgment

This work was supported by Grants-in-Aid for Scientific Research on Priority Area of Reactive Organometallics 05236101 and 05236102 from the Ministry of Education, Science and Culture, Japan.

## References and notes

[1] J.K. Stille, *Angew. Chem., Int. Edn. Engl.; 25* (1986) 508; T.N. Mitchell, *Synthesis*, (1992) 803, and references cited therein.
[2] Y. Hatanaka and T. Hiyama, *Synlett*, (1991) 845, and references cited therein.
[3] K. Yamamoto, A. Hayashi, S. Suzuki and J. Tsuji, *Organometallics, 6* (1987) 974; T. Tsumuraya and W. Ando, *Organometallics, 8* (1989) 2286; *9* (1990) 869; T. Hayashi, H. Yamashita, T. Sakakura, Y. Uchimaru and M. Tanaka, *Chem. Lett.*, (1991) 245; N.P. Reddy, T. Hayashi and M. Tanaka, *Chem. Lett.*, (1991) 677; K. Mochida, C. Hodota, H. Yamashita and M. Tanaka, *Chem. Lett.*, (1992) 1635; N. Chatani, N. Horiuchi and T. Hanafusa, *J. Org. Chem., 55* (1990) 3393; T.N. Mitchell, U. Schneider and B. Frohling, *J. Organomet. Chem., 384* (1990) C53.
[4] K. Ikenaga, S. Matsumoto, K. Kikukawa and T. Matsuda, *Chem. Lett.*, (1990) 185.
[5] A. Kanj, P. Meunier, B. Gautheron, J. Dubac and J.-C. Daran, *J. Organomet. Chem., 454* (1993) 51.
[6] E. Vedejs, A.R. Haight and W.O. Moss, *J. Am. Chem. Soc., 114* (1992) 6556.
[7] Colorless needles; melting point, 181.5–184.5°C. $^1H$ NMR ($CDCl_3$, 200 MHz) $\delta = 1.40$ (dd, $J = 7.0,6.6$ Hz, 6H,–$CH_2$–Ge–), 1.78 (dddd, $J = 7.0,6.6,6.2,5.7$ Hz, 6H,–$CH_2$–), 2.55

(dd, $J$ = 6.2, 5.8 Hz, 6H, $-CH_2-N-$). Gas chromatography–mass spectroscopy (70 eV): $m/e$ 250 ($M^+$), 214 ($M^+ - Cl$), 109, 84, 42. Anal. Found: C, 43.41; H, 7.05; N, 5.51. $C_9H_{18}NClGe$ calc.: C, 43.54; H, 7.31; N, 5.64%.

[8] Oily materials were obtained after usual work-up. Purified using gel permeation chromatography and showed satisfactory $^1H$ NMR spectra. For example, for butyl, $^1H$ NMR: $\delta$ 0.30–0.38 (m, 2H), 0.62(dd, $J$ = 6.6, 6.4 Hz, 6H), 0.81–0.89 (m, 3H), 1.20–1.28 (m, 4H), 1.46–1.58 (m, 6H), 2.40 (dd, $J$ = 5.9, 5.6 Hz, 6H) ppm. For allyl, $^1H$ NMR: $\delta$ 0.69 (dd, $J$ = 6.6, 6.4 Hz, 6H), 1.35 (dt, $J$ = 8.4, 1.4 Hz, 2H), 1.47–1.59 (m, 6H), 2.40 (dd, $J$ = 6.0, 5.6 Hz, 6H), 4.61 (dm, $J$ = 9.9 Hz, 1H), 4.68 (dm, $J$ = 16.9 Hz, 1H), 5.86(ddt, $J$ = 16.9, 9.9, 8.5 Hz, 1H) ppm. For phenyl, $^1H$ NMR: $\delta$ = 0.94 (dd, $J$ = 6.6, 6.4 Hz, 6H), 1.57–1.70 (m, 6H), 2.47 (dd, $J$ = 5.9, 5.7 Hz, 6H), 7.18–7.30 (m, 3H), 7.39–7.47 (m, 2H) ppm. For vinyl, $^1H$ NMR: $\delta$ = 0.75 (dd, $J$ = 6.6, 6.5 Hz, 6H), 1.49–1.62 (m, 6H), 2.42 (dd, $J$ = 5.9, 5.7 Hz, 6H), 5.42(dd, $J$ = 20.2, 4.0 Hz, 1H), 5.76 (dd, $J$ = 13.9, 4.0 Hz, 1H), 6.32 (dd, $J$ = 20.2, 13.9 Hz, 1H).

[9] A. Hallberg and C. Westerlund, *Chem. Lett.*, (1982) 1993.

[10] V. Farina and B. Krishnan, *J. Am. Chem. Soc., 113* (1991) 9585.

ELSEVIER

Journal of Organometallic Chemistry 508 (1996) 259–262

Journal of Organometallic Chemistry

# Electron density distribution in the vanadocene crystal on the basis of X-ray diffraction data at 108 K

M.Yu. Antipin [a,*], K.A. Lyssenko [a], R. Boese [b]

[a] *Institute of Organoelement Compounds Russian Academy of Sciences (INEOS), Vavilov St. 28, Moscow B-334, 117813, Russia*
[b] *Institüt für Anorganische Chemie der Universität-GH, Universitätsstr. 5–7, Essen, D-45117, Germany*

Received 14 July 1995

**Abstract**

Accurate molecular and crystal structure and experimental electron density distribution in the vanadocene single crystal were established on the basis of the precise X-ray diffraction data at 108 K. A characteristic asymmetry of the deformation electron density in the vicinity of the metal atom was found which is attributed to the different occupancies of the 3d-metal orbitals of the vanadium atom. A multipole analysis of the diffraction data was performed and the numerical values of the 3d-metal orbital occupancies in vanadocene were first calculated directly from these data. The results obtained are in agreement with the quantum-chemical calculations of vanadocene and other 3d-metallocenes.

*Keywords:* Vanadocene; X-ray structure; Charge density analysis

## 1. Introduction

3d-Metallocenes $Cp_2M$, where M = 3d-transition metal and $Cp = C_5H_5$ ligand, represent a very important class of organometallic compounds and the interest in their atomic and electronic structure still remains very high despite an almost 40 years history of these studies [1–9]. As an important result of these studies, a close structural similarity in the 3d-metallocenes was elucidated. Thus, the crystals of monoclinic $Cp_2Fe$, $Cp_2Co$, $Cp_2Ni$, and $Cp_2V$ were found to be isomorphous at room temperature and their crystal structures are very similar [10–13]. The electronic structure of the 3d-metallocene series may also be well explained in general features from the molecular-orbital (MO) diagram of ferrocene, the most important representative of these sandwich-like molecules, by subsequent removing of electrons from its occupied bonding and non-bonding $a_{1g}$ and $e_{2g}$ orbitals ($Cp_2Mn$, $Cp_2Cr$, $Cp_2V$), or adding electrons to the antibonding $e_{1g}$ orbital ($Cp_2Co$, $Cp_2Ni$) [14,15].

It is well established now, that direct information about electron density distribution in crystals may be obtained from precise X-ray diffraction data [16–18]. Nevertheless, the charge density analysis in the metallocene series was absent until now mainly due to the complicated nature of their crystal disorder [3–6], Jahn–Teller distorsions [19–21], and phase transitions on cooling the crystals [22,23]. We have found recently that the monoclinic structure of the vanadocene, $Cp_2V$ (**1**) is ordered at 108 K [24], and the first accurate electron density distribution study of the $Cp_2V$ crystal was undertaken at this temperature.

## 2. Results and discussion

The centrosymmetric $Cp_2V$ molecules in crystal have an ideal staggered conformation of the Cp-rings (Fig. 1), as was found earlier in the two X-ray structural studies of **1** at room temperature [12,13]. However, in these two studies an essential rotational disorder of the Cp-rings was noted that would forbid observation of accurate data on the molecular geometry and electron density distribution. The ordered nature of the $Cp_2V$ crystal structure at 108 K was proven in Ref. [24] by a careful analysis of the anisotropic displacement parameters. Thus, the largest eigenvalue $L_1$ of the molecular

* Corresponding author.

0022-328X/96/$15.00 © 1996 Elsevier Science S.A. All rights reserved
*SSDI* 0022-328X(95)05876-1

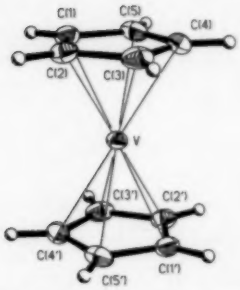


Fig. 1. General view of the vanadocene molecule in crystal with the representation of non-hydrogen atoms by the probability thermal ellipsoids ($p = 50\%$), and atom numbering scheme.

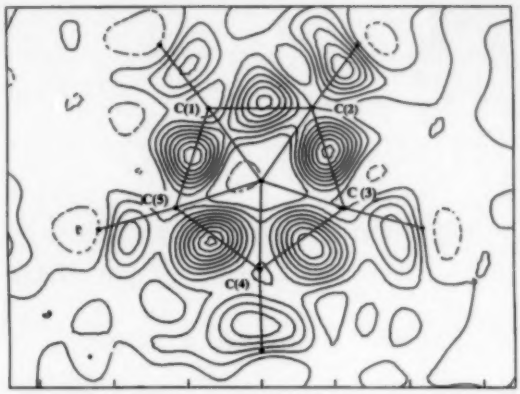


Fig. 2. Deformation electron density through Cp-ring plane. Contour intervals 0.05 e $Å^{-3}$, negative contours dashed.

libration tensor **L** in **1** was found to be 31°[2], that is the smallest value in the series of isomorphous $Cp_2Co$, $Cp_2Ni$, and $Cp_2V$ crystals at the same temperature.

The molecular geometry of **1** at 108 K is presented in Table 1. The V–C bond lengths are 2.260(1)–2.278(1) Å (mean value 2.269(6) Å) and C–C bond lengths 1.413(1)–1.423(1) Å (mean value 1.417(3) Å). The Cp-ring is planar within 0.001 Å and the distance from the metal atom to the ring center is 1.923 Å. These values, especially after correction for libration motion, are close to those found for vanadocene in the gas phase using the electron diffraction method: V–C 2.280(5) Å, C–C 1.434(3) Å, V-center of the ring 1.928(6) Å [25]. The C–H bond lengths are in the interval 0.94(2)–0.96(2) Å and displacements of these atoms from the carbon ring plane to the metal are small and hardly significant.

The deformation electron density (DED) map through the Cp-ring plane, obtained by a convential 'X–X' method, is shown in Fig. 2. Distinct positive DED peaks at the C–C bond centers and at the C–H bonds were found with the heights of 0.40–0.50 and 0.20–0.30 e $Å^{-3}$ respectively, indicating a rather good quality of the experimental data.

The typical DED section through the molecular symmetry plane, containing V, C(5), and C(5′) atoms, and the midpoints of the opposite C(2)–C(3) and C(2′)–C(3′) bonds of the ring is presented in Fig. 3. A characteristic asymmetry of the electron density distribution near the vanadium atom was observed, that is quite usual for transition metal complexes. In this section, two positive DED maxima with the heights of about 0.20 e $Å^{-3}$ are directed to the rings' centers, two other maxima being located in the V-containing plane almost parallel to the Cp-rings. The negative DED peaks (about −0.40 e $Å^{-3}$) were found along V–C and V-center C–C bond vectors. The general features of the DED maps through the other comparable sections were found to be almost the same. It is interesting to note some ellipticity of the DED sections through the middles of C–C bonds in the Fig. 3. This may reflect the contribution of the $\pi$-component in the corresponding bonds.

The section through the V-atom and parallel to Cp-ring planes is presented in Fig. 4. Four DED minima in the vicinity of the metal atom were located in this section together with the almost continuous 'ring-like' (centered at the V atom) distribution of the positive DED. The largest value of the DED maxima in this ring is equal to 0.35 e $Å^{-3}$. It should be noted that the DED picture near the metal atom in **1** is similar to that for centrosymmetrical triple-decker complex Cp–V–Bz–V–Cp (where $Bz = C_6H_6$) [16].

Table 1
Molecular geometry of vanadocene at 108 K (libration corrected bond lengths are also given)

| Bond | Bond length $d$ (Å) | Libration correction | Bond | Bond length $d$ (Å) | Libration correction | Bond | Angle (deg) |
|---|---|---|---|---|---|---|---|
| V–C(1) | 2.273(1) | 2.279 | C(1)–C(2) | 1.413(1) | 1.422 | C(2)–C(1)–C(5) | 108.5(1) |
| V–C(2) | 2.268(1) | 2.270 | C(2)–C(3) | 1.417(1) | 1.427 | C(1)–C(2)–C(3) | 107.7(1) |
| V–C(3) | 2.260(1) | 2.268 | C(3)–C(4) | 1.423(1) | 1.432 | C(2)–C(3)–C(4) | 108.1(1) |
| V–C(4) | 2.267(1) | 2.275 | C(4)–C(5) | 1.418(1) | 1.427 | C(3)–C(4)–C(5) | 107.7(1) |
| V–C(5) | 2.278(1) | 2.284 | C(1)–C(5) | 1.414(1) | 1.424 | C(1)–C(5)–C(4) | 108.0(1) |
| Mean | 2.269(6) | 2.275 | | 1.417(3) | 1.426 | Mean C–C–C | 108.0(3) |

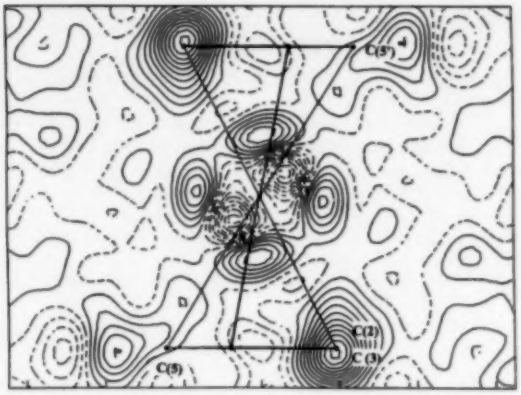


Fig. 3. DED section through the molecular symmetry plane, containing atoms V, C(5), C(5'), and midpoints of the opposite C(2)–C(3), and C(2')–C(3') bonds of the ring. Contours as in the Fig. 2.

The observed asphericity of the experimental DED distribution near the V-atom is caused by the preferential occupancy of the 3d-orbitals due to a relatively small overlap between the atomic 3d-metal and ligand orbitals, and agrees well with the MO treatment of the bonding in metallocenes. According to the numerous quantum-chemical calculations of these compounds (see for review in Ref. [15]), starting from the first MO calculation of the ferrocene by Shustorovitch and Dyatkina as early as 1961 [26], the metal 3d-orbitals, transforming as $e_{1g}$, $e_{2g}$, and $a_{1g}$ under axial molecular symmetry, will be split through the interaction with the corresponding ligand orbital combinations, and mainly metal 3d-molecular orbitals follow the sequence:

$$e_{2g}(d_{xy}, d_{x^2-y^2}) < a_{1g}(d_{z^2}) < e_{1g}(d_{xz,yz})$$

As a result, the $e_{1g}$ pair becomes antibonding, $e_{2g}$ bonding, and $a_{1g}$ nonbonding orbitals in 3d-metallocenes. It is essential that the $a_{1g}$ molecular orbital is localized at the metal atom with the pure $3d_{z^2}$ orbital contribution about 95%, but the metal contribution to the other $e_{2g}$ and $e_{1g}$ orbitals is smaller [15]. In accordance with this orbital sequence, the positive DED peaks directed to the ring centers (Fig. 3) should correspond to the occupied $3d_{z^2}$ orbital, and the 'ring-like' positive DED to the occupied $3d_{xy}$, and $3d_{x^2-y^2}$ orbitals, having essential atomic character.

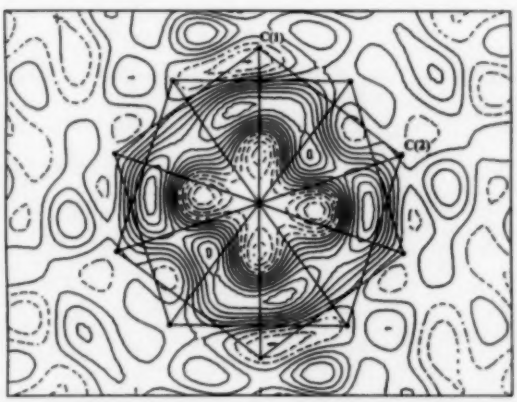


Fig. 4. DED section through V atom and parallel to Cp-ring plane. Contours as in the Fig. 2. The projection of the rings on this plane is shown for clarity with the C(1) and C(2) atoms numbering.

Table 2
3d-Occupancies in the vanadocene calculated from X-ray data in the multipole approximation

| d orbital | Population (e) | Population (%) |
|---|---|---|
| $d_{x^2-y^2}$ | 0.64(8) | 34 |
| $d_{xz} + d_{yz}$ | 0.00(3) | 0 |
| $d_{xy}$ | 0.60(5) | 32 |
| $d_{z^2}$ | 0.64(7) | 34 |

It is known, that numerical characteristics of the 3d-orbital occupancies of the central atom in the transition metal complexes may be evaluated from the analysis of X-ray diffraction data via refinement of these data in the multipole approximation [27,28]. This approach was used in the present paper for **1**, and results of the analysis are given in Table 2.

The results obtained agree well with the general features of the DED maps (see Figs. 3 and 4), and with other experimental and quantum-chemical data for vanadocene [29,30]. According to the electron density maps and multipole analysis, the ground state of the metal atom in **1** is the high-spin $^4A_{2g}$ one; that is in agreement with the spectral data (see Refs. [14,15]). The depopulation of the 3d-electron density in complex **1** should be noted. The total number of 3d-electrons is 1.88(7) instead of 3.0 for the spherical atom, and the most depopulated ones in comparison with the spherical atom are the $e_{1g}$ orbitals. This result was also mentioned for other 3d-metal complexes [28], and it may reflect some contribution of the covalent metal–ligand interaction. Thus, very recent valence level photoelectron cross-sections data for 3d-metallocenes, including vanadocene, give evidence for 3d-orbital covalency in the $e_{1g}$ orbitals [31]. For molecule **1**, the so-called back $\pi$-donation from the metal to the ligand may also be important.

## 3. Experimental and calculation details

Experimental diffraction data were obtained at 108 K for a single crystal of **1** with the linear dimensions about $0.3 \times 0.3 \times 0.3$ mm$^3$ using a four-circle Nicolet R3m/V diffractometer (monochromatized Mo K$\alpha$ radiation).

Crystals of **1** are monoclinic at 108 K: $a = 5.7208(6)$, $b = 8.211(1)$, $c = 8.831(1)$ Å $\beta = 90.94(1)°$, $V = 414.77(9)$ Å$^3$, $Z = 4$, space group $P2_1/n$.

The total number of 7105 reflections were measured using Wyckoff-type scan in the full sphere of the reciprocal space with $2\theta < 90°$. After averaging the data ($R_{int} = 0.025$) and empirical absorption correction (the min/max transmission coefficients were found to be 0.82/0.95), 2783 independent observed reflections with $|F| > 4.0\ \sigma(F)$ were used in the structure refinement by a full-matrix least squares to the final values of $R = 0.032$, $R_w = 0.038$, and GOF = 1.15 in the anisotropic–isotropic (H atoms) approximation. The quasi-high-order refinement using the weighting scheme of Dunitz and Seiler [32] with the $B = 5.0$ converged at $R = 0.031$, $R_w = 0.036$, and GOF = 1.18; H-atom parameters during this procedure were fixed. The high-order refinement of the structure using diffraction data with $\sin\theta/\lambda > 0.65$ Å$^{-1}$ was also carried out, and resulted in nearly the same atomic parameters as previous ones. DED maps were obtained with a conventional 'X–X' method using high-order refined atomic model and low-angle diffraction data ($\sin\theta/\lambda < 0.70$ Å$^{-1}$). All calculations were made with Micro-VAX-II computer using SHELXTL PLUS programs.

The multipole calculations were performed using the MOLLY program, adapted for a personal computer. The multipole population parameters were refined up to hexadecapole level ($l = 4$) for V and C atoms, and dipole level ($l = 2$) for H atoms with the inclusion the metal 4s-orbital contribution to the X-ray scattering; that resulted in the lowest $R$-values and goodness of fit ($R = 0.017$, $R_w = 0.027$, GOF = 0.98). The obtained multipole population coefficients were recalculated to the d-electron orbital occupancies using the procedure described in Ref. [28].

## Acknowledgments

This work was supported in part (M.Y.A. and K.A.L.) by the International Science Foundation (Grant M1F300). The authors are grateful to Professor Y.T. Struchkov (INEOS, Moscow) for his interest in this work.

## References

[1] J.D. Dunitz and L.E. Orgel, *Nature, 171* (1953) 121.
[2] J.D. Dunitz, L.E. Orgel and A. Rich, *Acta Crystallogr., 9* (1956) 373.
[3] P. Seiler and J.D. Dunitz, *Acta Crystallogr. B, 35* (1979) 1068.
[4] P. Seiler and J.D. Dunitz, *Acta Crystallogr. B, 35* (1979) 2020.
[5] P. Seiler and J.D. Dunitz, *Acta Crystallogr. B, 36* (1980) 2255.
[6] M.Yu. Antipin, R. Boese, N. Augart and G. Schmidt, *Struct. Chem., 4* (1993) 91.
[7] D. Braga and F. Grepioni, *Organometallics, 11* (1992) 711.
[8] D. Braga, *Chem. Rev., 92* (1992) 633.
[9] T.N. Doman, C.R. Landis and B. Bosnich, *J. Am. Chem. Soc., 114* (1992) 7264.
[10] W. Pfab and E.O. Fischer, *Z. Anorg. Allg. Chem., 274* (1953) 316.
[11] E. Weiss and E.O. Fischer, *Z. Anorg. Allg. Chem., 278* (1955) 219.
[12] M.Yu. Antipin, E.B. Lobkovsky, K.N. Semenenko et al., *Zh. Strukt. Khim., USSR, 20* (1979) 942.
[13] R.D. Rogers, J.L. Atwood, D. Foust and M.D. Rausch, *J. Cryst. Mol. Struct., 11* (1981) 183.
[14] A. Haaland, *Acc. Chem. Res., 12* (1979) 415.
[15] D.W. Clark and K.D. Warren, *Struct. Bonding, 39* (1980) 1.
[16] K. Angermund, K.H. Claus, R. Goddard and C. Cruger, *Angew. Chem., Int. Ed. Engl., 24* (1985) 237.
[17] P. Coppens, *Ann. Rev. Phys. Chem., 43* (1992) 663.
[18] G.A. Jeffrey and J.F. Piniella, *The Application of Charge Density Research to Chemistry and Drug Design*, Plenum, New York, 1991.
[19] J.H. Ammeter, N. Oswald and R. Bucher, *Helv. Chim. Acta, 58* (1975) 671.
[20] H. Eicher and H. Kohler, *Chem. Phys., 128* (1988) 297.
[21] R. Rai, *Physica B, 150* (1988) 414.
[22] J.W. Edwards, G.L. Kington and R. Mason, *Trans. Faraday, Soc., 56* (1960) 660.
[23] C. Sourisseau, G. Luccazeau, J.J. Dianoux and C. Poinsignon, *Mol. Phys., 48* (1983) 1367.
[24] M.Yu. Antipin and R. Boese, *Acta Crystallogr. B*, in press.
[25] E. Gard, A. Haaland, D.P. Novak and R. Seip, *J. Organomet. Chem., 88* (1975) 181.
[26] E.M. Shustorovitch and M.E. Dyatkina, *Zh. Strukt. Khim., USSR, 2* (1961) 49.
[27] N.K. Hansen and P. Coppens, *Acta Crystallogr. A, 34* (1978) 909.
[28] A. Holladay, P. Leung and P. Coppens, *Acta Crystallogr. A, 39* (1983) 377.
[29] R. Prins and J.D.W. van Voorst, *J. Chem. Phys., 49* (1968) 4665.
[30] D.R. Armstrong, R. Fortune and P.G. Perkins, *J. Organomet. Chem., 111* (1976) 197.
[31] J. Breeman, G. Cooper, J.C. Green et al., *J. Electron Spectrosc. Relat. Phenom., 66* (1–2) (1993) 101.
[32] J.D. Dunitz and P. Seiler, *Acta Crystallogr. B, 29* (1973) 589.

ELSEVIER

Journal of Organometallic Chemistry 508 (1996) 263–265

Journal of Organometallic Chemistry

Preliminary communication

# Hydride abstraction from ($\eta^2$-acetaldehyde)zirconocene dimer using $B(C_6F_5)_3$

Dirk Röttger, Stefanie Schmuck, Gerhard Erker *

*Organisch-Chemisches Institut der Universität Münster, Corrensstrasse 40, D-48149 Münster, Germany*

Received 27 June 1995

**Abstract**

$B(C_6F_5)_3$ reacts with the ($\eta^2$-acetaldehyde)zirconocene dimer (**4**) by hydride transfer from the methyl group of a $CH_3CHO$ ligand to boron. One of the metallaoxirane moieties of the dizirconium complex is then opened to give the salt $[(\eta^2\text{-}CH_3CHO)ZrCp_2 \cdot (H_2C{=}CHO)ZrCp_2]^+[HB(C_6F_5)_3]^-$ (**6**) that was isolated with an 80% yield.

*Keywords:* Aldehyde; Early transition metals; Group 4; Hydride; Zirconium

Under thermodynamic control ($\eta^2$-formaldehyde)-zirconocene forms a cyclic trimer that contains a central six-membered ring of alternating oxygen and zirconium atoms to three edges of which methylene groups are attached [1]. Under kinetic control the usually applied synthetic entry to the $[(\eta^2\text{-}CH_2O)ZrCp_2]_n$ complexes yields a corresponding cyclodimer (**2**) [2]. Here the $CH_2$ groups are attached to the edges of a central $Zr_2O_2$ four-membered metaloxide ring. These polymetallacycles have been used as molecular Fischer–Tropsch models. The $CH_2$ groups of for example **2** can be oligomerized by adding a trialkylborane catalyst [3]. In addition, many insertion reactions into the reactive Zr–$CH_2$ bonds of **2** have been realized [4]. The pronounced metallaoxirane character of the structural subunits of **2** was also utilized in a variety of ($\eta^2$-formaldehyde)-zirconocene transfer reactions leading to novel organometallic substrates [5] (for selected examples see Scheme 1).

In a similar way we have recently prepared the ($\eta^2$-acetaldehyde)zirconocene dimers (**4**). In this case a mixture of two diastereoisomers is obtained (of $C_1$ and $C_2$-symmetry respectively, in a 1.7 : 1 ratio under thermodynamic control). The dimetallatricyclic systems of **4** also contain reactive zirconium to carbon σ bonds that undergo the typical insertion chemistry [6]. In addition, the presence of methyl groups at the metallaoxirane rings allows for some reactions that have not been observed for the unsubstituted parent system **2**. These seem to make use of some typical "cyclopropane character" of the three-membered metallacyclic ring system in such Group 4 organometallic systems. We here describe a typical example, namely the reaction of the ($\eta^2$-acetaldehyde)zirconocene dimers **4** with the strong Lewis acid $B(C_6F_5)_3$ (Scheme 2).

The ($\eta^2$-acetaldehyde)zirconocene dimer (**4**) (kinetic 1 : 1.5 mixture of the *trans* and *cis* diastereoisomers) was dissolved in toluene and then treated with approximately twofold molar excess of tris(pentafluorophenyl)-borane at room temperature. The product precipitated from the solution and was isolated as an orange–yellow solid (**6**), yield about 500 mg (80%); melting point (differential scanning calorimetry), 47°C (decomposition). Anal. Found: C, 47.69, H, 2.90. $C_{42}H_{28}BF_{15}O_2Zr_2$ calc.: (1042.9) C 48.37, H 2.71%. The $^{11}B$ NMR spectrum (d, $^1J_{BH} = 90$ Hz at −25.5 ppm in $CD_2Cl_2$ solution at 64.2 MHz, 300 K) and the IR spectrum ($\nu_{(B-H)} = 2377$ cm$^{-1}$) revealed the presence of the hydridotris(pentafluorophenyl)borate anion [7,8]. The IR spectrum exhibits additional strong features at $\tilde{\nu} = 3121$, 2970, 2914, 2875, 1641, 1616, 1510, 1461, 1371, 1272, 1158, 1150, 1103, 1080, 1019, 976 and 813 cm$^{-1}$.

The newly formed compound **6** still contains one intact ($\eta^2$-acetaldehyde)zirconocene moiety inside the framework of the cationic dizirconocene complex. This is evident from the $^1H$ and $^{13}C$ NMR features of the $CH_3CHO$ group. $^1H$ NMR: $\delta$ 1.88 (d, $^3J = 6.2$ Hz, 3H,

* Corresponding author.

0022-328X/96/$15.00 © 1996 Elsevier Science S.A. All rights reserved
*SSDI* 0022-328X(95)05852-4

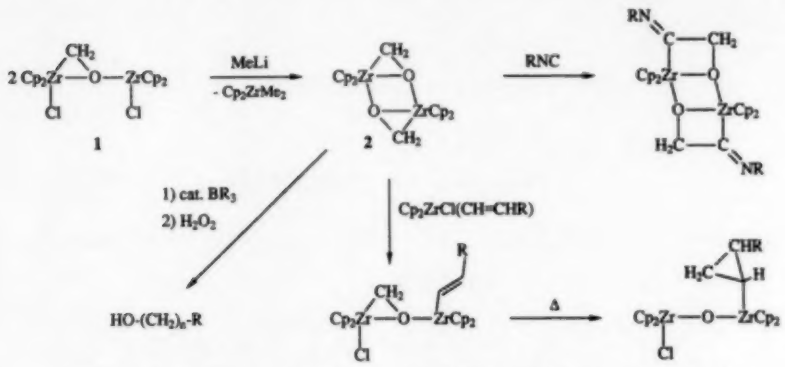


Scheme 1. Synthesis and selected reactions of the ($\eta^2$-formaldehyde)zirconocene dimer.

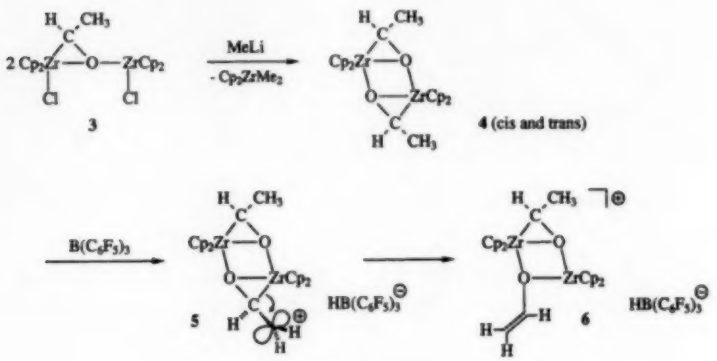


Scheme 2.

$CH_3$), 4.48 (q, $^3J$ = 6.2 Hz, 1H, CH) ppm. $^{13}$C NMR: $\delta$ 24.8 ($^1J_{CH}$ = 126 Hz, $CH_3$), 93.4 ($^1J_{CH}$ = 155 Hz, CHO) ppm. The methine coupling constant of $^1J_{CH}$ = 155 Hz is very typical of the metallaoxirane moiety [2–6]. The ($\eta^2$-$CH_3CHO$)Zr subunit contains a center of chirality. Therefore the cyclopentadienyl ligands at each bent metallocene group of the dinuclear complex **6** are diastereotopic. Accordingly, four $^1$H and $^{13}$C NMR Cp resonances are found. $^1$H NMR ($CD_2Cl_2$, 300 K) $\delta$ 6.53, 6.48, 6.06, 6.04 ppm. $^{13}$C NMR: $\delta$ 116.6, 116.4, 110.3, 110.1 ppm. The remaining signals of the $^1$H NMR spectrum of **6** exhibit a three proton AMX pattern ($\delta$ = 6.62, 4.50, 4.10 ppm with coupling constants $^3J$ = 13.7 and 6.0 Hz, $^2J$ = 2.8 Hz). We think that this vinyl group is connected to oxygen, which is in accord with the observed $^{13}$C NMR chemical shifts $\delta$ = 155.1 ($^1J_{CH}$ = 183 Hz, $-CH{=}CH_2$), 97.3 ($^1J_{CH}$ = 154 and 165 Hz, $-CH{=}CH_2$) ppm.

The formation of **6** can readily be explained if some metallaoxirane character of the ($\eta^2$-acetaldehyde)-zirconocene moiety is assumed. Hydride transfer from the methyl group to $B(C_6F_5)_3$ creates a heteroanalogous cyclopropylcarbinyl cation system **5** that might find some electronic stabilization in the bisected conformation [9] as depicted in Scheme 2. Subsequent cleavage of the adjacent endocyclic zirconium to carbon $\sigma$ bond seems to represent the most favorable pathway of stabilization of the intermediate **5**, that directly leads to the formation of the organometallic onium complex **6**. We conclude that this typical reaction of **4** with the hydride abstractor $B(C_6F_5)_3$ provides additional evidence of the pronounced metallaoxirane character of the ($\eta^2$-aldehyde)zirconocene species.

## Acknowledgments

Financial support from the Fonds der Chemischen Industrie, the Deutsche Forschungsgemeinschaft, and the Alfried Krupp von Bohlen und Halbach-Stiftung is gratefully acknowledged.

## References and notes

[1] K. Kropp, V. Skibbe, G. Erker and C. Krüger, *J. Am. Chem. Soc., 105* (1983) 3353.

[2] G. Erker, U. Hoffmann, R. Zwettler, P. Betz and C. Krüger, *Angew. Chem., 101* (1989) 644; *Angew. Chem., Int. Edn. Engl., 28* (1989) 630; G. Erker, F. Sosna and U. Hoffmann, *J. Organomet. Chem., 372* (1989) 41.

[3] G. Erker, S. Schmuck and U. Hoffmann, *J. Am. Chem. Soc., 113* (1991) 2330; for a related reaction see: R. Köster and M. Yalpani, *Angew. Chem., 95* (1985) 600; *Angew. Chem. Int. Edn. Engl., 24* (1985) 572.

[4] G. Erker, M. Mena, S. Werner and C. Krüger, *J. Organomet. Chem., 390* (1990) 323; G. Erker, M. Mena, C. Krüger and R. Noe, *J. Organomet. Chem., 402* (1991) 67; G. Erker, M. Mena, U. Hoffmann, B. Menjón and J.L. Petersen, *Organometallics, 10* (1991) 291; G. Erker, M. Mena, C. Krüger and R. Noe, *Organometallics, 10* (1991) 1201; G. Erker, F. Sosna, U. Hoffmann, R. Zwettler and C. Krüger, *J. Organomet. Chem., 367* (1989) C15.

[5] G. Erker, M. Bendix and R. Petrenz, *Organometallics, 13* (1994) 456; M. Bendix, M. Grehl, R. Fröhlich and G. Erker, *Organometallics, 13* (1994) 3366; G. Erker, S. Schmuck and M. Bendix, *Angew. Chem., 106* (1994) 2043; *Angew. Chem., Int. Edn. Engl., 33* (1994) 1955.

[6] S. Schmuck, G. Erker and S. Kotila, *J. Organomet. Chem.*, in press; F.R. Askham, K.H. Carrol and S.J. Alexander, *Organometallics, 12* (1994) 4810.

[7] B. Temme and G. Erker, *J. Organomet. Chem., 488* (1995) 177; X. Yang, C.L. Stern and T. Marks, *J. Am. Chem. Soc., 116* (1994) 10015.

[8] For other anion abstraction reactions of the $B(C_6F_5)_3$ reagent see: X. Yang, C.L. Stern and T.J. Marks, *J. Am. Chem. Soc., 113* (1991) 3623; X. Yang, C.L. Stern and T.J. Marks, *Angew. Chem., 104* (1992) 1406; *Angew. Chem., Int. Edn. Engl., 31* (1992) 1375; C. Pellecchia, A. Grassi and A. Immirzi, *J. Am. Chem. Soc., 115* (1993) 1160; D.J. Gillis, M.-J. Tudoret and M.C. Baird, *J. Am. Chem. Soc., 115* (1993) 2543; A.S. Guram and R.F. Jordan, *J. Org. Chem., 58* (1993) 5595; C. Pellecchia, A. Immirzi, A. Grassi and A. Zambelli, *Organometallics, 121* (1993) 4473; R. Quyoum, Q. Wang, M.-J. Tudoret and M.C. Baird, *J. Am. Chem. Soc., 116* (1994) 6435; R. Gómez, M.L.H. Green and J.L. Haggitt, *J. Chem. Soc., Chem. Commun.*, (1994) 2607; for applications of tris(pentafluorophenyl)borane in organic synthesis see: K. Ishihara, N. Hananki and H. Yamamoto, *Synlett*, (1993) 577 (1994) 963; T. Nagata, T. Toshihiro, T. Yamada, K. Imagawa and T. Mukaiyama, *Bull. Chem. Soc. Jpn., 67* (1994) 2614.

[9] R.F. Childs, R. Faggini, C.J. Lock, M. Mahendran and S.D. Zweep, *J. Am. Chem. Soc., 108* (1986) 1692; for reviews see: H.G. Richey, Jr., in G.A. Olah and P.v.R. Schleyer (eds.), *Carbonium Ions*, Vol. III, Wiley–Interscience, New York, 1972, Chapter 25; G.A. Olah, *Top. Curr. Chem., 80* (1979) 19.

ELSEVIER

Journal of Organometallic Chemistry 508 (1996) 267–269

Journal of Organometallic Chemistry

Preliminary communication

# Vergleichende Dimerisierung der Enantiomere von Oct-1-in-3-ol mit chiralen Rhodium-Phosphan-Komplexen

Hellmut Singer *, Michael Steigerwald

*Fachbereich Chemie und Pharmazie, Universität Mainz, J.J. Becherweg 34, D-55099 Mainz, Deutschland*

Eingegangen den 13. Juli 1995

**Abstract**

Three optically active phosphanes, $[(S)\text{-2-methylbutyl}]_{3-n}P[phenyl]_n$ (n = 0, 1, 2), were tested as ligands in rhodium(I) complexes to form catalysts for the enantioselective dimerisation of (R)- and (S)-oct-1-yn-3-ol. The catalytic reaction provides enantioselectivity for this type of C–C bond formation. For reactions at 45–75°C and depending on the P-ligand used the rates vary for both enantiomers from 6:1 to 50:1 in favour of the (S)-octynol.

**Zusammenfassung**

Drei optisch aktive Phosphane $[(S)\text{-2-Methylbutyl}]_{3-n}P[phenyl]_n$ (n = 0, 1, 2), wurden als Liganden in Rhodium(I)-Komplexen eingesetzt, um eine enantioselektive Dimerisierung von (R)- und (S)-Oct-1-in-3-ol zu erreichen. Die untersuchte Reaktion ergibt eine Enantioselektivität für diese Art der C–C Verknüpfung. Für Reaktionen von 45–75°C und abhängig vom eingesetzten P-Liganden differieren die Umsetzungsgeschwindigkeiten für beide Enantiomeren von 6:1 bis 50:1 zugunsten des (S)-Octinols.

*Keywords:* Catalysis; Chirality; Alkyne; Phosphine; Rhodium

## 1. Einleitung

Die Dimerisierung von α-Hydroxyacetylenen, katalisiert von Rhodium-Phosphan-Komplexen, war Gegenstand einiger Untersuchungen [1–4], deren Schwerpunkt die Variation der sterischen und elektronischen Eigenschaften der Phosphanliganden und der Substrate sowie des Rhodium-Phosphan-Verhältnisses darstellte. Das Hauptinteresse galt den aus diesen Variationen resultierenden qualitativen und quantitativen Veränderungen des Produktspektrums sowie daraus ableitbaren Aussagen zum Reaktionsablauf.

Ziel der vorliegenden Untersuchung [5] war es, einen ersten Vorstoß auf das Gebiet der Dimerisierung von chiralen α-Hydroxyacetylenen mit chiralen Rhodium-Phosphan-Komplexen zu unternehmen. Damit sollte untersucht werden, ob diese katalytische Reaktion einer C–C-Knüpfung sich für eine enantiomerenselektive Synthesen nutzen läßt. In Vorversuchen hatte sich gezeigt, daß Biphosphane als Liganden für die Dimerisierung von Alkinolen nicht zu aktiven Rhodiumkomplexen führen; danach war der Einsatz von chiralen Bisphosphanen nicht erfolgversprechend. Es wurde deshalb untersucht, ob einfache Phosphane mit einem Chiralitätszentrum in einem aliphatischen Substituenten am Phosphor geeignete Liganden für eine enantioselektive Dimerisierung darstellen.

Als α-Hydroxyacetylen wurde für dieses Projekt Oct-1-in-3-ol gewählt, dessen Enantiomere aus dem racemischen Gemisch isoliert wurden [6,7]. Die Rhodium-Phosphan-Komplexe wurden in situ aus Di-μ-chloro-bis-(1,5-hexadienrhodium(I)) [8,9] und $[(S)\text{-2-Methylbutyl-}]_{3-n}\text{-}[phenyl]_n$phosphanen (n = 0, 1, 2) [10,11] erzeugt und bei Reaktionstemperaturen von 45–75°C mit den Enantiomeren des Octinols in Toluol als Lösungsmittel umgesetzt. Während der Reaktion wurden Zeit-Umsatz-Bestimmungen durchgeführt.

Als Dimere entstanden in 1,4-Stellung (I) bzw. in 2,4-Stellung (II, Hauptprodukt) disubstituierte Enine.

Als Resultat ergab sich, daß (S)-Oct-1-in-3-ol im Vergleich zu seinem Enantiomeren, bei sonst konstanten Reaktionsbedingungen, mit $[(S)\text{-2-Methylbutyl}]_{3-n}$-$[phenyl]_n$phosphanen (n = 0, 1, 2) und Rhodium als Katalysatorelement schneller zu Dimeren abreagiert

* Corresponding author.

0022-328X/96/$15.00 © 1996 Elsevier Science S.A. All rights reserved
*SSDI* 0022-328X(95)05845-1

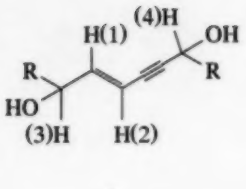


I

$R = C_5H_{11}$

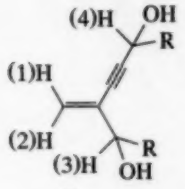


II

(Tabelle 1). Dieser Sachverhalt läßt sich mit den für verschiedene Reaktionstemperaturen bestimmten Geschwindigkeitskonstanten belegen. Die stärkste Differenzierung für die Umsetzung der enantiomeren Octinole ergibt sich für alle drei Phosphane bei 75°C als Reaktionstemperatur. Die aus den Geschwindigkeitskonstanten und den korrespondierenden Reaktionstemperaturen abgeleiteten Aktivierungsenergien weisen ebenfalls deutliche Differenzen auf. Damit wird es auch möglich sein, ausgehend von einem racemischen Gemisch, eines der enantiomeren Alkinole bevorzugt umzusetzen.

## 2. Experimenteller Teil

Die Reaktionsansätze wurden in mit Deckel und Teflonseptum verschraubbaren Reagenzgläsern (10 ml) durchgeführt. Die einzelnen Komponenten wurden in Form verdünnter toluolischer Lösungen bekannter Konzentration einpipettiert und auf ein Endvolumen von 5 ml aufgefüllt. In den Reaktionsansätzen lagen vor: 11 μmol Di-μ-chloro-bis-(1,5-hexadienrhodium(I)), 2,5 mmol (S)- oder (R)-Oct-1-in-3-ol, 373 μmol 1,2,4,5-Tetramethylbenzol (innerer Standard) und 131 μmol $[(S)\text{-2-Methylbutyl-}]_{3-n}[\text{phenyl}]_n$-phosphan (die Phosphane wurden spektroskopisch charakterisiert und ihre Reinheit gaschromatographisch bestätigt).

Die Ansätze wurden bei 75°C, 60°C und 45°C zur Reaktion gebracht. Zur Bestimmung von Zeit-Umsatz-Werten (Umsatz = abreagiertes Alkinol) wurden Proben durch die Septen Nach 15, 30, 45 und 60 Minuten entnommen und gaschromatographisch analysiert. Dazu wurde ein VEGA 2000 Gaschromatograph (Carlo Erba) mit einer 20 m Kapillarsäule der Firma ASS-Chem (Typ DB 1701, Filmdicke 0,2 μm, Innendurchmesser 0,18 mm) sowie ein Integrator der Firma Merck-Hitachi D 2000 benutzt.

Die Dimeren I und II wurden säulenchromatographisch abgetrennt, gereinigt und danach $^1$H-NMR-spektroskopisch in $CDU_3$ charakterisiert.

Hexadeca-7(*E*)-en-9-in-6,11-diol (Dimer I): 0.78 (m), 1.20 (m), 1.37 (m) und 1.57 (m) $R=C_5H_{11}$, 22H; 3.6 (s) OH; 3.99 (m) H(3); 4.33 (m) H(4); 5.60 (d, 15.9 Hz) H(2); 6.00 (dd, 15.9 und 6.0 Hz) H(1).

2-(1′-hydroxyhexyl)-deca-1-en-3-in-5-ol (Dimer II): 0.84 (m), 1.25 (m), 1.60 (m) $R=C_5H_{11}$, 22H; 3.6 (s) OH; 4.03 (t, 6.2 Hz) H(3); 4.39 (t, 6.3 Hz) H(4); 5.27 (schmales m), 5.31 (schmales m) H(1) und H(2).

## Literatur

[1] H. Singer, G. Wilkinson; *J. Chem. Soc. (A)*, (1968) 849.
[2] H.J. Schmitt, H. Singer, *J. Organomet. Chem.*, *153* (1978) 165.

Tabelle 1
Die für die Dimerisierung von (S)- und (R)-Oct-1-in-3-ol ermittelten Geschwindigkeitskonstanten und Aktivierungsenergien. R in den Phosphanen stellt den Substituenten (S)-2-Methylbutyl dar

| Octinol | Phosphan | Reaktionstemperatur [°C] | Aktivierungsenergie [kJ/mol] | Geschwindigkeitskonstante * $10^3$ [1/(mol Min)] | Umsatz des Monomeren nach 30 Min. [%] |
|---|---|---|---|---|---|
| (S) | $Ph_2PR$ | 75 | 26 | 33,5 | 64 |
| (S) | $Ph_2PR$ | 60 | 26 | 30,2 | 37 |
| (S) | $Ph_2PR$ | 45 | 26 | 14,5 | 16 |
| (S) | $PhPR_2$ | 75 | 32 | 34,9 | 67 |
| (S) | $PhPR_2$ | 60 | 32 | 24,9 | 26 |
| (S) | $PhPR_2$ | 45 | 32 | 12,5 | 15 |
| (S) | $PR_3$ | 75 | 30 | 39,1 | 65 |
| (S) | $PR_3$ | 60 | 30 | 30,1 | 29 |
| (S) | $PR_3$ | 45 | 30 | 14,9 | 16 |
| (R) | $Ph_2PR$ | 75 | 53 | 5,0 | 13 |
| (R) | $Ph_2PR$ | 60 | 53 | 2,4 | 11 |
| (R) | $Ph_2PR$ | 45 | 53 | 0,9 | 4 |
| (R) | $PhPR_2$ | 75 | 64 | 3,0 | 15 |
| (R) | $PhPR_2$ | 60 | 64 | 0,5 | 12 |
| (R) | $PhPR_2$ | 45 | 64 | 0,4 | 4 |
| (R) | $PR_3$ | 75 | 61 | 4,4 | 14 |
| (R) | $PR_3$ | 60 | 61 | 2,8 | 10 |
| (R) | $PR_3$ | 45 | 61 | 0,6 | 5 |

[3] H.-A. Schäfer, R. Marcy, Th. Rüping, H. Singer; *J. Organomet. Chem.*, *240* (1982) 17.
[4] Th. Rüping, H. Singer; *Inorg. Chim. Acta*, *131* (1987) 237.
[5] Michael Steigerwald; Dissertation, Fachbereich Chemie und Pharmazie der Johannes Gutenberg Universität Mainz (1994).
[6] S. Hashimoto, S. Kase, A. Suzuki, Y. Yanagiya, S. Ikegami; *Synth. Comm.*, *21* (1991) 833.
[7] Th. Künstler, D. Schollmeyer, H. Singer, M. Steigerwald; *Tetr. Asym.*, *4* (1993) 1645.
[8] G. Winkhaus, H. Singer; *Chem. Ber.*, *99* (1966) 3602.
[9] I.A. Zakharova, L.A. Leites, V.T. Aleksanyan; *J. Organomet. Chem.*, *72* (1974) 283.
[10] W.C. Davies, P.L. Pearse, W.J. Jones; *J. Chem. Soc.*, (1929) 1262.
[11] Houben-Weyl, *Methoden der organischen Chemie*, Georg Thieme; Band XII/1 (1963) 33 ff.

ELSEVIER

Journal of Organometallic Chemistry 508 (1996) 271–273

Journal of Organometallic Chemistry

Preliminary communication

# Crown compounds for anions. A polymeric complex of cyclic trimeric perfluoro-*o*-phenylenemercury with thiocyanate anion containing an infinite helical chain of alternating molecules of mercury-containing macrocycle and $SCN^-$ ions

I.A. Tikhonova, F.M. Dolgushin, A.I. Yanovsky, Yu.T. Struchkov, A.N. Gavrilova, L.N. Saitkulova, E.S. Shubina, L.M. Epstein, G.G. Furin, V.B. Shur *

*A.N. Nesmeyanov Institute of Organoelement Compounds of the Russian Academy of Sciences, Vavilov St. 28, Moscow 117813, Russia*

Received 24 July 1995

**Abstract**

It has been shown by IR spectroscopy that cyclic trimeric perfluoro-*o*-phenylenemercury $(o\text{-}C_6F_4Hg)_3$ is capable of binding thiocyanate anions in acetone solution, forming complexes whose composition is dependent on the ratio of reagents. In the interaction of $(o\text{-}C_6F_4Hg)_3$ with an equimolar amount of $[^nBu_4N]^+SCN^-$ in ethanol the complex formulated as $[(o\text{-}C_6F_4Hg)_3(SCN)]^-[^nBu_4N]^+$ has been isolated. An X-ray diffraction study of the complex has revealed that in the solid state it is polymeric and contains an infinite helical chain of alternating $(o\text{-}C_6F_4Hg)_3$ molecules and thiocyanate anions. Every $SCN^-$ ion in the complex is bonded to the mercury atoms of two neighbouring molecules of the macrocycle through the sulphur atom and forms with each of these molecules two relatively short Hg ··· S bonds and one considerably longer Hg ··· S bond.

*Keywords:* Mercury; Crown compounds; Macrocycle

As part of our continuing studies [1] of anion binding and catalytic properties of cyclic multidentate Lewis acids we have recently described [1b] the unusual complexes of bromide and iodide anions with cyclic trimeric perfluoro-*o*-phenylenemercury $(o\text{-}C_6F_4Hg)_3$ (**I**)

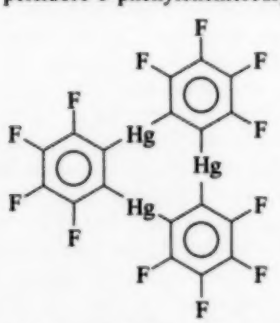

(I)

which contains three Hg atoms in a planar 9-membered cycle [2] [1]. The complexes are formulated as $[(o\text{-}C_6F_4Hg)_3X]^-$ (X = Br, I) and have (in the solid state) an unprecedented structure of polydecker bent sandwiches $[(\cdots \mathbf{I} \cdots X \cdots)_n]^{n-}$ wherein each halide anion is coordinated with six mercury atoms of two neighbouring molecules of **I**.

Here we report the ability of macrocycle **I** to bind thiocyanate anions effectively with formation of complexes whose composition is strongly dependent on the reagent ratio.

On addition of **I** to the excess of $[^nBu_4N]^+SCN^-$ in acetone at room temperature ($\mathbf{I}:SCN^- = 1:20–2$, $[SCN^-]_0 = 0.02$ M) the intensity of the $\nu_{CN}$ band of free thiocyanate anions (at 2056 $cm^{-1}$) in the IR spectrum decreases and two new $\nu_{CN}$ bands (at 2022 and 2075 $cm^{-1}$) appear indicating a complexation of $SCN^-$ with the mercury atoms of **I**. On raising the $\mathbf{I}:SCN^-$

* Corresponding author.

[1] For other works on binding of anions by cyclic multidentate Lewis acids see, e.g. Refs. [3–6].

0022-328X/96/$15.00 © 1996 Elsevier Science S.A. All rights reserved
*SSDI* 0022-328X(95)05965-2

molar ratio to 1:1, a band of free $SCN^-$ ions disappears whereas the intensities of $\nu_{CN}$ bands of complexed $SCN^-$ species increase. This is accompanied by a shift of a band at 2022 $cm^{-1}$ to 2014 $cm^{-1}$. The position of the other $\nu_{CN}$ band (at 2075 $cm^{-1}$) is virtually unaffected by raising the $I:SCN^-$ ratio. Use of excess **I** with respect to $SCN^-$ ($I:SCN^- = 20–2:1$, $[SCN^-]_0 = 0.002$ M) leads to a decrease in the intensities of the 2014 and 2075 $cm^{-1}$ bands and to the appearance of one more $\nu_{CN}$ band at 2044 $cm^{-1}$. These spectral changes are apparently due to the formation of complexes with different compositions in the solution.

When the reaction of **I** with an equimolar amount of $[^nBu_4N]^+SCN^-$ is carried out in ethanol ($[SCN^-]_0 = 0.02$ M) at 20°C, rapid precipitation of a fine crystalline colourless complex of the composition $[(o\text{-}C_6F_4Hg)_3(SCN)]^-[^nBu_4N]^+$ (**II**) occurs. The IR spectrum of acetone solution of the complex ($[\mathbf{II}]_0 = 0.02$ M) contains the above-mentioned $\nu_{CN}$ bands at 2014 and 2075 $cm^{-1}$ with the same intensity ratio (~1:4). The IR spectrum of **II** in Nujol mull differs markedly from that in acetone and shows two $\nu_{CN}$ bands of equal intensity at 2056 and 2096 $cm^{-1}$. A study of the Raman spectra of the single crystal of **II** (2057 and 2098 $cm^{-1}$) in polarized light has shown that the appearance of two $\nu_{CN}$ bands in the spectra of solid complex is caused by the Davydov splitting [7], hence, the value of ~2077 $cm^{-1}$ can be ascribed to the stretching vibrations of the CN bond of the thiocyanate ligand in **II**. The IR spectrum of $[^nBu_4N]^+SCN^-$ in Nujol mull displays the sole $\nu_{CN}$ band at 2056 $cm^{-1}$, i.e. coordination of the $SCN^-$ ion to **I** with formation of **II** increases the $\nu_{CN}$ frequency by 21 $cm^{-1}$. A band of $\nu_{SC}$ in the IR spectrum of **II** (Nujol mull) is observed at 668 $cm^{-1}$, which is 64 $cm^{-1}$ lower than the corresponding $\nu_{SC}$ frequency (732 $cm^{-1}$) in the spectrum of solid $[^nBu_4N]^+SCN^-$. Thus, the coordination of the $SCN^-$ ion to **I** probably leads to some strengthening of the CN bond of the thiocyanate ligand and to weakening of its SC bond.

An X-ray diffraction study of **II** [8] has shown that in the solid state the complex is polymeric $\{[(o\text{-}C_6F_4Hg)_3(SCN)]_n\}^{n-}$ and contains an infinite helical chain which is made up of alternating molecules of **I** and thiocyanate anions (Fig. 1). Every $SCN^-$ ion in the complex is bonded to the mercury atoms of two neighbouring molecules of the macrocycle through the sulphur atom and forms with each of these molecules two relatively short Hg···S bonds (3.06(1), 3.36(1) Å and 3.19(1), 3.36(1) Å) and one considerably longer Hg···S bond (3.74(1) and 3.87(1) Å; the sum of the Van der Waals radii of the Hg and S atoms is 2.1 + 1.85 = 3.95 Å [10]). A pronounced asymmetry of the sulphur atom coordination with the mercury atoms in **II** is apparently due to the steric repulsions between the CN fragment of the coordinated $SCN^-$ ion and the carbon and fluorine atoms of **I** which results in pushing

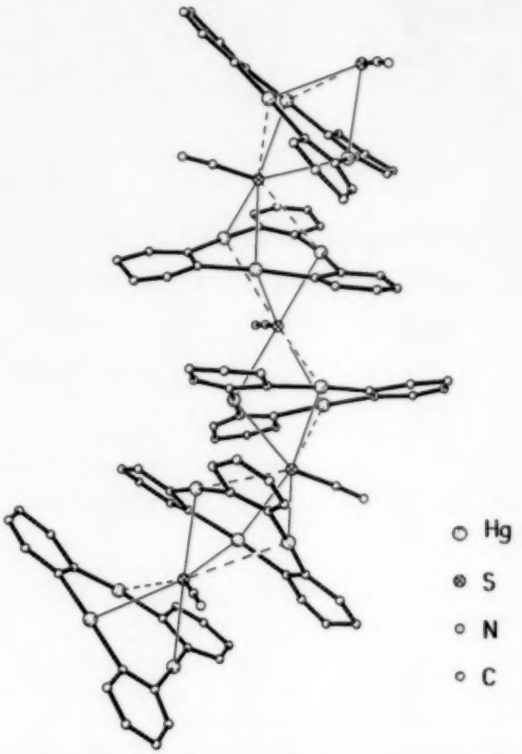


Fig. 1. The fragment of infinite polyanionic chain $\{[(o\text{-}C_6F_4Hg)_3(SCN)]_n\}^{n-}$ in the structure of **II**. The F atoms of phenylene rings are omitted for clarity.

the thiocyanate anion out of the space between the macrocycles. The above-mentioned complexes of **I** with iodide and bromide anions, which also have a polymeric structure $\{[(o\text{-}C_6F_4Hg)_3X]_n\}^{n-}$ in the solid state, are characterized by considerably more symmetrical coordination of the anionic centre with the Hg atoms.

The geometry of the thiocyanate ligand in **II** just as that of free $SCN^-$ ion is close to linear (the SCN bond angle in **II** is 173(4)°). Unfortunately, the limited accuracy of the X-ray experiment would not allow judgement on the influence of the complexation of $SCN^-$ with **I** on the CN bond length (1.10(5) Å in **II**). Nevertheless, some elongation of the SC bond in **II** (1.74(4) Å) as compared with the corresponding value for the free $SCN^-$ ion (e.g. 1.613 and 1.643 Å in the structures of trimethylsulfoxonium [11] and sodium [12] thiocyanates respectively) is obvious. It is consistent with the above-mentioned decrease in the $\nu_{SC}$ frequency in the IR spectra on transition from $[^nBu_4N]^+SCN^-$ to complex **II**.

Molecules of **I** in **II** exhibit, as a whole, considerable deviations from planarity (up to 0.4 Å), their mercury–carbon frameworks being non-planar as well (maximum

displacements from the mean planes are as large as 0.3 Å). Only the central 9-membered rings may be considered planar, although even these rings show noticeable deviations (up to 0.1 Å) from planarity. The mean planes of the neighbouring rings in the chain are non-parallel, forming the dihedral angle of 36.9°.

The S ··· N vector in **II** is inclined by 14.6 and 22.3° to the mean planes of the central 9-membered rings of two neighbouring molecules of **I**. Two adjacent $SCN^-$ groups in the polymeric chain of **II** are related by the $4_1$ symmetry operation and the S ··· N vector is almost normal to the *z*-axis of the unit cell. Therefore, the angle formed by the S ··· N vectors of the adjacent $SCN^-$ groups (89.7°) is close to 90°.

## Acknowledgements

This work was supported by the Russian Foundation for Basic Research (the Project codes 93-03-18342, 95-03-09365a and 94-03-08338) as well as by the International Science Foundation and Russian Government (Grant Nos. MMT 300 and MO4300).

## References and notes

[1] (a) V.B. Shur, I.A. Tikhonova, P.V. Petrovskii and M.E. Vol'pin, *Metalloorg. Khim, 2* (1989) 1431 (*Organomet. Chem. USSR, 2* (1989) 759);
(b) V.B. Shur, I.A. Tikhonova, A.I. Yanovsky, Yu.T. Struchkov, P.V. Petrovskii, S.Yu. Panov, G.G. Furin and M.E. Vol'pin, *J. Organomet. Chem., 418* (1991) C29; *Dokl. Akad. Nauk SSSR, 321* (1991) 1002;
(c) V.B. Shur, I.A. Tikhonova, F.M. Dolgushin, A.I. Yanovsky, Yu.T. Struchkov, A.Yu. Volkonsky, E.V. Solodova, S.Yu. Panov, P.V. Petrovskii and M.E. Vol'pin, *J. Organomet. Chem., 443* (1993) C19; *Dokl. Akad. Nauk, 328* (1993) 339;
(d) A.P. Zaraisky, O.I. Kachurin, L.I. Velichko, I.A. Tikhonova, G.G. Furin, V.B. Shur and M.E. Vol'pin, *Izvest. Akad. Nauk, Ser. Khim.*, (1994) 547;
(e) A.P. Zaraisky, O.I. Kachurin, L.I. Velichko, I.A. Tikhonova, A.Yu. Volkonsky and V.B. Shur, *Izvest. Akad. Nauk, Ser. Khim.*, (1994) 2047.

[2] (a) P. Sartori and A. Golloch, *Chem. Ber., 101* (1968) 2004;
(b) M.C. Ball, D.S. Brown, A.G. Massey and D.A. Wickens, *J. Organomet. Chem., 206* (1981) 265.

[3] (a) M. Newcomb, J.H. Horner and M.T. Blanda, *J. Am. Chem. Soc., 109* (1987) 7878;
(b) M. Newcomb, A.M. Madonic, M.T. Blanda and J.K. Judice, *Organometallics, 6* (1987) 145;
(c) M. Newcomb and M.T. Blanda, *Tetrahedron Lett., 29* (1988) 4261;
(d) M. Newcomb, J.H. Horner, M.T. Blanda and P.J. Squatritt, *J. Am. Chem. Soc., 111* (1989) 6294.

[4] M.E. Jung and H. Xia, *Tetrahedron Lett., 29* (1988) 297.

[5] (a) K. Jurkschat, H.G. Kuivila, S. Lui and J.A. Zubieta, *Organometallics, 8* (1989) 2755;
(b) K. Jurkschat, A. Rühlemann and A. Tzschach, *J. Organomet. Chem., 381* (1990) C53.

[6] (a) X. Yang, C.B. Knobler and M.F. Hawthorne, *Angew. Chem., Int. Ed. Engl., 30* (1991) 1507; *J. Am. Chem. Soc., 114* (1992) 380; *J. Am. Chem. Soc., 115* (1993) 4904;
(b) X. Yang, S.E. Johnson, S.I. Khan and M.F. Hawthorne, *Angew. Chem., Int. Ed. Engl., 31* (1992) 893;
(c) X. Yang, Z. Zheng, C.B. Knobler and M.F. Hawthorne, *J. Am. Chem. Soc., 115* (1993) 193.

[7] A.S. Davydov, *Uspekhi Fiz. Nauk, 3* (1964) 393

[8] Crystal data for **II**: $C_{35}H_{36}N_2F_{12}SHg_3$, $M = 1346.5$, tetragonal, space group $p4_12_12$, at −85°C, $a = 20.724(4)$, $c = 18.099(4)$ Å, $V = 7773(4)$ Å$^3$, $Z = 8$, $d_{calc.} = 2.301$ g cm$^{-3}$, $F(000) = 4992$. Intensity data were collected with a Syntex $P2_1$ diffractometer (−85°C, Mo K$\alpha$ radiation, $\theta/2\theta$ scan mode, $2\theta \leq 48°$, 3450 independent reflections, the empirical absorption correction ($\mu$(Mo K$\alpha$) = 119.6 cm$^{-1}$) based on the azimuthal scans of 18 reflections was applied). The structure was solved by direct method and refined by full-matrix least-squares in anisotropic (Hg, S, F and N), isotropic (C) approximation; no attempts for location of H atoms were undertaken. The absolute structure was determined by the Hamilton test at 99.5% probability ($R_{inv} = 0.0518$). The final refinement converged to $R = 0.0450$, $R_w = 0.0442$ and $S = 1.15$ for 1658 observed ($I > 3\sigma(I)$) independent reflections. All calculations were carried out on IBM PC using the SHELXTL PLUS programs [9]. Atomic coordinates, bond lengths and angles, and thermal parameters have been deposited at the Cambridge Crystallographic Data Centre.

[9] W. Robinson and G.M. Sheldrick, SHELX, in N.W. Isaacs and M.R. Taylor (eds.), *Crystallographic Computing — Techniques and New Technologies*, Oxford University Press, Oxford, UK, 1988, p. 366.

[10] S.S. Batsanov, *Zh. Neorg. Khim., 36* (1991) 3015.

[11] R. Puget, M. Jannin, R. Perret and C. DeBrauer, *Acta Cryst., C47* (1991) 2232.

[12] J.W. Bats, P. Coppens and A. Kvick, *Acta Cryst., B33* (1977) 1534.

ELSEVIER

Journal of Organometallic Chemistry 508 (1996) 275–279

Journal of Organometallic Chemistry

Preliminary communication

# Zur Elektronenstruktur metallorganischer Komplexe der f-Elemente XXXVIII ☆ Halbsandwich-Komplexe der Stöchiometrien (COT)Ln($HBpz_3$) und (COT)Ln[$HB(3,5\text{-}Me_2pz)_3$]-ideale Systeme für die experimentelle Bestimmung der Kristallfeld-Aufspaltungseffekte des Cyclooctatetraenyl-Liganden

Hanns-Dieter Amberger [a], Frank T. Edelmann [b]

[a] *Institut für Anorganische und Angewandte Chemie der Universität Hamburg, Martin-Luther-King-Platz 6, D-20146 Hamburg, Deutschland*
[b] *Chemisches Institut, Otto-von-Guericke Universität, Universitätsplatz 2, D-39106 Magdeburg, Deutschland*

Received 4 October 1995

**Abstract**

Because of the nearly negligible crystal field (CF) strength of $[HBpz_3]^-$ (pz = pyrazol-1-yl) and $[HB(3,5\text{-}Me_2pz)_3]^-$ ligands, respectively, the recently described (COT)Ln($HBpz_3$) and (COT)Ln[$HB(3,5\text{-}Me_2pz)_3$] complexes (COT = $\eta^8$-cyclooctatetraenyl) may be looked upon as simple $[Ln(COT)]^+$ moieties from the aspect of CF theory. The CF splitting pattern of $[Pr(COT)]^+$ could be derived on the basis of optical spectra and simulated by fitting the free parameters of an empirical Hamiltonian. The Slater and spin orbit coupling parameters are discussed in terms of covalency. The CF parameters obtained were inserted in the energy matrix of the spin-free $f^1$ case and the calculated orbital energies are compared with the predictions of previous MO calculations for $[Ce(COT)_2]^-$, $Ce(COT)_2$ and $U(COT)_2$.

*Keywords:* Praseodymium; Cyclooctatetraenyl; Optical spectra; Ligand field theory; MO calculations

## 1. Einführung

Die von Fischer aufgrund der Ergebnisse von Molekülorbital(MO)-Rechnungen postulierte Existenz von Bis($\eta^8$-cyclooctatetraenyl)uran(IV) ["Uranocen"; $U(COT)_2$] [1] veranlaßte Mitte der sechziger Jahre diverse Arbeitskreise zu Syntheseversuchen von COT-Verbindungen der f-Elemente. In der Tat gelang 1968 die Erstdarstellung von $U(COT)_2$ [2], 1970 die von $K[Ln(COT)_2]$ (Ln = Ce, Pr, Nd, Sm, Tb) [3] und 1976 die von $Ce(COT)_2$ [4]. Seitdem waren die f-Element-Metallocene Gegenstand zahlreicher physikalisch-chemischer Untersuchungen mit dem Ziel, die Elektronenstrukturen dieser Verbindungsklassen aufzuklären [5–10].

Wegen der Existenz eines Inversionszentrums und des damit verbundenen strengen Laporte-Verbotes sowie energetisch niedrig liegender Charge-transfer-Übergänge waren den optischen und magnetooptischen Untersuchungen im Bereich der f-f-Übergänge nur ein sehr begrenzter Erfolg beschieden [5–10]. Die verwertbaren Experimente für die Ableitung der zugrundeliegenden Kristallfeld (KF)-Aufspaltungsmuster erstreckten sich lediglich auf Bestimmungen der Temperaturabhängigkeit der paramagnetischen Suszeptibilität und der isotropen NMR-Verschiebungen ausgewählter Kerne mit geringen Kontaktanteilen sowie auf maximal zwei elektronische Raman-Übergänge bei $U(COT)_2$ [7,10–12].

Flankierend wurden zahlreiche Modellrechnungen unterschiedlicher Schwierigkeitsgrade durchgeführt [9

☆ XXXVII. Mitteilung siehe Lit. [23]. Herrn Prof. Dr. R.D. Fischer zum 60. Geburtstag gewidmet.

0022-328X/96/$15.00 © 1996 Elsevier Science S.A. All rights reserved
*SSDI* 0022-328X(95)06043-X

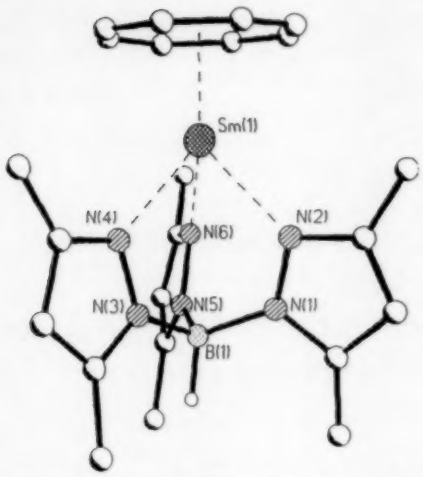


Abb. 1. Molekülstruktur von (COT)Sm[HB(3,5-$Me_2$pz)$_3$] [15].

10,13,14], die jedoch zu stark differierenden Ergebnissen führten (vgl. Abb. 1).

Die kürzlich beschriebenen (COT)Ln · L-Komplexe (Ln = Ce-Sm; L = Hydrotris(pyrazol-1-yl)borato [HBpz$_3$]$^-$, Hydrotris (3,5-dimethylpyrazol-1-yl)borato [HB($Me_2$pz)$_3$]$^-$) weisen kein Inversionszentrum auf [15], weshalb sich ihre KF-Aufspaltungsmuster in den optischen und magnetooptischen Spektren direkt widerspiegeln. Gemäß früheren Untersuchungen besitzt der [HBpz$_3$]$^-$- und damit auch der [HB($Me_2$pz)$_3$]$^-$-Ligand eine nahezu vernachlässigbare Ligandenfeldstärke [16]. Vom KF-theoretischen Standpunkt können die oben genannten Komplexe deshalb als weitgehend ungestörte [Ln(COT)]$^+$-Einheiten betrachtet werden, so daß nunmehr die einzigartige Chance besteht, die vom COT-Liganden verursachten KF-Effekte experimentell zu erfassen.

In der vorliegenden ersten Untersuchung geben wir dem zitronengelben 4f$^2$-System (COT) Pr[HB($Me_2$pz)$_3$] (**1**) den Vorzug, da hier die interessierenden f-f-Übergänge nicht durch intensive Charge-transfer-Banden verdeckt werden und diese Verbindung zudem gut fluoresziert, weshalb das zugrundeliegende KF-Aufspaltungsmuster durch Kombination absorptions- und lumineszenzspektroskopischer Befunde weitgehend lückenlos aufgestellt werden kann.

## 2. Experimentelles

Gepulvertes **1** wurde in Befolgung der in Lit. [15] angegebenen Arbeitsvorschrift hergestellt. Tieftemperatur-Absorptionsmessungen zeigten jedoch, daß **1**—je nach Syntheseversuch—mit ca. 5%–30% THF-Addukt verunreinigt war. Durch extrem langsames Abkühlen einer nahezu gesättigten Lösung des Rohproduktes von **1** in einer Mischung von Methylcyclohexan und Toluol im Verhältnis 2:1 resultierten zitronengelbe Kristalle (mit typischen Volumina von 1–3 mm$^3$) deren Absorptionsspektren die für das THF-Addukt charakteristischen Banden nicht mehr erkennen ließen.

## 3. Ergebnisse

Über Einzelheiten der optischen, magnetooptischen und magnetochemischen Messungen, deren Auswertung, die Ableitung des entsprechenden KF-Aufspaltungsmusters sowie dessen rechnerische Simulation unter Berücksichtigung der trigonalen Störung wird an anderer Stelle berichtet [17]. Hier soll zunächst die allgemeine Verfahrensweise kurz skizziert, dann die durch Anpassung des experimentell ermittelten KF-Aufspaltungsmusters erhalten Parameter hinsichtlich Bindungsfragen näher diskutiert und schließlich die erzielten experimentellen Ergebnisse mit den Voraussagen früherer Modellrechnungen verglichen werden.

Im Rahmen des sogenannten phänomenologischen oder parametrischen Ansatzes werden die offenen Parameter eines empirischen Hamilton-Operators $\hat{H} = \hat{H}_{fi} + \hat{H}_{KF}$ dem auf experimenteller Basis abgeleiteten KF-Aufspaltungsmuster der betreffenden Verbindung im Sinne der Methode der kleinsten Fehlerquadrate angepaßt [18]. Der Hamilton-Operator des freien Ions $\hat{H}_{fi}$ umfaßt bei Mehrelektronensystemen neben diversen kleineren Wechselwirkungen vor allem die interelektronische Abstoßung und die Spin-Bahn-Kopplung, die zu den Slater-Parametern $F^2$, $F^4$ und $F^6$ bzw. Zu dem Spin-Bahn-Kopplungsparameter $\zeta$ führen [18]. Das bei [Pr(COT)]$^+$ näherungsweise vorliegende KF der Symmetrie $C_{8v}$ gibt im Hamilton-Operator des KF ($\hat{H}_{KF}$) lediglich zu den Parametern $B_0^2$, $B_0^4$ und $B_0^6$ Anlaß [6,9].

Gemäß den experimentellen Befunden spalten bei **1** die (bei Annahme strenger $C_{8v}$-Symmetrie) zweifach entarteten KF-Zustände unter dem Einfluß des trigonalen Störfeldes des [HB($Me_2$pz)$_3$]$^-$-Liganden in zwei Komponenten mit maximalen Energieseparationen von 43 cm$^{-1}$ auf. Unter Vernachlässigung dieser Aufspaltungen konnte durch Schwerpunktbildung der beobachteten Bandenlagen in den Absorptions- und Lumineszenzspektren das KF-Aufspaltungsmuster des fiktiven Halbsandwich-Komplexes [Pr(COT)$_2$]$^+$ aufgestellt werden.

Durch Anpassung der offenen Parameter des oben erwähnten empirischen Hamilton-Operators gelang es, das so erhaltene KF-Aufspaltungsmuster mit einer r.m.s.-Abweichung von 31 cm$^{-1}$ bei 33 Zuordnungen rechnerisch zu reproduzieren. Die für Bindungsfragen und die Diskussion spektrochemischer Effekte relevanten Parameter $F^2$, $\zeta$, $B_0^2$, $B_0^4$ und $B_0^6$ nahmen dabei die Werte 66238, 748, −21, −3732 und 254 cm$^{-1}$ an.

Tabelle 1
Vergleich der Ligandenfeldstärken einiger repräsentativer $Pr^{III}$- bzw. $U^{IV}$-Verbindungen. (Alle Werte in $cm^{-1}$)

| Verbindung | $N_v/\sqrt{(4\pi)}$ | Literatur |
|---|---|---|
| $[Pr(COT)]^+$ | 1246 [a] | diese Arbeit |
| $[Pr(COT)_2]^-$ | 2492 [a] | diese Arbeit |
| $[Ce(COT)_2]^-$ | 503 [b] | [20] |
| $Ce(COT)_2$ | 5739 [b] | [21] |
| $U(COT)_2$ | 3928 [b,c] | [10] |
| $U(COT)_2$ | 9700 [b,c] | [13] |
| $U(COT)_2$ | 9238 [b] | [21] |
| $U(COT)_2$ | 1711 [b] | [20] |
| $U(COT)_2$ | 3234 [b] | [6] |
| $Cp_3Pr \cdot NCCH_3$ | 1003 [a] | [22] |
| $Cp_3La(NCCH_3)_2$:Pr | 1086 [a] | [23] |
| $Cp_3UCl$ | 2325 [a] | [24] |
| $[Cp_3U(NCBH_3)_2]^-$ | 2834 [a] | [25] |
| $Cs_2NaPrCl_6$ | 865 [a] | [26] |
| $Cs_2UCl_6$ | 2445 [a] | [27] |

[a] Auf experimenteller Grundlage abgeleitet.
[b] Auf der Basis von Modellrechnungen abgeleitet.
[c] S. Text.

## 4. Diskussion

Der Parameter $N_v/\sqrt{(4\pi)} = \sqrt{[\sum_{k,q}(B_q^k)^2/(2k+1)]}$ wird üblicherweise als ein Maß für die Größe der Ligandenfeldstärke betrachtet [19]. Nach Einsetzung der hier gefundenen Parameter $B_0^2$, $B_0^4$ und $B_0^6$ in obige Beziehung erhält man $N_v/\sqrt{(4\pi)} = 1246\ cm^{-1}$ für den Halbsandwich $[Pr(COT)]^+$ und damit in erster Näherung $2492\ cm^{-1}$ für den Vollsandwich $[Pr(COT)_2]^-$. In der Tabelle 1 wird dieser auf experimenteller Grundlage erhaltene Wert mit den auf Modellrechnungen basierenden Ergebnissen für $[Ce(COT)_2]^-$, $Ce(COT)_2$ [3] bzw. $U(COT)_2$ verglichen (vide infra). Zu Vergleichszwekken sind dort auch die "experimentellen" $N_v/\sqrt{(4\pi)}$-Werte einiger repräsentativer $Pr^{III}$- und $U^{IV}$-Verbindungen angegeben.

Offenbar ist der auf Experimenten beruhende Wert von $[Pr(COT)_2]^-$ nahezu um den Faktor fünf größer als der berechnete von $[Ce(COT)_2]^-$ [20] und bewegt sich teilweise im selben Rahmen wie der für $U(COT)_2$ erwartete und bei anderen $U^{IV}$-Verbindungen gefundene Betrag.

Um die Ligandenfeldstärke des COT- und des $\eta^5$-Cyclopentadienyl (Cp)-Liganden bei festgehaltenem Zentralion vergleichen zu können, wären die KF-Parameter des monomeren basenfreien $Cp'_3Pr$ ($Cp' = 1,3$-Bis(trimethylsilyl)cyclopentadienyl) [28] erforderlich. Da diese derzeit nicht in ausreichend verläßlicher Form verfügbar sind [29], wird hier auf die gesicherten KF-Parameter der Mono- und Bisacetonitriladdukte des Grundkörpers $Cp_3Pr$ zurückgegriffen [22,23] (vgl. Tabelle 1). Vernachlässigt man den Einfluß der Neutralbasen, dann ist die von den f-Funktionen des Pr-Zentralions "wahrgenommene", Ligandenfeldstärke eines COT-Ringes um den Faktor 3.5 stärker als die eines Cp-Ringes. Auf ein einziges C-Atom bezogen, ist die Ligandenfeldstärke beim COT-Ring immerhin noch mehr als doppelt so groß wie beim Cp-Liganden.

Die naheliegende Annahme, daß die erhöhte Ligandenfeldstärke des COT-Ringes durch einen deutlich größeren Grad an Kovalenz hervorgerufen wird, muß jedoch verworfen werden, da die nephelauxetischen Parameter $\beta = F^2_{(Komplex)}/F^2_{(freies\ Ion)}$, bzw. die relativistischen nephelauxetischen Parameter $\beta' = \zeta_{(Komplex)}/\zeta_{(freies\ Ion)}$, die als ein Maß für die Kovalenz einer Verbindung betrachtet werden [30], bei $[Pr(COT)]^+$ ($\beta = 0.922$, $\beta' = 0.977$), $Cp_3PrNCCH3$ ($\beta = 0.919$, $\beta' = 0.970$) [22] und $Cp_3La(NCCH_3)_2$:Pr ($\beta = 0.927$, $\beta' = 0.977$) [23] vergleichbar sind. Vielmehr dürfte der bei $[Ln(COT)]^+$ deutlich verringerte Ln-C-Abstand (259.5 pm bei $(COT)Sm(HBpz_3)$ [31], 276.3 pm bei triklinem $Cp_3Sm \cdot NCCH_3$ [32]) und die dabei exponentiell zunehmenden elektrostatischen Kräfte hierfür verantwortlich sein.

Die Einsetzung der mit dem Faktor zwei multiplizierten KF-Parameter von $[Pr(COT)]^+$ in die Energiematrix des spinfreien $f^1$-Problems (das einem KF der Symmetrie $D_{8h}$ ausgesetzt ist) [9] und deren anschließende Diagonalisierung führt zu den Energien der resultierenden f-Orbitale der Symmetrien $a_{2u}$, $e_{1u}$, $e_{2u}$ und $e_{3u}$ von $[Pr(COT)_2]^-$. In Abb. 2 wird das so erhaltene, für $[Pr(COT)_2]^-$ repräsentative Orbitalenergiediagramm mit ausgewählten berechneten MO-Schemata von $[Ce(COT)_2]^-$ [20], $Ce(COT)_2$ [21] und $U(COT)_2$ [6,10,20] verglichen.

In all diesen Schemata hat das überwiegend f-Charakter besitzende antibindende Orbital $e_{2u}$ (entsprechend den f-Funktionen $f_{xyz}$ und $f_{z(x^2-y^2)}$) die höchste Energie. Somit wird Streitwiesers Vision einer besonderes starken Wechselwirkung zwischen den Ringorbitalen der Rasse $e_{2u}$ und dem $f_{xyz}$- bzw. $f_{z(x^2-y^2)}$-Orbital [33] sowohl durch das Experiment als auch durch sämtliche Modellrechnungen bestätigt.

Es fällt auf, daß lediglich die jüngeren Modellrechnungen von Chang und Pitzer [10] sowie von Boerrigter et al. [13] für $U(COT)_2$ zu der gleichen energetischen Sequenz der f-Orbitale führen wie das Experiment für $[Pr(COT)]^+$ und somit auch für $[Pr(COT)_2]^-$. Es war naheliegend, auf der Grundlage der von Chang und Pitzer [10] bzw. Boerrigter et al. [13] [4] berechneten MO-Schemata von $U(COT)_2$ die KF-Parameter abzuschätzen und mit denen von $[Pr(COT)_2]^-$ zu vergle-

[3] Gemäß neuesten Modellrechnungen soll hier eine $f^1$-Konfiguration vorliegen [14].

[4] Das MO-Schema von Lit. [13] wurde in Abb. 2 nicht aufgenommen, da es den Rahmen der Graphik sprengen und somit zu einer unübersichtlichen Darstellung führen würde.

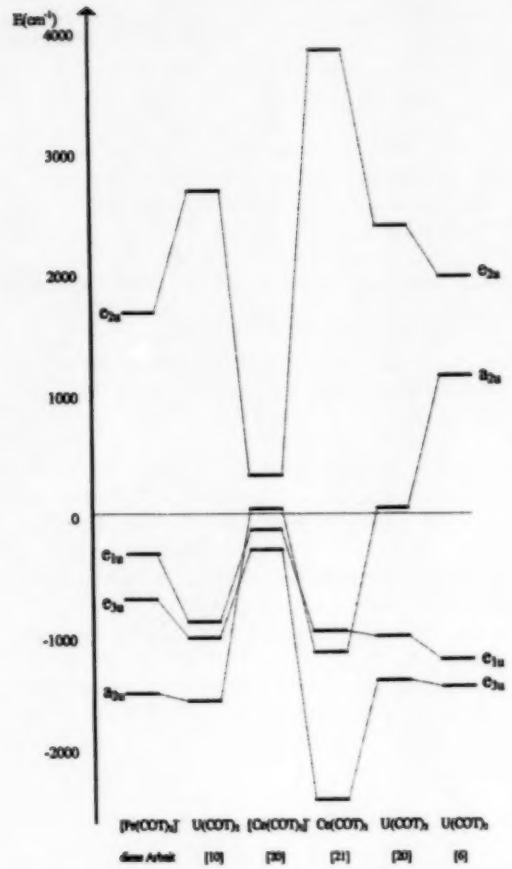


Abb. 2. Vergleich des auf experimenteller Basis abgeleiteten Orbitalenergieschemas des fiktven Komplexes $[Pr(COT)_2]^-$ mit den berechneten MO-Schemata von $[Ce(COT)_2]^-$, $Ce(COT)_2$ und $U(COT)_2$ im f-Energiebereich.

chen. Nach Gleichsetzung der berechneten Energien der f-ähnlichen Orbitale ($f^{-1}$ IVO-Rechnung der Tabelle 2, Lit. [10]; bzw. Abb. 2, Lit. [13] entnommen [5] mit den parameterbehafteten Orbitalenergien eines spinfreien f-Elektrons in einem KF von $D_{8h}$-Symmetrie [9] erhält man die in Tabelle 2 angegebenen KF-Parameter von $U(COT)_2$.

Offenbar ist in beiden Fällen—ähnlich wie bei $[Pr(COT)]^+$ und damit auch bei $[Pr(COT)_2]^-$—der mit negativem Vorzeichen versehene Parameter $B_0^4$ dominant, jedoch ist der Betrag von $B_0^4$ bei Boerrigter et al. um den Faktor 2.4 größer als bei Chang und Pitzer. Angesichts des Befundes, daß die Ligandenfeldstärke beim Gang von einer $Pr^{III}$- zu einer vergleichbaren

[5] Die entsprechenden numerischen Werte sind nach Auskunft der Autoren nicht mehr verfügbar.

Tabelle 2
Vergleich postulierter und angepaßter KF-Parameter. (Alle Werte in $cm^{-1}$)

| | $B_0^2$ | $B_0^4$ | $B_0^6$ | $N_v/\sqrt{4\pi}$ | |
|---|---|---|---|---|---|
| $U(COT)_2$ | −220 | −11779 | +2905 | 3928 | Chang/Pitzer [a] |
| $U(COT)_2$ | +223 | −28440 | +7465 | 9700 | Boerrigter et al. |
| $[Pr(COT)_2]^-$ | −42 | −7464 | +508 | 2492 | diese Arbeit |

[a] S. Text.

$U^{IV}$-Verbindung häufig um den Faktor drei vergrößerte Werte annimmt (vgl. Tabelle 1) und bei $[Pr(COT)_2]^-$ ein $N_v/\sqrt{4\pi}$-Wert von 2492 $cm^{-1}$ gefolgert wurde, dürften realistische $N_v/\sqrt{4\pi}$-Werte für $U(COT)_2$ in der Gegend von 7500 $cm^{-1}$ liegen, und sich die zugrundeliegenden KF-Parameter damit in der Mitte der in Tabelle 2 angegebenen Wertepaare bewegen.

## Dank

Diese Arbeit wurde von der Deutschen Forschungsgemeinschaft, dem Fonds der Chemischen Industrie sowie von der BASF AG, Ludwigshafen gefördert. Frau Dr. U. Kilimann und Herrn Dipl.-Chem. P. Porembs danken wir für die Synthesen der Proben, Herrn Dipl.-Chem. S. Jank für die Aufnahme der Spektren und Herrn Dr. H. Reddmann für quantenchemische Simulationen.

## Literatur

[1] R.D. Fischer, *Theor. Chim. Acta, 1* (1963) 418.
[2] A. Streitwieser, Jr. und U. Müller-Westerhoff, *J. Am. Chem. Soc., 90* (1968) 7364.
[3] F. Mares, K.O. Hodgson und A. Streitwieser, Jr., *J. Organomet. Chem., 24* (1970) C68.
[4] A. Greco, S. Cesca und G. Bertolini, *J. Organomet. Chem., 111* (1976) 321.
[5] D.G. Karraker, J.A. Stone, E.R. Jones, Jr. und N. Edelstein, *J. Am. Chem. Soc., 92* (1970) 4841.
[6] R.G. Hayes und N. Edelstein, *J. Am. Chem. Soc., 94* (1972) 8688.
[7] K.O. Hodgson, F. Mares, D.F. Starks und A. Streitwieser, Jr., *J. Am. Chem. Soc., 95* (1973) 8650.
[8] R.L. Mowery, *Diss. Abstr. Int., 37* (1977) 5112B.
[9] N.M. Edelstein, in T.J. Marks und R.D. Fischer (Hrsg.), *Organometallics of the f-Elements*, Reidel, Dordrecht, 1979.
[10] A.H. Chang und R.M. Pitzer, *J. Am. Chem. Soc., 111* (1989) 2500, und dort angegebene Literaturzitate.
[11] W.D. Luke und A. Streitwieser, Jr., in N.M. Edelstein (Hrsg.), *Lanthanide and Actinide Chemistry and Spectroscopy*, ACS Symposium Series 131, Washington DC, 1980.
[12] W. Jahn, K. Yünlü, W. Oroschin, H.-D. Amberger und R.D. Fischer, *Inorg. Chim. Acta, 95* (1984) 85.
[13] P.M. Boerrigter, E.J. Baerends und J.B. Snijders, *Chem. Phys., 122* (1988) 357.
[14] M. Dolg, P. Fulde, N. Stoll, H. Preuss, A. Chang und R.M. Pitzer, *Chem. Phys., 195* (1995) 71, und dort angegebene, Literaturzitate.

[15] U. Kilimann und F.T. Edelmann, *J. Organomet. Chem., 444* (1993) C15.
[16] M.V.R. Stainer und J. Takats, *Inorg. Chem., 21* (1982) 4050.
[17] H.-D. Amberger, H. Reddmann, S. Jank und F.T. Edelmann, in Vorbereitung.
[18] W.T. Carnall, J.V. Beitz, H. Crosswhite, K. Rajnak und J.B. Mann, in S.P. Sinha (Hrsg.), *Systematics and Properties of the Lanthanides*, Reidel, Dordrecht, 1982.
[19] F. Auzel und O.L. Malta, *J. Phys. (Paris), 105* (1983) 201.
[20] K.D. Warren, *Inorg. Chem., 14* (1975) 3095.
[21] N. Rösch und A. Streitwieser, Jr., *J. Am. Chem. Soc., 105* (1983) 7273.
[22] C. Apostolidis, B. Kanellakopulos, R. Klenze, H. Reddmann, H. Schulz und H.-D. Amberger, *J. Organomet. Chem., 426* (1992) 307.
[23] H.-D. Amberger, H. Reddmann und S. Jank, zur Veröffentlichung eingereicht bei *Spectrochim. Acta, Teil A.*
[24] H.-D. Amberger, H. Reddmann und N.M. Edelstein, *Inorg. Chim. Acta, 141* (1988) 313.
[25] H.-D. Amberger, H. Reddmann, G. Shalimoff und N.M. Edelstein, *Inorg. Chim. Acta, 139* (1987) 335.
[26] F.S. Richardson, M.F. Reid, J.J. Dollara und R.D. Smith, *J. Chem. Phys., 83* (1985) 3813.
[27] R.A. Satten, C.L. Schreiber und E.Y. Wong, *J. Chem. Phys., 42* (1965) 162.
[28] S.D. Stults, R.A. Andersen und A. Zalkin, *Organometallics, 9* (1990) 115.
[29] M. Sievers, H. Reddmann, H.-D. Amberger und R.D. Fischer, unveröffentlichte Ergebnisse.
[30] A.B.P. Lever, *Inorganic Electronic Spectroscopy*, Elsevier, Amsterdam, 1984 S. 738.
[31] U. Kilimann, *Dissertation*, Göttingen, 1994.
[32] M. Adam, H. Schultze und R.D. Fischer, *J. Organomet. Chem., 429* (1992) C1.
[33] A. Streitwieser Jr., U. Müller-Westerhoff, G. Sonnichsen, F. Mares, D.G. Morrell, K.O. Hodgson und C.A. Harmon, *J. Am. Chem. Soc., 95* (1972) 8644.

ELSEVIER

Journal of Organometallic Chemistry 508 (1996) 281

Journal of Organometallic Chemistry

# Book review

*Inorganic Chemistry of Main Group Elements*
R.B. King, VCH, New York, Weinheim, 1995, xix + 326 pages, DM115 £46.
ISBN 1-56081-679-1

To write a graduate-level textbook on the inorganic chemistry of the Main Group elements is to accept a colossal challenge. The subject is so wide-ranging and the topics to be covered so diverse that any book which is reasonable in length must appear to be superficial. In devising courses at university level many of us take the easy way out and cover 'selected topics' which we consider to be interesting or topical, but this approach quickly becomes dated as fashions change. Professor Bruce King has adopted a different strategy. He has attempted to cover the whole subject including all the topics which he thinks are important. He bases his account on the Periodic Table, with chapters on hydrogen, carbon, Si–Pb, nitrogen, P–Bi, chalogens, halogens and noble gases, boron, Al–Tl, alkali and alkaline earth metals, Zn–Hg, lanthanides and actinides. This is classical inorganic chemistry, taught in a traditional manner, but brought thoroughly up-to-date by reference to work published up to 1993. In most chapters there are brief, well-conceived sections on organometallic chemistry.

I think Professor King's judgments about the relative importance of the subjects he has covered are sound. He has included an astonishing amount of information and his clear, concise style is easy to read. Anyone looking for an introduction to an aspect of Main Group chemistry would do well to begin here. Inevitably, however, there is a breathlessness in the way the ground is covered; e.g. there is only one paragraph on gallium arsenide and only three on zeolites even though most university libraries have a shelf full of books on each topic. The size of Professor King's book is kept within bounds in two ways. First there is an excellent bibliography at the end of each chapter so that those wanting more know where to find it. Secondly the emphasis has been kept firmly on the descriptive, on facts rather than theory, on what happens rather than on why it happens. So there is little on what factors determine the relative stabilities of various oxidation states, on why some lone pairs are stereochemically active and others not, on thermochemical cycles, structural data or orbitals. Each chapter begins with a section entitled 'general aspects' including a good account of NMR-active nuclei for each element. This reflects the crucial part played nowadays by multinuclear NMR spectroscopy in studying the chemistry of Main Group elements. The other points are also mainly descriptive with little to relate the chemistry of the elements to the properties of their atoms. It is true that attempts to account for reactions and properties in this way are often simplified to the point where the explanations are facile and misleading, but the highly descriptive, systematic segregated approach which we find in this book tends to underplay the importance of trends in properties which inform much of the creative thinking of inorganic chemists. Since the author expects his readers to be familiar with fundamental ideas of chemical structure and bonding from previous courses perhaps this quibble does not matter too much. We are certainly given a well-balanced picture of the range and importance of Main Group chemistry and if this book encourages students to read widely and follow up particular topics in detail it will have served its purpose well.

**J.D. Smith**
*School of Chemistry and Molecular Sciences*
*University of Sussex*
*Brighton*
*BN1 9QJ*

0022-328X/96/$15.00 © 1996 Elsevier Science S.A. All rights reserved
*SSDI* 0022-328X(95)06013-8

ELSEVIER

Journal of Organometallic Chemistry 508 (1996) 283

Journal of Organometallic Chemistry

# Author Index of Volume 508

Acum, G.A., 137
Amberger, H.-D., 275
An, D.-L., 7
Ando, H., 49
Antipin, M.Yu., 259
Arancibia, A., 23
Asai, M., 121
Ascenso, J.R., 169
Azzaroni, F., 59

Baba, A., 49
Bermúdez, M.D., 53
Biscarini, P., 59
Boese, R., 259
Bordoni, S., 59
Bott, S.G., 91
Bryukhova, E.V., 129

Canovese, L., 101
Capon, J.-F., 1, 31
Carriedo, G.A., 23
Carrión, F.J., 53
Chou, Y.C., 183
Coville, N.J., 231
Crociani, B., 101

Delis, J.G.P., 109
Dias, H.V.R., 91
Díaz-Valenzuela, C., 23
Di Bianca, F., 101
Dolgushin, F.M., 39, 271
Du Plooy, K.E., 231
Du Toit, J., 231

Edelmann, F.T., 275
Elsevier, C.J., 109
Epstein, L.M., 271
Erker, G., 263

Fischer, R., 13
Fontana, A., 101
Fugami, K., 255
Fujiwara, M., 49
Furin, G.G., 271

García-Granda, S., 23
Gau, H.-M., 183
Gavrilova, A.N., 271
Gonçalves, I.S., 169
Gong, M.L., 183
Görls, H., 13

Goubitz, K., 109
Groot, A.M., 109

Hengge, E., 227
Herdtweck, E., 169
Herzog, U., 147

Jalón, F.A., 69
Jones, P.G., 53

Kameyama, M., 255
Käser, M., 219
Kergoat, R., 1, 31
Khotsyanova, T.L., 129
Kiefer, W., 153
Kizas, O.A., 39
Koch, J., 13
Koridze, A.A., 39
Kosugi, M., 255
Kratky, C., 195, 209
Krivykh, V.V., 39
Kunicki, A., 249
Kutschera, G., 195
Kuznetsov, S.I., 129

Le Berre-Cosquer, N., 1, 31
Leblanc, B., 31
Levendis, D.C., 231
Lin, J.T., 183
Longoni, G., 59
Lu, X., 83
Lyssenko, K.A., 259

Mays, M.J., 137
Mernyi, A., 209
Migita, T., 255
Mogi, E., 159

Otero, A., 69

Pasynkiewicz, S., 243
Pätzold, U., 147
Pérez-Carreño, E., 23
Pérez-Manrique, M., 69
Polzer, T., 153
Pruchnik, F., 75

Raithby, P.R., 137
Rodríguez, A., 69
Roewer, G., 147
Romão, C.C., 169
Röttger, D., 263
Rülke, R.E., 109

Sadowski, R., 249
Saitkulova, L.N., 271
Salzer, A., 219
Sato, M., 121, 159
Schenk, H., 109
Schmuck, S., 263
Schweder, B., 13
Semin, G.K., 129
Shiow, Y.-M., 183
Shubina, E.S., 271
Shur, V.B., 271
Singer, H., 267
Solan, G.A., 137
Souma, Y., 49
Steigerwald, M., 267
Struchkov, Yu.T., 39, 271

Tanaka, M., 49
Tanaka, Y., 255
Tanji, T., 255
Tikhonova, I.A., 271
Toyota, K., 7

Uguagliati, P., 101

Van Leeuwen, P.W.N.M., 109
Venturini, E., 59
Vicente, J., 53
Visentin, F., 101
Vorontsov, E.V., 39
Vrieze, K., 109

Wajda-Hermanowicz, K., 75
Walther, D., 13
Wang, S.Y., 183
Wang, Z., 91
Weissensteiner, W., 195, 209
Wen, Y.S., 183
Widhalm, M., 195, 209

Yanovsky, A.I., 39, 271
Yasunami, M., 7
Yoshida, A., 255
Yoshifuji, M., 7
Yutronic, N., 23

Zachara, J., 249
Zechmann, A., 227
Zhu, G., 83
Ziemkowska, W., 243
Zuber, M., 75

Elsevier Science S.A.

ELSEVIER

Journal of Organometallic Chemistry 508 (1996) 285–290

Journal of Organometallic Chemistry

# Subject Index of Volume 508

Acetylacetonato $\mu$-hydroxo complexes
Synthesis of some $\mu$-hydroxo-, phenoxo- and O,O-acetylacetonato-arylgold(III) complexes. Crystal structure of $[Au(C_6H_4NO_2-2)_2(\mu\text{-}OH)]_2 \cdot 2Et_2O$ (J. Vicente, M.D. Bermúdez, F.J. Carrión and P.G. Jones), 53

Acetylide complex
Preparation and some properties of Pt(II) ruthenocenylacetylide complexes (M. Sato and E. Mogi), 159

Acid halide
Reaction of pentaarylantimony with acid halide, aldehyde and ketone (M. Fujiwara, M. Tanaka, A. Baba, H. Ando and Y. Souma), 49

Aldehyde
Hydride abstraction from ($\eta^2$-acetaldehyde)zirconocene dimer using $B(C_6F_5)_3$ (D. Röttger, S. Schmuck and G. Erker), 263
Reaction of pentaarylantimony with acid halide, aldehyde and ketone (M. Fujiwara, M. Tanaka, A. Baba, H. Ando and Y. Souma), 49

Aliphatic diols
Reactions of trimethylaluminium with aliphatic diols (W. Ziemkowska and S. Pasynkiewicz), 243

Alkali metals
Preparation of Group 4 metal complexes of a bulky amido-fluorenyl ligand (H.V.R. Dias, Z. Wang and S.G. Bott), 91

Alkylidyne
The reactions of tricobalt alkylidyne complexes $[Co_3(\mu_3\text{-}CR)(CO)_9]$ (R = Me, $CO_2Me$) with the vinyl phosphine ligands $PPh_2CH=CH_2$ and *cis*-$Ph_2PCH=CHPPh_2$; crystal structure of $[Co_3(\mu_3\text{-}CCO_2Me)(\mu\text{-}Ph_2PCH=CHPPh_2)(CO)_7]$ (G.A. Acum, M.J. Mays, P.R. Raithby and G.A. Solan), 137

Alkyne
Vergleichende Dimerisierung der Enantiomere von Oct-1-in-3-ol mit chiralen Rhodium-Phosphan-Komplexen (H. Singer und M. Steigerwald), 267

Alkynyl
Comparison of the oxidation of dinuclear cyclopentadienyl iron diphosphine complexes with the bridging ligands –CN and $-C{=}C(CH_2)_2CN$ (G.A. Carriedo, A. Arancibia, C. Díaz-Valenzuela, N. Yutronic, E. Pérez-Carreño and S. García-Granda), 23

Allenylidene complexes
Synthesis of secondary allenylidene–molybdenum complexes with a ferrocenyl substituent from carbenium ions species stabilized by two organometallic moieties (J.-F. Capon, N. Le Berre-Cosquer, B. Leblanc and R. Kergoat), 31

Allyl transfer
Mechanism of oxidative allyl transfer from allylic ammonium cations to palladium(0) $\alpha$-diimine complexes (L. Canovese, F. Visentin, P. Uguagliati, F. Di Bianca, A. Fontana and B. Crociani), 101

Aluminium
Reactions of trimethylaluminium with aliphatic diols (W. Ziemkowska and S. Pasynkiewicz), 243
Synthesis, properties and crystal structure bis(cyclopentadienyl)-aluminium complex $[\eta^1\text{-}(C_5H_5)_2AlO\text{-}^iPr]_2$ (A. Kunicki, R. Sadowski and J. Zachara), 249

Amide
Preparation of Group 4 metal complexes of a bulky amido-fluorenyl ligand (H.V.R. Dias, Z. Wang and S.G. Bott), 91

Aminophosphines
Synthesis and molecular structure of enantiopure 1-(diphenylphosphino)-2,1′-[(1-*N*,*N*-dimethylamino)-1,3-propanediyl]-ferrocene and its palladium dichloride complex, a new ligand for enantioselective catalysts (A. Mernyi, C. Kratky, W. Weissensteiner and M. Widhalm), 209

Antimony
Reaction of pentaarylantimony with acid halide, aldehyde and ketone (M. Fujiwara, M. Tanaka, A. Baba, H. Ando and Y. Souma), 49

BPZM
Synthesis and spectroscopic studies of new hydridoruthenium complexes: catalytic reactions of [RuHCl(bpzm)(cod)] (bpzm = bis(pyrazol-1-yl)methane, cod = cycloocta-1,5-diene) (F.A. Jalón, A. Otero, A. Rodríguez and M. Pérez-Manrique), 69

Butyrolactone
Molecular oxygen promoted oxidative cleavage of carbon–palladium bonds — catalytic cyclization of allylic 2-alkynoates to $\alpha$-alkylidene-$\gamma$-butyrolactones by a $Pd^{II}$ complex (G. Zhu and X. Lu), 83

Carbenium ions
Reaction of sodium amalgam with carbenium ions species stabilised by two adjacent organometallic moieties (J.-F. Capon, N. Le Berre-Cosquer and R. Kergoat), 1
Synthesis of secondary allenylidene–molybdenum complexes with a ferrocenyl substituent from carbenium ions species stabilized by two organometallic moieties (J.-F. Capon, N. Le Berre-Cosquer, B. Leblanc and R. Kergoat), 31

Carbon monoxide
Insertion reactions involving palladium complexes with nitrogen ligands. I. Reactivity towards carbon monoxide of methylpalladium(II) complexes containing bidentate $\alpha$-diimine ligands: crystal structures of four methylpalladium (II) and acylpalladium(II) complexes (R.E. Rülke, J.G.P. Delis, A.M. Groot, C.J. Elsevier, P.W.N.M. Van Leeuwen, K. Vrieze, K. Goubitz and H. Schenk), 109

Carbonyl
Catalytic hydroformylation of (1*S*,5*S*)-(−)- and (1*R*,5*R*)-(+)-$\beta$-pinene: stereoselective synthesis and spectroscopic characterization of (1*S*,2*R*,5*S*)-, (1*S*,2*S*,5*S*)-, (1*R*,2*R*,5*R*)- and (1*R*,2*S*,5*R*)-10-formylpinane (F. Azzaroni, P. Biscarini, S. Bordoni, G. Longoni and E. Venturini), 59
Diphenylphosphine derivatives of $Co(NO)(CO)_3$, $Fe(NO)_2(CO)_2$ and $Mn(NO)(CO)_4$ (J.T. Lin, S.Y. Wang, Y.C. Chou, M.L. Gong, Y.-M. Shiow, H.-M. Gau and Y.S. Wen), 183
$^{55}Mn$ and $^{187}Re$ NQR spectral studies of modulation effects of mutual motions of electrons and atomic nuclei in cyclopentadienyl tricarbonyl manganese and rhenium complexes (G.K. Semin, S.I. Kuznetsov, E.V. Bryukhova and T.L. Khotsyanova), 129

Multiply substituted cyclopentadienyl metal complexes: I. Solid-state and solution conformational studies on ($\eta^5$-$C_5Me_4R$)Fe(CO)(L)I (R = H, $^t$Bu) (K.E. Du Plooy, J. Du Toit, D.C. Levendis and N.J. Coville), 231

Properties and reactivity of the new [$Ir_4$($\mu$-CO)$_3$(CO)$_5$($\mu$-$PR_3$)($PR_3$)$_2$] clusters, ($PR_3$ = $PPh_x pyl_{3-x}$, pyl = 2-pyridyl) (K. Wajda-Hermanowicz, F. Pruchnik and M. Zuber), 75

Reactions of (THF)W(CO)$_5$ with some diphosphenes carrying bulky aryl and phenoxy groups (D.-L. An, K. Toyota, M. Yasunami and M. Yoshifuji), 7

The reactions of tricobalt alkylidyne complexes [$Co_3$($\mu_3$-CR)(CO)$_9$] (R = Me, $CO_2$Me) with the vinyl phosphine ligands $PPh_2CH{=}CH_2$ and *cis*-$Ph_2PCH{=}CHPPh_2$; crystal structure of [$Co_3$($\mu_3$-$CCO_2Me$)($\mu$-$Ph_2PCH{=}CHPPh_2$)(CO)$_7$] (G.A. Acum, M.J. Mays, P.R. Raithby and G.A. Solan), 137

Carbonyl complexes

Optically active transition-metal complexes. III. Synthesis of optically active ($\eta^4$-aminodiolefin)tricarbonyl iron complexes. Kinetic resolution of a chiral amine by means of an optically active dienyl iron cation (M. Käser and A. Salzer), 219

Catalysis

Insertion reactions involving palladium complexes with nitrogen ligands. I. Reactivity towards carbon monoxide of methylpalladium(II) complexes containing bidentate α-diimine ligands: crystal structures of four methylpalladium (II) and acylpalladium(II) complexes (R.E. Rülke, J.G.P. Delis, A.M. Groot, C.J. Elsevier, P.W.N.M. Van Leeuwen, K. Vrieze, K. Goubitz and H. Schenk), 109

Katalytische Hydrierung von Halogenmonosilanen mit Tributylzinnhydrid (U. Pätzold, G. Roewer und U. Herzog), 147

Palladium-catalyzed reaction of 1-aza-5-germa-5-organobicyclo-[3.3.3]undecane with aryl bromide (M. Kosugi, T. Tanji, Y. Tanaka, A. Yoshida, K. Fugami, M. Kameyama and T. Migita), 255

Synthesis and spectroscopic studies of new hydridoruthenium complexes: catalytic reactions of [RuHCl(bpzm)(cod)] (bpzm = bis(pyrazol-1-yl)methane, cod = cycloocta-1,5-diene) (F.A. Jalón, A. Otero, A. Rodríguez and M. Pérez-Manrique), 69

Vergleichende Dimerisierung der Enantiomere von Oct-1-in-3-ol mit chiralen Rhodium-Phosphan-Komplexen (H. Singer und M. Steigerwald), 267

Catalyst

Synthesis and molecular structure of enantiopure 1-(diphenylphosphino)-2,1'-[(1-*N*,*N*-dimethylamino)-1,3-propanediyl]-ferrocene and its palladium dichloride complex, a new ligand for enantioselective catalysts (A. Mernyi, C. Kratky, W. Weissensteiner and M. Widhalm), 209

Charge density analysis

Electron density distribution in the vanadocene crystal on the basis of X-ray diffraction data at 108 K (M.Yu. Antipin, K.A. Lyssenko and R. Boese), 259

Chemoselective reaction

Reaction of pentaarylantimony with acid halide, aldehyde and ketone (M. Fujiwara, M. Tanaka, A. Baba, H. Ando and Y. Souma), 49

Chirality

Vergleichende Dimerisierung der Enantiomere von Oct-1-in-3-ol mit chiralen Rhodium-Phosphan-Komplexen (H. Singer und M. Steigerwald), 267

Chromium

Reactions of (THF)W(CO)$_5$ with some diphosphenes carrying bulky aryl and phenoxy groups (D.-L. An, K. Toyota, M. Yasunami and M. Yoshifuji), 7

Circular dichroism

Isomeric diphosphines of a heteroannularly bridged ferrocene: preparation, chromatographic separation and structure elucidation (G. Kutschera, C. Kratky, W. Weissensteiner and M. Widhalm), 195

Clusters

Properties and reactivity of the new [$Ir_4$($\mu$-CO)$_3$(CO)$_5$($\mu$-$PR_3$)($PR_3$)$_2$] clusters, ($PR_3$ = $PPh_x pyl_{3-x}$, pyl = 2-pyridyl) (K. Wajda-Hermanowicz, F. Pruchnik and M. Zuber), 75

Cobalt

Catalytic hydroformylation of (1*S*,5*S*)-(−)- and (1*R*,5*R*)-(+)-β-pinene: siereoselective synthesis and spectroscopic characterization of (1*S*,2*R*,5*S*)-, (1*S*,2*S*,5*S*)-, (1*R*,2*R*,5*R*)- and (1*R*,2*S*,5*R*)-10-formylpinane (F. Azzaroni, P. Biscarini, S. Bordoni, G. Longoni and E. Venturini), 59

Diphenylphosphine derivatives of Co(NO)(CO)$_3$, Fe(NO)$_2$(CO)$_2$ and Mn(NO)(CO)$_4$ (J.T. Lin, S.Y. Wang, Y.C. Chou, M.L. Gong, Y.-M. Shiow, H.-M. Gau and Y.S. Wen), 183

Cod

Synthesis and spectroscopic studies of new hydridoruthenium complexes: catalytic reactions of [RuHCl(bpzm)(cod)] (bpzm = bis(pyrazol-1-yl)methane, cod = cycloocta-1,5-diene) (F.A. Jalón, A. Otero, A. Rodríguez and M. Pérez-Manrique), 69

Complexes

Reactions of trimethylaluminium with aliphatic diols (W. Ziemkowska and S. Pasynkiewicz), 243

Cross-coupling

Palladium-catalyzed reaction of 1-aza-5-germa-5-organobicyclo-[3.3.3]undecane with aryl bromide (M. Kosugi, T. Tanji, Y. Tanaka, A. Yoshida, K. Fugami, M. Kameyama and T. Migita), 255

Crown compounds

Crown compounds for anions. A polymeric complex of cyclic trimeric perfluoro-*o*-phenylenemercury with thiocyanate anion containing an infinite helical chain of alternating molecules of mercury-containing macrocycle and $SCN^-$ ions (I.A. Tikhonova, F.M. Dolgushin, A.I. Yanovsky, Yu.T. Struchkov, A.N. Gavrilova, L.N. Saitkulova, E.S. Shubina, L.M. Epstein, G.G. Furin and V.B. Shur), 271

Crystal structure

Insertion reactions involving palladium complexes with nitrogen ligands. I. Reactivity towards carbon monoxide of methylpalladium(II) complexes containing bidentate α-diimine ligands: crystal structures of four methylpalladium (II) and acylpalladium(II) complexes (R.E. Rülke, J.G.P. Delis, A.M. Groot, C.J. Elsevier, P.W.N.M. Van Leeuwen, K. Vrieze, K. Goubitz and H. Schenk), 109

Multiply substituted cyclopentadienyl metal complexes: I. Solid-state and solution conformational studies on ($\eta^5$-$C_5Me_4R$)Fe(CO)(L)I (R = H, $^t$Bu) (K.E. Du Plooy, J. Du Toit, D.C. Levendis and N.J. Coville), 231

Preparation of Group 4 metal complexes of a bulky amido-fluorenyl ligand (H.V.R. Dias, Z. Wang and S.G. Bott), 91

Protonation of triosmium clusters $Os_3$(CO)$_9$($\mu$-CO)($\mu_3$-2$\sigma$,$\eta^2$-HC≡CR) and $Os_3$($\mu$-H)(CO)$_9$($\mu_3$-$\sigma$,2$\eta^2$-C≡CR) (R = $CH_2OH$, $CMe_2OH$, C(Me)=$CH_2$) (V.V. Krivykh, O.A. Kizas, E.V. Vorontsov, F.M. Dolgushin, A.I. Yanovsky, Yu.T. Struchkov and A.A. Koridze), 39

Synthesis and molecular structure of enantiopure 1-(diphenylphosphino)-2,1'-[(1-*N*,*N*-dimethylamino)-1,3-propanediyl]-ferrocene and its palladium dichloride complex, a new ligand for enantioselective catalysts (A. Mernyi, C. Kratky, W. Weissensteiner and M. Widhalm), 209

Synthesis of some μ-hydroxo-, phenoxo- and O,O-acetylacetonato-arylgold(III) complexes. Crystal structure of $[Au(C_6H_4NO_2-2)_2(\mu\text{-}OH)]_2 \cdot 2Et_2O$ (J. Vicente, M.D. Bermúdez, F.J. Carrión and P.G. Jones), 53

The reactions of tricobalt alkylidyne complexes $[Co_3(\mu_3\text{-}CR)(CO)_9]$ (R = Me, $CO_2Me$) with the vinyl phosphine ligands $PPh_2CH{=}CH_2$ and *cis*-$Ph_2PCH{=}CHPPh_2$; crystal structure of $[Co_3(\mu_3\text{-}CCO_2Me)(\mu\text{-}Ph_2PCH{=}CHPPh_2)(CO)_7]$ (G.A. Acum, M.J. Mays, P.R. Raithby and G.A. Solan), 137

Cyanide

Comparison of the oxidation of dinuclear cyclopentadienyl iron diphosphine complexes with the bridging ligands –CN and $-C{=}C(CH_2)_2CN$ (G.A. Carriedo, A. Arancibia, C. Díaz-Valenzuela, N. Yutronic, E. Pérez-Carreño and S. García-Granda), 23

Cyclization

Molecular oxygen promoted oxidative cleavage of carbon–palladium bonds — catalytic cyclization of allylic 2-alkynoates to α-alkylidene-γ-butyrolactones by a $Pd^{II}$ complex (G. Zhu and X. Lu), 83

Cyclooctatetraenyl

Zur Elektronenstruktur metallorganischer Komplexe der f-Elemente. XXXVIII. Halbsandwich-Komplexe der Stöchiometrien (COT)Ln(HBpz$_3$) und (COT)Ln[HB(3,5-Me$_2$pz)$_3$]-ideale Systeme für die experimentelle Bestimmung der Kristallfeld-Aufspaltungseffekte des Cyclooctatetraenyl-Liganden (H.-D. Amberger und F.T. Edelmann), 275

Cyclopentadienyl

Multiply substituted cyclopentadienyl metal complexes: I. Solid-state and solution conformational studies on $(\eta^5\text{-}C_5Me_4R)Fe(CO)(L)I$ (R = H, $^t$Bu) (K.E. Du Plooy, J. Du Toit, D.C. Levendis and N.J. Coville), 231

Synthesis, properties and crystal structure bis(cyclopentadienyl)-aluminium complex $[\eta^1\text{-}(C_5H_5)_2AlO\text{-}^i Pr]_2$ (A. Kunicki, R. Sadowski and J. Zachara), 249

Diphosphine

Isomeric diphosphines of a heteroannularly bridged ferrocene: preparation, chromatographic separation and structure elucidation (G. Kutschera, C. Kratky, W. Weissensteiner and M. Widhalm), 195

Early transition metals

Hydride abstraction from ($\eta^2$-acetaldehyde)zirconocene dimer using $B(C_6F_5)_3$ (D. Röttger, S. Schmuck and G. Erker), 263

EHMO calculations

Comparison of the oxidation of dinuclear cyclopentadienyl iron diphosphine complexes with the bridging ligands –CN and $-C{=}C(CH_2)_2CN$ (G.A. Carriedo, A. Arancibia, C. Díaz-Valenzuela, N. Yutronic, E. Pérez-Carreño and S. García-Granda), 23

Electrochemistry

Comparison of the oxidation of dinuclear cyclopentadienyl iron diphosphine complexes with the bridging ligands –CN and $-C{=}C(CH_2)_2CN$ (G.A. Carriedo, A. Arancibia, C. Díaz-Valenzuela, N. Yutronic, E. Pérez-Carreño and S. García-Granda), 23

Electron–nuclear motions

$^{55}Mn$ and $^{187}Re$ NQR spectral studies of modulation effects of mutual motions of electrons and atomic nuclei in cyclopentadienyl tricarbonyl manganese and rhenium complexes (G.K. Semin, S.I. Kuznetsov, E.V. Bryukhova and T.L. Khotsyanova), 129

Ferrocene

Synthesis and molecular structure of enantiopure 1-(diphenylphosphino)-2,1'-[(1-*N*,*N*-dimethylamino)-1,3-propanediyl]-ferrocene and its palladium dichloride complex, a new ligand for enantioselective catalysts (A. Mernyi, C. Kratky, W. Weissensteiner and M. Widhalm), 209

Synthesis of secondary allenylidene–molybdenum complexes with a ferrocenyl substituent from carbenium ions species stabilized by two organometallic moieties (J.-F. Capon, N. Le Berre-Cosquer, B. Leblanc and R. Kergoat), 31

Ferrocenophane

Reaction of sodium amalgam with carbenium ions species stabilised by two adjacent organometallic moieties (J.-F. Capon, N. Le Berre-Cosquer and R. Kergoat), 1

Ferrocenyl

Reaction of sodium amalgam with carbenium ions species stabilised by two adjacent organometallic moieties (J.-F. Capon, N. Le Berre-Cosquer and R. Kergoat), 1

Germanium

Palladium-catalyzed reaction of 1-aza-5-germa-5-organobicyclo-[3.3.3]undecane with aryl bromide (M. Kosugi, T. Tanji, Y. Tanaka, A. Yoshida, K. Fugami, M. Kameyama and T. Migita), 255

Gold

Synthesis of some μ-hydroxo-, phenoxo- and O,O-acetylacetonato-arylgold(III) complexes. Crystal structure of $[Au(C_6H_4NO_2-2)_2(\mu\text{-}OH)]_2 \cdot 2Et_2O$ (J. Vicente, M.D. Bermúdez, F.J. Carrión and P.G. Jones), 53

Group 4

Hydride abstraction from ($\eta^2$-acetaldehyde)zirconocene dimer using $B(C_6F_5)_3$ (D. Röttger, S. Schmuck and G. Erker), 263

Preparation of Group 4 metal complexes of a bulky amido-fluorenyl ligand (H.V.R. Dias, Z. Wang and S.G. Bott), 91

Halogenosilanes

Katalytische Hydrierung von Halogenmonosilanen mit Tributylzinnhydrid (U. Pätzold, G. Roewer und U. Herzog), 147

Heteroannularly-bridged ferrocene

Isomeric diphosphines of a heteroannularly bridged ferrocene: preparation, chromatographic separation and structure elucidation (G. Kutschera, C. Kratky, W. Weissensteiner and M. Widhalm), 195

Hydride

Hydride abstraction from ($\eta^2$-acetaldehyde)zirconocene dimer using $B(C_6F_5)_3$ (D. Röttger, S. Schmuck and G. Erker), 263

Synthesis and spectroscopic studies of new hydridoruthenium complexes: catalytic reactions of [RuHCl(bpzm)(cod)] (bpzm = bis(pyrazol-1-yl)methane, cod = cycloocta-1,5-diene) (F.A. Jalón, A. Otero, A. Rodríguez and M. Pérez-Manrique), 69

Hydroformylation

Catalytic hydroformylation of (1*S*,5*S*)-(−)- and (1*R*,5*R*)-(+)-β-pinene: stereoselective synthesis and spectroscopic characterization of (1*S*,2*R*,5*S*)-, (1*S*,2*S*,5*S*)-, (1*R*,2*R*,5*R*)- and (1*R*,2*S*,5*R*)-10-formylpinane (F. Azzaroni, P. Biscarini, S. Bordoni, G. Longoni and E. Venturini), 59

Hydrogenation

Katalytische Hydrierung von Halogenmonosilanen mit Tributylzinnhydrid (U. Pätzold, G. Roewer und U. Herzog), 147

Synthesis and spectroscopic studies of new hydridoruthenium complexes: catalytic reactions of [RuHCl(bpzm)(cod)] (bpzm = bis(pyrazol-1-yl)methane, cod = cycloocta-1,5-diene) (F.A. Jalón, A. Otero, A. Rodríguez and M. Pérez-Manrique), 69

Imine

Insertion reactions involving palladium complexes with nitrogen ligands. I. Reactivity towards carbon monoxide of methylpalladium(II) complexes containing bidentate α-diimine ligands: crystal structures of four methylpalladium (II) and acylpalladium(II) complexes (R.E. Rülke, J.G.P. Delis, A.M. Groot, C.J. Elsevier, P.W.N.M. Van Leeuwen, K. Vrieze, K. Goubitz and H. Schenk), 109

Indenyl complexes
Ring slippage in indenyl derivatives of molybdenum and tungsten (J.R. Ascenso, I.S. Gonçalves, E. Herdtweck and C.C. Romão), 169
Iridium
Properties and reactivity of the new $[Ir_4(\mu\text{-}CO)_3(CO)_5(\mu\text{-}PR_3)(PR_3)_2]$ clusters, ($PR_3 = PPh_xpyl_{3-x}$, pyl = 2-pyridyl) (K. Wajda-Hermanowicz, F. Pruchnik and M. Zuber), 75
Iron
Comparison of the oxidation of dinuclear cyclopentadienyl iron diphosphine complexes with the bridging ligands –CN and $-C{\equiv}C(CH_2)_2CN$ (G.A. Carriedo, A. Arancibia, C. Díaz-Valenzuela, N. Yutronic, E. Pérez-Carreño and S. García-Granda), 23
Diphenylphosphine derivatives of $Co(NO)(CO)_3$, $Fe(NO)_2(CO)_2$ and $Mn(NO)(CO)_4$ (J.T. Lin, S.Y. Wang, Y.C. Chou, M.L. Gong, Y.-M. Shiow, H.-M. Gau and Y.S. Wen), 183
Isomeric diphosphines of a heteroannularly bridged ferrocene: preparation, chromatographic separation and structure elucidation (G. Kutschera, C. Kratky, W. Weissensteiner and M. Widhalm), 195
Multiply substituted cyclopentadienyl metal complexes: I. Solid-state and solution conformational studies on $(\eta^5\text{-}C_5Me_4R)Fe(CO)(L)I$ (R = H, $^t$Bu) (K.E. Du Plooy, J. Du Toit, D.C. Levendis and N.J. Coville), 231
Optically active transition-metal complexes. III. Synthesis of optically active ($\eta^4$-aminodiolefin)tricarbonyl iron complexes. Kinetic resolution of a chiral amine by means of an optically active dienyl iron cation (M. Käser and A. Salzer), 219
Synthesis and molecular structure of enantiopure 1-(diphenylphosphino)-2,1'-[(1-*N*,*N*-dimethylamino)-1,3-propanediyl]-ferrocene and its palladium dichloride complex, a new ligand for enantioselective catalysts (A. Mernyi, C. Kratky, W. Weissensteiner and M. Widhalm), 209
Synthesis of secondary allenylidene–molybdenum complexes with a ferrocenyl substituent from carbenium ions species stabilized by two organometallic moieties (J.-F. Capon, N. Le Berre-Cosquer, B. Leblanc and R. Kergoat), 31
Synthetic studies of permethylcyclopentadienyl ruthenium(II) complexes involving dppf, (±)-BINAP and (±)-DIOP ligands (M. Sato and M. Asai), 121
Isomers
Reactions of trimethylaluminium with aliphatic diols (W. Ziemkowska and S. Pasynkiewicz), 243

Ketone
Reaction of pentaarylantimony with acid halide, aldehyde and ketone (M. Fujiwara, M. Tanaka, A. Baba, H. Ando and Y. Souma), 49
Kinetic resolution
Optically active transition-metal complexes. III. Synthesis of optically active ($\eta^4$-aminodiolefin)tricarbonyl iron complexes. Kinetic resolution of a chiral amine by means of an optically active dienyl iron cation (M. Käser and A. Salzer), 219
Kinetic studies
Mechanism of oxidative allyl transfer from allylic ammonium cations to palladium(0) α-diimine complexes (L. Canovese, F. Visentin, P. Uguagliati, F. Di Bianca, A. Fontana and B. Crociani), 101

Late transition metals
Insertion reactions involving palladium complexes with nitrogen ligands. I. Reactivity towards carbon monoxide of methylpalladium(II) complexes containing bidentate α-diimine ligands: crystal structures of four methylpalladium (II) and acylpalladium(II) complexes (R.E. Rülke, J.G.P. Delis, A.M. Groot, C.J. Elsevier, P.W.N.M. Van Leeuwen, K. Vrieze, K. Goubitz and H. Schenk), 109

Ligand bridged
Comparison of the oxidation of dinuclear cyclopentadienyl iron diphosphine complexes with the bridging ligands –CN and $-C{\equiv}C(CH_2)_2CN$ (G.A. Carriedo, A. Arancibia, C. Díaz-Valenzuela, N. Yutronic, E. Pérez-Carreño and S. García-Granda), 23
Ligand field theory
Zur Elektronenstruktur metallorganischer Komplexe der f-Elemente. XXXVIII. Halbsandwich-Komplexe der Stöchiometrien $(COT)Ln(HBpz_3)$ und $(COT)Ln[HB(3,5\text{-}Me_2pz)_3]$-ideale Systeme für die experimentelle Bestimmung der Kristallfeld-Aufspaltungseffekte des Cyclooctatetraenyl-Liganden (H.-D. Amberger und F.T. Edelmann), 275

Macrocycle
Crown compounds for anions. A polymeric complex of cyclic trimeric perfluoro-*o*-phenylenemercury with thiocyanate anion containing an infinite helical chain of alternating molecules of mercury-containing macrocycle and $SCN^-$ ions (I.A. Tikhonova, F.M. Dolgushin, A.I. Yanovsky, Yu.T. Struchkov, A.N. Gavrilova, L.N. Saitkulova, E.S. Shubina, L.M. Epstein, G.G. Furin and V.B. Shur), 271
Manganese
$^{55}Mn$ and $^{187}Re$ NQR spectral studies of modulation effects of mutual motions of electrons and atomic nuclei in cyclopentadienyl tricarbonyl manganese and rhenium complexes (G.K. Semin, S.I. Kuznetsov, E.V. Bryukhova and T.L. Khotsyanova), 129
Diphenylphosphine derivatives of $Co(NO)(CO)_3$, $Fe(NO)_2(CO)_2$ and $Mn(NO)(CO)_4$ (J.T. Lin, S.Y. Wang, Y.C. Chou, M.L. Gong, Y.-M. Shiow, H.-M. Gau and Y.S. Wen), 183
Mercury
Crown compounds for anions. A polymeric complex of cyclic trimeric perfluoro-*o*-phenylenemercury with thiocyanate anion containing an infinite helical chain of alternating molecules of mercury-containing macrocycle and $SCN^-$ ions (I.A. Tikhonova, F.M. Dolgushin, A.I. Yanovsky, Yu.T. Struchkov, A.N. Gavrilova, L.N. Saitkulova, E.S. Shubina, L.M. Epstein, G.G. Furin and V.B. Shur), 271
Metallocene
Preparation of Group 4 metal complexes of a bulky amido-fluorenyl ligand (H.V.R. Dias, Z. Wang and S.G. Bott), 91
MO calculations
Zur Elektronenstruktur metallorganischer Komplexe der f-Elemente. XXXVIII. Halbsandwich-Komplexe der Stöchiometrien $(COT)Ln(HBpz_3)$ und $(COT)Ln[HB(3,5\text{-}Me_2pz)_3]$-ideale Systeme für die experimentelle Bestimmung der Kristallfeld-Aufspaltungseffekte des Cyclooctatetraenyl-Liganden (H.-D. Amberger und F.T. Edelmann), 275
Molecular oxygen
Molecular oxygen promoted oxidative cleavage of carbon–palladium bonds — catalytic cyclization of allylic 2-alkynoates to α-alkylidene-γ-butyrolactones by a $Pd^{II}$ complex (G. Zhu and X. Lu), 83
Molybdenum
Reactions of $(THF)W(CO)_5$ with some diphosphenes carrying bulky aryl and phenoxy groups (D.-L. An, K. Toyota, M. Yasunami and M. Yoshifuji), 7
Ring slippage in indenyl derivatives of molybdenum and tungsten (J.R. Ascenso, I.S. Gonçalves, E. Herdtweck and C.C. Romão), 169
Synthesis of secondary allenylidene–molybdenum complexes with a ferrocenyl substituent from carbenium ions species stabilized by two organometallic moieties (J.-F. Capon, N. Le Berre-Cosquer, B. Leblanc and R. Kergoat), 31

Molybdenum clusters
Reaction of sodium amalgam with carbenium ions species stabilised by two adjacent organometallic moieties (J.-F. Capon, N. Le Berre-Cosquer and R. Kergoat), 1

Nitrosyl
Diphenylphosphine derivatives of $Co(NO)(CO)_3$, $Fe(NO)_2(CO)_2$ and $Mn(NO)(CO)_4$ (J.T. Lin, S.Y. Wang, Y.C. Chou, M.L. Gong, Y.-M. Shiow, H.-M. Gau and Y.S. Wen), 183
NMR spectroscopy
Properties and reactivity of the new $[Ir_4(\mu\text{-}CO)_3(CO)_5(\mu\text{-}PR_3)(PR_3)_2]$ clusters, ($PR_3 = PPh_xpyl_{3-x}$, pyl = 2-pyridyl) (K. Wajda-Hermanowicz, F. Pruchnik and M. Zuber), 75
Nuclear magnetic resonance
Multiply substituted cyclopentadienyl metal complexes: I. Solid-state and solution conformational studies on $(\eta^5\text{-}C_5Me_4R)Fe(CO)(L)I$ (R = H, $^t$Bu) (K.E. Du Plooy, J. Du Toit, D.C. Levendis and N.J. Coville), 231
Synthesis, properties and crystal structure bis(cyclopentadienyl)-aluminium complex $[\eta^1\text{-}(C_5H_5)_2AlO\text{-}^iPr]_2$ (A. Kunicki, R. Sadowski and J. Zachara), 249
Nuclear Quadrupole Resonance
$^{55}Mn$ and $^{187}Re$ NQR spectral studies of modulation effects of mutual motions of electrons and atomic nuclei in cyclopentadienyl tricarbonyl manganese and rhenium complexes (G.K. Semin, S.I. Kuznetsov, E.V. Bryukhova and T.L. Khotsyanova), 129

Optically active ligands
Optically active transition-metal complexes. III. Synthesis of optically active ($\eta^4$-aminodiolefin)tricarbonyl iron complexes. Kinetic resolution of a chiral amine by means of an optically active dienyl iron cation (M. Käser and A. Salzer), 219
Optical spectra
Zur Elektronenstruktur metallorganischer Komplexe der f-Elemente. XXXVIII. Halbsandwich-Komplexe der Stöchiometrien (COT)Ln($HBpz_3$) und (COT)Ln[$HB(3,5\text{-}Me_2pz)_3$]-ideale Systeme für die experimentelle Bestimmung der Kristallfeld-Aufspaltungseffekte des Cyclooctatetraenyl-Liganden (H.-D. Amberger und F.T. Edelmann), 275
Oxidation
Preparation and some properties of Pt(II) ruthenocenylacetylide complexes (M. Sato and E. Mogi), 159
Oxidative cleavage
Molecular oxygen promoted oxidative cleavage of carbon–palladium bonds — catalytic cyclization of allylic 2-alkynoates to α-alkylidene-γ-butyrolactones by a $Pd^{II}$ complex (G. Zhu and X. Lu), 83

Palladium
Insertion reactions involving palladium complexes with nitrogen ligands. I. Reactivity towards carbon monoxide of methylpalladium(II) complexes containing bidentate α-diimine ligands: crystal structures of four methylpalladium (II) and acylpalladium(II) complexes (R.E. Rülke, J.G.P. Delis, A.M. Groot, C.J. Elsevier, P.W.N.M. Van Leeuwen, K. Vrieze, K. Goubitz and H. Schenk), 109
Mechanism of oxidative allyl transfer from allylic ammonium cations to palladium(0) α-diimine complexes (L. Canovese, F. Visentin, P. Uguagliati, F. Di Bianca, A. Fontana and B. Crociani), 101
Palladium-catalyzed reaction of 1-aza-5-germa-5-organobicyclo-[3.3.3]undecane with aryl bromide (M. Kosugi, T. Tanji, Y. Tanaka, A. Yoshida, K. Fugami, M. Kameyama and T. Migita), 255
Palladium(II)
Molecular oxygen promoted oxidative cleavage of carbon–palladium bonds — catalytic cyclization of allylic 2-alkynoates to α-alkylidene-γ-butyrolactones by a $Pd^{II}$ complex (G. Zhu and X. Lu), 83
Palladium complex
Synthesis and molecular structure of enantiopure 1-(diphenylphosphino)-2,1′-[(1-*N*,*N*-dimethylamino)-1,3-propanediyl]-ferrocene and its palladium dichloride complex, a new ligand for enantioselective catalysts (A. Mernyi, C. Kratky, W. Weissensteiner and M. Widhalm), 209
Pentaarylantimony
Reaction of pentaarylantimony with acid halide, aldehyde and ketone (M. Fujiwara, M. Tanaka, A. Baba, H. Ando and Y. Souma), 49
Phosphine
Diphenylphosphine derivatives of $Co(NO)(CO)_3$, $Fe(NO)_2(CO)_2$ and $Mn(NO)(CO)_4$ (J.T. Lin, S.Y. Wang, Y.C. Chou, M.L. Gong, Y.-M. Shiow, H.-M. Gau and Y.S. Wen), 183
Properties and reactivity of the new $[Ir_4(\mu\text{-}CO)_3(CO)_5(\mu\text{-}PR_3)(PR_3)_2]$ clusters, ($PR_3 = PPh_xpyl_{3-x}$, pyl = 2-pyridyl) (K. Wajda-Hermanowicz, F. Pruchnik and M. Zuber), 75
Vergleichende Dimerisierung der Enantiomere von Oct-1-in-3-ol mit chiralen Rhodium-Phosphan-Komplexen (H. Singer und M. Steigerwald), 267
Phosphonium allenyl ligand
Protonation of triosmium clusters $Os_3(CO)_9(\mu\text{-}CO)(\mu_3\text{-}2\sigma,\eta^2\text{-}HC{=}CR)$ and $Os_3(\mu\text{-}H)(CO)_9(\mu_3\text{-}\sigma,2\eta^2\text{-}C{=}CR)$ (R = $CH_2OH$, $CMe_2OH$, $C(Me){=}CH_2$) (V.V. Krivykh, O.A. Kizas, E.V. Vorontsov, F.M. Dolgushin, A.I. Yanovsky, Yu.T. Struchkov and A.A. Koridze), 39
Phosphonium complexes
Protonation of triosmium clusters $Os_3(CO)_9(\mu\text{-}CO)(\mu_3\text{-}2\sigma,\eta^2\text{-}HC{=}CR)$ and $Os_3(\mu\text{-}H)(CO)_9(\mu_3\text{-}\sigma,2\eta^2\text{-}C{=}CR)$ (R = $CH_2OH$, $CMe_2OH$, $C(Me){=}CH_2$) (V.V. Krivykh, O.A. Kizas, E.V. Vorontsov, F.M. Dolgushin, A.I. Yanovsky, Yu.T. Struchkov and A.A. Koridze), 39
Phosphorus
Reactions of $(THF)W(CO)_5$ with some diphosphenes carrying bulky aryl and phenoxy groups (D.-L. An, K. Toyota, M. Yasunami and M. Yoshifuji), 7
Pinene
Catalytic hydroformylation of (1*S*,5*S*)-(−)- and (1*R*,5*R*)-(+)-β-pinene: stereoselective synthesis and spectroscopic characterization of (1*S*,2*R*,5*S*)-, (1*S*,2*S*,5*S*)-, (1*R*,2*R*,5*R*)- and (1*R*,2*S*,5*R*)-10-formylpinane (F. Azzaroni, P. Biscarini, S. Bordoni, G. Longoni and E. Venturini), 59
Platinum complex
Preparation and some properties of Pt(II) ruthenocenylacetylide complexes (M. Sato and E. Mogi), 159
Praseodymium
Zur Elektronenstruktur metallorganischer Komplexe der f-Elemente. XXXVIII. Halbsandwich-Komplexe der Stöchiometrien (COT)Ln($HBpz_3$) und (COT)Ln[$HB(3,5\text{-}Me_2pz)_3$]-ideale Systeme für die experimentelle Bestimmung der Kristallfeld-Aufspaltungseffekte des Cyclooctatetraenyl-Liganden (H.-D. Amberger und F.T. Edelmann), 275
Protonation
Protonation of triosmium clusters $Os_3(CO)_9(\mu\text{-}CO)(\mu_3\text{-}2\sigma,\eta^2\text{-}HC{=}CR)$ and $Os_3(\mu\text{-}H)(CO)_9(\mu_3\text{-}\sigma,2\eta^2\text{-}C{=}CR)$ (R = $CH_2OH$, $CMe_2OH$, $C(Me){=}CH_2$) (V.V. Krivykh, O.A. Kizas, E.V. Vorontsov, F.M. Dolgushin, A.I. Yanovsky, Yu.T. Struchkov and A.A. Koridze), 39
Pyridyl
Properties and reactivity of the new $[Ir_4(\mu\text{-}CO)_3(CO)_5(\mu\text{-}PR_3)(PR_3)_2]$ clusters, ($PR_3 = PPh_xpyl_{3-x}$, pyl = 2-pyridyl) (K. Wajda-Hermanowicz, F. Pruchnik and M. Zuber), 75

Rhenium
$^{55}$Mn and $^{187}$Re NQR spectral studies of modulation effects of mutual motions of electrons and atomic nuclei in cyclopentadienyl tricarbonyl manganese and rhenium complexes (G.K. Semin, S.I. Kuznetsov, E.V. Bryukhova and T.L. Khotsyanova), 129
Rhodium
Catalytic hydroformylation of (1*S*,5*S*)-(−)- and (1*R*,5*R*)-(+)-β-pinene: stereoselective synthesis and spectroscopic characterization of (1*S*,2*R*,5*S*)-, (1*S*,2*S*,5*S*)-, (1*R*,2*R*,5*R*)- and (1*R*,2*S*,5*R*)-10-formylpinane (F. Azzaroni, P. Biscarini, S. Bordoni, G. Longoni and E. Venturini), 59
Vergleichende Dimerisierung der Enantiomere von Oct-1-in-3-ol mit chiralen Rhodium-Phosphan-Komplexen (H. Singer und M. Steigerwald), 267
Ring slippage
Ring slippage in indenyl derivatives of molybdenum and tungsten (J.R. Ascenso, I.S. Gonçalves, E. Herdtweck and C.C. Romão), 169
Ring substituents
Multiply substituted cyclopentadienyl metal complexes: I. Solid-state and solution conformational studies on ($\eta^5$-$C_5Me_4R$)Fe(CO)(L)I (R = H, $^t$Bu) (K.E. Du Plooy, J. Du Toit, D.C. Levendis and N.J. Coville), 231
Ruthenium
Synthesis and spectroscopic studies of new hydridoruthenium complexes: catalytic reactions of [RuHCl(bpzm)(cod)] (bpzm = bis(pyrazol-1-yl)methane, cod = cycloocta-1,5-diene) (F.A. Jalón, A. Otero, A. Rodríguez and M. Pérez-Manrique), 69
Synthetic studies of permethylcyclopentadienyl ruthenium(II) complexes involving dppf, (±)-BINAP and (±)-DIOP ligands (M. Sato and M. Asai), 121
Ruthenocene
Preparation and some properties of Pt(II) ruthenocenylacetylide complexes (M. Sato and E. Mogi), 159

Silicon
Katalytische Hydrierung von Halogenmonosilanen mit Tributylzinnhydrid (U. Pätzold, G. Roewer und U. Herzog), 147
Six-electronic propargyl ligand
Protonation of triosmium clusters $Os_3(CO)_9(\mu\text{-}CO)(\mu_3\text{-}2\sigma,\eta^2\text{-}HC{\equiv}CR)$ and $Os_3(\mu\text{-}H)(CO)_9(\mu_3\text{-}\sigma,2\eta^2\text{-}C{\equiv}CR)$ (R = $CH_2OH$, $CMe_2OH$, $C(Me){=}CH_2$) (V.V. Krivykh, O.A. Kizas, E.V. Vorontsov, F.M. Dolgushin, A.I. Yanovsky, Yu.T. Struchkov and A.A. Koridze), 39
Spectroscopy
Reactions of trimethylaluminium with aliphatic diols (W. Ziemkowska and S. Pasynkiewicz), 243
Stereoselectivity
Catalytic hydroformylation of (1*S*,5*S*)-(−)- and (1*R*,5*R*)-(+)-β-pinene: stereoselective synthesis and spectroscopic characterization of (1*S*,2*R*,5*S*)-, (1*S*,2*S*,5*S*)-, (1*R*,2*R*,5*R*)- and (1*R*,2*S*,5*R*)-10-formylpinane (F. Azzaroni, P. Biscarini, S. Bordoni, G. Longoni and E. Venturini), 59
Molecular oxygen promoted oxidative cleavage of carbon–palladium bonds — catalytic cyclization of allylic 2-alkynoates to α-alkylidene-γ-butyrolactones by a $Pd^{II}$ complex (G. Zhu and X. Lu), 83
Steric effects
Multiply substituted cyclopentadienyl metal complexes: I. Solid-state and solution conformational studies on ($\eta^5$-$C_5Me_4R$)Fe(CO)(L)I (R = H, $^t$Bu) (K.E. Du Plooy, J. Du Toit, D.C. Levendis and N.J. Coville), 231
Tributylstannane
Katalytische Hydrierung von Halogenmonosilanen mit Tributylzinnhydrid (U. Pätzold, G. Roewer und U. Herzog), 147
Tricobalt
The reactions of tricobalt alkylidyne complexes $[Co_3(\mu_3\text{-}CR)(CO)_9]$ (R = Me, $CO_2Me$) with the vinyl phosphine ligands $PPh_2CH{=}CH_2$ and *cis*-$Ph_2PCH{=}CHPPh_2$; crystal structure of $[Co_3(\mu_3\text{-}CCO_2Me)(\mu\text{-}Ph_2PCH{=}CHPPh_2)(CO)_7]$ (G.A. Acum, M.J. Mays, P.R. Raithby and G.A. Solan), 137
Triosmium clusters
Protonation of triosmium clusters $Os_3(CO)_9(\mu\text{-}CO)(\mu_3\text{-}2\sigma,\eta^2\text{-}HC{\equiv}CR)$ and $Os_3(\mu\text{-}H)(CO)_9(\mu_3\text{-}\sigma,2\eta^2\text{-}C{\equiv}CR)$ (R = $CH_2OH$, $CMe_2OH$, $C(Me){=}CH_2$) (V.V. Krivykh, O.A. Kizas, E.V. Vorontsov, F.M. Dolgushin, A.I. Yanovsky, Yu.T. Struchkov and A.A. Koridze), 39
Tungsten
Reactions of $(THF)W(CO)_5$ with some diphosphenes carrying bulky aryl and phenoxy groups (D.-L. An, K. Toyota, M. Yasunami and M. Yoshifuji), 7
Ring slippage in indenyl derivatives of molybdenum and tungsten (J.R. Ascenso, I.S. Gonçalves, E. Herdtweck and C.C. Romão), 169

Vanadocene
Electron density distribution in the vanadocene crystal on the basis of X-ray diffraction data at 108 K (M.Yu. Antipin, K.A. Lyssenko and R. Boese), 259
Vinyl
The reactions of tricobalt alkylidyne complexes $[Co_3(\mu_3\text{-}CR)(CO)_9]$ (R = Me, $CO_2Me$) with the vinyl phosphine ligands $PPh_2CH{=}CH_2$ and *cis*-$Ph_2PCH{=}CHPPh_2$; crystal structure of $[Co_3(\mu_3\text{-}CCO_2Me)(\mu\text{-}Ph_2PCH{=}CHPPh_2)(CO)_7]$ (G.A. Acum, M.J. Mays, P.R. Raithby and G.A. Solan), 137
Vinylphosphine
The reactions of tricobalt alkylidyne complexes $[Co_3(\mu_3\text{-}CR)(CO)_9]$ (R = Me, $CO_2Me$) with the vinyl phosphine ligands $PPh_2CH{=}CH_2$ and *cis*-$Ph_2PCH{=}CHPPh_2$; crystal structure of $[Co_3(\mu_3\text{-}CCO_2Me)(\mu\text{-}Ph_2PCH{=}CHPPh_2)(CO)_7]$ (G.A. Acum, M.J. Mays, P.R. Raithby and G.A. Solan), 137

X-ray
Reactions of $(THF)W(CO)_5$ with some diphosphenes carrying bulky aryl and phenoxy groups (D.-L. An, K. Toyota, M. Yasunami and M. Yoshifuji), 7
X-ray diffraction
Synthesis, properties and crystal structure bis(cyclopentadienyl)-aluminium complex $[\eta^1\text{-}(C_5H_5)_2AlO\text{-}^iPr]_2$ (A. Kunicki, R. Sadowski and J. Zachara), 249
X-ray structure
Electron density distribution in the vanadocene crystal on the basis of X-ray diffraction data at 108 K (M.Yu. Antipin, K.A. Lyssenko and R. Boese), 259
Isomeric diphosphines of a heteroannularly bridged ferrocene: preparation, chromatographic separation and structure elucidation (G. Kutschera, C. Kratky, W. Weissensteiner and M. Widhalm), 195
Ring slippage in indenyl derivatives of molybdenum and tungsten (J.R. Ascenso, I.S. Gonçalves, E. Herdtweck and C.C. Romão), 169

Zirconium
Hydride abstraction from ($\eta^2$-acetaldehyde)zirconocene dimer using $B(C_6F_5)_3$ (D. Röttger, S. Schmuck and G. Erker), 263

# Instructions for Authors

## Submission of papers

Manuscripts (Regular Papers, Preliminary Communications and Priority Communications) should be submitted to one of the Regional Editors. Subject Reviews are published upon invitation by the Subject Reviews Editors.

*Regional Editors*

Professor R.B. King, Department of Chemistry, University of Georgia, Athens, GA 30602, USA.

Professor W.A. Herrmann, Anorganisch-chemisches Institut, Technische Universität München, Lichtenbergstrasse 4, D-85747 Garching, Germany.

Professor A. Nakamura, Department of Macromolecular Science, Faculty of Science, Osaka University, Toyonaka, Osaka 560, Japan.

Professor F. Mathey, Laboratoire de Chimie du Phosphore et des Métaux de Transition, Ecole Polytechnique, 91128 Palaiseau Cedex, France.

Professor D.M.P. Mingos, F.R.S., Imperial College, Department of Chemistry, South Kensington, London SW7 2AY, UK.

*Subject Reviews Editors*

Professor J.P. Oliver, Department of Chemistry, Wayne State University, Detroit, MI 48202, USA.

Professor G. van Koten, Department of Organic (Metal-Mediated) Synthesis, Utrecht University, Transitorium 3, Padualaan 8, NL-3584 CH Utrecht, The Netherlands.

*Book Reviews Editor*

Professor C. Eaborn, F.R.S., School of Molecular Sciences, University of Sussex, Brighton BN1 9QJ, UK.

Contributions are accepted on the understanding that authors have obtained the necessary authority for publication. Submission of an article is understood to imply that it is original and unpublished, and is not being considered for publication elsewhere. Upon acceptance of an article by the journal, the author(s) will be asked to transfer the copyright of the article to the publisher. This transfer will ensure the widest possible dissemination of information. A copyright transfer form will be sent to authors together with the proofs.

## Language

Papers will primarily be published in English. Papers in French or German can also be published, and should have an Abstract in English as well as the Resume or Zusammenfassung.

**Authors in Japan please note** that information about how to have the English of your paper checked, corrected and improved (*before submission*) is available from: Elsevier Science (Japan), 20-12 Yushima 3-chome, Bunkyo-ku, Tokyo 113; Tel: (030) 3833-3821; Fax: (03) 3836-3064.

## Manuscript preparation

Three copies of a Regular Paper, Preliminary Communication or Priority Communication should be submitted. Illustrations can be printed in colour when they are judged by the Editor to be essential to the presentation. The publisher and the author will each bear part of the extra costs involved. Further information concerning colour illustrations and the costs to the author can be obtained from the publisher. Further details concerning the preparation of manuscripts, illustrations, etc. are to be found in a leaflet available from Elsevier Science S.A., Avenue de la Gare 50, P.O. Box 564, 1001 Lausanne, Switzerland.

## Submission of electronic text

The final text may be submitted on a 3.5 in or 5.25 in diskette (in addition to a hard copy with original figures). Double density (DD) or high density (HD) diskettes are acceptable, but must be formatted to their capacity before the files are copied on to them. The main text, list of references, tables and figure legends should be stored in separate text files with clearly identifiable file names. The format of these files depends on the word processor used. WordPerfect 5.1 is the most preferable but for other formats please refer to the Instructions to Authors booklet. It is *essential* that the name and version of the wordprocessing program, type of computer on which the text was prepared, and format of the text files are clearly indicated.

The final manuscript may contain last minute corrections which are not included in the electronic text but such corrections must be clearly marked on the hard copy.

## Proofs

Authors will receive proofs which they are requested to return as soon as possible. No new material may be inserted in the text at the time of proof-reading.

All joint articles must indicate the name and full postal address (including telephone and telefax numbers) of the author to whom proofs should be sent.

## Offprints

Twenty-five offprints of each paper will be supplied free of charge to the author(s). Additional offprints may be ordered at prices shown on the offprint order form accompanying the proofs.

There are no page charges.

## Further information

All questions arising after acceptance of a paper, especially those concerning proofs, should be directed to Elsevier Editorial Services, Mayfield House, 256 Banbury Road, Oxford OX2 7DH, UK. (Tel: +44-1865-314900; Fax: +44-1865-314990)

© 1996 - Elsevier Science S.A. All rights reserved
0022-328X/96/$15.00
No part of this publication may be reproduced, stored in a retrieval system or transmitted in any form or by any means, electronic, mechanical, photocopying, recording or otherwise, without the prior written permission of the publisher, Elsevier Science S.A., P.O. Box 564, 1001 Lausanne, Switzerland.

Submission of an article for publication implies the transfer of the copyright from the author(s) to the publisher and entails the author(s) irrevocable and exclusive authorization of the publisher to collect any sums or considerations for copying or reproduction payable by third parties.

Upon acceptance of an article by the journal, the author(s) will be asked to transfer copyright of the article to the publisher. This transfer will ensure the widest possible dissemination of information.

**For Material Subject to US Copyright Law**

Special regulations for readers in the USA - This journal has been registered with the Copyright Clearance Center, Inc. Consent is given for copying of articles for personal or internal use, or for the personal use of specific clients. This consent is given on the condition that the copier pays through the Center the per-copy fee stated in the code on the first page of each article for copying beyond that permitted by Sections 107 or 108 of the US Copyright Law. The appropriate fee should be forwarded with a copy of the first page of the article to the Copyright Clearance Center, Inc., 222 Rosewood Drive, Danvers, MA 01923, USA. If no code appears in an article, the author has not given broad consent to copy and permission to copy must be obtained directly from the author. The fee indicated on the first page of an article in this issue will apply retroactively to all articles published in the journal, regardless of the year of publication. This consent does not extend to other kinds of copying, such as for general distribution, resale, advertising and promotion purposes, or for creating new collective works. Special written permission must be obtained from the publisher for such copying.

No responsibility is assumed by the Publisher for any injury and/or damage to persons or property as a matter of products liability, negligence or otherwise, or from any use or operation of any methods, products, instructions or ideas contained in the material herein.

♾ The paper used in this publication meets the requirements of ANSI/NISO 239.48-1992 (Permanence of Paper).

Printed in The Netherlands

**For:**

**All scientists wishing to keep abreast of developments in the chemistry of fluorine and its compounds**

# JOURNAL OF FLUORINE CHEMISTRY

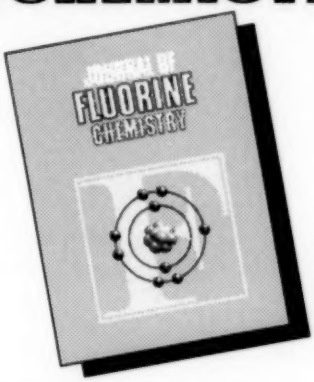


Commenced publication 1971/72
Published in 12 issues in 1995
ISSN 0022-1139

## AIMS AND SCOPE

The *Journal of Fluorine Chemistry* covers inorganic, organic, organometallic and physical chemistry and also includes papers on biochemistry and environmental industrial chemistry. In organic as well as in inorganic chemistry, fluorine and its compounds are important for fundamental investigations as well as for a great variety of industrial applications. This journal deals with all these aspects and serves both pure and applied research in the field. The *Journal of Fluorine Chemistry* contains original papers and preliminary communications describing research on the chemistry of fluorine and of compounds where that halogen exercises significant effects. Preparative and physico-chemical investigations as well as theoretical, structural and mechanistic aspects are covered. Review papers and fluorine chemistry syntheses are also published.

**Editors-in-Chief:**
**D.W.A. Sharp**
*University of Glasgow*
*Department of Chemistry*
*Glasgow, G12 8QQ*
*UK*

**J.C. Tatlow**
*30 Grassmoor Road*
*Kings Norton*
*Birmingham*
*B38 8BP*
*UK*

**ELSEVIER SCIENCE S.A.**
PO Box 564, 1001 Lausanne
Switzerland
tel. : +41 (21) 320 73 81
fax.: +41 (21) 323 54 44

*For customers in the USA and Canada:*
**ELSEVIER SCIENCE INC.**
Attn. Journal Information Center
PO Box 882
Madison Square Station, New York
NY 10159, USA
tel. : +1 (212) 633 3750
fax.: +1 (212) 633 3764

ELSEVIER

**JOURNAL OF FLUORINE CHEMISTRY**

JOM95

*Please send:*
- ❑ A free sample copy
- ❑ Instructions for authors
- ❑ Subscription information
- ❑ Advertising information

Name: _____
Company/Institute: _____
Street: _____ City: _____
Country: _____ Postal Code: _____
Date: _____ Signature: _____

0022-328X(19960208)508:1/2;1-8